# CHEMORECEPTION

# ADVANCES IN EXPERIMENTAL MEDICINE AND BIOLOGY



---

Recent Volumes in this Series

Volume 527
DEVELOPMENTS IN TRYPTOPHAN AND SEROTONIN METABOLISM
Edited by Graziella Allegri, Carlo V. L. Costa, Eugenio Ragazzi, Hans Steinhart, and Luigi Varesio

Volume 528
ADAMANTIADES-BEHÇET'S DISEASE
Edited by Christos C. Zouboulis

Volume 529
THE GENUS *YERSINIA*: Entering the Functional Genomic Era
Edited by Mikael Skurnik, José Antonio Bengoechea, and Kaisa Granfors

Volume 530
OXYGEN TRANSPORT TO TISSUE XXIV
Edited by Jeffrey F. Dunn and Harold M. Swartz

Volume 531
TROPICAL DISEASES: From Molecule to Bedside
Edited by Sangkot Marzuki, Jan Verhoef, and Harm Snippe

Volume 532
NEW TRENDS IN CANCER FOR THE 21ST CENTURY
Edited by Antonio Llombart-Bosch and Vicente Felipo

Volume 533
RETINAL DEGENERATIONS: Mechanisms and Experimental Theory
Edited by Matthew M. LaVail, Joe G. Hollyfield, and Robert E. Anderson

Volume 534
TISSUE ENGINEERING, STEM CELLS, AND GENE THERAPIES
Edited by Y. Murat Elçin

Volume 535
GLYCOBIOLOGY AND MEDICINE
Edited by John S. Axford

Volume 536
CHEMORECEPTION: From Cellular Signaling to Functional Plasticity
Edited by Jean-Marc Pequignot, Constancio Gonzalez, Colin A. Nurse, Nanduri R. Prabhakar, and Yvette Dalmaz

---

# CHEMORECEPTION

## From Cellular Signaling to Functional Plasticity

Edited by

Jean-Marc Pequignot
*CNRS—University Claude Bernard*
*Lyon, France*

Constancio Gonzalez
*University of Valladolid*
*Valladolid, Spain*

Colin A. Nurse
*McMaster University*
*Hamilton, Ontario, Canada*

Nanduri R. Prabhakar
*Case Western Reserve University*
*Cleveland, Ohio*

and

Yvette Dalmaz
*CNRS—University Claude Bernard*
*Lyon, France*

Springer Science+Business Media, LLC

Library of Congress Cataloging-in-Publication Data

International Symposium on Arterial Chemoreception (15th : 2002 : Lyon, France)
Chemoreception : from cellular signalling to functional plasticity / edited by Jean-Marc Pequignot ... [et al.].
p. ; cm. -- (Advances in experimental medicine and biology, ISSN 0065-2598 ; v. 536)
Includes bibliographical references and index.
ISBN 978-1-4613-4873-3 ISBN 978-1-4419-9280-2 (eBook)
DOI 10.1007/978-1-4419-9280-2
1. Chemoreceptors--Congresses. 2. Arteries--Congresses. I. Pequignot, Jean-Marc. II. Title. III. Series.
[DNLM: 1. Arteries--physiology--Congresses. 2. Chemoreceptors--physiology--Congresses. 3. Carotid Body--physiology--Congresses. 4. Cell Hypoxia--physiology--Congresses. 5. Oxygen--metabolism--Congresses. WG 510 I608c 2003]
QP455.I538 2002
612.1'33--dc22
2003054474

Proceedings of the XVth International Symposium on Arterial Chemoreception, held November 18–22, 2002, in Lyon, France

ISSN 0065-2598


Originally published by Kluwer Academic / Plenum Publishers, New York in 2003
Softcover reprint of the hardcover 1st edition 2003

http://www.wkap.nl/

10 9 8 7 6 5 4 3 2 1

A C.I.P. record for this book is available from the Library of Congress

# Preface

Since 1959, the International Society of Arterial Chemoreception (ISAC) has organized in a variety of countries fifteen scientific meetings devoted to the mechanisms of peripheral arterial chemoreception and chemoreceptor reflexes. After the meeting held in Philadelphia with Sukhamay Lahiri as president, ISAC membership elected Lyon (CNRS, University Claude Bernard, France) as the site of the XV$^{th}$ ISAC Symposium. The Symposium was effectively held in Lyon from the 18th to the 22nd of November 2002 and Jean-Marc Pequignot was its president. The organizers were Jean-Marc Pequignot and Yvette Dalmaz Lyon (CNRS, University Claude Bernard, France) and the Scientific Committee was formed by John Carroll (University of Arkansas for Medical Sciences, USA), Constancio Gonzalez (University of Valladolid, Spain), Prem Kumar (University of Birmingham, U.K.), Sukhamay Lahiri (University of Pennsylvania, Philadelphia, USA), Colin Nurse (McMaster University, Hamilton, Ontario, Canada), and Nanduri Prabhakar (Case Western University, Cleveland, Ohio, USA).

The Symposium in Lyon intended to follow the path opened in Philadelphia gathering people working at the interface of cellular and molecular biology with researchers in the more classical topics of chemoreception pathways and reflexes. The aim was to join experts with different perspectives. Along these lines, some participants are engaged in the exploration of the intimate mechanisms of oxygen sensing and cellular responses, with their work centered in a great number of preparations covering a broad spectrum from bacteria, to chemoreceptor cells or to central nervous systems neurons. Other participants in the Symposium are directing their efforts to define the responses elicited by alterations in oxygen availability, but the levels of their description are organs, systems or even entire organisms; this group of participants in the Symposium include

researchers dedicated to define the morphofunctional pathways linking the chemoreceptors and other oxygen sensing cells to the responding organs. The plasticity of the entire oxygen-sensing and effector machinery, triggered by continuous or intermittent exposure to altered oxygen levels also received special attention.. The plasticity was evidenced by modifications in the intimate molecular and cellular mechanisms, by changes in the anatomical pathways and functional responses seen in intact animals. These latest aspects brought our Symposium to the frontiers of physiology to meet the physiopathology and the mechanisms of disease. The Symposium program was built along these lines to accommodate the wide spectrum of participants.

In this Symposium we also wanted to make a tribute to Pierre Dejours (CNRS, Strasbourg, France). Pierre Dejours, who retired a few years ago, had a major part in the study of peripheral chemoreception. His investigations are considered as an important landmark that proved to be pivotal in the study of breathing regulation. Henry Gautier who was a close collaborator of Pierre Dejours presented a plenary lecture in his honor. The related chapter by Henry Gautier in this volume describes the steps of research work, which have led in particular to the so-called oxygen test or Dejours's test, classically used to assess the peripheral arterial chemosensitivty level in humans or animals, in neonates or adults.

As some of the most senior scientists in the field have pointed out, the Lyon Symposium has proven to be one of optimism: a great number of young investigators participated actively in the meeting and presented exciting results in various fields of chemoreception. Their successful contributions provided evidence for the growing interest of the international scientific community in the field of oxygen-sensing and chemoreception. A special session was organized to recognize the significant contributions of this new scientist generation and the ISAC membership awarded three prizes to Silvia Conde (New University of Lisbon, Portugal), Maria Garcia-Fernandez (University of Sevilla, Spain), and Michael G. Jonz (McMaster University, Hamilton, Ontario, Canada).

At a business meeting the ISAC council and the membership decided on the venue of the next ISAC symposium which is to be held in Sendai, Japan, in 2005, with Hisatake Kondo as its president. The following conference is to be held in Valladolid, Spain, in 2008, with Constancio Gonzalez as its president.

Several institutions provided funds for the organization of the XVth ISAC Symposium: Centre National de la Recherche Scientifique (CNRS), Institut National de la Recherche Médicale (INSERM), Université Claude Bernard Lyon I, Conseil Général du Rhône, Institut de Recherches Internationales Servier, Région Rhône-Alpes, Ville de Lyon. We are grateful

to all of them. Their generous financial support was essential to ensure the welcome of the participants. In particular, the support of Région Rhône-Alpes made it possible to publish this volume.

We are also very grateful to every participant who contributed scientifically and constructively to the fruitful discussions and the congenial atmosphere of the ISAC conference. Finally, we would like to thank especially Michele Chabrier ("Influence") who played a major role in the organization of the meeting and social program, Annick Brillant and Jacqueline Pequignot for the management of the editorial aspects of this volume.

The Editors,

*Jean-Marc Pequignot (Lyon, France)*
*Constancio Gonzalez (Valladolid, Spain)*
*Colin Nurse (Hamilton, Ontario, Canada)*
*Nanduri Prabhakar (Cleveland, Ohio, USA)*
*Yvette Dalmaz (Lyon, France)*

CONTENTS

**$O_2$ and $CO_2$ Sensing Mechanisms in Airway Chemoreceptors, Pulmonary Artery Smooth Muscle Cells and Other Oxygen-sensing Systems : Membrane Properties, Intracellular Metabolic and Genomic Events**

**Plasticity of Chemosensitivity Processes During Development: Transition at Birth and Delayed Effects**

**Plasticity of Chemosensitive Processes : Acclimatization to Intermittent Versus Chronic Hypoxia in Adult**

# Honoring Pierre Dejours : His Contribution to the Study of the Role of the Arterial Chemoreceptors in the Regulation of Breathing in Humans

HENRY GAUTIER
*Atelier de Physiologie Respiratoire, Faculté de Médecine Saint-Antoine ; 27, rue Chaligny 75012-Paris, France*

In the mid-fifties, Dejours became interested in the contribution of the arterial chemoreceptors in the regulation of breathing in humans. The role, but not the intimate mechanisms, of the receptors was relatively well known thanks to the experiments of recording of afferent activity and of electrical stimulation or denervation of afferent nerves but, for obvious reasons, these experiments could not be performed in humans. Human beings are provided with the same chemosensitive structures as laboratory animals and the fact that functional responses to respiratory stimuli (hypoxia and/or hypercapnia) are about the same in humans and experimental animals makes it likely that in human beings, the part played by the reflexogenic drive is the same as in animals.

Dejours (1957) asked the following question : *If a ventilatory oxygen drive does exist in humans under a given condition, how could it be demonstrated ?* The inhalation of a high oxygen mixture will suppress the drive and it is expected that ventilation should decrease. Conversely, the inhalation of a moderately hypoxic mixture will enhance the drive and an increase of ventilation would be anticipated. In practice, most physiologists have studied the expected changes in ventilation following a few minutes inhalation of a hyperoxic or hypoxic mixture.

Actually, at rest and at sea level, the ventilatory response to hyperoxic mixtures appears quite variable as shown in Table 1. However, it is important to emphasize that the response is definitely related to the duration of the exposure to hyperoxia. Indeed, if a high oxygen mixture is breathed for several minutes, ventilation does not change or even increases whereas, after only 1 or 2 minutes of hyperoxia, a significant reduction in ventilation is observed. Dejours (1957) realized that the method which consists in studying the ventilatory effects of pure oxygen inhalation after several minutes of such an inhalation is inadequate. In fact, a prolonged oxygen

*Chemoreception*, Edited by Pequignot et al.
Kluwer Academic/Plenum Publishers, New York, 2003

inhalation not only suppresses the oxygen drive but can and does provoke the change of many other factors which also act on ventilation, for instance : decrease of arterial pH due to an increase in oxyhemoglobin, change of alveolar and arterial $PCO_2$ and pH in the respiratory centers and possible circulatory changes such as in the cerebral blood flow. For these reasons, the observed change in ventilation represents only one aspect of a change in the oxygenation of the body, and it therefore cannot be interpreted simply in terms of oxygen drive.

*Table 1.* Effects of oxygen on ventilation in humans

| Authors | Number of subjects | $FIO_2$ % | Duration of exposure | % changes in ventilation |
|---|---|---|---|---|
| Shock and Soley (1940) | 33 | 100 | 20 min | + 13.4 |
| Dripps and Comroe (1947) | 33 | 100 | 6-8 min | + 7.6 |
| May(1957) | 15 | 60 | 10 min | + 0.4 |
| Loeschcke (1953) | 20 | 32 | 4 min | 0 |
| Dripps and Comroe (1947) | 32 | 100 | 1-2 min | - 3.1 |
| Loeschcke (1953) | 20 | 32 | 1 min | - 8.0 |
| May (1957) | 15 | 60 | 1 min | - 19.5 |

It is, however, possible to obtain a change in the oxygen drive almost free of secondary reactions. If in a given condition there is a chemoreflex oxygen drive (or more precisely a chemoreceptor hypoxic drive), the inhalation of a high oxygen mixture increases alveolar $PO_2$ at the first breath and after a few seconds, the blood with higher $PO_2$ flowing from the lungs perfuses the chemoreceptor carotid bodies, the activity of which should then decrease. Just at this time, a decrease in ventilation must be observed. With

such a method, most of the secondary factors are avoided because they are secondary in time. The inhalation of oxygen can be restricted to one or two breaths or can be prolonged for some time ; these techniques are referred to as the single-breath, double-breath or continuous oxygen test (Dejours *et al.*, 1958b).

In fact, the technique of the oxygen test is a particular application of a quite general method. Referring to the constancy of the *milieu interieur* put forward by Claude Bernard, Dejours (1962) indicates that : *Any new factor imposed upon an organism changes its equilibrium. In the early phase of the period of action of the disturbing agent, at the moment of maximal disruption, the transient variations observed in the organism can be related to it. But when the disturbing agent is applied for a prolonged time, many secondary reactions occur, generally tending to cancel out the disturbing effects of the factor of disequilibrium. These secondary reactions terminate eventually in a new state of equilibrium, the analysis of which is very complex.*

With the technique of the oxygen test, Dejours *et al.* (1957) observed that in normoxia, ventilation decreases transiently by about 10% after a delay of 10 seconds corresponding to the circulation time between the lung and the carotid body. If the subject is first made hypoxic by breathing an hypoxic mixture, the fall in ventilation following the oxygen test is much greater and the more hypoxic the subject, the greater the fall which is induced by 100% oxygen breathing (*e.g.* –13% with $FIO_2 = 0.17$ and –32% with $FIO_2 = 0.14$). Conversely, when the subject is made hyperoxic by breathing continuously a 33% oxygen mixture resulting in an alveolar $PO_2$ around 170 mmHg, the inhalation of 100% oxygen for one breath is not followed by any significant change in ventilation. This observation shows that the alveolar $PO_2$ threshold for oxygen stimulation of the chemoreceptors in human beings lies somewhere between 100 and 170 mmHg, a conclusion which agrees well with the data furnished by the direct recordings of chemoreceptor activity in animals as function of $PaO_2$.

It thus appears that the wave of hyperoxic blood, induced by the inhalation of 100% oxygen, suppresses the hypoxic chemoreceptor drive, resulting in a decrease in ventilation. This interpretation is based on the following considerations : a) In the awake dog, the same transient fall in ventilation is seen under otherwise identical conditions but it no longer occurs after chronic surgical chemodenervation (Bouverot *et al.*, 1965) ; b) In anaesthetized cats, 3 seconds after the start of oxygen breathing (*physiological or chemical denervation* of Dripps and Comroe, 1947), there occurs a decrease in ventilation together with a decrease in the chemoreceptor discharge recorded in the Hering's nerve (Leitner *et al.*, 1965) ; and c) Man has a functional arterial chemoreceptor system and,

indeed, Guz *et al.* (1966) showed in one unanaesthetized subject that vagus and glossopharyngeal nerve block by local anaesthesia resulted in almost complete abolition of the hyperventilation which occurs when breathing an hypoxic gas mixture. This experiment was the first to show in man that hypoxic hyperventilation had a chemoreflex origin.

It must be pointed out that the fall of ventilation recorded after the start of 100% oxygen breathing does not afford an accurate estimate of the magnitude of the ventilatory oxygen drive prior to the oxygen inhalation. Indeed, at the time when the maximal fall of ventilation is observed, $PO_2$ of the blood perfusing the carotid bodies may not be above the threshold of stimulation. If the oxygen inhalation is prolonged, arterial $PO_2$ reaches values much higher than the threshold of the chemoreceptors, but by that time, some secondary reactions have intervened, such as hypercapnia, which develops as soon as ventilation decreases after the start of 100% oxygen breathing.

The oxygen test that was just described above has been used at sea level by Dejours and his collaborators in various situations such as in man during muscular exercise (Dejours et al., 1958b), in premature and full-term newborn babies (Girard et al., 1960) and in different animal species such as birds (Bouverot and Leitner, 1972). During short-term acclimatization to an altitude of 3600m, a 50% fall in ventilation was consistently observed 15 to 20 seconds after a single-breath of 100% oxygen. This phenomenon demonstrated the existence of a strong oxygen drive which did not show any trend toward diminution during the period spent at altitude (Dejours *et al.*, 1959). Using also the oxygen test at altitude, we have confirmed the results of Dejours *et al.* and, in addition, we have shown that the decrease in ventilation was much smaller in subjects born and living permanently at altitude. We also confirmed that after a few minutes of 100% oxygen breathing, the ventilation was not significantly affected as indicated above (Lefrançois *et al.*, 1968).

The technique of the single-breath and its effects on the ventilation in the following seconds was not limited to the use of 100% oxygen. Indeed, Dejours and his collaborators used also single-breaths of nitrogen to provoke or enhance an hypoxic stimulus (Girard *et al.*, 1959). Likewise, $CO_2$-tests were also used in humans (Dejours *et al.*, 1958a) and dogs (Bouverot *et al.*, 1965). In the latter, this was done before and after carotid-denervation to determine the participation of the peripheral and central chemoreceptors in the ventilatory response to hypercapnia.

In short, the contribution of Pierre Dejours to the study of chemoreceptors was very important in the sixties and has initiated numerous studies. His investigations are now considered as a landmark that proved to be pivotal in the study of the regulation of breathing, particularly in humans

and, not surprisingly, references to Dejours's studies are often found in the literature (see for instance the recent work of Subramanian *et al.*, 2002).

According to the classical investigations of Dejours using the transient inhalation of oxygen or nitrogen, it was thought 40 years ago that the oxygen or rather the hypoxic drive was affecting ventilation through an *exclusive* action on arterial chemoreceptors. However, as indicated above, it was already known that when oxygen was breathed for several minutes, after the initial decrease in ventilation, a recovery and sometimes a hyperventilation could be observed. This recovery could not easily be explained and it was suggested that it was multifactorial in origin.

Since that time, numerous investigations carried out in laboratory animals and even in humans have definitively shown that exposure to various oxygen mixtures can affect ventilation and other functions by acting directly on the central nervous system. All these studies will not be rewiewed in this paper and only two examples will be mentioned as they are directly relevant to the control of breathing and are nowadays the subject of interesting projects which involve several neuro-modulators.

During acute exposure to hypoxia, ventilation increases to a peak. Immediately following this increase, ventilation decreases somewhat over the subsequent 10-30 minutes (Easton *et al.*, 1986). Although its intimate mechanisms are not fully understood, there is considerable experimental evidence that the decline in the ventilatory response to hypoxia, also named roll-off, reflects the effects of hypoxia on the central nervous system and probably involves the release of inhibitory neuro-modulators (see Bisgard and Neubauer, 1995). On the other hand, as indicated above, hyperoxia, after a brief hypoventilation, determines an increase in ventilation to or even above the control level. It seems quite remarkable that the secondary increase in ventilation observed during oxygen breathing appears as the opposite, the mirror image, of the ventilatory decline observed during hypoxia. Hence, it appears that hyperoxia has a central stimulatory component with a time-constant of a few minutes that can be masked by the abrupt decreased ventilatory drive of the chemoreceptors. This interpretation is supported by the fact that in intact conscious cats, *prolonged* oxygen breathing has no significant effects on ventilation whereas it induces a sustained hyperventilation after carotid-body denervation (Miller and Tenney, 1975 ; Gautier *et al.*, 1986). Finally, there are other results suggesting that hypoxia may also change ventilation and other functions such as body temperature regulation by acting directly on the central nervous system (Roux *et al.*, 2000). This is the case for the ventilatory depression consistently seen during hypoxia after carotid-body denervation in anaesthetized preparations whereas conscious carotid-body denervated

animals either showed no change in ventilation or actually hyperventilated when exposed to hypoxia (see Mortola and Gautier, 1995).

Another example concerns the interesting and intriguing effect of prior hyperoxia on the ventilatory response to hypoxia. It has been shown that the recovery process of the enhanced hypoxic depression by repeated hypoxic challenges in humans was slow in normoxic conditions as it required 30-60 minutes but this process could be accelerated by inhalation of 100% oxygen (Easton *et al.*, 1988). In addition, Honda *et al.* (1996) have recently shown, also in humans, that a short hyperoxic exposure before isocapnic hypoxia could potentiate the peak ventilatory response to hypoxia without modifying the late component of the biphasic ventilatory response. This was confirmed by Gozal (1998) in conscious freely behaving rats. Honda *et al.* speculated that central glutamate may be involved whereas the results of Gozal suggested that neuronal nitric oxide synthase may play an important role in such hypoxic ventilatory response potentiation by a previous hyperoxic exposure.

This review is limited to these recent studies in order to illustrate the fact that the mechanisms of action of hypoxia or hyperoxia on ventilation are far to be completely understood. However, it has now been demonstrated in numerous reports that these mechanisms involved several mediators or modulators at the periphery but also at the level of the central nervous system. It must be emphasized that all these recent studies do not contradict at all and rather help to explain the early findings of Pierre Dejours concerning the participation of the peripheral chemoreceptors in the regulation of breathing.

## REFERENCES

Bisgard, G.E., and Neubauer, J.A., 1995, Peripheral and central effects of hypoxia. In *Regulation of Breathing* (J.A. Dempsey and A.I. Pack, eds), Marcel Dekker, Inc, New York, pp.617-668.

Bouverot, P., Flandrois, R., Pucinelli, R., and Dejours, P., 1965, Etude du rôle des chémorécepteurs artériels dans la régulation de la respiration pulmonaire chez le chien éveillé. *Arch. Int. Pharmac.Thérap.* 157 : 257-271.

Bouverot, P., and Leitner, L.-M., 1972, Arterial chemorecptors in the domestic fowl. *Respir. Physiol.*15 : 310-320.

Dejours, P., 1957, Intérêt méthodologique de l'étude d'un organisme vivant à la phase initiale de rupture d'un équilibre physiologique. Compt. Rend. Acad. Sci. Paris 245 : 1946-1948.

Dejours, P., 1962, Chemoreflexes in breathing. *Physiol. Rev. 42 :* 335-358.

Dejours, P., Girard, F., Labrousse, Y., and Teillac, A., 1959, Etude de la régulation ventilation de repos chez l'Homme en haute altitude. *Rev. Fr. Etudes Clin. Biol. 4* : 115-127.

Dejours, P., Labrousse, Y., Raynaud, J., and Flandrois, R., 1958a, Etude du stimulus gaz carbonique de la ventilation chez l'Homme. *J. Physiol. Paris 50 :* 239-243.

Dejours, P., Labrousse, Y,, Raynaud, J., Girard, F., and Teillac, A., 1958b, Stimulus oxygène de la ventilation au repos et au cours de l'exercice musculaire, à basse altitude (50m), chez l'Homme. *Rev. Fr. Etudes Clin. Biol. 3 :* 105-123.

Dejours, P., Labrousse, Y., Raynaud, J., and Teillac, A., 1957, Stimulus oxygène chémoréflexe de la ventilation à basse altitude (50m) chez l'Homme. I Au repos. *J. Physiol. Paris 49 :* 115-124.

Dripps, R.D., and Comroe, J.H., Jr, 1947, The effect of the inhalation of high and low oxygen concentrations on respiration, pulse rate, ballisto-cardiogram and arterial oxygen saturation oximeter) of normal individuals. *Amer. J. Physiol.* 149 : *277-291.*

Easton, P. A., Slykerman, L.J., and Anthonisen, N.R., 1986, Ventilatory response to sustained hypoxia in normal adults. *J. Appl. Physiol.* 61 : 906-911.

Easton, P.A., Slykerman, L.J., and Anthonisen, N.R., 1988, Recovery of the ventilatory response to hypoxia in normal adults. *J. Appl. Physiol.* 64 : 521-528.

Gautier, H., Bonora, M., Gaudy, J.H., 1986, Ventilatory response of the conscious or anesthetized cat to oxygen breathing. *Respir. Physiol.* 65 : 181-196.

Girard, F., Lacaisse, A., and Dejours, P., 1960, Le stimulus $O_2$ ventilatoire à la période néonatale chez l'Homme. *J. Physiol. Paris* 52 : 108-109.

Girard, F., Teillac, A., Lefrançois, R., and Lacaisse, A., 1959, Etude du stimulus oxygène de la ventilation en hypoxie aiguë. *J. Physiol. Paris* 51 : 469-470.

Gozal, D., 1998, Potentiation of hypoxic ventilatory response by hyperoxia in the conscious rat :putative role of nitric oxide. *J. Appl. Physiol.* 85 : 129-132.

Guz, A., Noble, M.I.M., Widdicombe, J.G., Trenchard, D., and Mushin, W.W., 1966, Peripheral chemoreceptor block in man. *Respir. Physiol.* 1 : 38-40.

Honda, Y., Tani, H., Masuda, A., Kobayashi, T., Nishino, T., Kimura, H., Masuyama, S., and Kuriyama, T., 1996, Effect of prior $O_2$ breathing on ventilatory response to sustained isocapnic hypoxia in adult humans. *J. Appl. Physiol.* 81 : 1627-1632.

Lefrançois, R., Gautier, H., and Pasquis, P., 1968, Ventilatory oxygen drive in acute and chronic hypoxia. *Respir. Physiol.* 4 : 217-228.

Leitner, L.-M., Pagès, B., Pucinelli, R., and Dejours, P., 1965, Etude simultanée de la ventilation et des décharges des chémorécepteurs du glomus carotidien chez le chat. I Au cours d'inhalations brèves d'oxygène pur. Arch. Int. Pharmac. Thérap. 154 : 421-426.

Loeschcke, G.C., 1953, Spielen für die Ruheatmung des Menschen vom O2-Druck abhängige Erregungen des Chemoreceptoren eine Rolle *? Arch. ges.Physiol.* 257 : 349-362.

May, P., 1957, L'action immédiate de l'oxygène sur la ventilation chez l'homme normal. *Helv. Physiol. Acta* 15 : 230-240.

Miller, M.J., and Tenney, S.M., 1975, Hyperoxic hyperventilation in carotid-deafferented cats *Respir. Physiol.* 23 : 23-30.

Mortola, J.P., and Gautier, H., 1995, Interaction between metabolism and ventilation : Effects of respiratory gases and temperature. In Regulation of Breathing (J.A. Dempsey and A.I. Pack, eds*), Marcel Dekker, Inc, New York, pp.*1011-1064.

Roux, J.C., Peyronnet, J., Pascual, O., Dalmaz, Y., and Péquignot, J.C., 2000, Ventilatory and central neurochemical reorganisation of $O_2$ chemoreflex after carotid sinus nerve transection in rat. *J. Physiol. London 522 :* 493-501.

Shock, N.W., and Soley, M.H., 1940, Effect of breathing pure oxygen on respiratory volume in humans. *Proc. Soc. Exp. Biol. Med. 44 :* 418-420.

Subramanian, S., Erokwu, B., Han, F., Dick, T.E., and Strohl, K.P., 2002, L-NAME differentially alters ventilatory behavior in Sprague-Dawley and Brown Norway rats. J. *Appl. Physiol.* 93 : 984- 989.

# 2P Domain $K^+$ Channels : Novel Pharmacological Targets for Volatile General Anesthetics

AMANDA J. PATEL and ERIC HONORE
*From Institut de Pharmacologie Moléculaire et Cellulaire, CNRS-UMR6097, 660 route des Lucioles, Sophia Antipolis, 06560 Valbonne, France. Tel.: +33 (0)4 93 95 77 02/03 - Fax: +33 (0)4 93 95 77 04 - E-mail: honore@ipmc.cnrs.fr*

## 1. INTRODUCTION

Volatile anesthetics induce neuron hyperpolarization and consequent depression of the central nervous system (Nicoll and Madison, 1982; Berg-Johnsen and Langmoen, 1987; Franks and Lieb, 1988; el-Beheiry and Puil, 1989; Southan and Wann, 1989; MacIver and Kendig, 1991; Franks and Lieb, 1994; Harris *et al.*, 1995; Belelli *et al.*, 1999; Sirois *et al.*, 2000). Besides the well known potentiation of GABAA and glycine chloride channels (Harris *et al.*, 1995; Belelli *et al.*, 1999), evidence demonstrates that in both vertebrates and invertebrates, volatile anesthetics open background $K^+$ channels and thus increase the resting membrane potential (Franks and Lieb, 1988; Winegar *et al.*, 1996; Lopes *et al.*, 1998; Sirois *et al.*, 2000). For instance, in the mollusc Lymnea, halothane opens a class of baseline $K^+$ channels (IKAn) which hyperpolarize and silence pacemaker neurons (Franks and Lieb, 1988; Franks and Lieb, 1991; Lopes *et al.*, 1998). In *Aplysia* californica, halothane-mediated neuronal hyperpolarization is due to the opening of the background S type (serotonin-sensitive) $K^+$ channel (Winegar *et al.*, 1996). Similarly, opening of baseline acid-sensitive $K^+$ channels by volatile anesthetics produces rat hypoglossal and locus coeruleus neuron hyperpolarization (Sirois *et al.*, 1998; Sirois *et al.*, 2000).

Recent reports demonstrate that the volatile anesthetic-sensitive background $K^+$ channels belong to the family of mammalian $K^+$ channel subunits with four transmembrane segments and two P regions (Patel *et al.*, 1999; Gray *et al.*, 2000; Lesage *et al.*, 2000; Sirois *et al.*, 2000). Interestingly, the yeast 2P domain $K^+$ channel, which is characterized by eight, instead of four transmembrane segments, is also activated by volatile anesthetics demonstrating the conservation of this pharmacology (Ketchum *et al.*, 1995; Gray *et al.*, 1998). The mammalian 2P domain $K^+$ channel subunits are characterized by diverse patterns of expression and functional properties (Lesage and Lazdunski, 2000;

*Chemoreception*, Edited by Pequignot et al.
Kluwer Academic/Plenum Publishers, New York, 2003

Goldstein *et al.*, 2001; Patel and Honoré, 2001; Patel and Honoré, 2001; Patel and Honoré, 2001; Patel *et al.*, 2001). Volatile anesthetics selectively open human TREK-1, TREK-2, TASK-1, TASK-2 and TASK-3 channels (Patel *et al.*, 1999; Gray *et al.*, 2000; Lesage *et al.*, 2000; Meadows and Randall, 2001). On the contrary, local anesthetics reversibly inhibit the 2P domain $K^+$ channels (Patel *et al.*, 1998; Kindler *et al.*, 1999; Rajan *et al.*, 2000; Meadows and Randall, 2001). In the present report, the expression and properties of these anesthetic-sensitive $K^+$ channels are reviewed and their possible functional role in the mechanisms of anesthesia is discussed.

## 2. THE MAMMALIAN 2P DOMAIN $K^+$ CHANNELS

Mammalian $K^+$ channels belong to four main structural classes made of two, four, six and seven transmembrane segments (TMS) (Lesage and Lazdunski, 2000; Goldstein *et al.*, 2001; Patel and Honoré, 2001; Patel and Honoré, 2001; Patel and Honoré, 2001; Patel *et al.*, 2001). The common feature of all $K^+$ channels is the presence of a conserved motif called the P domain (the $K^+$ channel signature sequence or putative pore-forming region) which is part of the $K^+$ conduction pathway (Doyle *et al.*, 1998). The two, six and seven TMS classes are characterized by the presence of a single P domain while the most recently discovered class of four TMS subunits is characterized by the presence of a tandem of P domains (Lesage and Lazdunski, 2000; Goldstein *et al.*, 2001; Patel and Honoré, 2001; Patel and Honoré, 2001; Patel and Honoré, 2001; Patel *et al.*, 2001) (fig. 1).

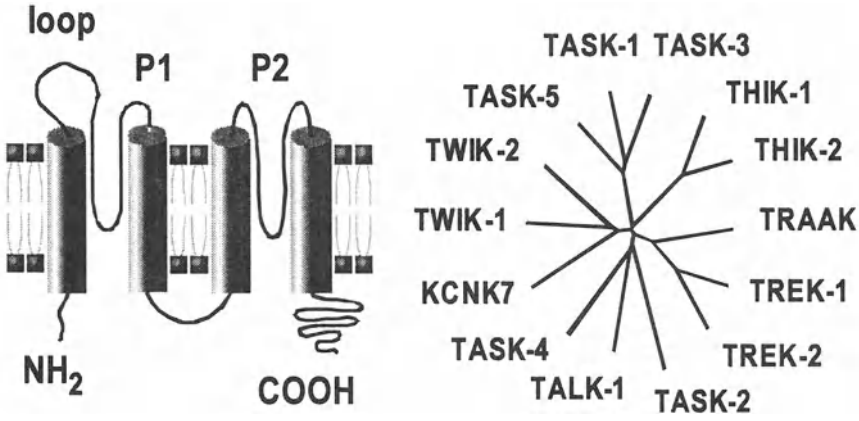


*Figure 1*: The human 2P domain $K^+$ channel subunits. Membrane topology of a background $K^+$ channel with four transmembrane segments and two P domains. Phylogenetic tree of the 14 human 2P domain $K^+$ channels.

Functional $K^+$ channels are tetramers of pore-forming subunits for the two, six and seven TMS classes and dimers in the case of the four TMS class (Lesage *et al.*, 1996; Lopes *et al.*, 2001).

The 2TMS/1P $K^+$ channels encode the inward rectifiers. These $K^+$ channels close with depolarization because of channel block by intracellular $Mg^{2+}$ and polyamines (for review Ruppersberg, 2000). The conductance increases upon hyperpolarization and consequently, the inward $K^+$ currents recorded at potentials below the equilibrium potential $EK^+$ (about -90 mV in a physiological $K^+$ gradient) are much larger than the outward $K^+$ currents recorded at depolarized potentials. Although, the amplitude of the outward currents flowing through the inward rectifiers is limited, they will have a major influence on the resting membrane potential (Hille, 1992). The voltage at which channel gating by intracellular $Mg^{2+}$ and polyamines occurs will set the range where the $K^+$ channel will influence the cell membrane potential. Because they are blocked at depolarized potentials, these channels will have a limited role in the initial repolarization of the action potential.

By contrast, the voltage-gated outward rectifiers encoded by the 6TMS/1P subunits, open upon depolarization. Depolarization is sensed by the positively charged fourth TMS which is coupled to activation gates. Opening of the voltage-gated $K^+$ channels is time-dependent (delayed rectifiers) and contributes to repolarize and terminate the action potential (Hille, 1992). Several voltage-gated $K^+$ channels are also characterized by a fast (N-type) inactivation process. The inactivation gate is the positively charged amino terminus of these specific subunits (ball and chain mechanism). The SK (6TMS/1P) and BK (7TMS/1P) channels are outward rectifiers which are opened by an increase in intracellular calcium. Additionally BK channels are activated by membrane depolarization.

The class of mammalian 4 TMS $K^+$ channel subunits has expanded to include 14 members (fig. 1). These subunits share the same structural motif with 4 TMS/2P, an extended M1P1 extracellular loop, and both amino- and carboxy- termini facing the cytosol. However, low sequence identity is found outside the pore domain (Lesage and Lazdunski, 2000; Goldstein *et al.*, 2001; Patel and Honoré, 2001; Patel and Honoré, 2001; Patel and Honoré, 2001; Patel *et al.*, 2001). The mammalian 2P domain $K^+$ channels are classified into five main structural subgroups: *i*) TWIK-1 (KCNK1), TWIK-2 (KCNK6) and KCNK7 (Lesage *et al.*, 1996; Chavez *et al.*, 1999; Pountney *et al.*, 1999; Salinas *et al.*, 1999; Patel *et al.*, 2000) (KCNK7 is not functional); *ii*) TASK-1 (KCNK3), TASK-3 (KCNK9) and TASK-5 (KCNK15) (TASK-5 is not functional) (Duprat *et al.*, 1997; Kim *et al.*, 1998; Leonoudakis *et al.*, 1998; Chapman *et al.*, 2000; Kim *et al.*, 2000; Rajan *et al.*, 2000); *iii*) TREK-1 (KCNK2), TREK-2 (KCNK10) and TRAAK (KCNK4) (Fink *et al.*, 1996; Fink *et al.*, 1998; Bang *et al.*, 2000; Lesage *et al.*, 2000); *iv*) TASK-2 (KCNK5),

TALK-1 (KCNK16) and TALK-2 (KCNK17) (also called TASK-4) (Reyes *et al.*, 1998; Gray *et al.*, 2000; Decher *et al.*, 2001; Girard *et al.*, 2001); *v*) THIK-1 (KCNK13) and THIK-2 (KCNK12) (Rajan *et al.*, 2000) (THIK-2 is not functional) (fig. 1). 2P domain $K^+$ channels have also been identified in Drosophila and *Caenorhabditis elegans* (Goldstein *et al.*, 1996; Wei *et al.*, 1996; Kunkel *et al.*, 2000). In the nematode, about 50 of 80 $K^+$ channel subunits belong to the 2P domain family (Wei *et al.*, 1996; Bargmann, 1998). In Drosophila 11 of 30 $K^+$ channel subunits belong to the 2P domain family (Rubin *et al.*, 2000). Very little conservation (<35%) is found between nematode, Drosophila and human sequences.

TWIK-1, the first mammalian 2P domain $K^+$ channel to be identified, self-associates to form disulfide-bridged homodimers (Lesage *et al.*, 1996). The extracellular M1P1 interdomain, predicted to form an amphipathic α helix, promotes self-dimerization. A cysteine located in this domain appears to be important for the dimerization of some, but not all 2P domain $K^+$ channels, for instance TASK-1 (Lesage *et al.*, 1996). Besides a role in self-dimerization, this large extracellular loop might also bind regulatory factors or extracellular ligands. A dimer contains 4P domains, which are essential in the formation of $K^+$ selective pores.

The 4TMS/2P subunits encode background $K^+$ channels. Background or leak $K^+$ channels are opened pores in the membrane and have no voltage- or time-dependency (Hille, 1992). Activation is instantaneous upon depolarization as the channels are always opened at rest. Because of an assymetrical physiological $K^+$ gradient (about 150 mM intracellular and 5 mM extracellular), the current to voltage relationship of a $K^+$ leak channel is predicted to be outwardly rectifying (Goldman, Hodgkin and Katz constant-field theory also called the open rectification) (Hille, 1992). In a symmetrical $K^+$ gradient, the current to voltage relationship of the leak channel is expected to be linear as observed for TASK-1, TRAAK and TALK-1. These $K^+$ channels thus behave as open rectifiers. Because of this leak characteristic, the background $K^+$ channels are expected to influence both the resting membrane potential (along with the inward rectifiers) and the repolarization phase of the action potential (along with the voltage-gated and $Ca^{2+}$-dependent outward rectifiers). Several 4TMS/2P background $K^+$ channels are however more than a simple open rectifier leak channel. For instance, TREK-1 is a $K^+$ channel which displays a strong outward rectification in a symmetrical $K^+$ gradient (Fink *et al.*, 1996; Patel *et al.*, 1998). This rectification is at least partly due to a voltage-dependent gating (Patel *et al.*, 1998; Bockenhauer *et al.*, 2001). Moreover, the activation of TASK-1, TASK-2 and TREK-2 is time-dependent (Reyes *et al.*, 1998; Gray *et al.*, 2000; Lesage *et al.*, 2000; Lopes *et al.*, 2000). On the contrary, TWIK-2 shows a mild inward rectification when recorded in a symmetrical $K^+$ gradient

(Patel *et al.*, 2000). Mild inward rectification is also typical to TWIK-1 and THIK-1 (Lesage *et al.*, 1996; Rajan *et al.*, 2000). TWIK-2 is additionally characterized by a time-dependent inactivation (Patel *et al.*, 2000). The various 4TMS/2P channels will differentially tune the resting potential and/or the action potential duration because of these particular rectification, time and voltage-dependent properties.

## 3. THE MECHANO-GATED TREK-1 AND TREK-2 $K^+$ CHANNELS ARE OPENED BY INHALATIONAL ANESTHETICS

Human TREK-1 is highly expressed in brain and ovary and to a lesser extent in kidney and small intestine (Patel *et al.*, 1999; Lesage *et al.*, 2000; Meadows *et al.*, 2000; Medhurst *et al.*, 2001). In human brain, TREK-1 shows the greatest expression in the caudate nucleus, the putamen, the spinal cord and the dorsal root ganglia (Lesage *et al.*, 2000; Medhurst *et al.*, 2001). Significant expression is also detected in both small and medium sized sensory neurons of mouse dorsal root ganglia (Maingret *et al.*, 2000). Human TREK-2 (78% of homology with TREK-1) is abundantly expressed in kidney and pancreas and more moderately in testis, brain, colon and small intestine (Bang *et al.*, 2000; Lesage *et al.*, 2000; Gu *et al.*, 2002). In human brain, TREK-2 shows the strongest expression in the caudate nucleus, the cerebellum, the corpus callosum and the putamen (Lesage *et al.*, 2000; Medhurst *et al.*, 2001). Some tissues only express TREK-1 (ovary) or TREK-2 (pancreas, colon) (Lesage *et al.*, 2000). Other tissues do not express these channels or only to very modest levels (heart, skeletal muscle, lung, blood leukocytes and spleen). Finally, some tissues present overlapping expression (brain, kidney, small intestine).

TREK-1 and TREK-2 channels are mechano-gated $K^+$ channels opened by membrane stretch (Patel *et al.*, 1998; Bang *et al.*, 2000; Lesage *et al.*, 2000; Maingret *et al.*, 2000). At the whole cell level, TREK-1 is modulated by cellular volume (Patel *et al.*, 1998; Maingret *et al.*, 2000). Mechanical force is believed to be transmitted directly to the channel *via* the lipid bilayer (Patel *et al.*, 1998; Maingret *et al.*, 1999). Lowering intracellular pH shifts the pressure-activation relationship of TREK-1 and TREK-2 toward positive values and ultimately leads to channel opening at atmospheric pressure (Maingret *et al.*, 1999; Lesage *et al.*, 2000). Acidosis essentially converts a TREK mechano-gated channel into a constitutively active background $K^+$ channel (Maingret *et al.*, 1999; Lesage *et al.*, 2000). TREK-1 is also gradually and reversibly opened by heat. A rise in temperature of 10°C enhances TREK-1 current amplitude by about 7 fold

(Maingret *et al.*, 2000). Finally, TREK-1, TREK-2 and TRAAK are reversibly opened by polyunsaturated fatty acids (PUFA) and lysophospholipids including arachidonic acid and lysophosphatidylcholine (Fink *et al.*, 1998; Patel *et al.*, 1998; Bang *et al.*, 2000; Lesage *et al.*, 2000; Maingret *et al.*, 2000). Deletional analysis demonstrates that the carboxy terminus, but not the amino terminus and the extracellular M1P1 loop, is critical for activation of TREK-1 by stretch, arachidonic acid, lysophospholipids, intracellular acidosis and temperature (Patel *et al.*, 1998; Maingret *et al.*, 1999; Maingret *et al.*, 2000). TREK-1 and TREK-2 activation are reversed by protein kinase A and protein kinase C stimulation (Fink *et al.*, 1996; Patel *et al.*, 1998; Lesage *et al.*, 2000; Maingret *et al.*, 2000; Maingret *et al.*, 2000). Protein kinase A-mediated phosphorylation of Ser333 in the carboxy terminus mediates TREK-1 closing (Patel *et al.*, 1998). TREK-1 and TREK-2 are insensitive to most of the classical $K^+$ channel blockers including $TEA^+$ (10 mM), 4-AP (3 mM), $Ba^{2+}$ (1 mM), glibenclamide (10 μM), charybdotoxin (1 μM) and apamin (10 μM). TREK-1 is reversibly blocked by $Gd^{3+}$ (30 μM), amiloride (2 mM) and chlorpromazine (1 μM) (Fink *et al.*, 1998; Patel *et al.*, 1998; Maingret *et al.*, 2000).

TREK-1 and TREK-2 are opened by chloroform, diethyl ether, halothane and isoflurane in transfected mammalian cells (Patel *et al.*, 1998; Patel *et al.*, 1999; Lesage *et al.*, 2000).Opening of these channels by anesthetics induces cell hyperpolarization. Interestingly, the other structurally and functionally related 2P domain $K^+$ channel TRAAK is insensitive to volatile anesthetics (Patel *et al.*, 1999). hTREK-1 is most sensitive to chloroform (2.3 fold increase in current amplitude at 1 mM), while halothane is the strongest opener of hTREK-2 (2.3 fold increase at 1 mM) (Patel *et al.*, 1999; Lesage *et al.*, 2000). In excised outside-out patches, the 48 pS TREK-1 channel is reversibly opened in a dose-dependent manner by chloroform and halothane (Patel *et al.*, 1999). No channel activity is observed in the absence of anesthetic, suggesting that volatile anesthetics convert inactive channels into active ones. Deletion of the amino terminus does not affect anesthetic-induced TREK-1 opening (Patel *et al.*, 1999). In contrast, deletion of the carboxy terminus at Thr 322 completely suppresses responses to both chloroform and halothane (Patel *et al.*, 1999). These results demonstrate that the carboxy terminus, but not the amino terminus, of TREK-1 is critical for anesthetic activation.

TREK-1 and TREK-2 share all the functional properties of the anesthetic-sensitive background $K^+$ channels in Lymnea pacemaker neurons and the S channel in *Aplysia* sensory neurons (Franks and Lieb, 1988; Winegar *et al.*, 1996; Lopes *et al.*, 1998). Both endogenous and cloned background $K^+$ channels are opened by volatile anesthetics in excised patches suggesting a direct mechanism of action (Winegar *et al.*, 1996; Patel *et al.*, 1999). Pure optical isomers of the volatile anesthetic isoflurane exhibit clear stereoselectivity in

activating background $K^+$ currents in pacemaker neurons of the Lymnea, (Franks and Lieb, 1991). The + isomer is more potent than the - isomer in hyperpolarizing neurons suggesting that volatile anesthetics act by direct binding to the protein rather than a nonspecific perturbation of lipids (Franks and Lieb, 1991). Although the stimulation by inhalational anesthetics seems to be direct, one cannot fully rule out possible indirect effects (Winegar *et al.*, 1996; Lopes *et al.*, 1998; Patel *et al.*, 1999). Indeed, it has been shown in Lymnea neurons, that although the activation of IKAn by volatile anesthetics is independent of the lipoxygenase and cyclooxygenase pathways, it might involve the cytochrome P450 pathway (Lopes *et al.*, 1998). Moreover, TREK-1 is not sensitive to volatile anesthetics when expressed in *Xenopus* oocytes (Gray *et al.*, 2000). These negative results may indicate that either a specific membrane environment and/or critical co-factors, which are absent in *Xenopus* oocytes but present in mammalian cells, may be required.

## 4. THE ACID-SENSITIVE BACKGROUND $K^+$ CHANNELS TASK-1 AND TASK-3 ARE OPENED BY VOLATILE ANESTHETICS

Human TASK-1 is particularly abundant in the pancreas and the placenta (Duprat *et al.*,1997). Lower levels of expression are found in brain>lung>prostate>heart>kidney>uterus>small intestine>colon. High levels of TASK-1 are found in cerebellar and olfactory granule cells, olfactory tubercles, scattered neurons through all layers of cerebral cortex, intralaminar thalamic nuclei, pontine nuclei and the locus coeruleus of the rat (Duprat *et al.*, 1997; Sirois *et al.*, 2000). Brainstem and spinal cord motorneurons display the strongest expression of TASK-1 (Sirois *et al.*, 2000). Motor nuclei with high levels of TASK-1 include facial, hypoglossal, ambigual and motor trigeminal as well as the vagal motor nucleus. TASK-1 is also particularly abundant in rat carotid body cells (Buckler *et al.*, 2000). In human brain, the strongest expression is found in the cerebellum, thalamus and pituitary gland (Medhurst *et al.*, 2001). TASK-1 is also particularly abundant in human dorsal root ganglia (Medhurst *et al.*, 2001). Human TASK-3, which is 62% identical to TASK-1, is largely and selectively expressed in the cerebellum (Chapman *et al.*, 2000; Medhurst *et al.*, 2001).

TASK-1 and TASK-3 $K^+$ currents are instantaneous (or at least very rapidly activating (Lopes *et al.*, 2000; Rajan *et al.*, 2000)) and non-inactivating (Duprat *et al.*, 1997; Kim *et al.*, 1998; Leonoudakis *et al.*, 1998; Kim *et al.*, 2000; Sirois *et al.*, 2000; Meadows and Randall, 2001). TASK-1 and TASK-3 are background $K^+$ currents which are very sensitive to variations in extracellular

pH (Duprat *et al.*, 1997; Leonoudakis *et al.*, 1998; Kim *et al.*, 2000; Rajan *et al.*, 2000; Sirois *et al.*, 2000; Meadows and Randall, 2001). Half of TASK-1 and TASK-3 channels are closed at a pH values of 7.3 and 6.5, respectively (Duprat *et al.*, 1997; Kim *et al.*, 1998; Leonoudakis *et al.*, 1998; Kim *et al.*, 2000; Sirois *et al.*, 2000; Meadows and Randall, 2001). TASK-1 is inhibited by $Zn^{2+}$, the local anesthetic bupivacaine, the anti-convulsant phenytoin, quinidine and $Ba^{2+}$ (Duprat *et al.*, 1997; Kim *et al.*, 1998; Leonoudakis *et al.*, 1998; Sirois *et al.*, 2000). It is, however, resistant to $TEA^{+}$ and 4-AP. TASK-1 is inhibited by receptors coupled to Gq proteins including the M3 muscarinic receptor (Millar *et al.*, 2000; Talley *et al.*, 2000). The second messenger involved in channel inhibition is still unknown. The endocannabinoid anandamide has recently been shown to be a direct and selective blocker of TASK-1 (Maingret *et al.*, 2001). TASK-3 is blocked by local anesthetics including lidocaine and bupivacaine, $Ba^{2+}$, quinidine but resistant to $TEA^{+}$ (Kim *et al.*, 2000; Rajan *et al.*, 2000; Meadows and Randall, 2001).

TASK-1 is opened by halothane > isoflurane but is insensitive to chloroform and partially inhibited by diethylether (Patel *et al.*, 1999; Sirois *et al.*, 2000). Halothane opens TASK-1 in the excised patch configuration despite a strong run down of channel activity upon excision (Patel *et al.*, 1999). Deletion of the last 147 amino acids in the carboxy terminus of TASK does not alter halothane sensitivity whereas further deletion kills channel activity. Fusing the carboxy terminus of TREK-1 restores basal but not anesthetic-stimulated activity demonstrating that the region located between residues 242 and 248 (VLRFMT) is critical for anesthetic sensitivity (Patel *et al.*, 1999; Talley and Bayliss, 2002).

A background $K^{+}$ current sets the resting membrane potential in type I carotid body chemoreceptor cells (Buckler, 1997; Buckler *et al.*, 2000). Reversible inhibition of this background $K^{+}$ current by hypoxia or acidosis induces membrane depolarization. Depolarization of type I cells leads to opening of voltage-gated $Ca^{2+}$ channels, increase in intracellular $Ca^{2+}$ and release of neurotransmitters (Lopez-Barneo, 1996). The released neurotransmitters stimulate sinus nerve endings and trigger the reflex increase in respiration. The endogenous background $K^{+}$ channel in type I cells shares the biophysical and pharmacological properties of TASK-1 (Buckler *et al.*, 2000). It is reversibly inhibited by mild external acidosis, time and voltage-independent, resistant to $TEA^{+}$ and 4-AP, but blocked by $Ba^{2+}$, $Zn^{2+}$, bupivacaine and quinidine. Moreover, the type I cell background $K^{+}$ current is enhanced by halothane but is insensitive to chloroform (Buckler *et al.*, 2000). Opening of TASK-1-like background $K^{+}$ channels in type I carotid body cells may be partially responsible for the suppression of hypoxic ventilatory drive under general anesthesia.

In rat somatic motoneurons, locus coeruleus neurons and cerebellar granule neurons, inhalational anesthetics similarly activate a background TASK-1-like conductance, causing membrane hyperpolarization and suppressing action potential discharge (Sirois *et al.*, 2000; Maingret *et al.*, 2001). These effects occur at clinically relevant anesthetic concentrations with the steep dose dependence expected for anesthetic effects of these compounds (Sirois *et al.*, 2000). External acidosis to pH 6.5 completely blocks the current activated by anesthetics (Sirois *et al.*, 2000; Maingret *et al.*, 2001). In motoneurons and cerebellar granule neurons opening of TASK-1 channels may contribute to anesthetic-induced immobilization, whereas in the locus coeruleus, it may support analgesic and hypnotic actions (Sirois *et al.*, 2000; Maingret *et al.*, 2001).

Application of 1 mM halothane reversibly potentiates human TASK-3 current amplitude by 66% (Meadows and Randall, 2001). The onset of halothane stimulation in *Xenopus* oocyte is rapid ($\tau$: 62 s) while full recovery takes as long as 5 minutes. By contrast, the neurosteroidal anesthetic alphaxolone inhibits TASK-3 (Meadows and Randall, 2001). Two other general anesthetics non-volatile agents, pentobarbital and ketamine do not affect significantly TASK-3 at a concentration of 100 $\mu$M (Meadows and Randall, 2001).

## 5. THE SPINAL CORD AND DORSAL ROOT GANGLION BACKGROUND $K^+$ CHANNEL TASK-2 IS OPENED BY INHALATIONAL ANESTHETICS

Human TASK-2 is found in high levels in kidney > pancreas > lung > placenta > brain (Reyes *et al.*, 1998). Although TASK-2 expression is weak in whole brain, it can be detected by PCR in rat spinal cord (Gray *et al.*, 2000). TASK-2 is found throughout the spinal cord in both ventral and dorsal sections (Gray *et al.*, 2000). Moreover, TASK-2 is expressed in human spinal cord as well as in dorsal root ganglia (Medhurst *et al.*, 2001). It produces non-inactivating, outwardly rectifying $K^+$ currents with activation potential thresholds that closely follow the $K^+$ equilibrium potential (Reyes *et al.*, 1998; Gray *et al.*, 2000). TASK-2 activation is time-dependent with a time constant of about 60 ms at 0 mV. TASK-2 currents are blocked by quinine and quinidine, but not by the classical $K^+$ channel blockers $TEA^+$, 4-AP, $Cs^+$ and $Ba^{2+}$ (Reyes *et al.*, 1998). TASK-2 is inhibited by external acidosis with a half-inhibition at pH 7.8 (Reyes *et al.*, 1998; Gray *et al.*, 2000). Application of volatile anesthetics causes a concentration-dependent increase in TASK-2 currents in a range overlapping MAC (Gray *et al.*, 2000). TASK-2 is more sensitive to halothane

than isoflurane (Gray *et al.*, 2000). Unlike TASK-1, TASK-2 is also stimulated by chloroform. Site-directed mutagenesis has been used to delete the carboxy terminus of TASK-2 (Gray *et al.*, 2000). The truncated TASK-2 channel does not express a spontaneous or volatile-anesthetic-evoked activity further demonstrating the critical role of the carboxy terminus in the function of 2P domain $K^+$ channels (Patel *et al.*, 1998; Patel *et al.*, 1999; Gray *et al.*, 2000).

## 6. VOLATILE ANESTHETIC-INHIBITED 2P DOMAIN $K^+$ CHANNELS

TWIK-2 is a background $K^+$ channel which is highly expressed in both visceral and vascular smooth muscle (Patel *et al.*, 2000). Human TWIK-2 is absent in the brain and in the cerebellum (Chavez *et al.*, 1999; Pountney *et al.*, 1999; Patel *et al.*, 2000; Medhurst *et al.*, 2001). However, a moderate to strong expression is found in the spinal cord and in the dorsal root ganglia (Medhurst *et al.*, 2001). Chloroform (300 μM) and halothane (750 μM) reversibly inhibit TWIK-2 by 32% and 27%, respectively (Patel *et al.*, 2000).

THIK-1 expression is ubiquitous with a substantial expression in some restricted areas of the rat brain (Rajan *et al.*, 2000). The strongest levels are found in the olfactory bulb granule cell layer, the lateral septal nucleus dorsal, the ventromedial hypothalamic nucleus, the thalamus reticular and reunions nuclei and finally the parabrachial nuclei (Rajan *et al.*, 2000). THIK-1 is a weak inward rectifier which is stimulated by arachidonic acid but inhibited by halothane with a IC50 value of 2.83 mM (Rajan *et al.*, 2000). Interestingly, 1 mM chloroform fails to affect THIK-1 (Rajan *et al.*, 2000).

Human TALK-1 is exclusively expressed in the pancreas (Girard *et al.*, 2001). Human TALK-2 is similarly found at high levels in the pancreas and is also present in liver, placenta, heart and lung (Girard *et al.*, 2001). TALK-1 and TALK-2 are background $K^+$ currents which are activated by alkaline pH, but are insensitive to arachidonic acid. Both channels are inhibited by 800 μM chloroform (-21% and -44%, respectively) and 800 μM halothane (-27% and -56%, respectively) (Decher *et al.*, 2001; Girard *et al.*, 2001). Interestingly, TALK-1 is not sensitive to 800 μM isoflurane while TALK-2 is stimulated (+58%) (Girard *et al.*, 2001).

## 7. CONCLUSIONS AND PERSPECTIVES

These recent findings provide strong evidence that 2P domain $K^+$ channels are sensitive molecular targets for volatile anesthetics. Together with the known modulation of neurotransmitter receptors (Harris *et al.*, 1995; Belelli *et al.*,

1999), activation of 2P domain $K^+$ channels will contribute to the hyperpolarizing action of general anesthetics (Patel *et al.*, 1999).

Opening of the 2P domain $K^+$ channels is agent specific. For instance, TREK-1, TREK-2 and TASK-2 are opened by chloroform, TASK-1, THIK-1 and TRAAK are unaffected, while TWIK-2, TALK-1 and TALK-2 are inhibited (Patel *et al.*, 1999; Gray *et al.*, 2000; Lesage *et al.*, 2000; Patel *et al.*, 2000; Rajan *et al.*, 2000; Girard *et al.*, 2001). Interestingly, TALK-2 is inhibited by chloroform and halothane while it is stimulated by isoflurane (Girard *et al.*, 2001). The volatile anesthetic-inhibited 2P domain $K^+$ channels including TWIK-2, THIK-1, TALK-1 and TALK-2 are mostly non-neuronal (THIK-1 is restricted to some brain areas) and strongly expressed in peripheral organs (Patel *et al.*, 2000; Rajan *et al.*, 2000; Girard *et al.*, 2001). TREK-1, TREK-2 and TASK-1 are more sensitive to halothane than isoflurane (Patel *et al.*, 1999; Lesage *et al.*, 2000). This difference in potency between the two volatile anesthetics indicates that opening of 2P domain $K^+$ channels will probably be prevalent during halothane-induced anesthesia. Clearly, further work is still necessary to map the putative anesthetic binding site and understand the role of the carboxy terminus in the mechanism of channel activation (Patel *et al.*, 1999).

Opening of 2P domain $K^+$ channels will have profound hyperpolarizing effects at both presynaptic and postsynaptic levels. Because of the leak behavior of the 2P domain $K^+$ channels, even moderate stimulation, as observed for clinical doses of volatile anesthetics, will have a major effect on the membrane potential (Lesage and Lazdunski, 2000; Goldstein *et al.*, 2001; Patel and Honoré, 2001; Patel and Honoré, 2001; Patel and Honoré, 2001; Patel *et al.*, 2001). The discovery of this class of anesthetic-sensitive $K^+$ channels with distinct patterns of expression, may provide a basis for how inhalational anesthetics depress the central nervous system (Patel *et al.*, 1999; Gray *et al.*, 2000; Lesage *et al.*, 2000; Medhurst *et al.*, 2001). These recent results contribute to the understanding of the molecular and cellular mechanisms of action of anesthetics.

## ACKNOWLEDGEMENTS

We are grateful to Pr. Michel Lazdunski for continual support. This work was supported by the Centre National de la Recherche Scientifique (CNRS, Boulevard Michel-Ange, Paris 75016).

# REFERENCES


Bang, H., Kim, Y. and Kim, D., 2000, TREK-2, a new member of the mechanosensitive tandem pore $K^+$ channel family. *J. Biol. Chem.* 275: 17412-17419.

Bargmann, C., 1998, Neurobiology of the *Caenorhabditis elegans* genome. *Science* 282: 2028-2033.

Belelli, D., Pistis, M., Peters, J.A. and Lambert, J.L., 1999, General anaesthetics action at transmitter-gated inhibitory amino acid receptors. *TIPS* 20: 496-502.

Berg-Johnsen, J. and Langmoen, I.A., 1987, Isoflurane hyperpolarizes neurones in rat and human cerebral cortex. *Acta Physiol. Scand.* 130: 679-685.

Bockenhauer, D., Zilberberg, N. and Goldstein, S.A., 2001, KCNK2: reversible conversion of a hippocampal potassium leak into a voltage-dependent channel. *Nat. Neurosci.* 4: 486-91.

Buckler, K., Williams, B. and Honoré, E., 2000, An oxygen-, acid- and anaesthetic-sensitive TASK-like background potassium channel in rat arterial chemoreceptor cells. *J. Physiol.* 525: 135-142.

Buckler, K.J., 1997, A novel oxygen-sensitive potassium current in rat carotid body type I cells. *J. Physiol.* 498: 649-662.

Chapman, C.G., Meadows, H.J., Godden, R.J., Campbell, D.A., Duckworth, M., Kelsell, R.E., Murdock, P.R., Randall, A.D., Rennie, G.I. and Gloger, I.S., 2000, Cloning, localisation and functional expression of a novel human cerebellum specific, two pore domain potassium channel. *Brain Res. Mol. Brain Res.* 82: 74-83.

Chavez, R.A., Gray, A.T., Zhao, B.B., Kindler, C.H., Mazurek, M.J., Mehta, Y., Forsayeth, J.R. and Yost, C.S., 1999, TWIK-2, a new weak inward rectifying member of the tandem pore domain potassium channel family. *J. Biol. Chem.* 274: 7887-7892.

Decher, N., Maier, M., Dittrich, W., Gassenhuber, J., Bruggemann, A., Busch, A.E. and Steinmeyer, K., 2001, Characterization of TASK-4, a novel member of the pH-sensitive, two-pore domain potassium channel family. *FEBS Lett.* 492: 84-9.

Doyle, D.A., Morais Cabral, J., Pfuetzner, R.A., Kuo, A., Gulbis, J.M., Cohen, S.L., Chait, B.T. and MacKinnon, R., 1998, The structure of the potassium channel: molecular basis of $K^+$ conduction and selectivity. *Science* 280: 69-77.

Duprat, F., Lesage, F., Fink, M., Reyes, R., Heurteaux, C. and Lazdunski, M., 1997, TASK, a human background $K^+$ channel to sense external pH variations near physiological pH. *EMBO J.* 16: 5464-5471.

el-Beheiry, H. and Puil, E., 1989, Postsynaptic depression induced by isoflurane in neocortical neurons. *Exp. Brain Res.* 75: 361-368.

Fink, M., Duprat, F., Lesage, F., Reyes, R., Romey, G., Heurteaux, C. and Lazdunski, M., 1996, Cloning, functional expression and brain localization of a novel unconventional outward rectifier $K^+$ channel. *EMBO J.* 15: 6854-6862.

Fink, M., Lesage, F., Duprat, F., Heurteaux, C., Reyes, R., Fosset, M. and Lazdunski, M., 1998, A neuronal two P domain $K^+$ channel activated by arachidonic acid and polyunsaturated fatty acid. *EMBO J.* 17: 3297-3308.

Franks, N.P. and Lieb, W.R., 1988, Volatile general anaesthetics activate a novel neuronal $K^+$ current. *Nature* 333: 662-664.

Franks, N.P. and Lieb, W.R., 1991, Stereospecific effects of inhalational general anesthetic optical isomers on nerve ion channels. *Science* 254: 427-430.

Franks, N.P. and Lieb, W.R., 1994, Molecular and cellular mechanisms of general anaesthesia. *Nature* 367: 607-614.

Girard, C., Duprat, F., Terrenoire, C., Tinel, N., Fosset, M., Romey, G., Lazdunski, M. and Lesage, F., 2001, Genomic and functional characteristics of novel human pancreatic 2P domain potassium channels. *Biochem. Biophys. Res. Commun.* 282: 249-256..

Goldstein, S.A., Price, L.A., Rosenthal, D.N. and Pausch, M.H., 1996, ORK1, a potassium-selective leak channel with two pore domains cloned from Drosophila melanogaster by expression in Saccharomyces cerevisiae. *Proc. Natl. Acad. Sci. USA* 93: 13256-13261.

Goldstein, S.A.N., Bockenhauer, D., O'Kelly, I. and Zilberg, N., 2001, Potassium leak channels and the KCNK family of two-P-domain subunits. *Nature Reviews/Neuroscience* 2: 175-184.

Gray, A.T., Winegar, B.D., Leonoudakis, D.J., Forsayeth, J.R. and Yost, C.S., 1998, TOK1 is a volatile anesthetic stimulated $K^+$ channel. *Anesthesiology* 88: 1076-1084.

Gray, A.T., Zhao, B.B., Kindler, C.H., Winegar, B.D., Mazurek, M.J., Xu, J., Chavez, R.A., Forsayeth, J.R. and Yost, C.S., 2000, Volatile anesthetics activate the human tandem pore domain baseline $K^+$ channel KCNK5. *Anesthesiology* 92: 1722-1730.

Gu, W., Schlichthorl, G., Hirsch, J.R., Engels, H., Karschin, C., Karschin, A., Derst, C., Steinlein, O.K. and Daut, J., 2002, Expression pattern and functional characteristics of two novel splice variants of the two-pore-domain potassium channel TREK-2. *J. Physiol.* 539: 657-668.

Harris, R.A., Mihic, S.J., Dildy-Mayfield, J.E. and Machu, T.K., 1995, Actions of anesthetics on ligand-gated ion channels: role of receptor subunit composition. *Faseb J.* 9: 1454-1462.

Hille, B., 1992, Ionic channels of excitable membranes. *Sinauer Associates Inc* Sunderland, Massachusetts.

Ketchum, K.A., Joiner, W.J., Sellers, A.J., Kaczmarek, L.K. and Goldstein, S.A.N., 1995, A new family of outwardly rectifying potassium channel proteins with two pore domains in tandem. *Nature* 376: 690-695.

Kim, D., Fujita, A., Horio, Y. and Kurachi, Y., 1998, Cloning and functional expression of a novel cardiac two-pore background $K^+$ channel (cTBAK-1). *Circ. Res.* 82: 513-518.

Kim, Y., Bang, H. and Kim, D., 2000, TASK-3, a new member of the tandem pore $K^+$ channel family. *J. Biol. Chem.* 275: 9340-9347.

Kindler, C.H., Yost, C.S. and Gray, A.T., 1999, Local anaesthetic inhibition of baseline potassium channels with two pore domains in tandem. *Anesthesiology* 90: 1092-1102.

Kunkel, M.T., Johnstone, D.B., Thomas, J.H. and Salkoff, L., 2000, Mutants of a temperature-sensitive two-P domain potassium channel. *J. Neurosci.* 20: 7517-7524.

Leonoudakis, D., Gray, A.T., Winegar, B.D., Kindler, C.H., Harada, M., Taylor, D.M., Chavez, R.A., Forsayeth, J.R. and Yost, C.S., 1998, An open rectifier potassium channel with two pore domains in tandem cloned from rat cerebellum. *J. Neurosci.* 18: 868-877.

Lesage, F., Guillemare, E., Fink, M., Duprat, F., Lazdunski, M., Romey, G. and Barhanin, J., 1996, TWIK-1, a ubiquitous human weakly inward rectifying $K^+$ channel with a novel structure. *EMBO J.* 15: 1004-1011.

Lesage, F. and Lazdunski, M., 2000, Molecular and functional properties of two-pore-domain potassium channels. *Am. J Physiol. Renal Physiol* 279: F793-801.

Lesage, F., Reyes, R., Fink, M., Duprat, F., Guillemare, E. and Lazdunski, M., 1996, Dimerization of TWIK-1 $K^+$channel subunits *via* a disulfide bridge. *EMBO J.* 15: 6400-6407.

Lesage, F., Terrenoire, C., Romey, G. and Lazdunski, M., 2000, Human TREK2, a 2P domain mechano-sensitive $K^+$ channel with multiple regulations by polyunsaturated fatty acids, lysophospholipids, and Gs, Gi, and Gq protein-coupled receptors. *J. Biol. Chem.* 275: 28398-28405.

Lopes, C.M., Gallagher, P.G., Buck, M.E., Butler, M.H. and Goldstein, S.A., 2000, Proton block and voltage gating are potassium-dependent in the cardiac leak channel Kcnk3. *J. Biol. Chem.* 275: 16969-16978.

Lopes, C.M., Zilberberg, N. and Goldstein, S.A., 2001, Block of Kcnk3 by protons. Evidence that 2-P-domain potassium channel subunits function as homodimers. *J. Biol. Chem* 276: 24449-24452.

Lopes, C.M.B., Franks, N.P. and Lieb, W.R., 1998, Actions of general anaesthetics and arachidonic acid pathway inhibitors on $K^+$ currents activated by volatile anaesthetics and FMRFamide in molluscan neurones. *Br. J. Pharmacol.* 125: 309-318.

Lopez-Barneo, J., 1996, Oxygen-sensing by ion channels and the regulation of cellular functions. *Trends Neurosci.* 19: 435-40.

MacIver, M.B. and Kendig, J.J., 1991, Anesthetic effects on resting membrane potential are voltage-dependent and agent-specific. *Anesthesiology* 74: 83-88.

Maingret, F., Lauritzen, I., Patel, A., Heurteaux, C., Reyes, R., Lesage, F., Lazdunski, M. and Honoré, E., 2000, TREK-1 is a heat-activated background $K^+$ channel. *EMBO J.* 19: 2483-2491.

Maingret, F., Patel, A., Lazdunski, M. and Honoré, E., 2001, The endocannabinoid anandamide is a direct and selective blocker of the background $K^+$ channel TASK-1. *EMBO J.* 20: 47-54.

Maingret, F., Patel, A.J., Lesage, F., Lazdunski, M. and Honore, E., 1999, Mechano- or acid stimulation, two interactive modes of activation of the TREK-1 potassium channel. *J Biol Chem* 274: 26691-6.

Maingret, F., Patel, A.J., Lesage, F., Lazdunski, M. and Honoré, E., 2000, Lysophospholipids open the two P domain mechano-gated $K^+$ channels TREK-1 and TRAAK. *J. Biol. Chem.* 275: 10128-10133.

Meadows, H.J., Benham, C.D., Cairns, W., Gloger, I., Jennings, C., Medhurst, A.D., Murdock, P. and Chapman, C.G., 2000, Cloning, localisation and functional expression of the human orthologue of the TREK-1 potassium channel. *Pflugers Arch.* 439: 714-722.

Meadows, H.J. and Randall, A.D., 2001, Functional characterisation of human TASK-3, an acid-sensitive two-pore domain potassium channel. *Neuropharmacology* 40: 551-9.

Medhurst, A.D., Rennie, G., Chapman, C.G., Meadows, H., Duckworth, M.D., Kelsell, R.E., Gloger, II and Pangalos, M.N., 2001, Distribution analysis of human two pore domain potassium channels in tissues of the central nervous system and periphery. *Brain Res Mol Brain Res.* 86: 101-114.

Millar, J.A., Barratt, L., Southan, A.P., Page, K.M., Fyffe, R.E., Robertson, B. and Mathie, A., 2000, A functional role for the two-pore domain potassium channel TASK-1 in cerebellar granule neurons. *Proc. Natl. Acad. Sci. USA* 97: 3614-3618.

Nicoll, R.A. and Madison, D.V., 1982, General anaesthetics hyperpolarize neurons in the vertebrate central nervous system. *Science* 217: 1055-1057.

Patel, A.J. and Honoré, E., 2001, Anesthetic-sensitive 2P domain $K^+$ channels. *Anesthesiology* 95: 1013-1025.

Patel, A.J. and Honoré, E., 2001, Molecular Physiology of oxygen-sensitive potassium channels. *Eur. Resp. J.* 118: 221-227.

Patel, A.J. and Honoré, E., 2001, Properties and modulation of mammalian 2P domain $K^+$ channels. *Trends Neurosci.*24: 339-46.

Patel, A.J., Honoré, E., Lesage, F., Fink, M., Romey, G. and Lazdunski, M., 1999, Inhalational anaesthetics activate two-pore-domain background $K^+$ channels. *Nature Neurosci.* 2: 422-426.

Patel, A.J., Honoré, E., Maingret, F., Lesage, F., Fink, M., Duprat, F. and Lazdunski, M., 1998, A mammalian two pore domain mechano-gated S-like $K^+$ channel. *EMBO J.* 17: 4283-4290.

Patel, A.J., Lazdunski, M. and Honoré, E., 2001, Lipid and mechano-gated 2P domain $K^+$ channels. *Curr Opin Cell Biol* 13: 422-8.

Patel, A.J., Maingret, F., Magnone, V., Fosset, M., Lazdunski, M. and Honore, E., 2000, TWIK-2, an inactivating 2P domain K+ channel. *J Biol Chem* 275: 28722-30.

Pountney, D.J., Gulkarov, I., Vega-Saenz de Miera, E., Holmes, D., Saganich, M., Rudy, B., Artman, M. and Coetzee, W.A., 1999, Identification and cloning of TWIK-originated similarity sequence (TOSS): a novel human 2-pore $K^+$ channel principal subunit. *FEBS Lett.* 450: 191-196.

Rajan, S., Wischmeyer, E., Karschin, C., Preisig-Muller, R., Grzeschik, K.H., Daut, J., Karschin, A. and Derst, C., 2000, THIK-1 and THIK-2, a novel subfamily of tandem pore domain $K^+$ channels. *J. Biol. Chem.* 276: 7302-7311.

Rajan, S., Wischmeyer, E., Liu, G.X., Preisig-Muller, R., Daut, J., Karschin, A. and Derst, C., 2000, TASK-3, a novel tandem pore-domain acid-sensitive $K^+$ channel: an extracellular histidine as pH sensor. *J. Biol. Chem.* 275: 16650-16657.

Reyes, R., Duprat, F., Lesage, F., Fink, M., Farman, N. and Lazdunski, M., 1998, Cloning and expression of a novel pH-sensitive two pore domain potassium channel from human kidney. *J. Biol. Chem.* 273: 30863-30869.

Rubin, G.M., Yandell, M.D. and Wortman, J.R., 2000, Comparative genomics of the eukaryotes. *Science* 287: 2204-2215.

Ruppersberg, J.P., 2000, Intracellular regulation of inward rectifier K+ channels. *Pflugers Arch* 441: 1-11.

Salinas, M., Reyes, R., Lesage, F., Fosset, M., Heurteaux, C., Romey, G. and Lazdunski, M., 1999, Cloning of a new mouse two-P domain channel subunit and a human homologue with a unique pore structure. *J. Biol. Chem.* 274: 11751-11760.

Sirois, J.E., Lei, Q., Talley, E.M., Lynch, C., 3rd and Bayliss, D.A., 2000, The TASK-1 two-pore domain $K^+$ channel is a molecular substrate for neuronal effects of inhalational anesthetics. *J. Neurosci.* 20: 6347-6354.

Sirois, J.E., Pancrazio, J.J., Lynch, C. and Bayliss, D.A., 1998, Multiple ionic mechanisms mediate inhibition of rat motoneurones by inhalation anaesthetics. *J. Physiol.* 512.3: 851-862.

Southan, A.P. and Wann, K.T., 1989, Inhalation anaesthetics block accommodation of pyramidal cell discharge in the rat hippocampus. *Br. J. Anaesth.* 63: 581-586.

Talley, E.M. and Bayliss, D.A., 2002, Modulation of TASK-1 (Kcnk3) and TASK-3 (Kcnk9) potassium channels: volatile anesthetics and neurotransmitters share a molecular site of action. *J. Biol; Chem* 277: 17733-42.

Talley, E.M., Lei, Q., Sirois, J.E. and Bayliss, D.A., 2000, TASK-1, a two-pore domain $K^+$ channel, is modulated by multiple neurotransmitters in motoneurons. *Neuron* 25: 399-410.

Wei, A., Jegla, T. and Salkoff, L., 1996, Eight potassium channel families revealed by the *C. elegans* genome project. *Neuropharmacology* 35: 805-829.

Winegar, B.D., Owen, D.F., Yost, C.S., Forsayeth, J.R. and Mayeri, E., 1996, Volatile general anesthetics produce hyperpolarization of *Aplysia* neurons by activation of a discrete population of baseline pot.assium channels. *Anesthesiology* 85: 889-900.

# $Ca^{2+}$ responses to hypoxia are mediated by $IP_3$-R on $Ca^{2+}$ store depletion

SUKHAMAY LAHIRI, ARIJIT ROY, JINQUING LI, ANIL MOKASHI, and SANTHOSH M. BABY
*Department of Physiology, University of Pennsylvania Medical Center, Philadelphia, PA 19104-6085 USA*

## 1. INTRODUCTION

Inositol 1,4, 5-triphosphate ($IP_3$) is generated from the hydrolysis of phosphatidylinositol 4, 5-triphosphate ($PIP_2$) which is a component of plasma membrane. $IP_3$ acts as a messenger to link with receptors $IP_3$-Rs which are located on intracellular $Ca^{2+}$ stores, such as the endoplasmic reticulum (ER) (Belousov et al., 1995; Berridge, 1993). The ER also often shares the same domain of the mitochondria which have a low affinity, high-capacity for $Ca^{2+}$ uptake mechanism, and $Ca^{2+}$ concentrations influence mitochondrial metabolism (Duchen, 2000). Thus, $IP_3$-Rs are an ideal candidate for $Ca^{2+}$-related cellular functions. Rizzuto et al. (1993) have shown that $[Ca^{2+}]_m$ increases rapidly and transiently upon stimulation with agonists coupled to $IP_3$-R generation. This leads to high $[Ca^{2+}]_i$ close to $IP_3$-R and sensed by mitochondria. Conversely, metabolites generated by energy production may influence $IP_3$-mediated $Ca^{2+}$ dynamics. Depletion of cellular energy resources leads to the accumulation of cytoplasmic reduced NADH (Veech et al., 1970). Hypoxia decreases mitochondrial respiration by inhibiting the terminal step in the electron transport chains, provoking a rapid rise in intracellular $Ca^{2+}$ (Biscoe and Duchen, 1990; Kaplin et al., 1996; McCormack et al., 1990). Hypoxia also increases cytoplasmic NADH levels as a result of enhanced glycolysis (Yager et al., 1991). Also, NADH selectively stimulates the release of $Ca^{2+}$ mediated by $IP_3$-R (Ferris and Snyder, 1992).

*Chemoreception*, Edited by Pequignot et al.
Kluwer Academic/Plenum Publishers, New York, 2003

The role of $IP_3$ has been looked into for carotid body chemoreception simply because $Ca^{2+}$ is an important player in the scenario. Pokorski and Stroszander (1997), using ATP as an agonist, showed that $IP_3$ played a role in the hypoxic signal transduction in the carotid body. Gonzalez's laboratory (Rigual et al., 1999), on the other hand, showed that hypoxia inhibited synthesis of $IP_3$ in the whole carotid body. These observations reached opposite conclusions. Our strategy was to inhibit the $IP_3$-Rs, and examine the effects on $Ca^{2+}$ release and subsequently the effects of hypoxia and hypercapnia, and also on the chemosensory discharge. Inhibitors and blockers have been used successfully as tools to explore the biological functions, as we will see later in this symposium (Wyatt and Buckler, 2003; Ortega-Saenz et al., 2003). We used cell permeant 2-APB (2-amino ethoxdiphenyl borate) to block $Ca^{2+}$ release from the $IP_3$-Rs pathway in the ER- mitochondria complex, and examine the effects on global $[Ca^{2+}]$ in glomus cells, and sensory responses of the rat carotid body.

## 2. HYPOTHESES

### 2.1 Hypothesis One

One scenario was that glomus cell membrane stimulation by hypoxia would lower $K^+$ conductance, leading to membrane depolarization and opening of voltage-gated $Ca^{2+}$ channels, followed by $Ca^{2+}$ entry and $[Ca^{2+}]_i$ rise, and eventually the chemosensory discharge (Lopez-Barneo et al., 2001).

### 2.2 Hypothesis Two

Another scenario was that $IP_3$-Rs which would mobilize $Ca^{2+}$ from intracellular stores and blockade of $IP_3$-Rs would inhibit the $Ca^{2+}$ release. Accordingly, blockade of $IP_3$-Rs should leave the mechanism described under 2.1 intact, and either should not matter with respect to $[Ca^{2+}]_i$ response to hypoxia. In that case, $Ca^{2+}$ influx mediated by the mechanisms postulated under 2.1 would continue to occur.

The hypercapnic $[Ca^{2+}]$ response, however, would not be affected by 2-APB because it does not have any influence on the membrane which alone determines the hypercapnic response.

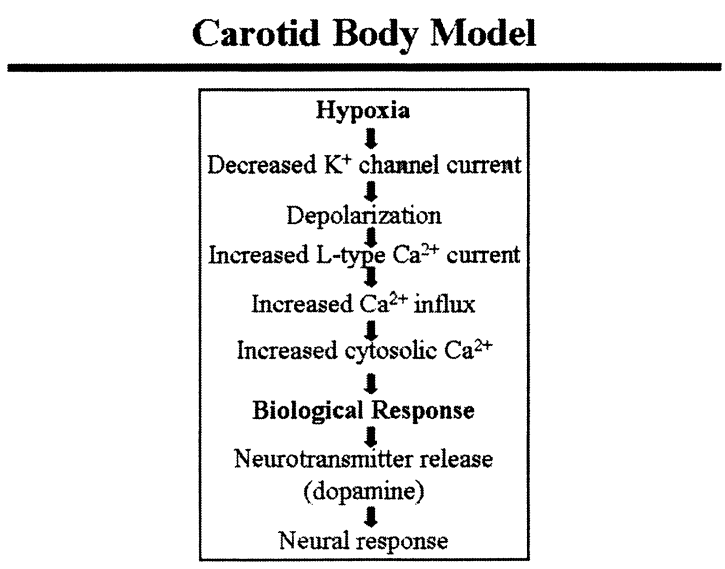


*Figure 1.* Hypothesis 1. Hypoxic $Ca^{2+}$ response: membrane model of carotid body glomus cell.

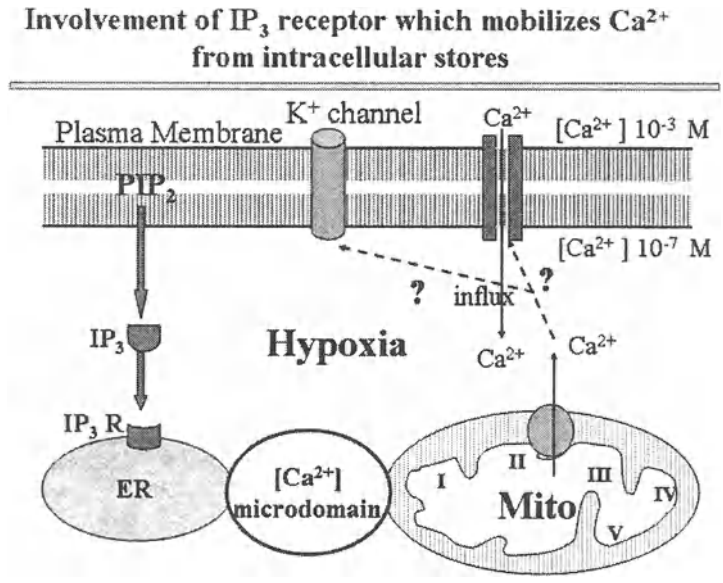


*Figure 2.* Hypothesis 2. Hypoxic $Ca^{2+}$ response: ER-mitochondrial $Ca^{2+}$-store depletion model.

# 3. METHODS

## 3.1 Isolation of Cells

Rat glomus cells were isolated and kept in culture (up to 24 h.). The cells were then incubated with Fura-2-AM (5μM) for measuring $Ca^{2+}$ with excitation at 340 nm and 380 nm and emission at 510 nm. Hypoxia (10-15 Torr) was used in the superfusate replacing normoxia ($Po_2$ • 120 Torr) and hypercapnia ($Pco_2$ • 60 Torr) replacing the normocapnia ($Pco_2$ • 30 Torr).

## 3.2 Measurement of Chemosensory Discharges

Chemosensory discharges were measured with the usual technique (Roy et al., 2000). The effects of hypoxia ($Po_2$ • 28-30 Torr) were measured by perfusing the carotid body with $CO_2$-$HCO_3^-$ buffer equilibrated at $Pco_2$ • 30 Torr (pH • 7.4). The hypercapnic responses ($Pco_2$ • 55-60 Torr) were measured at $Po_2$ of • 120 Torr).

# 4. RESULTS

## 4.1 Identification of Glomus Cells

Carotid body glomus cells which were 12-24 h old were demonstrated by tyrosine hydroxylase fluorescence. The $[Ca^{2+}]_i$ response was tested with hypoxia. These tests established the identity of the glomus cells of rat carotid body (not shown at the symposium and not here).

## 4.2 Responses of $Ca^{2+}$

$[Ca^{2+}]_i$ responses to hypoxia were inhibited (almost, except for 10%) by 2-APB (100 μM) but not to hypercapnia (Fig. 3). These responses were summarized, which were shown at the symposium. The characteristics of the responses were essentially similar to those exhibited by oligomycin (5 μg/ml) (not shown here). Thus, the influx of $Ca^{2+}$ from the extracellular space was inhibited by both 2-APB and oligomycin, and both blocked the reaction initiated at ER-mitochondrial complex.

### 4.3 Sensory Responses

The sensory responses almost duplicated the $[Ca^{2+}]_i$ responses (not shown).

## 5. DISCUSSION

### 5.1 Mitochondrial Inhibitors

Mitochondrial inhibitors inhibited the hypoxic calcium responses of glomus cells. This is consistent with the observations that mitochondrial inhibitors decreased the K-conductance of glomus cell membrane (Buckler & Vaughn-Jones; 1998; Wyatt and Buckler, 2003).

The blockade of $IP_3$-Rs at the ER-mitochondrial complex blocked the hypoxic $Ca^{2+}$ response of the glomus cells leaving the hypercapnic response intact. The [ $Ca^{2+}$] responses mimicked the sensory response of the carotid body to metabolic inhibitors (Buckler and Vaughan-Jones, 1998; Daudu et al., 2000; Mulligan and Lahiri, 1982).

### 5.2 Blockade of Responses

All these results are consistent with the idea that $IP_3$-Rs blockers inhibited the mitochondrial $[Ca^{2+}]$ responses. Thus, mitochondria somehow communicate with the plasma membrane. Here we show that blockade of $IP_3$-Rs blocked the hypoxic response. Thus, the blockade of hypoxic $Ca^{2+}$-responses is common to both, suggesting that blockade of $IP_3$.R must block the mitochondrial hypoxic response, regardless of the mechanism of effect of 2-APB (Hajnoczky et al., 2000).

### 5.3 Stored Calcium

We measured $[Ca^{2+}]_i$ with normal extracellular $[Ca^{2+}]_o$ of 2.2 mM. With the removal of extracellular $[Ca^{2+}]$ the stored calcium will probably be depleted gradually and $[Ca^{2+}]_i$ response would be minimal. In any case, with extracellular zero $[Ca^{2+}]$, influx of $Ca^{2+}$ will be zero, and would not serve the purpose of testing the hypothesis. With $Ca^{2+}$-channel blocker, influx of $Ca^{2+}$ will also be zero, and that should not serve the purpose either.

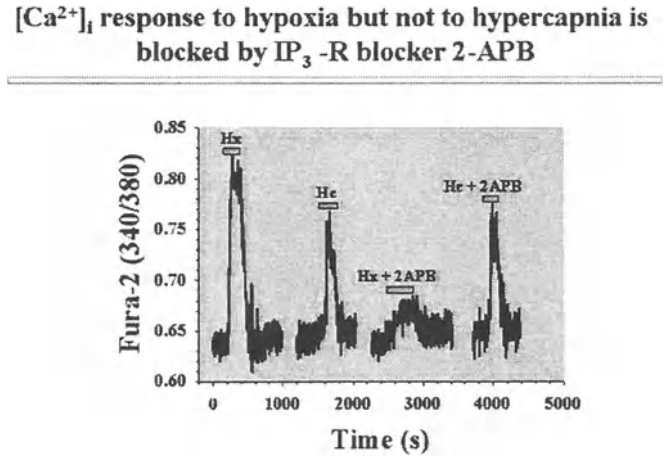


*Figure 3.* Calcium responses to hypoxia (Hx) and hypercapnia (Hc). 2APB inhibited the hypoxic response leaving hypercapnic response intact.

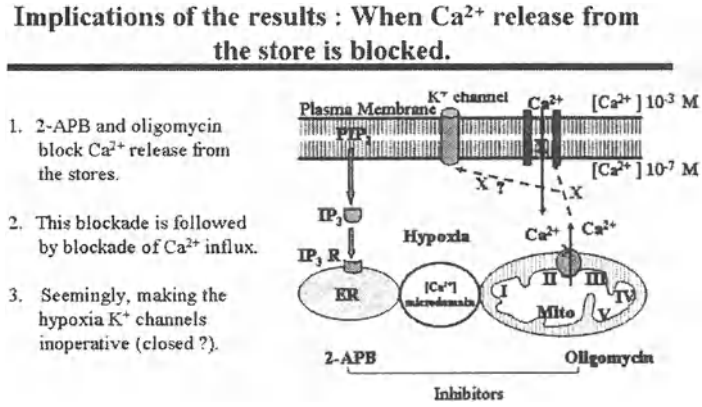


*Figure 4.* Capacitative calcium entry during hypoxia is blocked by 2-APB and oligomycin at ER-mitochondria complex; calcium store depletion is blocked by the inhibitors.

## 5.4 Role of $Ca^{2+}$

With the available data, we present the model involving the role of the calcium store and extracellular $Ca^{2+}$ in hypoxic responses. This message from the internal cellular store is communicated to the membrane which increases the $Ca^{2+}$ influx (capacitative $Ca^{2+}$ entry) (Putney, 1997). With the blockade of $Ca^{2+}$ store depletion, the message to the membrane is blocked. This blockade of $Ca^{2+}$ influx also turns off the hypoxia-sensitive $K^+$ channels (Fig. 4).

The response to hypercapnia remains intact because hypercapnia does not involve the $Ca^{2+}$ store and also it affects different $K^+$ channels than hypoxic sensitive $K^+$ channels.

# 6. CONCLUSION

We showed that blockade of ER-mitochondria $Ca^{2+}$ store depletion practically inhibited the influx of extracellular $Ca^{2+}$. The implications of these results were discussed in terms of $Ca^{2+}$-store depletion and $Ca^{2+}$ influx. This could be considered as evidence for the capacitative $Ca^{2+}$ entry theory of Putney (1997).

# ACKNOWLEDGEMENTS

This work was supported by grants: R-37-HL-43413-12, RO1-HL-50180-10, T32-HL-07027-27, ONR N00014-01-1-0948-02. We are grateful to Mary Pili for her secretarial assistance.

# REFERENCES

Belousov A., Godfraind JM, Krnjevic K (1995). Internal $Ca^{2+}$ stores involved in anoxic responses of rat hippocampal neurons. J. Physiol. 486: 547-556.

Berridge MJ (1993). Inositol trisphosphate and calcium signaling. Nature 361: 315-325.

Biscoe TJ (1990). Responses of type I cells dissociated from the rabbit carotid body to hypoxia. J. Physiol. 428: 39-59.

Buckler KJ, Vaughan-Jones RD (1998). Effects of mitochondrial uncoupler on intracellular calcium, pH and membrane potential in rat carotid body type I cells. J. Physiol. 513: 819-833.

Daudu PA, Rozanov C, Roy A, Mokashi A, Lahiri S (2000). Effects of 2, 4-dinitrophenol (DNP) on the relationship between the chemosensory activities of the rat carotid body and intracellular calcium of glomus cells. Adv. Exptl. Med. Biol. 475: 655-661.

Duchen MR (2000). Mitochondria and calcium: from cell signaling to cell death. J. Physiol. 529: 57-68.

Ferris CD, Snyder SH (1992). Inositol 1, 4, 5-trisphosphate-activated calcium channels. Ann. Rev. Physiol. 54: 469-488.

Hajnoczky G, Csordas G, Krishnamurthy R, Szalai G (2000). Mitochondrial calcium signaling driven by the $IP_3$ receptor. J. Bioenergetics and Biomembranes 32: 15-25.

Kaplin AI, Snyder SH, Linden DJ (1996). Reduced nicotinamide adenine dinucleotide-selective stimulation of inositol 1, 4, 5-trisphosphate receptors mediates hypoxic mobilization of calcium. J. Neuroscience 16: 2002-2011.

Lopez-Barneo J, Pardel R, Ortega-Saenz P (2001). Cellular mechanisms of oxygen sensing. Annu. Rev. Physiol. 63: 259-287.

McCormack JG, Halestrap AP, Denton RM (1990). Role of calcium ions in regulation of mammalian intramitochondrial metabolism. Physiol. Rev. 70: 391-425.

Mulligan E, Lahiri S (1982). Separation of carotid body chemoreceptor responses to $O_2$ and $CO_2$ by oligomycin and antimycin A. Amer. J. Physiol. 242: C200-C206.

Ortega-Saenz P, Garcia-Fernandez M, Pardal R, Lopez-Barneo J. Responsiveness to hypoxia of carotid body glomus cells is independent of mitochondrial electron flow but occluded by rotenone. XVth International ISAC Symposium. (2003 in press).

Pokorski M, Strosznajder R. (1997). ATP activates phospholipase C in the cat carotid body in vitro. J. Physiol. Pharmacol. (48) 3: 443-450.

Putney JW (1997). Type 3 inositol 1, 4, 5-triphosphate-activated calcium channels. Annu. Rev. Physiol. 54: 469-488.

Rigual R, Teresa M, Cachero G, Rocher A, .Gonzalez C. (1999). Hypoxia inhibits the synthesis of phosphoinositides in the rabbit carotid body. Eur. J. Physiol. 437: 839-845.

Rizzuto R, Brini M, Murgia M, Pozzan T (1993). Microdomains with high $Ca^{2+}$ close to $IP_3$-sensitive channels that are sensed by neighboring mitochondria. Science 262: 744-747.

Roy A, Rozanov C, Mokashi A, Lahiri S. (2000). $Po_2$-$Pco_2$ stimulus interaction in $[Ca^{2+}]_i$ and CSN activity in the adult rat carotid body. Resp. Physiol. 122: 15-26.

Veech RL, Raijman L, Krebs HA (1970). Equilibrium relations between the cytoplasmic adenine nucleotide system and nicotinamide adenine nucleotide system in rat liver. Biochem. J. 117: 499-503.

Wyatt CN, Buckler KJ.The effect of mitochondrial inhibitors on membrane currents in isolated neonatal rat carotid body type I cells. XVth International ISAC Symposium. (2003 in press).

Yager JY, Brucklacher RM, Vannucci RC (1991). Cerebral oxidative metabolism and redox state during hypoxia-ischemia and early recovery in immature rats. Am J Physiol 261: 12132-12136.

# Functional Identification of Kvα Subunits Contributing to the $O_2$-Sensitive $K^+$ Current in Rabbit Carotid Body Chemoreceptor Cells

LÓPEZ-LÓPEZ, J.R., PÉREZ-GARCÍA, M.T., SANZ-ALFAYATE, G., OBESO ANA. and GONZALEZ CONSTANCIO

*Instituto de Biología y Genética Molecular (IBGM), Universidad de Valladolid y Consejo Superior de Investigaciones Científicas (CSIC); Departamento de Bioquímica y Biología Molecular y Fisiología, Facultad de Medicina, Valladolid, Spain.*

## 1. INTRODUCTION

Carotid body (CB) chemoreceptors are the major contributors to the hyperventilatory responses to acute hypoxia. Low $PO_2$ inhibits K channel activity of chemoreceptor cells, inducing a depolarization-mediated neurotransmitter release that elicits the ventilatory response (Gonzalez *et al.*, 1994). Although $O_2$-sensitive $K^+$ currents were described in rabbit CB chemoreceptor cells several years ago (López-Barneo *et al.*, 1988), the molecular identity of the underlying K channels remains unresolved.

K channels belong to a large and diverse protein family (Coetzee *et al.*, 1999). As $O_2$-sensitive $K^+$ currents in rabbit CB chemoreceptor cells are voltage-dependent, fast inactivating and $Ca^{2+}$-independent (Ganfornina and López Barneo, 1992), we have searched for the presence in the CB of K channels encoding currents with these electrophysiological properties. So far, six different Kv subunits (Kv1.4, Kv3.3-4 and Kv4.1-3) have been reported to exhibit those properties when expressed in heterologous expression systems (Coetzee *et al.*, 1999; Rudy and McBain, 2001). Combining molecular biology, histochemistry, and electrophysiological techniques, we have determined the presence of those subunits in rabbit chemoreceptor cells (Sanchez *et al.*, 2002), and we have explored their functional contribution to the $O_2$-sensitive current.

## 2. METHODS

### 2.1 CB chemoreceptor cells isolation and culture

Rabbit CBs were obtained and enzymatically dispersed as previously described

*Chemoreception*, Edited by Pequignot et al.
Kluwer Academic/Plenum Publishers, New York, 2003

(Sanchez *et al.*, 2002). Isolated cells were plated onto poly-L-lysine-coated coverslips with DMEM/5% FBS medium, and maintained in culture at 37ºC for up to 72 h.

**2.2. Kv channels mRNA and protein detection in chemoreceptor cells.** Conventional RT-PCR methods were used to test the presence of Kv transcripts in CB cells. We have cloned and sequenced fragments of those subunits whose rabbit sequences were not available (Sanchez *et al.*, 2002). To analyze the expression and the cellular distribution of channel subunits within the CB, we have combined the use of immunocytochemistry with *in situ* hybridization techniques (Sanchez *et al.*, 2002).

**2.3. Electrophysiological methods.** Ionic currents were recorded at room temperature (20-25ºC) using the whole-cell configuration of the patch-clamp technique. Current recordings and data acquisition were made as previously described (Pérez-García *et al.*, 2000). The composition of the bath solution was (mM): 141 NaCl, 4.7 KCl, 1.2 $MgCl_2$, 1.8 $CaCl_2$, 10 glucose, 10 HEPES, (pH 7.4 with NaOH) and the pipette solution was (mM): 125 KCl, 4 $MgCl_2$, 10 HEPES, 10 EGTA, 5 MgATP; pH 7.2 with KOH. Ionic currents were recorded by 500 ms voltage steps to +40 mV from a holding potential of -80 mV applied every 15s. Electrodes were dipped in an antibody-free pipette solution and then back filled with the pipette solution containing the antibody of interest (0.2 μg/ml). In order to eliminate artefacts due to changes in the seal, a 10 ms prepulse to -100 mV was applied prior to the step to +40 mV (see figure 1A). The current response to the prepulse was used to calculate the access resistance (Ra) and the membrane resistance (Rm) applying the membrane test algorithms described elsewhere (pCLAMP, Axon Instruments). Cells without stable values of Ra were discarded for analysis. Data analysis were performed with ORIGIN 4.0 (Microcal Inc.). Pooled data are expressed as mean $\pm$ standard error of the mean (SEM). Statistical comparisons between groups of data were carried out with the two-tailed Student t test for unpaired data, and values of $p<0.05$ were considered statistically different.

## 3. RESULTS AND DISCUSSION

**3.1. Expression and distribution of fast inactivating K channels in rabbit carotid body.** We have previously tested the presence of each Kv transcript in rabbit CB using RT-PCR with unique primers designed from rabbit sequences

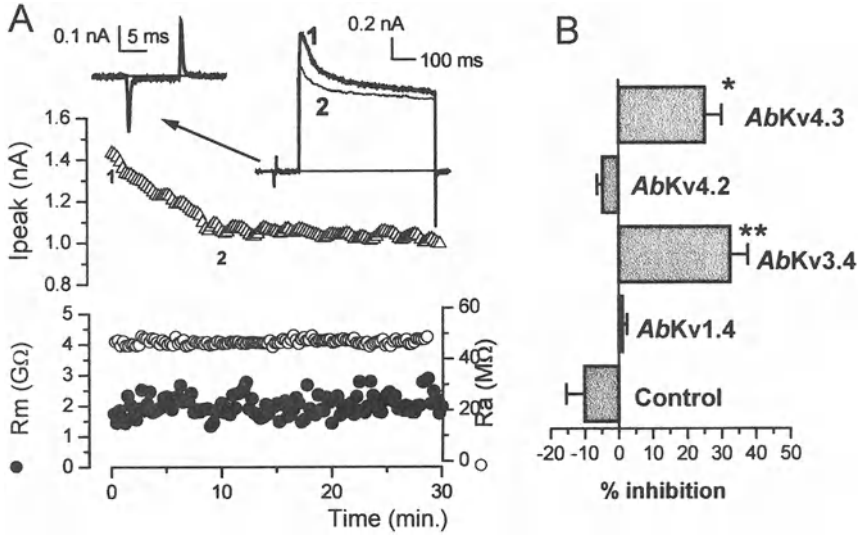


***Figure 1***. Antibody blocking experiments. (A) The upper graph shows the time course of the peak current amplitude in a cell perfused with antiKv4.3 in the pipette solution. Representative traces at the beginning of the recording (1, thick line) and after 10 min of dialysis (2, dotted line) are shown in the inset, as well as the seal-conditions control recordings for each trace. The calculated membrane resistance (Rm) and access resistance (Ra) in each pulse along the 30 min of recording are illustrated in the lower graph. (B) Average inhibition of peak current with the indicated antibodies. Inhibition was calculated as $100.(1-I/I_0)$, where $I_0$ is the initial amplitude of the current (t=0) and I is the current amplitude after 10 min of recording.*$p<0.01$; **$p<0.001$. Each bar is the average of 4-10 experiments.

(Sanchez *et al.*, 2002). Those results showed the transcription of Kv1.4, 3.4, 4.1 and the long form of Kv4.3, but not Kv3.3 or 4.2. To demonstrate the presence of particular Kv subunits in chemoreceptor cells, we analyzed their cellular distribution with immunocytochemistry when antibodies were commercially available, and *in situ* hybridization (in the case of Kv4.1, which antibody is not available). We have concluded that rabbit CB chemoreceptor cells express Kv3.4, 4.1 and 4.3. However, not all the TH positive cells showed Kv3.4 expression, suggesting that Kv3.4 is expressed only in a subpopulation of chemoreceptor cells. A summary of our results is shown in table I.

| Kv α subunit | mRNA expression | Protein expression | TH co-localization |
|---|---|---|---|
| **Kv1.4** | Yes | Yes | No |
| **Kv3.3** | No | ND | ND |
| **Kv3.4** | Yes | Yes | Yes |
| **Kv4.1** | Yes | ND | Yes |
| **Kv4.2** | No | No | No |
| **Kv4.3** | Yes | Yes | Yes |

*Table 1* RT-PCR, immunocytochemistry and *in situ* hybridization confirms the expression in chemoreceptor cells of three fast inactivating Kv subunits: Kv3.4, Kv4.1, and Kv4.3. No Kv3.3 or Kv4.2 transcription is detected in the CB, while the Kv1.4 subunit is present only in nerve terminals. ND = not determined.

**3.2. Antibody blockade of $K^+$ currents in rabbit CB chemoreceptor cells.** To elucidate the contribution of Kv3.4 and Kv4.3 subunits to the $K^+$ currents of chemoreceptor cells, we assayed the efficiency of antiKv antibodies to block these currents. Whole-cell voltage-clamp experiments were performed including antiKv1.4, 3.4, 4.2, or 4.3 antibodies in the patch pipette. Control cells where either recorded in the absence of antibody, in the presence of another unrelated antibody such as anti-myosin, or in the presence of a goat anti-mouse serum, to exclude non-specific effects. Figure 1A shows representative traces obtained in one CB chemoreceptor cell in the presence of antiKv4.3. After 10 min of dialysis, the current decreased irreversibly. Recordings for as long as 30 min did not increase significantly the observed inhibition. Average effects of the different antibodies applied are shown in figure 1B. AntiKv1.4 and antiKv4.2 did not change outward currents after several minutes of recording, while both the antiKv3.4 and 4.3 produced a significant reduction in $I/I_0$, indicating that Kv3.4 and Kv4.3 subunits contribute to the fast inactivating $K^+$ current of chemoreceptor cells.

**3.3. Effect of hypoxia on $K^+$ currents in the presence of antiKvα antibodies.** We have also used the immunological blockade of $K^+$ currents as a tool for assaying the role of the different Kv subunits on the hypoxic inhibition of the whole $K^+$ current. This approach has been used recently to demonstrate the $O_2$-sensitivity of Kv1.2 in PC12 cells (Conforti *et al.*, 2000). Our results show that hypoxia could still decrease the remaining $K^+$ current in a significant manner after blocking Kv subunit-specific components by any antibody addition (Figure2). However, when we express the effect of hypoxia as percentage of

inhibition of the total current, hypoxic inhibition is significantly smaller in the presence of antiKv4.3, suggesting that Kv4.3 channels contribute to the $O_2$-sensitive current.

In contrast, antiKv3.4 treatment tends to increase hypoxic inhibition, although not significantly. The lack of an estimation of the affinity of the antibodies, and the unavailability of antiKv4.1, does not allow us to infer clear-cut conclusions about the quantitative contribution of the different Kv channel subunits to the $O_2$-sensitive $K^+$ current. Nevertheless, our data suggest a lack of effect of $O_2$ on Kv3.4 channels. This conclusion could explain the observed trend to an increase in the effect of hypoxia in the presence of antiKv3.4, because if some proportion of the $O_2$-insensitive current has been blocked by the antibody, the $O_2$-sensitive current would represent a larger proportion of the remaining current.

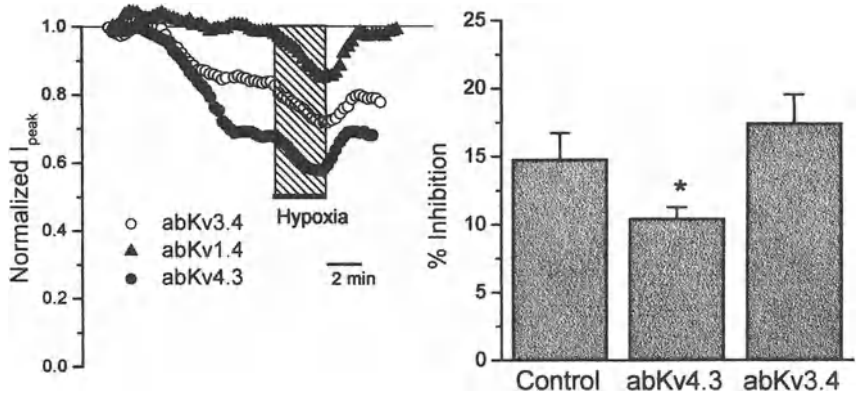


***Figure 2*** *A*ntibody blockade and hypoxic inhibition of $K^+$ currents. Left panel shows the time course of the peak current amplitude in 3 different cells in the presence of the indicated antibody in the pipette solution. Hypoxia was applied when indicated. The average data obtained in 3-7 cells in each condition are represented on the right part of the figure as percentage of inhibition of the peak current amplitude. The effect of hypoxia was calculated as the ratio $I_{hypoxia}$ / $I_{control}$, being $I_{control}$ the mean value of the current amplitude before and after hypoxic stimulation. * $p<0.05$.

These experiments indicate that while both, Kv4.3 and Kv3.4 contribute to the transient outward $K^+$ current of chemoreceptor cells, only Kv4.3 seems to be modulated by low $PO_2$. This observation is in agreement with previous data from our group showing the ubiquitous expression of both Kv4.3 and Kv4.1 in

chemoreceptor cells (Sanchez *et al.*, 2002) and the functional consequences of Kv4 knockout (Pérez-García *et al.*, 2000). Adenoviral infection of CB cells with dominant-negative Kv4 constructs leads to a reduction of the transient $K^+$ currents, depolarises the cells and makes them unresponsive to hypoxia. We present here further evidence implicating Kv4 channels as components of the $O_2$-sensitive $K^+$ currents, specifically demonstrating the contribution of Kv4.3. We can not estimate the quantitative contribution of Kv4.3 to the macroscopic current, but we can be fairly confident regarding the specificity of the immunological blockade. We have studied the effect of antiKv4.3 on the K currents of HEK cells transfected with Kv4.3, and we found a decrease in the peak current amplitude of 59±7% (n=5). Also, we show that antiKv4.2 does not affect the amplitude of the $K^+$ currents of chemoreceptor cells (figure 1B) or the magnitude of its hypoxic inhibition (data not shown). Altogether, these data suggest that intracellular perfusion with antiKv4 antibodies has a blocking effect specific for the subfamily member.

Taken together, our data clearly prove a role for Kv3.4 and Kv4.3 channels as molecular constituents of the transient outward $K^+$ current of rabbit CB chemoreceptor cells, and identify Kv4.3 as one of the putative components of the $O_2$-sensitve $K^+$ current. These conclusions also open interesting questions to explore and understand the structural requirements of oxygen sensitivity. The key issue is to elucidate if Kv4 subunits sense $O_2$ themselves, or if other regulatory subunits are required to confer $O_2$-sensitivity to the channels.In fact, the increasing number of reports regarding $O_2$ modulation of very different channels (Pérez-García and López-López, 2000; Patel and Honore, 2001), together with the expression of Kv4 channels in non chemoreceptor tissues, makes more likely the hypothesis of an $O_2$-sensor capable to interact with the channel or with an accessory subunit.

## ACKNOWLEDGMENTS

We want to thank María Llanos for technical assistance. This work was supported by Spanish DGICYT Grants BFI2001/1713 to C.G., and BFI2001-1691 to J.R.L.L. and a VA001/01 grant from the Junta de Castilla y León to M.T.P.G and Red RESPIRA (FISS).

# REFERENCES

Barry, D. M. and Nerbonne, J. M. (1996). Myocardial potassium channels: electrophysiological and molecular diversity. *Annu Rev Physiol* 58:363-394.

Coetzee, W. A., Amarillo, Y., Chiu, J., Chow, A., Lau, D., McCormack, T., Moreno, H., Nadal, M. S., Ozaita, A., Pountney, D., Saganich, M., Vega-Saenz, d. M., and Rudy, B. (1999). Molecular diversity of $K^+$ channels. *Ann N Y Acad Sci* 868: 233-285.

Conforti, L., Bodi, I., Nisbet, J. W., and Millhorn, D. E. (2000). $O_2$-sensitive $K^+$ channels: role of the Kv1.2 -subunit in mediating the hypoxic response. *J Physiol (Lond)* 524:783-793.

Ganfornina, M. D. and López Barneo, J. (1992). Gating of $O_2$-sensitive $K^+$ channels of arterial chemoreceptor cells and kinetic modifications induced by low $PO_2$. *J Gen Physiol* 100:427-455.

Gonzalez, C., Almaraz, L., Obeso, A., and Rigual, R. (1994). Carotid body chemoreceptors: from natural stimuli to sensory discharges. *Physiol Rev* 74:829-898.

López-Barneo, J., López-López, J. R., Ureña, J., and Gonzalez, C. (1988). Chemotransduction in the carotid body: $K^+$ current modulated by $PO_2$ in type I chemoreceptor cells. *Science* 241:580-582.

Patel, A. J. and Honore, E. (2001). Molecular physiology of oxygen-sensitive potassium channels. *Eur Respir J* 18:221-227.

Pérez-García, M. T. and López-López, J. R. (2000). Are Kv channels the essence of $O_2$ sensing? *Circ Res* 86:490-491.

Pérez-García, M. T., López-López, J. R., Riesco, A. M., Hoppe, U. C., Marban, E., Gonzalez, C., and Johns, D. C. (2000). Viral gene transfer of dominant-negative Kv4 construct suppresses an $O_2$- sensitive $K^+$ current in chemoreceptor cells. *J Neurosci* 20:5689-5695.

Rudy, B. and McBain, C. J. (2001). Kv3 channels: voltage-gated $K^+$ channels designed for high-frequency repetitive firing. *Trends Neurosci* 24:517-526.

Sanchez, D., Lopez-Lopez, J. R., Perez-Garcia, M. T., Sanz-Alfayate, G., Obeso, A., Ganfornina, M. D., and Gonzalez, C. (2002). Molecular identification of Kvalpha subunits that contribute to the oxygen-sensitive $K^+$ current of chemoreceptor cells of the rabbit carotid body. *J Physiol (Lond)* 542:369-382.

# Carotid Body Chemoreceptor Activity in Mice Deficient in Selected Subunits of NADPH Oxidase

L. HE[1], J. CHEN[1], B. DINGER[1], K. SANDERS[2], K. SUNDAR[2], J. HOIDAL[2] and S. FIDONE[1]

*Departments of [1]Physiology and [2]Medicine, University of Utah School of Medicine, Salt Lake City, UT, USA*

## 1. INTRODUCTION

Exposure of the carotid body to hypoxia elicits increased neural activity in the carotid sinus nerve (CSN), and reflex cardio-pulmonary adjustments which mitigate the adverse effects of hypoxemia. Increased carotid body activity occurs at relatively moderate arterial $PO_2$, in contrast to the severe hypoxia required to elicit metabolic and functional adjustments in non-$O_2$ sensing tissues (S.J.Fidone *et al.*, 1997). Chemosensory type I cells derived from neuroectoderm are responsible for this exquisite sensitivity, and numerous laboratories have reported that low $PO_2$ inhibits the conductance of a variety of voltage sensitive and voltage-insensitive $K^+$-channels in these cells. Yet the molecular mechanism underlying the $PO_2$ modulation of cell currents remains uncertain and controversial (H.Acker *et al.*,1994, A.M.Riesco-Fagundo *et al.*,2001). Various heme proteins have been proposed as primary $O_2$ sensors, and one set of data in particular suggests the involvement of a multi-component cytochrome b-containing NADPH oxidase which may be similar if not identical to the superoxide generating enzyme commonly found in phagocytic cells (H.Acker *et al.*, 1994).

*Chemoreception*, Edited by Pequignot et al.
Kluwer Academic/Plenum Publishers, New York, 2003

According to this hypothesis superoxide anion ($O_2^{-}\bullet$) is generated intracellularly in proportion to available $O_2$, and $K^+$-channels are modulated by $H_2O_2$ formed from $O_2^{-}\bullet$ by the action of cytosolic ZnCu superoxide dismutase (ZnCuSOD).

For many years it has been known that large quantities of $O_2^{-}X$ are produced by phagocytic cells as part of an extracellular killing mechanism (i.e., the respiratory burst) activated in response to invading micro-organisms. Phagocytic NADPH oxidase is a complex enzyme comprised of two trans-membrane and four cytosolic subunits. The large 91 kD glycoprotein ($gp91^{phox}$; phox: phagocytic oxidase) and a 22 kD protein ($p22^{phox}$) form a membrane bound cytochrome b558 (B.M Babior *et al.*, 1999, H.Sauer *et al.*, 2001). Immunologic stimulation initiates a protein kinase C (PKC)-dependent process in which cytosolic subunits, including $p67^{phox}$, $p40^{phox}$, $p47^{phox}$ and a small GTPase (Rac-1 or Rac-2), unite at the membrane to form the active enzyme. An electron is then transferred from NADPH to $O_2$, thus forming $O_2^{-}X$ plus $NADP^+$( B.M Babior *et al.*, 1999, H.Sauer *et al.*,2001). Despite recent advances in demonstrating the importance of reactive oxygen species (ROS; i.e., $O_2^{-}\bullet$ and $H_2O_2$) in cell signaling (H.Sauer *et al.*, 2001, V.J. Thannickal *et al.*, 2000), perplexing conceptual issues have arisen in applying the phagocytic form of the oxidase as a model $O_2$-sensor. Toxic amounts of $O_2^{-}X$ are produced primarily on the extracellular side of the plasma membrane (B.M Babior *et al.*,1999, H.Sauer *et al* 2001), a location entirely inconsistent with the action of an intracellular messenger. In addition, the phagocytic enzyme is inactive in resting phagocytic cells, which does not support the notion that ROS production can be up- or down-regulated by local $PO_2$. However, in non-phagocytic cells numerous recent studies have shown that NADPH oxidase is constitutively active, and produces low levels of $O_2^{-}X$ (J.M Li *et al* 2002, V.J. Thannickal *et al.*, 2000). For example, vascular endothelial cells contain an NADPH oxidase in which cytochrome b558 and the cytosolic subunits are preassembled on cytoskeletal elements in the perinuclear region, where they are engaged in constitutive production of intracellular ROS (J.M Li *et al.*, 2002). Like other messenger molecules (i.e., cyclic AMP, cyclic GMP, inositol phosphates and nitric oxide), ROS have been shown to affect specific targets within local cellular compartments (G. Pani *et al.*, 2001), frequently involving cysteine and methionine residues which are highly labile targets for oxidation/reduction (V.J. Thannickal *et al.*, 2000, D.Xu *et al.*, 2002). Changes in the redox state

at these sites has been demonstrated to critically alter important effector molecules including $K^+$-channels (T.Hoshi *et al.*, 2001, X.D.Tang *et al.*, 2001). Moreover, recent studies have indicated the involvement of ROS generated by NADPH oxidase in cell signaling in the lung. $K^+$-channels in $O_2$-sensitive neuroepithelial body (NEB) cells (X.W. Fu *et al* 2000, I.O'Kelly *et al.*,2000, D.Wang *et al.*, 1996) are activated by low concentrations of $H_2O_2$, and hypoxia-evoked depression of channel activity is occluded in the presence of oxidase inhibitors, suggesting that the oxidase is a key enzyme which couples local $PO_2$ to cell activity (X.W. Fu *et al* .,2000, D.Wang *et al.*, 1996).

## 2. $O_2$-SENSING IN NADPH OXIDASE DEFICIENT MICE

Gene-deleted mice deficient in $gp91^{phox}$ (J.D Pollock *et al.*,1995) or $p47^{phox}$ (S.H Jackson *et al.*, 1995) subunits of NADPH oxidase were originally generated to establish animal models of granulomatous disease, an inherited disorder characterized by the absence of the respiratory burst in neutrophils. In recent studies we used these strains to examine the NADPH oxidase hypothesis of $O_2$-sensing in carotid body. Our initial findings using the $gp91^{phox}$-deleted animals demonstrated that resting and hypoxia-evoked carotid sinus nerve (CSN) activity was identical in normal versus gene-deleted preparations. Likewise, nerve activity evoked by the classical chemoreceptor stimulant, nicotine, did not differ between the two strains of mice (L.He *et al.*,2002). We also demonstrated that low-$O_2$-mediated depression of whole-cell $K^+$-currents, and hypoxia-evoked $Ca^{2+}$-responses were indistinguishable in normal and gene-deleted type I cells (L.He *et al.*, 2002). These results agreed with earlier studies which demonstrated normal hypoxia-evoked responses in pulmonary artery smooth muscle (S.L.Archer *et al.*,1999), but they conflicted with the elimination of $K^+$-current $O_2$-sensitivity in NEB cells following deletion of the $gp91^{phox}$-gene (X.W. Fu *et al.*,2000).

Although results from the carotid body refuted the participation of $gp91^{phox}$ in the chemoreceptor response, they did not rule out the possibility that ROS production in type I cells was mediated by a gene homolog (G.Cheng *et al.*, 2001). Consistent with this notion were the results of experiments evaluating chemoreceptor activity in mice lacking expression of the

cytosolic $p47^{phox}$ subunit which demonstrated increased chemoreceptor activity (figure 1). Compared with wild-type mice, resting CSN activity was marginally (but significantly, $p<0.05$) increased in the $p47^{phox}$-deleted preparations, but markedly increased by hypoxia (K.A Sanders *et al.*, 2002). These findings supported studies of the hypoxic ventilatory response (HVR) in unanesthetized unrestrained mice in which breathing 10% $O_2$ elicited a 20% increase in wild-type mice, but a doubling of ventilation in the $p47^{phox}$-deleted animals (K.A Sanders *et al.*, 2002 ). Supporting data from preliminary experiments indicate that low-$O_2$ elicits enhanced depression of $K^+$-currents and elevated $Ca^{2+}$-responses in type I cells from $p47^{phox}$ gene-deleted animals.

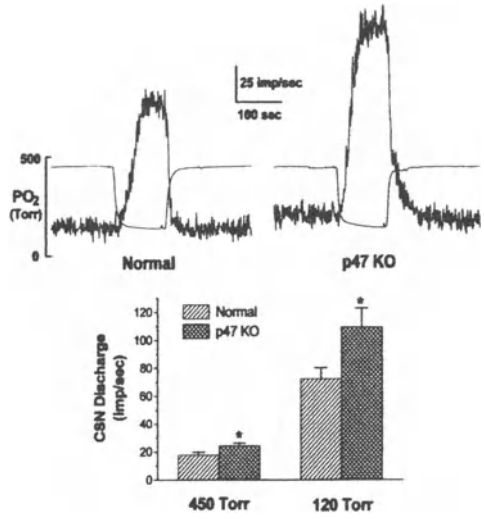


*Figure 1.* Carotid sinus nerve (CSN) activity in wild-type and $p47^{phox}$-null mutant mice. Upper panel shows slightly elevated resting neural activity and markedly enhanced hypoxia-evoked discharge in a preparation from an oxidase-deficient mouse (p47 KO) vs. a normal mouse. Superimposed trace indicates bath $PO_2$. Summary data for resting and evoked activity in lower panel. (Data re-plotted from K.A Sanders *et al* 2002, with permission.)

## 3. THE ROLE OF ROS IN CAROTID BODY $O_2$-SENSING

The differing effects of $gp91^{phox}$- versus $p47^{phox}$-gene deletion on carotid body function suggest that a homolog of the NADPH oxidase of phagocytes participates in chemotransduction. However, the data presently available do not clarify the precise role of the enzyme in the transduction cascade. The original hypothesis of NADPH oxidase involvement in $O_2$-sensing postulates that hypoxia would decrease ROS production in type I cells

(H.Acker *et al.*, 1994), but the relationship between $PO_2$ and ROS levels in type I cells has not been firmly established. In other cells and tissues hypoxia can increase or decrease ROS production in either mitochondria or via NADPH oxidase (I.O'Kelly *et al.*, 2000, G.B Waypa *et al.*, 2001). In addition, the target of ROS in type I cells is an unknown and critical factor in determining the effect of NADPH oxidase on cell activity. Recent studies have indicated that voltage-sensitive $K^+$-channels in type I cells are modulated by hypoxia via a mechanism independent of soluble factors such as ROS (A.M. Riesco-Fagundo *et al.*, 2001). Thus ROS do not appear to be necessary for cell activation. On the other hand, if hypoxia enhances NADPH oxidase activity, elevated ROS levels may increase the open probability of $K^+$-channels thus facilitating cell repolarization. Such a scheme is consistent with elevated CSN activity in $p47^{phox}$-gene deleted animals. Clarification of these issues must await future measurements of the effect of hypoxia on NADPH oxidase activity, and evaluation of the interaction of ROS with the chemotransduction machinery in type I cells.

## ACKNOWLEDGMENTS

Supported by the Office of Research and Development, Medical Research Service, Department of Veterans Affairs; National Institutes of Health Specialized Center of Research Project P50 HL-50153, and National Institute of Neurological Disorders and Stroke Grants NS 12636 and NS 07938

## REFERENCES

H.Acker, 1994 Mechanisms and meaning of cellular oxygensensing in the organism, *Respir.Physiol.* 95(1):1.

S.L.Archer, H.L.Reeve, E.Michelakis, L.Puttagunta, R.Waite, D.P.Nelson, M.C.Dinauer, and E.K.Weir, 1999 $O_2$ sensing is preserved in mice lacking the gp91 phox subunit of NADPH oxidase, *Proc.Natl.Acad.Sci.USA* 96:7944.

B.M.Babior, 1999 NADPH oxidase: An update, *Blood* 93(5):1464

G.Cheng, Z.Cao, X.Xu, E.G.Van Meir, and J.D.Lambeth, 2001 Homologs of gp91*phox*: cloning and tissue expression of Nox3, Nox4 and Nox5 , *Gene* 269:131.

S.J.Fidone, C.Gonzalez, L.Almaraz, and B.Dinger, 1997 Cellular mechanisms of peripheral chemoreceptor function, *in: "The Lung: Scientific Foundations"*, R.G.Crystal and J.B. West, et.al. eds., Lippincott-Raven Publishers , Philadelphia

X.W.Fu, D.Wang, C.A.Nurse, M.C.Dinauer, and E.Cutz, 2000, NADPH oxidase is an $O_2$ sensor in airway chemoreceptors: Evidence from $K^+$ current modulation in wild-type and oxidase-deficient mice, *PNAS* 97(8):4374

L.He, J.Chen, B.Dinger, K.Sanders, K.Sundar, J.Hoidal, and S.Fidone, 2002, Characteristics of carotid body chemosensitivity in NADPH oxidase-deficient mice, *Am.J.Physiol.Cell.Physiol.* 282:C27

T.Hoshi and S.H.Heinemann, 2001, Topical review: Regulation of cell function by methionine oxidation and reduction, *J.Physiol.* 531.1:1

S.H.Jackson, J.I.Gallin, and S.M.Holland, 1995, The p47phox mouse knock-out model of chronic granulomatous disease, *J.Exp.Med.* 182(3):751.

J.-M.Li and A.J.Shah, 2002, Intracellular localization and preassembly of the NADPH oxidase complex in cultured endothelial cells, *J.Biol.Chem.* 277(22):19952.

I.O'Kelly, A.Lewis, C.Peers, and P.J.Kemp, 2000, $O_2$ sensing by airway chemoreceptor-derived cells: Protein kinase C activation reveals functional evidence for involvement of NADPH oxidase, *J.Biol.Chem.* 275(11):7684

G.Pani, B.Bedogni, R.Colavitti, R.Anezvino, S.Borrello, and T.Galeotti, 2001, Cell compartmentalization in redox signaling, *IUBMB Life* 52:7

J.D.Pollock, D.A.Williams, M.A.C.Gifford, L.L.Li, X.Du, J.Fisherman, S.H.Orkin, C.M.Doerschuk, and M.C.Dinauer, 1995, Mouse model of x-linked chronic granulmatous disease, an inherited defect in phagocyte superoxide production, *Nature Genetics* 9:202.

A.M.Riesco-Fagundo, M.T.Pérez-Garc¸a, and J.R.Lpez-Lpez, 2001,$O_2$ modulates large-conductance $Ca^{2+}$-dependent $K^+$ channels of rat chemoreceptor cells by a membrane-restricted and CO-sensitive mechanism, *Circ.Res.* 89:430

K.A.Sanders, K.M.Sundar, L.He, B.Dinger, S.Fidone, and J.R.Hoidal, 2002, Role of components of the phagocytic NADPH oxidase in oxygen sensing, *J.Appl.Physiol.* 93(4) :1357.

H.Sauer, M.Wartenberg, and J.Hescheler, 2001, Reactive oxygen species as intracellular messengers during cell growth and differentiation, *Cell.Physiol.Biochem.* 11:173.

X.D.Tang, H.Daggett, M.Hanner, M.L.Garcia, O.B.McManus, N.Brot, H.Weissbach, S.H.Heinemann, and T.Hoshi, 2001, Oxidative regulation of large conductance calcium-activated potassium channels, *J.Gen.Physiol.* 117:253.

V.J.Thannickal and B.L.Fanburg, 2000, Reactive oxygen species in cell signaling, *Am.J.Physiol.Lung Cell.Mol.Physiol.* 279:L1005.

D.Wang, C.Youngson, V.Wong, H.Yeger, M.C.Dinauer, E.Vega-Saenz De Miera, B.Rudy, and E.Cutz, 1996, NADPH-oxidase and a hydrogen peroxide-sensitive $K^+$ channel may function as an oxygen sensor complex in airway chemoreceptors and small cell lung carcinoma cell lines, *Proc.Natl.Acad.Sci.USA* 93:13182.

G.B.Waypa, N.S.Chandel, and P.T.Schumacker, 2001, Model for hypoxic pulmonary vasoconstriction involving mitochondrial oxygen sensing, Circ.Res. 88:1259

D.Xu, I.I.Rovira, and T.Finkel, 2002, Oxidants painting the Cysteine Chapel: Redox regulation of PTPs, *Developmental Cell* 2:251

# Glucose Sensing Cells in the Carotid Body

MARÍA GARCÍA-FERNÁNDEZ, PATRICIA ORTEGA-SÁENZ, RICARDO PARDAL, and JOSÉ LÓPEZ-BARNEO*

*Laboratorio de Investigaciones Biomédicas. Hospital Universitario Virgen del Rocío, Universidad de Sevilla, E-41013, Seville, Spain.*

## 1. INTRODUCTION

As neurons utilize almost exclusively glucose as energy source, brain function depends critically on a steady glucose supply (Martin et al., 1994; Auer et al., 1998). Acute hypoglycemia is counterbalanced by sympathetic activation to increase glucose delivery to blood (Cryer et al., 1981; Cane et al., 1986; Gerich and Campbell, 1988). This homeostatic response is essential for life and particularly important for insulin-treated diabetics, however the underlying mechanisms and site(s) of peripheral blood glucose control remain unknown (Cane et al., 1986; Amiel et al., 1987; Hoffman et al., 1999). Although the existence of glucose-sensitive neurons in the hypothalamus and other areas of the brain is well documented (Biggers et al., 1989; Routh, 2002), there is considerable evidence supporting the existence of peripheral glucose sensors, which are necessary for the proper counterregulatory responses to hypoglycemia. Systemic glucoreceptors have been proposed to exist at the liver, pancreas, portal vein, and carotid bodies (Alvarez-Buylla and Alvarez Buylla, 1988; Donovan et al., 1991; Hevener et al., 2000; Koyama et al., 2000, 2001), nevertheless the physiological role of these glucose sensitive regions is controversial and the glucose sensing cells have not been identified. The carotid

*Chemoreception*, Edited by Pequignot et al.
Kluwer Academic/Plenum Publishers, New York, 2003

bodies are strategically located chemosensory organs, connected to the brain centers involved in glucose homeostasis, whose stimulation produces sympathetic activation and the output of hepatic glucose (Alvarez-Buylla and Alvarez-Buylla, 1988; 1994; Zinker et al., 1994). In addition, surgical resection of the carotid bodies and surrounding tissues impairs the counterregulatory neuroendocrine responses to insulin-induced mild hypoglycemia (Koyama et al., 2000) and to exercise (Koyama et al., 2001). Based on these precedents we have studied whether glomus cells, the $O_2$-responsive elements in the carotid body (see for a review López-Barneo et al., 2001), are glucose sensors. Herein, we briefly summarize our recent work on the characterization of glucose-sensitive cells in the carotid body. We propose that carotid body glomus cells are multimodal receptors, which serve to integrate information about blood chemical variables ($O_2$, $CO_2$, glucose and others) to activate counterregulatory responses.

## 2. ACTIVATION OF GLOMUS CELLS BY LOW GLUCOSE

The carotid body is composed of innervated clusters of glomus cells that when activated release dopamine and other transmitters to stimulate afferent sensory fibers (see López-Barneo et al., 2001). We have used for these experiments a thin slice preparation that retains the carotid body structure and preserves the characteristic response of glomus cells to hypoxia (Pardal et al., 2000). Carotid body sections of ~150 μm thick were maintained in culture medium (DMEM) at 37°C in a 5% $CO_2$ incubator and placed on a recording chamber, mounted on the stage of an upright microscope, where it was continuously perfused by gravity (flow 1 to 2 ml/min) with a solution containing (in mM) 117 NaCl, 4.5 KCl, 23 $NaHCO_3$, 1 $MgCl_2$, 2.5 $CaCl_2$, 5 Glucose and 5 Sucrose. Exposure of glomus cells in these slices to a glucose-free solution (replacing 5 mM glucose for sucrose) induced a secretory activity that was monitored by amperometry (Pardal et al., 2000; Pardal and López-Barneo, 2002) (Fig. 1A, top). Single exocytotic events appeared as spike-like signals, indicating the release of catecholamines from individual vesicles. The magnitude of the secretory response was estimated from the sum of the time integral of the secretory events (cumulative secretion in Fig. 1A bottom), which represents a value of electric charge proportional to the number of catecholamine molecules oxidized (Ureña et al., 1994). The average rate of secretion during the last minute of exposure to low glucose (1870±386 fC/min, n=14 cells) was over 20 times that of the control condition (88±45 fC/min, n=14) (Fig. 1B). The effect of low glucose on glomus cells was concentration-dependent. At an $O_2$ tension ($PO_2$) of 150 mmHg, a condition used in most experiments to

suppress the $O_2$-sensitive activation pathway (see below), the cells were almost silent in 5 mM glucose. When glucose was lowered to 2 mM catecholamine release became appreciable and increased in proportion with the degree of glucopenia (Figures 1C&D).

Catecholamine secretion induced by glucose-free solutions was totally suppressed by the addition of 0.2 mM $Cd^{2+}$ to the extracellular solution (Fig. 1E). Therefore, these results indicate that low glucose-induced transmitter secretion in glomus cells depends on extracellular $Ca^{2+}$ influx through voltage-dependent channels of the plasma membrane.

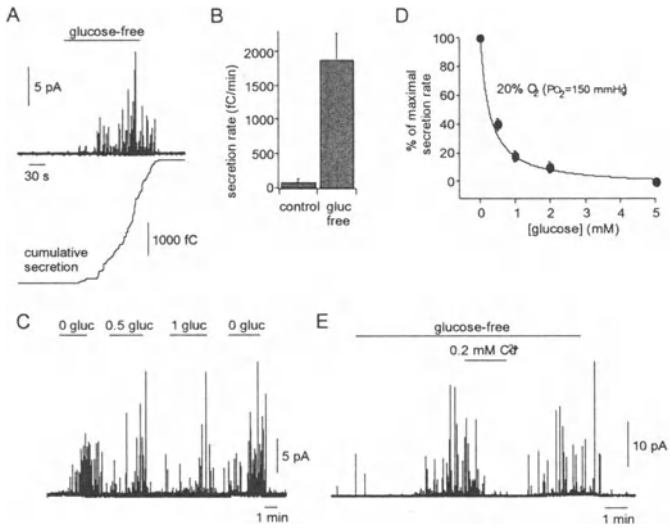


*Figure 1.* Secretory response of glomus cells to low glucose. A. Top. Amperometric signal illustrating the increase of secretory activity in a glomus cell exposed to a glucose-free solution. Each spike corresponds to the release of a catecholaminergic vesicle. Bottom. Cumulative secretion signal (in femtocoulombs) resulting from the time integral of the amperometric recording. B. Average secretion rate (mean ± s.d., in fC/min) in cells exposed to 5 (control) and 0 (glucose-free) mM glucose. C. Secretory response of a single glomus cell to various levels of low glucose. D. Secretory activity (expressed in the ordinate as percentage of maximal secretion rate in each experiment) as a function of extracellular glucose concentration. $PO_2$ in the experiments was 150 mmHg. Each data point is the mean±standard deviation of measurements in three cells subjected to the complete experimental protocol. Solid line was drawn by eye. E. Reversible suppression of low glucose-evoked secretory activity by application of 0.2 mM $Cd^{2+}$ to the extracellular solution.

## 3. GLOMUS CELLS ARE MULTIMODAL CHEMORECEPTORS

Exposure of glomus cells to low glucose is a stimulus that, as does hypoxia, increases cell excitability. Thus, we expected an enhancement in sensitivity to low glucose for cells exposed to reduced $PO_2$ as well as augmentation of the secretory response when the two conditions were present simultaneously. Fig. 2A shows that the typical response of glomus cells to hypoxia (switching from an external solution bubbled with air, $PO_2$ ~150 mmHg, to another bubbled with nitrogen, $PO_2$ ~20 mmHg) was markedly potentiated in 0 mM glucose. The mean secretory rate measured in cells exposed to low $PO_2$ (~20 mmHg) or to glucose-free solutions (1789±439 fC/min, n=8 and 1870±386 fC/min, n=14, respectively) increased to 4400±1300 fC/min (n=8) when the two stimuli were applied together (Fig. 4B). Owing to the additive effects of hypoxia and glucopenia, the dependence of glomus cell secretion on glucose concentration, studied initially at $PO_2$ of 15 mmHg (see above), was displaced toward higher glucose levels when $PO_2$ was maintained at 90 mmHg, an $O_2$ tension comparable to that in the arterial blood irrigating the rat carotid body in vivo (Fig. 2C). Thus, at physiological low $PO_2$ glomus cell secretory activity is significantly modulated by extracellular glucose in the concentration range (2 to 5 mM) that includes the values observed in common hypoglycemic situations (Dunn-Meynell et al., 2002; Routh et al., 2002).

Our findings strongly suggest that carotid body glomus cells are physiological low-glucose detectors that transduce glucose levels into variable rates of transmitter release. Although the existence of peripheral glucosensors presumably located in the liver or portal vein has been proposed (Donovan et al., 1991, 1994), the strategically located carotid bodies may be of special importance for brain homeostasis as neurons are particularly vulnerable to the simultaneous lack of glucose and oxygen (Martin et al., 1994; Auer, 1998). The function of glomus cells as combined $O_2$ and glucose sensors, in which the two stimuli potentiate each other, is surely advantageous to facilitate activation of the counterregulatory measures in response to small reductions of any of the regulated variables. Impairment of low-glucose sensing by carotid body glomus cells might contribute to the susceptibility of insulin-dependent diabetic patients to hypoglycemia (Heverner et al., 1997; Koyama et al., 2000). In conclusion, glomus cells are integrated metabolic sensors with a novel role as low-glucose detectors thus helping prevent neuronal damage by acute hypoglycemia. These cells, known to be activated by hypoxia and hypercapnia, (see Fig. 3), represent

a typical example of multimodal chemoreceptors in which several stimuli converge to activate secretion.

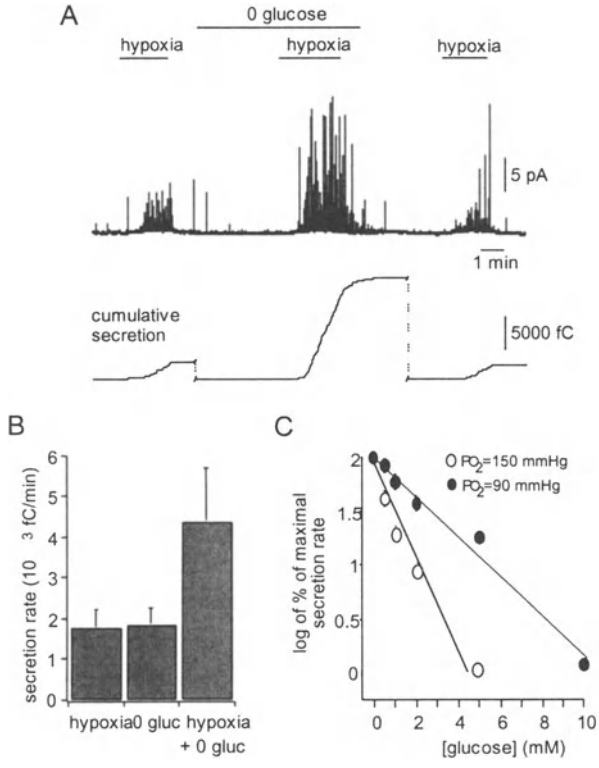


*Figure 2.* Increased sensitivity to low glucose by exposure to low $PO_2$. A. Potentiation of the secretory response to 0 mM glucose in a cell exposed to hypoxia ($PO_2$ ~20 mmHg). Secretion rates during the three successive responses to hypoxia are 1837, 5816 and 1729 fC/min, respectively. Resetting of the integrator used to calculate the cumulative secretion signal is indicated by dotted lines. B. Average secretion rates (in fC/min) in cells exposed to low $PO_2$ (~20 mmHg; 1780±439, n=8), 0 glucose (1870±386, n=14) and the two conditions simultaneously (4400±1300, n=8). C. Logarithm of maximal secretion rate (ordinate) as a function of glucose concentration at two different $PO_2$ values. Straight lines are fitted by eye. Each data point is the mean±standard deviation of 3 to 5 measurements in three cells. Solid line was drawn by eye.

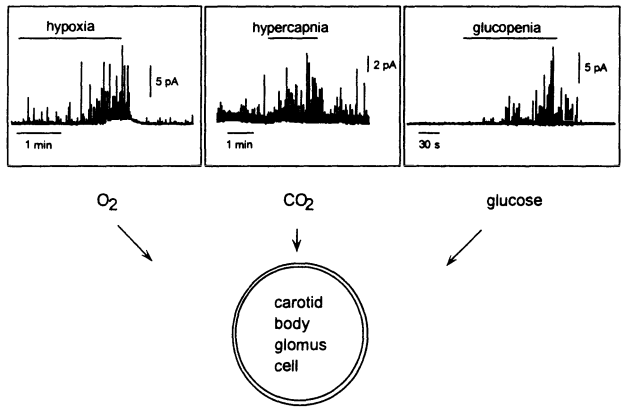


*Figure 3.* Carotid body chemoreceptors glomus cells are multimodal. Representation of responses in a glomus cell to various stimuli, which converge to evoke secretion. Hypoxia ($PO_2$ ~20 mm Hg); Hypercapnia (10% $CO_2$), and glucopenia (0 mM glucose).

## ACKNOWLEDGEMENTS

Research in the authors' laboratory is supported by grants from the Consejería de Salud of the Andalusian Government and the Areces Foundation. M. García-Fernández received a FPU fellowship from the Spanish Ministry of Education. J. López-Barneo received the "Ayuda a la Investigación 2000" of the Juan March Foundation.

## REFERENCES

Alvarez-Buylla, R. and Alvarez-Buylla, E.R. (1988). Carotid sinus receptors participate in glucose homeostasis. *Respir. Physiol.* 72, 347-360.

Alvarez-Buylla, R. and Alvarez-Buylla, E.R. (1994). Changes in blood glucose concentration in the carotid body sinus modify brain glucose retention. *Brain Res.* 654, 167-170.

Amiel, S.A., Tamborlane, W.V., Simonson, D.C. and Sherwin, R.S. (1987). Defective glucose counterregulation after strict glycemic control of insulin-dependent diabetes mellitus. *N. Eng. J. Med.* 316, 1376-1383.

Auer, R.N. (1998). Insulin, blood glucose levels, and ischemic brain damage. *Neurology* Suppl 3, S39-43.

Biggers, D.W., Myers, S.R., Neal, D., Stinson, R., Cooper, N.B., Jaspan, J.B., Williams, P.E., Cherrington, A.D. and Frizzell, R.T. (1989). Role of brain in counterregulation of insulin-induced hypoglycemia in dogs. *Diabetes* 38, 7-16.

Cane, P., Artal, R. and Bergman, R. N. (1986). Putative hypothalamic glucoreceptors play no essential role in the response to moderate hypoglycemia. *Diabetes* 35, 268-277.

Cryer, P.E. (1981). Glucose counterregulation in man. *Diabetes* 30, 261-264.

Donovan, C.M., Halter, J. B. And Bergman, R. N. (1991). Importance of hepatic glucoreceptors in sympathoadrenal response to hypoglycemia. *Diabetes* 40, 155-158.

Donovan, C.M., Hamilton-Wessler, M., Halter, J. B. and Bergman, R. N. (1994). Primacy of liver glucosensors in the sympathetic response to progressive hypoglycemia. *Proc. Natl. Acad. Sci. 'USA* 91, 2863-2867

Dunn-Meynell, A.A., Routh, V.H., Gaspers, L- and Levin, B.E. (2002). Glucokinase is the likely mediator of glucosensing in both glucose-excited and glucose-inhibited central neurons. *Diabetes* 51, 2056-2065.

Gerich, J.E. and Campbell, .PJ. (1988). Overview of counterregulation and its abnormalities in diabetes mellitus and other conditions. *Diabetes Metab Rev.* 4, 93-111.

Hevener, A.L., Bergman, R.N., and Donovan, C.M. (1997). Novel glucosensor for hypoglycemic detection localized to the portal vein. *Diabetes* 46, 1521-1525.

Hevener, A.L., Bergman, R.N. and Donovan, C.M. (2000). Portal vein afferents are critical for the sympathoadrenal response to hypoglycemia. *Diabetes* 49, 8-12.

Hoffman, R.P., Hausberg, M., Sinkey, C.A. and Anderson, E.A. (1999). Hyperglycemia without hyperinsulinemia produces both sympathetic neural activation and vasodilation in normal humans. *J. Diabetes Comp.* 13, 17-22.

Koyama, Y., Coker, R.H., Stone, E.E., Lacy, D.B., Jabbour, K., Williams, E. and Wasserman, D.H. (2000). Evidence that carotid bodies play an important role in glucoregulation in vivo. *Diabetes* 49, 1434-1442.

Koyama, Y., Coker, R.H., Denny, J., Lacy, D.B., Jabbour, K., Williams, E. and Wasserman, D.H. (2001). Role of carotid bodies in the control of the neuroendocrine response to exercise. *Am. J. Physiol. Endocrinol. Metab.* 281, E742-E748.

López-Barneo, J., Pardal, R.. and Ortega-Sáenz, P. (2001). Cellular mechanisms of oxygen sensing. *Annu. Rev. Physiol.* 63, 259-287.

Martín, R.L., Lloyd, H.G. and Cowan, A.I. (1994). The early events of oxygen and glucose deprivation: setting the scene for neuronal death? *Trends Neurosci.* 17, 251-257.

Pardal, R., Ludewig, U., García-Hirschfeld, J. and López-Barneo, J. (2000). Secretory responses of intact glomus cells in thin slices of rat carotid body to hypoxia and tetraethylammonium. *Proc. Natl. Acad. Sci. USA* 97, 2361-2366.

Pardal, R. and López-Barneo, J. (2002). Low glucose-sensing cells in the carotid body. *Nat Neurosci.* 5, 197-198.

Routh, V.H. (2002). Glucose-sensing neurons: Are they physiologically relevant? *Physiol. Behav.* 76, 403-413.

Ureña, J., Fernández-Chacón, R., Benot, A.R., Álvarez de Toledo, G. and López-Barneo, J. (1994). Hypoxia induces voltage-dependent $Ca^{2+}$ entry and quantal dopamine secretion in carotid body glomus cells. *Proc. Natl. Acad. Sci. USA* 91, 10208-1021

Zinker, B.A., Nandaran, K., Wilson, R., Lacy, D. B. and Wasserman, D. H. (1994). Acute adaptation of carbohydrate metabolism to decreased arterial $PO_2$. *Am. J. Physiol.* 266, E921-E929

# Effect of Mitochondrial Inhibitors on Type I Cells

CHRISTOPHER N. WYATT and KEITH J. BUCKLER
*University Laboratory of Physiology, Parks Road, Oxford. OX1 3PT.*

## 1. INTRODUCTION

Inhibitors of mitochondrial function have been known to be stimulants of the carotid body for many decades. Recent experiments have demonstrated that in isolated neonatal rat type I cells both hypoxia and mitochondrial uncouplers inhibit background $K^+$ currents. This leads to membrane depolarisation and voltage gated $Ca^{2+}$ entry (Buckler, 1997; Buckler and Vaughan-Jones, 1998). Since these data are consistent with a role for mitochondria in oxygen sensing, we have determined whether other mitochondrial inhibitors mimic the effects of hypoxia on the type I cells.

## 2. METHODS

Rats aged 10-15 days were anaesthetised with 4% halothane; carotid bodies were removed and the rats decapitated. Type I cells were isolated enzymically as described before (Buckler, 1997). Electrophysiological experiments were conducted using the perforated patch clamp technique at 35°C. Currents were evoked by holding cells at -70 mV then stepping to -100 mV and ramping to -40 mV over a 300 ms period at 0.5 Hz.

For experiments recording intracellular $Ca^{2+}$, cells were loaded with the calcium fluorophore Indo-1AM, 2.5 μM for 30 min at room temperature.
All solutions were made up in bicarbonate buffered tyrode gassed with 95% air / 5% $CO_2$. Hypoxia (approximately 6 Torr) was induced by gassing solutions with 95% $N_2$ / 5% $CO_2$.

*Chemoreception*, Edited by Pequignot et al.
Kluwer Academic/Plenum Publishers, New York, 2003

## 3. RESULTS

The effects of 4 inhibitors of electron transport and one inhibitor of ATP synthase on intracellular calcium $[Ca^{2+}]_i$ levels was investigated. Hypoxia is known to cause a rapid and reversible rise in $[Ca^{2+}]_i$ in type I cells. All five compounds tested; rotenone, myxathiazol, antimycin A, cyanide and oligomycin evoked a rapid rise in $[Ca^{2+}]_i$ and this rise was greatly attenuated by the removal of extracellular $Ca^{2+}$ in a manner similar to that observed with hypoxia. See Fig 1 for an example recording.

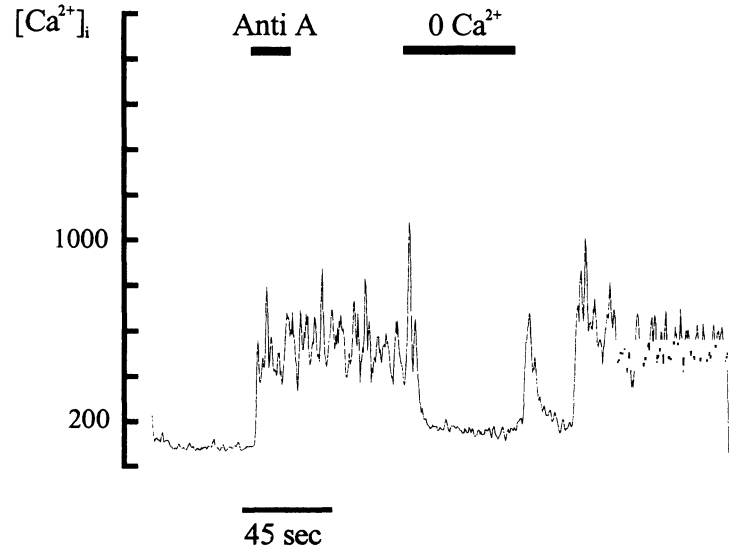


*Figure 1.* The effect of 500nM antimycin A on intracellular calcium in the presence and absence of extracellular calcium

All inhibitors tested significantly reduced membrane conductance: NaCN (2mM) from 359 ± 57 to 136 ± 34 pS (n = 7, mean ± SEM, P< 0.005, paired Student's t test); rotenone (1 μM) from 285 ± 31 to 108 ± 49 pS (n = 8, P< 0.002); myxathiazol (100nM) from 312 ± 43 to 30 ± 62 pS (n = 6, P< 0.01) and oligomycin (2.5 μg $ml^{-1}$) from 324 ± 28 to 105 ± 24 pS (n = 8, P< 0.0001).

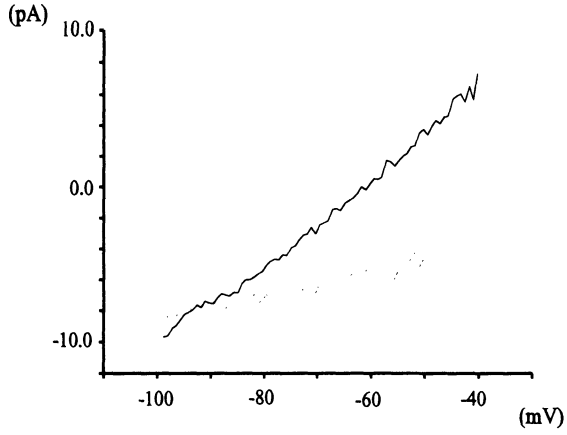


*Figure 2.* The effect of rotenone on membrane currents

Inhibitor sensitive currents were shifted in a positive direction by increasing extracellular $[K^+]$ from 4.5 to 20 mM indicating that they were due, in part to inhibition of a background current.

Under current clamp conditions, both rotenone (1 μM) and cyanide (2mM) depolarised cells from –49.4 ± 2.9 to –26.4 ± 2.6 mV (n = 9, P< 0.0001) and from –59.8 ± 1.8 to –41.7 ± 1.1 mV (n = 10, P< 0.0001) respectively. This resulted in significant rises in $[Ca^{2+}]_i$ which could be significantly attenuated if the cells were voltage clamped at –70 mV.

Interestingly, hypoxia caused no further inhibition to currents exposed to NaCN, rotenone and FCCP at concentrations that completely prevent oxidative phosphorylation.

## 4. CONCLUSION

These data suggest either a common or convergent transduction mechanism for the effects of both hypoxia and mitochondrial inhibitors.

In addition they indicate that mitochondria play a vital role in the oxygen-dependent regulation of background $K^+$ channels in type-1 cells. Whether the mitochondria form a crucial part of the oxygen sensing mechanism or simply act to supply ATP to the sensing mechanism remains to be determined.

## ACKNOWLEDGEMENTS

This work was supported by the MRC.

## REFERENCES

Buckler KJ. 1997, A novel oxygen-sensitive potassium current in rat carotid body type I cells. *J. Physiol.*; 498: 649- 62

Buckler KJ, Vaughan-Jones RD. 1998, Effects of mitochondrial uncouplers on intracellular calcium, pH and membrane potential in rat carotid body type I cells. *J Physiol.* ; 513 (Pt 3): 819-33.

# Ascorbate in the Carotid Body

ANETA DYMECKA[1], MAGDALENA MARCZAK[1], AHLAM RAMADAN[1], PIOTR SUCHOCKI[2], AND MIECZYSŁAW POKORSKI[1]
*[1]Department of Respiratory Research, Medical Research Center, Polish Academy of Sciences, Warsaw and [2]Department of Drug Analysis, Warsaw Medical University, Warsaw, Poland*

## 1. INTRODUCTION

In previous work, we found that ascorbic acid (AA) or ascorbate is present in the carotid body of the cat (Pokorski and Gonet, 1997), the animal that, as opposed to man and other primates, is capable of synthesizing ascorbate (Chatterjee, 1973). The content of ascorbate is decreased in the hypoxic carotid body, which implies the compound might be involved in the chemosensing process, although the determinants of such an involvement remain unraveled.

A drawback of AA is that, as a hydrophilic compound, it cannot penetrate the phospholipid cellular membranes, where signaling pathways reside. A lipid-soluble form of ascorbate, such as ascorbyl-6-palmitate (AP), should overcome this problem, which also could give a better perspective on the role of ascorbate in chemoreception, if only such a form carried ascorbate over into the carotid body. Therefore, in the present study we set out to compare the accumulation of ascorbate in the carotid body tissue, following chronic ingestion of AP or AA by cats. The results presented herein are an expanded version of the carotid body fragment of a study published by us elsewhere (Pokorski *et al,* 2003).

## 2. MATERIALS AND METHODS

The carotid bodies were obtained from adult cats of either sex. The animals

*Chemoreception*, Edited by Pequignot et al.
Kluwer Academic/Plenum Publishers, New York, 2003

were housed at a local animal house and were on a commercial, ascorbate-free diet (Pet Specialties, Inc., Dana Point, CA) before the commencement of the study. AP - 600 mg/kg daily - as a suspension in milk or AA in the equimolar dose, dissolved in milk, each in a 15 ml volume was given by gavage for 6 consecutive days. The carotid bodies were dissected the day after the supplementation had ended from a surgical approach in the neck under α-chloralose and urethane (35 and 800 mg/kg, respectively). Control carotid bodies were dissected from untreated cats. The study was approved by a local Ethics Committee.

The carotid body tissue was subjected to the extraction procedure consisting of homogenization in chloroform:MeOH (2:1, v/v) under ice cooling and protection from light. Tissue samples were analyzed by an HPLC method (Shimadzu assembly, Kyoto, Japan). The mobile phase eluent: MeOH and 0.02 mol/l phosphate buffer (6:5 v/v) was pumped at 1 ml/min through a Supelcosil LC-NH2 25 x 4.6 mm column. The injection volume was 20 µl and the UV detection of peaks was at 255 nm. Calibration peaks produced from AA standards, 10 µg AA/1 ml chloroform:MeOH, were used to calculate the concentration of ascorbate in biological samples.

## 3. RESULTS

Fig. 1 shows an example of the HPLC trace from a carotid body sample, prepared from a control, untreated cat. The ascorbate peak eluted at 6 min and was clearly separable from other peaks, whose exact nature was beyond the scope of this study. The identity of the ascorbate peak was confirmed by coelution of the peaks with the known standard added to the carotid body sample, which enhanced the peak, and by the elution of the standard alone at the same time point (see Fig. 2 for details). From the standard peak (ST), the ascorbate content in the carotid body sample (SA) was quantified. Fig. 2 displays a comparison of this content in the samples obtained from AP-treated (Panel A) and untreated (Panel B) cats. After AP, the ascorbate content amounted to 465 µg/g wet weight of carotid body tissue (peak SA in Panel A), which was a considerable increase over 15 µg/g noted in the untreated cat (peak SA in Panel B).

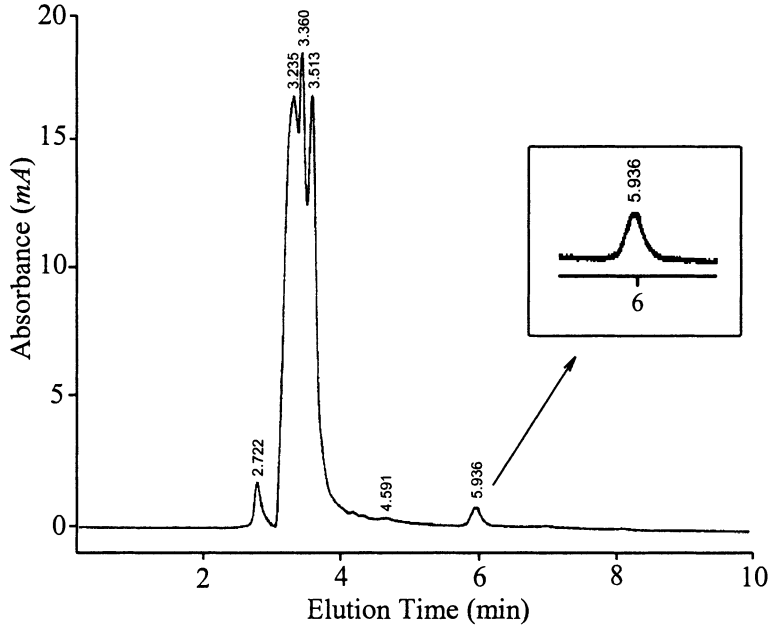


*Figure 1.* HPLC elution profiles in cat carotid body homogenate. The inset shows a 3-fold magnification of the region containing ascorbate, identified and confirmed by applying the relevant standards. Measurement conditions: injection vol. 20 µl, mobile phase: MeOH+0.02 mol/l PB (6:5), column 25x4.6 mm, flow rate 1 ml/min, UV detection at 255 nm.

The latter amount represents the endogenous level of ascorbate in the carotid body. On average, ascorbate content amounted to 6±3 (SE) µg/g in untreated, 58±10µg/g in AA-treated, and 636±146 µg/g in AP-treated carotid body tissues. The ascorbate content was significantly higher in the AP than in the AA group (unpaired t-test) and in either was higher than in the untreated group (one-way Anova) ($P<0.05$).

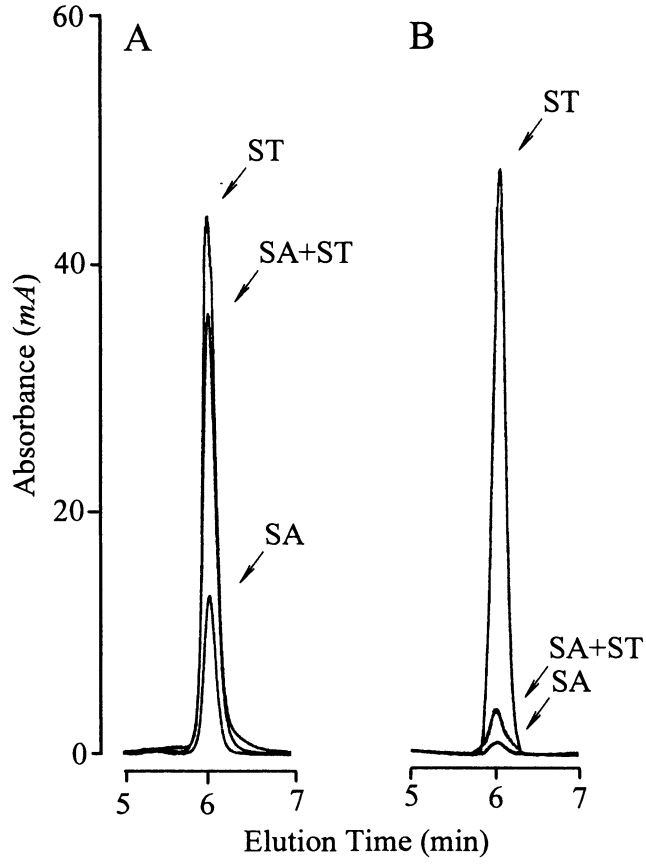


*Figure 2.* Chromatograms of ascorbate in carotid bodies of the ascorbyl palmitate-treated (A) and untreated (B) cats. SA, biological sample; ST, standard; SA+ST, coelution of the peaks with the standard added individually to the carotid body samples. Measurement conditions as in Fig. 1.

## 4. DISCUSSION

This study demonstrates two main points: (i) ascorbate was recovered from the carotid body after ingestion of AP, a lipophilic derivative of ascorbate and (ii) AP boosts the accumulation of ascorbate in the carotid body. AP seems thus the

superior form of ascorbate delivery. The results of this study corroborate our previous findings on ascorbate in the cat carotid body (Pokorski and Gonet, 1997). In that study, the presence of ascorbate in the carotid body was inferred from the electron spin resonance signal that had the characteristics of an in vitro ascorbyl radical. The radical must have originated from ascorbate in vivo. In the present study we quantified, from the chromatographic profiles, the endogenous ascorbate content in the normoxic carotid body. This content was in a range of 0.5-15 μg/g of tissue, not an insubstantial amount compared with other tissues (Horning, 1975).

The role of ascorbate in the carotid body is unclear. Ascorbate delivered by AP is liable to become more efficiently available for the processes taking place in the membrane portions of the cell. This notion is supported by the findings of Ross *et al.* (1999) who showed that AP binds to erythrocyte membranes, where it retains its reducing and antioxidant properties as an intact molecule. Accumulation of ascorbate in the carotid body implies a role, which could go beyond its possible action to protect the plasma membrane integrity, jeopardized by hypoxia. Ascorbate, especially its reducing power, could be operative in the hypoxia-sensing process. Ascorbate has the capability to interact with virtually all putative mechanisms of carotid chemoreception, such as the redox signaling pathway, fatty acid transport across mitochondrial membranes, neurotransmitter synthesis and release, or the expression of HIV-1 factor. The possibility of a functional role is strengthened by the elaboration of ascorbate found in the hypoxic carotid body (Pokorski and Gonet, 1997). The exact nature of the ascorbate role could not be discerned in the present study, as it would require another study design.

We conclude that the uptake ability for ascorbate is greater in the carotid body when it is delivered by the lipophilic AP. Accumulation of ascorbate in the carotid body gives a fuller view of the organ. How exactly ascorbate coalesces into the makings of a hypoxic response remains to be established.

## ACKNOWLEDGMENTS

This study was supported by the statutory budget of the Polish Academy of Sciences Medical Research Center. Results reported herein expand the carotid body part of the studies published by us in *J Biomed Sci 10:193-198; 2003.*

## REFERENCES

Pokorski M, Gonet B. Hypoxia depletes ascorbate in the cat carotid body. *Respir Physiol* 107:213-218; 1997.

Chatterjee IB. Evolution and the biosynthesis of ascorbic acid. *Science* 182:1271-1272, 1973.

Pokorski M, Marczak M, Dymecka A, Suchocki P. Ascorbyl palmitate as a carrier of ascorbate into neural tissue. *J Biomed Sci* 10:193-198; 2003.

Horning D. Distribution of ascorbic acid, metabolites and analogues in man and animals. *Ann NY Acad Sci* 258:103-118; 1975.

Ross D, Mendiratta S, Qu Z, Cobb CE, May JM. Ascorbate 6-palmitate protects human erythrocytes from oxidative damage. *Free Rad Biol Med* 26:81-89; 1999.

# Studies on Glomus Cell Sensitivity to Hypoxia in Carotid Body Slices

PATRICIA ORTEGA-SÁENZ, MARÍA GARCÍA-FERNÁNDEZ, RICARDO PARDAL, ELEUTERIO ALVAREZ#, and JOSÉ LÓPEZ-BARNEO*

*Laboratorio de Investigaciones Biomédicas. Hospital Universitario Virgen del Rocío, Universidad de Sevilla, E-41013, Seville, Spain.*

## 1. INTRODUCTION

Oxygen sensing is a fundamental biological process present in almost all life forms (for reviews see Bunn and Poyton, 1996; López-Barneo et al., 2001). In mammals, the survival in acute hypoxia requires fast respiratory and cardiocirculatory adjustments to ensure sufficient $O_2$ supply to the most critical organs such as the brain or the heart. The main $O_2$ sensor mediating the acute responses to hypoxia is the carotid body (CB), a minute bilateral organ at the bifurcation of the carotid artery innervated by afferent chemosensory fibers. In conditions of hypoxemia, the CBs stimulate the brainstem respiratory centers to evoke hyperventilation. Glomus, or type I, cells are electrically excitable (Duchen et al., 1988, López-Barneo et al., 1988) and constitute the major $O_2$-sensitive elements of the CB (López-Barneo et al., 1988, Delpiano and Hescheler, 1989; Peers 1990; Stea and Nurse, 1991, Buckler, 1997). It is broadly accepted that hypoxia signaling in these cells requires the inhibition of $O_2$-sensitive potassium channels of the plasma membrane, which leads to depolarization, external $Ca^{2+}$ influx, and release of the transmitters that activate

*Chemoreception*, Edited by Pequignot et al.
Kluwer Academic/Plenum Publishers, New York, 2003

the afferent sensory fibers (López- Barneo et al., 1993; Ureña et al., 1994; Buckler and Vaughan-Jones, 1994; Carpenter et al., 2000; Pardal et al., 2000). This basic scheme of chemotransduction has also been proposed to operate in other $O_2$-sensitive neurosecretory systems, such as cells in the lung neuroepithelial bodies (Youngson et al., 1993), chromaffin cells of the adrenal medulla (Thompson and Nurse, 1998), or PC-12 cells (Zhu et al., 1996).

Besides the recent developments in glomus cell physiology, whether the $O_2$ sensitive membrane electrical events are directly involved in the chemosensing process is still debated (for example, see Lahiri et al., 1998). In addition, the molecular nature of the $O_2$ sensor in the CB is unknown. A major challenge to the understanding of CB $O_2$ sensing is the reproducibility of results, as we have repeatedly observed that the $O_2$-sensitivity is a labile characteristic easily disrupted by the enzymatic treatment and/or mechanical dispersion of the cells. We have developed a slice preparation of these organs to study the $O_2$-sensitivity of glomus cells. We have shown that CB slices are amenable for patch-clamp experiments and allow to perform physiological and pharmacological studies at the cellular level in almost optimal conditions. Herein we describe the basic responses of glomus cells in the slices to hypoxia. We also summarize experiments designed to test whether $O_2$-sensitivity of CB cells is altered by inhibition of nitric oxide (NO) synthesis or protein hydroxylation.

## 2. GLOMUS CELL $O_2$-SENSING IN CAROTID BODY SLICES

Carotid body sections of ~150 μm thick were maintained in culture medium at 37°C in a 5% $CO_2$ incubator. For the experiments a slice was transferred to the recording chamber mounted on the stage of an upright microscope, where it was continuously perfused by gravity (flow 1 to 2 ml/min) with a solution containing (in mM) 117 NaCl, 4.5 KCl, 23 $NaHCO_3$, 1 $MgCl_2$, 2.5 $CaCl_2$, 5 Glucose and 5 Sucrose. The entire recording set-up was maintained at a temperature between 34 and 37°C. The control (normoxic) solution was bubbled with a gas mixture of 5% $CO_2$, 20% $O_2$, and 75% $N_2$ ($PO_2$ ~150 mmHg), and the hypoxic solution with 5% $CO_2$, and 95% $N_2$ ($PO_2$ in the chamber ~20 mmHg). After switching from normoxia to hypoxia, complete equilibration of the new solution in the chamber required between 1 and 2 minutes (for details, see Pardal et al., 2000).

As described in dispersed rat cells (Peers, 1990; Wyatt and Peers, 1995; López-López et al., 1997) the amplitude of macroscopic voltage-dependent $K^+$ currents recorded in glomus cells in the slices was reversibly reduced when exposed to low $PO_2$. Typical recordings of $O_2$-sensitive currents as well as the peak current/voltage relationship in the normoxic and hypoxic conditions are shown in Fig. 1A. Note that the effect of hypoxia is preferentially seen with depolarizations between -10 and +30 mV, voltages at which $Ca^{2+}$-dependent $K^+$ channels are maximally activated due to transmembrane $Ca^{2+}$ influx.

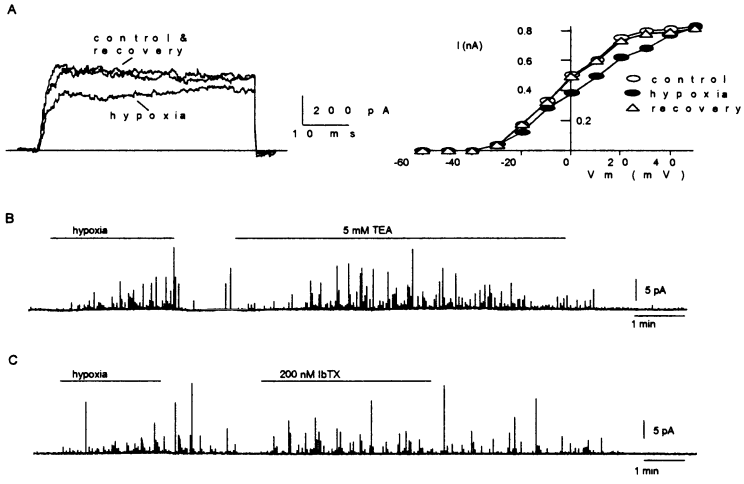


*Figure 1.* Responses of carotid body glomus cells to hypoxia. A. Left. Superimposed macroscopic $K^+$ currents from a glomus cell elicited by depolarizing pulses from –80 mV to the indicated voltage in the three experimental conditions (control, low $PO_2$ and recovery). Note the reversible reduction of the current by hypoxia ($PO_2$ ~20 mmHg). Right. Peak current amplitude-voltage relationship measured in the same cell. The pipette solution contained (in mM): 125 KCl, 4 $MgCl_2$, 4 MgATP, 10 Hepes, 10 EGTA, pH 7.2. B & C. Secretory responses of intact glomus cells to hypoxia and to the $K^+$ channel blockers tetraethylammonium (TEA) and iberiotoxin (IbTX).

We also have characterized the neurosecretory responses to hypoxia and $K^+$ channel blockers of glomus cells in the slices using the amperometric detection of catecholamines (Pardal et al., 2000). Single secretory events were recorded by the application of a polarized 10-μm carbon-fiber electrode near the surface of a

glomus cell. Representative examples of exocytotic responses of glomus cells in the slice to hypoxia are shown in Fig. 1 B and C. Spike-like signals, that resulted from the fusion of single vesicles, were reversibly evoked upon exposure to low $PO_2$. On the average the frequency of secretory events elicited by hypoxia was 49±19 spikes/min (n=24 cells) and the secretory rate 1710±270 femtocoulombs (fC)/min (n=17 cells). Note that blockers of the maxi-K channels, as tetraethylammonium (TEA) and iberiotoxin (IbTX), evoked secretory responses qualitatively similar to those elicited by low $PO_2$.

## 3. INHIBITION OF NO SYNTHESIS AND SENSITIVITY TO HYPOXIA OF GLOMUS CELLS

Nitric oxide (NO) is known to participate in the chemosensory response of the CB to hypoxia (for review, see Prabhakar, 1999). The hypoxic response of the chemoreceptors is modulated by NO presumably produced either by the vascular endothelium or by microganglial neurons located within the CB or along neighboring glossopharyngeal and carotid sinus nerves. NO is produced in the CB during hypoxia and depresses the afferent chemosensory activity (Fung et al., 2001). Conversely, inhibition of NO synthase (NOS) increases the response to hypoxia (Chugh et al., 1994; Wang et al., 1994; Trzebski et al., 1995). Besides its modulatory effect on CB activity, NO has been suggested to play a more general role in $O_2$ sensing since it binds at the heme group of cytochrome C and reduces the affinity of the enzyme for $O_2$ (Brown and Cooper, 1994; Cleeter et al., 1994; Schweitzer and Richter, 1994). It has been proposed that NO produced during hypoxia might act on cytochrome C at mitochondrial complex IV to reduce $O_2$ consumption, thus cells could adjust their metabolic rate (and possibly other functions) to the availability of $O_2$ (Clementi et al., 1999).

Based on these precedents we tested to see whether inhibition of NO synthesis in CB slices alters the sensitivity to hypoxia of glomus cells. These experiments were done on slices incubated with L-$N^G$-nitroarginine-methylester (L-NAME) a potent inhibitor of NOS that at 500 μM completely abolishes NO production in the CB (Fung et al., 2001) and other tissues (Clementi et al., 1999). An experiment was also done with the NOS inhibitor Nω-nitro-L-arginine (L-NNA) (500 μM) with similar results. Fig. 2A illustrates the secretory response to hypoxia of a cell that had been incubated with L-NAME for 40 min prior the experiment. Cells treated with L-NAME responded normally to depolarization

with high external $K^+$ and generated a secretory burst in response to hypoxia (1332±688 fC/min, n=4) similar to that observed in normal cells (see above). Fig. 2B illustrates with another experiment the response of glomus cells to the acute (10 min) exposure to L-NAME. In most cases, the NOS antagonist induced by itself some secretory activity but it did not prevent a further increase in secretion during exposure to hypoxia. These results indicate that inhibition of NO synthesis does not alter the sensitivity to hypoxia of glomus cells. Therefore, the interaction of NO and cytochrome C, proposed to be a form of $O_2$ sensing in some cells (Clementi et al., 1999), does not seem to be a fundamental $O_2$-sensitive mechanism involved in CB chemotransduction. Our observations are, however, in fair agreement with the potentiation of the response to hypoxia by L-NAME described in whole CB preparations and therefore compatible with a modulatory role of NO on the chemosensory response of CB cells to hypoxia (Chugh et al., 1994; Wang et al., 1994; Trzebski et al., 1995; Prabhakar, 1999).

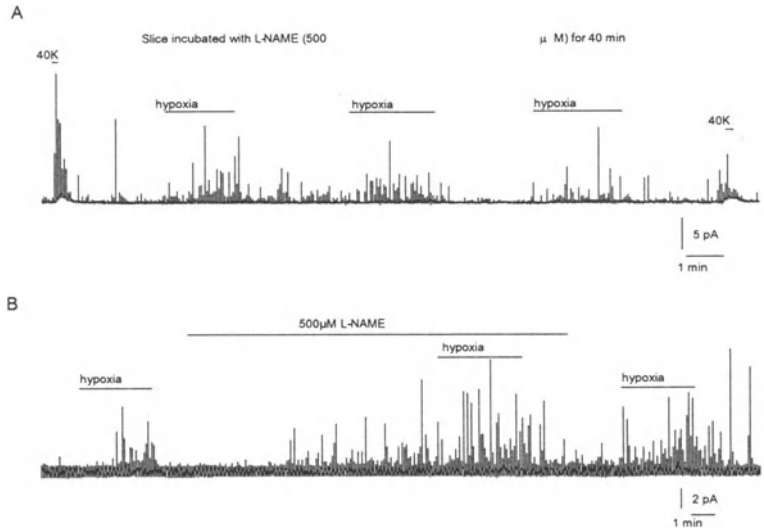


*Figure 2*. Effect of inhibition of NO synthesis on the sensitivity of glomus cells to low $PO_2$. A. The secretion of catecholamines is monitored by amperometry in a slice exposed to L-NAME for 40 min before the experiment. B. Acute effect of incubation with L-NAME, which did not prevent the response to hypoxia of the cell. Secretion rate in L NAME (605 fC/min) increased to 2268 fC/min on exposure to low $PO_2$.

## 4. INHIBITION OF PROTEIN HYDROXYLATION AND SENSITIVITY TO HYPOXIA OF GLOMUS CELLS

Besides the acute cardiocirculatory reflexes to hypoxia mediated by the CB and other organs, there are chronic responses to hypoxia which depend on the expression of a wide repertoire of oxygen-sensitive genes with roles in diverse cellular functions such as angiogenesis, red blood cell production, glucose and energy metabolism, apoptosis and cell proliferation (Bunn and Poyton, 1996; Lopez-Barneo et al., 2001; Semenza, 2001). The chronic cellular responses to hypoxia, studied in great detail in the past few years, are mediated by ubiquitously expressed hypoxia-inducible transcription factors (HIFα) (Semenza, 2001). Stabilization and transcriptional activity of HIFα depend on oxygen-dependent prolyl and asparaginyl hydroxylases. In the absence of $O_2$, the lack of critical OH groups in specific amino acids of the HIFα molecule facilitates its transcriptional activity and prevents its degradation by the proteasome (Jaakola et al., 2001; Ivan et al., 2001; Lando et al., 2002). Heterozygous HIF1-α knock out mice have alterations in the acute responses of CB to hypoxia (Kline et al., 2002), thus we designed experiments to test whether inhibition of HIF hydroxylation alters the sensitivity of glomus cells to low $PO_2$. We used for the experiments the drug dimethyloxalylglycine (DMOG), a membrane permeant competitive inhibitor of oxoglutarate, the substrate of the hydroxylases, that completely inhibits protein hydroxylation and induces gene expression in normoxia (Jaakola et al., 2001). Fig. 3 illustrates a representative experiment performed on slices exposed to 1 mM DMOG for 90 min (60 min in the culture medium at 37 °C and 30 additional min in the recording chamber). DMOG elicited by itself a small secretory activity but did not prevent the exocytotic response of the cell to hypoxia. In cells treated with DMOG, low $PO_2$ induced secretion rates between 1500 and 2500 fC/min, values within the same range of those measured in the absence of DMOG (see above). These data suggest that protein hydroxylation does not participate in the acute response to hypoxia of glomus cells.

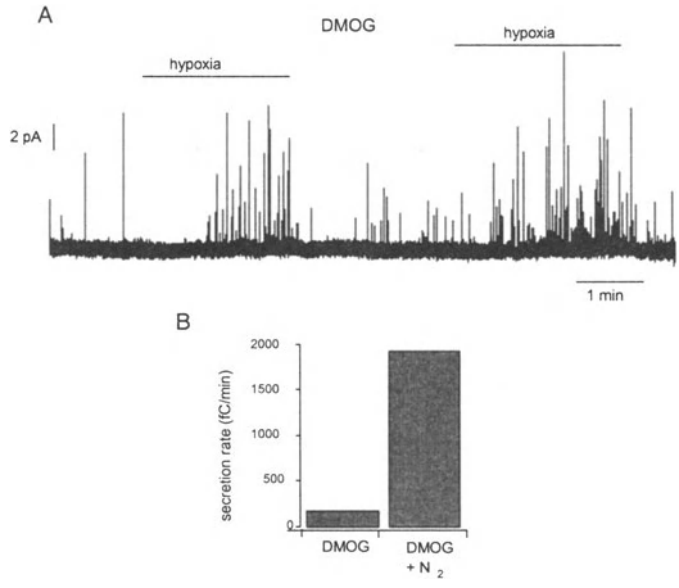


*Figure 3.* Inhibition of protein hydroxylation and sensitivity of glomus cells to hypoxia. A. Secretory response to hypoxia of a cell bathed in a solution with 1 mM dimethyloxalylglycine (DMOG). Prior the experiment, the slice had been incubated for 90 min in a solution with 1 mM DMOG. B. Average secretion rate (in femtocoulombs/min, measured during the last minute before switching to the new solution) of the two exposures to hypoxia shown in the figure.

## ACKNOWLEDGEMENTS

Research in the authors' laboratory is supported by grants from the Consejería de Salud of the Andalusian Government and the Areces Foundation. J. López-Barneo received the "Ayuda a la Investigación 2000" of the Juan March Foundation.

## REFERENCES

Brown G.D. and Cooper, C.E. (1994). Nanomolar concentrations of nitric oxide reversibly inhibit synaptosomal respiration by competing with oxygen and cytochrome oxidase *FEBS Lett.* 356, 295-298.

Buckler, K.J. (1997). A novel oxygen-sensitive potassium current in rat carotid body type I cells. *J. Physiol,* 498, 649-662.

Buckler, K.J. and Vaughan-Jones, R.D. (1994). Effects of hypoxia on membrane potential and intracellular calcium in rat neonatal carotid body type I cells. *J. Physiol.* 476, 423-428.

Bunn, H.F. and Poyton, R.O. (1996). Oxygen sensing and molecular adaptations to hypoxia. *Physiol. Rev.* 76, 839-885.

Carpenter, E., Hatton, C.J. and Peers, C. (2000). Effects of hypoxia and dithionite on catecholamine release from isolated type I cells of the rat carotid body. *J. Physiol.* 523, 719-729.

Chugh, D.K., Katayama, M., Mokashi, A., Bebout, D.E., Ray, D.K. and Lahiri, S. (1994). Nitric oxide-related inhibition of carotid chemosensory nerve activity in the cat. *Respir. Physiol.* 97, 147-156.

Cleeter, M.W., Cooper, J.M., Darley-Usmar, V.M., Moncada, S. and Schapira, A.H. (1994). Reversible inhibition of cytochrome c oxidase, the terminal enzyme of the mitochondrial respiratory chain, by nitric oxide. Implications for neurodegenerative diseases. *FEBS Lett.* 345, 50-54.

Clementi, E., Brown, G.C., Foxwell, N. and Moncada, S. (1999). On the mechanism by which vascular endothelial cells regulate their oxygen consumption. *Proc. Natl. Acad. Sci. USA* 96, 1559-1562.

Delpiano, M.A. and Hescheler, J. (1989). Evidence for a $PO_2$-sensitive $K^+$ channel in the type-I cell of the rabbit carotid body. *FEBS Lett.* 249, 195-198.

Duchen, M.R., Caddy, K.W.T., Kirby, G.C., Patterson, D.L., Ponte, J. and Biscoe, T.J. (1988). Biophysical studies of the cellular elements of the rabbit carotid body. *Neurosci.* 26, 291-311.

Fung, M.L., Ye, J.S. and Fung. P.C.W. (2001). Acute hypoxia elevates nitric oxide generation in rat carotid body in vitro. *Pflügers Arch. Eur. J. Physiol.* 442, 903-909.

Ivan, M., Kondo, K., Yang, H., Kim, W., Valiando, J., Ohh, M., Salic, A., Asara, J.M., Lane, W.S. and Kaelin, W.G. (2001). HIFalpha targeted for VHL-mediated destruction by proline hydroxylation: implications for $O_2$ sensing. *Science* 292, 464-468

Jaakola, P., Mole, D.R., Tian, Y-M., Wilson, M.I., Gielbert, J., Gaskell, S.J., Von Kriegsheim, A., Hebestreit, H.F., Mukherji, M., Schofield, C.J., Maxwell, P.H., Pugh, C.W. and Ratcliffe, P. (2001) Targeting of HIF- to the von Hippel-Lindau ubiquitylation complex by $O_2$-regulated prolyl hydroxylation *Science* 292, 468-472.

Kline, D.D., Peng, Y.J., Manalo, D.J., Semenza, G.L., Prabhakar, N.R.. (2002). Defective carotid body function and impaired ventilatory responses to chronic hypoxia in mice partially deficient for hypoxia- inducible factor 1 alpha. *Proc. Natl. Acad. Sci. USA*. 99, 821-826.

Lahiri, S., Roy, A., Rozanov, C., Mokashi, A. (1998). $K^+$-current modulated by $PO_2$ in type I cells in rat carotid body is not a chemosensor. *Brain Res.* 794, 162-165.

Lando, D., Peet, D.J., Whelan, D.A., Gorman, J.J. and Whitelaw, M.L. (2002) Asparragine hydroxilation of the HIF transactivation domain: a hypoxic swith *Science* 295, 858-861

López-Barneo, J., López-López, J.R., Ureña, J., González, C. (1988). Chemotransduction in the carotid body: $K^+$ current modulated by $PO_2$ in type I chemoreceptor cells. *Science 242, 580-582.*

López-Barneo, J., Benot, A.R., Ureña, J. (1993). Oxygen sensing and the electrophysiology of arterial chemoreceptor cells. *News Physiol. Sci.* 8, 191-195.

López-Barneo, J., Pardal, R., Ortega-Sáenz, P. (2001). Cellular mechanisms of oxygen sensing. *Annu. Rev. Physiol.* 63, 259-287.

López-López, J.R., González, C., Pérez-García, M.T. (1997). Properties of ionic currents from isolated adult rat carotid body chemoreceptor cells: effect of hypoxia. *J. Physiol.*. 499, 429-441.

Pardal, R., Ludewig, U., García-Hirschfeld, J., López-Barneo, J. (2000). Secretory responses of intact glomus cells in thin slices of rat carotid body to hypoxia and tetraethylammonium. *Proc. Natl. Acad. Sci. USA* 97, 2361-2366.

Peers, C. (1990). Hypoxic suppression of $K^+$ currents in type I carotid body cells: selective effect on the $Ca^{2+}$-activated $K^+$ current. *Neurosci. Lett.* 119, 253-256.

Prabhakar, N.R. (1999). NO and CO as second messengers in oxygen sensing in the carotid body. *Respir. Physiol.* 115, 161-168.

Semenza, G.L. (2001) HIF-1 and mechanisms of hypoxia sensing. *Curr. Opin. Cell Biol.* 13, 167-171

Schweitzer, M. and Richter, C. (1994). Nitric oxide potently and reversibly deenergizes mitochondria at low oxygen tension. *Biochem. Biophys. Res. Commun.* 204, 169-175.

Stea, A., Nurse, C.A. (1991). Whole-cell and perforated-patch recordings from $O_2$-sensitive rat carotid body cells grown in short- and long-term culture. *Pflügers Arch. Eur. J. Physiol.* 418, 93-101. Thompson, R.J., Nurse, C.A. (1998). Anoxia differentially modulates multiple $K^+$ currents and depolarizes neonatal rat adrenal chromaffin cells. *J. Physiol.* 512, 421-434.

Trzebski, A., Sato, Y., Suzuki, A. and Sato, A. (1995). Inhibition of nitric oxide synthesis potentiates the responsiveness of carotid chemoreceptors to systemic hypoxia in the rat. *Neurosci. Lett.* 190, 29-32.

Ureña, J., Fernández-Chacón, R., Benot, A.R., Álvarez de Toledo, G., López-Barneo, J. (1994). Hypoxia induces voltage-dependent $Ca^{2+}$ entry and quantal dopamine secretion in carotid body glomus cells. *Proc. Natl. Acad. Sci. USA* 91, 10208-10211.

Wang, Z.Z., Stensaas, L.J., Bredt, D.S., Dinger, B. and Fidone, S.J. (1994). Localization and actions of nitric oxide in the cat carotid body. *Neurosci.* 60, 275-286.

Wyatt, C.N., Peers, C. (1995). $Ca^{+2}$-activated $K^+$ channels in isolated type I cells of the neonatal rat carotid body. *J. Physiol.* 483, 559-565.

Youngson, C., Nurse, C., Yeger, H., Cutz, E. (1993. Oxygen sensing in airway chemoreceptors. *Nature* 365, 153-155.

Zhu, W.H., Conforti, L., Czyzyk-Krzeska, M.F., Millhorn, D.E. (1996). Membrane depolarization in PC-12 cells during hypoxia is regulated by an $O_2$-sensitive $K^+$ current. *Am. J. Physiol.* 271, C658-C665.

# An Unusual Cytochrome $a_{592}$ with Low $PO_2$ Affinity correlates with Afferent Discharge in the Carotid Body

CHRISTINE HUCKSTORF*, TINO STRELLER* and HELMUT ACKER#
*Institute of Physiology, University of Rostock, Gertrudenstr. 9, D-18057Rostock, Germany; #Max-Planck-Institute of Molecular Physiology, Otto-Hahn-Str. 11, D-44227 Dortmund, Germany

## 1. INTRODUCTION

The carotid body (CB) located at the carotid artery bifurcation informs the central nervous system about arterial $pO_2$ changes. The CB response to hypoxic stimuli includes augmented transmitter release and increased generation of action potentials in the carotid sinus nerve (CSN). Until now the molecular and cellular mechanisms of the oxygen sensing signal cascade are not clear. Cellular oxygen sensing processes are believed to be initiated by specialised cytochromes (Bunn and Poyton, 1996; Lopez-Barneo *et al.*, 2001). In recent studies (Lahiri and Acker, 1999; Lahiri *et. al*, 1999) simultaneous recordings of rat CB light absorption spectra and chemoreceptor discharge were used to characterize heme proteins as primary oxygen sensor. Redox spectra were deconvoluted by means of redox differential spectra of isolated non mitochondrial cytochrome $b_{558}$ and mitochondrial cytochromes $c_{550}$, $b_{563}$ and the cytochrome c oxydase (CCO) peaking at 603 nm. Mathematically deconvolution fitted very closely to experimental spectra in the wavelength range between 520 and 570 nm confirming the contribution of cytochromes $b_{558}$, $c_{550}$ and $b_{563}$ in the carotid body tissue. However, the wavelength range between 570 and 620 nm normally dominated by cytochrome aa3 of the CCO (absorbance peak at 603 nm) was fitted only partly indicating an additional component.

*Chemoreception*, Edited by Pequignot et al.
Kluwer Academic/Plenum Publishers, New York, 2003

The aim of the present study was to characterize this additional cytochrome contributing to the hypoxia induced absorption spectra of the rat carotid body. By experimental and mathematical deconvolution of light absorption spectra we could identify a cytochrome a peaking at 592 nm suggesting the CB CCO to be very specialized concerning the electron pathway within complex IV.

## 2. METHODS AND RESULTS

### 2.1 *In vitro* Carotid Body

Carotid bodies including the carotid sinus nerve were removed, dissected free of connecting tissue and rinsed with saline in order to free the organ of red cells as described previously (Lahiri *et al.*, 1999). CB were placed in a superfusion chamber on an opaque bench containing small holes of diameters similar to that of the organs. It was superfused with isotonic salt solution (in mM: NaCl 128, KCL 5.6 glucose 27.5, Hepes 7, $NaHCO_3$ 10, $CaCl_2$ 2.1) equilibrated with different $O_2/N_2/CO_2$ mixtures to adjust oxygen tensions to various levels, or with CO or with different cyanide ($CN^-$) concentrations at pH about 7.4. Saline flowed through the chamber at 60 ml/min. Temperature was maintained at 36°C. In some cases, the right and left cervical and nodose ganglia were also removed from the animals, serving as control tissue.

### 2.2 Light absorption spectra

Superfusion chamber was mounted on the stage of a light microscope (Olympus). White light from a halogen bulb (12 V, 100 W) passing through an objective (40x) transilluminated the CB for 10 s every minute. Absorption changes at different wavelength occurring when light is passing CB tissue were recorded by a photodiode-array spectrometer (MCS 210, Zeiss, Köln, FRG) connected to the third ocular of a trinocular head of the microscope via a light guide. Difference spectra were obtained by subtracting the first recorded so-called reference spectrum in the superfusion medium equilibrated with 28.8 % $O_2$, 4 % $CO_2$ and 67.2 % $N_2$ (aerobic steady state) from those obtained under reducing conditions, produced by equilibrating saline with different concentrations of $N_2$, $O_2$, CO or cyanide (CN) at constant $CO_2$ (4 %). The recorded difference spectra could be described mathematically within a wavelength range of 510 – 630 nm by means of the redox spectra of isolated mitochondrial cytochromes $c_{550}$, $b_{563}$ and CCO

cytochrome $a3_{603}$ as well as non mitochondrial cytochrome $b_{558}$ (Lahiri *et al.*, 1999). For deconvolution of CB spectra a fifth component was required. This component was detected in CB tissue by forming the difference spectrum hypoxia ($PO_2$ = 60 mmHg) minus $CN^-$ (100 µM) versus aerobic steady state ($PO_2$ = 200 mmHg) as described to isolate photometrically cytochrome a of CCO with an absorption peak at 605 nm (Liao and Palmer, 1996) and called cytochrome $a_{592}$ concerning its absorbance peak at 592 nm. The difference spectra of the 5 cytochromes were normalized (peak maximum = 1.0) and than varied in size until their sum resulted in a superposition curve that fits as good as possible to the experimental curve. Their sizes reflect the contribution of each cytochrome to the whole spectrum. These contributions, when given as percent of their sum (so called relative spectral weights), allow to compare different spectra concerning the reduction state of cytochromes.

CB were exposed to a 5 min period of $PO_2$ = 100 mmHg (n = 5), 80 mmHg (n = 7), 60 mmHg (n = 8), respectively or to anoxia (n = 4) produced by adding sodium dithionite (100 mM) to the saline ($PO_2$ = 0 mmHg). Spectral analysis was performed on spectra recorded after three min hypoxia. Within the wavelength range of 530 – 630 nm, spectra are composed of two broad absorption peaks. Spectral deconvolution between 510 and 570 nm revealed high contribution of cytochrome $c_{550}$ and $b_{563}$, and a lower but significant contribution of cytochrome $b_{558}$. Between 570 and 630 nm a high contribution of cytochrome $a3_{603}$ and a lower but significant contribution of cytochrome $a_{592}$ was detectable. However, unlike the other cytochromes which relative spectral weights behaved rather independent on hypoxic level, the relative spectral weight of cytochrome $a_{592}$ decreased significantly from 15.4 % at the lowest hypoxic level of $PO_2$ = 100 mmHg to 9.7 % at 80 mmHg and 7.6 % at 60 mmHg (Fig. 1). Under anoxia the contribution of cytochrome $a_{592}$ was nearly undetectable.

CB were exposed for 3 min to saline superfusion with different cyanide concentrations of 10 - 100 µM. Spectral analysis was performed on the second and third recorded spectrum. Similar to hypoxia cytochrome $a_{592}$ was necessary for an optimal deconvolution of spectra recorded at lower $CN^-$ concentrations. The relative spectral weight of cytochrome $a_{592}$ decreased significantly from 7.8 % at 10 µM $CN^-$ to 0.4 % at 100 µM. The relative spectral weights of the other 4 cytochromes did not show any significant dependence on $CN^-$ levels.

Comparative light absorption measurements were carried out on cervical and nodose ganglia (n = 8). Similar to CB tissue light absorption spectra of ganglion tissue showed two distinct peaks during exposure to 3 min hypoxia ($PO_2$ = 80 mmHg). One peak in the wavelength range between 520 and 570 nm could be fitted by cytochromes $c_{550}$, $b_{558}$ and $b_{563}$, the other peak in the

wavelength range between 570 and 620 nm was found to be identical with cytochrome $a3_{603}$. Exposure to $CN^-$ (100 µM) evoked stable absorption spectra mainly composed of cytochromes $a3_{603}$ and $c_{550}$ (Table 1)

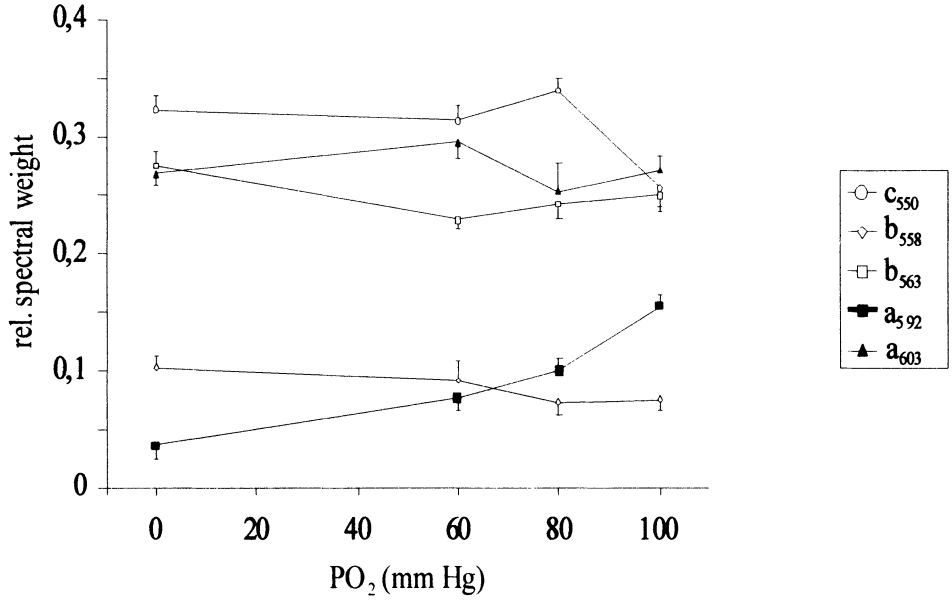


*Figure 1.*, Relationship between different $PO_2$ values in the superfusion medium and spectral weight factors (%) of the different cytochromes to fit experimental light absorption spectra. Cytochrome $a_{592}$ only (thick solid lines) shows a nonlinear dependence with increasing reducing conditions while the spectral weight factor of the other cytochromes is constant with increasing reduction: $c_{550}$ (dashed lines), $b_{558}$ (thin solid lines), $b_{563}$ (dotted lines) and $a_{603}$ (dashed-dotted lines).

*Table 1.* Relative spectral weights of the cytochromes during several stimulation types of carotid body (CB) and ganglion (cervical or nodose) tissue (GG). n.d.= not detectable.

| Stimulation | Cytochromes (rel. spectral weight + standard dev. in % ) | | | | |
|---|---|---|---|---|---|
| | $c_{550}$ | $b_{558}$ | $b_{563}$ | $a_{592}$ | $a3_{603}$ |
| CB hypoxia (80 mm Hg) | 33.8 ± 2.5 | 7.2 ± 3.0 | 24.0 ± 3.3 | 9.8 ± 2.9 | 25.1 ± 6.5 |
| CB CN (100 µM) | 55.0 ± 5.4 | 4.7 ± 2.9 | 7.4 ± 1.6 | 0.4 ± 0.9 | 32.3 ± 3.8 |
| GG hypoxia (80 mm Hg) | 35.4 ± 5.2 | 6.6 ± 3.3 | 19.4 ± 3.7 | n.d. | 36.7 ± 3.1 |
| GG CN (100 µM) | 52.3 ± 2.9 | 1.1 ± 0.9 | 5.7 ± 2.5 | n.d. | 39.6 ± 2.5 |

## 2.3 Chemoreceptor nervous discharge

Simultaneously to spectral recordings of CB tissue chemoreceptor afferent discharge from the whole carotid sinus nerve was recorded with a suction glass microelectrode (Lahiri *et al.*, 1999). The recorded signal was amplified and passed by a band filter (10 Hz – 3 kHz). Subsequently discharge peaks were extracted using a window discriminator (WPI, Berlin, FRG) and counted every second providing time series of counting rates during a stimulation period considered as afferent chemoreceptor discharge signal. Stimulation of CB tissue by hypoxia, CO or $CN^-$ induced an increase in afferent chemoreceptor discharge signal which time course was characterized by a first transient phasic component changing into a rather stable and constant tonic component. Therefore, afferent signals were median filtered and mathematically deconvoluted into a phasic (rapidly adapting) and a tonic (slowly adapting) weight (Streller *et al.*, 2002). The tonic weight of the reaction was quantified as the relative contribution of the tonic component to the whole signal, resulting in a tonic weight of 100 % for exclusive tonic afferent signal and 0 % for exclusive phasic ones.

The time course of CSN afferent signal was analysed for 5 min periods of $PO_2$ = 100 mmHg (n = 8), 80 mmHg (n = 7), 60 mmHg (n = 6) and for anoxia (n = 4). The phasic component of nerve reaction dominated the more the stronger the level of hypoxia was, whereas the contribution of the tonic component to chemoreceptor discharge decreased significantly ($p < 0.01$) from 77.0 % at 100 mmHg via 48.8 % at 80 mmHg to 34.6 % at 60 mmHg. Under anoxia ($PO_2$ = 0 mmHg) CSN activity showed a transient phasic component with subsequent complete suppression resulting in a tonic component of 0 %. Figure 2 represents the relation of tonic weight of the afferent nerve discharge signal to spectral weight of the cytochrome $a_{592}$ in dependence on $PO_2$ level correlating with high significance ($p < 0.01$).

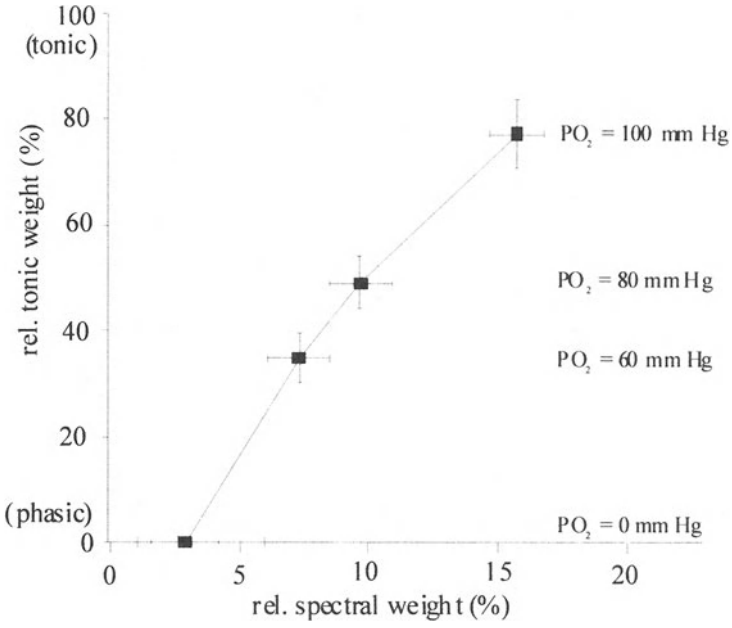


*Figure 2.* Tonic weight of chemoreceptor discharge signal versus spectral weight of cytochrome $a_{592}$ at different levels of hypoxia in the medium superfusing CB.

The time course of CSN afferent signal was analysed for increasing cyanide concentrations of 10 - 100 µM. The reaction was dominated by the tonic component at lower $CN^-$ concentrations and by the phasic component at higher concentrations being expressed in significant decrease in tonic weight ($p < 0.01$) with increasing $CN^-$ concentrations from 88.3 % at 10 µM to 7.0 % at 100 µM $CN^-$.

Stimulation of CB by CO (PCO = 500 mmHg) under normoxia ($PO_2$ = 200 mmHg) evoked tonic chemoreceptor discharge that is inhibited while CB tissue was transilluminated (Fig. 3) due to light induced photolytic release of CO from cytochrome a3 binding. Furthermore, figure 3 shows that the photolytic effect on CO stimulated CSN discharge is inhibited or even reversed at a $PO_2$ of 60 mmHg (n = 6) as well as at 30 µM $CN^-$ (n = 4) in the superfusion medium and time course is more phasic.

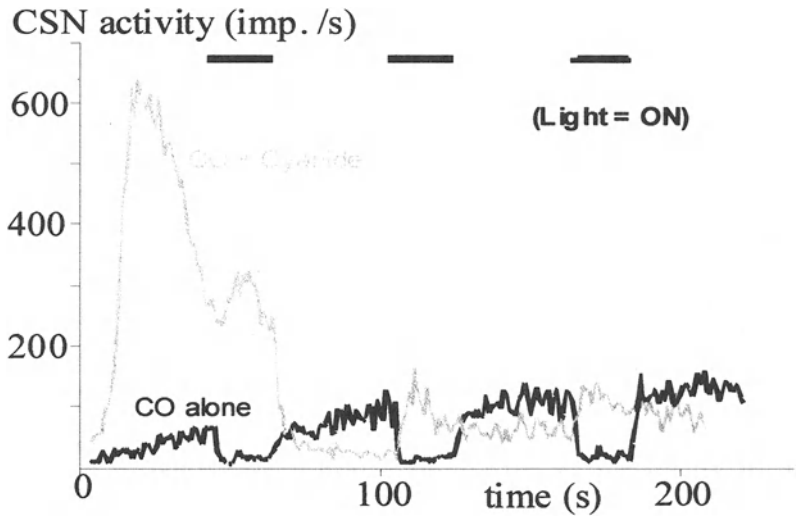


*Figure 3.* Photolysis of chemoreceptor discharge during CB exposure to CO (PCO = 500 mmHg) under normoxia (black curve) and inhibited photolysis during additional exposure (A) to hypoxia (PO2 = 60 mm Hg, grey curve). The black bars on top depict phases of CB transillumination with bright light.

## 3. DISCUSSION

This study describes the relationship between cytochrome redox state as measured by light absorption spectra and carotid body chemoreceptor discharge under different levels of $O_2$, $CN^-$ and CO. The spectra achieved were composed of mitochondrial cytochromes $c_{550}$, $b_{563}$, $a_{592}$, $a3_{603}$ and non mitochondrial cytochrome $b_{558}$. The change in optical density of difference spectra is mainly related to the changed redox state of cytochromes as compared to the control state. Consequently, spectral weights of cytochromes with low control reduction state increase approximately proportional to increasing reducing conditions leading to constant spectral weight values. Spectral weight of a cytochrome being already reduced at control will diminish in proportion to the other cytochromes at increasing reducing conditions. Among the five cytochrome components which are necessary for deconvolution of CB spectra only the cytochrome $a_{592}$ correlates with decreasing $PO_2$ and increasing $CN^-$ concentrations by diminishing its spectral weight. Furthermore, there is correlation between cytochrome $a_{592}$ and tonic afferent discharge in response to binding of CCO ligands $O_2$, $CN^-$ and CO. The results suggest cytochrome $a_{592}$ as particular

sensitive to changes at higher $PO_2$ range and lower $CN^-$ concentrations and as a part of CCO.

When assuming cytochrome $a_{592}$ as the cyanide insensitive cytochrome a component of CB CCO the absorption maximum is shifted from normally 605 nm (Liao and Palmer, 1996) to 592 nm. A similar shift for cytochrome a is described in *Paracoccus denitrificans* as a result of a single amino acid mutation (Kannt *et al.*, 1999) causing a drastically lowered mid point potential. This unusual low mid point potential suggests that cytochrome $a_{592}$ does not participate in the main electron transfer within CCO (Fig. 4). At the basis of the results obtained by chemosensor stimulations with the cytochrome $a3_{603}$ ligands CO and $CN^-$, it seems conceivable that there is a parallel electron pathway from cytochrome $a_{592}$ which is changed already at mild hypoxia, leading to changes in mitochondrial membrane potential (MTP), calcium release and subsequent afferent discharge.

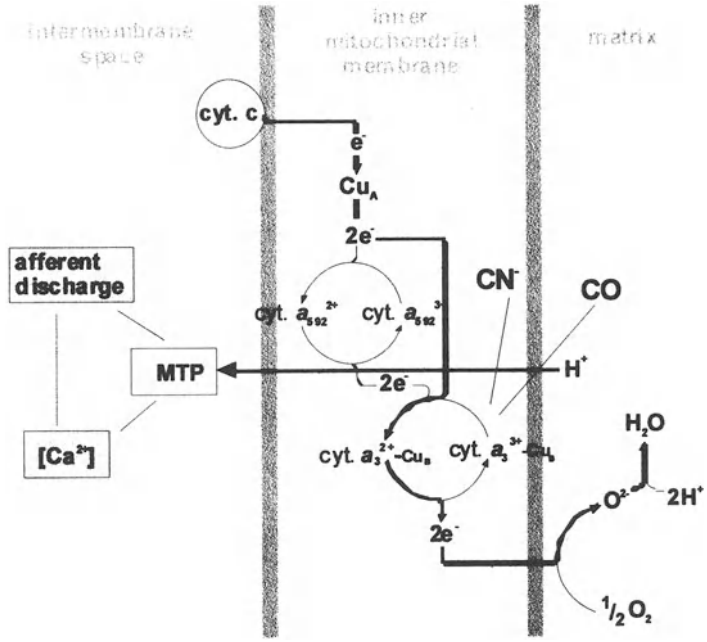


*Figure 4.* CCO cytochrome model of CB oxygen sensing: In parallel to the main pathway of electrons from cytochrome c via CuA to the binuclear center a3-CuB, there is a secondary pathway via a592. This pathway is, in contrast to the main pathway, sensitive to weak hypoxia, and coupled to transmembrane proton pumping and in generation of the transfer potential (MTP). Due to electron bypassing cytochrome $a_{592}$ dominating with an apparent low $PO_2$ and $CN^-$ affinity triggers MTP changes and hence intracellular calcium levels in a nonlinear fashion.

## 4. CONCLUSION

Dominance of direct electron transfer from $Cu_A$ to cytochrome a3-$Cu_B$ bypassing cytochrome a might suggest cytochrome $a_{592}$ as a cytochrome with an apparent low $PO_2$ affinity. The results support the hypothesis of a cytochrome $a_{592}$, which is unique in the carotid body and, as part of the mitochondrial CCO, is involved in triggering the afferent chemosensor discharge.

## REFERENCES

Bunn, H.F., and Poyton, R.O., 1996, Oxygen sensing and molecular adaptation to hypoxia., *Physiol. Rev.* 76: 839-885

Lopez-Barneo, J., Pardal, R., and Ortega-Saenz, P., 2001, Cellular mechanism of oxygen sensing. , *Ann. Rev. Physiol.* 63: 259-287

Lahiri, S., and Acker, H., 1999, Redox-dependent binding of CO to heme protein controls P(O2)-sensitive chemoreceptor discharge of the rat carotid body. *Respir. Physiol.* 115: 169-177

Lahiri, S., Ehleben, W., and Acker, H., 1999, Chemoreceptor discharges and cytochrome redox changes of the rat carotid body: role of heme ligands *PNAS* 96: 9427-9432

Streller, T., Huckstorf, C., Pfeiffer, C., and Acker, H. 2002, Unusual cytochrome a592 with low PO2 affinity correlates as putative oxygen sensor with rat carotid body chemoreceptor discharge, *FASEB J* 16: 1277-1279

# A Reevaluation of the Mechanisms Involved in the Secretion of Catecholamine Evoked by 2,4-Dinitro-Phenol from Chemoreceptor Cells of the Rabbit Carotid Body

ROCHER A., GEIJO E.*, CACERES AI., GONZALEZ CONSTANCIO,and ALMARAZ L.*

*Instituto de Biología y Genética Molecular, Departamento de Bioquímica y Biología Molecular y Fisiología, Facultad de Medicina. Universidad de Valladolid/CSIC. *Instituto de Neurociencias, Departamento de Fisiología, Facultad de Medicina. Universidad de Elche/ CSIC.*

## 1. INTRODUCTION

Dinitrophenol (2,4 dinitrophenol; DNP) was early identified as a potent stimulant of the carotid body (CB; Shen and Hauss, 1939). DNP acts directly upon chemoreceptor cells promoting an increase in the intracellular calcium concentration and the release of catecholamine (CA); both responses are strongly dependent on the presence of $Ca^{2+}$ and $Na^{+}$ in the extracellular media (Obeso *et al.*, 1989; Rocher *et al.*, 1991; Buckler and Vaughan-Jones, 1998). The uncoupling effects of DNP have also been studied in chemoreceptor cells: DNP produces an activation of glucose consumption and a decrease in the mitochondrial membrane potential (Obeso *et al.*, 1989; Buckler and Vaughan-Jones, 1998). Mitochondrial uncouplers such as DNP, carbonyl cyanide m-chlorophenylhydrazone (CCCP) or carbonylcyanide p-(trifluoromethoxy)-phenylhydrazone (FCCP), are protonophores that produce intracellular acidification in several cell types including chemoreceptor cells (Grinstein and Rothstein, 1986; Tretter *et al.*, 1998; Buckler and Vaughan-Jones, 1998; Park *et al.*, 2002). An intracellular acidification followed by consecutive activation of $Na^{+}/H^{+}$ and $Na^{+}/Ca^{2+}$ exchanger was proposed by our group as the mechanism that triggers exocitosis during DNP stimulation in the adult rabbit CB (Rocher *et al.*, 1991; Gonzalez *et al.*, 1994). In rat neonatal chemoreceptor cells, however, it was found that DNP induces membrane depolarization by inhibiting a background, voltage-insensitive, $K^{+}$ current (Buckler and Vaughan-Jones, 1998). In addition to suppress this current, DNP also activates a yet uncharacterized inward current. In this model, an "unknown link" between DNP-induced mitochondrial depolarization and plasmalemmal $K^{+}$-channels inhibition was put forward. In this paper, we have restudied the effects of DNP on rabbit

*Chemoreception*, Edited by Pequignot et al.
Kluwer Academic/Plenum Publishers, New York, 2003

chemoreceptor cells looking for the presence in this preparation of membrane depolarization. Results show that the secretion of CA induced by DNP in the rabbit CB is mostly the result of the entry of calcium to the cell via depolarization-activated calcium channels. In the discussion we reevaluate our previous data and hypothesis on the mechanism of DNP stimulation of the CB at the light of our new data. Though the nature of the membrane current targeted by DNP in rabbit CB has not been investigated, our results indicate that in adult rabbit CB chemoreceptor cells operate trough similar mechanisms than in neonatal rat CB chemoreceptor cells.

## 2. MATERIAL AND METHODS

**2.1 Surgery.** Adult New Zealand rabbits were used in these experiments. The animals were anesthetized with sodium pentobarbitone (30-40 mg/Kg, i.v.), the carotid bifurcations excised and the carotid bodies cleaned of surrounded tissue under dissecting microscope. The protocols were approved by the Institutional Animal Care and Use Committee of the Universities of Valladolid and Elche.

**2.2 $^3$H-catecholamine release experiments.** The endogenous deposits of CA of the CBs were isotopically labeled with $^3$H by incubating the organs in a medium containing 20 μM-[3,5-$^3$H]tyrosine, 1 mM ascorbic acid, and 100 μM-DL-6-methyl-5,6,7,8-tetrahydropterine (see Rocher et al., 1991, for details). After labeling, individual CBs were placed in vials containing 1 ml of solution (in mM: NaCl, 116; $NaHCO_3$, 24: KCl, 5; $CaCl_2$, 2; $MgCl_2$, 1; Hepes, 10; glucose, 5; pH 7.4) equilibrated with 20% $O_2$/5% $CO_2$, rest $N_2$. The solutions were renewed every 10 minutes and analyzed for their content in $^3$H-CA by adsortion in alumina and posterior counting of the eluates in a scintillation spectrometer. As shown in Figure 1, each CB was stimulated by incubating it in the presence of DNP during two 10 min periods (S1 and S2). In the experimental CB, the calcium antagonists were present in the media 10 min prior and during the presentation of the second stimulus. The evoked release of $^3$H-CA (cpm above basal release) obtained in the second stimulation period (S2) was divided by that obtained in the first one (S1) and the mean S2/S1 ratio obtained in control CB was compared with that obtained in the experimental (drug-treated) organ. Data are expressed as mean ± SE. Statistical significance of the observed differences was assessed using Student's *t* test for unpaired data.

**2.3 Electrophysiological recordings.** Chemoreceptor cells from rabbit CB were enzymatically dispersed and plated on poly-L-lysine-coated coverslips as previously described (Rocher *et al.*, 1999). Coverslips were placed on a thermostatized recording chamber (Warners Instrument) and superfused by gravity at a rate of 1.5-2 ml/min. Extracellular solution (in mM: NaCl, 116; $NaHCO_3$, 24; KCl, 5; $CaCl_2$, 2; $MgCl_2$, 1; HEPES, 10; glucose, 5; pH 7.4 equilibrated with 5% $CO_2$ /95% $O_2$) was preheated at 36°C and maintained between 33-35°C in the recording chamber. Borosilicate glass electrodes were filled with a solution containing (in mM): potassium gluconate, 95; KCl, 40; HEPES, 10; $MgCl_2$, 2; EGTA 5, pH 7.3 containing 100-150 µg/ml of nystatin. The liquid junction potential, refered to a Ag-AgCl pellet, was 7-9 mV and data are not corrected for it. Electrophysiological recordings were conducted using a RK 300 amplifier (Bio-Logic). The data were filtered at 2 KHz. Pulse generation, acquisition and data analysis were performed with the pClamp software (version 8.1).

## 3. RESULTS

**3.1 The release of $^3$H-catecholamine evoked by DNP is mediated by activation of voltage-dependent calcium channels.** Chemoreceptor cells of the rabbit CB lack low voltage-activated calcium channels but express L-, N-, P/Q- and resistant or R-type calcium channels (Overholt *et al.*, 1997). To investigate the possible participation of these channels in the release of $^3$H-CA induced by DNP, we studied the effect of cadmium (200 µM), a non-specific blocker of the high voltage-activated calcium channels, nisoldipine and ω-conotoxin MVIIC on this secretory response. Nisoldipine, a specific blocker of L-type calcium channels, was used at 2 µM, and ω-conotoxin MVIIC at 3 µM, a concentration high enough to block N- and P/Q-type channels (Olivera *et al.*, 1994). Figure 1 shows the time course of the release of $^3$H-CA from four representatives CB incubated during two 10 min periods (S1 and S2) in the presence of 100 µM DNP. Part A shows the release from a control CB: it can be seen the typical decay of the evoked response to a second application of the stimulus. In twelve control CB the evoked release in S2/S1 ratio was 0.63 ± 0.04. Part B, C and D show the time course of the release of $^3$H-CA from three CB incubated in the presence of different blockers of calcium channels during the second stimulation with DNP. The presence of 200 µM $CdCl_2$ (Figure 1B) dramatically reduced the release response to 20% of its control value (S2/S1 ratio was 0.61 ± 0.03 in control CB and 0.12 ± 0.06 in $Cd^{2+}$-treated CB; $p<0.001$; $n=4$). Nisoldipine

alone reduced the release response by 62% (Figure 1C) and when added in combination with ω-conotoxin MVIIC (Figure 1D), the secretory response further declined to a value only 18% of that obtained in control CB (S2/S1 ratios were: 0.66 ± 0.09 in control *vs* 0.25 ± 0.03 in nisoldipine-treated CB, and 0.61± 0.07 in control *vs* 0.11± 0.02 in nisoldipine plus ω-conotoxin MVIIC-treated CB; $p< 0.05$ and 0.001 respectively; n=4 in every experimental group). These results show that more than 80% of the release of $^3$H-CA induced by DNP is mediated by calcium entering the cell through voltage-activated calcium channels and therefore indicate that chemoreceptor cells should be depolarized

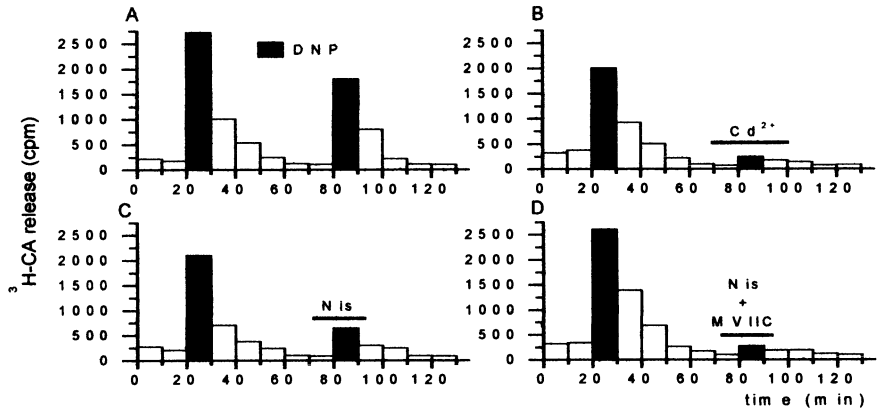


by this metabolic uncoupler.

*Figure 1.* Effect of different blockers of voltage-activated calcium channels on the release of $^3$H-CA induced by DNP in the rabbit carotid body (CB). Time course of the release of $^3$H-CA from four different CB. The CBs were incubated in control bicabonate-buffered solution in the absence (□) and in the presence (■) of 100 μM DNP. Antagonists of calcium channels were present in the incubation media at the times indicated by horizontal lines. $Cd^{2+}$: 200 μM $CdCl_2$; Nis: Nisoldipine 2μM and MVIIC: ω-conotoxin MVIIC 3 μM.

**3.2 DNP depolarizes rabbit CB chemoreceptor cells and decreases membrane conductance.** Figure 2A shows the membrane potential recorded in a representative chemoreceptor cell by the perforated-patch technique under current-clamp conditions (Im=0). The cell displayed a stable membrane potential of -52 mV during superfusion with a bicarbonate-buffered media and the addition of DNP (200 μM) produced a rapid depolarization to -37 mV. Upon returning to control conditions, membrane potential recovered with a time

course similar to that displayed during DNP-induced activation. In some cells, a transitory hyperpolarization was observed after the elimination of DNP from the superfusion media. In five cells, mean resting membrane potential was –54 ± 3 mV (range –47 to –62 mV) and DNP decreased this value to –37 ± 2 mV (range –45 to –32 mV). Average depolarization obtained in these cells during DNP superfusion was 17 ± 3 mV.

Figure 2B shows current flowing through the membrane of a chemoreceptor cell under voltage-clamp conditions. The cell shown in the figure was voltage-clamped at –50 mV (the same voltage that displayed under current-clamp conditions) and 50 ms voltage pulses to –70 mV were applied to the cell at a frequency of 2 Hz. In concordance with the depolarization produced by DNP, during membrane voltage-clamping the venom induced an inward current with a time course similar to that obtained in the current-clamp experiments. Average inward current induced by DNP in three voltage-clamped cells at –50 mV was –18 ± 4 pA (range –12 to –26 pA). Figure 2B also shows that DNP reduces membrane conductance in chemoreceptor cells measured from the response to

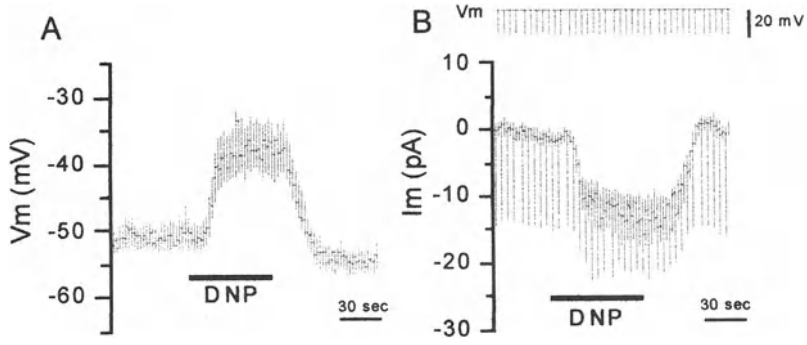


*Figure 2.* Effect of DNP on membrane potential and membrane current of isolated chemoreceptor cells. A. Recording of membrane potential in a single cell in current-clamp mode (Im=0). B. Recording of membrane current in a single cell voltage-clamped at –50 mV and subjected to 50 ms voltage pulses to –70 mV. In both cases recordings were performed by the perforated-patch technique. DNP (200 μM) was present in the media at the time indicated by the horizontal lines.

depolarizing pulses to –70 mV. In the three cells studied, average membrane conductance (measured between –50 to –70 mV) in control bicarbonate-buffered solution was 1083 ± 274 pS and decreased to 410 ± 51 pS during DNP superfusion. These results indicate that DNP depolarizes chemoreceptor cells of the rabbit CB by closing some type(s) of ionic channels.

## 4. DISCUSSION

The present work shows that DNP depolarizes rabbit chemoreceptor cells and that the bulk of the secretion of CA induced by the venom results from the entry of calcium to the cell through high-voltage activated calcium channels.

Previous work has shown that both, the release of CA and the increase in intracellular calcium induced by DNP are highly dependent on the presence of $Ca^{2+}$ in the extracellular media (Rocher *et al.*, 1991; Buckler and Vaughan-Jones, 1998). However, the pathway for the calcium entry into the cell during this type of stimulation has not been clearly established. Activation of voltage-dependent calcium channels during DNP stimulation is strongly suggested by our data showing that the release of CA induced by DNP is reduced by 80% in the presence of 200 μM $Cd^{2+}$ and by data in rat chemoreceptor cells showing a similar reduction in DNP-induced $Ca^{2+}_i$ increase in the presence of 2 mM $Ni^{2+}$ (Buckler and Vaughan-Jones, 1998). However, although these divalent cations are well known blockers of voltage-activated calcium channnels, it should not be forgotten that, at the above concentrations, they display a significant inhibitory effect on the $Na^+/Ca^{2+}$ exchanger (Iwamoto and Shigekawa, 1998), a mechanism proposed as putative calcium entry pathway during DNP stimulation (Rocher *et al.*, 1991). To discard this possibility, we tested the effect of specific organic calcium channels antagonists on the secretory response. The participation of L-type calcium channel is supported by the 62% inhibition of the observed secretion in the presence of 2 μM nisoldipine. These data are not in accordance with previous data from our laboratory showing that the release of CA induced by DNP was insensitive to dihydropyridines. This discrepancy is probably due to the fact that in the first study we used nisoldipine at 625 nM, a concentration probably too low to saturate L-type channels (Overholt *et al.*, 1997). Our present data also indicate that the remaining calcium-sensitive response observed after L-type channels blockade should be mediated by activation of P/Q-type and/or N-type channels because it was blocked when 3 μM ω-conotoxin MVIIC was applied in combination with nisoldipine. We tend to think that P/Q-type are the involved channels in the response because ω-conotoxin GVIA, a specific antagonist of N-type channels, did not modify the secretion of CA induced by

either hypoxia or high $K^+_e$ (Rocher, Almaraz and Gonzalez, unpublished observations) suggesting that N-type channels are not linked to exocitosis of CA in the rabbit CB. In rat there is an important fraction of DNP-induced $Ca^{2+}_i$ increase resistant to L-type channel blockade (Buckler and Vaughan-Jones, 1998), but the type of $Ca^{2+}$ channels responsible for it has not been studied.

The data on secretion presented here evidence that DNP is activating high-voltage activated calcium channels in rabbit chemoreceptor cells and also indicate that the venom depolarizes these cells. According to the data on secretion, we consistently found a reversible membrane depolarization during superfusion of chemoreceptor cells with DNP. In addition, in voltage-clamp experiments we observed that the venom induced an inward current associated with a decrease in membrane conductance. We have not investigated the nature of the ionic current affected by DNP but the inhibition of a $K^+$ channel is compatible with the data. Since membrane conductance was measured at membrane potential between –50 and –70 mV from holding potentials of –50 mV, the hypothetical $K^+$-current inhibited by DNP should be active at these potential values. Therefore, it is possible that a background $K^+$ conductance is the target of DNP in rabbit CB as it has been found in rat chemoreceptor cells (Buckler and Vaughan-Jones, 1998).

In the model that we published in 1991 (Rocher *et al.*, 1991), we proposed that DNP acting as a protonophore would acidify the cell promoting the entry of $Na^+$ to the cell in exchange by $H^+$. The release of CA will then be triggered by the entry of $Ca^{2+}$ through the $Na^+/Ca^{2+}$ exchanger working in the reversal mode. The data supporting this hypothesis could be now reevaluated at the light of the results presented in this work, particularly regarding to three points: i) the insensitivity of the secretory response to dihydropyridines and the lack of knowledge, at that time, of the existence of P/Q-type calcium channels led as to postulate that DNP did not depolarize chemoreceptor cells; the data presented in this paper clearly show that this is not the case; ii) the involvement of $Na^+/H^+$ exchanger in the DNP-induced secretory response was proposed on the basis of the blocking effect of ethylisopropylamiloride (EIPA) on this evoked release of CA; with our new data, this effect can now be assigned to the inhibitory effect of this drug on L-type calcium channels (Garcia *et al.*, 1990) and, iii) the involvement of the $Na^+/H^+$ exchanger was also supported by the intense $Na^+$-dependence of the DNP-induced release of CA; however, other mechanisms may explain these data. For example, the membrane current sensitive to DNP may carry $Na^+$ as it has been found for the inward current induced by FCCP in vascular endothelial cells (Park et al., 2002) or may be $Na^+$-dependent as it is the case for some type of background $K^+$-channels (Lesage and Lazdunski, 2000).

Alternatively, the removal of $Na^+$ from the extracellular medium could hyperpolarize chemoreceptor cells (Buckler and Vaughan-Jones, 1994; Carpenter et al., 2000; Carpenter and Peers, 2001) bringing membrane potential to values closer to the equilibrium potential of a hypothetical DNP-sensitive $K^+$ current; this effect will make smaller the effect of the venom on membrane potential and therefore on CA secretion. Finally, it should be recalled that the percentage of the secretory response blocked by calcium antagonists is similar to that blocked by extracellular calcium removal (Rocher et al., 1991). These results do not support the possibility that other calcium entry pathways, as the $Na^+/Ca^{2+}$ exchanger, contribute in a significant manner to elevate $Ca^{2+}_i$ and secretion during DNP stimulation. While the DNP-induced depolarization will be favourable for $Ca^{2+}$ influx through the exchanger, the entry of calcium by the membrane calcium channels will have the opposite effect.

## ACKNOWLEDGEMENTS

The authors are grateful to Ms. María Llanos Bravo for technical assistance. This work was supported by Spanish DGICYT Grants BFI2002-03467 to E.Geijo, BFI2001-1713 to C.Gonzalez and RED RESPIRA (FISS).

## REFERENCES

Buckler, KJ. and Vaughan-Jones, RD. (1998). Effects of mitochondrial uncouplers on intracellular calcium, pH and membrane potential in rat carotid body type I cells. *J Physiol* 513:819-833.

Buckler, KJ. and Vaughan-Jones, RD. (1994). Effects of hypercapnia on membrane potential and intracellular calcium in rat carotid body type I cells. *J Physiol* 478: 157-171.

Carpenter, E., Hatton, CJ. and Peers, C. (2000). Effects of hypoxia and dithionite on catecholamine release from isolated type I cells of the rat carotid body. *J Physiol* 523:719-729.

Carpenter, E. and Peers C. (2001). A standing Na+ conductance in rat carotid body type I cells. *Neuroreport* 12:1421-1425.

Garcia, ML., King, VF., Shevell, JL., Slaughter, RS., Suarez-Kurtz, G., Winquist, RJ. and Kaczorowski, GJ. (1990). Amiloride analogs inhibit L-type calcium channels and display calcium entry blocker activity. *J Biol Chem* 265:3763-3771.

Gonzalez, C., Almaraz, L., Obeso, A. and Rigual, R. (1994). Carotid body chemoreceptors: from natural stimuli to sensory discharges. *Physiol Rev* 74: 829-898.

Grinstein, S. and Rothstein, A. (1986). Mechanisms of regulation of the Na+/H+ exchanger. *J Membr Biol* 90:1-12.

Iwamoto, T. and Shigekawa, M. (1998). Differential inhibition of $Na^+/Ca^{2+}$ exchanger isoforms by divalent cations and isothiourea derivative. *Am J Physiol.* 275: C423-C430.

Lesage, F. and Lazdunski, M. (2000). Molecular and functional properties of two-pore-domain potassium channels. *Am J Physiol Renal Physiol* 279: F793-F801.

Obeso, A., Almaraz, L. and Gonzalez, C. (1989). Effects of cyanide and uncouplers on chemoreceptor activity and ATP content of the cat carotid body. *Brain Res* 481: 250-257.

Olivera, BM., Miljanich, GP., Ramachandran, J. and Adams, ME. (1994). Calcium channel diversity and neurotransmitter release: the omega-conotoxins and w-agatoxins. *Annu Rev Biochem* 63:823-867.

Overholt, JL. and Prabhakar, NR. (1997). Ca2+ current in rabbit carotid body glomus cells is conducted by multiple types of high-voltage-activated Ca2+ channels. *J Neurophysiol* 78:2467-2474.

Park, KS., Jo, I., Park, K., Bae, SW., Rhim, H., Suh, SH., Park, J, Zhu, H., So, I. and Kim, KW. (2002). FCCP depolarizes plasma membrane potential by activating proton and Na+ currents in bovine aortic endothelial cells. *Pflugers Arch* 443:344-352.

Rocher, A., Gonzalez, C. and Almaraz, L. (1999). Adenosine inhibits L-type Ca2+ current and catecholamine release in the rabbit carotid body chemoreceptor cells. *Eur J Neurosci* 11:673-681.

Rocher, A., Obeso, A., Gonzalez, C. and Herreros, B. (1991). Ionic mechanisms for the transduction of acidic stimuli in rabbit carotid body glomus cells. *J Physiol.* 433:533-548.

Shen, TC. and Hauss, WH. (1939). Influence of dinitrophenol, dinitroortocresol and paranitrophenol upon the carotid sinus chemoreceptors of the dog. *Arch Int Pharmacodyn Ther* 63:251-258.

Tretter, L, Chinopoulos, C. and Adam-Vizi, V. (1998). Plasma membrane depolarization and disturbed Na+ homeostasis induced by the protonophore carbonyl cyanide-p-trifluoromethoxyphenyl-hydrazon in isolated nerve terminals. *Mol Pharmacol* 53:734-741.

# Enhancing Effect of Vasopressin on the Hyperglycemic Response to Carotid Body Chemoreceptor Stimulation

*Role of metabolic variables.*

[1,2]SERGIO A. MONTERO, [1]ALEXANDER YARKOV, [1]MÓNICA LEMUS, [3]HERÓN MENDOZA, [4]VICTORIA VALLES, [1,5]ELENA R. DE ÁLVAREZ-BUYLLA and [1]RAMÓN ÁLVAREZ-BUYLLA. †

*[1]Centro Universitario de Investigaciones Biomédicas and [2]Fac. de Medicina, Universidad de Colima, [3]Fac. de Medicina, Universidad Autónoma de Tamaulipas, [4]Depto. de Diabetes, Inst. Nac. de Nutrición y Ciencias Médicas "Salvador Zubirán", [5]CINVESTAV, México.*

## 1. INTRODUCTION

Glucose homeostasis, a fundamental process for life, is controlled at multiple levels. Glucose sensitive receptors in the brain, portal vein, liver, pancreas and carotid bodies (Álvarez-Buylla and Roces de Álvarez-Buylla, 1994) provide afferent information to central nervous system (CNS) about the glucose concentration in different regions of the body. In the CNS, this input is integrated by the hypothalamus and the nucleus of the tractus solitarius (NTS) (Adachi *et al.*, 1995). Additionally, there is evidence that carotid body receptors (CBR) are also sensitive to changes in blood glucose concentration (Álvarez-Buylla and Roces de Álvarez-Buylla, 1994; López-Barneo *et al.*, 2001) and afferent impulses from these receptors induce a reflex response on glucose levels: 1) by enhancing glucose production by the liver, and 2 by promoting glucose retention by the brain. Carotid bodies play an important role in the insulin-induced counterregulatory response to mild hypoglycemia (Koyama *et al.*, 2000). The efferent pathway for these reflexes is not fully understood, but previous experiments identify the neurohypophysis and adrenal glands as necessary for the hyperglycemic reflex initiated by NaCN stimulation, and suggest that the effects of these two glands on CBR hyperglycemic reflex are humoral (Álvarez-Buylla *et al.*, 1997). This is supported by the finding that the neurohypophyseal hormone arginine-vasopressin (AVP) has a modulatory role on glucose metabolism during stress, and that an increase of vasopressin plasma levels is observed after perfusion of the carotid sinus with deoxygenated blood, a method similar to NaCN stimulation (Share and Levy, 1966). In addition,

*Chemoreception*, Edited by Pequignot et al.
Kluwer Academic/Plenum Publishers, New York, 2003

hypophysectomy leads to adrenal cortical atrophy and hypoglycemia (Wurtman *et al.*, 1968). We have previously hypothesized that pituitary AVP may be involved in the hyperglycemic reflex initiated by CBR stimulation. In this paper we extend the study to the role of glucose in regulating AVP at the level of NTS (Yarkov *et al.*, 2001), and suggest that this peptide may facilitate hyperglycemic reflexes elicited by CBR stimulation. We show that AVP can directly trigger a hyperglycemic reflex similar to that obtained after CBR stimulation. We suggest that AVP may interact with vasopressin receptors located in the NTS, liver, adrenal cells and pancreas to stimulate the secretion of epinephrine (E) and glucagon.

## 2. METHODS

### 2.1 Animals and Surgical Procedures

Experiments were performed on adult male Wistar rats (280-300 g weight) fasted for 12 h. Anesthesia was induced by intraperitoneal administration of sodium pentobarbital (3 mg/100 g) which was supplemented by a continuous intraperitoneal infusion of 2 drops/min of the anesthetic at a concentration of 63 mg/100 ml in 0.9 % NaCl, so that no pain responses to paw pinching were observed, but the eye palpebral reflex was present. Respiration and body temperature were artificially maintained. All procedures performed on animals were in accordance with the National Research Council Guide for the Care and Use of Laboratory Animals (NCR Pub., 1996). Bilateral adrenalectomies (ADX) were performed by a dorsal access 3 days before the experiment. To obtain blood samples catheters were inserted into the femoral artery and jugular sinus (via the right external jugular vein) (Fig. 1A). In some experiments the catheter in jugular sinus was also used to inject drugs. The correct placement of the catheters was verified at the end of each experiment during autopsy. In normal rats the coeliac trunk was chosen to reach the hepatic territory, a catheter was introduced into the thoracic aorta, via the abdominal aorta, above the coeliac trunk (Guarner and Alvarez-Buylla, 1991) (Fig. 1A), and it was attached to a the syringe pump for infusions (Baby Bee, BAS, Indiana, USA). The time of experimental injections was considered as t=0 (indicated as an arrow in the figures). At blood collection time 0.15 mL of arterial blood and 0.15 mL of venous blood were collected, at two basal values and 6 experimental values after the injections in the first series of experiments or 3 experimental

values in the second series (Fig. 1). Brain glucose retention (BGR) was determined between glucose concentration in the abdominal aorta and glucose concentration in the jugular sinus.

### 2.1.1 CBR Stimulation

The circulation in the carotid sinus (CS) was isolated from general circulation during injections of NaCN (5 μg/100 g in 0.1 ml saline) as a bolus through a 27 gauge needle and a catheter (Clay Adams PE-10) placed in the common carotid artery below the isolated carotid sinus to avoid baroreceptors stimulation (Fig.1A). Both the left external carotid artery (beyond the lingual branch) and the internal carotid near the jugular foramen were temporarily occluded (15-20 sec) to prevent NaCN solution from entering the brain. (Alvarez-Buylla and Alvarez-Buylla, 1988).

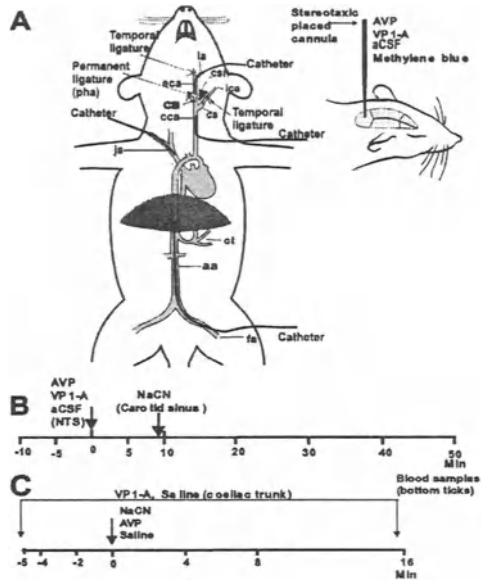


*Figure 1.* Diagram illustrating: (**A**) the placement of catheters and ligatures to locally perfuse the carotid body receptors (CBR) for stimulation (by injecting NaCN), the placement of catheters to obtain blood samples, and the stereotaxic cannula for central injections; (**B** and **C**) experimental protocols. aa, abdominal aorta; CSF, artificial cerebrospinal fluid; AVP, arginine vasopressin; **CB**, carotid body; cca, common carotid artery; cs, carotid sinus; csn, carotid sinus nerve; ct, coeliac trunk; eca, external carotid artery; fa, femoral artery; ica, internal carotid artery; js, jugular sinus; la, lingual artery; VP1-A, vasopressin antagonist.

### 2.1.2 Microinjections into the NTS

After making an occipital craniotomy, the head was fixed in a stereotaxic apparatus (David Kopf Instruments,Stoelting, Illinois, USA), a glass micropipette with a tip diameter of 50-60 μm was inserted into the left NTS (P=12.7 mm, L=1.45 mm, V=7.7 mm) (Paxinos and Watson, 1986). All the substances were injected by a micropump at a rate of 100 nL/30 sec (Yarkov *et al.,* 2001). At the end of each experiment the micropipette tip was identified by injecting methylene blue (1 %, same volume) (Fig.1A). The rats were killed with an intravenous dose of sodium pentobarbital (50 mg/kg) the brain was removed and immediately frozen for further histological verification at 40 μm thick sections in a cryostat (Fig. 2).

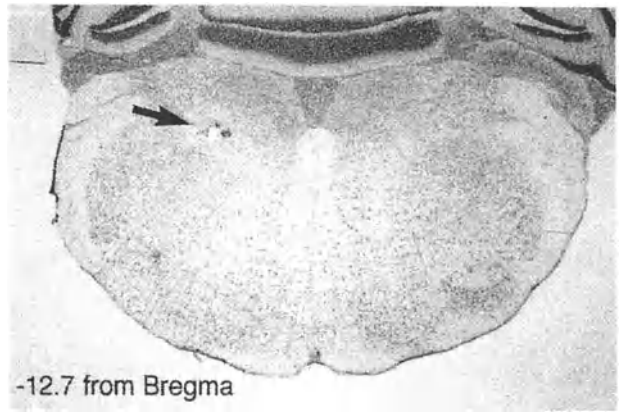


*Figure 2.* Representative frontal section of brain stem of rats that received the injections of AVP, VP1-A or aCSF into the nucleus of the tractus solitarius (NTS) (arrow). Sections were stained with Cresyl –violet.

## 2.2 Drugs

The drugs used in this study were: Sodium cyanide (NaCN) (see CBR stimulation). [Arg8]-vasopressin (AVP, Sigma Chemical Co., St. Louis MO, USA) and [β-mercapto-β,β-cyclopentamethylene-propeonyl$^{1}$, *O*-Met-Tyr$^{2}$, Arg$^{8}$]-Vasopressin (VP1-A; AVP-antagonist, Sigma, Chemical Co., St. Louis MO, USA). Compounds were dissolved in artificial cerebrospinal fluid (aCSF; 147 mM NaCl, 4mM KCl, 1.2 mM $CaCl_2$ and 1 mM $MgCl_2$) immediately before application. In control experiments the same volume of artificial cerebrospinal fluid (aCSF) or saline alone were injected (Fig. 1 **B** and **C**).

## 2.3 Analytical Methods

Glucose concentration in blood samples was measured by the glucose-oxidase method (Beckman Autoanalyzer, Fullerton CA, USA) in μmol/mL units. Epinephrine in plasma (E) was measured by HPLC in pg/mL units. Glucagon concentration in plasma was measured by RIA in pg/mL units. The data are expressed as means ± SE , the statistical comparisons were performed using Student's t-test and analysis of variance (ANOVA) for repeated measurements, comparisons in all cases were done between experimental values and controls.

## 2.4 Experimental Protocol

Animals were subjected to one of the following procedures: (a) aCSF injections into NTS 9 min before CBR stimulation, control experiments (n=10); (b) AVP (10 pmol/100 nL) injections into the NTS 9 min before CBR stimulation (n=6); (c) VP1-A (100 pmol/100 nL) injections into the NTS 9 min before CBR stimulation (n=5); (d) CBR stimulation during a VP1-A (2.5 nmol/100g/min) or saline (as control) infusions (21 min) into the coeliac trunk (n=10); (e) AVP (15 pmol/100g) injections into the jugular sinus in normal rats (n=5) and ADX rats (n=5); f) AVP (5 pmol/100g/min) infusion (16 min) into the coeliac trunk in normal rats (n=5) and ADX rats (n=5).

# 3. RESULTS

## 3.1 CBR Stimulation after AVP in NTS

Direct administration of AVP (10 pmol) into the NTS 9 min before CBR stimulation with NaCN (5 μg/100 g), resulted in a significantly higher concentration of blood glucose when compared to their respective controls (aCSF injection). Arterial blood glucose rapidly increased, reaching a maximum value at 20 min ($P<0.01$) and the hyperglycemia was maintained for the duration of the experiment. Significantly higher arterial concentration was only observed until 30 min ($P<0.5$) (n=6) (Fig. 3A). When brain glucose retention (BGR) was calculated, significant increases (compared to controls) were observed at 10 and 20 min after AVP ($P<0.01$ and $P<0.05$) (Fig. 3B). The effect on glucagon concentration in blood was not significant (n=6, Table 1). In contrast to the results seen with AVP, injection of the VP1-A (100 pmol) had no significant effects on blood glucose concentration (n=5, Fig. 4A), but glucagon concentration decreased significantly ($P<0.05$) (Table 1). When BGR was calculated significant decreases were obtained after VP1-A at 30, 40 and 50 min postinjection ($P<0.01$) (Fig. 4B).

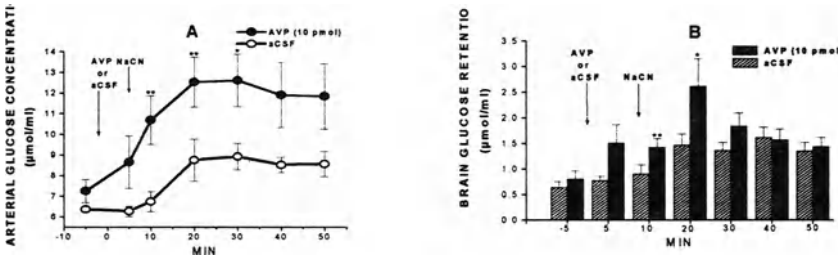


*Figure 3.* Changes in arterial glucose concentration (**A**) and brain glucose retention (**B**) after carotid body receptor stimulation with cyanide (NaCN) injected into the vascularly isolated carotid sinus, pretreatment with AVP (10 pmol) (n=6) or aCSF (n=10) in normal rats as indicated. The values are means ± SEM. *Significantly different from control-aCSF data (*P<0.05,**P<0.01 ANOVA for repeated measures).

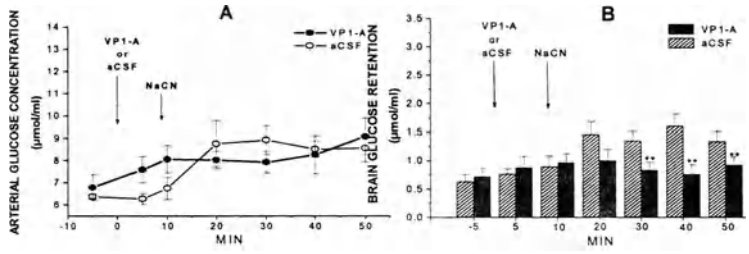


*Figure 4.* Changes in arterial glucose concentration (**A**) and brain glucose retention (**B**) after carotid body receptor stimulation with cyanide (NaCN) into the vascularly isolated carotid sinus, pretreatment with VP1-A (100 pmol) (n=5) or aCSF (n=10) in normal rats as indicated. The values are means ± SEM. *Significantly different from control-aCSF data (**P<0.01 ANOVA for repeated measures)

When AVP and VP1-A effects were compared, a significant diminution was observed on arterial glucose concentration and on BGR after CBR stimulation preceded by VP1-A (P<0.01) (Fig. 5). These experiments confirmed the receptor nature of AVP effect observed above

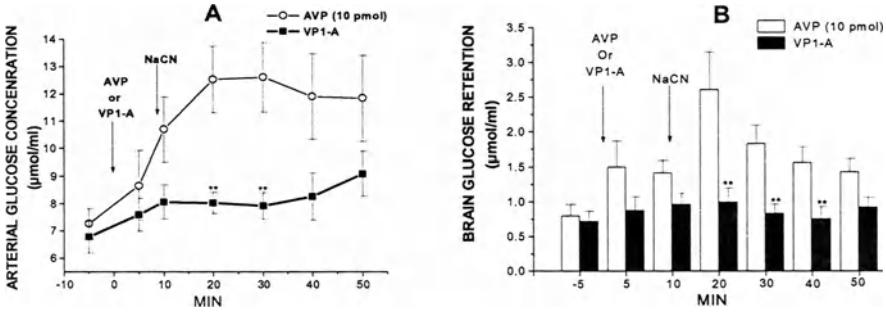


*Figure 5.* Changes in arterial glucose concentration (**A**) and brain glucose retention (**B**) after carotid body receptor stimulation with cyanide (NaCN) injected into the vascularly isolated carotid sinus, pretreatment with AVP 10 (pmol) (n=6) or VP1-A (100 pmol) (n=5) in normal rats as indicated. The values are means ± SEM. *Significantly different from AVP data (**P<0.01 ANOVA for repeated measures).

*Table 1.* Changes in circulating glucose and glucagon concentrations after CBR stimulation pretreatment with aCSF, AVP or VP1-A in the NTS in normal rats as indicated.

| | aCSF+NaCN (n=10) | | AVP+NaCN (n=6) | | VP1-A+NaCN (n=5) | |
|---|---|---|---|---|---|---|
| MIN | Gluc (μmol/ml) | GN (pg/ml) | Gluc (μmol/ml) | GN (pg/ml) | Gluc (μmol/ml) | GN (pg/ml) |
| -5 | 6.4±0.1 | 159±25 | 7.3±0.6 | 56±7 | 6.7±0.5 | 151±35 |
| +20 | 8.8±1.0* | 225±22* | 12.5±1** | 66±30 | 7.3±0.3 | 75±22* |

AVP, arginine vasopressin; aCSF, artificial cerebrospinal fluid; GN, glucagon; Gluc, glucose; NaCN, sodium cyanide; VP1-A, vasopressin antagonist. Significantly different from its basal sample (-5 min time) *P<0.05, **P<0.01. aCSF, AVP and VP1-A were injected a t=0 min, NaCN was injected at t=9 min.

## 3.3 CBR Stimulation during VP1-A Infusion into the Hepatic Territory

To study whether hepatic receptors to AVP participate in these reflexes, we stimulated CBR with NaCN (5 μg/100 g) simultaneously with an infusion of an antagonist to V1a receptors in the liver.

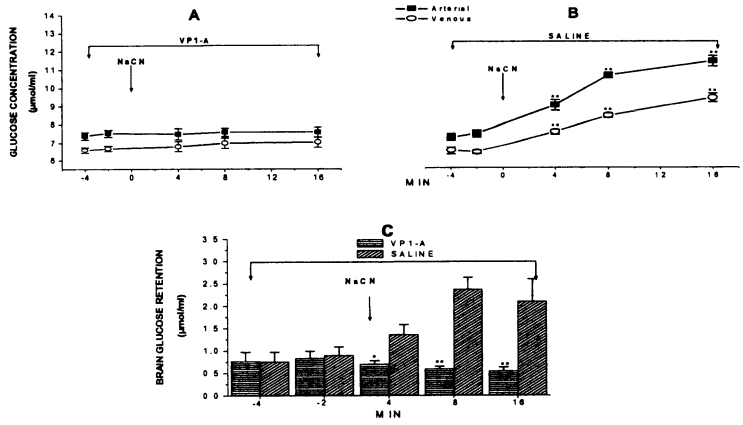


*Figure 6.* Changes in glucose concentration (**A** and **B**) and brain glucose retention (**C**) after carotid body receptor stimulation with cyanide (NaCN) injected into the vascularly isolated carotid sinus, during a VP1-A (2.5 nmol/100 g/min) (**A**, n=5) or saline infusions (**B**, n=5) into the coeliac trunk (hepatic territory) in normal rats. The values are means ± SEM. *Significantly different from control-saline data (**P<0.01, *P<0.05 Student's t-test).

*Table 2.* Changes in circulating glucose and epinephrine concentration after CBR stimlation or AVP injection into the jugular sinus in normal and ADX rats.

| | Normal rats | | | | | | ADX rats | |
|---|---|---|---|---|---|---|---|---|
| | NaCN (n = 5) | | SALINE (n = 5) | | AVP (n = 5) | | AVP (n = 5) | |
| MIN | Gluc (μmol/ml) | E (pg/ml) | Gluc (μmol/ml) | E (pg/ml) | Gluc (μmol/ml) | E (pg/ml) | Gluc (μmol/ml) | E (pg/ml) |
| - 5 | 6.4 ± 0.1 | 65± 14 | 6.3± 0.3 | 59± 11 | 6.7 ± 0.5 | 55± 11 | 6.5 ±0.3 | 36 ±4 |
| + 10 | 8.8± 10 | 157± 28** | 6.6± 0.5 | 67± 9 | 9.7± 0.3** | 191±25** | 6.9± 0.6 | 35± 2 |

ADX, adrenalectomized; AVP, arginine vasopressin; E, epinephrine, Gluc, glucose; NaCN, sodium cyanide. * Significantly different from its basal sample (-5mn time) *P<0.05, **P<0.01

VP1-A (2.5 nmol/100 g/min) into the coeliac trunk abolished the hyperglycemic reflex to NaCN, when compared with control rats in which an infusion of saline was made (Fig. 6**A** and 6**B**). In the same way, VP1-A significantly decreased the retention of glucose caused by anoxic stimulus at 4, 8 and 16 min postinjection (P<0.05 and P<0.01) (Fig. 6**C**).

To further analyze the interaction of AVP with vasopressin receptors located in adrenal cells, and the resulting secretion of epinephrine (E), in the next series of experiments we infused AVP (5 pmol/100 g/min) into normal and ADX rats. In these conditions AVP caused an increase in arterial glucose concentration similar in both cases (Fig. 7), indicating, that at least in part, in the effector mechanism for this hyperglycemic reflex, AVP has a direct action on the liver, without adrenal participation. AVP also increased E levels in a similar way to CBR stimulation (Table 2).

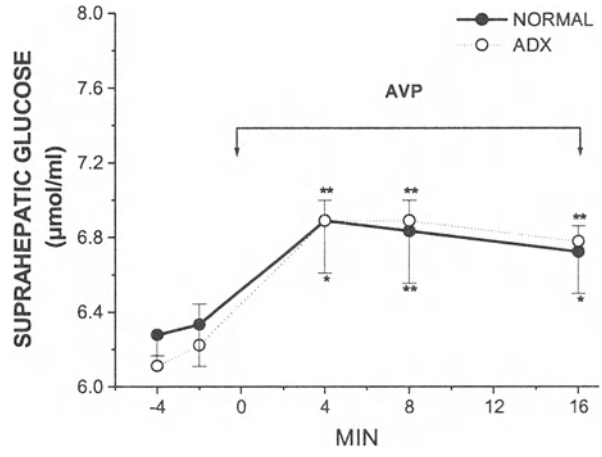


*Figure 7* Changes in suprahepatic glucose concentration during an AVP (5 pmol/100 g/min) infusion into the coeliac trunk in normal (n=5) and adrenalectomized rats (ADX) (n=5). The values are means ± SEM. *Significantly different from normal data (**P<0.01,*P<0.05 Student's t-test)

## 4. DISCUSSION

These data indicate that AVP participates in the hyperglycemic reflex and brain glucose retention, elicited by CBR stimulation. When chemoreceptors from the vascularly isolated carotid sinus were stimulated with NaCN after a local application of AVP (10 pmol) into the NTS, the hyperglycemic reflex was enhanced and significant differences were observed at 1, 11 and 21 min after CBR stimulation compared to control experiments in which aCSF was injected into the NTS prior to CBR stimulation (Fig. 3). It is well established that AVP is widely distributed in the CNS (De Vries *et al.,* 1995). In the hypothalamus AVP plays a central role in glucose regulation (Gomez et al., 1997) and neurons from the paraventricular nuclei have a prominent AVPergic projection to the NTS. Our previous studies show that a local application of AVP into the NTS resulted in a pronounced and rapid increase in arterial blood glucose level and in BGR (Yarkov *et al.,* 2001) and this effect was abolished by an AVP receptor antagonist.

In this study the preadministration of VP1-A 9 min before CBR stimulation was found to decrease the BGR responses to CBR stimulation (Fig. 4). This effect was more evident when AVP and VP1-A data were compared (Fig. 5). Central injections of AVP preceding CBR stimulation also increased glucagon levels in plasma, whereas VP1-A decreased glucagon concentrations without altering glucose levels (Table 1). These results suggested that AVP also exerts a direct stimulatory action on pancreatic cells (Spruce *et al.,* 1985). Above results indicate that AVP effects are mediated by VP1-A sensitive receptors (V1a) (Ostrowsky *et al.*, 1994) and further indicate that the actions of AVP are locally restricted to specific neurons in the NTS (Hegarty and Felder, 1997). The activation of AVPergic system of the hypothalamus may also play a feedforward role to increase the glucose level in blood and BGR (Yarkov *et al.*, 2001).

In order to examine the peripheral action of AVP, and its possible role on hyperglycemic reflex, adrenals and hepatic participation were analyzed in the second series of experiments. In our experiments circulating concentrations of E also rose significantly after the anoxic stimulus or after AVP injections in the jugular sinus, but adrenalectomy abolished these reflex responses (Table 2). AVP has a direct action on rat adrenal medulla (Grazzini *et al.,* 1998) promoting E secretion which in turn increases glucose levels in plasma. In ADX rats an infusion of AVP in the coeliac trunk (directly to the hepatic territory) produced similar results to those obtained in normal rats, increasing suprahepatic glucose levels (Fig. 7). It is well known that AVP has an inductive role to directly stimulate hepatic glycogenolysis (Hems *et al.,* 1978). When VP1-A was infused into the hepatic territory, the hyperglycemic response and BGR increase elicited by CBR stimulation were abolished (Fig. 6). These results indicate that, at least in part, AVP has a direct action on the liver to promote glycogenolysis after CBR stimulation. We cannot discount that some of the effects are mediated through a direct autonomic outflow to the liver and that secretions from the adrenals are only permissive for this response (Rosen et al., 1983); however, this finding argues for a greater role of the liver.

In summary, the present study demonstrates that NTS administration of AVP results in an enhancement of hyperglycemic reflex initiated by NaCN stimulation of the CBR acting on hepatic, pancreatic and on adrenal receptors to modify glucose retention by the brain.

## ACKNOWLEDGEMENTS

We thank Dr. Jeanette Hyer and Dr. Arturo Alvarez-Buylla, UCSF, USA for revision of the manuscript. This project was supported by the Consejo Nacional de Ciencia y Tecnología, México 29569-N.

## REFERENCES

Adachi A, Kobashi M, Funahashi M. (1995) Glucose-responsive neurons in the brainstem. *Obes. Res.* 5: 735-740.

Alvarez-Buylla R., Alvarez-Buylla E. (1988) Carotid sinus receptors participate in glucose homeostasis. *Respir. Physiol.* 72:347-360.

Alvarez-Buylla R, Alvarez-Buylla de ER, Mendoza H, Montero SA, Alvarez-Buylla A. (1997) Pituitary and adrenals are required for hyperglycemic reflex initiated by stimulation of CBR with cyanide. *Am J Physiol* 272: R392-R399.

Alvarez-Buylla, R, Roces de Alvarez-Buylla, E. (1994) Changes in blood glucose concentration in the carotid body-sinus modify brain glucose retention. *Brain Res.*, 654: 167-170.

De Vries GJ, Buijs RM, Van Leeuwen FW, Caffé AR, Swaab DF. (1985) The vasopressinergic innervation of brain in normal an castrated rat. *J. Comp. Neurol.* 233: 236-254.

Gomez F, Chapleur M, Fernette B, Burlet C, Nicolas J-P. Burlet A. (1997) Arginine vasopressin (AVP) depletion in neurons of the suprachiasmatic nuclei affects the AVP content of the paraventricular neurons and stimulates adrenocorticotrophic hormone release. *J. Neurosci. Res*, 50: 565-574.

Grazzini E, Boccara G, Joubert D, Trueba M, Durroux T, Guillon G, Gallo-Payet N, Chouinard L, Payet MD, Serradeil Le Gal C. (1998) Vasopressin regulates adrenal functions by acting through different vasopressin receptor subtypes. *Advan. Exp. Med. Biol.* 449: 325-334.

Guarner V, Alvarez-Buylla R. (1991) Changes in brain glucose retention produced by the stimulation of an insulin-sensitive reflexogenic zone in rats. *J. Auton. Nerv. Syst.* 34:89-94.

Hegarty AA, Felder RB. (1997) Vasopressin and V1-receptor antagonists modulate the activity of NTS neurons receiving baroreceptor input. *Am. J. Physiol.* 273: 143-152.

Hems DA, Rodrigues LM, Whitton PD. (1978) Rapid stimulation by vasopressin, oxytocin and angiotensin II of glycogen degradation in hepatocyte suspensions. *Biochem.* J. 172: 311-317.

Koyama Y, Cocker RH, Stone EE, Lacy DB, Jabbour K, Williams PE, Wasserman DH. (2000) Evidence that carotid bodies play an important role in glucoregulation in vivo. *Diabetes* 49: 1434-1442.

López-Barneo J, Parda, R, Ortega-Sáinz P. (2001) Cellular mechanism of oxygen sensing. *Annu. Rev. Physiol.* 63: 259-287.

Ostrowski NL, Lolait, SJ, Young WS. (1994) Cellular localization of vasopressin V1a receptor messenger ribonucleic acid in adult male rat brain, pineal, and brain vasculature, *Endocrinol.* 135: 1511-1528.

Paxinos G, Watson C. (1986) The Rat Brain in Stereotaxic Coordinates. *New York: Academic Press,*

Rosen SG, Clutter WE, Shah SD, Miller JP, Bier DM, Cryer PE. (1983) Direct α-adrenergic stimulation of hepatic glucose production in human subjects. *Am J Physiol* 245: E616-E626.

Share L, Levy MN. (1966) Effect of carotid chemoreceptor stimulation on plasma antidiuretic hormone titer. *Am. J. Physiol.* 210:157-161.

Spruce BA., McCulloch AJ, Burd J, Orskov H, Heaton A, Baylis PH, and Alberti KGMM. (1985) The effect of vasopressin infusion on glucose metabolismin man. *Clin. Endocrinol.* 22: 463-468.

Wurtman RJ, Casper A, Pohorecky LA, Bartter FC. (1968) Impaired secretion of epinephrine in response to insulin among hypophysectomized dogs. *Proc. Natl. Acad. Sci.* USA 61:522-528.

Yarkov, A., Montero, S., Lemus, M., de Alvarez-Buylla, ER., Alvarez-Buylla R. (2001) Arginine-vasopressin in nucleus of the tractus solitarius induce hyperglycemia and brain glucose retention. *Brain Res.* 902: 212-222.

# Immunohistochemical Study of the Carotid Body During Acute Hypoxia

KAZUO OHTOMO[1], YOSHIAKI HAYASHIDA[2], KOHKO FUKUHARA[3], HIDEKI NANRI[4], MASAHARU IKEDA[4], and KATSUAKI YOSHIZAKI[5]

*[1]Department of Anatomy, and [5]Department of Physiology, School of Health Science, Faculty of Medicine, Akita University, Akita 010-8543, Japan; [2]Department of System Physiology, and [4]Department of Health Development, University of Occupational and environmental Health, Kitakyushu 807-8555, Japan; [3]Department of Anatomy, School of Medicine, Faculty of Medicine, Akita University, Akita 010-8543, Japan*

## 1. INTRODUCTION

The carotid body is known to function as a chemoreceptor that is sensitive to inadequate oxygenation (hypoxia), hypercapnia and increased acidity in the arterial blood supply. Its regulatory effect is considered to be dependent on the ratio of oxygen to carbon dioxide. Differences in the plasma concentrations of these gases are measured by peripheral and central chemoreceptors located in the carotid body and brainstem, respectively. The carotid body consists basically of a parenchymal mass of clusters and strands of granular chromaffin type I glomus cells surrounded by nongranular type II glomus cells, with sinusoidal capillaries in close contact with both cell types. Afferent nerve fibers from the sinus branch of the glossopharyngeal nerve and postganglionic fibers of the sympathetic cervical ganglia form a dense network in contact with the type 1 cells. Some free nerve endings are present in the pericapillary space. Excitatory impulses generated in these fibers – suspected to be true chemoreceptor nerve endings – are transmitted to the vasomotor center of the medulla oblongata. The glomus cells, classed as AUDP cells, are polygonal with light, round nuclei, abundant mitochondria and free ribosomes, a well developed ergastoplasm, and a Golgi apparatus. The expression of SP-22 protein is reported to be enhanced about 1.5- to 4.6-fold when bovine aortic endothelial cells (BAEC) are exposed to various types of oxidative stress, including mitochondrial respiratory inhibitors

*Chemoreception*, Edited by Pequignot et al.
Kluwer Academic/Plenum Publishers, New York, 2003

which increase the generation of superoxide in the mitochondria. BAEC with an increased level of the mitochondrial protein SP-22 resulting from mild oxidative stress become tolerant to subsequent intense oxidative stress. *SP-22 is reported to be a member of the thioredoxin-dependent peroxidase family, suggesting that it may be one of the components of the antioxidant system in mitochondria, which are the major sites where reactive oxygen intermediates are generated (*Araki *et al.*, 1999*).*

An attractive and widely accepted tool for mapping multisynaptic neuronal pathways is Fos immunohistochemistry (Dragunow and Faull, 1989; Bullit, 1990). Expression of the proto-oncogene c-fos is considered to be a marker of activation of individual neurons after synaptic activation and $Ca^{2+}$ influx through voltage-sensitive $Ca^{2+}$ channels (Morgan and Curran, 1991; Sheng and Greenberg, 1990). The protein product of c-fos, the nuclear protein Fos, is induced rapidly and transiently, remains in the cell nucleus at elevated concentration for several hours, and can be detected immunohistochemically with antibodies. In several studies, Fos immunohistochemistry has been used to map neuronal pathways involved in the physiological responses to hypoxia and hypercapnia (Teppema *et al.*,1997). (Erickson and Millhorn 1994) and (Larnicol *et al.*, 1994) studied the expression of c-fos in the brainstem during hypoxia in rats and cats.

In the present study, the effects of acute isocapnic hypoxia on the rat carotid body and glomus cells were examined by immunohistochemistry. The primary antibodies used were raised against two antioxidant enzymes, SP-22 and thioredoxin (Trx), which constitute the Trx-dependent antioxidant system in mitochondria of mammalian cells, and c-fos protein, which is understood to play a pivotal role in the transduction of extracellular signals occurring after changes in gene expression.

## 2. MATERIALS AND METHODS

Fourteen adult male Wistar rats were placed in an air-tight acrylic chamber (volume about 140 l), and exposed to acute isocapnic hypoxia supplied with a gas mixture of 10% $O_2$ and 3-4% $CO_2$ in $N_2$ for 1, 3, 6, 12, 24, and 48 h, respectively. The animals were maintained under standard temperature and lighting conditions with free access to food and water. The flow of these gases was regulated by a flowmeter, and the $O_2$ and $CO_2$ levels in the box were monitored with a gas analyzer (Respina 1H26, NEC Sanei, Japan). This hypoxic condition was previously confirmed to be isocapnic to rats (Hayashida *et al.*,1996). As a control, two Wistar rats were placed in an ordinary air-conditioned room.

## 2.1 Tissue preparation for immunohistochemistry

Each animal was deeply anesthetized by intraperitoneal injection of sodium pentobarbital (50 mg/kg), and perfused through the heart with physiological saline solution containing heparin, followed by 2% paraformaldehyde and 0.2% saturated picric acid solution in 0.1 M phosphate buffer, pH 7.4. The carotid bodies were removed and post-fixed for one day in the same fixative. After rinsing in 10 mM phosphate-buffered saline (PBS) (pH 7.4), the specimens were incubated with 30% sucrose in PBS for one day. Cryostat 10-μm-thick serial sections were then cut and mounted on silane-coated slides.

## 2.2 Immunohistochemistry

After quenching endogenous peroxidase activity by incubating the sections with 0.3% $H_2O_2$, the sections were incubated with antibodies against SP-22, Trx, or c-fos diluted (1:2,000) in a solution of 1% bovine albumin in 10 mM PBS (pH 7.4) at room temperature (RT) for 1 day and then incubated with goat anti-rabbit IgG (1:200; Jackson ImmunoResearch, USA) in 10 mM PBS (pH 7.4) at RT for 2 h. They were then incubated with rabbit peroxidase-antiperoxidase complex (1:200; Dako, Denmark) in 10 mM PBS (pH 7.4) at RT for 2 h. Each incubation was carried out in a moist chamber. After each incubation, the sections were rinsed (3 x 10 min each) with 10 mM PBS (pH 7.4). The bound peroxidase was visualized by incubating the sections with 0.05% 3,3'-diaminobenzidine tetrahydrochloride (Sigma, USA) in 50 mM Tris HCl buffer (pH 7.5) containing 0.01% $H_2O_2$ at RT for 10 min (Graham and Karnovsky, 1966). These sections were finally dehydrated through a graded ethanol series (50%-100%), and mounted on Peamount (Fisher, USA).

# 3. RESULTS

The grades of immunoreactivity of the SP-22, Trx and c-fos antibodies for each exposure time are summarized in Table 1.

*Table1.* Grades of immunoreactivity with SP-22, Trx and c-fos antibodies of glomus cells in the carotid body of control rats, and rats exposed to isocapnic hypoxia for various periods.

| | control | 1 h | 3 h | 6 h | 12 h | 24 h | 48 h |
|---|---|---|---|---|---|---|---|
| SP-22 | + | + | + | + | + | ++ | ++ |
| Trx | ++ | ++ | ++ | ++ | ++ | +++ | +++ |
| c-fos | + | + | + | + | ++ | ++ | ++ |

## 3.1 SP-22 immunoreactivity

Under isocapnic hypoxia, the immunoreactivity of mitochondrial protein SP-22 antibody was localized in the glomus cells and numerous nerve fibers of the rat carotid body.

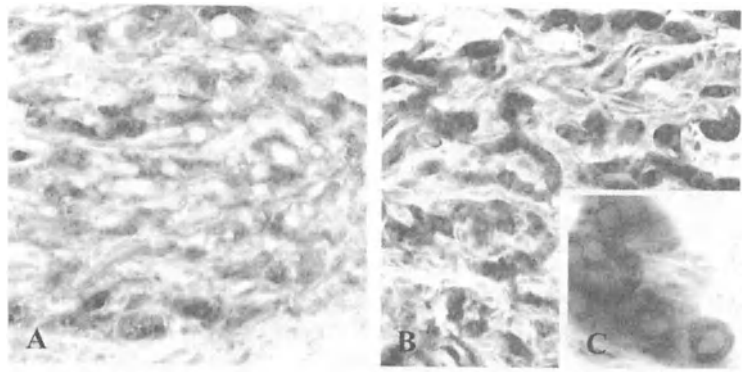


*Fig.1,* SP-22 immunoreactive glomus cells in the rat carotid body exposed to isocapnic hypoxia for 12 h (A) and 24 h (B, C). A part of B is shown at a higher magnification in the C.

The immunoreactivity in glomus cells appeared as dot- or strand-like reaction products in the cytoplasm (Figure 1C ). These reaction products became especially intense after 24 and 48 h exposure to isocapnic hypoxia (Table 1 and Figures 1A,1B,1C).

## 3.2 Trx immunoreactivity

The immunoreactivity of Trx antibody was similar to that of SP-22 antibody after all exposure times, although the overall reaction intensity was slightly stronger (Table 1, Figures 2A,2B).

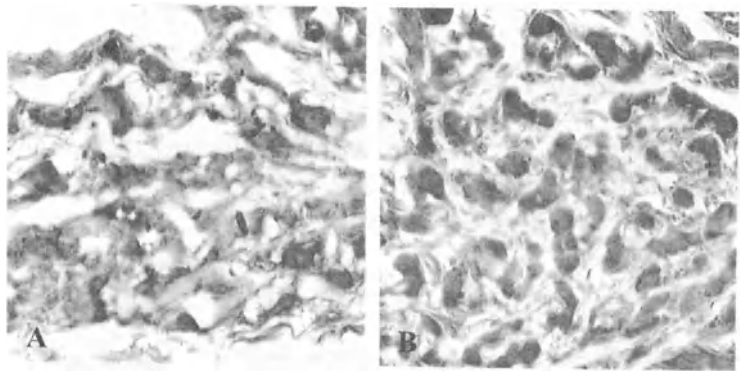


*Fig. 2,* Trx immunoreactive cells in the rat carotid body exposed isocapnic hypoxia for 12 h (A) and 24 h (B).

## 3.3 c-fos immunoreactivity

The immunoreactivity of c-fos antibody was localized in the glomus cells of the rat carotid body (Figures 3A,3B). The overall immunoreaction was weaker than those of the Sp-22 and Trx antibodies (Figures 1A,1B,1C,2A,2B,3A,3B), but showed a definite increase at 12 h of exposure to isocapnic hypoxia (Figures 3A,3B).

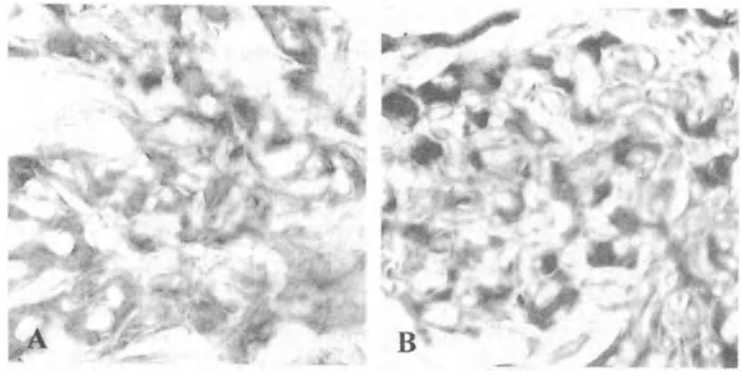


*Fig. 3,* c-fos immunoreactive glomus cells in the rat carotid body exposed to isocapnic hypoxia for 6 h (A) and 12 h (B).

## 4. DISCUSSION

Effects of varying concentrations of oxygen and carbon dioxide on glomus cells of the carotid body were first demonstrated by (Pietruschka *et al.*, 1977) in cells cultured for 3 days under either hypoxic or hypercapnic conditions. Outgrowth of cultured cells was more active in the presence of 10% than in 5% $CO_2$. In a 5% $CO_2$ atmosphere, the outgrowth of glomus cells was most pronounced at $O_2$ concentrations between 2% and 7.5%. Under extreme hypoxic conditions no differentiated cells were observed in the presence of 5% $CO_2$, whereas some were observed in 10% $CO_2$. Morphological determination of mitochondrial and cytoplasmic volume densities showed that membrane potential ($V_m$) was reduced by 5% $CO_2$ under extremely hypoxic conditions. No effect of $O_2$ concentration on $V_m$ was seen with 10% $CO_2$. Marked differences in the number of dense-cored vesicles were observed in individual glomus cells. Only cells grown in the presence of 5% $CO_2$ and 0% $O_2$ lacked dense-cored vesicles.( Fernando *et al.*, 1992) and (Araki *et al.*, 1999) have demonstrated the oxidant-mediated induction of Trx and SP-22, which constitute the TRX-dependent antioxidant system in mammalian cells. In the present study, SP-22 and Trx showed an intense immunoreaction in animals exposed to hypoxic conditions for more than 24 h. These findings suggest that mitochondrial sensitivity to these proteins in glomus cells is increased after exposure to hypoxia for this period. (Hellstrom *et al.*,1976) found that hypoxia selectively depleted the dopamine content of the rat carotid body, and that sectioning of the sinus nerve shortened the duration of this depletion; 30 min after exposure to hypoxia, dopamine levels were reduced to about one-third. Control levels of dopamine were already found 2 h after the experiment. Release of dopamine in response to hypoxic stimulation has also been shown to occur in vitro in the carotid body of the rabbit (Fidone *et al.*, 1982). (Blumcke *et al.*,1967) using fluorescence histochemistry demonstrated a decrease of catecholamine concentration after severe hypoxia in 9-16-day-old and adult rats. The immunoreactivities of the proteins investigated in the present study differed from those of the above neurotransmitters, and the results suggested that the Trx-dependent peroxidase family constitutes one of the main antioxidant systems in mitochondria, which are a major site of reactive oxygen intermediate generation.

In most other organs, hypoxia induces Fos expression, albeit more generally than hypercapnia (Teppema, 1997). However, in the present study, Fos expression was increased after exposure to hypoxia for 12 h, suggesting that Fos regulates the expression of the Trx-dependent perioxidase family.

The present study showed that rats were able to adapt to mild hypoxia. In

rats exposed to isocapnic hypoxia for 24 hours, the glomus cells of the carotid body exhibited intense Trx- and SP-22-like immunoreactivity. In the case for c-fos, animals exposed to the same conditions for 12 hours showed the most intense immunoreactivity. These results suggest that the glomus cells of the carotid body are affected by hypoxia, and that gene expression precedes the changes in both of the antioxidant enzymes themselves.

## REFERENCES

Araki, M., Nanri, H., Ejima, K., Murasato., Y., Fujiwara, T., Nakashima, Y. and Ikeda, M. 1999, Antioxident function of the mitochondorial protein SP-22 in the cardiovascular system. *J. Biol. Chem.* 274, 2271-2278.

Blumcke, S., Rode, J. and Niedorf, H. R. 1967, The carotid body after oxygen deficiency. Z. *Zellforsch.* 80, 52-77.

Bullit, E. 1990, Expression of c-fos-like protein as a marker for neuronal activity following noxious stimulation in the rat. *J. Comp. Neurol.* 296, 517-530.

Dragunow, M. and Faull, R. 1989, The use of c-fos as a metabolic marker in neuronal pathway tracing. *J. Neurosci. Meth.* 29, 261-265.

Erickson, J. T. and Millhorn, D. E. 1994, Hypoxia and electrical stimulation of the carotid sinus nerve induce fos-like immunoreactivity within catecholaminergic and serotonergic neurons of the rat brainstem. *J. Comp. Neurol.* 348, 161-182.

Fernando, M. R., Nanri, H., Yoshitake, S., Nagata-Kuno, K. and Minalkami, S. 1992, Thioredoxin regenerates proteins inactivated by oxidative stress in endothelial cells. *Eur. J. Biochem.* 209, 917-922.

Fidone, S. J., Gonzalez, C. and Yoshizaki, K. 1982, Effects of low oxygen on release of dopamine from the rabbit carotid body in vitro. *J. Physiol.* 333, 93-110.

Graham, R. C. and Karnovsky, M.j. 1966, The early stages of injected horsradish peroxidase in the proximal tubles on mouse kidney: Ultrastructural cytochemistry by a new technique. *J. Histochem. Cytochem.* 14, 291-302.

Hayashida, Y., Hirakawa, H., Nakamura, T. and Maeda, M. 1996, Chemorecepters in autonomic responses to hypoxia in conscious rat. *Adv. Exp. Med. Biol.* 410, 439-442.

Hellstrom, S., Hanbauer, I. and Costa, AE. 1976, Selective decrease of dopamine content in rat carotid body following exposure to hypoxic conditions. *Brain Res.* 118, 352-355 .

Larnicol, N., Wallois, F., Berquin, P., Gros, F. and Rose, D. 1994, c-fos-like immunoreactivity in the cat's neuraxis following moderate hypoxia or hypercapnia. *J. Physiol.* 88, 81-88.

Morgan, J. I. and Curran, T. 1991, Stimulus-transcription coupling in the nervous system: Involvement of the inducible proto-oncogenes fos and jin. *Annu. Rev.Neurosci.* 14, 421-451.

Pietruschka, F., Schafer, D. and Lubbers, D. W. 1977, Effect of oxygen and carbon dioxide on the differentiation of chemosensitive cells (carotid body) in primary tissue culture. *Drug Res.* 27, 450-451.

Sheng, M. and Greenberg, M. E. 1990, The regulation and function of c-fos and other immediate early genes in the nervous system. *Neuron* 4, 477-485.

Teppema, L. J., Veening, J. G., Kranenburug, A., Dahan, A., Berkenbosch, A. and Olievier, C. 1997, Expression of c-fos in the rat brainstem after exposure to hypoxic and to normoxic and hyperoxic hypercapnia. *J. Comp. Neurol.* 388, 169-190.

# Effect of HERG-like Potassium Channel Blocker on the Carotid Body Chemoreception

SHINOBU OSANAI, TORU TAKAHASHI, HITOSHI NAKANO, YOSHINOBU OHSAKI, and KENJIRO KIKUCHI

*First Department of Medicine, Asahikawa Medical College 2-1-1-1 Midorigaoka Higashi, Asahikawa 078-8510, Japan*

## 1. INTRODUCTION

It has been hypothesized that an oxygen sensitive $K^+$ channel ($KO_2$) on the glomus cell plays a central role in hypoxic chemoreception (López-Barneo *et al.*, 1988). This hypothesis, known as "the membrane model", states that hypoxia inhibits conductance of the $KO_2$ channel, leading to depolarization of the cell membrane. Subsequently, the depolarization induces opening of voltage-dependent $Ca^{2+}$ channels and the resultant $Ca^{2+}$ influx. Finally, released neurotransmitters stimulate the terminals of afferent fibers (López-Barneo, 1996).

However, various electrophysiological and pharmacological findings made objection against the membrane hypothesis (for review see Gonzalez *et al.*, 1994; Lahiri *et al.*, 2001). Especially, despite inhibiting $K^+$ current of glomus cell membrane, pharmacological agents such as TEA, 4-AP, and charybdotoxin cause no significant changes in basal carotid sinus nerve (CSN) activity or hypoxic response. Moreover, the $KO_2$ are not active at the reported resting potentials of glomus cells.

On the other hand, the voltage-dependent $K^+$ channels belonging to the ether-à-go-go family are widely expressed in various mammalian organs including cells of neural crest origin (Warmke and Ganetzky 1994; Shi *et al.*,1997). The chief feature of HERG current is a unique inward rectification mechanism, which can contribute to the resting membrane

*Chemoreception*, Edited by Pequignot et al.
Kluwer Academic/Plenum Publishers, New York, 2003

potential in various cell types. Recently, it has been reported that a HERG-like current contributes to control the resting membrane potential of glomus cells, and a specific blocker of HERG-like $K^+$ channel increases intracellular $Ca^{2+}$ in isolated glomus cells and augments the CSN activity (Overholt *et al.*, 1997). Accordingly, HERG-like $K^+$ channel on glomus cell is suitable for a prime candidate for $O_2$ sensing.

The aim of the present study was to investigate whether dofetilide, a potent and specific HERG-like $K^+$ channel blocker (Jurkiewicz and Sanguinetti, 1993), modulates carotid body chemoreception via the same signalling pathway as hypoxia. We thus examined whether extracellular $Ca^{2+}$ was required for the carotid body response to dofetilide.

## 2. METHODS

### Animals and surgical procedures

The Animal Experiment Committee of Asahikawa Medical College approved the present study. Domestic white rabbits, weighing 3.1 to 3.6 kg, were anaesthetized with pentobarbital sodium (30 mg/kg, i.v.) and urethane (1200 mg/kg, i.p.). Isolated perfused carotid bodies were prepared as described in a previous paper (Osanai *et al.*, 1997). In brief, a catheter was inserted into the common carotid artery and all other vessels were tied off, except for the veins. After the CSN was dissected from the glossopharyngeal nerve, the carotid artery bifurcation with the carotid body was immediately removed. The isolated carotid body was perfused with a normoxic and normocapnic solution (pH ~ 7.40, $PCO_2$ ~ 35 mmHg, $PO_2$ ~ 135 mmHg) from a constant-pressure (approximately 65 mmHg) gravity driven reservoir. The temperature of the perfusion chamber and of the fluid reservoirs was maintained by circulating warm water at 37.0 ± 0.5°C. The CSN was desheathed and the nerve fibers were hooked onto bipolar platinum electrodes. Neural discharges were recorded using a differential amplifier with a notch filter (50Hz). The impulses were monitored by an oscilloscope and counted with an electronic amplitude discriminator and a frequency meter. Carotid chemosensory activity was recorded on a printer and transferred to a data acquisition system.

### Materials

The perfusate was a modified Tyrode's solution containing 112 mM NaCl, 4.7 mM KCl, 2.2 mM $CaCl_2$, 1.1 mM $MgCl_2$, 21.4 mM $NaHCO_3$, 5.0 mM HEPES, 5.0 mM glucose, 22.0 mM sodium glutamate, and 4 mg/mL

dextran. For experiments requiring $Ca^{2+}$-free solution, $Ca^{2+}$ was omitted and an equal amount of $Mg^{2+}$ was added to the solution. The normoxic and hypoxic solutions were equilibrated by bubbling with compressed gas, containing 5% $CO_2$ in 21% $O_2$, and 5% $CO_2$ in 3% $O_2$, respectively. Dofetilide was dissolved in 2 ml of dimethyl sulfoxide and stored. They were freshly diluted to adequate concentrations.

## Protocols

(1)The CSN activity was measured with exposure to various dofetilide concentrations (0, 0.1, 1, 10 ?M, n = 6). (2)The effects of both hypoxia (pH ~ 7.40, $PCO_2$ ~ 35 mmHg, $PO_2$ ~ 25 mmHg) and dofetilide on carotid chemoreception were tested in control solution and $Ca^{2+}$-free solution (n = 6).

## Data analysis

Results are presented as the mean ± SEM. Statistical significance was assessed using the Students two-tailed paired *t*-test for comparison between control and treatment groups. P was considered significant at < 0.05.

# 3. RESULTS

The administration of dofetilide increased the frequency of CSN impulses in a dose-dependent manner (Fig. 1). The effect of hypoxia and dofetilide on CSN activity in $Ca^{2+}$-free solution is illustrated in Fig. 2. After switching to a $Ca^{2+}$-free solution, the CSN response to hypoxia was decreased. Contrary, the response to dofetilide was maintained after switched to the $Ca^{2+}$-free solution. The effects of $Ca^{2+}$-free solution on CSN responses to hypoxic and dofetilide are summarized in Fig. 3. Although the $Ca^{2+}$-free solution decreased CSN response to hypoxia, dofetilide stimulated carotid sinus activity under the $Ca^{2+}$-free condition.

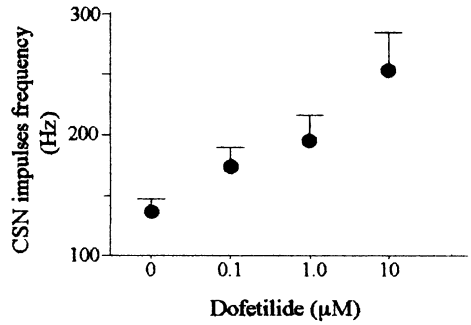


*Figure 1.* Effects of dofetilide on the carotid sinus nerve (CSN) activity. Dofetilide increases CSN impulse frequency in dose-dependent manner.

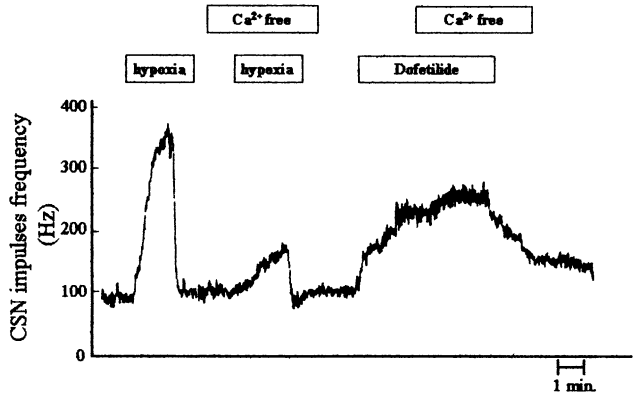


*Figure 2.* Representative record of carotid sinus nerve (CSN) activity. Hypoxia ($Po_2$ ~ 25 mmHg) stimulates CSN activity under normal condition. In the absence of $Ca^{2+}$, CSN response to hypoxia is decreased. Effect of dofetilide (10 μM) on the CSN activity is not reduced by $Ca^{2+}$-free condition.

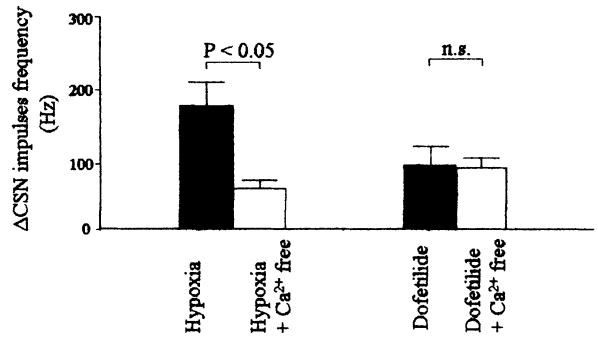


*Figure 3.* Effects of hypoxia ($Po_2$ ~ 25 mmHg) and dofetilide (10 μM) on carotid sinus nerve (CSN) activity under normal condition and $Ca^{2+}$-free condition. ΔCSN = increase of CSN impulse from control condition.

## 4. DISCUSSION

In the present study, the CSN response to hypoxia is dependent on the $Ca^{2+}$ concentration of perfusate, but nonetheless, the effect of dofetilide is independent on the $Ca^{2+}$ concentration. Our result indicates that the effect of dofetilide is different from physiological mechanism of hypoxic chemotransduction in the carotid body. Although (Overholt *et al.*, 2000) described that dofetilide increases $Ca^{2+}$ in cytosol of glomus cells, they did not show the origin of $Ca^{2+}$. If $Ca^{2+}$ influx is not required with the effect of dofetilide, it may increase cytosol $Ca^{2+}$ from intracellular storage of the glomus cells. Therefore, the source of cytosol $Ca^{2+}$ increased by dofetilide will be critical to understand its pharmacological effects.

It has been reported that $Ba^{2+}$, nonspecific inhibitor of background $K^+$ current, leads to depolarization of glomus cell (Buckler et al. 1999) and augments CSN activity (Donnelly., 1997). In addition, $Ba^{2+}$ inhibits HERG-like $K^+$ current (Overholt *et al.*, 2000). Noteworthy, stimulated CSN activity by $Ba^{2+}$ has been observed under $Ca^{2+}$ free condition (Rozanov *et al.*, 2001). From these resemblances, it is possible that the pharmacological effects of dofetilide are similar to the effect of $Ba^{2+}$ on the glomus cell. Also, (Rozanov *et al.*, 2001) have shown that $Ba^{2+}$-stimulated CSN activity is not affected by $Cd^{2+}$ and oligomycin, which inhibit the CSN response to hypoxia. Therefore, they suggested that $Ba^{2+}$ might have direct effect on the afferent fibers. This suggestion may also apply to dofetilide.

## 5. CONCLUSION

The stimulatory effect of dofetilide is different from the hypoxic chemoreception in the carotid bodies.

## REFERENCES

Buckler K.J., 1999, Background leak $K^+$ currents and oxygen sensing in carotid body type 1 cells. *Respir. Physiol.* 115: 179-187.

Donnelly, D.F., 1997, Are oxygen dependent $K^+$ channels essential for carotid body chemotransduction? Respir. Physiol. 110: 211-218.

Jurkiewicz, N.K., and Sanguinetti, M.C., 1993, Rate-dependent prolongation of cardiac action potentials by a methanesulfonanilide class III antiarrythmic agent. Specific block of rapidly activating delayed rectifier $K^+$ current by dofetilide. *Circ. Res.* 72: 75-83.

Gonzalez, C., Almaraz, L., Obeso, A., and Rigual, R., 1994, Carotid body chemoreceptors: from natural stimuli to sensory discharges. *Physiol. Rev.* 74: 829-898.

Lahiri, S., Rozanov, C., Roy, A., Storey, B., and Buerk, D.G., 2001, Regulation of oxygen sensing in peripheral arterial chemoreceptors. *Int. J. Biochem. Cell Biol.* 33: 755-774.

López-Barneo, J., López-López, J.R., Ureña, J., and González, C., 1988, Chemotransduction in the carotid body: $K^+$ current modulated by $Po_2$ in type I chemoreceptor cells. *Science* 241: 580-582.

López-Barneo, J., 1996, Oxygen-sensing by ion channels and the regulation of cellular functions. *Trends Neurosci.* 19: 435-440.

Osanai, S., Buerk, D.G., Mokashi, A., Chugh, D.K., and Lahiri, S., 1997, Cat carotid body chemosensory discharge (*in vitro*) is insensitive to charybdotoxin. *Brain Res.* 747: 324-327.

Overholt, J.L., Ficker, E., Yang, T., Shams, H., Bright, G.R., and Prabhakar, N.R., 2000, HERG-Like potassium current regulates the resting membrane potential in glomus cells of the rabbit carotid body. *J. Neurophysiol.* 83: 1150-1157.

Rozanov, C., Roy, A., Mokashi, A., Daudu, P., and Lahiri, S., 2001, Barium-stimulated chemosensory activity may not reflect inhibition of background voltage-insensitive $K^+$ channels in the rat carotid body. *Brain Res.* 897: 1-8.

Shi W., Wymore, R.S., Wang, H., Pan, Z., Cohen, I.S., McKinnon, D., and Dixon, J.E., 1997, Identification of two nervous system-specific members of the *erg* potassium channel gene family. *J. Neurosci.* 17: 9423-9432.

Warmke, J.W., and Ganetzky, B. 1994, A family of potassium channel genes related to *eag* in *Dorsophilia* and mammals. *Proc. Natl. Acad. Sci.* USA 91, 3438-3442.

# The Effect of Methanandamide on Isolated Type I Cells

CHRISTOPHER N. WYATT and KEITH J. BUCKLER
*University Laboratory of Physiology, Parks Road, Oxford. OX1 3PT. UK.*

## 1. INTRODUCTION

Previous work from this laboratory has demonstrated that hypoxia inhibits a TASK-1 like background $K^+$ current in isolated neonatal rat carotid body type I cells. This inhibition leads to membrane depolarisation and voltage gated $Ca^{2+}$ entry (Buckler, 1997; Buckler *et al*, 2000). Maingret *et al* (2000) have demonstrated that the endocannabinoid anandamide was a direct and selective blocker of TASK-1. Therefore, in this study we have investigated the actions of anandamide and its analogue methanandamide on isolated type I cells.

## 2. METHODS

Rats aged 10-15 days were anaesthetised with 4% halothane; carotid bodies were removed and the rats decapitated. Type I cells were isolated enzymically as described before (Buckler, 1997). Electrophysiological experiments were conducted using the perforated patch clamp technique at 35°C. Currents were evoked by holding cells at -70 mV then stepping to -100 mV and ramping to -40 mV over a 200 ms period at 0.5 Hz.
For experiments recording intracellular $Ca^{2+}$, cells were loaded with the calcium fluorophore Indo-1AM, 2.5 μM for 30 min at room temperature.
All solutions were made up in bicarbonate buffered tyrode gassed with 95% air / 5% $CO_2$. Hypoxia (approximately 6 Torr) was induced by gassing solutions with 95% $N_2$ / 5% $CO_2$.

*Chemoreception*, Edited by Pequignot et al.
Kluwer Academic/Plenum Publishers, New York, 2003

# 3. RESULTS

Hypoxia (6 Torr) caused rapid, robust and reversible rises in intracellular calcium ($[Ca^{2+}]_i$): 844 ± 208 nM (n = 5, mean ± SEM, P< 0.02 Students paired t test) whereas 3 μM anandamide (a concentration known to inhibit TASK-1) evoked no rise in $[Ca^{2+}]_i$ in these cells. See Figure 1.

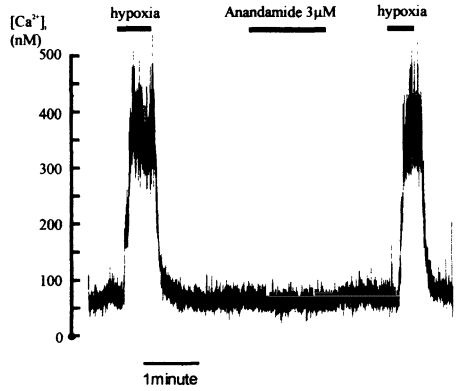


*Figure 1.* An example trace from a type I cell loaded with indo-1AM showing the effects of hypoxia and anandamide

25mM $K^+$ evoked a rise in $[Ca^{2+}]_i$ of 2696 ± 165 nM (n = 6, P< 0.0001). This rise was significantly inhibited by 3.0 μM methanandamide, 76.6 ± 7.7% (n = 6, P< 0.0003). See Figure 2.

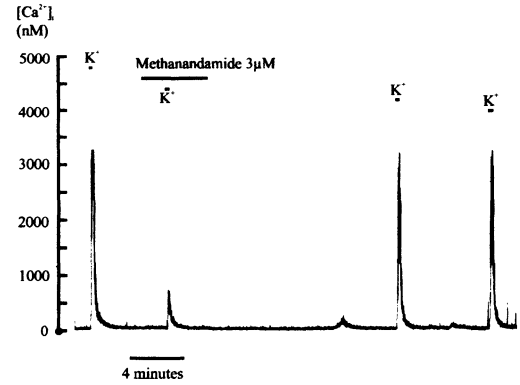


*Figure 2.* An example recording from a cell loaded with indo-1AM. 25mM potassium causes robust rises in intracellular calcium, this is inhibited by methanandamide

The effect of methanandamide on resting membrane conductance was determined using whole cell perforated patch clamp recording. Methanandamide 3 μM significantly reduced resting membrane conductance measured between -60 mV and -50 mV from 311 ± 25.1 pS to 182 ± 22.7 pS (n = 13, P< 0.0001). The reversal potential of the methanandamide sensitive current was approximately -80mV. See fig 3.

In addition it was also noticed that when both methanandamide and hypoxia were applied to the same type I cells no additional inhibition by methanandamide was observed over that caused by hypoxia alone (n = 5), see fig 4A. The hypoxia sensitive current however was significantly inhibited by methanandamide (see fig 4B). At –40 mV methanandamide reduced the hypoxia sensitive current from 9.2 ± 4.1 pA to 2.7 ± 3.9 pA (n = 5, P< 0.02) at -40 mV, see fig 4B.

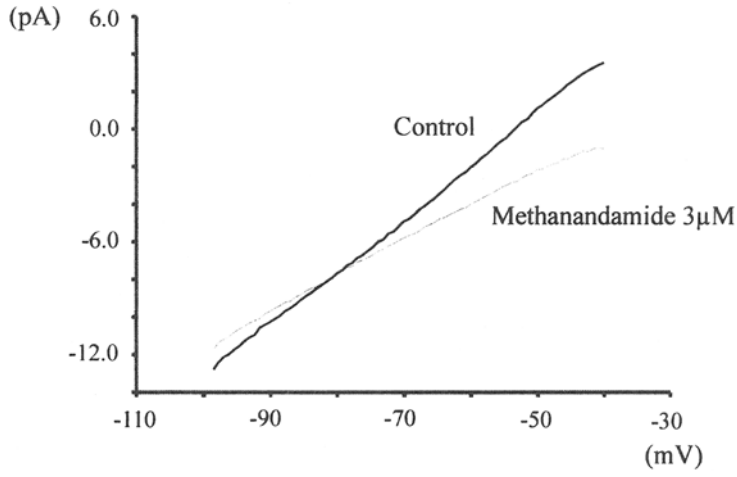


*Figure 3.* The effect of methanandamide on membrane currents in type I cells

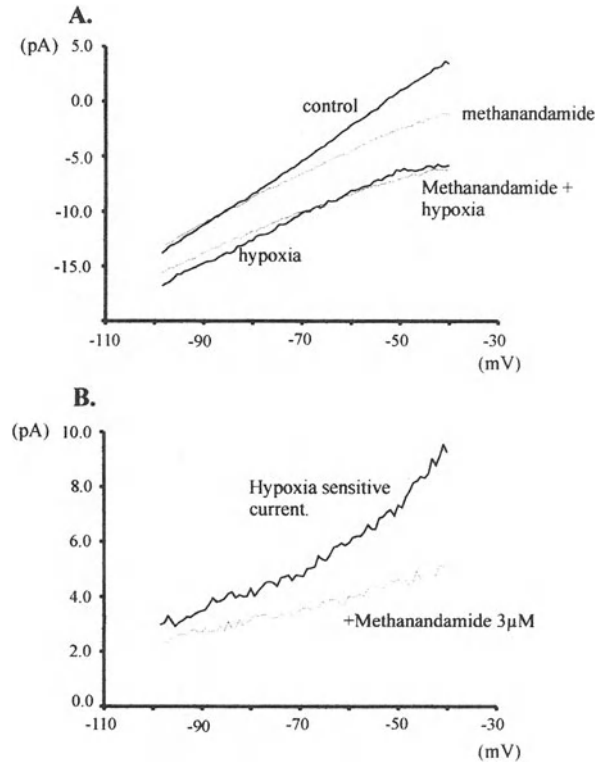


*Figure 4.* A. The effect of methanandamide on membrane currents in the presence and absence of hypoxia. B. Subtracted currents showing the effect of methanandamide on the hypoxia sensitive current

## CONCLUSION

These data indicate that 3 μM methanandamide inhibits type I cell resting membrane conductance. The reversal potential of the methanandamide sensitive current (-80 mV) suggests that this effect is due to the inhibition of a background potassium current. We propose that this is the same background K-current as that inhibited by hypoxia since, in the presence of hypoxia the effect of methanandamide was almost completely abolished. Given these observations, methanandamide might be expected to cause a

membrane depolarisation and voltage gated calcium entry. We did not however observe any increase in intracellular calcium upon application of methanandamide. This is probably explained by fact that methanandamide also appears to inhibit voltage gated calcium entry in these cells as evidenced from the marked reduction in the calcium response to other depolarising stimuli (high K fig 2).

In summary this study has shown that the oxygen sensitive background K-current in type-1 cells is also inhibited by methanandamide a known blocker of TASK-1. This gives further support to the hypothesis that the background oxygen sensitive K-current of type-1 cells is mediated via TASK-like K-channels.

## ACKNOWLEDGEMENTS

This work was supported by the MRC.

## REFERENCES

Buckler KJ, Williams BA, Honore E. 2000, An oxygen-, acid- and anaesthetic-sensitive TASK-like background potassium channel in rat arterial chemoreceptor cells. *J. Physiol.* ;525 Pt 1:135-42.

Buckler KJ, Vaughan-Jones RD. 1998, Effects of mitochondrial uncouplers on intracellular calcium, pH and membrane potential in rat carotid body type I cells. *J. Physiol.*;513 ( Pt 3):819-33

Maingret F, Patel AJ, Lazdunski M, Honore E. 2001, The endocannabinoid anandamide is a direct and selective blocker of the background K(+) channel TASK-1 *EMBO J.*;20(1-2):47-54

# Doxapram Stimulates Carotid Body with Different Mechanisms from Hypoxic Chemotransduction

TORU TAKAHASHI, SHINOBU OSANAI, HITOSHI NAKANO, YOSHINOBU OHSAKI, and KENJIRO KIKUCHI
*First Department of Medicine, Asahikawa Medical College 2-1-1-1 Midorigaoka Higashi, Asahikawa 078-8510, Japan*

## 1. INTRODUCTION

Although it has been known that doxapram has stimulus effect on the carotid body (Mitchell and Herbert, 1975; Nishino, 1982), the mechanism has not yet been explained at the cellular or receptor level. Peers and Wyatt described the electrophysiological effects of doxapram on $K^+$ channels on glomus cells and doxapram can inhibit the $K^+$ current of the glomus cells (Peers, 1991; Wyatt and Peers, 1994). They forwarded a hypothesis that doxapram modulates carotid body chemoreception via the same signaling pathway as "the membrane model of $O_2$ sensing" (for review see López-Barneo, 1996).

The aim of the present study was to investigate this hypothesis. We thus examined whether extracellular $Ca^{2+}$ was required for the carotid body response to hypoxia and/or doxapram. In addition, we studied the effects of various $K^+$ channel activators on carotid body chemoreception. By way of pharmacological tools, we used NS-1619 as a large-conductance $Ca^{2+}$-activated $K^+$ ($BK_{Ca}$) channel activator (Olsen, 1994) and halothane as a TASK-like background $K^+$ channel (TASK-1) activator (Buckler, 2000).

*Chemoreception*, Edited by Pequignot et al.
Kluwer Academic/Plenum Publishers, New York, 2003

## 2. METHODS

Animals and surgical procedures. Male domestic white rabbits, weighing 3.0 to 3.5 kg, were anesthetized with pentobarbital sodium and urethane. Isolated perfused carotid bodies were prepared as described in a previous paper (Osanai, 1997). The isolated carotid body was perfused with a normoxic and normocapnic solution from a constant-pressure (approximately 65 mmHg) gravity driven reservoir. Neural discharges were recorded using a differential amplifier with a notch filter (50Hz). The impulses were monitored by an oscilloscope and counted with an electronic amplitude discriminator and a frequency meter.

Materials. The perfusate was a modified Tyrode's solution (pH $\approx$ 7.40, $P_{CO_2} \approx 35$ mmHg, $P_{O_2} \approx 135$ mmHg). For experiments requiring $Ca^{2+}$-free solution, $Ca^{2+}$ was displaced by an equal amount of $Mg^{2+}$. The normoxic and hypoxic solutions were equilibrated by bubbling with compressed gas, containing 5% $CO_2$ in 21% $O_2$, and 5% $CO_2$ in 3% $O_2$, respectively. Drugs were freshly prepared prior to use. Doxapram hydrochloride was diluted to the desired concentration in Tyrode's solution. NS-1619 and halothane were dissolved in 2 ml of dimethyl sulfoxide and stored. They were freshly diluted to adequate concentrations.

Protocols. (1) The effects of both hypoxia ($P_{O_2} \approx 25$ mmHg) and doxapram (20 μM) on carotid chemoreception were tested in control solution and $Ca^{2+}$-free solution (n = 6). (2) We then compared the effects of NS-1619 (30-μM, n = 6) and halothane (100 μM, n = 6) on the carotid body response to hypoxia and doxapram.

Data analysis. Results are presented as the mean ± SEM. Statistical significance was assessed using the Students two-tailed paired *t*-test for comparison between control and treatment groups.

## 3. RESULTS

The effects of $Ca^{2+}$-free solution on carotid body responses to hypoxic and doxapram are summarized in Fig. 1. The $Ca^{2+}$-free solution decreased carotid body chemoreceptor responses to hypoxia and doxapram.

The effects of NS-1619 on responses of the carotid body to hypoxia and doxapram are shown in Fig. 2. Application of NS-1619 did not change the CSN response to hypoxia. The carotid body response to hypoxia with NS-1619 was similar to that of the control. However, the CSN responses to doxapram were partially decreased by co-administration of NS-1619.

The administration of halothane decreased CSN activity under normoxic conditions. In addition, the CSN responses to hypoxia and doxapram were significantly blocked by halothane (Fig. 3).

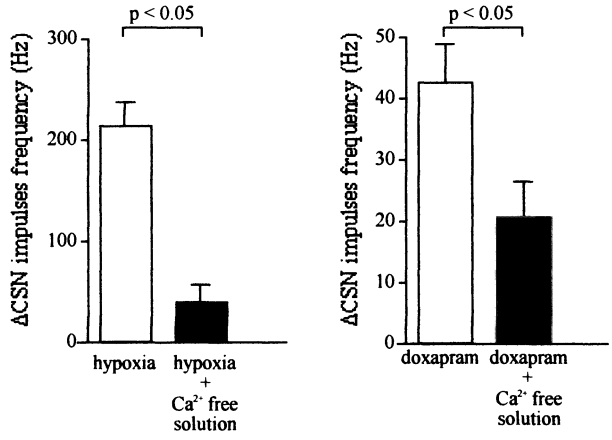


*Figure 1.* Carotid sinus nerve (CSN) responses to hypoxia and doxapram under control condition and $Ca^{2+}$ -free condition. ΔCSN, increase from control; Open bars, control solution; Shaded bars, $Ca^{2+}$ -free solution.

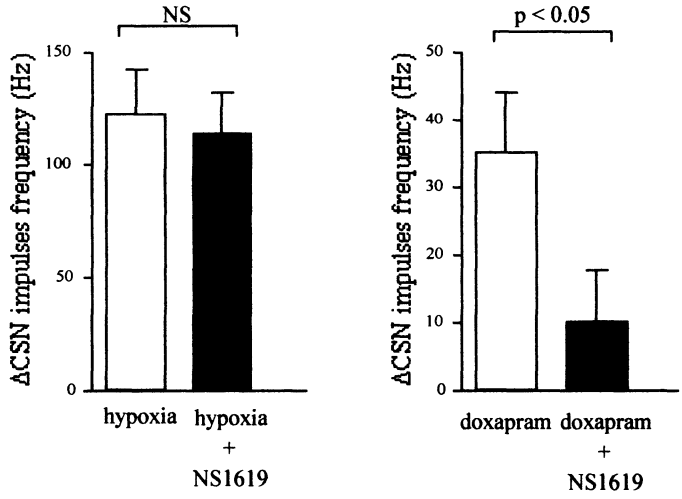


*Figure 2.* Effects of NS-1619 on carotid sinus nerve (CSN) responses to hypoxia and doxapram. ΔCSN, increase from control; Open bars, control solution; Shaded bars, $Ca^{2+}$ -free solution.

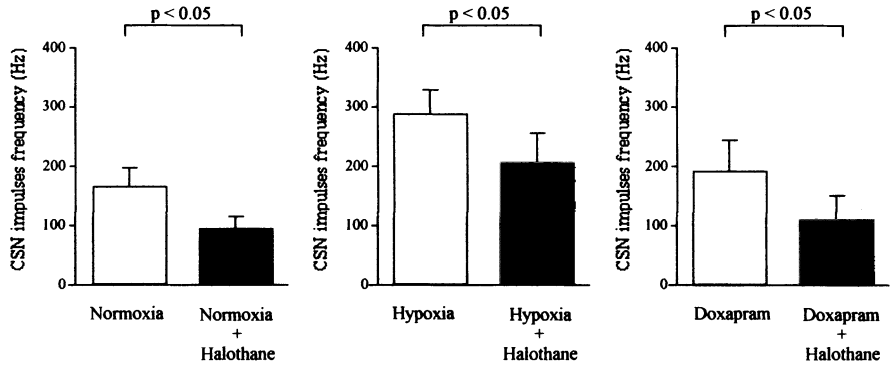


*Figure 3.* Effects of halothane on carotid sinus nerve (CSN) response to hypoxia and doxapram. Open bars, control solution; Shaded bars, $Ca^{2+}$ -free solution.

## 4. DISCUSSION

Our data with regard to the $Ca^{2+}$-dependent effects of doxapram and hypoxia on the carotid body are similar to that of a previous study in which doxapram and hypoxia were observed to cause a similar release in neurotransmitter from isolated glomus cells (Anderson-Beck, 1995). However, as discussed below, doxapram likely stimulates carotid body via a different mechanism from hypoxic chemotransduction.

Doxapram has been reported to inhibit both $Ca^{2+}$-insensitive and $Ca^{2+}$-sensitive $K^+$ channels on glomus cells (Wyatt, 1994). The $Ca^{2+}$-sensitive $K^+$ channels were sensitive to voltage and inhibited by charybdotoxin (CTX), which is a selective $BK_{Ca}$ channel blocker. The present study showed partial inhibition of the effects of doxapram on the carotid body with NS-1619, which supports the results of previous reports. However, the response of the carotid body to hypoxia was not influenced by NS-1619 in the present study. This provides strong evidence that the effects of doxapram differ from those of hypoxia with regard to carotid body chemotransduction.

Buckler et al. have reported expression of oxygen- and acid-sensitive background $K^+$ channels, which are likely to be TASK1-like channels, in glomus cells (Buckler, 2000). They have also shown stimulation of $K_{O_2}$ current by halothane. Therefore, it has been suggested that carotid body chemosensitivity to hypoxia may be inhibited by administration of halothane.

Interestingly, halothane has been found to reduce the hypoxic ventilatory response (Hirshman, 1977; Davies, 1982). In the present study, the effect of halothane on carotid body chemosensory responses to hypoxia is consistent with the observations of previous reports. However, halothane has been observed to reduce carotid body excitation by nicotine (Davies, 1982). It is possible that the depressive effect of halothane is not specific to hypoxic chemotransduction.

## 5. CONCLUSION

We conclude that doxapram might increase chemosensory discharge via inhibition of $BK_{Ca}$ current within the carotid body. However, this mechanism may differ from that which governs hypoxic chemotransduction of the carotid body.

## REFERENCES

Anderson-Beck R, Wilson L, Brazier S, Hughes IE, and Peers C. Doxapram stimulates dopamine release from the intact rat carotid body in vitro. Neurosci Lett 187: 25-28, 1995.

Buckler KJ, Williams BA, and Horore E. An oxygen-, acid- and anaesthetic-sensitive TASK-like background potassium channel in rat arterial chemoreceptor cells. J Physiol (Lond.) 525: 135-142, 2000.

Davies RO, Edwards Jr. MW, and Lahiri S. Halothane depresses the response of carotid body chemoreceptors to hypoxia and hypercapnia in the cat. Anesthesiology 57: 153-159, 1982.

Hirshman CA, McCullough RE, Cohen PJ, and Weil JV. Depression of hypoxic ventilatory response by halothane, enflurane and isoflurane in dogs. Br J Anaesth 49: 957-963, 1977.

López-Barneo J, López-López JR, Ureña J, and González C. Chemotransduction in the carotid body. Science 241: 580-582, 1988.

López-Barneo J. Oxygen-sensing by ion channels and the regulation of cellular functions. Trends Neurosci 19: 435-440, 1996.

Mitchell RA, and Herbert DA. Potencies of doxapram and hypoxia in stimulating carotid-body chemoreceptors and ventilation in anesthetized cats. Anesthesiology 42: 559-566, 1975.

Nishino T, Mokashi A, and Lahiri S. Stimulation carotid chemoreceptors and ventilation and doxapram in the cat. J Appl Physiol 52: 1261-1265, 1982.

Olsen SP, Munch E, Moldt P, and Drejer J. Selective activation of Ca2+-dependent K+ channels by novel benzimidazolone. Eur J Pharmacol 251: 53-59, 1994.

Osanai S, Buerk DG, Mokashi A, Chugh DK, and Lahiri S. Cat carotid body chemosensory discharge (in vitro) is insensitive to charybdotoxin. Brain Res 747: 324-327, 1997.

Peers C. Effects of doxapram on ionic currents recorded in isolated type I cells of the neonatal rat carotid body. Brain Res 568: 116-122, 1991.

Wyatt CN, and C Peers. Ca2+-activated K+-channels from isolated type I carotid body cells of the neonatal rat. Adv Exp Med Biol 360: 159-161, 1994.

# Neuromuscular Blocking Agents and Carotid Body Oxygen Sensing

MALIN JONSSON, STEN G. E. LINDAHL and LARS I. ERIKSSON

*Department of Anesthesiology and Intensive Care Medicine, Karolinska Hospital and Institute, Stockholm, Sweden*

## 1. INTRODUCTION

Ventilatory depression is the leading cause behind anesthesia related postoperative morbidity and mortality worldwide (Lunn *et al.*, 1983). Residual effects of muscle relaxants and general anesthetics are frequently associated with postoperative ventilatory failure and hypoxia. It is known that the ventilatory response to acute hypoxia is mainly mediated by afferent input from peripheral chemoreceptors of the carotid body and from the aortic arch. However, the mechanism behind oxygen sensing of the carotid bodies is not fully known. Recent studies show that hypoxia may block the leak-type potassium channel inducing a depolarisation of the cell membrane of the type I (glomus) cell. This seems to open voltage-gated calcium channels with an inward flux of calcium that result in a release of excitatory neurotransmitters. The activation of the type 1 cell chemotransmission causes an increased activity in the carotid sinus nerve (CSN) which finally gives rise to an increased ventilation.

Several neurotransmitters have been shown to play an important role in the chemotransmission, the most important being dopamine, acetylcholine and possibly substance P (Prabhakar, 2000).

*Chemoreception*, Edited by Pequignot et al.
Kluwer Academic/Plenum Publishers, New York, 2003

There is strong evidence that play an essential role in the chemotransmission of the carotid body. An increased release of acetylcholine has been found during hypoxia, exogenous applied acetylcholine and nicotine increase CSN activity and nicotinic antagonists reduce the CSN activity to hypoxia (Fitzgerald *et al.,* 2000). In addition, the α4 and α7 subunit of the neuronal nicotinic *acetylcholine* receptor (nAChR) have been found in the carotid body and afferent system (Ishizawa *et al.,* 1996; Shirahata *et al.,* 1998) and α2, α3, α4, α5, β2, β4 subunits have been found in total carotid body mRNA (Cohen G, 2002).

Muscle relaxants are used in anesthesia and intensive care to facilitate intubation of the trachea, to provide optimal conditions for the surgeon and in the intensive care unit during certain procedures and to facilitate advanced mechanical ventilation to patients with severe lung failure. Clinically used muscle relaxants have their preferred affinity to the muscle type nAChR and have traditionally been thought to have a very low ganglionic blocking properties. Recent information do not support that neuromuscular blocking agents lack affinity to the neuronal type nAChR (Tassonyi *et al.,* 2002). In contrast, there are evidence that even low concentrations of a neuromuscular blocking compound bind to the neuronal type nAChR that in the very low clinical range even may facilitate channel opening rather than cause an inhibition (Cardone *et al.*, 1994; Chiodini *et al.,* 2001).

## 2. MUSCLE RELAXANTS AND HYPOXIC VENTILATORY RESPONSE IN HUMANS

The clinically used muscle relaxant vecuronium was shown to depress the hypoxic ventilatory response during poikilocapnia and isocapnia in partially paralysed human volunteers (Eriksson *et al.,* 1992; Eriksson *et al.,* 1993). Furthermore, using subparalysing doses of three different muscle relaxants (atracurium, pancuronium and vecuronium) a 30 % reduction in HVR was found (Eriksson, 1996). In the rabbit, a close carotid body injection of vecuronium reduced phrenic nerve activity during hypoxia (Wyon *et al.,* 1996) which may suggest that vecuronium affect the carotid body oxygen sensing during hypoxia.

## 3. MUSCLE RELAXANTS AND CAROTID BODY RESPONSE TO HYPOXIA

To further investigate vecuroniums effect on the carotid body response to hypoxia an *in situ* rabbit chemoreceptor single fibre preparation was used. Single chemoreceptor activity was measured during normoventilation and at four different levels of isocapnic hypoxia before and after 0.1 mg and 0.5 mg vecuronium given systemically. The single fibre chemoreceptor activity to hypoxia was reduced after both 0.1 and 0.5 mg of vecuronium, and the response was reversible (Wyon *et al.*, 1998). Interestingly, these observations occurred at clinically relevant concentrations of vecuronium in the rabbit as demonstrated by simultaneous mechanomyographical recordings of the time course of neuromuscular blockade of the lower limb (Wyon, *et al.*, 1998).

## 4. MUSCLE RELAXANTS AND CHOLINERGIC TRANSMISSION IN THE CAROTID BODY

Based on the above we hypothesized that vecuronium depress the carotid body response to hypoxia due to a blockade of neuronal nAChRs in the carotid body.

Adult New Zealand White rabbits were anesthetized with 50-60 mg pentobarbitone I.V. and tracheostomized. The carotid body and adjacent carotid sinus nerve (CSN) were removed and put into a perfusion chamber. The carotid body was perfused and superfused with modified Tyrodes buffer solution at constant pressure, temperature (37 ± 0.5 ºC) and normocapnia. Samples were taken at regular intervals from the perfusion chamber for analysis of pH, $PCO_2$, $PO_2$, sodium and potassium. Before and after the end of each experiment a hypoxic test was done to assure stability and validity of the preparation over time.

The carotid body was then stimulated with a bolus dose of 500 µg nicotine at regular 30 minute intervals. Registrations were made from the whole CSN and the response were measured as an increase in chemoreceptor discharge frequency (Hz). The method is presented more in detail elsewhere (Jonsson *et al.*, 2002). The preparation was perfused with one of two different types of muscle relaxants, atracurium 28.1 µM or vecuronium 10 µM. Boluses of nicotine were given before after 30 minutes perfusion of one of the relaxant and after a 30 minutes wash-out period.

The nicotine-induced carotid body chemoreceptor response was reduced by 70 ± 30 and 66 ± 19 % (SEM) ($P<0.05$) after perfusion with atracurium and vecuronium respectively, and the depression was reversible after both drugs (Figure 1) (Jonsson *et al.*, 2002). We therefore concluded that atracurium and vecuronium depress nicotine-induced carotid body chemoreceptor response.

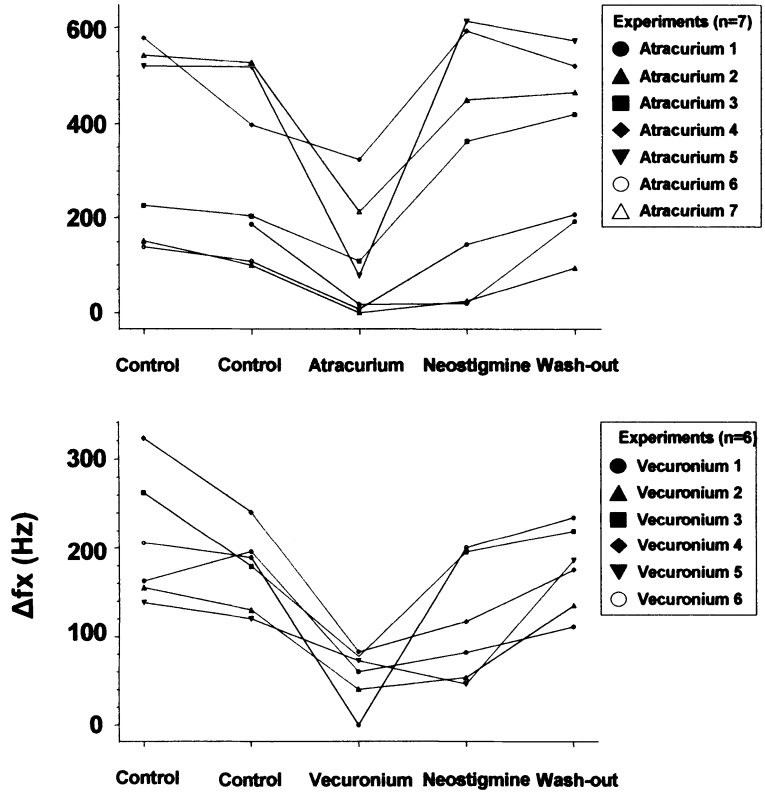


*Figure 1:* Individual chemoreceptor responses to repeated doses of 500μg of nicotine. Initially duplicated controls, after 30 minutes of atracurium respectively vecuronium perfusion, after neostig-mine and finally after 30 minutes wash-out. $\Delta f_X$ = peak $f_X$ - baseline $f_X$

From Jonsson et al 2002 with permission from *Acta Anaesthesiologica Scandinavica.*

## 5. DISCUSSION

We have in a series of experiments showed that 1) clinically used muscle relaxants reduce HVR in humans, 2) a close carotid body injection of vecuronium reduce phrenic nerve activity during hypoxia, 3) vecuronium depress carotid body single fibre chemoreceptor response to hypoxia and 4) nicotine-induced carotid body chemoreceptor activity are depressed by atracurium and vecuronium. Igarashi et al have made similar findings in the carotid body of the rat, showing that vecuronium depress chemoreceptor activity to hypoxia, acetylcholine and to nicotine (Igarashi *et al.*, 2002). Moreover, unpublished observations by our group indicate that there is a dose-dependent relationship between the dose of muscle relaxants and the reduction in chemoreceptor response to nicotine and furthermore that equipotent concentrations of the two different muscle relaxants atracurium and vecuronium depress chemoreceptor activity to the same extent. We therefore speculate that commonly used muscle relaxants have an affinity to neuronal nAChRs in the carotid body. In anesthetic practise it is important to avoid residual neuromuscular block because of the absence of defence against hypoxia. And moreover, the serious consequences of using muscle relaxants in animal experiments investigating the function of carotid body oxygen sensing must be kept in mind.

## ACKNOWLEDGEMENTS

This work was supported by grants from The Medical Research Council (project numbers K2000-04X-13404-01A and K2001-73X-10401-09A), The Karolinska Institute Funds, The AGA AB Research Fund and the Stockholm County Council.

## REFERENCES

Cardone, C., Szenohradszky, J., Yost, S., and Bickler, P. E. (1994). *Anesthesiology* 80, 1155-61; discussion 29A.

Chiodini, F., Charpantier, E., Muller, D., Tassonyi, E., Fuchs-Buder, T., and Bertrand, D. (2001).

*Anesthesiology* 94, 643-51.

Cohen G, H. Z.-Y., Grailhe R, Gallego J, Gaultier C, Changeux J-P, Lagercrantz H. (2002). *PNAS.*

Eriksson, L. I. (1996). *Acta Anaesthesiol Scand* 40, 520-3.

Eriksson, L. I., Lennmarken, C., Wyon, N., and Johnson, A. (1992). *Acta Anaesthesiol Scand* 36, 710-5.

Eriksson, L. I., Sato, M., and Severinghaus, J. W. (1993). *Anesthesiology* 78, 693-9.

Fitzgerald, R. S., Shirahata, M., and Wang, H. Y. (2000). *Adv Exp Med Biol* 475, 485-94.

Igarashi, A., Amagasa, S., Horikawa, H., and Shirahata, M. (2002). *Anesth Analg* 94, 117-22, table of contents.

Ishizawa, Y., Fitzgerald, R. S., Shirahata, M., and Schofield, B. (1996). *Adv Exp Med Biol* 410, 253-6.

Jonsson, M., Kim, C., Yamamoto, Y., Runold, M., Lindahl, S. G., and Eriksson, L. I. (2002). *Acta Anaesthesiol Scand* 46, 488-94.

Lunn, J. N., Hunter, A. R., and Scott, D. B. (1983). *Anaesthesia* 38, 1090-6.

Prabhakar, N. R. (2000). *J Appl Physiol* 88, 2287-95.

Shirahata, M., Ishizawa, Y., Rudisill, M., Schofield, B., and Fitzgerald, R. S. (1998). *Brain Res* 814, 213-7.

Tassonyi, E., Charpantier, E., Muller, D., Dumont, L., and Bertrand, D. (2002). *Brain Res Bull* 57, 133-50.

Wyon, N., Eriksson, L. I., Yamamoto, Y., and Lindahl, S. G. (1996). *Anesth Analg* 82, 1252-6.

Wyon, N., Joensen, H., Yamamoto, Y., Lindahl, S. G., and Eriksson, L. I. (1998). *Anesthesiology* 89, 1471-9.

# The Pulmonary Interstitium: An Introductory Review

GIUSEPPE MISEROCCHI

*Dipartimento di Medicina Sperimentale, Ambientale e Biotecnologie Mediche*
*Università di Milano-Bicocca, Via Cadore 48 20052 MONZA - ITALY*

## 1. INTRODUCTION

The lung tissue serves the main function of gas diffusion. Diffusion for oxygen at alveolar level can be estimated at some 6 x $10^{8}$ liters over a life span, a tremendous amount, requiring specific morphofunctional adaptations of the lung tissue. The air-blood barrier displays in fact two features optimising gas diffusion: it is very thin, about 0.1-0-5 μm due to its delicate structure and furthermore the extravascular space reflects a condition of minimum hydration, in fact one may think of the pulmonary interstitium as a functionally "dry" tissue space. The minimum amount of interstitial water depends upon the dynamic equilibrium established between fluid filtration through a low permeability microvascular district and a powerful lymphatic drainage. Such equilibrium results in a subatmospheric hydraulic pressure of the interstitial space of the order of – 10 $cmH_2O$ (Miserocchi *et al.*, 1990).

*Chemoreception*, Edited by Pequignot et al.,
Kluwer Academic/Plenum Publishers, New York, 2003

## 2. INTERSTITIAL LUNG EDEMA

A major failure of the respiratory function occurs when extravascular water increases as in lung edema. Although a lot is known on the distribution of extravascular water in frank edema, informationon the early phase of fluid accumulation has been acquired only recently. This was made possible by adopting experimental methods causing a slow increase in extravascular lung water that allowed to describe the early events leading to formation of interstitial edema. Three models were used: slow infusion of saline solution (hydraulic type of edema), single bolus injection of elastase (lesional type of edema), exposure to hypoxia (increased permeability edema)(Miserocchi *et al.*, 2001a; Miserocchi *et al.*, 2001b; Negrini *et al.*,1998; Passi *et al.*, 1998; Passi *et al.*, 1999). The study considered the perturbations induced on the macromolecular organisation of the extracellular matrix, on the morphological structure of the air-blood barrier and on the involvement of endothelial cells in this process. In all the models used the increased microvascular fluid filtration occurring in the early phase of interstitial edema, caused an increase in hydraulic interstitial pressure up to about 5 $cmH_2O$.

## 3. MACROMOLECULAR STRUCTURE AND MECHANICAL COMPLIANCE OF THE INTERSTITIAL MATRIX

The study of the early phase of edema development was considered important to elucidate the early mechanisms involved in either tissue repair or, conversely, severe tissue lesion. The increase in interstitial pressure reveals a strong resistance of the lung tissue to an increase in extravascular water. The compliance of the lung tissue, as measured from the ratio between the change in interstitial volume to the change in interstitial pressure is about twenty fold lower as compared to other tissues. The increase in interstitial pressure clearly represents a protective factor against edema development as it opposes further filtration. Proteoglycans are the main matrix molecules controlling the hydration state of the interstitial matrix. These molecules are responsible for two important aspects of interstitial fluid dynamics: they control the sieving properties of the basement membrane and they also provide a low mechanical compliance of the pulmonary interstitium. Perlecan and syndecan are heparansulphate proteoglycans found in the basement membrane and in cell membrane. The copolymeric nature of these proteoglycans chains accounts for specific

interaction properties in basement membrane organisation, receptor function and cell-cell and cell-matrix interactions. Versican is a large chondroitin sulfate proteoglycan found in interstitial matrix where it forms aggregates with hyaluronic acid. Versican possesses a high number of anion charges allowing to display marked hydrophilic properties to control the hydration level of the interstitial space. Despite the fact that proteoglycans represent important "tissue safety factors" against the development of edema, it was found that even a modest increase in interstitial water (about 10-15%) leads to partial fragmentation of these molecules and to a loss of their binding properties to other macromolecules of the matrix (Miserocchi *et al.*, 2001a; Miserocchi *et al.*, 2001b; Negrini *et al.*,1998; Passi *et al.*, 1998; Passi *et al.*, 1999). Fragmentation may reflect either the breaking of non-covalent bonds due to increased parenchymal forces and/or to activation of metalloproteases MMP-2 and MMP-9. In particular, we could demonstrate the presence of a form of MMP-9 expressed by neutrophils (Miserocchi *et al.*, 2001b; Passi *et al.*, 1998; Passi *et al.*,1999). Thus, despite the strong resistance of pulmonary tissue to an increase in extravascular water, yet, even a small increase in hydration state leads to partial fragmentation of the interstitial matrix; therefore pulmonary tissue cells ought to face the functional role of matrix replacement. Severe edema certainly results as a consequence of massive fragmentation of matrix proteoglycans (Miserocchi *et al.* 2001a).

## 4. BIOCHEMISTRY OF ENDOTHELIAL PLASMAMEMBRANES

We wished to further investigate the condition of mild interstitial edema because it represents a critical equilibrium between matrix degradation and deposition provided by cellular activation. We focused on the cellular involvement, particularly the composition of plasma membranes that are known to be sensitive to alterations in chemical and physical stimuli of the environment surrounding the cells. A biochemical study carried on the endothelial cells (Palestini *et al.*, 2002) showed that mechanical stimuli elicited by a modest increase in extravascular water caused significant changes in composition and structure of the plasma membrane. In fact, the increase in interstitial pressure occurring in interstitial edema was found to induce an increase in plasma membrane cholesterol and phosphorus content, suggesting an increase in membrane surface area. Furthermore, NOS activity doubled. These biochemical changes were related to an increase in vesicular formation, in particular caveolae. Caveolae are plasma membrane invaginations about 50-70 nm in

diameter, representing a site for signal transduction but also involved in transcytosis. The biochemical modifications could be related to an increase in fluidity of plasmamembranes. Thus, the suggestion was that mechanical stimuli influencing signal transduction, either at cell surface or through the cytoskeleton, lead to the release of cytokines and other mediators. Endothelial cells, representing the interface sensing both vascular and parenchymal signals, may be primarily involved to trigger transcription factors and protein expression that in turn influence either matrix deposition and tissue repair or, conversely, activate proteases leading to severe tissue damage.

## 5. MORPHOMETRY

A morphometric study (Conforti *et al,* 2002) also showed that in interstitial edema, water accumulation can be detected both in the thin and in the thick portion of the air-blood barrier. In fact, the thickness of the basement membrane of the thin portion of the air-blood barrier was found to increase by 25% while the thickness of the thick portion increased by 35% leading to an increase in interfibrillar distance from 60 to 100 nm. This widening was significantly greater in the more dependent regions of the lung.

## REFERENCES

Conforti, E., Fenoglio, C, Bernocchi, G., Bruschi, O., and Miserocchi, G., 2002, Morpho-functional analysis of lung tissue in mild interstitial edema. *Am. J. Physiol. Lung Cell. Mol. Physiol.* 282: L766-L774.

Miserocchi, G., Negrini, D., and Gonano, C., 1990, Direct measurements of interstitial pulmonary pressure in in-lung with intact pleural space. *J. Appl. Physiol.* 69(6), 2168-2174.

Miserocchi, G., Negrini, D., Passi, A., and De Luca, G., 2001a, Development of lung edema: interstitial fluid dynamics and molecular structure. *News Physiol. Sc.* 16:66-71.

Miserocchi, G., Passi, A., Negrini, D., Del Fabbro, M., and De Luca, G., 2001b, Pulmonary interstitial pressure and tissue matrix structure in acute hypoxia. *Am. J. Physiol. Lung Cel. Mol. Physiol.*. 280:L881-L887.

Negrini, D., Passi, A., De Luca, G, and Miserocchi, G., 1998, Proteoglycan involvement during development of lesional pulmonary edema. *Am. J. Physiol. Lung Cell. Mol. Physiol.* 274: L203-L211.

Palestini,P., Calvi, C., Conforti, E., Botto, L., Fenoglio, C., and Miserocchi, G., 2002, Composition,cell,biophysical properties, and morphometry of plasmamembranes in pulmonary interstitial edema. *Am. J. Physiol. Lung Cel. Mol. Physiol.* 282: L1382-L1390.

Passi, A., Negrini, D., Albertini, R., De Luca, G., and Miserocchi, G., 1998, Involvement of lung interstitial proteoglycans in development of hydraulic- and elastase-induced edema. *Am. J. Physiol. Lung Cell. Mol. Physiol.* 275:L631-L635.

Passi, A., Negrini, D., Albertini, R., Miserocchi, G., and De Luca, G., 1999, The sensitivity of versican from rabbit lung to gelatinase A (MMP-2) and B (MMP-9) and its involvement in the development of hydraulic lung edema. *FEBS letters* 456: 93-96.

# Regulation of $K^+$ Currents by CO in Carotid Body type I Cells and Pulmonary Artery Smooth Muscle Cells

PREM KUMAR[1], ERIC DUBUIS[2], and CHRISTOPHE VANDIER[2]

*[1]Department of Physiology, The Medical School, University of Birmingham, Birmingham B15 2TT, UK. [2]Laboratoire de physiopathologie de la paroi arterielle (LABPART), Faculte de Medecine, 2 bis Boulevard Tonnelle, 37032 Tours, France.*

## 1. INTRODUCTION

Potassium channels are a diverse group of proteins that control membrane excitability and their regulation can influence cell signalling through the modulation of calcium entry. A subset of these channels appears to be particularly sensitive to oxygen tension and these play an important role in the regulation of arterial blood gas tensions. In pulmonary arterial smooth muscle cells, $K^+$ channel activity is linked to contractile tone. Factors that regulate the activity of these channels therefore have a major influence upon blood vessel diameter and therefore on pulmonary artery (PA) blood pressure, thus altering regional ventilation -perfusion ratios in the lung. In carotid body (CB) type I cells, $K^+$ channel activity is linked to the secretion of a variety of putative neurotransmitter and regulation of these channels therefore influences carotid sinus nerve activity and thus cardiorespiratory control. In both systems, hypoxia decreases the activity of a variety of $K^+$ channels, some of which regulate the resting membrane potential. In CB type I cells and in PA smooth muscle cells, hypoxia decreases the activity of the TASK-1 channel (a background $K^+$ channels in type one cells and probably $K_N$ channels in PA (Gurney *et al.*, 2002)), large conductance $Ca^{2+}$-activated ($BK_{Ca}$) channels and/or voltage-activated (Kv) channels depending on species and experimental conditions (Lopez-Barneo *et al.*, 2001).

*Chemoreception*, Edited by Pequignot et al.
Kluwer Academic/Plenum Publishers, New York, 2003

In both In both cases, however, these $K^+$ channels seem to act more as effectors than sensors of the decreased oxygen tension. A better knowledge of the identity of these sensors which seem to differ between PA smooth muscle cells and CB type I cells as well as the mechanism by which they regulate of $K^+$ channel activity is of potential clinical importance in the understanding of a variety of pathological process such as pulmonary hypertension for which there is presently very poor therapeutics. It could be envisaged that drugs could be developed to stimulate selectively the opening of $K^+$ channels by acting upon the relation between specific sensors and $K^+$ channels thus providing, for example, a new class of selective vasodilators.

## 2. A CO-SENSITIVE HAEM PROTEIN AS A SENSOR OF THE HYPOXIC RESPONSE

The diatomic gas, carbon monoxide (CO) is endogenously produced by haem oxygenase (HO) which catalyses the oxidative cleavage of haem to CO, iron and biliverdine (Tenhunen *et al.*, 1968). Three isoforms of HO have been identified; an inducible isoform, HO-1 (induced by hypoxia) and two constitutive isoforms, HO-2 and HO-3 (Durante and Schafer, 1998). CO binds non-covalently to ferrous haem groups in haemoglobin, myoglobin, certain cytochromes and other haem proteins. There may exist a role for endogenous CO-haemoglobin binding in the transport and excretion of CO and perhaps in the facilitation of $O_2$ release as was postulated for another diatomic gas, nitric oxide (Hobbs *et al.*, 2002). CO is a relatively inert biological compound with ligand binding to iron-containing, reduced haemproteins being its major chemical interaction. The primary toxicity of CO is due to its high affinity binding to haemoglobin, locking the compound in the oxy conformation and decreasing oxygen unloading to tissues. This toxicity is perhaps an unfortunate consequence of industrialisation and the production of high quantities of exogenous CO. Nevertheless, exogenous CO at a variety of tensions can and have been used as a good tool to support the hypothesis that oxygen sensors are haem proteins. In this brief review we summarise some of the main findings obtained by ourselves and others on the interaction between CO-induced effects and membrane $K^+$ channels in both CB type I cells and PA smooth muscle cells.

### 2.1 A High PCO/PO2 ratio mimics the effect of acute hypoxia on $K^+$ currents in CB Type I Cells

CO when applied at a high partial pressure relative to $O_2$ has long been known to act like hypoxia by decreasing oxygen consumption in the carotid body and increasing sinus nerve discharge in both multi-fibre and single-fibre recordings and in both *in vivo* and *in vitro* preparations (Conway *et al.*,

1997; Joels and Neil, 1962; Lahiri *et al.*, 1995; Lahiri *et al.*, 1993; Osanai *et al.*, 1996). This effect is photolabile, being largely, but not completely inhibited by light, suggesting an action upon mitochondrial cytochromes, most likely through the formation of a CO-complex with cytochrome $a_3$ as confirmed with photometry studies (Wilson *et al.*, 1994). The CO effect upon sinus nerve discharge is dependent upon extracellular $Ca^{2+}$ and, more crucially, upon voltage gated $Ca^{2+}$ entry (Barbe *et al.*, 2002). This suggests an action via neurotransmitter release and, indeed, high tensions of CO have been shown to cause the release of dopamine from type I cells (Buerk *et al.*, 1997). In contrast, however, to the effect upon discharge, the effect of CO upon dopamine release is not affected by light and this has been suggested to indicate a photolabile effect of CO upon chemoafferent nerve endings (Lahiri and Acker, 1999). No direct evidence for this suggestion has yet been provided, and whilst it may be that transmitters other than dopamine are involved, the effect of CO upon transmitter release does itself suggest that there is an additional effect upon type I cells.

The first studies on isolated type I cells and CO used rabbit type I cells and demonstrated that CO could act like $O_2$ rather than like a lack of $O_2$ in that CO could reverse the action of hypoxia upon membrane $K^+$ currents (Lopez-Lopez and Gonzalez, 1992). This study and a subsequent one in rat type I cells (Riesco-Fagundo *et al.*, 2001) thus concluded that carotid body cells contained a membrane bound haem protein that might act as a sensor of oxygen desaturation – an idea mooted previously by Lloyd and colleagues (Lloyd *et al.*, 1968) based upon the similarity in shape of the oxygen-haemoglobin desaturation curve and the response curve of the carotid body to hypoxia. Indeed, if $P_{CO}/P_{O_2}$ ratios of 1 or less are used, the sensitivity of the carotid body to $CO_2$ is reduced (Conway *et al.*, 1997)– an effect also not dissimilar to that of $O_2$ alone. Presumably, in these experiments, the degree of CO used was not sufficient to inhibit mitochondrial electron transport and decrease $O_2$ consumption.

If a $P_{CO}/P_{O_2}$ ratio of greater than 2 is used, however, effects similar to hypoxia can be observed (Barbe *et al.*, 2001; Barbe *et al.*, 2002). Thus, in type I cells isolated from adult rat carotid bodies, we demonstrated that CO could cause a readily reversible depolarisation of around 10mV from the resting membrane potential but, critically, only when these current clamp experiments were performed using the perforated patch configuration where cell access is obtained through the use of the antibiotic, amphotericin B. In cells examined with the standard, whole cell configuration, CO was without effect and we took this to suggest an absolute requirement for intracellular signalling based upon the idea that the whole cell but not the perforated patch configuration would give rise to significant intracellular dialysis. The

depolarising effect of CO was, however, not photolabile. This was confirmed in studies where current-voltage relations between –90 and +30mV were determined in isolated type I cells, demonstrating a similar *ca.* 10mV magnitude, rightward shift in the position of the zero current crossing and a decrease of ca. 40% in the resting membrane conductance between –50 and –60mV– effects that were not photolabile. The reversal potential of the CO effect was shifted as predicted by increasing external [$K^+$] and the effect was not blocked by a solution containing TEA, 4-AP, $Ni^{2+}$ and zero $Ca^{2+}$. Taken together, these findings, we suggested, demonstrated that high tensions of CO could act in a non-photolabile, reversible manner upon type I cell mitochondria leading to an intracellular signal-dependent inactivation of a number of $K^+$ currents including those carried through background leak (presumably TASK-1; (Buckler *et al.*, 2000)) channels.

## 2.2 Chronic low ratio of CO/O2 increases $K^+$ currents and prevents Chronic Hypoxia decrease of $K^+$ currents

PA smooth muscle cells have a high input resistance in the resting state (reported as 18 GOhms by Evans et *al.*(1996) and 4.7 GOhm by Park et *al.*, (1997)) that corresponds to low ionic channel activity near the resting membrane potential. As a consequence of the opening or closure of just a few channels can cause a substantial change in membrane potential and thus modification of arterial tone. On the other hand, PA smooth muscle cells have a high density of $BK_{Ca}$ channels and Kv channels. Both of these channels regulate the resting membrane potential of PA smooth muscle cells (Bae *et al.*, 1999; Osipenko *et al.*, 1998; Vandier *et al.*, 1998) and $BK_{Ca}$ is suspected to act as a feedback mechanism in the regulation of $Ca^{2+}$ entry (Brayden and Nelson, 1992); thus they are important in regulating pulmonary arterial tone (Standen and Quayle, 1998) and a deregulation of these $K^+$ channels could change reactivity of vascular smooth muscle.

It's well known that prolonged exposure to alveolar hypoxia (chronic hypoxia) induces physiological pulmonary vascular remodeling that results in the development of pulmonary hypertension (Reeves *et al.*, 1979). A hallmark of pulmonary hypertension is an increase of pulmonary vascular resistance with sustained pulmonary vasoconstriction *via* depolarization of PA smooth muscle cells (Shimoda *et al.*, 2000). This hypoxia-induced membrane depolarization was mainly due to reduced expression of $\alpha$ subunit protein of Kv (Platoshyn *et al.*, 2001; Wang *et al.*, 1997) and of decreased $BK_{Ca}$ channels activity (Peng *et al.*, 1997).

Acute exposure to CO has been shown to activate $BK_{Ca}$ channels in tail artery smooth muscle cells of rats (Wang *et al.*, 1997) and, in the pulmonary

circulation, exogenous CO decreases vascular resistance (Duke and Killick, 1952) and inhibits hypoxic pulmonary vasoconstriction (Tamayo *et al.*, 1997) probably by a direct vasorelaxing effect of CO on smooth muscle cells (Steinhorn *et al.*, 1994). Nevertheless, there is no direct evidence that CO is able to increase $BK_{Ca}$ in PA smooth muscle cells. Furthermore, the physiological and pathological importance of endogenous CO on $K^+$ channel functions had not been studied directly. Indeed, only studies using blockers of HO to inhibit endogenous CO production and were performed and only in systemic vessels (Kaide *et al.*, 2001; Liu *et al.*, 1999; Zhang *et al.*, 2001). Recently, we demonstrated that chronic CO (rats were placed in an exposure chamber inflated by an air-CO mixture for 3 weeks at 530 p.p.m) increases $BK_{Ca}$ currents which hyperpolarized resistance PA smooth muscle cells (Dubuis *et al.*, 2002). Furthermore, the resting membrane potential of PA smooth muscle cells isolated from chronic CO-exposed rats was more negative than controls and this was associated with a decrease of membrane resistance in these cells. Chronic CO also hyperpolarized the membrane potential of pressurized PA vessels and blockers of $BK_{Ca}$ depolarized membranes of smooth muscle cells from arteries isolated from chronic CO-exposed rats but not those from normal rats suggesting a control of the resting membrane potential by $BK_{Ca}$ in chronic CO-exposed rats.

Sustained activation or overexpression of HO-1 prevents the development of hypoxic pulmonary hypertension (Christou *et al.*, 2000; Minamino *et al.*, 2001) and exogenous CO activates $BK_{Ca}$ currents. Thus, we speculate that chronic CO could prevent chronic hypoxic pulmonary hypertension in rats by increasing the functionality of $BK_{Ca}$ channels. We demonstrated this point and showed that if chronic hypoxia induced a significant increase of membrane resistance of PA smooth muscle cells, this effect was prevented in cells isolated from chronic hypoxic rats exposed to CO, an effect linked to an increase of $BK_{Ca}$ currents.

## 3. CONCLUSION

Like hypoxia, CO can also modulate a variety of $K^+$ currents in two different oxygen sensing cell types; CB type I cells and PA smooth muscle cells. This action of CO is most likely mediated through complex formation with an oxygen sensing-haem protein(s) that may be located in both intra- and extra-mitochondrial locations. Opposite effects of this gas on $K^+$ currents can be obtained by using different $PCO/PO_2$ ratios, indicating that CO can be used as a tool to mimic hypoxia in the CB or as oxygen in the prevention of hypoxic pulmonary vasoconstriction in the PA circulation.

## ACKNOWLEDGEMENTS

This work was supported by grants from The Wellcome Trust and l'Agence De l'Environnement et de la Maîtrise d'Energie (ADEME).

## REFERENCES

Bae, Y.M., Park, M.K., Lee, S.H., Ho, W.K., and Earm, Y.E., 1999, Contribution of Ca2+-activated K+ channels and non-selective cation channels to membrane potential of pulmonary arterial smooth muscle cells of the rabbit. *J Physiol* 514: 747-58.

Barbe, C., Al-Hashem, F., Conway, A.F., Dubuis, E., Vandier, C., and Kumar, P., 2001, Effect of carbon monoxide on whole cell currents of the isolated rat carotid body type I cell. *J Physiol* 533: 108P-109P.

Barbe, C., Al-Hashem, F., Conway, A.F., Dubuis, E., Vandier, C., and Kumar, P., 2002, A possible dual site of action for carbon monoxide-mediated chemoexcitation in the rat carotid body. *J Physiol* 543: 933-45.

Brayden, J.E., and Nelson, M.T., 1992, Regulation of arterial tone by activation of calcium-dependent potassium channels. *Science* 256: 532-5.

Buckler, K.J., Williams, B.A., and Honore, E., 2000, An oxygen-, acid- and anaesthetic-sensitive TASK-like background potassium channel in rat arterial chemoreceptor cells. *J Physiol* 525 Pt 1: 135-42.

Buerk, D.G., Chugh, D.K., Osanai, S., Mokashi, A., and Lahiri, S., 1997, Dopamine increases in cat carotid body during excitation by carbon monoxide: implications for a chromophore theory of chemoreception. *J Auton Nerv Syst* 67: 130-6.

Christou, H., Morita, T., Hsieh, C.M., Koike, H., Arkonac, B., Perrella, M.A., and Kourembanas, S., 2000, Prevention of hypoxia-induced pulmonary hypertension by enhancement of endogenous heme oxygenase-1 in the rat. *Circ Res* 86: 1224-9.

Conway, A.F., Pepper, D.R., and Kumar, P., 1997, Dose-dependent modulation of carotid body CO2-O2 interaction by carbon monoxide. *J Physiol* 504: 201P-202P.

Dubuis, E., Gautier, M., Melin, A., Rebocho, M., Girardin, C., Bonnet, P., and Vandier, C., 2002, Chronic carbon monoxide enhanced IbTx-sensitive currents in rat resistance pulmonary artery smooth muscle cells. *Am J Physiol Lung Cell Mol Physiol* 283: L120-9.

Duke, H.N., and Killick, E.M., 1952, Pulmonary vasomotor responses of isolated perfused cat lung to anoxia. *J Physiol* 117: 303-316.

Durante, W., and Schafer, A.I., 1998, Carbon monoxide and vascular cell function (Review). *Int J Mol Med* 2: 255-262.

Gurney, A.M., Osipenko, O.N., MacMillan, D., and Kempsill, F.E., 2002, Potassium channels underlying the resting potential of pulmonary artery smooth muscle cells. *Clin Exp Pharmacol Physiol* 29: 330-3.

Hobbs, A.J., Gladwin, M.T., Patel, R.P., Williams, D.L., and Butler, A.R., 2002, Haemoglobin: NO transporter, NO inactivator or NOne of the above? *Trends Pharmacol Sci* 23: 406-11.

Joels, N., and Neil, E., 1962, The action of high tensions of carbon monoxide on the carotid chemoreceptors. *Archives Internationales de Pharmacodynamie et de Thérapie* 139: 528-534.

Kaide, J.I., Zhang, F., Wei, Y., Jiang, H., Yu, C., Wang, W.H., Balazy, M., Abraham, N.G., and Nasjletti, A., 2001, Carbon monoxide of vascular origin attenuates the sensitivity of renal arterial vessels to vasoconstrictors. *J Clin Invest* 107: 1163-71.

Lahiri, S., and Acker, H., 1999, Redox-dependent binding of CO to heme protein controls P(O2)-sensitive chemoreceptor discharge of the rat carotid body. *Respir Physiol* 115: 169-77.

Lahiri, S., Buerk, D.G., Chugh, D., Osanai, S., and Mokashi, A., 1995, Reciprocal photolabile O2 consumption and chemoreceptor excitation by carbon monoxide in the cat carotid body: evidence for cytochrome a3 as the primary O2 sensor. *Brain Res* 684: 194-200.

Lahiri, S., Iturriaga, R., Mokashi, A., Ray, D.K., and Chugh, D., 1993, CO reveals dual mechanisms of O2 chemoreception in the cat carotid body. *Respir Physiol* 94: 227-40.

Liu, H., Mount, D.B., Nasjletti, A., and Wang, W., 1999, Carbon monoxide stimulates the apical 70-pS K+ channel of the rat thick ascending limb. *J Clin Invest* 103: 963-70.

Lloyd, B.B., Cunningham, D.J.C., Goode, R.C., Joels, N., and Neil, E., 1968, Depression of hypoxic hyperventilation in man by sudden inspiration of carbon monoxide. In *Arterial Chemoreceptors* (R. W. Torrance, eds), Blackwell, Oxford, pp. 145-148.

Lopez-Barneo, J., Pardal, R., and Ortega-Saenz, P., 2001, Cellular mechanism of oxygen sensing. *Annu Rev Physiol* 63: 259-87.

Lopez-Lopez, J.R., and Gonzalez, C., 1992, Time course of K+ current inhibition by low oxygen in chemoreceptor cells of adult rabbit carotid body. Effects of carbon monoxide. *FEBS Lett* 299: 251-4.

Minamino, T., Christou, H., Hsieh, C.M., Liu, Y., Dhawan, V., Abraham, N.G., Perrella, M.A., Mitsialis, S.A., and Kourembanas, S., 2001, Targeted expression of heme oxygenase-1 prevents the pulmonary inflammatory and vascular responses to hypoxia. *Proc Natl Acad Sci U S A* 98: 8798-803.

Osanai, S., Chugh, D.K., Mokashi, A., and Lahiri, S., 1996, Stimulus interaction between CO and CO2 in the cat carotid body chemoreception. *Brain Res* 711: 56-63.

Osipenko, O.N., Alexander, D., MacLean, M.R., and Gurney, A.M., 1998, Influence of chronic hypoxia on the contributions of non-inactivating and delayed rectifier K currents to the resting potential and tone of rat pulmonary artery smooth muscle. *Br J Pharmacol* 124: 1335-7.

Peng, W., Hoidal, J.R., Karwande, S.V., and Farrukh, I.S., 1997, Effect of chronic hypoxia on K+ channels: regulation in human pulmonary vascular smooth muscle cells. *Am J Physiol* 272: C1271-8.

Platoshyn, O., Yu, Y., Golovina, V.A., McDaniel, S.S., Krick, S., Li, L., Wang, J.Y., Rubin, L.J., and Yuan, J.X., 2001, Chronic hypoxia decreases K(V) channel expression and function in pulmonary artery myocytes. *Am J Physiol Lung Cell Mol Physiol* 280: L801-12.

Reeves, J.T., Wagner, W.W., Jr., McMurtry, I.F., and Grover, R.F., 1979, Physiological effects of high altitude on the pulmonary circulation. *Int Rev Physiol* 20: 289-310.

Riesco-Fagundo, A.M., Perez-Garcia, M.T., Gonzalez, C., and Lopez-Lopez, J.R., 2001, O(2) modulates large-conductance Ca(2+)-dependent K(+) channels of rat chemoreceptor cells by a membrane-restricted and CO-sensitive mechanism. *Circ Res* 89: 430-6.

Shimoda, L.A., Sham, J.S., and Sylvester, J.T., 2000, Altered pulmonary vasoreactivity in the chronically hypoxic lung. *Physiol Res* 49: 549-60.

Standen, N.B., and Quayle, J.M., 1998, K+ channel modulation in arterial smooth muscle. *Acta Physiol Scand* 164: 549-57.

Steinhorn, R.H., Morin, F.C., and Russell, J.A., 1994, The adventitia may be a barrier specific to nitric oxide in rabbit pulmonary artery. *J Clin Invest* 94: 1883-8.

Tamayo, L., Lopez-Lopez, J.R., Castaneda, J., and Gonzalez, C., 1997, Carbon monoxide inhibits hypoxic pulmonary vasoconstriction in rats by a cGMP-independent mechanism. *Pflugers Arch* 434: 698-704.

Tenhunen, R., Marver, H.S., and Schmid, R., 1968, The enzymatic conversion of heme to bilirubin by microsomal heme oxygenase. *Proc Natl Acad Sci U S A* 61: 748-55.

Vandier, C., Delpech, M., and Bonnet, P., 1998, Spontaneous transient outward currents and delayed rectifier K+ current: effects of hypoxia. *Am J Physiol* 275: L145-54.

Wang, J., Juhaszova, M., Rubin, L.J., and Yuan, X.J., 1997, Hypoxia inhibits gene expression of voltage-gated K+ channel alpha subunits in pulmonary artery smooth muscle cells. *J Clin Invest* 100: 2347-53.

Wang, R., Wu, L., and Wang, Z., 1997, The direct effect of carbon monoxide on KCa channels in vascular smooth muscle cells. *Pflugers Arch* 434: 285-91.

Wilson, D.F., Mokashi, A., Chugh, D., Vinogradov, S., Osanai, S., and Lahiri, S., 1994, The primary oxygen sensor of the cat carotid body is cytochrome a3 of the mitochondrial respiratory chain. *FEBS Lett* 351: 370-4.

Zhang, F., Kaide, J., Wei, Y., Jiang, H., Yu, C., Balazy, M., Abraham, N.G., Wang, W., and Nasjletti, A., 2001, Carbon monoxide produced by isolated arterioles attenuates pressure-induced vasoconstriction. *Am J Physiol Heart Circ Physiol* 281: H350-8.

# Ionotropic Receptors in Pulmonary Neuroepithelial Bodies (NEB) and their Possible Role in Modulation of Hypoxia Signalling

ERNEST CUTZ , X.W. FU and CA. NURSE[†]

*Division of Pathology, Department of Paediatric Laboratory medicine, The Research Institute, The Hospital for Sick Children and University of Toronto, Toronto, Ontario, Canada M5G 1X8.*
*[†]Department of Biology, McMaster University, Hamilton, Ontario, Canada L8S 4K1*

## 1. INTRODUCTION

The neuroepithelial bodies (NEB) are specialized pulmonary structures composed of clusters of innervated amine- and peptide-containing cells, widely distributed within airway mucosa of human and animal lung (Lauweryns *et al.*, 1972). NEB cells are preferentially located at or near airway bifurcations, a site ideally suited for sensing changes in airway gas concentration. NEB cells express a membrane-bound $O_2$ sensor protein, NADPH oxidase, which appears to function in association with $O_2$ sensitive $K^+$ channels (Wang *et al.*, 1996; Fu *et al.*, 1999, 2002). In these specialized receptor cells, hypoxia inhibits $Ca^{2+}$–dependent and $Ca^{2+}$-independent $K^+$ channels, leading to an increase in cell firing or a facilitation of membrane depolarization (Youngson *et al.*, 1993). These events are proposed to stimulate neurotransmitter release, which in turn activates second order vagal chemoafferent neurons (Fu *et al.*, 2001). The candidate neurotransmitters involved in chemotransduction of hypoxia stimulus in NEB cells are similar to those proposed for the carotid body glomus cells i.e., serotonin (5-HT), acetycholine (ACh) and ATP (Zhang and Nurse, 2000). Earlier studies reported hypoxia-induced 5-HT release from NEB cells in vivo in neonatal rabbits, and in cultures of NEB cells isolated from

*Chemoreception*, Edited by Pequignot et al.
Kluwer Academic/Plenum Publishers, New York, 2003

rabbit fetal lungs (Cutz *et al.*, 1993, Lauweryns *et al.*, 1972). More recently, using a highly sensitive carbon fiber amperometry technique we have shown hypoxia-induced 5-HT release directly from rabbit NEB cells in fresh lung slices with a graded response to different levels of hypoxia (Fu *et al,*. 2002). Mophological studies demonstrated co-localization of 5-HT and 5-$HT_3$-R immunoreactivity in the same NEB cell (Fu *et al.*, 2001). Recent studies have shown that both human and rodent bronchial epithelial cells express nAChR containing α3, α5, α7 and β2 or β4 subunits (Maus *et al,*. 1998). Other studies on monkey lungs have reported localization of nAChR α7 subunit in airway epithelial cells as well as in NEB cells (Sekhon *et al.*,,1999). In the rat, the efferent cholinergic (VACHT-immunoreactive) fibers appear to innervate NEB cells, as well as TH-immunopositive postganglionic sympathetic nerve fibres (Brouns, *et al.*, 2000). We report here morphological and electrophysiological evidence that the nAChR β2 and α7 subunits are co-expressed in the same NEB cells, giving rise to a heterogeneous population of ion channels. Thus, NEB cells may act as a modulator of cell proliferation under conditions of chronic nicotine exposure. This could be critical during lung development since the release of 5-HT and other peptides from NEB cells could affect adjacent bronchovascular structures by targeting airway and/or vascular smooth muscle cells and associated nerve endings (Cutz and Jackson, 1999).

## 2. RESULTS AND DISCUSSION

### 2.1 NEB cells in mammalian lung express functional serotonin-type 3 (5-$HT_3$) receptor

We demonstrated expression of 5-$HT_3$-R mRNA in NEB cells in the lungs of different mammals (hamster, rabbit, mouse and human). Dual immunocytochemistry (for 5-HT and 5-$HT_3$-R) and confocal microscopy localized 5-$HT_3$-R on NEB cell plasma membrane. The electrophysiological characteristics of 5-$HT_3$-R in NEB cells were studied in fresh slices of neonatal hamster lung using whole-cell patch clamp technique. Application of 5-HT (10-100 μM) and 5-$HT_3$-R agonist 2-methyl-5HT (10-100 μM) induced inward currents in a concentration-dependent manner. The 5-HT induced current was blocked (76.5 ± 5.9% n= 10) by specific 5-$HT_3$-R antagonist ICS 205-930 (50 μM), while ketanserin (5-$HT_2$ receptor antagonist) and p-MPP (5- $HT_{1A}$, antagonist) had minimal effects. Forskolin had no effect on desensitization and amplitude of 5-HT induced current. The reduction of $Ca^{2+}$ and $Mg^{2+}$ in the extracelluar solution enhanced the amplitude of the 5-HT induced current because of slower desensitization (Fu

*et al.*, 2001). These studies raise the possibility that 5-$HT_3$-R in NEB cells may function as autoreceptors which modulate hypoxic signaling via autocrine or paracrine mechanisms. In order to test this idea, we examined the effects of hypoxia on the release of serotonin (5-HT) from intact NEB cells in neonatal rabbit lung slices preparation (Fu *et al.*, 2002). The secretory response of NEB cells exposed to hypoxia was studied in the presence of ICS 205 930 (50 μM), a specific 5-$HT_3$-R blocker. The mean amperometric spike frequency was reduced from 0.38 ± 0.05 Hz (n=12) in hypoxia alone to 0.12 ± 0.04 Hz (n =7, $p<0.05$) in hypoxia plus ICS 205 930 , corresponding to ~68% inhibition of the response (Fig.1). This finding suggests that during hypoxia activation of 5-$HT_3$ autoreceptors facilitates 5-HT release from NEB cells by a positive feedback mechanism (Fu *et al.*, 2002).

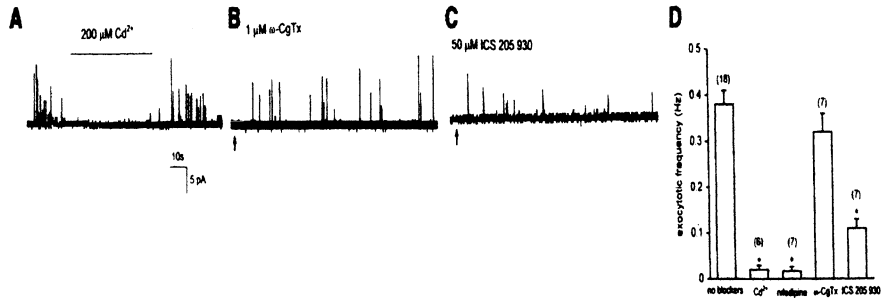


*Figure 1. Effects of $Ca^{2+}$ channels blockers and 5-$HT_3$-R blocker on hypoxia-induced secretory reponses.* ***A****, Example of amperometric recording of exocytosis evoked from NEB cell following exposure to hypoxia ($pO_2$ =18 mmHg). Exocytosis was abolished by switching solution to one of the same $pO_2$ but also containing 200 μM $Cd^{2+}$.* ***B****, Example of amperometric recording of exocytosis evoked from NEB cell following exposure to N-type $Ca^{2+}$ blocker, 1 μM ω-CgTx.* ***C****, Example of amperometric recording of exocytosis evoked from NEB cell following exposure to 5-$HT_3$-R blocker, 50 μM ICS 205 930.* ***D****, Bar graph showing mean frequency of exocytosis evoked by hypoxia (no blockers) in the presence of different selective blockers of voltage-gated $Ca^{2+}$ channels and 5-HT-$_3$-R blocker. Cells were exposed either $Cd^{2+}$ (200 μM), or nifedipine (2 μM) or –CgTx (1 μM), and ICS 205 930 ( 50 μM ), as indicated at each bar. Each bar represents mean ± SEM determined from the number of cells indicated in parentheses (* $p < 0.05$) (from Fu et al., 2002).*

## 2.2 Expression of functional nicotinic acetylcholine receptors in NEB cells of neonatal hamster lung

We used non-isotopic *in situ* hybridization method to localize mRNA for β2 subunit of nAChR in NEB cells. Double label immunofluoresence technique confirmed co-expression of β2 and α7 subunits of nAChR in NEB cells, and β2 and α7 co-expression with 5-HT, a marker of NEB cells (Fu *et al.*, 2001).

The electrophysiological characteristics of nAChR in NEB cells were studied using whole-cell patch-clamp technique on fresh lung slices. Application of nicotine (0.1μM ~ 100μM) evoked inward currents that were concentration-dependent ($EC_{50}$ = 3.8μM; Hill Coefficient = 1.1). Acetycholine (100μM) and nicotine (50μM) produced two types of currents. In most NEB cells, nicotine-induced currents had a single desensitization component that was blocked by mecamylamine (Mec, 50μM) and dihydro-β-erythroidine (DHβE, 50μM). In some NEB cells, nicotine-induced current had two components, one with fast and the second with slowly desensitizing kinetics. The fast component was selectively blocked by methyllycacotine (MLA,10 nM), whereas both components were inhibited by Mec. Choline (0.5 mM) also induced an inward current that was abolished by 10 nM MLA. It has been previously reported that in cat glomus cells the ACh-induced inward current was enhanced by mild hypoxia, suggesting that nicotinic ACh receptors may be sensitive to oxygen tension (Shirahata and Shaw, 1999). To test whether or not the same is true for $O_2$-sensitive NEB cells we have studied the effects of 100 μM ACh plus mild hypoxia ($pO_2$ =75 mmHg) or severe hypoxia ($pO_2$ = 20 mmHg). We observed no significant changes in ACh-induced inward current under these conditions. The mean amplitude was 305.7 ± 19.4 pA (n=4) after perfusion of 100 μM ACh plus mild hypoxia. The mean amplitude after perfusion of 50 μM ACh alone and ACh plus severe hypoxia solution ($pO_2$ = 20 mmHg) were 217.5 ± 25.3 pA and 220.2 ± 25.3 pA(n=4) , respectively (Fig.2). Therefore, ACh- evoked inward currents in NEB cells do not appear to be modulated by hypoxia. These studies suggest that NEB cells in neonatal hamster lung express functional heteromeric α3/β2 and α7 nAChR, and that cholinergic mechanisms could modulate NEB chemoreceptor function under normal and pathological conditions.

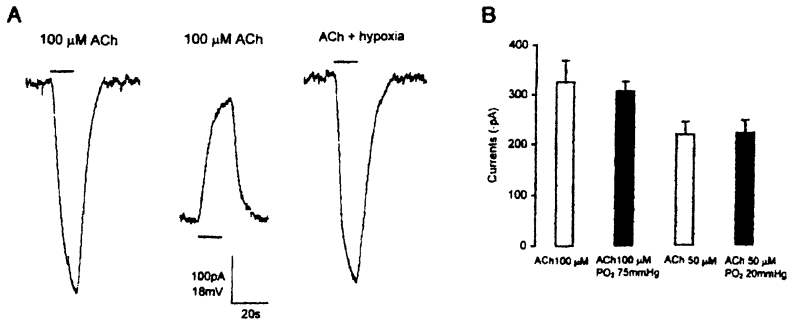


*Figure 2. Effects of ACh on whole-cell current and membrane potential in NEB cells* ***A****, ACh (100 μM) induced a rapid inward current. Under current-clamp, ACh evoked depolarization of membrane potential. hypoxia ($pO_2$=75 mmHg) failed to change ACh-induced current. Holding potential was –60 mV.* ***B****, hypoxia ($pO_2$=75 mmHg, and $pO_2$=20 mmHg) had no significant effect on 100 μM or 50μM ACh induced inward currents. Each bar presents 4 cells.*

## 2.3 Innervation of NEB and Possible Model of Hypoxia Chemotransduction

The nature and origin of intraepithelial nerve endings in contact with NEB cells have been investigated in rabbit neonatal lungs using electron microscopy and various vagotomy procedures (Lauweryns *et al.*, 1985). The predominant or type-1 nerve endings, rich in mitochondria, were interpreted as afferent sensory fibers of vagal origin with the cell bodies residing in the nodose ganglion. The less frequent, type 2 fibers, containing small agranular vesicles and suggestive of efferent-like activity were interpreted as axon collaterals, which could modulate secretory activity of NEB cells. Recent studies using various neuroendocrine and neural markers with an aid of confocal microscopy revealed a complex neural network innervating NEB. In adult Wistar rat, three different sensory fiber populations have been identified (Brouns *et al.*, 2000). The predominant nerve population was represented by vagal afferents immunoreactive for Calbindin D28K or $P_2X_3$ purinoreceptors. The second population of nerve fibers, immunoreactive for CGRP was derived from the spinal ganglia, whereas the third component was represented by nNOS immunoreactive nerve fibers originating from peribronchial ganglia.

These data suggest complex neural regulation of NEB activity, reminiscent of the carotid body. At the level of hypoxia chemotransduction, combining data from studies on sensory innervation of NEB and expression of ionotropic receptors the following model can be envisaged (Fig.3). A hypothetical axon reflex proposed for NEB consists of an afferent (A) limb, shown as 1 to 3, while the efferent (E) limb is designated as 4 and 5. Airway hypoxia ($pO_2$) is detected by $O_2$ sensor located on apical membrane which triggers neurotransmitter release (i.e. 5-HT) via exocytosis of dense core granules at synapses with afferent-like nerve endings (1). This in turn would depolarize the nerve ending. This wave of depolarization would involve all nerve endings that are in cytoplasmic continuity (2,3). The depolarization of morphologically efferent-like (E) nerve ending (3) may result in activation of post-synaptic nACh-R triggering neurotransmitter release at the base of NEB cells (5) with local paracrine effects on airway or vascular smooth muscle or adjacent pulmonary cells. Theoretically, efferent discharge could also trigger exocytosis at the intra corpuscular nerve ending (5). Similarly presynaptic $5HT_3$-R on NEB cell membrane could be activated (interrupted arrows) further enhancing neurotransmitter release and thus amplifying the hypoxia signal. All or none action potential could arise in the afferent vagal nerve fibres projecting to the brain stem if the generator potential reaches a threshold value (6). This model could also explain a possible dual role for NEB as airway chemoreceptors affecting the respiratory control and also as

local paracrine regulators of pulmonary function including airway and vascular tone as well as the growth and differentiation during lung development (Sunday and Cutz, 2002). Hypoxia could be the critical signal with NEB playing a central role in pulmonary physiology and pathophysiology.

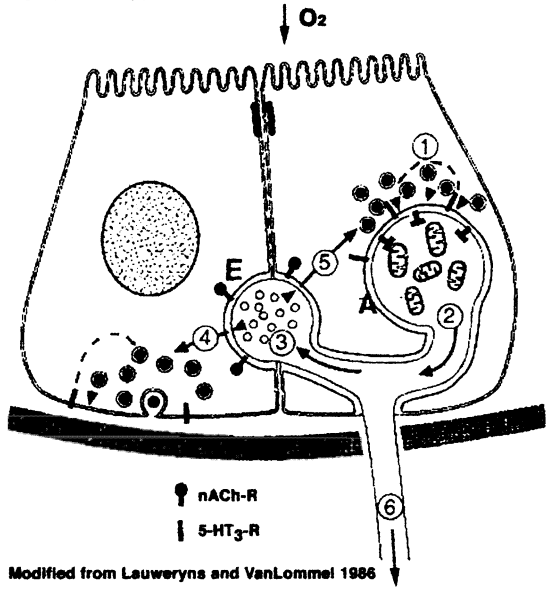


*Figure. 3. (for legend see text)*

## 3. CONCLUSIONS

Our studies demonstrate expression of functional 5-$HT_3$-R in NEB cells of mammalian lungs. In NEB cells, 5-$HT_3$-R may function as an autoreceptor since these cells are a known source of 5-HT in the lung. During hypoxia, activation of 5-$HT_3$ autoreceptors facilitates 5-HT release from NEB cells by a positive feedback mechanism. We provide morphological and electrophysiological evidence that NEB cells in neonatal hamster lung express functional nAChR β2 and α7 subunits co-expressed in the same NEB cell, giving rise to a heterogeneous population of ion channels. ACh- evoked inward currents in NEB cells do not appear to be modulated by hypoxia. The expression of postsynaptic or presynaptic nAChRs α3/ β2 and α7 subunits in NEB cells indicate that ACh could function as an excitatory transmitter modulating the responses of NEB cells and also possibly regulate the 5-HT release. Therefore, cholinergic mechanisms could modulate NEB chemoreceptor function under normal and pathological conditions.

A possible model of hypoxia chemotransduction in NEB provides an explanation for their dual role as airway chemoreceptors involved in respiratory control and as local paracrine regulators of pulmonary function.

## ACKNOWLEDGEMENTS

Work supported by grants from CIHR (MOP-12742, MGP-15270) and Canadian Cystic Fibrosis Foundation.

## REFERENCES

Brouns, I.,Adriaensen, D.,Burnstock, G., Timmermans, J.P., 2000 *Am.J. Respir. Cell Mol. Biol* .23:52-61.

Cutz, E., Spiers, V. and Yeger, H. 1993, *Ana. Rec.* 236:41-52.

Cutz, E. and Jackson, A. 1999, *Respi.r Physiol.* 115:201-14.

Fu, X.W., Nurse, C.A., Wang, Y.T. and Cutz, E. 1999, *J .Physiol.* 514:139-150.

Fu, X. W., Wang, D., Pan, J., Farragher, S.M., Wong, V. & Cutz, E., 2001, *Am. J. Physiol* 281, L931-940.

Fu, X.W., Nurse, C.A., Wong, V and Cutz, E., 2002, *J.Physiol*, 539, pp 503-510.

Fu, X.W., Jackson, A., Wang, D. and Cutz, E. 2001,
Http:/www.neur.affil.edu/post/AAA.html

Lauweryns, J.M, VanLommel A, Dom RJ., 1985, *J. Neurol. Sci* 195; 67:81-92.

Lauweryns, J.M., Cokelaere, M. & Theunyck, P., 1972, *Zeitschrift Fur Zellforshung* 135,569-592.

Maus, ADJ., Pereira, E. FR., Karachunski, P.I., Horton, R.M., Navaneetham, D., Mackin, K., Cortes, W.S., Albuqerque, E.X. and Conti-Fine, M. 1998, *Molecular Pharmacology* 54:779-788.

Shirahata, M. and Sham, J S K., 1999, *Jap. J.Physiol.* 49: 213-228.

Sekhon, H.S,, Jia, Y., Raab, R., Kuryatov, A., Pankow, J. F., Whitsett, J.A., Lindstrom, J. and Spindel, E.R., 1999, *J. Clin. Invest.* 103 :637-647.

Sunday, M.E. and Cutz, E., 2000, Role of neuroendocrine cells in fetal and postnatal lung. In *Endocrinology of the Lung* (Mendelson CR,ed) Humana Press, Totowa, N.J. p 299-336.

Wang, D., Youngson, C., Wong, V., Yeger, H., Dinauer, M., Vega-saenz de miera, E., Rudy, B, & Cutz, E., 1996, *Pro.Nat.Acad.Sci. USA* 93, 13182-13187.

Youngson, C., Nurse, C.A., Yeger, H. & Cutz, E., 1993, *Nature* 365, 153-155.

Zhang, M., Zhong, H., Vollmer, C. and Nurse, C.A.., 2000, *J. Physiol*, 525 pp 143-158.

Zhang, M. and Nurse C.A., 2000, *Brain Res.*872:199-203.

# Mitochondrial Complex II is Essential for Hypoxia-induced ROS Generation and Vasoconstriction in the Pulmonary Vasculature

RENATE PADDENBERG, ANNA GOLDENBERG, PETRA FAULHAMMER, RUEDIGER C. BRAUN-DULLAEUS* and WOLFGANG KUMMER

*Institute for Anatomy and Cell Biology, Justus-Liebig-University, 35385 Giessen, Germany*
**Department of Internal Medicine, Justus-Liebig-University, 35385 Giessen, Germany*

## 1. INTRODUCTION

In the pulmonary vasculature hypoxia induces vasoconstriction and vascular remodelling. By directing the blood flow away from poorly ventilated regions of the lung perfusion is matched to ventilation. However, persistent activation of these mechanisms causes pulmonary hypertension. Up to now both the molecular structure of the oxygen sensor and the subsequent signalling cascade are still under debate. A role as early mediator of the hypoxic response is discussed for reactive oxygen species (ROS). However, the data presented in the literature about the hypoxic regulation of ROS generation are controversial. The aim of our study was to investigate the production of ROS by cells of small intrapulmonary arteries under conditions of normoxia and hypoxia. The source of normoxic and hypoxic ROS generation was characterized by application of inhibitors of the individual complexes of the mitochondrial respiratory chain. Additionally, the requirement of functional mitochondrial complex II for hypoxic pulmonary vasoconstriction was determined by videomorphometric analysis of small intrapulmonary vessels in precision cut lung slices.

*Chemoreception*, Edited by Pequignot et al.
Kluwer Academic/Plenum Publishers, New York, 2003

## 2. RESULTS AND DISCUSSION

### 2.1 Hypoxia-induced increase in ROS production by cells of intrapulmonary vessels

ROS production by cells of small intrapulmonary vessels was investigated in precise cut murine lung sections (1). These lung slices were incubated for 3 h at normoxia (21% $O_2$, 5% $CO_2$, 74% $N_2$) or hypoxia (1% $O_2$, 5% $CO_2$, 94% $N_2$) in presence of the fluorescent indicator 2′,7′-dichlorofluorescein diacetate (DCF-DA). In the confocal laser scanning microscope single ROS producing cells became visible as bright spots within the vascular walls (Fig. 1A). A quantitative analysis revealed that hypoxia significantly increased the number of ROS generating cells per vessel (Fig. 1B).

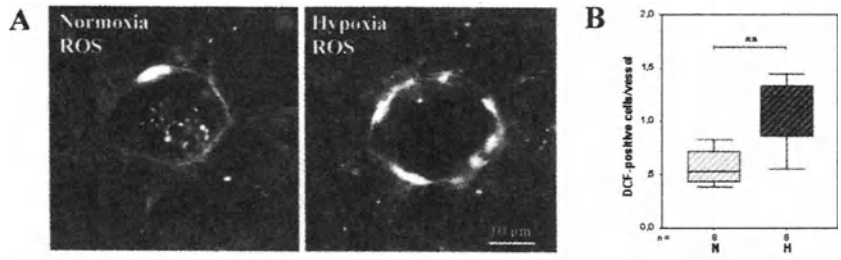


*Figure 1:* Confocal laser scanning micrographs of ROS generating cells in walls of intrapulmonary vessels as detected by application of DCF-DA (**A**). A quantitative analysis of the number of positive cells/vessel in lung sections cultured at normoxia (N) or at hypoxia (H) is presented in (**B**). In the boxplots the median, the 25% and 75% percentiles as well as minimum and maximum values are shown. n=number of independent experiments. **p<0.01 (Mann-Whitney-test).

### 2.2 Identification of mitochondria as source of ROS production

A number of enzymes such as NADPH-oxidases and the xanthine/xanthine oxidase system as well as mitochondria are known to generate ROS in a controlled way (2). To identify the source of ROS in cells of the pulmonary vasculature, lung sections were incubated in presence of rotenone, an inhibitor of complex I of the mitochondrial respiratory chain. Rotenone nearly completely blocked ROS production indicating that normoxic and hypoxic ROS generation occurred by mitochondria (Fig. 2).

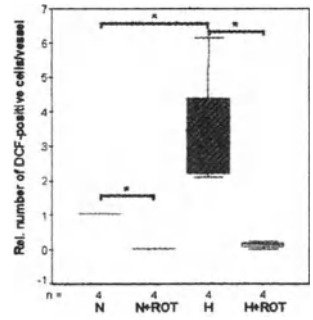


*Figure 2:* Suppression of normoxic (N) and hypoxic (H) ROS production in pulmonary vascular cells by rotenone (ROT), an inhibitor of complex I of the mitochondrial respiratory chain. The mean of normoxia of each experiment was normalized to 1, data are presented as boxplots. n=number of independent experiments. *p<0.05 (Mann-Whitney-test).

## 2.3 Essential role of complex II in oxygen dependent regulation of ROS production

To further characterize normoxic and hypoxic ROS production the effects of the following inhibitors of the respiratory chain were tested: i) 3-nitroproprionic acid (3-NPA), an irreversible inhibitor of complex II, ii) thenoyltrifluoroacetone (TTFA) which disturbs the electron transfer from complex II to ubiquinone, iii) antimycin A (AA), a substance blocking the Q-cycle of complex III, and iv) sodium azide, an inhibitor of complex IV. Fig. 3 gives a schematic illustration of the structure of the mitochondrial respiratory chain and the sites of inhibition by the substances listed.

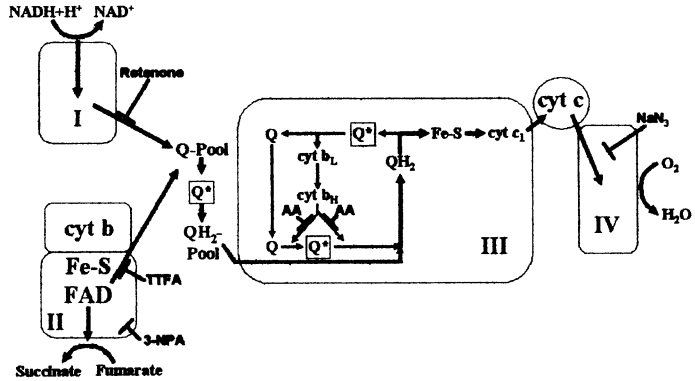


*Figure 3:* Scheme illustrating the structure of the mitochondrial respiratory chain and the sites of inhibition by rotenone, TTFA, 3-NPA, AA and $NaN_3$. Roman numerals: complexes I to IV. Cyt $b_L$, $b_H$, c and $c_1$: cytochromes $b_L$, $b_H$, c and $c_1$; Fe-S: iron-sulphur protein; Q: ubiquinone; $QH_2$: ubiquinol; Q* : ub[sem]quinone, a free radical intermediate considered to donate electrons to $O_2$ for ROS generation.

The findings on the effects of the inhibitors on the number of ROS generating cells/vessel under conditions of normoxia and hypoxia are summarized in table 1.

*Table 1:* Effects of inhibition of the individual complexes of the respiratory chain on the number of ROS generating cells per vessel. ⬇ : decrease; [⬇] weak decrease; +/-: no effect

| Inhibitor | Target | Normoxia | Hypoxia |
|---|---|---|---|
| Rotenone (Rot) | complex I | ⬇ | ⬇ |
| 3-Nitroproprionic acid (3-NPA) | complex II | +/- | ⬇ to normoxia |
| Thenoyltrifluoroacetone (TTFA) | complex II | [⬇] | ⬇ to normoxia |
| Antimycin A (AA) | complex III | ⬇ | ⬇ |
| Sodium azide ($NaN_3$) | complex IV | +/- | +/- |

Inhibition of complex I by rotenone and of complex III by AA reduced both normoxic and hypoxic ROS generation. Blockade of complex II by 3-NPA or TTFA had no or only weak effects on normoxic ROS generation whereas hypoxic ROS production was reduced to the level observed at normoxia. Sodium azide, an inhibitor of complex IV, had no effect on ROS production at either condition. Based on these results we concluded that complexes I and III are necessary for ROS generation both at normoxia and hypoxia whereas complex IV is not involved in this process. The most interesting finding was that in presence of complex II inhibitors selectively the hypoxia-induced increase in ROS production was prevented. This indicates that complex II plays an essential role in the oxygen-dependent regulation of ROS generation.

## 2.4 Hypoxia-induced switch in the function of complex II from succinate dehydrogenase (SDH) to fumarate reductase

Complex II is a component both of the Krebs-cycle and of the mitochondrial respiratory chain. It is composed of a peripheral domain located in the mitochondrial matrix and an anchor domain spanning the inner mitochondrial membrane. Complex II catalyses the dehydrogenation of succinate of fumarate, and electrons generated by this reaction are employed for the reduction of ubiquinone to ubiquinol. However, under certain conditions complex II can also act as fumarate reductase resulting in a reverse flow of the electrons from ubiquinol to fumarate (3).

To clarify which function of complex II – SDH or fumarate reductase - is responsible for the hypoxia-induced increase in ROS production incubations were performed in presence of an excess of SDH substrate succinate compared to glucose. As shown in Fig. 4 succinate reduced hypoxic but not normoxic ROS generation.

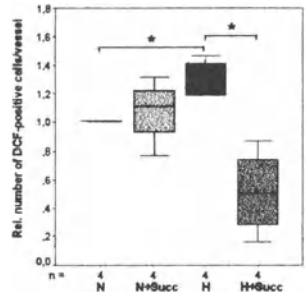


*Figure 4:* Application of an excess of succinate, the substrate of SDH, prevented the hypoxia-induced increase in the number of ROS generating cells/vessel. Data are presented as boxplots, the mean of normoxia of each experiment was normalized to 1. n=number of independent experiments. *p<0.05 (Mann-Whitney-test).

Employing an enzyme-histochemical technique the dependence of SDH-activity on oxygen was investigated (Fig. 5A). For that purpose incubations were performed at air (normoxia) or in a nitrogen atmosphere (hypoxia). A quantitative analysis of the relative staining intensities revealed that already at normoxia cells of the vascular walls exhibited a distinctly lower SDH-activity than Clara cells of the respiratory epithelium. This activity was further reduced by hypoxia (Fig. 5B).

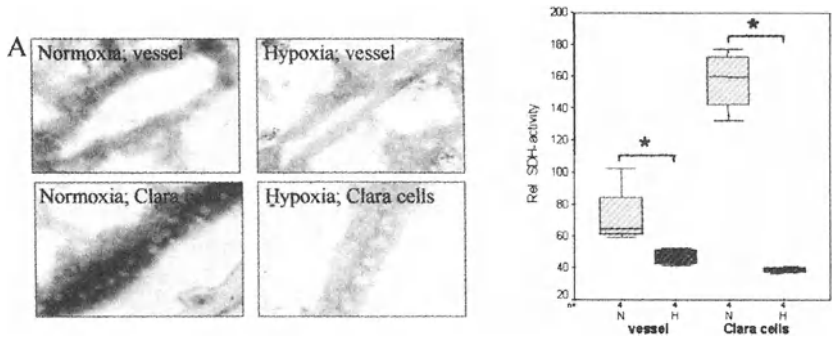


*Figure 5:* Enzyme-histochemical detection of hypoxia-induced reduction of SDH-activity in cells of intrapulmonary vessels and in Clara cells. The reactions were performed at air (normoxia; N) or in a nitrogen atmosphere (hypoxia; H). In (**A**) SDH-activity is shown in original micrographs, and in (**B**) the results of a quantitative analysis are given. n=number of independent experiments. *$p<0.05$ (Mann-Whitney-test).

Our data of the histochemical assay and the inhibitory effect of succinate argue against a function of complex II as SDH. We suppose, that at hypoxia complex II acts as fumarate reductase. Part of the electrons generated at complex I are now flowing to complex II and are used for the reduction of fumarate to succinate. In Fig. 6 a model is given describing the oxygen dependent change in the directionality of the electron flow at complex II.

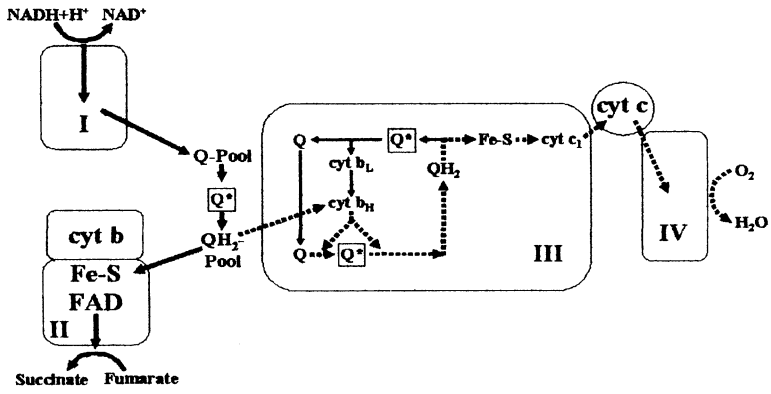


*Figure 6:* Proposed model describing an oxygen dependent change in the directionality of the electron flow at complex II of the mitochondrial respiratory chain. At hypoxia, the activity of complex II is switched from SDH to fumarate reductase; now fumarate also acts as terminal electron acceptor, receiving its electrons from ubiquinol generated by complex I. Abbreviations as in Figure 3.

## 2.5 Suppression of hypoxic pulmonary vasoconstriction (HPV) by complex II inhibitors

Murine lung sections were used to investigate the requirement of functional complex II for HPV. For that purpose videomorphometric analysis of small intrapulmonary vessels (inner diameter 30-80 μm) was performed. The sections were incubated for 10 min in normoxic gassed medium to allow adaptation to the flow-through incubation chamber, then the vessels were dilated with nitroprusside sodium to standardize the starting conditions, and subsequently the drug was removed by a normoxic wash. Then the lung sections were either incubated in hypoxic gassed medium or in hypoxic medium supplemented with the complex II inhibitor TTFA. After 40 min the sections were washed with normoxic gassed medium and finally incubated with the thromboxane analogon U46619 as a positive control for constriction capacity. Exposure to hypoxia resulted in a significant reduction of the luminal area of the vessels indicative of HPV. This reaction was completely blocked by TTFA whereas the contraction induced by U46619 was not effected (Fig. 7). Comparable results were obtained with 3-NPA, another inhibitor of complex II. Obviously, HPV demands functional complex II.

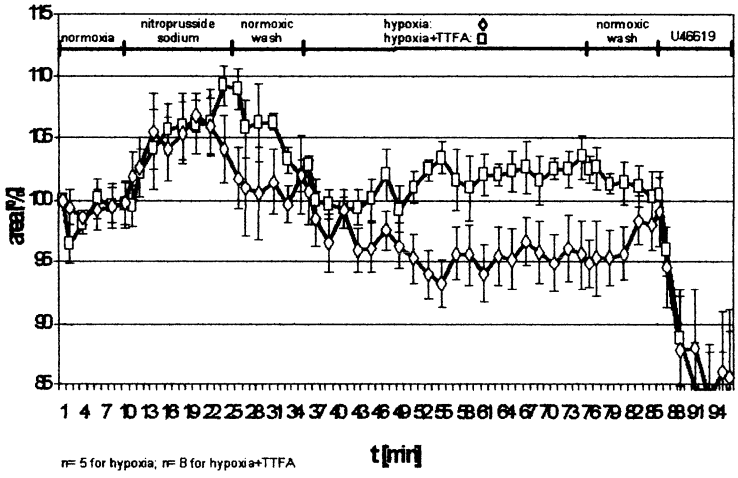


*Figure 7*: Videomorphometric analysis of intrapulmonary vessels. Exposure to hypoxic gassed medium induced a decrease in the luminal area of the vessels indicative of HPV ( ◊ ). This reaction was suppressed by the complex II inhibitor TTFA ( □).

## 3. SUMMARY

Hypoxia induces an increase in the ROS generation by cells of small intrapulmonary vessels. Based on our results we suppose that this is caused by a switch in the catalytic activity of mitochondrial complex II from succinate dehydrogenase to fumarate reductase. Functional complex II is also necessary for hypoxic pulmonary vasoconstriction.

## ACKNOWLEDGEMENTS

This research was supported by the Deutsche Forschungsgemeinschaft (SFB 547, project C1)

## REFERENCES

Held, H.D., Martin, C., and Uhlig S., 1999, Characterization of airway and vascular responses in murine lungs. *Br. J. Pharmacol.*. 126: 1191-1199.

Ullrich, V., and Bachschmid, M., 2000, Superoxide as a messenger of endothelial function. *Biochem. Biophys. Res. Commun.* 278: 1-8.

Hägerhäll, C., 1997, Succinate:quinine oxidoreductases. Variations on a conserved theme. *Biochim. Biophys. Acta* 1320: 107-141.

# Regulation of the Hypoxia-inducible Transcription Factor HIF-1 by Reactive Oxygen Species in Smooth Muscle Cells

RACHIDA SIHAM BEL AIBA, AGNES GÖRLACH

*Experimental Pediatric Cardiology, German Heart Center Munich at the Technical University Munich, Lazarettstr. 36, 80636 Munich, goerlach@dhm.mhn.de*

## 1. HIF-1, A TRANSCRIPTION FACTOR STIMULATED BY HYPOXIA

Hypoxia is able to activate the expression of a number of genes that are important for the cell to adapt to low oxygen conditions such as erythropoietin, vascular endothelial growth factor (VEGF) or plasminogen activator inhibitor-1 (PAI-1). The major transcription factor involved in the gene induction by hypoxia is the hypoxia-inducible factor-1 (HIF-1) (Semenza *et al.*, 2001) which consists of two subunits, HIF-1α and HIF-ß also known as ARNT. While the ARNT protein is readily found in the cell, the HIF-1α protein is undetectable under normoxic conditions. In fact, under normal oxygen conditions, this protein is modified by prolyl and asparaginyl hydroxylation, ubiquitinylated and degradated by the proteasome. During hypoxia, hydroxylase activity is reduced, thus allowing HIF-1α protein levels to increase (Kaelin, 2002). The HIF-1α protein can then translocate to the nucleus, interact with the ARNT subunit, bind to specific DNA binding sites named hypoxia response elements (HRE) and finally induce transcription of the target genes.

*Chemoreception*, Edited by Pequignot et al.
Kluwer Academic/Plenum Publishers, New York, 2003

## 2. HIF-1, A TRANSCRIPTION FACTOR RESPONSIVE TO THROMBIN UNDER NORMOXIC CONDITIONS

In addition to hypoxia, increased HIF-1α levels are also observed under normoxic conditions. In smooth muscle cells (SMC), the coagulation factor thrombin, known to be a potent activator of many SMC functions (Patterson *et al*, 2001), is able to increase HIF-1α protein levels in a time- and concentration-dependent manner (Gorlach *et al.*, 2001). As shown in Fig. 1, two hours of thrombin stimulation is sufficient to obtain a maximum increase of HIF-1α protein levels.

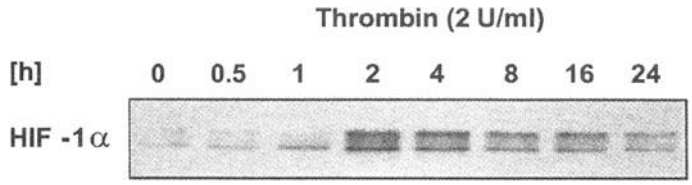


*Figure 1:* Smooth muscle cells were treated with thrombin (2U/ml) for several time points. HIF-1α expression was evaluated by Western Blot using a primary antibody directed against the human HIF-1α subunit.

Moreover, thrombin stimulation results in the nuclear translocation of HIF-1α (Fig. 2A) and in an increase in HIF-1 activity. Electrophoretic mobility shift assays (EMSA) and supershift analysis showed that HIF-1α is part of the complex binding to the HRE in response to thrombin (Gorlach *et al*, 2001). In addition, reporter gene assays, performed with several luciferase constructs containing HREs demonstrated that the HIF-1 activity is increased by thrombin stimulation to the same extent than by hypoxia. These findings indicate that thrombin is able to elevate HIF-1α levels and to activate the HIF-1 pathway in SMC. Increased HIF-1α protein levels have now also been observed under normoxia in response to other activators of G-protein-coupled receptors such as angiotensin II (Richard *et al.*, 2000) or after treatment with growth factors and cytokines acting via receptor tyrosine kinases such as platelet-derived growth factor and transforming growth factor-ß1 (Gorlach *et al.*, 2001), epidermal growth factor (Zhong *et al.*, 2000), insulin (Kietzmann *et al*, 2002) and insulin-like growth factor (Zelzer *et al.*, 1998), hepatocyte growth factor (Tacchini *et al.*, 2001), fibroblast growth factor-2 (Li et *al.*, 2002) or interleukin-1ß and tumor necrosis factor-α (Hellwig-Burgel *et al.*, 1999, Sandau *et al.*, 2001).

## 3. HIF-1α IS REGULATED BY REACTIVE OXYGEN SPECIES

Although activation of the HIF-1 pathway under normoxic conditions has now been observed frequently, the mechanisms underlying these responses remain unclear and may be similar or different to the mechanisms of activation by hypoxia. Reactive oxygen species (ROS) have been implicated to play an important, although to date not completely understood, role in hypoxic activation of the HIF-1 pathway (Michiels *et al.,* 2002). Indeed, recent evidence accumulates that generation of low amounts of ROS as well as changes in the cellular levels of ROS essentially participate in cell signaling (Martindale & Holbrook, 2002). Thus, ROS have been recognized to provide a potential link between receptor activation and stimulation of intracellular signaling cascades in response to hormones, growth factors and cytokines. Indeed, thrombin has been shown to activate ROS formation in SMC, and this response was significantly inhibited by treatment with the antioxidant vitamin C (Gorlach *et al.,* 2001, Brandes *et al.,* 2001). Pretreatment with vitamin C or N-acetylcysteine also abrogated thrombin-stimulated HIF-1α protein levels (Figure 2B). Moreover, HIF-1α nuclear translocation and HIF-1 reporter gene activity stimulated by thrombin were abolished by antioxidant treatment (Figure 2A), showing that the thrombin-induced HIF-1α levels are ROS-dependent. Indeed, antioxidant treatment also prevented thrombin-stimulated upregulation of the HIF-1 target genes VEGF and PAI-1 (Bassus *et al.,* 2001, Gorlach *et al.,* 2001). Consistently, antioxidants prevented HIF-1α expression elevated by angiotensin II (Richard *et al.,* 2000), HGF (Tacchini *et al.,* 2001) or TNF-α (Sandau *et al.,* 2001) further supporting a critical role of ROS in regulating the HIF-1 pathway.

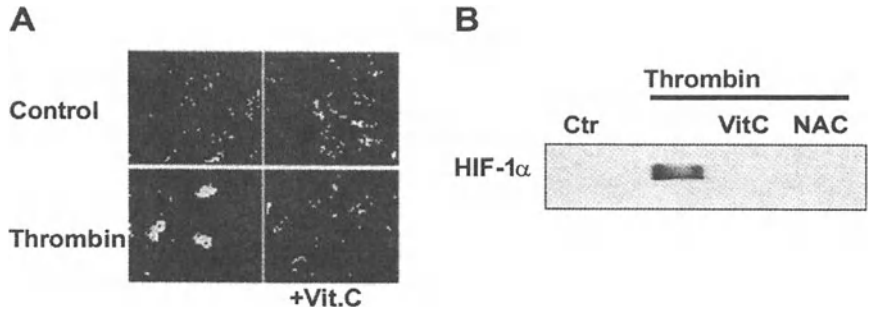


*Figure 2:* Smooth muscle cells were treated with vitamin C (VitC, 100μM) or N-acetylcysteine (NAC, 100mM) prior stimulation with thrombin (2U/ml). **A)** HIF-1α immunofluorescence with an antibody against human HIF-1α. **B)** HIF-1α protein levels evaluated by Western Blot analysis.

This assumption was further substantiated by experiments where SMC were exposed to increasing concentrations of $H_2O_2$. Western Blot analysis showed that low $H_2O_2$ concentrations (10μM) maximally increased HIF-1α protein levels, whereas higher $H_2O_2$ concentrations (100μM) decreased HIF-1α levels (Figure 3).

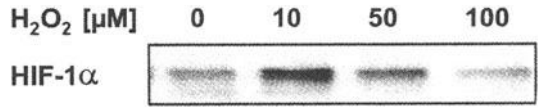


*Figure 3:* Smooth muscle cells were treated with increasing $H_2O_2$ concentrations. HIF-1α expression was evaluated by Western Blot using a primary antibody directed against the human HIF-1α subunit.

## 4. HIF-1: A TARGET OF THE NADPH OXIDASE

Several systems are able to generate ROS. In SMC, NADPH oxidases were proposed to contribute considerably to agonist-induced ROS formation (Griendling *et al.,* 2000). This enzyme is composed of several subunits including p22phox, p47phox, p67phox and the GTPase Rac (Babior et al., 1999). Two recently identified proteins, Nox1 and Nox4, which are homologous to the neutophil gp91phox NADPH oxidase component, may also be required for ROS production in SMC (Lambeth, 2002). The importance of p22phox in agonist-induced ROS production and gene expression has been demonstrated in SMC stimulated with thrombin (Gorlach *et al.,* 2001, Gorlach *et al.,* 2002). Using p22phox antisense oligonucleotides or antisense cDNA, p22phox expression was prevented. Concomitantly, thrombin-stimulated ROS production was significantly decreased in p22phox antisense–transfected SMC compared with cells transfected with p22phox scrambled oligonucleotides (Fig. 4A). Furthermore, compared to SMC transfected with p22phox scrambled oligonucleotides, thrombin-induced HIF-1α protein levels were significantly diminished in p22phox antisense–transfected cells (Figure 4B). Moreover, p22phox antisense treatment inhibited the upregulation of the HIF-1 target genes VEGF and PAI-1 by thrombin, indicating that the NADPH oxidase is involved in the activation of the HIF pathway leading to the upregulation of the HIF-1 target genes VEGF and PAI-1 (Figure 4C &D).

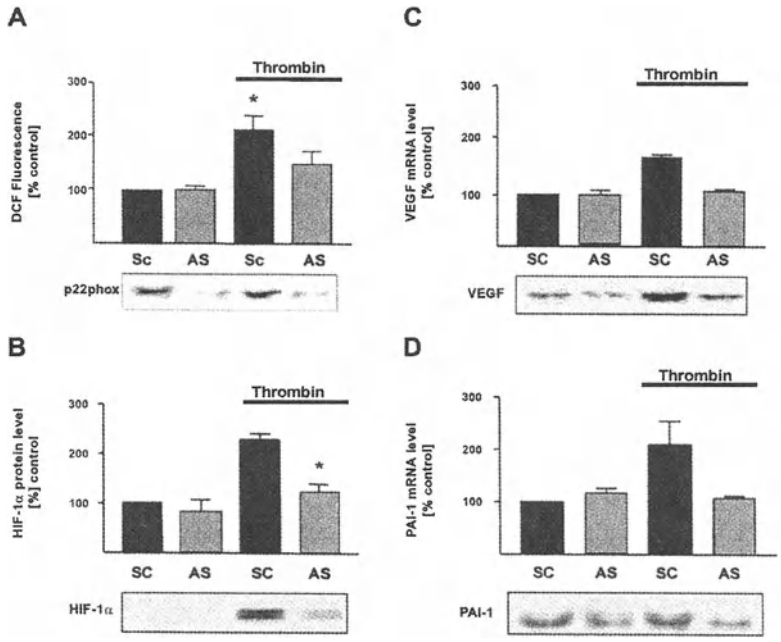


*Figure 4:* Smooth mucle cells were transfected with p22phox scrambled (SC) or antisense (AS) oligonucleotides. **A)** The formation of reactive oxygen species was measured by dichlorofluorescein (DCF) fluorescence after stimulation with thrombin (2U/ml) and Northern Blot analysis was performed using cDNA probe for rat p22phox. **B)** Western Blot analysis was performed as in Figure 1. **C)** Northern blot analysis was performed with cDNA probes for rat VEGF, and **D)** for rat PAI-1.

## 5. ROS-DEPENDENT SIGNALLING PATHWAYS REGULATE THE HIF PATHWAY

Thrombin has been shown to activate multiple pathways in SMC including MAP kinases and phosphatidyl-inositol-3 kinase (PI3K)-dependent pathways such as protein kinase B (PKB) (Patterson *et al.,* 2001, Herkert *et al.,* 2002). These pathways are also stimulated by $H_2O_2$. Moreover, ROS and the NADPH oxidase are specifically involved in thrombin-stimulated kinase activation in SMC: Pretreatment with antioxidants or p22phox antisense oligonucleotides prevented thrombin-induced activation of p38 MAP kinase (p38MAPK) and PKB. However, this treatment had no effect on thrombin-stimulated activation of ERK1/2, indicating that the NADPH oxidase specifically mediates thrombin-induced p38MAPK and PKB activation (Herkert *et al.,* 2002). Similar observations were made in response to angiotensin II (Kyaw *et al.,* 2001). Activation of p38MAPK and PKB is also

involved in thrombin-induced stimulation of the HIF-1 pathway. Treatment with inhibitors of p38 MAP kinase or PI3K prevented thrombin-stimulated HIF-1α protein induction whereas inhibitors of the ERK1/2 pathway had no effect (Gorlach *et al.,* 2001). Moreover, thrombin-induced upregulation of the HIF target genes PAI-1 and VEGF was also sensitive to inhibition of p38MAPK and PI3K/PKB, but was insensitive to inhibition of the ERK1/2 (Gorlach *et al.,* 2001).

## 6. CONCLUSION

The transcription factor HIF-1 is essential not only for hypoxic gene regulation, but is also centrally involved in the cellular response to thrombin, growth factors and cytokines. ROS, which are derived from an NADPH oxidase in SMC, play an important role in regulating expression and activity of HIF under non-hypoxic conditions by specifically activating p38 MAP kinase and PKB (Fig. 5). Whereas the mechanisms involved in hypoxic stabilization of the HIF-1α protein and activation of the HIF-1 pathway are increasingly elucidated, the exact mechanisms underlying the elevated levels of HIF-1α protein observed under non-hypoxic conditions in response to thrombin or other agonists are not completely clear. However, ROS and ROS-dependent pathways appear to play a role in controlling the HIF pathway under both, hypoxic and non-hypoxic, conditions, further supporting the assumption that HIF-1 is a transcription factor tightly regulated by ROS and the cellular redox state.

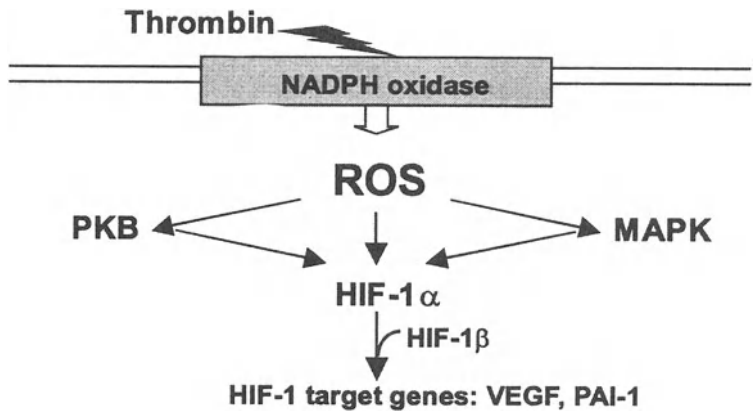


*Figure 5:* Thrombin regulation of HIF

# REFERENCES

Babior, B.M., 1999, NADPH oxidase: an update. *Blood* **93**: 1464-1476.

Bassus, S., Herkert, O., Kronemann, N., Gorlach, A., Bremerich, D., Kirchmaier, C.M., Busse, R., Schini-Kerth, V.B., 2001, Thrombin causes vascular endothelial growth factor expression in vascular smooth muscle cells: role of reactive oxygen species. *Arterioscler Thromb Vasc Biol* **21**: 1550-1555.

Brandes, R.P., Viedt, C., Nguyen, K., Beer, S., Kreuzer, J., Busse, R., Gorlach, A., 2001, Thrombin-induced MCP-1 expression involves activation of the p22phox-containing NADPH oxidase in human vascular smooth muscle cells. *Thromb Haemost* **85**: 1104-1110.

Gorlach, A., Diebold, I., Schini-Kerth, V.B., Berchner-Pfannschmidt, U., Roth, U., Brandes, R.P., Kietzmann, T., Busse, R., 2001, Thrombin activates the hypoxia-inducible factor-1 signaling pathway in vascular smooth muscle cells: Role of the p22(phox)-containing NADPH oxidase. *Circ Res* **89**: 47-54.

Gorlach, A., Kietzmann, T., Hess, J., 2002, Redox Signaling through NADPH Oxidases: Involvement in Vascular Proliferation and Coagulation. *Ann N Y Acad Sci* **973**: 505-507.

Griendling, K.K., Sorescu, D., Ushio-Fukai, M., 2000, NAD(P)H oxidase: role in cardiovascular biology and disease. *Circ Res* **86**: 494-501.

Hellwig-Burgel, T., Rutkowski, K., Metzen, E., Fandrey, J., Jelkmann, W., 1999, Interleukin-1beta and tumor necrosis factor-alpha stimulate DNA binding of hypoxia-inducible factor-1. *Blood* **94**: 1561-1567.

Herkert, O., Diebold, I., Brandes, R.P., Hess, J., Busse, R., Gorlach, A., 2002, NADPH oxidase mediates tissue factor-dependent surface procoagulant activity by thrombin in human vascular smooth muscle cells. *Circulation* **105**: 2030-2036.

Kaelin WG Jr., 2002, How oxygen makes its presence felt. *Genes Dev* **16**: 1441-1445.

Kietzmann, T., Samoylenko, A., Roth, U., Jungermann K., 2002, Hypoxia-Inducible Factor-1 And Hypoxia Response Elements Mediate the Induction of Plasminogen Activator Inhibitor-1 Gene Expression by Insulin in Primary Rat Hepatocytes. *Blood Sep 12, DOI 10.1182/blood-2002-06-1693*

Kyaw, M., Yoshizumi, M., Tsuchiya, K., Kirima, K., Tamaki, T., 2001, Antioxidants inhibit JNK and p38 MAPK activation but not ERK 1/2 activation by angiotensin II in rat aortic smooth muscle cells. *Hypertens Res* **24**: 251-261.

Lambeth, J.D., 2002, Nox/Duox family of nicotinamide adenine dinucleotide (phosphate) oxidases. *Curr Opin Hematol* **9**: 11-17.

Li, J., Shworak, N.W., Simons, M., 2002, Increased responsiveness of hypoxic endothelial cells to FGF2 is mediated by HIF-1alpha-dependent regulation of enzymes involved in synthesis of heparan sulfate FGF2-binding sites. *J Cell Sci* **115**: 1951-1959.

Martindale, J.L., Holbrook, N.J., 2002, Cellular response to oxidative stress: signaling for suicide and survival. *J Cell Physiol* **192**: 1-15.

Michiels, C., Minet, E., Mottet, D., Raes, M., 2002, Regulation of gene expression by oxygen: NF-kappaB and HIF-1, two extremes. *Free Radic Biol Med* **33**: 1231-1242.

Patterson, C., Stouffer, G.A., Madamanchi, N., Runge, M.S., 2001, New tricks for old dogs: nonthrombotic effects of thrombin in vessel wall biology. *Circ Res* **88**: 987-997.

Richard, D.E., Berra, E., Pouyssegur, J., 2000, Nonhypoxic pathway mediates the induction of hypoxia-inducible factor 1alpha in vascular smooth muscle cells. *J Biol Chem* **275**: 26765-26771.

Sandau, K.B., Zhou, J., Kietzmann, T., Brune, B., 2001, Regulation of the hypoxia-inducible factor 1alpha by the inflammatory mediators nitric oxide and tumor necrosis factor-alpha in contrast to desferroxamine and phenylarsine oxide. *J Biol Chem* **276**: 39805-39811.

Semenza, G.L., 2001, Hypoxia-inducible factor 1: oxygen homeostasis and disease pathophysiology. *Trends Mol Med* 7:345-350.

Tacchini, L., Dansi, P., Matteucci, E., Desiderio, M.A., 2001, Hepatocyte growth factor signalling stimulates hypoxia inducible factor-1 (HIF-1) activity in HepG2 hepatoma cells. *Carcinogenesis* **22**: 1363-1371.

Zelzer, E., Levy, Y., Kahana, C., Shilo, B.Z., Rubinstein, M., Cohen, B., 1998, Insulin induces transcription of target genes through the hypoxia-inducible factor HIF-1alpha/ARNT. *EMBO J* **17**: 5085-5094.

Zhong, H., Chiles, K., Feldser, D., Laughner, E., Hanrahan, C., Georgescu, M.M., Simons, J.W., Semenza, G.L., 2000, Modulation of hypoxia-inducible factor 1alpha expression by the epidermal growth factor/phosphatidylinositol 3-kinase/PTEN/AKT/FRAP pathway in human prostate cancer cells: implications for tumor angiogenesis and therapeutics. *Cancer Res* **60**: 1541-1545.

# $O_2$-Sensing Mechanisms in Efferent Neurons to the Rat Carotid Body

VERÓNICA A. CAMPANUCCI, IAN M. FEARON AND COLIN A. NURSE
*Department of Biology, McMaster University, Hamilton, Ontario, Canada L8S 4K1*

## 1. INTRODUCTION

$O_2$-sensing by mammalian cells is a fundamental process that is important for adaptation to variable physiological situations. The mammalian carotid bodies (CB) are peripheral chemoreceptors which monitor blood levels of $Po_2$, $Pco_2$ and pH (González *et al.*, 1994; Prabhakar, 2000; López-Barneo *et al.*, 2001). As a result they can initiate or modify respiratory reflexes in order to maintain $PO_2$ homeostasis. Inhibition of $K^+$ channels appears to be an important step in CB chemotransduction during hypoxia (Peers, 1997; López-Barneo *et al.*, 2001). It is known that under certain conditions the responses of the CB to specific stimuli can be altered. Chemoreceptor inhibition is the mechanism by which the CB responses are reduced during chemical stimulation, leading to an inhibition of chemoreceptor discharge. Nitric oxide (NO) has been implicated as an important neurotransmitter in the efferent inhibition of rat CB chemoreceptors during hypoxia (Wang *et al.*, 1993; 1994a & b; 1995a & b; Höhler *et al.*, 1994). An extensive plexus of NO synthase (NOS)-containing nerve fibers projects to the CB and is formed by sensory fibers from the petrosal ganglion and autonomic fibers from neurons located near the junction of the glossopharyngeal (GPN) and carotid sinus (CSN) nerves (Wang *et al.*, 1993).

Several studies have focussed on the effects of NO on CB chemoreceptor cells, but much less is known about the properties of NO-producing autonomic neurons in the GPN and CSN branches, and particularly how they

*Chemoreception*, Edited by Pequignot et al.
Kluwer Academic/Plenum Publishers, New York, 2003

become activated. In the present study we tested the hypothesis that GPN neurons are themselves $O_2$-sensitive, thereby providing a pathway by which they could produce CB chemoreceptor inhibition during hypoxia. Interestingly, our findings based on whole-cell recordings indicate that these neurons express a background $K^+$ conductance sensitive to hypoxia and the volatile anaesthetic halothane.

# 2. METHODS

## 2.1 Cell culture

Sections of the glossopharyngeal nerve (GPN), extending from its intersection with the carotid sinus nerve (CSN) to a region ~5 mm distal to the intersection, were dissected from Wistar rat pups (10-14 days old). The sections were pooled, digested with enzyme and mechanically dissociated to produce dispersed GPN neurons that were grown on a thin layer of Matrigel. The solutions and culture procedures were identical to those described elsewhere (Zhong *et al.*, 1997).

## 2.2 Perforated patch recording

The methods for obtaining nystatin perforated-patch recordings of membrane potential (current clamp) and ionic currents (voltage clamp) from GPN neurons were identical to those previously described (Zhong *et al.*, 1997). Patch pipettes were filled with intracellular recording solution of the following composition (mM): K-Gluconate 105, KCl 30, Hepes 10, NaCl 5, $CaCl_2$ 2, pH adjusted to 7.2 with KOH, plus 500 $\mu g.ml^{-1}$ nystatin. The extracellular recording solution contained (mM): NaCl 135, KCl 5, Hepes 10, glucose 10, $CaCl_2$ 2, $MgCl_2$ 2, pH adjusted to 7.4 with NaOH at RT. Some experiments, designed to dissect the $O_2$-sensitive $K^+$ current ($IKO_2$), were carried out in $Ca^{2+}$ free extracellular recording solution containing different concentrations of $K^+$ ($Na^+$ substituted) and in mM: Hepes 10, glucose 10, $MgCl_2$ 2, $NiCl_2$ 2, pH adjusted to 7.4 with KOH or NaOH at RT. Various types of $K^+$ currents (as indicated in the text) were blocked using the following drugs: tetraethylammonium (TEA, 5-30 mM), 4-aminopyridine (4-AP, 2-5 mM), barium (BaCl, 10 mM) and quinidine (1 mM). To block voltage-dependent $Na^+$ currents, tetrodotoxin (TTX, 1 μM) was added to the bathing solution. The volatile anesthetic 2Bromo-2chloro-1,1,1trifluoroethane (halothane; 5-10 mM) was added to the extracellular

solution in some experiments. Hypoxia ($Po_2$ ~ 15 mmHg) was generated by bubbling 100 % $N_2$ into the perfusion reservoir.

# 3. RESULTS

## 3.1 Hypoxia-sensitivity in GPN neurons

Perforated patch whole-cell recordings were carried out on GPN neurons usually within 1-2 days of isolation. As shown in Fig. 1A, hypoxia reversibly inhibited outward currents in GPN neurons at positive test potentials; this response can be observed in example traces and the corresponding I-V plot (Fig. 1A). This effect of hypoxia persisted in physiological solution containing the classical $K^+$ channel blockers TEA (5 mM) and 4-AP (2 mM; Fig. 1B), suggesting involvement of a background or 'leak' current.

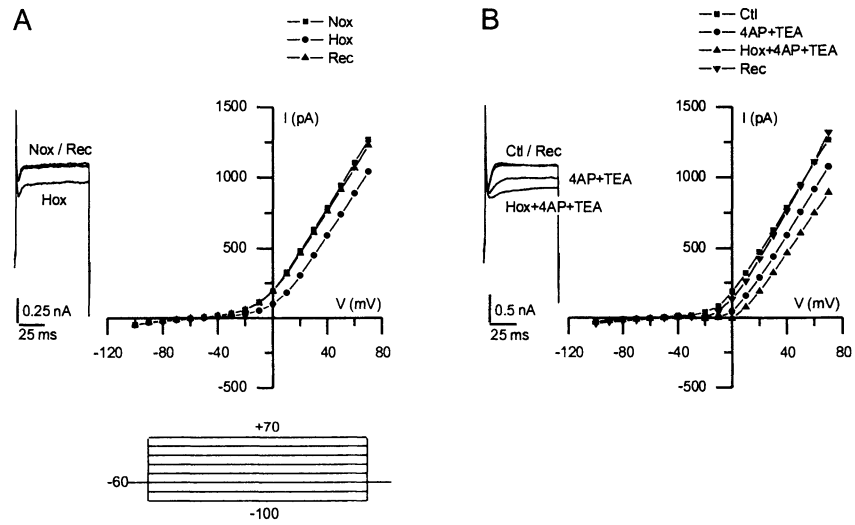


*Figure 1.* Electrophysiological responses of cultured GPN neurons to hypoxia. A, traces show a representative example of the reversible reduction in the macroscopic outward current recorded in a GPN neuron after exposure to hypoxia in physiological extracellular $K^+$ (5 mM) solution, during step to +40 mV. Corresponding I-V plot of the current during normoxia (Nox), hypoxia (Hox) and recovery (Rec) is shown on right. B, traces show a representative example of the response to hypoxia in physiological solution containing 4-AP (2mM) and TEA (5 mM) during step to +40 mV; corresponding I-V plot shows current during normoxia and hypoxia in the presence of 4-AP and TEA.

## 3.2 Instantaneous 'leak' currents in GPN neurons

To enhance the magnitude of 'leak' currents and to facilitate quantification of the hypoxia-sensitive component, voltage clamp recordings were carried out in high $K^+$ external solutions containing 1 μM TTX, 30 mM TEA, 5 mM 4-AP and 2 mM $Ni^{2+}$ to block voltage-dependent currents. Representative current traces, typical of instantaneous 'leak' currents, are shown in Fig. 2A for a cell exposed to this solution in symmetrical $K^+$ (135 mM) conditions. The hypoxia-sensitive difference current ($IKO_2$), obtained by subtracting the current recorded in hypoxia from that in normoxia (Fig. 2A), reversed near 0 mV, the $K^+$ equilibrium potential, and the I-V relation displayed little voltage dependence (Fig. 2A). Interestingly, $IKO_2$ was sensitive to the volatile anaesthetic halothane (Fig. 2B), which occluded the response to hypoxia. Moreover, $IKO_2$ was also inhibited by quinidine, barium and weakly by extracellular acidification in symmetrical $K^+$ solutions (data not shown).

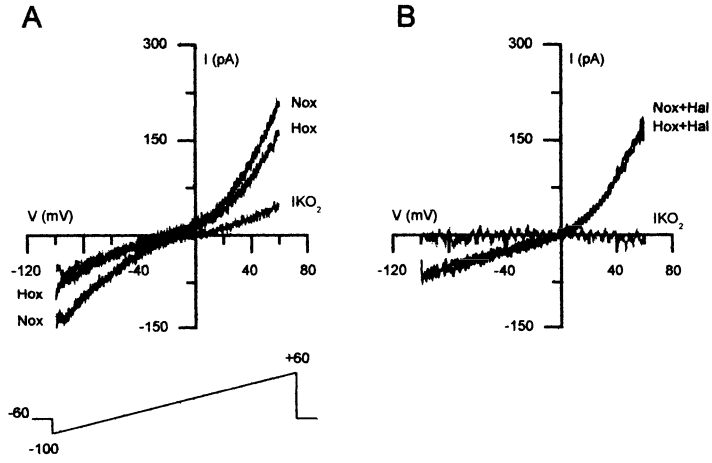


*Figure 2.* Electrophysiological properties of the background hypoxia-sensitive $K^+$ current ($IKO_2$) in GPN neurons. A, ramp traces show a representative example of background or 'leak' currents before (Nox) and during (Hox) hypoxia, recorded in symmetrical high $K^+$ solution (135 mM) containing TTX (1 μM), 4-AP (5 mM), TEA (30 mM) and $Ni^{2+}$ (2 mM; substituted for $Ca^{2+}$). Trace in grey shows the hypoxia-sensitive 'difference' current ($IKO_2$), obtained by subtracting the current density during hypoxia from that during normoxia. In B, experimental procedure as in A, but with the volatile anaesthetic halothane (Hal, 5-10 mM) present. Note, occlusion of $IKO_2$ in the presence of this agent.

## 3.3 Effect of hypoxia and halothane on neuronal excitability

Under current clamp conditions, constant (near-threshold) depolarizing current pulses were injected in order to test whether or not hypoxia increased excitability of GPN neurons. As shown in Fig. 3A, hypoxia increased probability of neuronal firing, and the effect was mimicked by application of the volatile anaesthetic halothane (Fig. 3B).

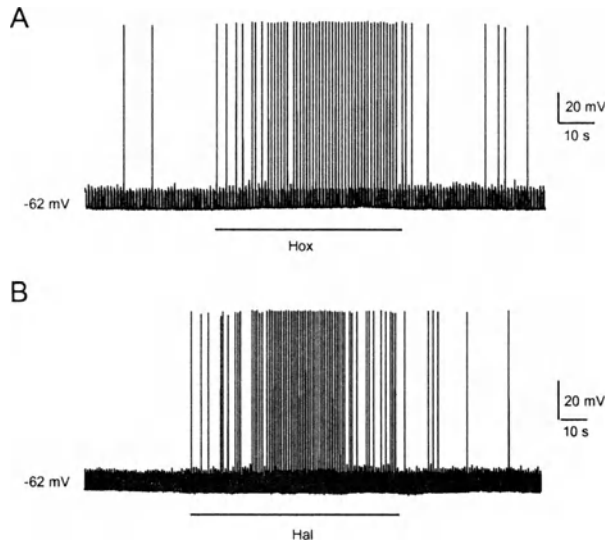


*Figure 3.* Effect of hypoxia and halothane on the membrane potential and excitability in GPN neurons. Under current clamp conditions, during injection of constant (near-threshold) depolarizing current pulses, hypoxia (A, Hox) and halothane (B, Hal) reversibly increased probability of neuronal firing.

# 4. DISCUSSION

The present study reveals an $O_2$-sensing mechanism in peripheral neurons that are thought to be involved in efferent inhibition of the rat carotid body (CB) (Wang *et al.*, 1993; 1994a & b; 1995a & b; Höhler *et al.*, 1994). The $O_2$-sensitive current expressed in GPN neurons arises from $K^+$-selective background channels that were insensitive to classical voltage-dependent $K^+$ channel blockers (Goldstein *et al.*, 2001). The volatile anaesthetic halothane inhibited $IKO_2$ and increased neuronal excitability,

effects that are opposite to those expected for the currently known $O_2$-sensitive members of the background $K^+$ family, TASK1 (Buckler *et al.*, 2000; Plant *et al.*, 2002) and TASK3 (O'Kelly *et al.*, 1999; Hartness *et al.*, 2001). The $O_2$-sensitive current expressed in GPN neurons was inhibited by halothane, a pharmacological characteristic shared with two members of the background $K^+$ channel family, THIK1 (kcnk13; Rajan *et al.*, 2001) and TWIK2 (kcnk6; Patel *et al.*, 2000). However, TWIK2 is reported to be insensitive to inhibition by barium in symmetrical $K^+$ solutions, which is inconsistent with our observations on the $O_2$-sensitive background $K^+$ current in GPN neurons.

Therefore, our studies raise the possibility of a novel $O_2$-sensing mechanism in GPN neurons mediated by a halothane-inhibited background $K^+$ conductance. However, further molecular identification of this conductance will be necessary to clarify which member(s) of the background $K^+$ channel family is responsible for conferring $O_2$-sensitivity.

## ACKNOWLEDGEMENTS

This work was supported by research grants from CIHR and The Canadian SIDS Foundation.

## REFERENCES

Buckler KJ, Williams BA, Honoré E (2000). An oxygen-, acid- and anaesthetic-sensitive TASK-like background potassium channel in rat arterial chemoreceptor cells. *J Physiol* 525, 135-142.

Goldstein SA, Bockenhauer D, O'Kelly I & Zilberberg N (2001). Potassium leak channels and the KCNK family of two-P-domain subunits. *Nat Rev Neurosci* 2, 175-184.

González C, Almaraz L, Obeso A & Rigual R (1994). Carotid body chemoreceptors: from natural stimuli to sensory discharges. *Physiol Rev* 74, 829-898.

Hartness ME, Lewis A, Searle GJ, O'Kelly I, Peers C & Kemp PJ (2001). Combined antisense and pharmacological approaches implicate hTASK as an airway $O_2$- sensing $K^+$ channel. *J Biol Chem* 276, 26499-26508.

Höhler B, Mayer B & Kummer W (1994). Nitric oxide synthase in the rat carotid body and carotid sinus. *Cell Tissue Res* 276, 559-564.

López-Barneo J, Pardal R & Ortega-Saenz P (2001). Cellular mechanism of oxygen sensing. *Annu Rev Physiol* 63, 259-287.

O'Kelly I, Stephens RH, Peers C & Kemp PJ (1999). Potential identification of the $O_2$-sensitive $K^+$ current in a human neuroepithelial body-derived cell line. *Am J Physiol* 276, L96-L104.

Patel AJ, Maingret F, Magnone V, Fosset M, Lazdunski M, Honoré E (2000). TWIK-2, an inactivating 2P domain K+ channel. *J Biol Chem* 275, 28722-28730.

Peers C (1997). Oxygen-sensitive ion channels. *Trends Pharmacol Sci* 18, 405-408.

Plant LD, Kemp PJ, Peers C, Henderson Z & Pearson HA (2002). Hypoxic depolarization of cerebellar granule neurons by specific inhibition of TASK-1. *Stroke* 33, 2324-2328.

Prabhakar NR (2000). Oxygen sensing by the carotid body chemoreceptors. *J Appl Physiol* 88, 2287-2295.

Rajan S, Wischmeyer E, Karschin C, Preisig-Muller R, Grzeschik KH, Daut J, Karschin A & Derst C (2001). THIK-1 and THIK-2, a novel subfamily of tandem pore domain $K^+$ channels. *J Biol Chem* 276, 7302-7311.

Wang ZZ, Bredt DS, Fidone SJ, Stensaas LJ (1993) Neurons synthesizing nitric oxide innervate the mammalian carotid body. *J Comp Neuro* 336, 419-432.

Wang ZZ, Dinger BG, Stensaas LJ, Fidone SJ (1995a) The role of nitric oxide in carotid chemoreception. *Biol Signals* 4, 109-116.

Wang ZZ, Stensaas LJ, Bredt DS, Dinger B, Fidone SJ (1994a) Localization and actions of nitric oxide in the cat carotid body. *Neuroscience* 60, 275-286.

Wang ZZ, Stensaas LJ, Bredt DS, Dinger BG, Fidone SJ (1994b) Mechanisms of carotid body inhibition. *Adv Exp Med Biol* 360, 229-235.

Wang ZZ, Stensaas LJ, Dinger BG, Fidone SJ (1995b) Nitric oxide mediates chemoreceptor inhibition in the cat carotid body. *Neuroscience* 65, 217-229.

Zhong H, Zhang M & Nurse CA (1997). Synapse formation and hypoxic signalling in co-cultures of rat petrosal neurones and carotid body type 1 cells. *J Physiol* 503, 599-612.

# Amyloid Peptide-Mediated Hypoxic Regulation of $Ca^{2+}$ Channels in PC12 Cells

CHRIS PEERS, KIM N. GREEN and JOHN P. BOYLE
*Institute for Cardiovascular Research, Worsley Medical and Dental Building, University of Leeds, Leeds LS2 9JT, UK.*

## 1. INTRODUCTION

The incidence of dementias such as Alzheimer's Disease (AD) is dramatically increased in patients who have previously suffered prolonged hypoxic or ischemic episodes. Such episodes commonly arise as a consequence of cardiovascular dysfunctions such as stroke (Tatemichi *et al.*, 1994; Kokmen *et al.*, 1996; Moroney *et al.*, 1996). This clear link between hypoxic / ischemic episodes and increased incidence of AD strongly suggests that reduction in local $O_2$ levels may be capable of precipitating this increasingly widespread disease.

A hallmark feature of AD is the increased appearance of amyloid β peptides (AβPs; reviewed by Mattson, 1997; Selkoe, 2001), cleavage products derived from amyloid precursor protein (APP; Glenner & Wong, 1984; Masters *et al.*, 1985). APP is one of only a few gene products whose expression is increased following a period of cerebral ischemia (Kogure & Kato, 1993; Koistinaho *et al.*, 1996). The major (non-amyloidogenic) cleavage product of APP, sAPPα, is neuroprotective (Mattson, 1997; Selkoe, 2001), and so increased expression of APP may be considered a defence mechanism against ischemia. However, increased APP levels would also provide increased substrate for formation of toxic AβPs (Mattson, 1997; Selkoe, 2001) and, indeed, AβP production is increased following ischemia (Yokoto *et al.*, 1996; Jendroska *et al.*, 1997).

Mechanisms underlying the neuronal toxicity of AβPs remain to be fully resolved, but involve disruption of $Ca^{2+}_i$ homeostasis (Mattson, 1997; Fraser *et al.*, 1997) and free radical damage (Behl *et al.*, 1994; Schubert *et al.*,

*Chemoreception*, Edited by Pequignot et al.
Kluwer Academic/Plenum Publishers, New York, 2003

1995). In addition, other studies have shown that AβPs disrupt $Ca^{2+}_i$ homeostasis by forming $Ca^{2+}$-permeable pores or channels (Arispe *et al.*, 1996; Kawahara *et al.*, 1997; Rhee *et al,* 1998) which may account for increased central synaptic activity.

Here, we describe the effects of prolonged hypoxia on $Ca^{2+}$ influx pathways in catecholamine secreting PC12 cells. This study was prompted by our previous finding that chronic hypoxia (10% $O_2$, 24h) leads to excessive stimulus-evoked neurosecretion due to the emergence of a $Cd^{2+}$-resistant $Ca^{2+}$ influx pathway tightly coupled to the exocytotic machinery (Taylor *et al.*, 1999).

# 2. METHODS

## 2.1 Cell culture and chronic hypoxia

PC12 cells were cultured in RPMI 1640 culture medium (containing L-glutamine) as previously described (Taylor *et al.*, 1999; Taylor & Peers, 1999). Cells were incubated at 37°C in a humidified atmosphere of 5% $CO_2$/95% air and passaged every 7 days. Cells exposed to chronic hypoxia were treated identically, except that for 24h prior to experiments they were transferred to a humidified incubator equilibrated with 10% $O_2$, 5% $CO_2$ and 85% $N_2$. Following this period in chronic hypoxia, cells were exposed to room air for no longer than 1h before experimentation. Amyloid peptides used in this study were dissolved in sterile Ultrapure water and stored frozen in aliquots until required, so that they only underwent one freeze-thaw cycle before being applied directly to the cells. Gel electrophoresis of peptide samples revealed that they were applied to cells in the unaggregated form.

## 2.2 Patch-clamp recording

Cells were plated onto coverslips, fragments of which were subsequently placed in a perfusion chamber and perfused with a solution of composition (in mM): NaCl 110, CsCl 5, $MgCl_2$ 0.6, $BaCl_2$ 20, Hepes 5, glucose 10 and tetraethylammonium-Cl 20 (pH 7.4). Osmolarity of the perfusate was adjusted to 300mOsm by addition of sucrose. Patch pipettes (5-7MΩ resistance) were filled with a solution of (in mM): CsCl 130, EGTA 1.1, $MgCl_2$ 2, $CaCl_2$ 0.1, NaCl 10, Hepes 10 and $Na_2ATP$ 2 (pH 7.2). After establishing the whole-cell configuration, cells were voltage-clamped at –80mV and whole cell capacitance determined from analogue compensation. To evoke whole-cell $Ca^{2+}$ channel currents, 200ms voltage ramps were

applied from –100mV to +100mV at a frequency of 0.2Hz (Green & Peers, 2001). Evoked currents were filtered at 1kHz, digitised at 2kHz and stored on computer for off-line analysis. All results are presented as mean ± s.e.m. current densities spanning the voltage range –60mV to +60mV, which covers their full activation range, and statistical analysis performed using unpaired Student's t-tests. All data tested were taken from current densities measured at +20mV (where I-V relationships were maximal).

## 3. RESULTS AND DISCUSSION

Figure 1 plots whole cell $Ca^{2+}$ channel currents obtained from cells cultutred normoxically, hypoxically or in the presence of AβPs, as indicated. Clearly, as compared with control cells, current densities measured in hypoxic cells were significantly greater, as were those observed in cells pre-incubated with AβPs. Such enhancement was perhaps as anticipated, given the enhancement of evoked secretion seen in cells exposed to hypoxia and AβPs reported previously (Taylor *et al.*, 1999). However, given that the $Ca^{2+}$ dependent secretory response seen in hypoxic and AβP-treated PC12 cells was only suppressed by ~60% in the presence of $Cd^{2+}$ (whereas responses in control cells were completely inhibited by $Cd^{2+}$ (Taylor *et al.*, 999), the near complete inhibition of current by $Cd^{2+}$ was perhaps unexpected.

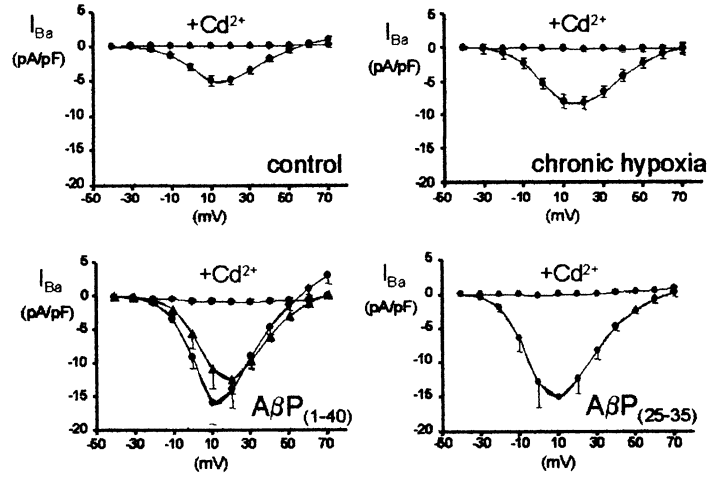


*Figure 1. Hypoxia and AβPs augment $Ca^{2+}$ channel currents in PC12 cells.* Whole-cell current density versus voltage plots measured in four cell groups as indicated, in the absence and presence (+$Cd^{2+}$) of 200μM $Cd^{2+}$. Note the augmentation of current densities in hypoxic and AβP-treated cells (100nM, 24h, except bottom left, triangles represent 20nM treatment) as compared with controls, and the near complete inhibition of inward currents in each case in the presence of $Cd^{2+}$. Data plotted are mean ± s.e.m. current densities taken from at least 8 cells in each case.

Closer inspection of currents recorded in hypoxic and AβP-treated cells revealed that small inward currents were detectable, and that these could be inhibited by the monoclonal antibody, 3D6, raised against the N'-terminus of AβP (Figure 2). Such currents were not detected in control cells (Green & Peers, 2001). Thus both hypoxia and AβPs were able to induce an inward $Ca^{2+}$ current in PC12 cells that could be inhibited by the 3D6 antibody. Given that these currents are so small in amplitude, it is likely that the underlying channels are linked closely to the secretory apparatus, since they are likely to cause only very local, sub-membraneous rises of $[Ca^{2+}]_i$. It is noteworthy that these small currents are not in themselves large enough to account for the overall augmentation of currents as shown in Figure 1. To investigate this further, the pharmacological properties of $Ca^{2+}$ currents were examined.

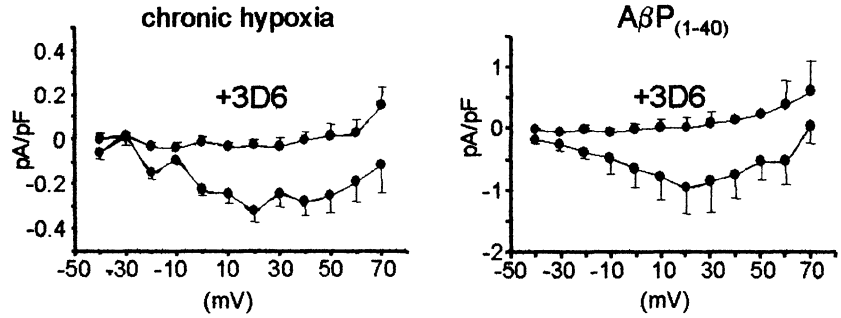


*Figure 2. $Cd^{2+}$ resistant $Ca^{2+}$ currents in hypoxic and AβP-treated PC12 cells.* Whole-cell current density versus voltage plots measured in hypoxic and AβP-treated PC12 cells as indicated in the presence of 200μM $Cd^{2+}$, and also, where indicated, following co-incubation with the monoclonal antibody, 3D6. Data plotted are mean ± s.e.m. current densities taken from at least 8 cells in each case.

Figure 3 reveals that the selective inhibitor of L-type $Ca^{2+}$ channels, nifedipine, caused ~ 40% inhibition of currents in controls cells, indicating that L-type channels give rise to this fraction of total current recorded. In marked contrast, the same concentration of nifedipine caused ~80% inhibition of currents recorded in hypoxic cells and cells exposed to AβPs. Furthermore, the residual, nifedipine-resistant currents detected in all four cell groups tested were similar in magnitude. This finding strongly suggests that hypoxia and AβP treatment, in addition to inducing a $Cd^{2+}$-resistant $Ca^{2+}$ current (Figure 2), also caused a selective up-regulation of L-type $Ca^{2+}$ channels in PC12 cells.

The present findings provide direct evidence that chronic hypoxia causes marked enhancement of $Ca^{2+}$ influx into PC12 cells, and that these effects are

closely mimicked by exposure of cells to AβPs associated with Alzheimer's disease. Two distinct effects are revealed; firstly a $Cd^{2+}$ resistant $Ca^{2+}$ influx pathway, which may be formed by aggregates of amyloid peptides themselves, since the could be blocked by an anti-amyloid peptide antibody (Figure 2); secondly, a selective up-regulation of L-type $Ca^{2+}$ channels which are normally expressed by these cells. Both effects are likely to cause excessive $Ca^{2+}$ influx into these cells following excitation, and so are likely to contribute to the disturbance of $Ca^{2+}$ homeostasis which is commonly associated with the neurodegeneration of Alzheimer's disease.

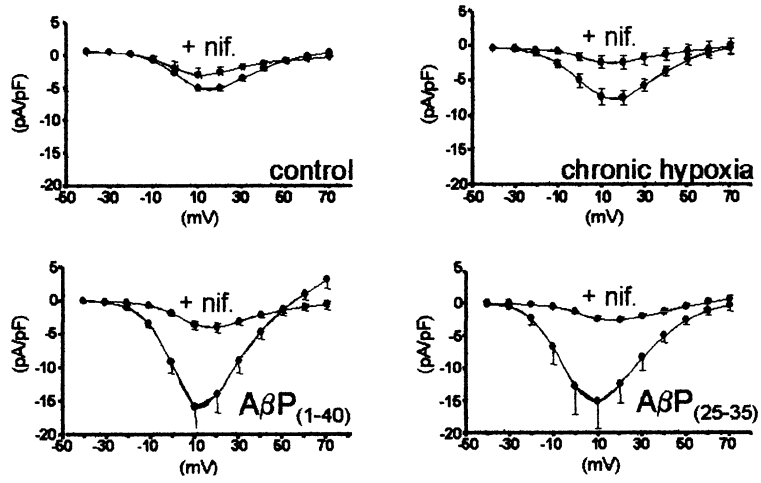


*Figure 3. Nifedipine-sensitivity of $Ca^{2+}$ currents in PC12 cells.*
Whole-cell current density versus voltage plots measured in four cell groups as indicated, in the absence and presence (+ nif.) of 2μM nifedipine. Data plotted are mean ± s.e.m. current densities taken from at least 8 cells in each case.

## ACKNOWLEDGEMENTS

This work was supported by the Medical Research council and the Wellcome Trust.

## REFERENCES

Arispe, N., Pollard, H.B. and Rojas, E., 1996, $Zn^{2+}$ interaction with Alzheimer amyloid beta protein calcium channels. *Proc.Natl.Acad.Sci.USA* 93: 1710-1715.

Behl, C., Davis, J.B., Lesley, R. and Schubert, D., 1994, Hydrogen peroxide mediates amyloid beta protein toxicity. *Cell* 77: 817-827.

Fraser, S.P., Suh, Y.-H. and Djamgoz, M.B.A., 1997, Ionic effects of the Alzheimer's disease beta-amyloid precursor protein and its metabolic fragments *Trends Neurosci.* 20: 67-72.

Glenner, G.G. and Wong, C.W., 1984, Alzheimer's disease: initial report of the purification and characterization of a novel cerebrovascular amyloid protein. *Biochem.Biophys. Res. Comm.* 120: 885-890.

Green, K.N. and Peers, C., 2001, Amyloid β peptides mediate hypoxic augmentation of $Ca^{2+}$ channels. *J. Neurochem.* 77: 953-956.

Jendroska, K., Hoffmann, O.M. and Patt, S., 1997, Amyloid beta peptide and precursor protein (APP) in mild and severe brain ischemia. *Ann.N.Y.Acad. Sci.* 826: 401-405.

Kawahara, M., Arispe, N., Kuroda, Y. and Rojas, E., 1997, Alzheimer's disease amyloid beta-protein forms $Zn^{2+}$-sensitive, cation selective channels across excised membrane patches from hypothalamic neurons. *Biophys. J.* 73: 67-75.

Kogure, K. and Kato, H., 1993, Altered gene expression in cerebral ischemia. *Stroke* 24: 2121-2127.

Kokmen, E., Whisnant, J.P., O'Fallon, W.M., Chu, C.P. and Beard, C.M., 1996, Dementia after ischemic stroke: a population-based study in Rochester, Minnesota (1960-1984). *Neurology* 46: 154-159.

Koistinaho, J., Pyykonen, I., Keinanen, R. and Hokfelt, T., 1996, Expression of beta-amyloid precursor protein mRNAs following transient focal ischemia. *Neuroreport* 7: 2727-2731.

Masters, C.L., Multhaup, G., Simms, G., Pottgiesser, J., Martins, R.N. and Beyreuther, K., 1985, Neuronal origin of a cerebral amyloid: neurofibrillary tangles of Alzheimer's disease contain the same protein as the amyloid of plaque cores and blood vessels. *EMBO J.* 4: 2757-2763.

Mattson, M.P.,1997, Cellular actions of β-amyloid precursor protein and its soluble and fibrillogenic derivatives. *Physiol. Rev.* 77: 1081-1132.

Moroney, J.T., Bagiella, E., Desmond, D.W., Paik, M.C., Stern, Y. and Tatemichi, T.K., 1996, Risk factors for incident dementia after stroke. Role of hypoxic and ischemic disorders. *Stroke* 27, 1283-1289.

Rhee, S.K., Quist, A.P. and Lal, R., 1998, Amyloid β protein (1-42) forms calcium-permeable, $Zn^{2+}$-sensitive channel. *J. Biol. Chem.* 273: 13379-13382.

Schubert, D., Behl, C., Lesley, R., Brack, A., Dargusch, R., Sagara, Y. and Kimura, H., 1995, Amyloid peptides are toxic via a common oxidative mechanism. *Proc. Natl. Acad. Sci. USA* 92: 1989-1993.

Selkoe, D.J., 2001, Alzheimer's disease: genes, proteins and therapy. *Physiol. Rev.* 81: 741-766.

Tatemichi, T.K., Paik, M., Bagiella, E., Desmond, D.W., Stern, Y., Sano, M. Hauser, W.A. and Mayeux, R., 1994, Risk of dementia after stroke in a hospitalized cohort: results of a longitudinal study. *Neurology* 44: 1885-1891.

Taylor, S.C., Batten, T.F.C. and Peers, C., 1999, Hypoxic enhancement of quantal catecholamine secretion: evidence for the involvement of amyloid β-peptides. *J. Biol. Chem.* 274: 31217-31223.

Yokota, M., Saido, T.C., Tani, E., Yamaura, I. and Minami, N., 1996, Cytotoxic fragment of amyloid precursor protein accumulates in hippocampus after global forebrain ischemia. *J. Cereb.Blood Flow Metab.* 16: 1219-1223.

# Role of ROS and NO in Hypoxia-induced Increase in Tyrosine Hydroxylase-messenger RNA in PC12 cells

WOLFGANG KUMMER, BRIGITTE HÖHLER, ALEXANDRA SELL, JÖRG HÄNZE*, UWE PFEIL and ANNA GOLDENBERG

*Institute for Anatomy and Cell Biology, Justus-Liebig-University, 35385 Giessen, Germany*
**Department of Internal Medicine, Justus-Liebig-University, 35385 Giessen, Germany*

## 1. INTRODUCTION

Paraganglia such as the carotid body and retroperitoneal paraganglia constitute a protective system against the adverse effects of hypoxia by measuring arterial $pO_2$ and initiating appropriate reflexes. One of these protective reflexes is release of catecholamines into the blood stream by retroperitoneal paraganglia and the fetal adrenal medulla. Concomitant to this release, catecholamine synthesis is enhanced by hypoxia-induced increase in transcription of the rate-limiting enzyme of catecholamine synthesis, i.e. tyrosine hydroxylase (TH). A tumor cell line derived from a rat adrenal medullary tumor, PC12 cells, is a suitable model to study this hypoxia-induced increased TH gene transcription (Czyzyk-Krzeska *et al.*, 1994; Kroll and Czyzyk-Krzeska, 1998).

Work on other, non-paraganglionic cell types and different hypoxia-responsive genes has recently identified crucial steps in the final pathway linking hypoxia to activation of transcription. A key position is held by the transcription factor HIF (hypoxia-inducible factor), and mechanisms have been best investigated for the isoform HIF-1α. It is constitutively expressed but also constitutively degraded by the proteasomal pathway under normoxic conditions. The signal for being directed towards ubiquitylation and subsequent proteasomal degradation is hydroxylation at a critical prolyl residue by a family of newly

*Chemoreception*, Edited by Pequignot et al.
Kluwer Academic/Plenum Publishers, New York, 2003

discovered HIF prolyl hydroxylases (Ivan *et al.*, 2001; Jaakola *et al.*, 2001; Epstein *et al.*, 2001; Bruick and McKnight, 2001). Under conditions of hypoxia, this prolyl hydroxylation ceases, thus allowing HIF-1α to form a dimer with ARNT (aryl hydrocarbon receptor nuclear translocator) and, subsequently, to activate transcription. The mechanisms by which prolyl hydroxylation is diminished under hypoxia are currently not fully understood. An obvious possibility is offered by the requirement of molecular oxygen for the hydroxylation reaction, so that diminished availability of oxygen might simply reduce enzymatic activity (Ivan *et al.*, 2001; Jaakola *et al.*, 2001; Epstein *et al.*, 2001). However, there are also other pathways known of HIF activation which are less understood and cannot be linked to diminished oxygen supply. Cytokines lead to HIF stabilization even under normoxic conditions, and increased production of reactive oxygen species (ROS) and NO have been found to be involved in this activation pathway (Sandau *et al.*, 2001; Haddad, 2002). We have recently demonstrated an increased generation of ROS in hypoxia-exposed PC12 cells (Höhler *et al.*, 1999) and an increased generation of NO in neuronal cells (Henrich *et al.*, 2002). On this background, we asked in the present study whether PC12 cells also respond to hypoxia by an increased NO production, and whether hypoxic ROS and NO production are linked to the hypoxia-induced TH mRNA increase in PC12 cells.

## 2. RESULTS AND DISCUSSION

### 2.1 Mitochondria are the source of hypoxia-induced increase in ROS production by PC12 cells

ROS production by PC12 cells was investigated at exposure for 1 h to normoxia (21% $O_2$, 5% $CO_2$, 74% $N_2$) or hypoxia (1% $O_2$, 5% $CO_2$, 94% $N_2$) using the fluorescent indicators 2′,7′-dichlorofluorescein diacetate (DCF-DA) or dihydrorhodamine 123, and confocal laser scanning microscopy. As reported previously (Höhler *et al.*, 1999), ROS production increased in PC12 cells during exposure to hypoxia. The hypoxia-induced increase in intracellular fluorescence was sensitive to application of the flavoprotein inhibitor diphenyleniodonium (DPI, 20 μM), to the superoxide scavenger nitrobluetetrazolium (NBT; 1 mM), and to the cell membrane permeable superoxide scavenger, Mn(III)-tetrakis(1-methyl-4-pyridyl)-porphyrin (MnTMPyP, 50 μM), but insensitive to the

hydroxyl radical scavenger dimethylthiourea (DMTU, 10 mM) and the NO-synthase (NOS) inhibitor NG-monomethyl-L-arginine (L-NMMA, 200 μM). Thus, the fluorescence indicators demonstrated an hypoxia-induced increase in superoxide generated by a flavoprotein while formation of hydroxyl radicals or NO-derived radicals such as peroxynitrite did not contribute to enhanced fluorescence signals.

In two series of experiments designed to discriminate between mitochondrial and extra-mitochondrial ROS generation, mitochondria were identified as the source of hypoxia-induced ROS production in PC12 cells. 1) The anion channel blocker 4,4'-diisothiocyanostilbene-2,2' disulfonate was administered at 200 μM in order to prevent exit from intramitochondrially produced superoxide through the inner mitochondrial membrane, and subsequently, into the cytoplasm (Beavis and Davatol-Hag, 1996). Under this condition, a hypoxia-induced intracellular increase was neither observed using the indicator DCF-DA nor using dihydrorhodamine 123, indicating that mitochondrially generated superoxide could not react with the dye located in the cytoplasm and was dismutated intramitochondrially. 2) More direct evidence was provided by blocking mitochondrial translation by application of thiamphenicol over a period of 5 days (Kroon *et al.*, 1976). The efficacy of this treatment was demonstrated by immunolabelling of PC12 cells with cytochrome c-oxidase antiserum. The mitochondrially encoded cytochrome c-oxidase was readily demonstrable in untreated cells while almost no immunoreactivity was detected in thiamphenicol-treated cells. In addition, rotenone (2.5 μM), a blocker of complex I of the respiratory chain which raises normoxic ROS production in PC12 cells (Höhler *et al.*, 1999) failed to do so in thiamphenicol-treated cells, demonstrating lack of electron transport in the respiratory chain in this experimental condition. Thiamphenicol-treated cells did not respond to hypoxia with an increased ROS-generation, showing that an intact mitochondrial respiratory chain is required for the hypoxia-induced increased in ROS production by PC12 cells.

## 2.2 Neither ROS production nor an intact mitochondrial respiratory chain are required for hypoxia-induced TH gene transcription in PC12 cells

PC12 cells were exposed for 6 h to either normoxia or hypoxia (1% $O_2$), and TH mRNA was quantified by hybridization of slot blots and densitometry as

described before (Höhler *et al.*, 1999). Under these conditions, a 2fold increase in TH mRNA was observed, and this increase was fully sensitive to the flavoprotein inhibitor DPI, thereby confirming and extending previous studies in which 5% $O_2$ were applied (Czyzyk-Krzeska *et al.*, 1994; Höhler *et al.*, 1999). None of the ROS scavengers tested, however, could prevent this hypoxia-induced increase in TH mRNA. These ROS scavengers were NBT (1 mM), ebselen (2 μM), DMTU (5-10 mM), MnTMPyP (50 μM), superoxide dismutase (130 U/ml), and catalase (1000 U/ml). Only when using NBT the hypoxia-induced increase was not as pronounced as in controls but it was still significantly present. PC12 cells that had been treated with thiamphenicol and did not respond to hypoxia with an increased ROS production still responded to hypoxia with an increase in TH mRNA that was indistinguishable from that shown by untreated cells. Hence, neither ROS production nor mitochondrially encoded proteins are necessary for hypoxic upregulation of TH mRNA in PC12 cells.

## 2.3 PC12 cells respond to hypoxia with an increased production of NO

In view of our recent observation that sensory neurons respond to hypoxia with an increased NO production by endothelial NOS (Henrich *et al.*, 2002) we investigated whether PC12 cells 1) also contain NOS isoforms, and 2) increase NO production during hypoxia. Using RT-PCR with two different intron-spanning primer pairs (exons 21/22 and 23/24), endothelial NOS specific products were amplified from PC12 cells. Confirming previous immunohistochemical (Dötsch *et al.*, 1997) and RT-PCR data (Onoue *et al.*, 2002), also neuronal NOS specific products were amplified by RT-PCR. Applying the NO-sensitive indicator, diaminofluorescein-2 diacetate, and confocal laser scanning microscopy, NO production has recently been described in PC12 cells (Lopez-Figueroa *et al.*, 2000). Using this compound in an experimental set-up as described for ROS measurements, we observed an hypoxia-induced increase in NO production that was sensitive to the NOS inhibitor, L-NMMA. Thus, PC12 cells contain NOS isoforms and respond to hypoxia with an increased NO production.

## 2.4 Hypoxia-induced NO production is not linked to enhanced TH gene transcription

TH mRNA was quantified by real-time RT-PCR (iCycler, Biorad, Germany) after 6 h exposure of PC12 cells to either normoxia or hypoxia (1% $O_2$). Fully in accordance with the data obtained by densitometry of hybridized slot blots, a hypoxia-induced twofold increase in TH mRNA was measured using this technique. Again in line with the densitometric experiments, the hypoxia-induced increase in TH mRNA could be entirely blocked by the flavoprotein inhibitor DPI. The general NOS inhibitor L-NMMA, however, did not prevent the hypoxia-induced increase in TH mRNA. Applying a luciferase-based HRE (hypoxia-responsive element) reporter gene assay (see Hänze *et al.*, this volume) increased binding activity of the transcription factor HIF could be demonstrated in PC12 cells under the present conditions of hypoxia, and this effect was also not inhibited by L-NMMA. Finally, external application of the NO donor sodium nitroprusside did not increase TH mRNA, as it would be predicted if the hypoxia-induced increase in NO production were linked to TH gene transcription, but rather resulted in a trend towards lower TH mRNA levels as measured by slot blot hybridization/densitometry. Collectively, these data show that hypoxic upregulation of TH gene expression in PC12 cells is not induced by the simultaneously occurring increased generation of NO. Entirely consistent with this concept are the recent observations that various NO donors suppress the hypoxic accumulation of HIF-1α in PC12 cells (Agani *et al.*, 2002), and that NO activates HIF-prolyl hydroxylase in Hep3B cells (Wang *et al.*, 2002).

# 3. CONCLUSION

PC12 cells respond to hypoxia with an increased generation of both ROS, originating from mitochondria, and NO. However, neither this increased radical formation nor the presence of proteins encoded by the mitochondrial genome, and hence an intact mitochondrial electron transport chain, are required for HIF stabilization and the resulting increased in TH mRNA in PC12 cells.

## ACKNOWLEDGEMENTS

This research was supported by the Deutsche Forschungsgemeinschaft (SFB 547, project C1).

## REFERENCES

Agani, F.H., Puchowicz, M., Chavez, J.C., Pichiule, P., and LaManna, J.C., 2002, Role of nitric oxide in the regulation of HIF-1α expression during hypoxia. *Am. J. Physiol. Cell Physiol.* 283: C178-C186.

Beavis, A.D., and Davatol-Hag, H., 1996, The mitochondrial inner membrane anion channel is inhibited by DIDS. *J. Bioenerg. Biomembr.* 28: 207-214.

Bruick, R.K., and McKnight, S.L., 2001, A conserved family of prolyl-4-hydroxylases that modify HIF. *Science* 294: 1337-1340.

Czyzyk-Krzeska, M.F., Furnari, B.A., Lawson, E.E., and Millhorn, D.E., 1994, Hypoxia increases rate of transcription and stability of tyrosine hydroxylase mRNA in pheochromocytoma (PC12) cells. *J. Biol. Chem.* 269: 760-764.

Dötsch, J., Hänze, J., Dittrich, K., Demirakca, S., Haberberger, R., and Rascher, W., 1997, Stimulation of neuropeptide Y release in rat pheochromocytoma cells by nitric oxide. *Eur. J. Pharmacol.* 331: 313-317.

Epstein, A.C.R., Gleadle, J.M., McNeill, L.A., Hewitson, K.S., O'Rourke, J., Mole, D.R., Mukherji, M., Metzen, E., Wilson, M.I., Dhanda, A., Tian, Y.-M., Masson, N., Hamilton, D.L., Jaakola, P., Barstead, R., Hodgkin, J., Maxwell, P.H., Pugh, C.W., Schofield, C.J., and Ratcliffe, P.J., 2001, *C. elegans* EGL-9 and mammalian homologs define a family of dioxygenases that regulate HIF by prolyl hydroxylation. *Cell* 107: 43-54.

Haddad, J.J., 2002, Recombinant human interleukin (IL)-1β-mediated regulation of hypoxia-inducible factor-1α (HIF-1α) stabilization, nuclear translocation, and activation requires an antioxidant/reactive oxygen species (ROS)-sensitive mechanism. *Eur. Cytokine Netw.* 13: 250-260.

Henrich, M., Hoffmann, K., König, P., Gruß, M., Fischbach, T., Göedcke, A., Hempelmann, G., and Kummer, W., 2002, Sensory neurons respond to hypoxia with NO production associated to mitochondria. *Mol. Cell. Neurosci.* 20: 307-322.

Höhler, B., Lange, B., Holzapfel, B., Goldenberg, A., Hänze, J., Sell, A., Testan, H., Möller, W., and Kummer, W., 1999, Hypoxic upregulation of tyrosine hydroxylase gene expression is paralleled, but not induced, by increased generation of reactive oxygen species in PC12 cells. *FEBS Lett.* 457: 53-56.

Ivan, M., Kondo, K., Yang, H., Kim, W., Valiando, J., Ohh, M., Salic, A., Asara, J.M., Lane, W.S., and Kaelin *jr.*, W.G., 2001, HIFα targeted for VHL-mediated destruction by proline hydroxylation: implications for $O_2$ sensing. *Science* 292: 464-468.

Jaakola, P., Mole, D.R., Tian, Y.-M., Wilson, M.I., Gielbert, J., Gaskell, S.J., von Kriegsheim, A., Hebestreit, H.F., Mukherji, M., Schofield, C.J., Maxwell, P.H., Pugh, C.W., and Ratcliffe, P.J., 2001, Targeting of HIF-α to the von-Hippel-Lindau ubiquitylation complex by $O_2$-regulated prolyl hydroxylation. *Science* 292: 464-468.

Kroll, S.L., and Czyzyk-Krzeska, M.F., 1998, Role of $H_2O_2$ and heme-containing $O_2$ sensors in hypoxic regulation of tyrosine hydroxylase gene transcription. *Am. J. Physiol.* 274: C167-C174.

Kroon, A.M., Vries, H., and Nijhof, W., 1976, Protein synthesis in heart mitochondria: mechanism and metabolic aspects. *Acta Cardiol.* 31: 1-13.

Lopez-Figueroa, M.O., Caamano, C., Morano, M.I., Ronn, L.C., Akil, H., and Watson, S.J., 2000, Direct evidence of nitric oxide presence within mitochondria. *Biochem Biophys. Res. Commun.* 272: 129-133.

Onoue, S., Endo, K., Yajima, T., and Kashimoto, K., 2002, Pituitary adenylate cyclase activating polypeptide regulates the basal production of nitric oxide in PC12 cells. *Life Sci.* 71: 205-214.

Sandau, K.B., Zhou, J., Kietzmann, T., and Brüne, B., 2001, Regulation of the hypoxia-inducible factor 1α by the inflammatory mediators nitric oxide and tumor necrosis factor-α in contrast to desferroxamine and phenylarsine oxide. *J. Biol. Chem.* 276: 39805-39811.

Wang, F., Sekine, H., Kikuchi, Y., Takasaki, C., Miura, C., Heiwa, O., Shuin, T., Fujii-Kurijama, Y., and Sogawa, K., 2002, HIF-1α-prolyl-hydroxylase: molecular target of nitric oxide in the hypoxic signal transduction pathway. *Biochem. Biophys. Res. Commun.* 295: 657-662.

# Oxygen Sensing by Human Recombinant Tandem-P Domain Potassium Channels

[1]PAUL J KEMP, [2]CHRIS PEERS, [1]PAULA MILLER, and [1]ANTHONY LEWIS

*[1]School of Biomedical Sciences and [2]Institute for Cardiovascular Research, Worsley Medical and Dental Building, University of Leeds, Leeds LS2 9JT, UK.*

## 1. INTRODUCTION

Oxygen sensing in many tissues is crucially dependent upon hypoxia-evoked suppression of $K^+$ channel activity (Kemp *et al.*, 2003; Lopez-Barneo *et al.*, 2001; Peers, 1997; Patel and Honore, 2001; Peers & Kemp, 2001). This is particularly true of the prospective airway $O_2$ sensor, the neuroepithelial body of the lung (Youngson *et al.*, 1993; Cutz and Jackson, 1999), their immortalised cellular counterpart (H146 cells - O'Kelly *et al.*, 1998; O'Kelly *et al.*, 2000b; O'Kelly *et al.*, 2000a; Hartness *et al.*, 2001; O'Kelly *et al.*, 1999; Kemp *et al.*, 2003) and the arterial $O_2$ sensor, the carotid body (Lopez-Barneo *et al.*, 1988; Peers, 1990; Buckler, 1997). In addition, the $K^+$ channels almost certainly contribute to hypoxic vasoconstriction of the pulmonary vasculature ( Post *et al.*, 1992; Weir & Archer, 1995; Osipenko *et al.*, 2000 Coppock *et al.*, 2001;) although the full extent and nature of their involvement is still somewhat controversial (Ward & Aaronson, 1999). Although each tissue and model system expresses a cell-specific gamut of $K^+$ channels, central to $O_2$ sensory transduction in several is hypoxic inhibition of members of the gene family encoding tandem P-domain ($K_{2P}$) $K^+$ channels. Such background $K^+$ channels contribute to the maintenance of resting membrane potential in cells where they are expressed and ascription of specific $K_{2P}$ channels to cellular hypoxic responses have been shown directly in the airway chemosensing model H146 cells (Hartness *et al.*, 2001) – TASK3) and inferred in carotid body glomus cells (Buckler *et al.*, 2000) – TASK1) and arteriolar smooth muscle of the pulmonary circulation(Gurney *et al.*, 2002) - TASK1 or TASK3). The current exception

*Chemoreception*, Edited by Pequignot et al.
Kluwer Academic/Plenum Publishers, New York, 2003

to this potentially unifying theme in acute $O_2$ sensing is the native neuroepithelial body, where involvement of $K_{2P}$ channels has not been robustly investigated other than by demonstration immunohistochemically of the TASK2 protein (Kemp *et al.*, 2003).

In addition to the reports of $K_{2P}$ inhibition by hypoxia in specialised cells, recent evidence from work in native tissue has suggested strongly that hypoxic regulation of $K_{2P}$ channels (TASK1 in cerebellar granule cells (Plant *et al.*, 2002) and TASK3 in cortical pyramidal cells (Kemp *et al.*, 2002b)) is also crucial to the neuronal responses observed when $O_2$ is reduced to levels consistently observed in pathological conditions such as stroke. Such observations in the central nervous system are particularly important because of recent proposals that certain $K_{2P}$ channels (specifically TREK1) may be involved in neuronal protection (Maingret *et al.*, 1999) and may, as such, represent rational therapeutic targets for alleviation of brain injury during conditions characterised by neuroexcitotoxicity.

To investigate the mechanism of oxygen-sensing by these background $K^+$ channels, we have produced HEK293 cell lines which express stably one of three human members of the tandem P domain $K^+$ channel family known to be expressed in cells which demonstrate $O_2$ sensitivity: hTASK1, hTASK3 and hTREK1. All three of these channels are acutely inhibited by hypoxia. Importantly, there is clear overlap between effects of the major modulatory influences of these channels (acid-base status for TASK1/3 and arachidonic acid for TREK1) and reduced $O_2$ which suggests that the structural requirements for regulation by hypoxia may co-localise significantly with those required for modulation by acid-base status and arachidonic acid.

## 2. METHODS

### 2.1 Cell culture and transfection

Wild type HEK293 cells were maintained in Earle's minimal essential medium (containing L-glutamine) supplemented with 10% (v/v) fetal calf serum, 1% antibiotic antimycotic, 1% non-essential amino acids and gentamicin (50 mg $ml^{-1}$) in a humidified incubator gassed with 5% $CO_2$/95% air. Cells were passaged every 7 days in a ratio of 1:25 using divalent cation-free phosphate buffered saline (PBS). Open-reading frames of cloned hTASK1 (KCNK3 - (Duprat *et al.*, 1997)), hTASK3 (KCNK9, - (Kim *et al.*, 2000)) and hTREK1 (KCNK2 - (Meadows *et al.*, 2000)) were ligated into either pcDNA3.1-$V_5$/$His_6$-TOPO (hTASK1 and hTASK3) or pcDNA3.1-TOPO (hTREK1), transfected into HEK 293 cells using Superfect™ transfection reagent and selected with 1mg.$ml^{-1}$ G418 sulphate, as previously described ( Meadows *et al.*, 2000; Lewis *et al.*, 2001;). As the vector

employed for hTASK1 and hTASK3 contained $V_5$ and $His_6$ peptide epitopes, immunocytochemical verification of protein expression was possible without the use of channel-specific antibodies; specific hTREK antibodies are commercially available. 24 hours before transfection, wild-type HEK293 cells were plated at *circa* 80% confluency. 10μg of channel-pcDNA3.1/TOPO construct was diluted with medium containing neither serum nor antibiotics, 50μl of transfection reagent was added and the mixture incubated for 10 minutes at room temperature to allow complex formation. Medium was aspirated and cells were washed with $Mg^{2+}/Ca^{2+}$-free phosphate buffered saline (PBS). After 10 minutes, 5ml of the conditioned medium was added to the transfection solution and this was then added to the cells and incubated at 37°C for 3 hours, before the transfection solution was removed, the cells washed once with PBS, and fresh medium added. After 48 hours, wild-type medium was replaced by selection medium which contained $1mg.ml^{-1}$ G418. Selection medium was replaced every 7 days. After 4 weeks, single colonies were isolated by adhering sterile cloning rings to the bottom of the flask using vacuum grease and cells contained within each ring were isolated by adding 200μl PBS with 10% trypsin at 37°C for 2 min before adding 200μl fetal calf serum to inactivate the trypsin. Cells were triturated and transferred into selection medium. Each clone was characterised for channel expression by patch clamp analysis of membrane currents, immunocytochemistry and RT-RCR (as appropriate).

## 2.2 Patch-clamp analyses

Cells were grown for 24 hours on glass coverslips before being transferred to a continuously perfused ($5ml.min^{-1}$) recording chamber (volume *circa.* 200μl) mounted on the stage of an inverted microscope. The perfusate was composed of (in mM): 135 NaCl, 5 KCl, 1.2 $MgCl_2$, 5 HEPES, $CaCl_2$ 2.5, 10 D-glucose (pH 7.4). Whole cell $K^+$ currents were recorded at room temperature (21 ± 1°C) using a pipette solution composed of (in mM): 10 NaCl, 117 KCl, 2 $MgSO_4$, 11 HEPES, EGTA 11, $CaCl_2$ 1, 2 $Na_2ATP$ (pH 7.2). When filled with this solution, pipettes were of resistance 3-7 MΩ. Hypoxic solutions were bubbled with $N_2$ for at least 30 minutes prior to perfusion of cells, which produced no shift in either internal or external pH. $pO_2$ was measured using a polarized carbon fibre electrode (Mojet *et al.*,1997), to be 30-40 mmHg. Normoxic solutions were equilibrated with room air. Patch-clamp recordings were made using an Axopatch 200B amplifier and Digidata 1323 A/D interface. To evoke whole-cell $K^+$ currents, cells were clamped at a holding potential of –70mV, and voltage ramps from -100 mV to 0mV (1000ms, 0.1Hz) followed by 100ms steps to 0 mV and +60 mV were applied. Data are shown as example traces

or mean ± S.E.M plots. Cell attached recordings were obtained using patch pipettes filled with standard extracellular solution. In these experiments, pipette potential was held at 0mV, and 1s voltage ramps (from +30mV to –130mV, which mimics the whole-cell voltage protocol in which resting membrane potential was clamped to –70mV) were applied at a frequency of 0.1Hz.

# 3. RESULTS AND DISCUSSION

To date, three recombinant $K_{2P}$ channels have been shown to be sensitive to ambient $pO_2$; these are hTASK1 (KCNK3 - (Lewis *et al.*, 2001)), hTASK3 (KCNK9) and hTREK1 (KCNK2 -(Kemp *et al.*, 2002a)

## 3.1 Expression and $O_2$-sensitivity of human TASK1

Stable expression of hTASK1 was verified using RT-PCR and immunocytochemistry (data not shown, see Lewis *et al.*, 2001). Whole-cell $K^+$ currents of cells stably expressing hTASK1 were, as anticipated, extremely sensitive to extracellular pH, within the physiological range ($IC_{50}$ ~ 7.0). All cells expressing this signature pH-sensitivity were acutely modulated by $pO_2$; reduction of $pO_2$ from 150mmHg to <40mmHg (at pH 7.4) caused rapid and reversible suppression of pH-sensitive $K^+$ currents(Figure 1A). Furthermore, these two regulatory signals clearly acted at the same channel, since the magnitude of the $O_2$-sensitive current was dependent on the extracellular pH (Figure 1B, C). These data represent the first direct verification that hTASK1 is $O_2$-sensitive and reinforce the idea that this $K^+$ channel is key to $O_2$ sensing in chemoreceptors, as suggested in carotid body (Buckler *et al.*, 2000) and central neurones (Plant *et al.*, 2002).

## 3.2 Expression and $O_2$-sensitivity of human TASK3

Stable expression of hTASK3 was verified using RT-PCR and immunocytochemistry (data not shown, see Kemp *et al.*, 2002a) and we have demonstrated that this channel is acutely inhibited by hypoxia (Figure 1D and Kemp *et al.*, 2002a). This observation lends weight to the argument that hTASK3 is the $O_2$-sensitive $K^+$ channel in the NEB cell model, as previously suggested by antisense loss-of-function experiments (Hartness *et al.*, 2001).

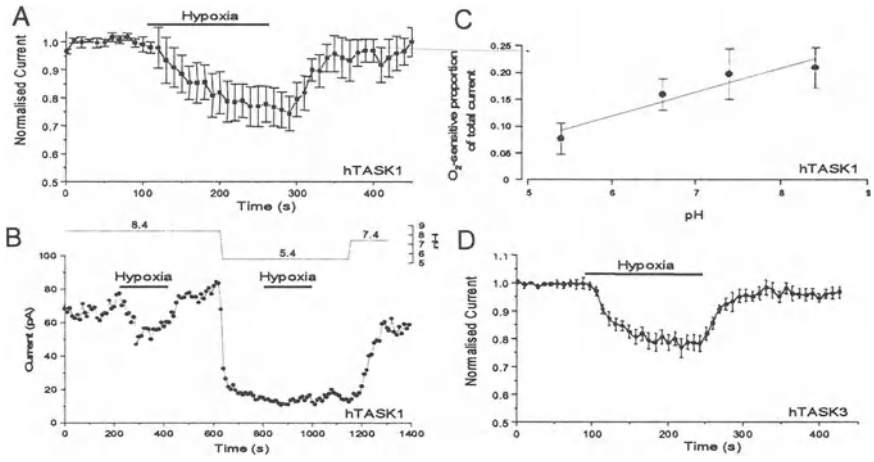


*Figure 1. Stable transfection in HEK293 cells of recombinant hTASK channels and the effect of acute hypoxia thereon.*

(A) Normalized mean time-series plot of the effect of hypoxia on hTASK1 currents measured at 0mV at a $pH_o$ of 7.4. (B) Typical time-series plot showing the effect of hypoxia on hTASK1 currents in a cell perfused with bath solution at $pH_o$ values indicated on the top-right axis. (C) Mean inhibition of hypoxia (as a proportion of the total current measured in $pH_o$ = 7.4) plotted against $pH_o$, demonstrating interactivity of these two modulators. (D) Normalized mean time-series plot of the effect of hypoxia on hTASK3 currents measured at 0mV at a $pH_o$ of 7.4. Periods of exposure to hypoxic perfusate in all panels are indicated by the horizontal bars.

## 3.3 Expression and $O_2$-sensitivity of human TREK1

In central neuronal tissues, another member of the $K_{2P}$ family, hTREK1 (KCNK2), is highly expressed (Medhurst *et al.*, 2001). Acute hypoxia ($pO_2$ = 20mmHg) causes a rapid and reversible inhibition of whole-cell TREK1 $K^+$ current in stably transfected HEK293 cells (Figure 2A, B). In accordance with previous studies, hTREK1 $K^+$ current was enhanced by arachidonic acid in a concentration-dependent manner (Figure 2A, B), (Miller *et al.*, 2003) with maximal enhancement (*circa* 2.5-fold augmentation) observed at a concentration of 10μM. Importantly, acute hypoxia almost completely prevented augmentation of whole cell $K^+$ currents by arachidonic acid (Figure 2A, B). The ability of arachidonic acid to augment currents – and of hypoxia to abrogate this effect – was also observed in cell-attached patches (Figure 2C, D). (Miller *et al.*,2003). These data indicate that hypoxia interacts with hTREK-1, possibly at a site recognized as common to the activation of these channels by agents, including arachidonic acid. Since brain $pO_2$ is as low as 20mmHg, these findings also suggest that the recruitment of activated TREK channels to facilitate neuroprotection (cell hyperpolarization) is probably not possible at ambient brain $O_2$ levels.

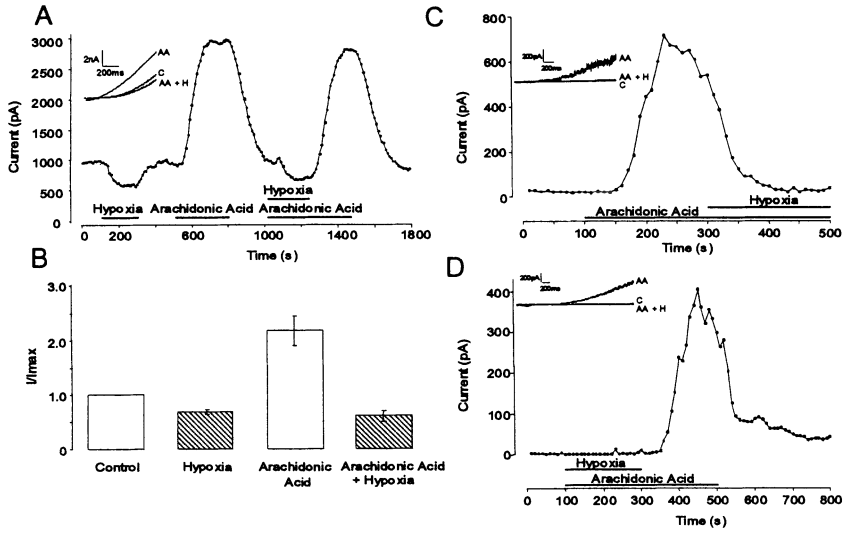


*Figure 2. The effects of acute hypoxia and arachidonic acid on hTREK1 $K^+$ currents.*

(A) Typical time-series plot of the effects of hypoxia and/or 10μM arachidonic acid on hTREK1 whole cell $K^+$ currents measured at 0mV. (B) Mean, normalised data showing the effects of hypoxia and/or 10μM arachidonic acid. (C, D) Typical time-series plots showing the effects of hypoxia and/or 10μM arachidonic acid on hTREK1 cell-attached $K^+$ currents in exemplar cells perfused with arachidonic acid before (C) or during (D) bath hypoxia. Periods of exposure to agents are indicated by the horizontal bars.

## 4. CONCLUSION

$O_2$-sensitive $K^+$ channels have been described and studied in specialised native chemosensory tissues (carotid body, neuroepithelial body and pulmonary arteriole), immortalised cellular models (H146 cells and PC12 cells) and non-specialised tissues (central neurones) where they contribute to cell resting potential. Each tissue and cell type is characterised by a different array of these $K^+$ channels and their inhibition by hypoxia contributes to the physiological response to acute episodes of reduced $O_2$ availability. Although data derived from native tissue is useful, it needs to be combined with the new information garnered from studies which employ recombinant $K^+$ channels in strictly defined cellular environments in order for the full picture to emerge.

This work was funded by The Wellcome Trust and The British Heart Foundation

## 5. REFERENCES


Buckler, K. J., 1997, A novel oxygen-sensitive potassium channel in rat carotid body type I cells. *J.Physiol.* 498, 649-662.

Buckler, K. J., Williams, B. A., & Honore, E., 2000, An oxygen-, acid- and anaesthetic-sensitive TASK-like background potassium channel in rat arterial chemoreceptor cells. *J.Physiol.* 525, 135-142.

Coppock, E. A., Martens, J. R., & Tamkun, M. M., 2001, Molecular basis of hypoxia-induced pulmonary vasoconstriction:role of voltage-gated $K^+$ channels. *Am.J.Physiol.* 281, L1-L8.

Cutz, E. & Jackson, A., 1999, Neuroepithelial bodies as airway oxygen sensors. *Respir.Physiol.* 115 , 201-214.

Duprat, F., Lesage, F., Fink, M., Reyes, R., Heurteaux, C., & Lazdunski, M., 1997, TASK, a human background $K^+$ channel to sense external pH variations near physiological pH. *EMBO J.* 16, 5464-5471.

Gurney, A. M., Osipenko, O. N., MacMillan, D., & Kempsill, F. E., 2002, Potassium channels underlying the resting potential of pulmonary artery smooth muscle cells. *Clin.Exp.Pharmacol.Physiol* 29, 330-333.

Hartness, M. E., Lewis, A., Searle, G. J., O'Kelly, I., Peers, C., & Kemp, P. J., 2001, Combined antisense and pharmacological approaches implicate hTASK as an airway $O_2$ sensing $K^+$ channel. *J.Biol.Chem.* 276, 26499-26508.

Kemp, P. J., Lewis, A., Miller, P., Chapman, C. G., Meadows, H., & Peers, C., 2002a, Oxygen sensing by two members of the human tandem P domain $K^+$ channel family. *FASEB J.* 16, A61.

Kemp, P. J., Plant, L. D., Peers, C., & Pearson, H. A., 2002b, Acute hypoxia inhibits an acid-sensitive leak $K^+$ conductance in primary cultures of rat neocortical pyramidal neurones which is not TASK1. *FASEB.J* 16, A61.

Kemp, P. J., Searle, G. J., Hartness, M. E., Lewis, A., Miller, P., Williams, S. E., Wootten, P., Adriaensen, D., & Peers, C., 2003, Acute oxygen sensing in cellular models:relevance to physiology of pulmonary neuroepithelial and carotid bodies. *Anat.Rec.* 270, 41-50.

Kim, Y., Bang, H., & Kim, D., 2000, TASK-3, a new member of the tandem pore $K^+$ channel family. *J.Biol.Chem.* 275, 9340-9347.

Lewis, A., Hartness, M. E., Chapman, C. G., Fearon, I. M., Meadows, H. J., Peers, C., & Kemp, P. J., 2001, Recombinant hTASK1 is an $O_2$-sensitive $K^+$ channel. *Biochem.Biophys.Res.Comm.* 285, 1290-1294.

Lopez-Barneo, J., Lopez-Lopez, J. R., Urena, J., & Gonzalez, C., 1988, Chemotransduction in the carotid body: $K^+$ current modulated by $PO_2$ in type I chemoreceptor cells. *Science* 241, 580-582.

Lopez-Barneo, J., Pardal, R., & Ortega-Saenz, P., 2001, Cellular mechanism of oxygen sensing. *Ann.Rev.Physiol.* 63, 259-287.

Maingret, F., Patel, A. J., Lesage, F., Lazdunski, M., & Honore, E., 1999, Mechano- or acid stimulation, two interactive modes of activation of the TREK-1 potassium channel. *J.Biol.Chem.* 274, 26691-26696.

Meadows, H. J., Benham, C. D., Cairns, W., Gloger, I., Jennings, C., Medhurst, A. D., Murdock, P., & Chapman, C. G., 2000, Cloning, localisation and functional expression of the human orthologue of the TREK-1 potassium channel. *Pflugers Arch* 439, 714-722.

Medhurst, A. D., Rennie, G., Chapman, C. G., Meadows, H., Duckworth, M. D., Kelsell, R. E., Gloger, I. I., & Pangalos, M. N., 2001, Distribution analysis of human two pore domain potassium channels in tissues of the central nervous system and periphery. *Brain Res.Mol.Brain Res.* 86, 101-114.

Miller,P., kemp,PJ.,Lewis, A.,Chapman, SG.,& Meadows, H. J., 2003, Hypoxia inhibits the recombinant tandem P domain K+ channel, hTREK1, and excludes its activation by arachidonic acid or stretch *J. Physiol.* 548.31-37

Mojet, M. H., Mills, E., & Duchen, M. R., 1997, Hypoxia-induced catecholamine secretion in isolated newborn rat adrenal chromaffin cells is mimicked by inhibition of mitochondrial respiration. *J.Physiol.* 504, 175-189.

O'Kelly, I., Lewis, A., Peers, C., & Kemp, P. J., 2000a, $O_2$ sensing by airway chemoreceptor-derived cells: protein kinase C activation reveals functional evidence for involvement of NADPH oxidase. *J.Biol.Chem.* 275, 7684-7692.

O'Kelly, I., Peers, C., & Kemp, P. J., 1998, Oxygen-sensitive $K^+$ channels in neuroepithelial body-derived small cell carcinoma cells of the human lung. *Am.J.Physiol.* 275, L709-L716.

O'Kelly, I., Peers, C., & Kemp, P. J., 2000b, Oxygen sensing by model airway chemoreceptors: Hypoxic inhibition of $K^+$ channels in H146 cells. *Adv.Exp.Med.Biol.* 475, 611-622.

O'Kelly, I., Stephens, R. H., Peers, C., & Kemp, P. J., 1999, Potential identification of the oxygen sensitive $K^+$ current in a human neuroepithelial body-derived cell line. *Am.J.Physiol* 276, L96-L104.

Osipenko, O. N., Tate, R. J., & Gurney, A. M., 2000, Potential role for kv3.1b channels as oxygen sensors. *Circ.Res.* 86, 534-540.

Patel, A. J. & Honore, E., 2001, Molecular physiology of oxygen-sensitive channels. *Euro.Respir.J.* 18, 221-227.

Peers, C., 1997, Oxygen-sensitive ion channels. *Trends Pharmacol.Sci.* 18, 405-408.

Peers, C., 1990, Hypoxic suppression of $K^+$ currents in type-I carotid-body cells - selective effect on the $Ca^{2+}$-activated $K^+$ current. *Neurosci.Lett.* 119, 253-256.

Peers, C. & Kemp, P.J., 2001, Acute oxygen sensing: Diverse but convergent mechanisms in airway and arterial chemoreceptors. *Respir. Res.* 2, 145-149.

Plant, L. D., Kemp, P. J., Peers, C., Henderson, Z., & Pearson, H. A., 2002, Hypoxic depolarization of cerebellar granule neurons by specific inhibition of TASK-1. *Stroke* 33, 2324-2328.

Post, J. M., Hume, J. R., Archer, S. L., & Weir, E. K., 1992, Direct role for potassium channel inhibition in hypoxic pulmonary vasoconstriction. *Am.J.Physiol.* 262, C882-C890.

Ward, J. P. & Aaronson, P. I., 1999, Mechanisms of hypoxic pulmonary vasoconstriction: can anyone be right? *Respir.Physiol.* 115, 261-271.

Weir, E. K. & Archer, S. L., 1995, The mechanism of acute hypoxic pulmonary vasoconstriction: the tale of two channels. *FASEB J.* 9, 183-189.

Youngson, C., Nurse, C., Yeger, H., & Cutz, E., 1993, Oxygen sensing in airway chemoreceptors. *Nature* 365, 153-155.

# Oxygen Sensing by Human Recombinant Large Conductance,Calcium-activated Potassium Channels

## *Regulation by acute hypoxia*

[1]PAUL J KEMP, [2]CHRIS PEERS AND [1]ANTHONY LEWIS
*[1]School of Biomedical Sciences and [2]Institute for Cardiovascular Research, Worsley Medical and Dental Building, University of Leeds, Leeds LS2 9JT, UK.*

## 1. INTRODUCTION

Although $O_2$-sensitive tissues express a wide variety of channel types (Lopez-Barneo *et al.*, 2001; Peers & Kemp, 2001), central to the cellular mechanism of $O_2$ sensing in many is hypoxic suppression of large conductance $Ca^{2+}$-activated $K^+$ channels (maxiK, $BK_{Ca}$ or *Slo* channels). Thus, hypoxic inhibition of maxiK channels has been demonstrated in carotid body (Peers, 1990; Pardal *et al.*, 2000; Riesco-Fagundo *et al.*, 2001), pulmonary smooth muscle (Cornfield *et al.*, 1996), chromaffin cells (Thompson & Nurse, 1998), and other non-chemosensory tissues such as central neurones (Liu *et al.*, 1999; Jiang & Haddad, 1994b). Contribution of this channel type to carotid body, chromafin cell and central neuronal function is well supported although some controversy still surrounds their involvement in pulmonary vasoconstriction (Ward & Aaronson, 1999) where there is also good evidence for both delayed rectifier (Tristani-Firouzi *et al.*, 1996) and tandem P domain $K^+$ channels in the response (Gurney *et al.*, 2002); the later observation is fully supported by our recent report of $O_2$ sensitivity of the tandem P domain channel, hTASK1, in a recombinant mammalian system similar to that employed in the present study (Lewis *et al.*, 2001).

Although it has been suggested that the mechanism of hypoxic regulation of $K^+$ channels in general, and maxiK channels in particular, may involve $O_2$-dependent modulation of cellular redox potential, the nature of the sensor is still unclear and the mechanism whereby decreased $pO_2$ evokes channel inhibition in different tissues remains controversial. Indeed, there are

*Chemoreception*, Edited by Pequignot et al.
Kluwer Academic/Plenum Publishers, New York, 2003

varying reports which have suggested involvement of either cytosolic factors (e.g. (Wyatt & Peers, 1995)) or direct channel modulation (e.g. (Liu *et al.*, 1999; Riesco-Fagundo *et al.*, 2001; Jiang & Haddad, 1994a)). In favour of potential regulation by cellular redox state are recent data demonstrating activation of these channels by oxidising agents in a recombinant cellular system (Tang *et al.*, 2001) and their inhibition by reduced glutathione in rat hippocampal neurones (Soh *et al.*, 2001). However, since hypoxic regulation of recombinant maxiK channels of known molecular identity have not been studied to date, it is difficult to assess the contribution that tissue-specificity, species-differences, splice variation and subunit stoichiometry have to the final modulation by $O_2$ of natively expressed maxiK channels. To address some of these concerns, we have employed HEK293 cells stably co-expressing identified α- and β- subunits of a human maxiK channel in order to examine the $O_2$-sensitivity of these recombinant $K^+$ channels at the single channel level.

This work was funded by The Wellcome Trust and The British Heart Foundation

## 2. METHODS

### 2.1 Cell culture and chronic hypoxia

Human embryonic kidney 293 (HEK 293) cells which express human brain αβ maxiK channels (Ahring *et al.*, 1997) were maintained in Earle's minimal essential medium (containing L-glutamine) supplemented with 10 % fetal calf serum, 1% antibiotic antimycotic, 1% non-essential amino acids and 0.2% in a humidified incubator gassed with 5% $CO_2$/95% air. Cells were passaged every 7 days in a ratio of 1:25 using $Ca^{2+}$- and $Mg^{2+}$-free phosphate-buffered saline. The co-expressed α- and β-subunits were KCNMA1 (Genbank accession number U11717) and KCNMB1 (Genbank accession number U42600), respectively. For the experiments described herein, cells were cultured for up to 3 days on glass coverslips at 37°C in water-saturated environments of 21% $O_2$/5% $CO_2$/74% $N_2$ ($pO_2$ ~ 143 mmHg – "Normoxia").

### 2.2 Patch-clamp recording

Cells were transferred to a continuously perfused (5ml.min$^{-1}$) recording chamber mounted on the stage of an inverted microscope. For inside-out, excised patch clamp recordings, the standard bath solution was composed of (in mM): 10 NaCl, 117 KCl, 2 $MgCl_2$, 11 N-2-hydroxyethylpiperazine-N'-

ethanesulfonic acid (HEPES), pH 7.2 with $Ca^{2+}$ buffered to 30 nM, 100 nM, 300 nM, 1 μM and 100 μM using ethylene glycol-bis(β-aminoethyl ether)-N,N,N', N'-tetraacetic acid (EGTA), and $CaCl_2$ in appropriate ratios. The $Na^+$-rich pipette solution was composed of (in mM): 135 NaCl, 5 KCl, 1.2 $MgCl_2$, 5 HEPES, $CaCl_2$ 2.5, 10 D-glucose (pH 7.4). The $K^+$-rich pipette solution was composed of (in mM): 10 NaCl, 117 KCl, 2 $MgCl_2$,, 2.0 $CaCl_2$ (pH 7.2). To evoke macro-patch $K^+$ currents, one of four protocols (Vh = -70mV) was employed: 1) *standard ramp,* voltage ramps from -100 mV to +60 mV (2 s, 0.1 Hz); 2) *extended ramp,* –70 mV holding potential, voltage ramps from -100 mV to +200 mV (2 s, 0.1 Hz); 3) *activating step,* –70 mV holding potential, voltage steps from holding to between 0 mV and +50 mV in 10 mV increments (100 ms, 0.1 Hz) and; 4) *deactivating step,* –70mV holding potential, voltage step from holding to 130 mV (50 ms) followed by steps in the range –70 mV to –130 mV in 10 mV increments (1 s, 0.1Hz).

Solutions which were employed to produce *acute* hypoxia were bubbled with $N_{2(g)}$ for at least 30 min. prior to perfusion of cells; this produced no shift in pH. $pO_2$ was measured (at the cell) using a polarized carbon fibre electrode (Mojet *et al.*, 1997) to be 25-40 mmHg. Normoxic solutions were equilibrated with room air. All $K^+$ currents were recorded at a bath temperature of 22 ± 0.5 °C. Current recordings were made using an Axopatch 200B amplifier and Digidata 1320 A/D interface.

## 3. RESULTS and DISCUSSION

The continuous current recording shown in Figure 1A clearly demonstrates that acute hypoxia evokes a dramatic and reversible reduction in patch activity.. All patches demonstrated such depression (Figure 1B,

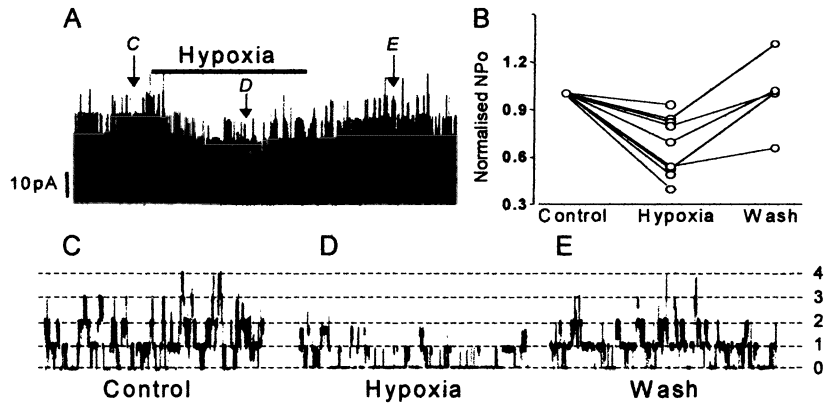


*Figure 1. Hypoxic suppression of single maxiK channel activity.*
(A) Current recording (360s) from an inside-out, excised membrane patch in asymmetrical solutions ($[Ca^{2+}]_i$=300 nM, Vh=+50 mV). Period of hypoxia shown by horizontal bar. (B) Normalised *NPo* values from 9 separate cells under the conditions described in (*A*) as defined. (C) (D) and (E) Single channel currents on an extended time-base (200 ms per trace) from the recording shown in (*A*) at the arrows.

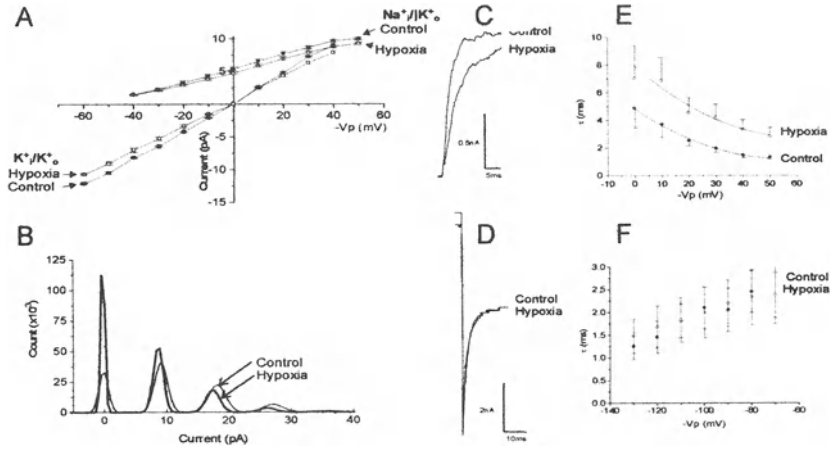


*Figure. 2 Hypoxic modulation of single channel conductance and activation.*
(A) Single channel I-V relationships in normoxia (*control - solid symbols*) and hypoxia (*open symbols*) with either $Na^+$-rich (*circles,* n = 6) or $K^+$-rich pipette solutions (*squares,* n = 4) with $[Ca^{2+}]_i$ = 300 nM. (B) Exemplar all-points histogram taken from a patch which was bathed in the asymmetrical solutions as above (Vh = at +50mV) in normoxia (*control – fine line*) and hypoxia (*bold line*). (C) Activation current (from Vh = +50mV) in the presence (*hypoxia)* and absence (*control*) of hypoxia. (D) Exemplar deactivating tail current (stepped from 130 mV to –130 mV) in the presence (*hypoxia)* and absence (*control*) of hypoxia. (E) Voltage-dependence of mean activation time constants in the presence (*hypoxia – open symbols*) and absence (*control – closed symbols*) of hypoxia (n = 10). (F). Voltage-dependence of mean deactivation time constants in the presence (*hypoxia – open symbols*) and absence (*control – closed symbols*) of hypoxia (n = 5). All recordings were performed in asymmetrical solutions with 1 μM $[Ca^{2+}]_i$.

32.0± 6.5% inhibition, n = 9, P<0.01). Traces shown in Figure 1 C, D and E (200 ms – arrows on Figure 1A) exemplify this reduction in channel activity evoked by hypoxia and demonstrate clearly that hypoxic inhibition of maxiK currents does not have an absolute requirement for soluble cytosolic factors.

In symmetrical $K^+$-rich solutions ($Ca^{2+}{}_i$ = 300 nM), hypoxia significantly (P < 0.05, n = 4) reduced single channel conductance by ~ 12 % from 215.4 ± 2.0 pS to 188.5 ± 10 pS (Figure 2A). Similarly, in asymmetrical solutions, conductance was also reduced by hypoxia (Figure 2A). This observation of reduced unitary conductance is highlighted in Figure 2B where the channel amplitudes, calculated from all-points histograms of an exemplar patch (asymmetrical solutions at +50 mV), are seen to be reduced at all open levels. In order to study activation/deactivation at test potentials which were on the rising phase of the current-voltage relationship, we employed inside-out patches in 1μM $Ca^{2+}{}_i$. All activating and deactivating currents were best described by a single exponential function. Under these conditions, hypoxia

significantly decreased the rate of activation at all test potentials (Figure 2C and E, n = 10, P < 0.02). In contrast, deactivation was unaffected by hypoxia (Figure 2D and F).

Figure 3 illustrates the dependence of hypoxic channel inhibition on

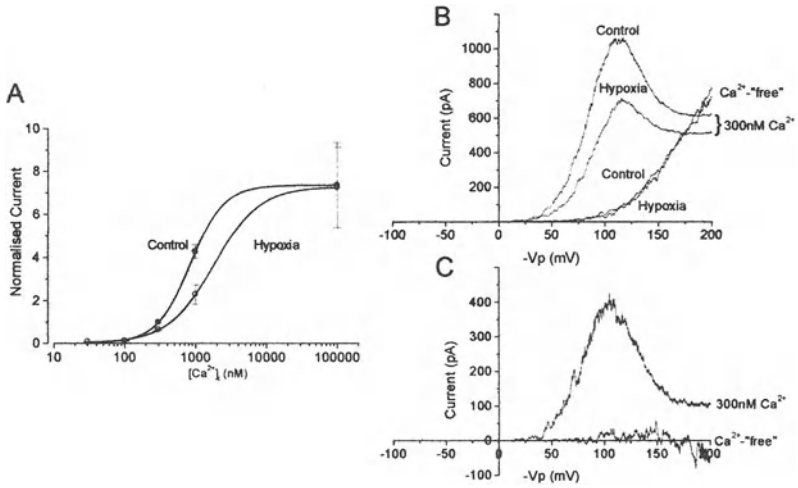


*Figure 3. $Ca^{2+}{}_i$- and voltage-dependence of hypoxic channel inhibition.*
(A). Dependence of currents (measured at +50 mV) on $[Ca^{2+}]_i$ in normoxia (filled circles) and hypoxia (open circles). (B) Effect of hypoxia in the extended voltage range in the presence (*300 nM*) and absence (*$Ca^{2+}$-"free"*) of $[Ca^{2+}]_i$. (C) Hypoxia-sensitive currents in the presence (*300 nM*) and absence (*"$Ca^{2+}$-free"*) $[Ca^{2+}]_i$. Data for B and-C are representative of four such recordings.

$[Ca^{2+}]_i$. Thus, at low $[Ca^{2+}]_i$, hypoxia had no significant effect on channel activity (Measured at +50mV – Figure 3A). However, as $[Ca^{2+}]_i$ was raised to 300 nM and 1 μM, channel inhibition became apparent. The calculated $EC_{50}$ values were 840 ± 15 nM in normoxia vs. 1805 ± 112 nM in hypoxia. Hypoxic inhibition was not supported at high $[Ca^{2+}]_i$ (Figure 3A). The data in Figure 3 suggest that hypoxia evokes channel inhibition by either increasing the voltage threshold for channel activation and/or decreasing $Ca^{2+}$ sensitivity of the channels. To distinguish between these possibilities, we employed the extended ramp protocol to evoke similar degrees of channel activity, albeit at different voltages, regardless of $[Ca^{2+}]_i$. When $[Ca^{2+}]_i$ was less than 1 nM, the large depolarising ramp was able to evoke activity which was not significantly different from that in the presence of 300 nM at +200 mV (Figure 3B – control). Most importantly, in the presence

of 300 nM $[Ca^{2+}]_i$, hypoxia caused a significant decrease in current at all activating potentials (Figure 3B – hypoxia) whereas hypoxic current suppression was completely absent when $[Ca^{2+}]_i$ below 1 nM; subtracted, hypoxia-sensitive currents in the "absence" and presence of $[Ca^{2+}]_i$ are plotted in Figure 3C. These data suggest strongly that hypoxia inhibits maxiK channels by reducing their $Ca^{2+}$ sensitivity – a notion which was confirmed by demonstrating that hypoxia was without effect at a saturating concentration of $Ca^{2+}{}_i$ in the extended ramp protocol (data not shown).

Our findings demonstrate directly that the human α/β maxiK channel heteromer is an $O_2$-sensitive $K^+$ channel and support strongly the notion that hypoxic inhibition of this channel occurs primarily via a reduction in $Ca^{2+}$-sensitivity with an additional, minor reduction in unitary conductance.

## REFERENCES

Ahring, P. K., Strobaek, D., Christophersen, P., Olesen, S. P., & Johansen, T. E., 1997, Stable expression of the human large-conductance $Ca^{2+}$-activated $K^+$ channel alpha- and beta-subunits in HEK293 cells. *FEBS Lett.* 415, 67-70.

Gurney, A. M., Osipenko, O. N., MacMillan, D., & Kempsill, F. E., 2002, Potassium channels underlying the resting potential of pulmonary artery smooth muscle cells. *Clin. Exp. Pharmacol. Physiol* 29, 330-333.

Jiang, C. & Haddad, G. G., 1994a, A direct mechanism for sensing low oxygen levels by central neurons. *Proc.Natl.Acad.Sci.USA* 91, 7198-7201.

Jiang, C. & Haddad, G. G., 1994b, Oxygen deprivation inhibits a $K^+$ channel independently of cytosolic factors in rat central neurons. *J.Physiol.* 481, 15-26.

Lewis, A., Ashford, M. L. J. Ashford, C. Peers & P. J. Kemp, 2002, Hypoxia inhibits human recombinant maxi $K^+$ channels by a mechanism which is membrane delimited and $Ca^{2+}$-sensitive. *J. Physiol.* 540, 771-780.

Liu, H., Moczydlowski, E., & Haddad, G. G., 1999, $O_2$ deprivation inhibits $Ca^{2+}$-activated $K^+$ channels via cytosolic factors in mice neocortical neurons. *J.Clin.Invest.* 104 , 577-588.

Lopez-Barneo, J., Pardal, R., & Ortega-Saenz, P., 2001, Cellular mechanism of oxygen sensing. *Ann.Rev.Physiol.* 63, 259-287.

Mojet, M. H., Mills, E., & Duchen, M. R., 1997, Hypoxia-induced catecholamine secretion in isolated newborn rat adrenal chromaffin cells is mimicked by inhibition of mitochondrial respiration. *J.Physiol.* 504, 175-189.

Pardal, R., Ludewig, U., Garcia-Hirschfeld, J., & Lopez-Barneo, J., 2000, Secretory responses of intact glomus cells in thin slices of rat carotid body to hypoxia and tetraethylammonium. *Proc.Natl.Acad.Sci.U.S.A* 97, 2361-2366.

Peers, C., 1990, Hypoxic suppression of $K^+$ currents in type-I carotid-body cells - selective effect on the $Ca^{2+}$-activated $K^+$ current. *Neurosci.Lett.* 119, 253-256.

Peers, C. & Kemp, P. J., 2001, Acute oxygen sensing: diverse but convergent mechanisms in airway and arterial chemoreceptors. *Respir.Res* 2, 145-149.

Riesco-Fagundo, A. M., Perez-Garcia, M. T., Gonzalez, C., & Lopez-Lopez, J. R., 2001, $O_2$ modulates large-conductance $Ca^{2+}$-dependent $K^+$ channels of rat chemoreceptor cells by a membrane-restricted and CO-sensitive mechanism. *Circ.Res.* 89, 430-436.

Soh, H., Jung, W., Uhm, D. Y., & Chung, S., 2001, Modulation of large conductance calcium-activated potassium channels from rat hippocampal neurons by glutathione. *Neurosci Lett* 298, 115-118.

Tang, X. D., Daggett, H., Hanner, M., Garcia, M. L., McManus, O. B., Brot, N., Weissbach, H., Heinemann, S. H., & Hoshi, T., 2001, Oxidative regulation of large conductance calcium-activated potassium channels. *J.Gen.Physiol.* 117, 253-274.

Thompson, R. J. & Nurse, C. A., 1998, Anoxia differentially modulates multiple $K^+$ currents and depolarizes neonatal rat adrenal chromaffin cells. *J.Physiol.* 512, 421-434.

Tristani-Firouzi, M., Reeve, H. L., Tolarova, S., Weir, E. K., & Archer, S. L., 1996, Oxygen-induced constriction of rabbit ductus arteriosus occurs via inhibition of a 4-aminopyridine-, voltage-sensitive potassium channel. *J.Clin.Invest.* 98, 1959-1965.

Ward, J. P. & Aaronson, P. I., 1999, Mechanisms of hypoxic pulmonary vasoconstriction: can anyone be right? *Respir.Physiol.* 115, 261-271.

Wyatt, C. N. & Peers, C., 1995, $Ca^{2+}$-activated $K^+$ channels in isolated type-I cells of the neonatal rat carotid-body. *J.Physiol.* 483, 559-565.

# Potential Oxygen Sensing Pathways in the Zebrafish Gill

MICHAEL G. JONZ, IAN M. FEARON and COLIN A. NURSE
*Department of Biology, McMaster University, Hamilton, Ontario, Canada L8S 4K1*

## 1. INTRODUCTION

Regulation of arterial partial pressure of oxygen ($P_{O_2}$) during periods of hypoxia ensures adequate delivery of $O_2$ to systemic tissues. Peripheral $O_2$ chemoreceptors in mammals, such as carotid body glomus cells and neuroepithelial bodies of the lung, respond to hypoxia with a reduction of $K^+$ current (López-Barneo *et al.*, 1988; Youngson *et al.*, 1993; see also Thompson *et al.*, 1997). This cellular response is thought to initiate hyperventilation and other physiological adaptations to hypoxia through $Ca^{2+}$-dependent neurosecretion and activation of post-synaptic pathways (González *et al.*, 1994; López-Barneo *et al.*, 2001). In water-breathing vertebrates, such as teleost fish, hypoxia induces hyperventilation, bradycardia and an increase in gill vascular resistance, and these responses arise principally from peripheral $O_2$ chemoreceptors (Burleson *et al.*, 1992). However, $O_2$-sensitive cells mediating these responses have not been identified.

The gill arches are innervated by branches of the glossopharyngeal (IX) and vagus (X) nerves (Nilsson, 1984) and contain numerous gill filaments that each give rise to a series of respiratory lamellae. Serotonergic neuroepithelial cells (NECs) reside in the epithelium of gill filaments exposed directly to the respiratory water flow in all fish species examined so far, and contain dense-cored vesicles at the ultrastructural level (Dunel-Erb *et al.*, 1982; Bailly *et al.*, 1992; Zaccone *et al.*, 1994; Zaccone *et al.*, 1997). In addition, extracellular recordings from afferent fibres of IX and X cranial nerves indicated the presence of $O_2$ chemoreceptors within the fish gill (Burleson and Milsom, 1993; Milsom and Brill, 1986). Although the

*Chemoreception*, Edited by Pequignot et al.
Kluwer Academic/Plenum Publishers, New York, 2003

available evidence suggests that gill NECs may represent a group of peripheral $O_2$ chemoreceptors, confirmation of this hypothesis awaits electrophysiological characterisation of the effects of hypoxia on these cells.

The objectives of this investigation were to identify NECs and possible pathways through which these potential $O_2$ chemoreceptors may function in the gills of zebrafish (*Danio rerio*), and to determine if these cells are $O_2$-sensitive. With the aid of a zebrafish-specific neuronal marker, confocal microscopy and voltage-clamp experiments, our preliminary results lead us to propose that NECs of fish may be phylogenetic precursors of mammalian $O_2$ chemoreceptors.

## 2. MATERIALS AND METHODS

### 2.1 Confocal Immunofluorescence

Adult zebrafish were obtained from local commercial sources and maintained in an aquarium at 28°C on a 14 h light/dark cycle (Westerfield, 2000). Animals were quickly stunned with a blow to the head and decapitated. Gills were removed and washed in phosphate-buffered solution (PBS) containing (in mM): NaCl, 137; $Na_2HPO_4$, 15.2; KCl, 2.7; $KH_2PO_4$, 1.5; pH 7.8 (Bradford *et al.*, 1994). Tissue was fixed by immersion in 4% paraformaldehyde in PBS at 4°C overnight and permeabilised in PBS containing 1% fetal calf serum and 0.5% Triton X-100 for 48 h at 4°C. Gill arches were prepared as whole mounts and treated with primary antisera against a zebrafish neuron-specific antigen (zn-12, 1:25), the synaptic vesicle protein SV2 (1:200, Developmental Studies Hybridoma Bank) or serotonin (5-HT, 1:250, Sigma) for 24 h. Antiserum against zn-12 acts as a general neuronal marker in the zebrafish (Trevarrow *et al.*, 1990) and 5-HT has been used to label neuroepithelial cells (NECs) of the fish gill (Dunel-Erb *et al.*, 1982). Tissue was treated with secondary antisera conjugated with fluorescent markers FITC (1:50, Jackson Laboratories) or Alexa 594 (1:100, Molecular Probes) at 23°C for 1 h in darkness. Arches were mounted on glass microscope slides in Vectashield (Vector Laboratories) to prevent photobleaching. Tissue specimens were examined with a confocal scanning system (Radiance 2000, Biorad) equipped with Ar and HeNe lasers with peak outputs of 488 and 543 nm, respectively. Tissue was scanned in optical sections separated by 0.2-1 μm and composite images of these sections were produced. Images were converted to grayscale and colour-inverted so that immunofluorescent structures appeared as black on a white background.

## 2.2 Electrophysiology

Zebrafish gill cells were dissociated, plated in glass-bottom culture dishes coated with poly-L-lysine and maintained in L-15 medium (supplemented with 2% penicillin/streptomycin and 10% fetal calf serum) for 24-48 h. The presence of NECs *in vitro* was verified by 5-HT and SV2 immunoreactivity (as above), and Neutral Red (NR) was used as a vital marker for 5-HT-containing cells (Youngson *et al.*, 1993). The whole-cell, voltage-clamp technique (Hamill *et al.*, 1981) was used to monitor ionic currents in NR-positive cells. Recordings were obtained using an EPC 9 amplifier (Heka Electronics) and digitally converted using an AD/DA converter with an ITC-16 interface and Pulse software (Heka Electronics). Glass electrodes were pulled on a vertical pipette puller (PP-83, Narishige) with a tip resistance of 5-8 MΩ. Electrodes were fire-polished and filled with intracellular recording solution containing the following (mM): KCl, 135; NaCl, 5; $CaCl_2$, 0.1; EGTA, 11; HEPES, 10; Mg-ATP, 2; pH 7.2 (Thompson *et al.*, 1997). Junction potentials (~5 mV) were subtracted and seal resistance was typically 1-10 GΩ. Extracellular recording solution contained the following (mM): NaCl, 135; KCl, 5; $CaCl_2$, 2; $MgCl_2$, 2; glucose, 10; HEPES, 10; pH 7.4 (Thompson *et al.*, 1997). Normoxic (150 mmHg) and hypoxic (20 mmHg, equilibrated with 100% $N_2$) extracellular solutions were perfused into the bath at a flow rate of 4 ml/min. NR-positive cells were held at –60 mV and ionic currents were evoked by changing the membrane potential from –100 mV to 60 mV over 1 s following a ramp protocol. Outward current was recorded before and after a 2 min application of hypoxia.

# 3. RESULTS

## 3.1 Confocal Immunofluorescence

Neuroepithelial cells (NECs) expressed 5-HT and were located in gill epithelia (Fig. 1A). Two major groups of NECs were identified based on location and morphology: large, irregular-shaped NECs of the filament epithelium and small, spherical NECs of the lamellar epithelium (Fig. 1A). A zn-12-immunoreactive (IR) nerve bundle composed of extrinsic nerve fibres entered the filaments and extended zn-12-IR nerve fibres to innervate NECs of the respiratory lamellae (Fig. 1B). A second zn-12-IR nerve bundle ran distally from the base of the filament beneath the basal lamina and was

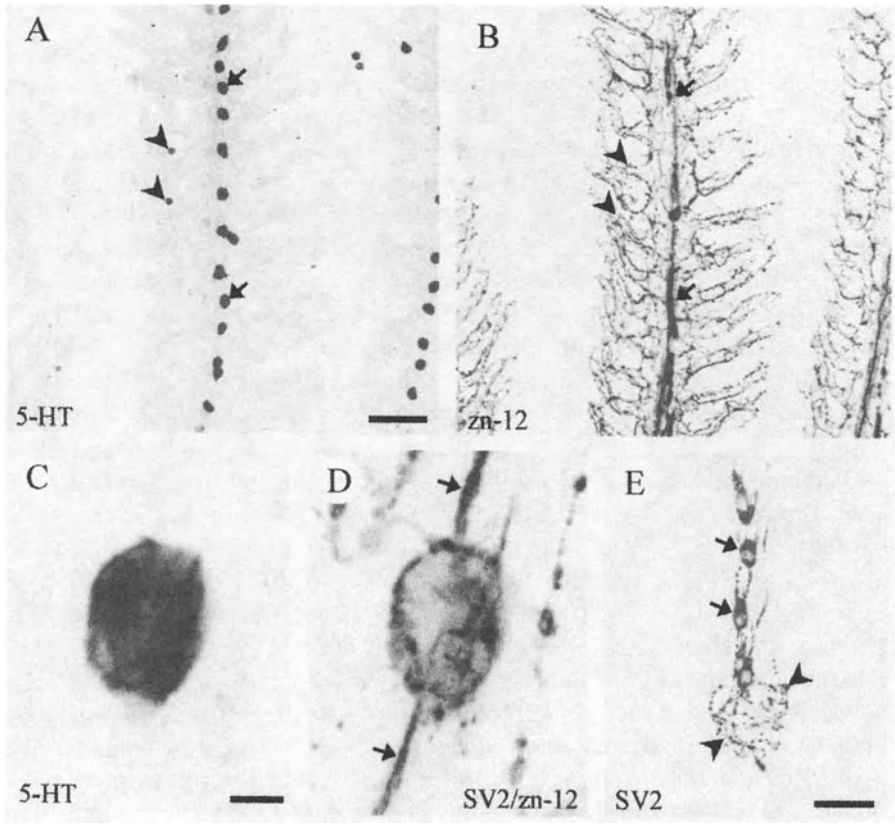


*Figure 1.* Confocal immunofluorescence of neuroepithelial cells (NECs) of the zebrafish gill and associated innervation. **A:** Serotonin-immunoreactive (5-HT-IR) NECs situated in epithelia of a gill filament (arrows) and respiratory lamellae (arrowheads). Scale bar 25 μm. **B:** Same tissue as in A, showing only zn-12 immunoreactivity. Two adjacent zn-12-IR nerve bundles (arrows) innervate NECs of the filament and extend zn-12-IR nerve fibres (arrowheads) to NECs of the lamellae. **C:** Higher magnification of a 5-HT-IR NEC of the filament epithelium. Scale bar 2.5 μm. **D:** Same cell as in C is SV2-IR and is innervated by a zn-12-IR intrinsic nerve bundle (arrows). **E:** Intrinsic SV2-IR neurons (arrows) of the proximal gill filament are multipolar and send processes distally toward filament NECs and proximally toward the base of the efferent filament artery (not shown) where SV2-IR nerve endings (arrowheads) were found. Scale bar 25 μm.

associated with NECs of the filament epithelium (Fig. 1B). At higher magnification, 5-HT-IR NECs contained SV2-IR synaptic vesicles and were intimately associated with zn-12-IR nerve bundles (Fig. 1C, D). These nerve bundles were of intrinsic origin and arose from a group of SV2-IR multipolar neurons of the proximal filament that also formed SV2-IR nerve endings surrounding the efferent filament artery (Fig. 1E).

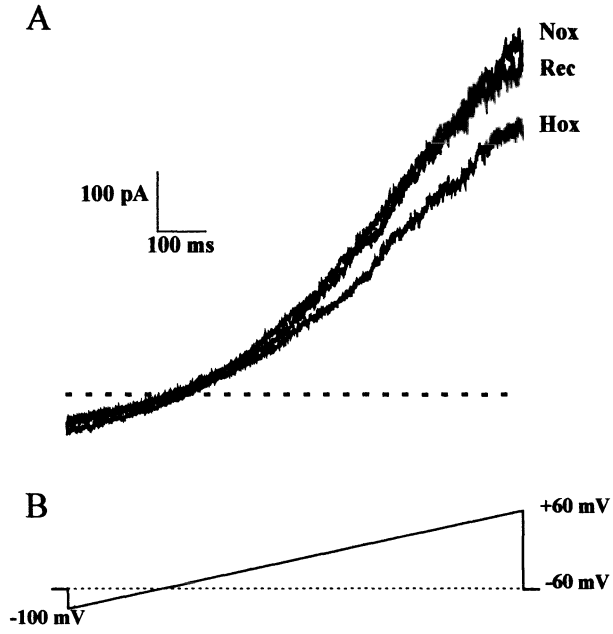


*Figure 2.* Hypoxia inhibits outward $K^+$ current in a Neutral Red-positive cell. **A:** Whole-cell, voltage-clamp recordings showing reversible reduction of $K^+$ current when normoxic solution (Nox) was replaced with hypoxic solution (Hox). Rec, recovery. **B:** Ramp protocol used for recordings in A. Cell was held at –60 mV and membrane potential was ramped over 1 s.

## 3.2 Electrophysiology

Zebrafish gill cells labelled with NR expressed an $O_2$-sensitive outward $K^+$ current. The replacement of normoxic solution with hypoxic solution during voltage-clamp recording resulted in a reversible decrease in outward $K^+$ current, noticeable at positive test potentials during ramp depolarisations (Fig. 2A, B). Outward current was restored after reperfusion with normoxic solution.

# 4. DISCUSSION

This study has identified serotonergic NECs of the zebrafish gill filaments and lamellae that contain synaptic vesicles, as evidenced by SV2 immunoreactivity. As concluded in previous studies (Dunel-Erb *et al.*, 1982; Bailly *et al.*, 1992) this suggests a neurosecretory role for NECs in the gill. Furthermore, stimulation of NECs by hypoxia induced exocytosis (Dunel-Erb *et al.*, 1982). Neuroepithelial cells of the respiratory lamellae received innervation from extrinsic neurons, possibly ganglionic, which suggests that

stimulation of lamellar NECs by hypoxia may lead to activation of afferent post-synaptic pathways and changes in ventilation and heart rate. In support of this proposal, an afferent discharge was recorded from fibres of cranial nerves IX and X innervating isolated gill arches exposed to hypoxia *in vitro* (Burleson and Milsom, 1993; Milsom and Brill, 1986). Conversely, NECs of the filaments were associated with fibres of intrinsic neurons that also formed nerve endings on the base of the efferent filament artery. This artery returns oxygenated blood to the systemic circulation and may represent a major site at which gill blood flow is regulated during stimulation of filament NECs by hypoxia. Despite implications of our morphological evidence that NECs may act as $O_2$ chemoreceptors, we do not rule out a possible neuroendocrine role of gill NECs.

The reversible inhibition of an $O_2$-sensitive $K^+$ current by hypoxia in NR-positive, presumptive NECs of the zebrafish gill is reminiscent of the response of $O_2$ chemoreceptors in mammals (López-Barneo *et al.*, 1988; Youngson *et al.*, 1993; Thompson *et al.*, 1997). These data raise the possibility that NECs of the fish gill may be involved in the $O_2$ sensing pathway and respiratory regulation, and are phylogenetically related to mammalian $O_2$ chemoreceptors.

## ACKNOWLEDGEMENTS

The authors wish to thank Cathy Vollmer for expert technical advice, and Verónica Campanucci, Dr. Mike O'Donnell, Dr. Chris Wood and Dr. Scott Kelly for suggestions. We also acknowledge the Natural Sciences and Engineering Research Council (NSERC) of Canada for funding through an operating grant to C.A.N. and a postgraduate scholarship to M.G.J.

## REFERENCES

Bailly, Y., Dunel-Erb, S. and Laurent, P. (1992). The neuroepithelial cells of the fish gill filament: indolamine-immunocytochemistry and innervation. *Anat Rec* 233:143-161.

Bradford, C.S., Sun, L., Collodi, P. and Barnes D.W. (1994). Cell cultures from zebrafish embryos and adult tissues. *Mol Mar Biol Biotechnol* 3:78-86.

Burleson, M.L. and Milsom, W.K. (1993). Sensory receptors in the first gill arch of rainbow trout. *Resp Physiol* 93:97-110.

Burleson, M.L., Smatresk, N.J. and Milsom, W.K. (1992). Afferent inputs associated with cardioventilatory control in fish. In: Hoar WS, Randall DJ, Farrell AP, editors: Fish Physiology, Vol. XIIB. San Diego: Academic Press. p 389-426.

Dunel-Erb, S., Bailly, Y. and Laurent, P. (1982). Neuroepithelial cells in fish gill primary lamellae. *J Appl Physiol: Resp Environ Exercise Physiol* 53:1342-1353.

González, C., Almaraz, L., Obeso, A. and Rigual, R. (1994). Carotid body chemoreceptors: from natural stimuli to sensory discharges. *Physiol Rev* 74:829-898.

Hamill, O.P, Marty, A., Neher, E., Sakmann, B. and Sigworth, F.J. (1981). Improved patch-clamp techniques for high-resolution current recording from cells and cell-free membrane patches. *Pflügers Arch* 391:85-100.

López-Barneo, J., Pardal, R. and Ortega-Sáenz, P. (2001). Cellular mechanisms of oxygen sensing. *Annu Rev Physiol* 63:259-287.

López-Barneo, J., López-López, J.R., Ureña, J. and Gonzalez, C. (1988). Chemotransduction in the carotid body: $K^+$ current modulated by $Po_2$ in type I chemoreceptor cells. *Science* 241: 580-582.

Milsom, W.K. and Brill, R.W. (1986). Oxygen sensitive afferent information arising from the first gill arch of yellowfin tuna. *Resp Physiol* 66:193-203.

Nilsson, S. (1984). Innervation and pharmacology of the gills. In: Hoar WS, Randall DJ, editors: Fish Physiology, Vol. XA. San Diego: Academic Press. p 185-227.

Thompson, R.J., Jackson, A. and Nurse, C.A. (1997). Developmental loss of hypoxic chemosensitivity in rat adrenomedullary chromaffin cells. *J Physiol* 498: 503-510.

Trevarrow, B., Marks, D.L. and Kimmel, C.B. (1990). Organization of hindbrain segments in the zebrafish embryo. *Neuron* 4:669-679.

Youngson, C., Nurse, C., Yeger, H. and Cutz, E. (1993). Oxygen sensing in airway chemoreceptors. *Nature* 365:153-155.

Westerfield, M. (2000). The Zebrafish Book. A Guide for the Laboratory Use of Zebrafish (*Danio rerio*). 4th ed. Eugene: University of Oregon Press.

Zaccone, G., Fasulo, S. and Ainis, L. (1994). Distribution patterns of the paraneuronal endocrine cells in the skin, gills and the airways of fishes as determined by immunohistochemical and histological methods. *Histochem J* 26:609-629.

Zaccone, G., Fasulo, S., Ainis, L. and Licata, A. (1997). Paraneurons in the gills and airways of fishes. *Microsc Res Tech* 37:4-12.

# Sensory Neurons of Rat and Mice Dorsal Root Ganglia Respond to Hypoxia with Increased NO Generation

MICHAEL HENRICH[1,2] PETER KÖNIG[2], MARCO GRUß[1,3], TAMARA FISCHBACH[2], AXEL GÖDECKE[4], GUNTER HEMPELMANN[1] and WOLFGANG KUMMER[2]

*[1]Department of Anaesthesiology, Intensive Care and Pain Therapy, Justus-Liebig-University, D-35385 Giessen, Germany; [2]Institute for Anatomy and Cell Biology, Justus-Liebig-University, D-35385 Giessen, Germany; [3]Institute for Physiology, Justus-Liebig-University, D-35385 Giessen, Germany; [4]Institute for Physiology, Heinrich-Heine University, D-40225 Düsseldorf, Germany*

## 1. INTRODUCTION

Studies on *Drosophila* larvae have added nitric oxide (NO) as another endogenous intracellular signalling molecule mediating hypoxia-induced adaptations (Wingrove and O'Farrell, 1999; DiGregorio *et al.*, 2001). In mammalian cells, exogenously applied NO is able to interfere with the signalling cascades that are activated by low oxygen tension. NO treatment under normoxic conditions stabilizes hypoxia-inducible factor-1α (HIF-1α), the major transcription factor involved in hypoxia-regulated gene expression, and promotes its DNA-binding activity and downstream gene expression (Genius and Fandrey, 2000; Kimura *et al.*, 2000; Palmer et al., 2000; Sandau *et al.*, 2001). It is currently unclear, whether this effect is due to an interaction of NO with the iron containing HIF-modulating enzyme, HIF-prolyl-hydroxylase (Ivan *et al.*, 2001; Jaakkola *et al.*, 2001) or whether NO acts via a different pathway. Under hypoxic conditions, however, partly opposing effects of exogenously applied NO have been reported (Liu *et al.*, 1998; Huang *et al.*, 1999; Sogawa *et al.*,1998). One possible explanation is that NO may react with ROS formed during hypoxia to yield compounds

*Chemoreception*, Edited by Pequignot et al.
Kluwer Academic/Plenum Publishers, New York, 2003

such as peroxynitrite that do not stimulate HIF-1α (Semenza, 2001). Similarly, the effect of NO on the skeletal muscle calcium release channel is critically dependent on $pO_2$ (Eu *et al.*, 2000). None of these studies reported on the endogenous production of NO under these conditions.

## 1.1 Sensory neurons of lumbar dorsal root ganglia

In this study we investigated sensory neurons in slices of lumbar dorsal root ganglia (DRG) from mice and rats. These ganglia contain large sensory neurons with high biosynthetic capacity and with long axonal processes depending on an energy consuming axonal transport, which both require a constant oxygen supply. These sensory neurons are devoid of synapses at their cell bodies. Since a) synaptic input is a main regulator of NO synthesis, and b) enhanced synaptic transmitter release is one of the earliest events under hypoxia, these characteristics allow to evaluate hypoxic regulation of neuronal NO directly without interfering influences of synaptic input. The detection of NO by the NO-sensitive dye DAF-2DA and its recording by confocal laser scanning microscopy (CLSM) allowed to distinguish the neuronal NO production from that of other cell types (e.g. satellite cell, Schwann cells, endothelial cells).

# 2. SENSORY NEURONS OF RAT AND MICE DRG RESPOND TO HYPOXIA WITH ENHANCED NO-PRODUCTION

Slices of rat lumbar DRG were exposed to either normoxic (21% $O_2$) or hypoxic (1% $O_2$) gas concentrations for 1 h. After this exposure period the DAF-2T-fluorescence was evaluated for each neuron separately and expressed as grey value on a limited scale from 0-255. Under hypoxia the DAF-2T-fluorescence in the neurons increased significantly compared to normoxic culture conditions. The specificity of DAF-2DA for NO was demonstrated by the application of the general NOS-inhibitor L-NMMA. This inhibitor completely prevented the hypoxia-induced increase in neuronal NO production and reduced the DAF-2T-fluorescence in normoxia, thereby demonstrating a basal normoxic neuronal NO production.

### 2.1 Hypoxic NO generation requires extracellular calcium and depends on the activity of voltage-gated calcium channels

Calcium is the strongest activator of constitutively expressed NOS isoforms. Accordingly, experiments carried out in calcium-free medium revealed that the hypoxia-induced increase in NO generation depends on extracellular calcium. Further pharmacological experiments elucidated an involvement of voltage-gated channels in the hypoxic activation of NO production. The pharmacological inhibition of voltage-gated calcium channels by either $Ni^{2+}$or $Cd^{2+}$ or by verapamil or nifedipine prevented the hypoxia-induced increase in NO generation. The normoxic NO generation remained unaltered by the pharmacological inhibition of voltage-gated calcium channels.

## 3. NO-PRODUCTION IS ASSOCIATED TO MITOCHONDRIA

The subcellular compartment of the hypoxic NO generation was determined by a photoconversion technique in which an electron dense DAB reaction product was generated at the site of DAF-2T-fluorescence, and by subsequent processing of the tissue for electron microscopy. In the minority of neurons which were exposed to normoxia a weak labelling of mitochondrial membrane was observed. In contrast to that the inner mitochondrial membranes were intensely stained in all neurons which were exposed to hypoxia. Omission DAF-2DA from the culture medium led to a mitochondrial staining under neither normoxic nor hypoxic conditions.
This membrane labelling of the DAB conversion product specifically indicates the location where the fluorescent indicator DAF-2T is generated by endogenous NO. This was confirmed by simultaneous inhibition of endogenous NO generation by L-NMMA and exogenous application of the NO donor SNP. This treatment led to an enhanced DAF-2T fluorescence in the neurons but not to a mitochondrial DAB-membrane labelling after photoconversion, indicating that accumulation of DAF-2T or DAB at mitochondrial membranes is not an intrinsic property of these reagents but due to a local endogenous NO production at these sites.

## 4. NOS ISOFORMS IN SENSORY NEURONS

Using the NADPH-diaphorase technique as a general indicator for NOS activity without distinguishing between isoforms, all neurons in rat and murine DRG were stained with the reaction product NBT. Only a few neurons showed an intense staining whereas the majority was weakly stained in a dot-like distribution pattern with gradual differences between individual neurons. This staining demonstrated that all sensory neurons of lumbar DRG express at least one NOS isoform. Subtyping of isoforms was achieved by immunohistochemistry using antibodies against all three NOS isoforms. In the minority of the neurons the neuronal NOS was diffusely distributed in the cell bodies sparing the nucleus, similar to the intensely NBT-stained neurons. The inducible NOS was entirely absent in all neurons investigated. In contrast to that the endothelial NOS was distributed in the cell bodies of all neurons in a dot-like pattern. The neuronal expression of endothelial NOS was confirmed by single cell RT-PCR using two different intron-spanning primer pairs. Also, dot-like NADPH-diaphorase activity was missing in neurons from endothelial $NOS^{-/-}$ mice.

### 4.1 Subcellular distribution of NOS isoforms

On the ultrastructural level, NADPH-diaphorase reactivity was found in the cytoplasm and at the smooth ER and the nuclear membrane in the minority of the cells. In the majority of the neurons, the reaction product was located at those compartments of the smooth ER which were associated to mitochondria. Using immunohistochemistry at the ultrastructural level, the neuronal NOS was found to be diffusely distributed in a minority of cell bodies, confirming the light microscopic immunohistochemical findings and the NADPH-diaphorase staining on the ultrastructural level. In contrast to this, the endothelial NOS was located in all neurons investigated located at compartments of the smooth ER in association to mitochondria. Occasionally, it was also found at the nuclear membrane. This staining pattern correlated with that for NADPH-diaphorase activity in the majority of DRG neurons.

## 5 ENDOTHELIAL NOS IS ACTIVATED BY HYPOXIA

Sensory neurons of wild type mice responded to hypoxia with an significant increase in NO generation compared to normoxic conditions.

DRG neurons of neuronal $NOS^{-/-}$ mice were still able to enhance the NO production under hypoxia significantly and to the same extent as those from wild type mice. On the opposite to that, sensory neurons of endothelial $NOS^{-/-}$ mice failed to respond to hypoxia by an increased NO generation. Thus the endothelial NOS is the isoform that is responsible for the hypoxia-induced increase in NO generation.

# 6 CONCLUSION

The present study demonstrated that sensory neurons respond to hypoxia with an increased NO generation. The responsible NOS isoform is the endothelial NOS which is expressed by all neurons. It is specifically located at juxtamitochondrial compartments of the smooth ER. Using a photoconversion technique and electron microscopy we provide evidence that NO is also juxtamitochondrially released and is targeted to the inner mitochondrial membrane. The hypoxic activation of eNOS requires extracellular calcium and depends on the activity of voltage-gated calcium channels. The present data provide evidence for a hypoxia-activated cascade which results in enhanced juxtamitochondrial NO generation by the endothelial NOS, thereby contributing to resistance against hypoxia by interfering with mitochondrial function (cf. Beltrán *et al.*, 2000).

# ACKNOWLEDGEMENTS

We thank Andreas Scholz, Giessen, for providing samples of neuronal cytoplasm collected during intracellular recording experiments and Silke Wiegand, Martin Bodenbenner and Gerhard Kripp for skillful technical assistance. This study was supported by the DFG (SFB 547, project C1; GK 534).

# REFERENCES

Beltrán, B., Mathur, A., Duchen, M.R., Erusalimsky, J.D., and Moncada, S., 2000, The effect of nitric oxide on cell respiration: A key to understand its role in cell survival or death. *Proc. Natl. Acad. Sci. USA* 97: 14602-14607.

DiGregorio, P.J., Ubersax, J.A., and O'Farrell, P.H., 2001, Hypoxia and nitric oxide induce a rapid, reversible cell cycle arrest of the Drosophila syncytial divisions. *J. Biol. Chem.* 276: 1930-1937.

Eu, J.P., Sun, J., Xu, L., Stamler, J.S., and Meissner, G., 2000, The skeletal calcium release channel: coupled $O_2$ sensor and NO signalling functions. *Cell* 102: 499-509.

Genius, J., and Fandrey, J., 2000, Nitric oxide affects the production of reactive oxygen species in hepatoma cells: implications for the process of oxygen sensing. *Free Radic. Biol. Med.* 29: 515-521.

Huang, L.E., Willmore, W.G., Gu, J., Goldberg, M.A., and Bunn, H.F., 1999, Inhibition of hypoxia-inducible factor 1 activation by carbon monoxide and nitric oxide. Implications for oxygen sensing and signaling. *J. Biol. Chem.* 274: 9038-9044.

Ivan, M., Kondo, K., Yang, H., Kim, W., Valiando, J., Ohh, M., Salic, A., Asara, J.M., Lane, W.S., and Kaelin, W.G.Jr., 2001, HIFα targeted for VHL-mediated destruction by proline hydroxylation: Implications for $O_2$ sensing. *Science* 292: 464-468

Jaakkola, P., Mole, D.R., Tian, Y-M., Wilson, M.I., Gielbert, J., Gaskell, S.J., von Kriegsheim, A., Hebestreit, H.F., Mukherji, M., Schofield, C.J., Maxwell, P.H., Pugh, C.W., and Ratcliffe, P.J., 2001, Targeting of HIF-α to the von Hippel-Lindau ubiquitylation complex by $O_2$-regulated prolyl hydroxylation. *Science* 292: 468-472

Kimura, H., Weisz, A., Kurashima, Y., Hashimoto, K., Ogura, T., D'Acquisto, F., Addeo, R., Makuuchi, M., and Esumi, H., 2000, Hypoxia response element of the human vascular endothelial growth factor gene mediates transcriptional regulation by nitric oxyde: control of hypoxia-inducible factor-1 activity by nitric oxide. *Blood* 95: 189-197.

Liu, Y., Christou, H., Morita, T., Laughner, E., Semenza, G.L., and Kourembanas, S., 1998, Carbon monoxide and nitric oxide suppress the hypoxic induction of vascular endothelial growth factor gene via the 5' enhancer. J. Biol. Chem. 273: 15257-15262.

Palmer, L.A., Gaston, B., and Johns, R.A., 2000, Normoxic stabilization of hypoxia-inducible factor-1 expression and activity: redox-dependent effect of nitrogen oxides. *Mol. Pharmacol.* 58: 1197-1203.

Sandau, K.B., Fandrey, J., and Brüne, B., 2001, Accumulation of HIF-1α under the influence of nitric oxide. *Blood* 97: 1009-1015.

Semenza, G. L., 2001, HIF-1 and mechanisms of hypoxia sensing. *Curr. Opinion Cell Biol.* 13: 167-171.

Sogawa, K., Numayama-Tsuruta, K., Ema, M., Abe, M., Abe, H., and Fujii-Kuriyama, Y., 1998, Inhibition of hypoxia-inducible factor 1 activity by nitric oxide donors in hypoxia. *Proc. Natl. Acad. Sci. USA* 95: 7368-7373.

Wingrove, J.A. and O'Farrell, P.H., 1999, Nitric oxide contributes to behavioral, cellular, and developmental responses to low oxygen in Drosophila. *Cell* 98: 150-114.

# Molecular Mechanisms of Oxygen-Induced Regulation of $Na^+/K^+$ Pump

ANNA BOGDANOVA[1*]; OMOLARA O. OGUNSHOLA[1]; CHRISTIAN BAUER[2], MIKKO NIKINMAA[3]and MAX GASSMANN[1]

*Institute of Veterinary Physiology[1], Institute of Physiology[2] University of Zürich, Zürich Switzerland; Laboratory of Animal Physiology Department of Biology University of Turku, Turku, Finland[3]*

## 1. INTRODUCTION

$Na^+/K^+$ pump is deactivated under hypoxic conditions in many cell types, including neurons, cardiac myocytes, hepatocytes, alveolar epithelial cells and chromaffin cells of adrenal medulla (Erecinska and Silver, 2001; Inoue *et al,* 1999; Suzuki *et al.*, 1999; Ziegelhoffer *et al.,* 2000). The ability of the pump to respond to hypoxic conditions with reversible deactivation coupled to a decrease in passive permeability of cell membrane to sodium and potassium preserves cell integrity and ATP levels during prolonged hypoxic periods in hypoxia-tolerant species such as western painted turtle and ground squirrel (Buck & Hochachka, 1993; MacDonald & Storey, 1999). On the other hand, in cells with high passive permeability to inorganic cations deactivation of the pump results in a rapid dissipation of transmembrane gradients, passive accumulation of $Na^+$, cell swelling and finally lysis. Rapid decrease in ATP levels, particularly in cells with activemetabolism and ATP production, is believed to be a major course of $Na^+/K^+$ ATPase deactivation under hypoxic conditions (Fig 1). This is clearly true for neurons where ATP depletion under hypoxic conditions occurs within minutes, followed by a decrease in $Na^+/K^+$ pump activity and consequent membrane depolarization, swelling and necrosis. However, deactivation of the

*Chemoreception*, Edited by Pequignot et al.
Kluwer Academic/Plenum Publishers, New York, 2003

pump in response to ischemic hypoxia also occurs in cardiac myocytes where the ATP fuelling the pump is mostly, if not entirely, of glycolytic origin (Ziegelhoffer., 2000). Therefore, along with ATP depletion other mechanisms must be involved in hypoxia-induced deactivation of $Na^+/K^+$ pump. As one such mechanism, it has been suggested that deactivation of $Na^+/K^+$ pump would result from increased production of reactive oxygen species (ROS), because of mitochondrial uncoupling under hypoxic conditions (Chandel *et al.*, 1997; Chandel and Schumacker, 2000; Duranteau *et al.*, 1998), and consecutive oxidation of the pump. However, whereas deactivation of the pump by brief hypoxic treatment is reversible, oxidative treatments cause irreversible inhibition of the pump (Boldyrev and Bulygina, 1997; Dobrota *et al.*, 1999; Ferrari *et al.*, 1991; Huang, Wang and Askari, 1992; Kurella *et al.*, 1997). One more parameter, affected by hypoxia-reoxygenation is cellular redox status, characterised by GSH and GSSG levels.

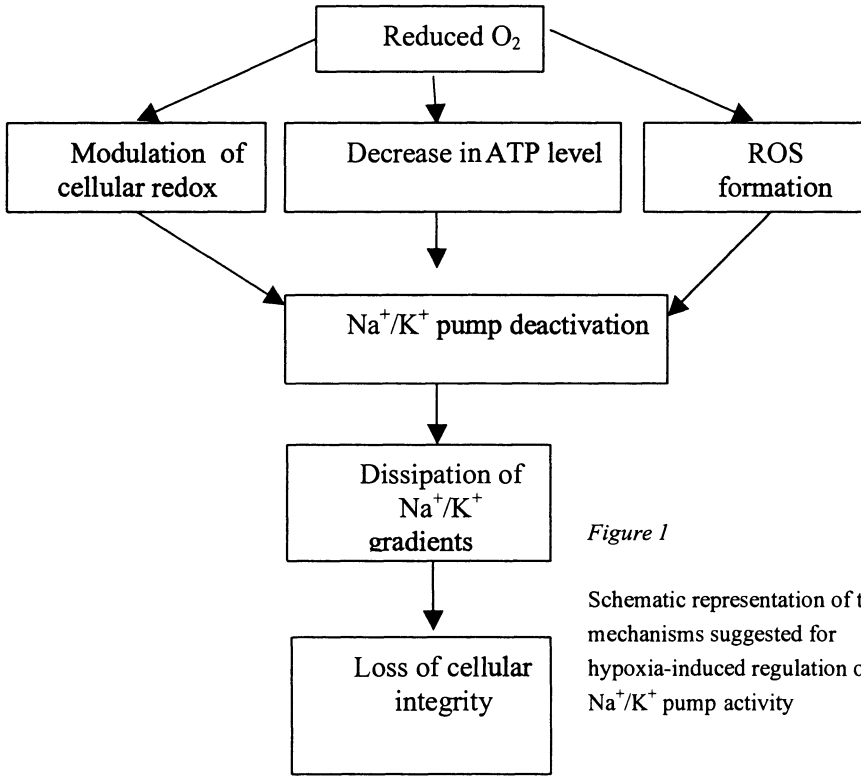


*Figure 1*

Schematic representation of the mechanisms suggested for hypoxia-induced regulation of $Na^+/K^+$ pump activity

Furthermore, data on hypoxia-induced ROS production are contradictory. In the present paper we have attempted to evaluate the roles of ROS and cellular redox status in hypoxia-induced inhibition of $Na^+/K^+$ ATPase.

## 2. RESULTS AND DISCUSSION

### 2.1 Effect of acute hypoxic exposure on $Na^+/K^+$ pump performance and cellular ATP

We have used mouse erythrocytes and trout hepatocyte primary cultures to evaluate $Na^+/K^+$ pump activity as well as ATP levels and ROS production rates under normoxic and hypoxic conditions. $^{86}Rb$ was used to evaluate active $K^+$ influx into the cells. As can be seen from Fig 2 in both cell types $Na^+/K^+$ ATPase was the only potassium transport pathway responding to a decrease in $pO_2$. This contrasts with findings on oxygen-sensitivity of $Na^+/H^+$ exchanger and $K^+$-$Cl^-$ cotransporter in red blood cells of different species, suggesting tissue- and species-specificity of oxygen-induced responses (Gibson, Cossins & Ellory, 2000). Its activity reduced to about a half of its initial level in mouse red blood cells and to about one third in trout hepatocytes under hypoxic conditions (Fig 2). Hypoxia-induced deactivation of the transporter was rapid (within minutes) and was not associated with a concomitant decrease in cellular ATP. In mouse erythrocytes lacking mitochondria ATP level did not change under hypoxic conditions during 1 h incubation. In trout hepatocytes ATP depletion occurs (Krumschnabel, *et al.*, 2001), but its time course is much slower than that of $Na^+/K^+$ pump deactivation. Therefore, hypoxia-induced $Na^+/K^+$ pump deactivation in either erythrocytes or hepatocytes cannot be explained by cellular ATP depletion.

### 2.2 Reversibility of hypoxic effect

An important feature of hypoxia-induced deactivation of $Na^+/K^+$ pump is its reversibility. Activity of the pump could be at least partially restored in mouse erythrocytes by 20 min of reoxygenation. Recovery of $Na^+/K^+$ ATPase activity was also shown in hypoxic ventricular myocyte preparations (Van Emous *et al.*, 2001; Ziegelhoffer *et al.*, 2000). In hibernating animals such as ground squirrel or in the hypoxia-tolerant turtle, hypoxia-induced $Na^+/K^+$ ATPase deactivation is also reversible (Buck and Hochachka, 1993; Hochachka and Lutz, 2001; MacDonald and Storey, 1999). When combined with a decrease in passive

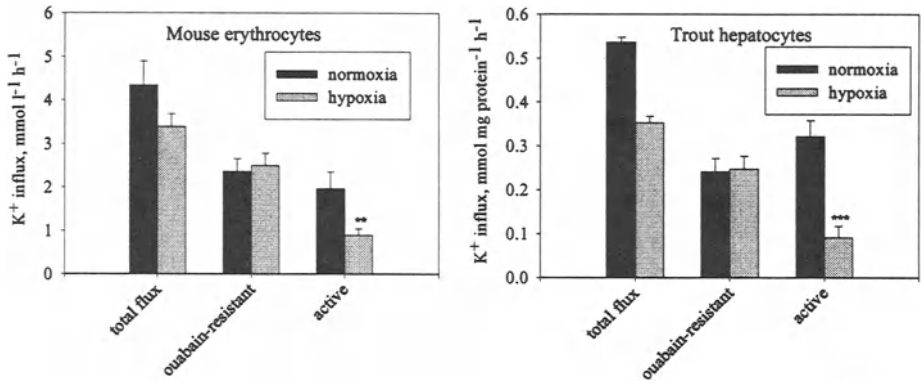


*Figure 2.* Hypoxia-induced deactivation of $Na^+/K^+$ pump in trout hepatocytes and mouse erythrocytes. Both hepatocyte primary culture (1-3 hours after isolation) and erythrocytes were pre-equilibrated in suspension for 10 min under hypoxic conditions (1% $O_2$) before $^{86}Rb$ was added to evaluate $K^+$ ($^{86}Rb$) uptake during 5 min incubation. $K^+$($^{86}Rb$) fluxes were measured with and without 1 mM ouabain. Data are means of 5 independent experiments ± SEM.

permeability of plasma membrane to sodium and potassium this reversible decrease in the pump activity is a powerful adaptive strategy since it helps to reduce ATP consumption under hypoxic conditions by 50-70%. In erythrocytes hypoxia-induced deactivation of the pump could be reversed when intracellular $Na^+$ levels increased (Bogdanova, unpublished data). This important feature protected the cells from $Na^+$ overload as a result of passive $Na^+$ intake.

## 2.3 ROS formation as a function of $pO_2$

We used fluorescent dye $H_2$DCDCF to follow ROS production in hepatocyte primary cultures using microfluorescent live imaging. Cells were preconditioned on poly-lysine-coated coverslips overnight before the experiment started. After 20 min preloading at 21% $O_2$ with the dye in the presence or in the absence of 5 mM mercaptopropyonyl glycine (MPG), ROS scavenger, the oxygen level of perfusion medium was decreased to 1% $O_2$ and cells preequilibrated at these hypoxic conditions for 20 more minutes. To avoid dye leakage, the perfusion medium was recycled and constantly flushed with gas mixture of defined $pO_2$. Oxygenation level was increased gradually from 1 to 50 % $O_2$ and consequent ROS production was monitored. Fluorescence recording started when steady state readings for

hypoxic conditions was achieved. As shown in Fig. 3 ROS levels in the cells were proportional to the level of oxygenation. In the presence of MPG ROS production was virtually abolished. Incubation of the cells for 1 hour under hypoxic conditions resulted in a slow increase in cellular fluorescence. Overall this increase was much smaller than the one induced by reoxygenation. Hence, although there is some ROS production under hypoxic conditions, the production is smaller than at higher oxygen levels and therefore, cannot be the cause of $Na^+/K^+$ pump deactivation by hypoxia.

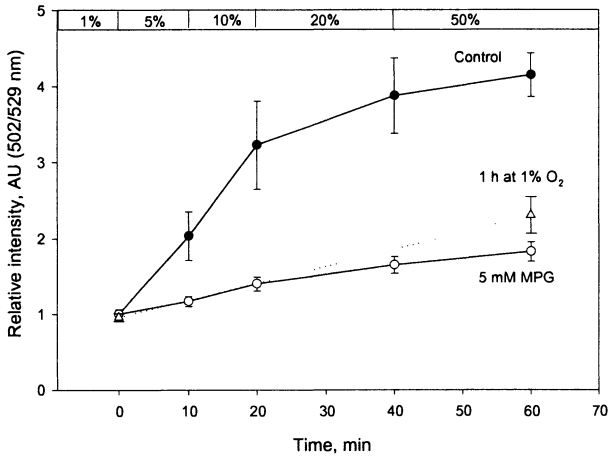


*Figure 3* ROS formation as a function of $pO_2$ in trout hepatocytes. For details on experimental procedures see Raberg et al (Rabergh et al. 1994). Presented are averaged values on fluorescence take during the last 3 min of exposure. Data are means for 15 individual cells from 4 different fishes

A decrease in ROS production in hypoxic conditions is in line with our earlier observations on oxygen-induced regulation of $K^+$-$Cl^-$ cotransporter (KCC) and $Na^+/H^+$ exchanger (NHE) in trout erythrocytes *et al.*, We have shown that treatment of the cells with ROS scavenger MPG could mimic hypoxic responses. Furthermore, copper-induced catalysis of Fenton reaction, where hydroxyl radicals are produced under hypoxic conditions is able to trigger reoxygenation response in KCC.

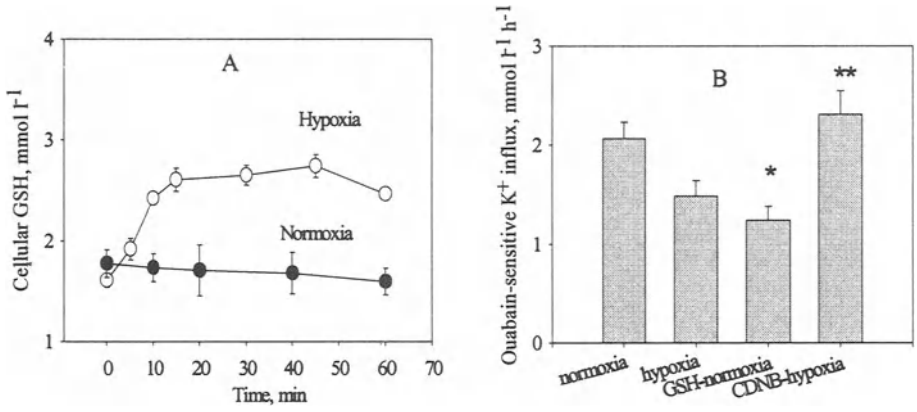


*Figure 4.* Hypoxia-induced increase in GSH levels in mouse erythrocytes. GSH-induced regulation of $Na^+/K^+$ pump. A. Mouse erythrocytes were incubated in a tonometer at 1% $O_2$ for 60 min. Samples of cell suspension were taken at various time-points and GSH measured as described (Benesch, Benesch & Yung, 1973). Values are means of 5 independent experiments ± SEM. B. Ouabain-sensitive $K^+(^{86}Rb)$ influx into mouse erythrocytes under normoxic (± 5 mM GSH, 30 min preequilibration) or hypoxic (± 0.3 mM CDNB, added at at the beginning of hypoxic exposure, 15 min prior to flux evaluation) conditions. Values are means of 4-6 independent experiments ± SEM.

Since the above findings suggest that reducing conditions (i.e. conditions in which ROS formation is reduced) are associated with hypoxia, we further investigated hypoxia-induced changes in reduced glutathione (GSH) levels in cells where rapid hypoxia-induced deactivation of the $Na^+/K^+$ pump occurs.

## 2.4 Cellular GSH changes in response to hypoxic insult

In mouse erythrocytes GSH levels were a function of $pO_2$ in the incubation medium (Fig 4A). Kinetics of increase in GSH levels was consistent with those for $Na^+/K^+$ pump deactivation. In hypoxia, depletion of GSH up to "normoxic" levels using conjugating agent CDNB abolished the deactivation of the pump (Fig 4B). Moreover, incubation of cells with 5 mM GSH for 30 min caused a significant decrease of the pump activity already at normoxic conditions.

Rapid increase in cellular GSH levels in response to acute hypoxic exposure has been shown to occur in several cell types (Niknahad *et al.,,* 1995; Reeve *et al.,* 2001). With regard to ion transport, earlier studies have indicated that a decrease in cellular GSH level is associated with an inhibition of $K^+$-$Cl^-$ cotransporter, $Na^+/H^+$ exchanger and $Na^+/K^+$ pump (Cutaia and Parks, 1994; Haddock *et al.*, 1995; Lauf, Adragna and Agar, 1995). In contrast, no data are available on the effect of increase in GSH concentration on ion transport. However, the present studies link an increase in cellular GSH level to an inhibition $Na^+/K^+$ pump. It is thus possible that cellular GSH level is of crucial importance in modulation of activity of a number of transporters by oxygen.

## 2.5 Possible mechanisms of oxygen-induced regulation of $Na^+/K^+$ pump activity

Although the present studies suggest an important role of GSH in hypoxia-induced deactivation of $Na^+/K^+$ pump, its exact mechanism remains unclear. GSH may directly regulate redox state of thiols of alpha and beta-subunits of $Na^+/K^+$ pump. On the other hand, since phosphorylation is an important element in the control of the pump activity, involved in reversible deactivation of the enzyme under conditions of limited oxygen and food supply such as hypoxia or hibernation (Graham *et al.*, 1993; Kiroytcheva *et al.*,1999; MacDonald and Storey, 1999), it is possible that kinases/phosphatases involved in regulation of $Na^+/K^+$ pump activity may be redox sensitive.

# 3. CONCLUDING REMARKS

Our results show that the rapid deactivation of $Na^+/K^+$ pump in hypoxia is associated with a rapid increase in cellular GSH levels. Rapid reversible deactivation of $Na^+/K^+$ pump under hypoxic conditions is advantageous for the cells facing limited oxygen supply since ATP consumption is decreased. Members of the signalling pathways leading to GSH-induced responses of the transporter remain to be revealed.

# ACKNOWLEDGMENTS

This study was supported by Swiss National Foundation for MG, Olga Mayenfisch Foundation for AB and by the Academy of Finland, Research Council for the Environmental and Natural Resources for MN and AB.

# REFERENCES


Benesch, R.E., Benesch, R., Yung, S., 1973, *Anal Biochem* 55:245-8.

Bogdanova, A.Y., Nikinmaa, M. 2001, *J Gen Physiol* 117:181-90.

Boldyrev, A.A., Bulygina, E.R. 1997, *Ann N Y Acad Sci* 834:666-8.

Buck, L.T., Hochachka, P.W. 1993, *Am J Physiol* 265:R1020-5.

Chandel, N.S., Budinger, G.R., Choe, S.H., Schumacker, P.T. 1997, *J Biol Chem* 272:18808-16.

Chandel, N.S., Schumacker, P.T. 2000, *J Appl Physiol* 88:1880-9.

Cutaia, M., Parks, N. 1994, *Am J Physiol* 267:L649-59.

Dobrota, D., Matejovicova, M., Kurella, E.G., Boldyrev, A.A. 1999, *Cell Mol Neurobiol* 19:141-9.

Duranteau, J., Chandel, N.S., Kulisz, A., Shao, Z., Schumacker, P.T. 1998, *J Biol Chem* 273:11619-24.

Erecinska, M., Silver, I.A. 2001, *Respir Physiol* 128:263-76.

Ferrari, R., Ceconi, C., Curello, S., Cargnoni, A., Alfieri, O., Pardini, A., Marzollo, P., Visioli, O. 1991, *Am J Med* 91:95S-105S.

Gibson, J.S., Cossins, A.R., Ellory, J.C. 2000, *J Exp Biol* 203:1395-407.

Graham, E., Mishra, O.P., Delivoria-Papadopoulos, M. 1993, *Neurosci Lett* 153:93-7.

Haddock, P.S., Woodward, B., Hearse, D.J. 1995, *J Mol Cell Cardiol* 27:1185-94.

Hochachka, P.W., Lutz, P.L. 2001, *Comp Biochem Physiol B Biochem Mol Biol* 130:435-59.

Huang, W.H., Wang, Y., Askari, A. 1992, *Int J Biochem* 24:621-6.

Inoue, M., Fujishiro, N., Imanaga, I. 1999, *J Physiol* 519:385-96.

Kiroytcheva, M., Cheval, L., Carranza, M.L., Martin, P.Y., Favre, H., Doucet, A., Feraille, E. 1999, *Kidney Int* 55:1819-31.

Krumschnabel, G., Manzl, C., Schwarzbaum, P.J. 2001, *J Exp Biol* 204:3943-51.

Kurella, E., Kukley, M., Tyulina, O., Dobrota, D., Matejovicova, M., Mezesova, V., Boldyrev, A. 1997, *Ann N Y Acad Sci* 834:661-5.

Lauf, P.K., Adragna, N.C., Agar, N.S. 1995, *Am J Physiol* 269:C234-41.

MacDonald, J.A., Storey, K.B. 1999, *Biochem Biophys Res Commun* 254:424-9.

Nikinmaa, M. 2002, *Comp Biochem Physiol A Mol Integr Physiol* 133:1.

Nikinmaa, M., Bogdanova, A.Y., Lecklin, T. 2002, *Acta Physiol Scand* in press

Niknahad, H., Khan, S., O'Brien, P.J. 1995, *Chem Biol Interact* 98:27-44.

Rabergh, C.M., Ziegler, K., Isomaa, B., Lipsky, M.M., Eriksson, J.E. 1994, *Am J Physiol* 267:G380-6.

Reeve, H.L., Michelakis, E., Nelson, D.P., Weir, E.K., Archer, S.L. 2001, *J Appl Physiol* 90:2249-56.

Suzuki, S., Noda, M., Sugita, M., Ono, S., Koike, K., Fujimura, S. 1999, *J Appl Physiol* 87:962-8.

Van Emous, J.G., Vleggeert-Lankamp, C.L., Nederhoff, M.G., Ruigrok, T.J., Van Echteld, C.J. 2001, *Am J Physiol Heart Circ Physiol* 280:H2189-95.

Ziegelhoffer, A., Kjeldsen, K., Bundgaard, H., Breier, A., Vrbjar, N., Dzurba, A. 2000, *Gen Physiol Biophys* 19:9-47.

# The Paraganglia of the Rat Superior Laryngeal Nerve

KRIS HUGHES, MARK PICKERING, DEIRDRE M. O'LEARY, AIDAN BRADFORD, RONAN G. O'REGAN and JAMES F.X. JONES

*Department of Human Anatomy and Physiology, University College Dublin, Earlsfort Terrace, Dublin 2, Irealnd.*

## 1. INTRODUCTION

The chemoreceptor function of the aortic bodies (AB) was discovered before that of the carotid bodies (CB) in the dog (see Daly, 1997 for excellent historical overview). Whilst the reflex respiratory and cardiovascular effects of CB stimulation are well described in many vertebrates including humans, the reflex effects of AB stimulation have been less well studied (Marshall, 1994). This is partly explained by the technical difficulties associated with selective perfusion of the AB chemoreceptors. In one of the few studies of this type Daly and Ungar (1966) succeeded in selective perfusion of the two groups of chemoreceptors in the anaesthetized dog. It was found that the respiratory action of the CB was much greater (sevenfold on average) than the AB, whilst the potency of reflex vasoconstriction of hindlimb was equal. This data is particularly valuable because the comparison was made using the natural stimulus of hypoxaemic blood. More recently, experiments in the cat by Daly and Jones (1998) showed that in many animals AB stimulation using cyanide was without respiratory effect but produced a potent constriction of the femoral vasculature. Furthermore, Jones and Daly (1997) observed that whilst the primary cardiac chronotropic action of the AB was weaker than the CB, the dromotropic actions were of equal magnitude. Clearly the study of reflex actions of chemoreceptors other than the CB should include recording of parameters other than respiration. This fundamental point has been missed in many studies of chemoreceptor paraganglia conducted by respiratory physiologists (see Brophy *et al.* 1999 for elaboration). Whilst there have been studies of the reflex action of rat CB stimulation on the cardiovascular

*Chemoreception*, Edited by Pequignot et al.
Kluwer Academic/Plenum Publishers, New York, 2003

system (Marshall, 1994) there appear to be none related to the reflex action of chemoreceptors other than the CB. As we will show here paraganglia of the superior laryngeal nerve (SLN) may be an important group of peripheral arterial chemoreceptors in the rat. One of the few studies which examined cardiovascular changes evoked by isocapnic hypoxia in the rat, unfortunately utilised a procedure for sinoaortic denervation which included cutting both SLNs (Hirakawa *et al.* 1997).

## 1.1 The SLN paraganglion

The aortic nerve of rat was initially believed to contain only baroreceptor fibres until Brophy *et al.* (1999) produced the first recordings of chemoreceptors in this small nerve *in vivo*. However the amount of glomus tissue in this nerve is quite small (unpublished observations: JFX Jones). McDonald and Blewett (1981) reported that the rat had a substantial distribution of chemoreceptor like tissue outside the usual AB territories. These sites include the recurrent and superior laryngeal nerves (RLN and SLN). It is to be emphasised that in humans collections of chemoreceptor tissue resembling that of the rat can be found on the SLN and RLN (Hervonen *et al.* 1978;Plenat *et al.* 1988;Lack *et al.* 1978;Dahlquist 1986). The paraganglia of rat laryngeal nerves are small aggregations of small intensely fluorescent cells surrounded by vascular glomi (Dahlqvist, 1986). They share a number of morphological features with the larger paraganglia of the ninth cranial nerve (carotid bodies) (McDonald and Haskell, 1985). In the present study we have examined these structures with a two stain perfusion technique and attempted to record electrophysiologically from single fibres of the SLN *in vitro*.

# 2. EXPERIMENTAL DESIGN AND METHODS

## 2.1 Morphological studies

Following deep anaesthesia with chloroform, a midsternotomy was performed and the animals (n=8; 212-320g male Wistar rats) killed humanely by exsanguination. The left ventricle of the heart was cannulated using a 21G needle (the tip of which had been modified by bevelling). The paraganglia were highlighted by constant pressure intracardiac perfusion (100mmHg) of the vital dye neutral red (300ml of 1% w/v in normal saline), and then the vasculature was filled with an insoluble precipitate of Berlin Blue (500 ml of 0.1% w/v in normal saline). Both dyes were filtered using

Whatman No. 1 filter paper immediately prior to use and perfused at 37°C to avoid vessel constriction. The left and right RLN and SLN were removed after dissection along their entire lengths. The nerves were prepared as wholemounts, squash mounted on microscopy slides in normal saline and immediately photographed with a JVC digital camera (0.5 inch CCD).

A separate group of animals were used to test whether the paraganglia contained biogenic amines (n=9; 236-373g male Wistar rats). The animals were prepared exactly as described above except that the heart was only perfused with Berlin Blue (it was discovered that neutral red interfered with the following fluorescence protocol). After perfusion the nerves were placed in sucrose-phosphate-glyoxylic acid (SPG) solution for 3 hours (10.7 g sucrose, 4.8g potassium phosphate and 1.5 g glyoxylic acid in 150 ml distilled water, pH 7.4 adjusted with NaOH). The nerves were removed from solution, blotted and placed on glass slides. Once air-dried the specimens were heated to 95°C for 5 minutes in an oven and subsequently mounted in liquid paraffin. A laser confocal microscope was used to excite the specimens (488nm blue light) and the emission wavelength was 522nm, green-yellow light. Optical sections were captured at 5μm slice thickness and each section enhanced four times with Kalman filtering.

## 2.2 Analysis

The criteria for identification of paraganglia included a heavily stained red oblate ellipsoidal structure containing a Berlin Blue sinusoidal vasculature. SCION imaging software was used to measure cross-sectional area and calibrated in both X and Y directions to correctly account for the pixel aspect ratio of every image. Statistical analysis of histogram data was performed using the Kolmogorov-Smirnov test and parametric group data analysed with student's t test and the non-parametric data with the Mann Whitney U-test. Statistical significance was assumed when $p<0.05$.

## 2.3 Single fibre recording of chemoreceptors

Male Wister rats (n=3; weighing 246-253g) were killed quickly and humanely by personnel trained in the procedure (according to Institutional Animal Ethics Committee guidelines).

The right SLN was quickly removed from the animal and transferred to warm (37° C) oxygenated Krebs solution. It was pinned out on Sylgard using 50μm Tungsten wire (Fig. 1.) and superfused at 5ml/min with HEPES buffered Tyrode solution (37°C ;$PO_2$ approximately 150mmHg). Single fibre recordings were made from the cut end of the main nerve trunk with glass suction microelectrodes. The signal was amplified and filtered (Neurolog System) and digitised with an A/D convertor (CED1401). Spike2 software (Cambridge Electronic Design) was be used to discriminate and sort spike shapes. We conducted a search for spontaneously firing units and a second

glass electrode containing cyanide (1 mg $ml^{-1}$) dissolved in phosphate buffered solution (pH 7.4) was used to deliver this chemostimulant in close proximity to the glomus (5µl by pressure ejection)(Fig. 1.).

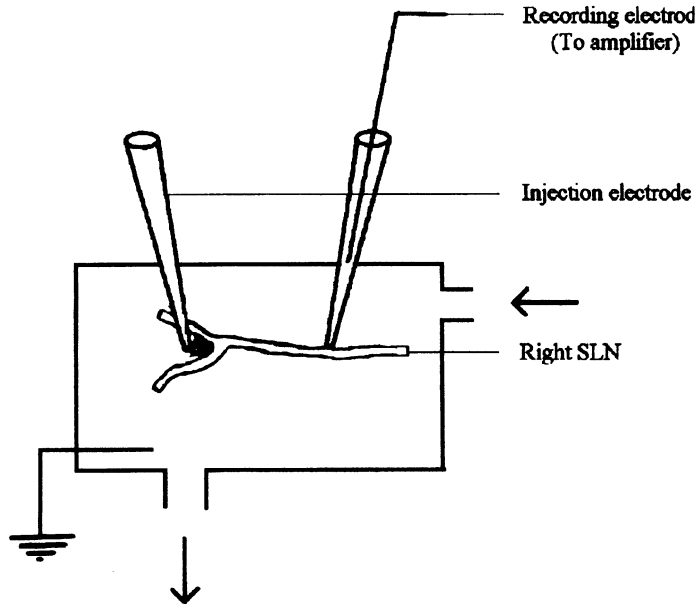


*Figure 1.*Diagram of in vitro SLN paraganglion preparation. Arrows indicate the direction of the superfusate. One glass electrode is used for single fibre recording and the other glass electrode is used for microinjection of chemostimulants.

## 3. RESULTS

The simple two stain perfusion technique produced clear, highly circumscribed red spots in and adjacent to vagal nerve trunks (Fig. 2). The red spots were surrounded by blue capillary sinusoids. We found no evidence of a portal vasculature between adjacent glomi, and the inflow vessels were formed of vasa nervorum in the interior of the nerve. In contrast, venous outflow vessels appeared to be located outside the epineurium. The cross sectional area (18,090 ± 13,928 $\mu m^2$; mean ± S.D.) of 86 paraganglia (in recurrent and superior laryngeal nerves) was measured in 8 Wistar rats. The area-frequency distribution of the paraganglia was found to be significantly different to a normal distribution (Kolmogorov -Smirnov test). The mean cross sectional area of the SLN paraganglia was greater than that that of the recurrent laryngeal nerve (RLN), and this explained why the

*Figure 2.*Photomontage of an SLN paraganglion wholemount preparation. The abundant glomus tissue is stained with the vital dye Neutral Red which is taken up selectively by the paraganglia. The vasculature is filled with Berlin Blue. Calibration bar is 500 μm.

grouped data were not normally distributed. There was no significant asymmetry in the paraganglia areas when left RLN+SLN were compared to right RLN +SLN (Mann-Whitney U-test, $p>0.05$). The SPG method for localizing biogenic amines showed that both the SLN and RLN glomi contained highly fluorescent aggregations of small cells. Larger fluorescent cells were commonly seen scattered along the nerve trunks outside of the glomi and may be mast cells containing histamine.

In order to test whether the SLN glomus tissue was chemosensitive, an isolated *in vitro* preparation of nerve and paraganglia was perfected. A total of 15 single units were recorded in 3 rats. Eleven of 15 units (6, 5 and 4 units per rat) were sensitive to sodium cyanide (discharge increased significantly from $0.08 \pm 0.04$ to $19.5 \pm 4.2$ Hz; Student's paired t-test) delivered in close proximity to the main glomus as a bolus of 5 µl (1mg $ml^{-1}$) from a glass micropipette.

All values quoted are mean ± S.E.M. unless otherwise stated.

## 4. DISCUSSION

The morphometric analysis of this study highlights the SLN as containing one of the largest paraganglion of the Xth nerve. McDonald and Haskell (1985) have also described the morphology and blood supply to this SLN paraganglion. Our results are in broad agreement with theirs but they reported that the afferent feeding vessel to the SLN paraganglia was a branch of the main ipsilateral carotid body artery. We did not trace the afferent vessels back far enough to confirm or refute this interesting observation.
Experiments on rat laryngeal afferents (and on SLN of other species) do not mention the presence of arterial chemoreceptor fibres in this nerve (Sant'Ambrogio and Sant'Ambrogio, 1991; Widdicombe 1986; Sekizawa and Tsubone, 1991). The reason for this may relate to the peculiar vascular geometry of the SLN glomi. The afferent arterial supply runs in the interior of the nerve itself, so that the act of sectioning the SLN to perform fibre splitting *in vivo* destroys the vascular supply of the paraganglia. In addition, past studies have concentrated on laryngeal luminal stimuli with altered gas composition of inspired and expired air being the focus of attention (Bradford *et al.* 1993). Our preliminary data on an isolated superfused SLN paraganglion preparation dodges this problem and has produced evidence that the SLN paraganglion is a chemoreceptor. Some caution must be exercised however, since we have not tested the physiological stimulus of hypoxia.

The results of this study are important because chronic hypoxaemia is an end product of many diverse disorders of the pulmonary gas exchanger. The internal sensors of oxygen are poorly understood from the point of view of reflex cardiovascular regulation. There have been no studies in human or rat which examine the reflex regulation of the cardiovascular system by arterial chemoreceptors other than the carotid body. Textbooks of physiology and respiratory medicine commonly adopt the chemoreceptor

arrangement of the dog, with carotid and aortic bodies in humans depicted as having the distribution, function and reflex action found in the canine.

## ACKNOWLEDGEMENTS

The work from this laboratory was supported by a Marie Curie Fellowship of the European Community Program, IHP, under the contract number HPMD-CT-2000-00041, and University College Dublin. We are also indebted to the Wellcome Trust (UK) for the specialised equipment used in these studies.

## REFERENCES

Bradford, A., Nolan, P., O' Regan, R.G. and McKeogh, D. 1993, Carbon dioxide-sensitive superior laryngeal nerve afferents in the anaesthetized cat. *Exp. Physiol.* 78(6): 787-798.

Brophy, S., Ford, T.W., Carey, M. and Jones, J.F., 1999, Activity of aortic chemoreceptors in the anaesthetized rat. *J. Physiol.* 514(3): 821-828.

Dahlqvist, A., 1986, Recurrent laryngeal nerve and its paraganglia. A structural and biochemical study. PhD Thesis, University of Umea Press, Sweden.

Daly, M. and Ungar, A., 1966, Comparison of the reflex responses elicited by stimulation of the separately perfused carotid and aortic body chemoreceptors in the dog. *J. Physiol.* 182(2): 379-403.

Daly, M. De Burgh 1997, Peripheral arterial chemoreceptors and respiratory-cardiovascular integration. *Monographs of the Physiological Society*, Oxford Medical Publications.

Daly MD. and Jones JF. 1998, Respiratory modulation of carotid and aortic body reflex left ventricular inotropic responses in the cat. *J. Physiol.* 509(3): 895-907.Hervonen, A., Partanen, S., Vaalasti, A., Partanen, M., Kanerva, L. and Alho H., 1978,

The distribution and endocrine nature of the abdominal paraganglia of adult man.*Am. J. Anat.* 153(4): 563-72.

Hirakawa, H., Nakamura, T. and Hayashida, Y., 1997, Effect of carbon dioxide on autonomic cardiovascular responses to systemic hypoxia in conscious rats. *Am. J. Physiol.* 273(2 Pt 2): R747-754.

Jones, J.F. and de Burgh Daly, M., 1997, Reflex cardiac dromotropic responses to stimulation of the carotid and aortic chemoreceptors in the anaesthetized cat. *J. Physiol.* 502(2): 461-467.

Lack, E.E., 1978, Hyperplasia of vagal and carotid body paraganglia in patients with chronic hypoxemia. *Am. J. Pathol.* 91(3): 497-516.

Marshall, J.M., 1994, Peripheral chemoreceptors and cardiovascular regulation. *Physiol. Rev.* 74(3): 543-594.

McDonald, D.M. and Blewett, R.W., 1981, Location and size of carotid body-like organs (paraganglia) revealed in rats by the permeability of blood vessels to Evans blue dye. *J. Neurocytol.* 10(4): 607-643.

McDonald, D.M. and Haskell, A. 1985, Vascular geometry of arterial chemoreceptors: learning about the carotid body by studying paraganglia of the superior laryngeal nerve. In *Chemoreceptors in Respiratory Control* ,edited by Ribeiro J.A. and Pallot D.J., pp39-49. Croom Helm, London and Sydney.

Plenat, F., Leroux ,P., Floquet, J. and Floquet, A., 1988, Intra and juxtavagal paraganglia: a topographical, histochemical, and ultrastructural study in the human. *Anat. Rec.* 221(3):743-753.

Sant'Ambrogio, G. and Sant'Ambrogio, F.B., 1991, Reflexes from the airway, lung, chest wall, and limbs. In *The Lung: Scientific Foundations* edited by R.G. Crystal, J.B. West et al. Raven Press Ltd., New York.

Sekizawa, S. and Tsubone, H., 1991, The respiratory activity of the superior laryngeal nerve in the rat. *Respir. Physiol.* 86(3): 355-368.

Widdicombe, J.G., 1986, Sensory innervation of the lungs and airways. *Prog. Brain Res.* 67: 49-64.

# Dye and Electric Coupling between Carotid Nerve Terminals and Glomus Cells

R.G. JIANG and CARLOS EYZAGUIRRE
*Department of Physiology, University of Utah School of Medicine, Salt Lake City, UT, USA*

## 1. INTRODUCTION

Synaptic blockers are rather ineffective in blocking the carotid nerve discharge elicited by "natural" stimuli such as hypoxia, hypercapnia or acidity. At the same time, these drugs are quite effective in eliminating the effects produced by exogenous applications of excitatory transmitters. It is likely that the release of multiple transmitters by the natural stimuli prevents a single synaptic blocker from being effective. However, we propose an additional mechanism for this failure: electric coupling between carotid nerve terminals and glomus cells via gap junctions.

Gap junctions occur between glomus cells, between glomus and sustentacular cells, and between sustentacular cell processes (McDonald, 1981; Abudara *et al.*, 1999, 2000; Kondo and Iwasa, 1996), which results in electric coupling between glomus cells (Monti-Bloch *et al.*, 1993). In addition, Kondo and Iwasa (1996) have described some special unions within the chemical synapse between glomus cells and carotid nerve terminals that were thought to be gap junctions. More recently, however, Kondo (2002) has cast some doubts about his earlier findings.

This physiological study was inspired by the original description of Kondo and Iwasa (1996) and will show suggestive evidence that, indeed, there is

*Chemoreception*, Edited by Pequignot et al.
Kluwer Academic/Plenum Publishers, New York, 2003

coupling between carotid nerve terminals and glomus cells (see also, Eyzaguirre *et al.*, 2002).

## 2. METHODS

Carotid bodies were excised from Sprague-Dawley rats (both male and female) weighing 60-200 g, anesthetized with intraperitoneal injections of sodium pentobarbital (50 mg/kg). The organs were placed in a lucite chamber through which flowed a physiological solution equilibrated with 100% $O_2$. The $pO_2$ of the saline was 300 Torr at pH 7.43.

The preparations were mounted on the stage of an inverted microscope and viewed with phase-contrast or Hoffmann optics. For stimulation and recording, two microelectrodes filled with 3 M KCl (tip resistance 20-40 MΩ), were mounted on one micromanipulator and lowered into the tissue for simultaneous intracellular penetration of one glomus cell and a nerve ending. The electrodes were connected to independent amplifiers that allowed current delivery and the recording of voltages produced in the nerve terminals and cells. Under current clamping (or voltage recordings), a pulse delivered to Cell 1 elicited a voltage drop ($V_1$) in this cell. In coupled cells, voltages were also detected in coupled Cell 2 because a voltage drop occurred across the intercellular junction ($\Delta Vj$). Consequently, the electrode lodged in Cell 2 registered $E_2$, which was smaller than $V_1$. The degree of coupling was established as the coupling coefficient ($K_c$) equal to $E_2/V_1$.

Glomus cells were identified by immuno fluorescence staining for TH. Tissues were fixed in 4% paraformaldehyde for 15-18 h at 4°C or 1 h at room temperature. After washing with TBST (50 mM Tris-HCl, 150 mM NaCl, 0.3% Triton X-100, pH 7.6), the tissue was treated with 2% goat serum in TBST for 1 h at room temperature. Then, the tissues were incubated in the primary antibody, which was rabbit anti-tyrosine hydroxylase (CHEMOCON), for 15-18 h at 4°C. This antibody was diluted 1:500 in TBST plus 2% goat serum. The secondary antibody was Texas Red goat anti-rabbit IgG (Vector Laboratories), diluted 1:100 in 50 mM TBS (Tris-HCl and 150 mM NaCl, pH 7.6). Tissues were incubated in the secondary antibody for 30 min at room temperature and washed with TBS before being covered with Vectashield placed on a cover glass slip.

To identify stimulated and recorded nerve endings and glomus cells, we used electrodes made from two-barrel borosilicate glass tubing with filaments (WPI). One barrel was filled with 3 M KCl (2-10 MΩ) for stimulation and

recording. For microejections, the other barrel was filled with 5% Lucifer Yellow (Lucifer Yellow CH, Lithium salt, Molecular Probes) in 150 mM LiCl. When the double-barrel microelectrode was inserted into a cell, dye ejection was accomplished with 100 ms negative current pulses (1-50 nA) delivered through the dye-filled barrel and applied for 1-5 min at 100 ms intervals. After dye ejection, the tissue was fixed and examined with a confocal microscope (Zeiss LSM 510). Images were acquired in the green and red channels by Argon and HeNe lasers and viewed as series of optical sections of from 0.8 to 4 μm. All images were processed with LSM 5 Examiner and Adobe PhotoDeluxe. It was possible to independently examine the green (LY) and red (TH) images, or to superimpose them.

## 3. RESULTS

Fig. 1 shows an experiment in which a nerve terminal was impaled with a double barrel microelectrode (upper left diagram). One barrel contained 3 M KCl to record the ongoing electrical activity of the terminal, which is presented at the bottom of the figure. The resting potential was about –65 mV over which there were small deflections. At 50 sec there was a spontaneous slow depolarization topped by faster but still relatively small deflections. At about 80 sec there was a much larger and slow depolarization accompanied by much larger and short bursts of activity.

The electric potentials here presented are typical of carotid nerve terminal activity that was originally described by Hayashida *et al.* (1980) and labelled small depolarizing potentials (sdps). Consequently, in all likelihood, the impaled structure was a carotid nerve terminal. Based on this assumption, we injected Lucifer Yellow through the other barrel of the electrode.

After preparing the tissue for TH staining, to view the background glomus cells, the preparation was taken to a confocal microscope to examine the LY injection site. The picture on the upper right side of the illustration shows the result of this observation. The injected site appears as a bright spot (yellow in the original) and the dye spread to adjoining glomus cells (dark in this picture, but red in the original). Therefore, there was dye coupling between a carotid nerve terminal and the adjoining glomus cells. It was possible to successfully perform several other similar experiments.

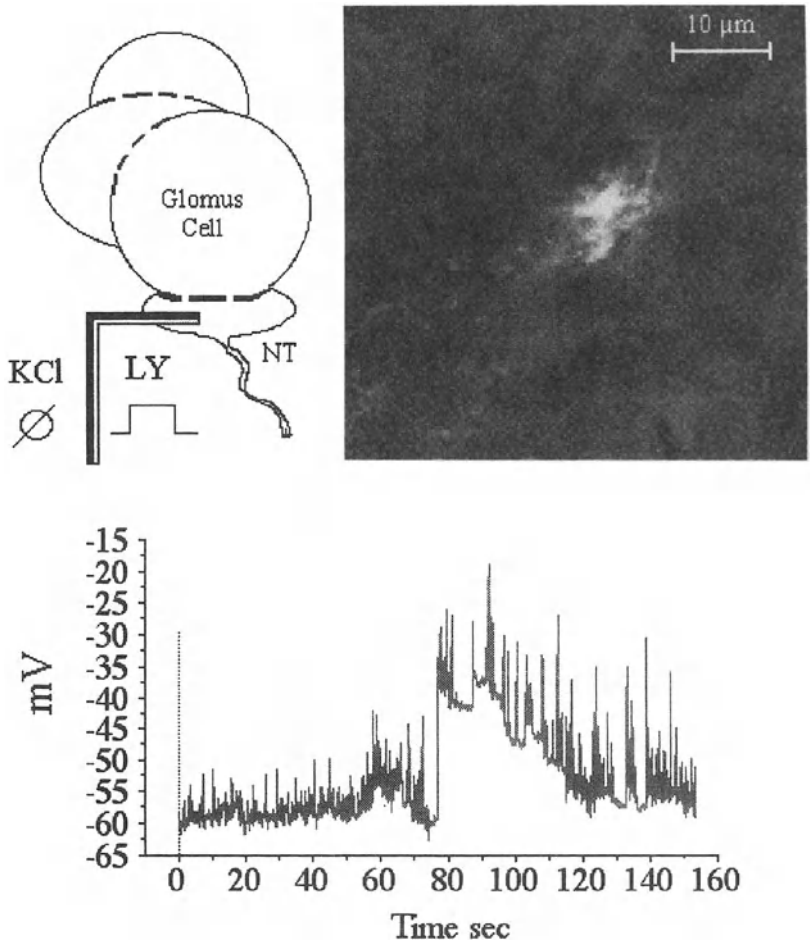


*Figure 1.* Upper left diagram shows a nerve terminal (NT) impaled with a double barrel microelectrode. One barrel is filled with 3 M KCl for recording (ø) and the other contains Lucifer Yellow (LY) for staining the recorded structure. Upper right, confocal image of Lucifer Yellow staining of impaled and recorded nerve terminal. Note that the dye spreads from the injected spot toward adjoining glomus cells that were stained for tyrosine hydroxylase (TH), which appear dark in this picture. They were red in the original. Lower record, recordings of sdps from the impaled nerve terminal.

To detect electric coupling between glomus cells and carotid nerve terminals, we performed experiments similar to that shown in Fig. 2.

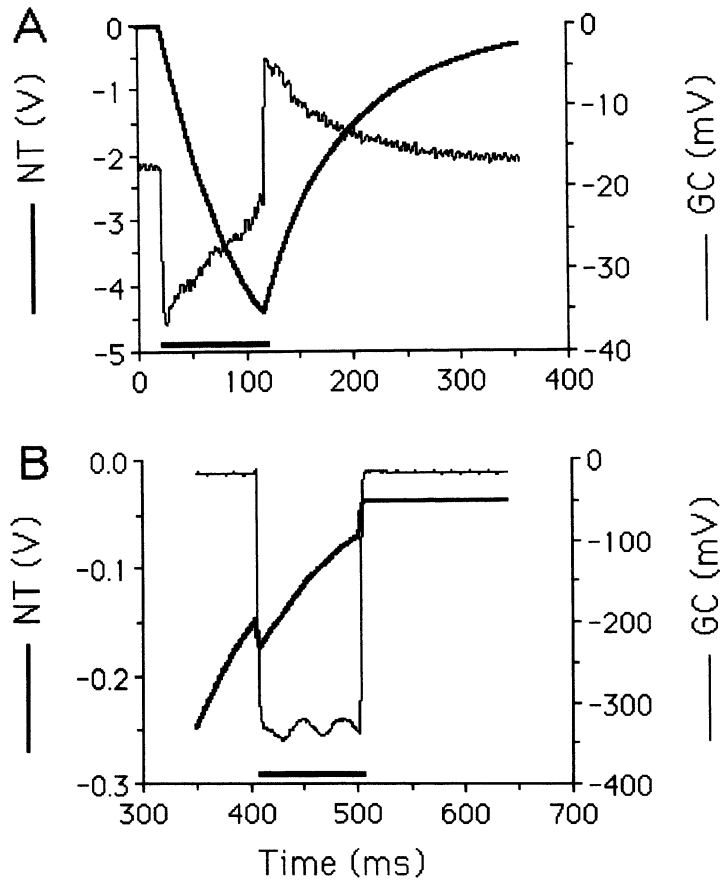


*Figure 2.* A, a negative current pulse (2 nA, horizontal bar at the bottom) applied to a nerve terminal elicits a large negative potential in this structure (left ordinate and thick trace) and a smaller negative deflection in the coupled glomus cell (right ordinate and thin trace). B, is a continuation of A. A 2 nA negative current pulse (horizontal bar at bottom) elicits a negative deflection in the glomus cell (right ordinate and thin trace) and a smaller deflection in the nerve terminal. Note that the glomus cell pulse was applied while the nerve terminal recuperated from the pulse previously applied to the nerve. More details in the text.

A nerve terminal and an adjoining glomus cell were simultaneously impaled for stimulation and recording. The thick trace in A shows the effect of a 2 nA negative current pulse (bottom horizontal bar) applied to a nerve terminal (later morphologically identified as such) and the accompanying voltage transfer to a glomus cell (thin trace). Note the high input resistance ($R_o$) of the terminal, which prevented full development of the potential change. $R_o$ was higher than 2 GΩ. B, was taken during the recovery of the nerve ending hyperpolarization when a 2 nA current pulse was delivered to the glomus cell. Note the negative break in the recovery curve of the terminal. The input resistance of the glomus cell was about 150 MΩ, much lower than that of the nerve terminal.

The coupling coefficient ($K_c$) from nerve to cell was 0.008, whereas that from cell to nerve was 0.47. Thus, coupling from cell to nerve was much higher than from nerve to cell. This difference in coupling direction seemed to be the general rule for positive and negative current pulses.

## 4. CONCLUSIONS

In spite of Kondo's (2002) reservations about the presence of gap junctions between glomus cells and carotid nerve terminals, our results strongly suggest that they do occur. There was spread of dye to the glomus cells when a nerve terminal was injected with Lucifer Yellow. Also, current injected into one of these elements was transferred to the other, although current diffused more easily from cell to nerve terminal. We do not have a ready explanation for this difference. It means, however, that electric events in glomus cells (depolarization or hyperpolarization) are more easily transferred to the nerve terminal than phenomena occurring in the nerve ending.

Current spread from glomus cells to nerve terminals may make it impossible for specific synaptic blockers to effectively eliminate the effects of "natural" stimuli if these agents act mainly on the glomus cells. Also, release of multiple transmitters complicates things further when only one specific blocker is employed.

A definitive answer to the occurrence of coupling between glomus cells and nerve terminals will be available when connexins are explored and found, using the electronmicroscope.

## ACKNOWLEDGEMENTS

Work supported by NIH grant NS 07938.

## REFERENCES

Abudara, V., Garcés, G., and Sáez J.C., 1999, Cells of the carotid body express connexin43 which is up-regulated by cAMP. *Brain Res.* 849: 25-33.

Abudara V., Eyzaguirre, C., and Sáez, J.C., 2000, Short- and long-term regulation of rat carotid body gap junctions by cAMP. Identification and regulation of connexin43, a gap junction subunit. *Adv. Exper. Med. Biol.* 475: 359-370.

Eyzaguirre, C., Jiang, R.G., and Abudara,V., 2002, Electric and dye coupling between rat carotid body cells and between these cells and carotid nerve endings. In: Oxygen Sensing: Responses and Adaptation to Hypoxia. (S. Lahiri, G. Semenza and N. Prabhakar, eds). Marcel Dekker, NY (in press).

Hayashida, Y., Koyano, H., and Eyzaguirre, C., 1980, An intracellular study of chemosensory fibers and endings. *J. Neurophysiol.* 44: 1077-1088.

Kondo, H., and Iwasa, H., 1996, Re-examination of the carotid body ultrastructure with special attention to intercellular membrane appositions. *Adv. Exper. Med. Biol.* 410: 45-50.

Kondo, H., 2002, Are there gap junctions between chief (Glomus, Type I) cells in the carotid body chemoreceptor ? *Microsc. Res.Tech.* 59: 227-233.

McDonald, D.M., 1981, Peripheral chemoreceptors: Structure-function relationships of the carotid body. In: Regulation of Breathing. (T.F. Hornbein, ed.). Marcel Dekker, NY, pp 105-319.

Monti-Bloch, L., Abudara, V., and Eyzaguirre, C., 1993, Electrical communication between glomus cells of the rat carotid body. *Brain Res.* 622: 119-131.

# Neurotransmitter Relationships in the Hypoxia-challenged Cat Carotid Body

ROBERT S. FITZGERALD, HAY-YAN (JACK) WANG, SERABI HIRASAWA, and MACHIKO SHIRAHATA

*Departments of Environmental Health Sciences (Division of Physiology), Physiology, Medicine, and Anesthesiology/Critical Care Medicine. The Johns Hopkins Medical Institutions Baltimore, MD 21205 USA*

## 1. INTRODUCTION

The most fundamentally necessary substrate for life is oxygen.The human organism cannot be without it for more than a few minutes without doing irreversible damage to neural structures. This substrate is used to oxidize glucose, which process provides the organism with the energy required for all of life's processes. Well-appreciated is the fact that the carotid body is the principal detector of systemic hypoxia. The aortic bodies also play a role, but appear to be in humans at least considerably less important. We have learned in this conference that the carotid body also increases its neural output to the nucleus tractus solitarius in response to reduced glucose in blood or perfusion fluids.It is therefore somewhat amusing as well as frustrating that even though 250 years have passed since the first report of the carotid body in 1743, the precise steps describing how this all-important structure sends its message to the nucleus tractus solitarius continue to remain mysterious.Generations of investigators have tried to determine these mechanisms. And though considerable progress has been made, no definitive answer can yet be provided.

*Chemoreception*, Edited by Pequignot et al.
Kluwer Academic/Plenum Publishers, New York, 2003

Currently accepted assumptions include a necessary role for neurotransmitters released from the carotid body's glomus cells.These bind to "post-synaptic" receptors on the afferent neurons abutting on the glomus cells, provoking a depolarization which travels centrad. Two key questions seem to be the focus of present-day investigation: (1) How is the glomus cell depolarized so as to allow the entry of calcium and subsequent release of the neurotransmitters? (2) What are the excitatory and modulatory neurotransmitters?

Over the last 10 years we have tried to establish acetylcholine (ACh) as an excitatory neurotransmitter, at least in the cat carotid body. We chose the cat because previously we had, along with many other investigators, described in this species many cardiopulmonary reflex responses to hypoxia which to some degree involved the carotid bodies (and/or aortic bodies). It seemed appropriate to determine in this species how this oxygen sensor detected the absence of this all-important substrate. It seems equally important to determine the mechanisms involved in the carotid body's response to hypoglycemia. They may differ from those operating during hypoxia.

We focused on ACh in spite of the opinion of some early investigators. Corneille Heymans, who won the Nobel Prize in 1938 for his discovery of the role of carotid mechanisms in the control of the cardiopulmonary system, thought that ACh had nothing whatever to do with the excitation of the carotid body by normal stimuli (Heymans, et al, 1958). Other very distinguished physiologists shared that opinion. However, we felt that the work of an opposing coterie of early investigators, specifically the "Swedish Group" of Liljestrand, von Euler, Zotteman and their colleagues, had data which was very persuasive in support of ACh as an excitatory neurotransmitter (for overview cf. Fitzgerald, 2000). Subsequently the "Utah Group" of Eyzaguirre, Fidone, Zapata, Dinger, and their many colleagues also added evidence supporting an excitatory role for ACh. More recently, Nurse and his colleagues have reported data strongly indicative of a critical excitatory role for ACh in the hypoxic stimulation of their reconstructed rat carotid body (Nurse et al, 1999; Zhang et al, 2000). Alcayaga, Iturriaga, Zapata and their colleagues have also contributed support (Alcayaga et al, 1998).

We have demonstrated that perfusion of the cat carotid body with a hemicholinium-containing solution for 10 min preceding a hypoxic challenge significantly reduced the neural output in response to that stimulus (Fitzgerald et al, 1996). This suggested that the synthesis of ACh may have been inhibited; the results corroborated previous studies. Vesamicol is an agent which inhibits the packaging of ACh into vesicles. We have demonstrated that including this agent in a perfusion also significantly reduced the neural output in response to hypoxia

(Fitzgerald et al., 1996). Postsynaptically we blocked putative nicotinic receptors with several cholinergic receptor antagonists and observed the reduction of hypoxia-induced neural output (Fitzgerald et al., 1994,1997). Added to these pharmacological interventions we performed a variety of experiments to detect and locate cholinergic receptors. Several of our findings are reported in this symposium. Fluorometric studies to detect the behavior of intracellular calcium and patch clamp experiments to demonstrate the effect of cholinergic agonists on membrane voltages and currents have all been consistent in demonstrating a key excitatory role for ACh. And recently we have demonstrated the release of ACh from in vitro cat carotid bodies in response to hypoxia (Fitzgerald et al., 1999).

Several criteria need fulfillment in order to establish a substance as a neurotransmitter (Fitzgerald, 2000). If one accepts these, our several studies, integrated with the many valuable results of previous and contemporary investigators, would seem to warrant the status of neurotransmitter for ACh, firmly...at least in the cat and rat. Quite possibly other substances might also pass the criteria test.

Hence, the "Cholinergic Hypothesis", we feel, is in place and our current efforts have been to extend the Hypothesis. The current hypothesis being tested is: ***The well-established hypoxia-induced release of catecholamines is at least partially modulated by cholinergic mechanisms.*** Again we have only used the cat.

## 2. MATERIALS AND METHODS AND RESULTS

### 2. 1. Muscarinic Modulation of Hypoxia-induced Catecholamine Release

Carotid bodies were removed from deeply anesthetized cats,cleaned in an ice-cold Krebs Ringer bicarbonate solution (KRB) containing cholinesterase inhibitors. They were next bubbled for 30 min at 37° C in 170 μL of the solution which was 40 μM for L-DOPA, a catecholamine precursor.After this conditioning incubation each carotid body was placed in a separate Eppendorf tube containing 85 μL KRB. One served as control; its contralateral mate was challenged with a cholinergic inhibitor.

The M1 muscarinic receptor inhibitor 1 μM pirenzepine provoked a signficant reduction in the recovery of dopamine (DA) from the medium

compared to the control carotid body. Norepinephrine recovery was also reduced. Our pirenzepine data suggested the possibility that the hypoxia-induced release of ACh acted upon glomus cell M1 receptors. Since presynaptic M1 receptors enhance the release of ACh and other neurotransmitters, blocking M1s would reduce the amount of DA and NE released as well as the release of ACh, compared to a control.

Further analysis of the data revealed that the impact of pirenzepine and methoctramine on NE release appeared to be greater than their impact on the release of DA and its metabolites. Pirenzepine reduced the hypoxia-induced release of NE from the treated carotid body to 66% of that released by the control carotid body. Methoctramine increased NE's release from the treated carotid body to 140% of its control. The reduction and enhancement values for DA and its metabolites were to 84% ($P = 0.014$ *vs* NE) and to 121% ($P = 0.102$ *vs* NE) of the control release values, respectively (Wang et al, 2002).

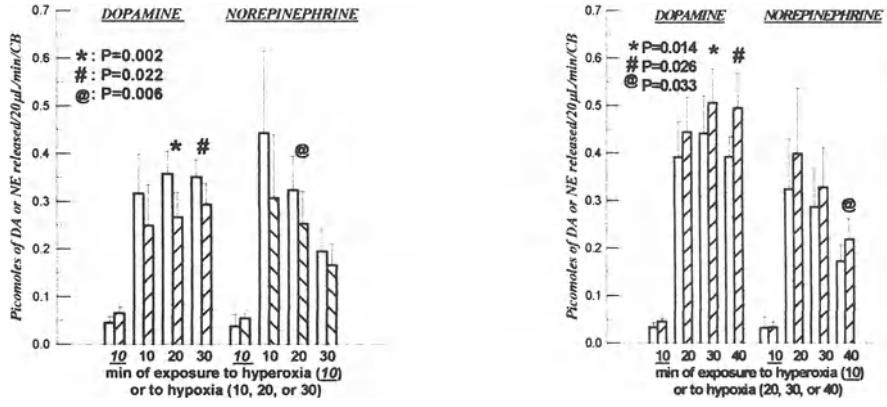


*Figure 1.* The left panel shows the effect of the M1 muscarinic receptor blocker,1.0 µM pirenzepine; the right, the effect of 1.37 µM methoctramine, the M2 muscarinic receptor blocker. Open bars = control carotid bodies; hatched bars= blocker-treated carotid bodies. (n=11)

An interesting but unexpected phenomenon appeared upon closer inspection of the control values seen in Figure 1. The release of DA was independent of the

duration of hypoxia, whereas the release of NE decreased significantly as the duration of the hypoxic exposure increased.

## 2.2. Nicotinic Modulation of Hypoxia-induced Catecholamine Release

Having detected the presence of α3, α4, β2 subunits of the neuronal nicotinic receptors on carotid body glomus cells (cf. Hirasawa et al, this conference), we tested the effect of one of the more specific nicotinic receptor antagonists, dihydro-β-erythroidine (DHβE). Figure 2 clearly shows a significant reduction in the hypoxia-induced release of DA at all concentrations of the antagonist, whereas DHβE did not attenuate the hypoxia-induced release of NE.

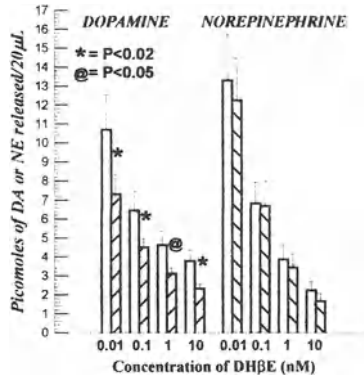


*Figure 2.* DHβE signicantly reduced the hypoxia-induced release of DA, but has no significant effect on the hypoxia-induced release of NE. (n = 7).

## 3. DISCUSSION

The Cholinergic Hypothesis is currently well-supported, and the data above seem to support the new hypothesis.Our own recent studies and several of the reports in this conference address the issue of interrelationships among putative neurotransmitters involved in the chemotransduction of hypoxia. Our current focus has been and continues to be establishing a cholinergic-catecholaminergic

interrelationship in the carotid body. Bairam and her colleagues (2000) using a different preparation also found that cholinergic agonists delivered exogenously controlled the release of catecholamines. That cholinergic mechanisms are found to control catecholaminergic release in the carotid body is not altogether surprising. The autonomic nervous system controls the heart's stroke volume and rate with a balance and interaction of the sympathetic and parasympathetic nervous systems on the heart and on each other. In the central nervous system there are several instances of muscarinic and nicotinic modulation of dopamine and noradrenaline release (Clarke et al., 1996; DeKlippel et al., 1993; P. Izurieta-Sanchez et al, 2000; Smolders et al., 1997). One study suggested a potential source for the difference between release patterns for DA and NE. Presynaptic nicotinic receptors associated with striatal DA terminals differed pharmacologically from those on hippocampal NE terminals. Nigrostriatal DA neurons expressed mainly $\alpha 4$, $\alpha 5$, and $\beta 2$ nicotinic receptor subunits, while hippocampal NE neurons expressed $\alpha 3$, $\beta 2$, and $\beta 4$ subunits. This situation is consistent with the reports of several other glomus cell heterogeneities. It seems entirely possible that not all glomus cells have exactly the same complement of neurotransmitters nor the same set of nicotinic receptors. Further study of neurotransmitter interrelationships will undoubtedly help to bring greater clarity to these interactions so fundamental to the chemotransduction of hypoxia, and perhaps reveal clues as to the mechanisms involved in the transduction of hypoglycemia.

## ACKNOWLEDGEMENT

This study was supported by HL50712 and HL61596

## REFERENCES

Alcayaga J., Iturriaga R., Varas R., Arroyo J., Zapata P., 1998. Selective activation of carotid nerve fibers by acetylcholine applied to the cat petrosal ganglion in vitro. *Brain Res.* 786: 47-54.

Bairam A., Neji H., Marchal F., 2000. Cholinergic dopamine release from the in vitro rabbit carotid body. *J. Appl. Physiol.* 88: 1737-1744.

Clarke P., Reuben M., 1996. Release of $^{3}$H-noradrenaline from rat hippocampal synaptosomes by nicotine: mediation by different nicotinic receptor subtypes from striatal $^{3}$H-dopamine release. *Br. J. Pharmacol.* 117: 595-606.

DeKlippel N., Sarre S., Ebinger G., Michotte Y., 1993. Effect of $M_1$- and $M_2$-muscarinic drugs on striatal dopamine release and metabolism: an in vivo microdialysis study comparing normal and 6-hydroxy-dopamine-lesioned rats. *Brain Res.* 630:57-64.

Fitzgerald R.S., 2000. Oxygen and carotid body chemotransduction: the cholinergic hypothesis – a brief history and new evaluation. *Respir. Physiol.* 120: 89-104.

Fitzgerald R.S., Shirahata M., 1994. Acetylcholine and carotid body excitation during hypoxia in the cat. *J. Appl. Physiol.* 76: 1566-1574.

Fitzgerald R.S., Shirahata M., Ide T., 1997. Further cholinergic aspects of carotid body chemotransduction of hypoxia in cats. *J. Appl. Physiol.* 82: 819-827.

Fitzgerald R.S., Shirahata M., Ishizawa Y., 1996. The presynaptic component of a cholinergic mechanism in the carotid body chemotransduction of hypoxia in the cat. *Adv. Exp. Med. Biol.* 410: 245-252.

Fitzgerald R.S., Shirahata M., Wang H-Y., 1999. Acetylcholine release from cat carotid bodies. *Brain Res.* 841: 53-61.

Heymans C., Neil E., 1958. Reflexogenic Areas of the Cardiovascular System, p. 191. Boston: Little & Brown.

Izurieta-Sanchez P., Sarre S., Ebinger G., Michotte Y., 2000. Muscarinic antagonists in substantia nigra influence the decarboxylation of L-dopa in striatum. *Eur. J. Pharmacol.* 399: 151-160.

Nurse C.A., Zhang M., 1999. Acetylcholine contributes to hypoxic chemotransmission in co-cultures of rat type I cells and petrosal neurons. *Respir. Physiol.* 115: 189-199.

Smolders I., Bogaert L., Ebinger G., Michotte Y., 1997. Muscarinic modulation of striatal dopamine, glutamate, and GABA release, as measured with in vivo microdialysis *J. Neurochem.* 68: 1942-1948.

Wang H-Y. (Jack), Fitzgerald R., 2002. Muscarinic modulation of hypoxia-induced release of catecholamines from the cat carotid body. *Brain Res.* 927: 122-137.

Zhang M., Zhong H., Vollmer C., Nurse C.A., 2000. Co-release of ATP and ACh mediates hypoxic signalling at rat carotid body chemoreceptors. *J. Physiol. Lond.* 525: 143-158.

# ACH Differentially Modulates Voltage-gated K Channels in Glomus Cells between DBA/2J and A/J Strains of Mice

SHIGEKI YAMAGUCHI[1,2], TOMOKO HIGASHI[1], YUICHI HORI[3], and MACHIKO SHIRAHATA[1]

*Departments of Environmental Health Sciences, Johns Hopkins Bloomberg School of Public Health, Baltimore, USA[1]; Departments of Anesthesiology[2] and Physiology[3], Dokkyo University School of Medicine, Mibu, Japan*

## 1. INTRODUCTION

The hypoxic ventilatory response (HVR) among individuals varies widely (Eisele *et al.*, 1992; Vizek *et al.*, 1987; Weil *et al.*, 1970) and genetic factors significantly contribute to these variations (Kawakami *et al.*, 1982; Nishimura *et al.*, 1991). A study using several inbred strains of mice indicates that genetic determinants apparently influence the HVR (Tankersley *et al.*, 1994) DBA/2J mice demonstrated the highest HVR and the A/J mice the lowest HVR. These data suggest that genetically regulated differences exist in the system controlling the hypoxic ventilatory response. A major hypoxic chemosensor is the carotid body. Recently, we have found morphological and functional differences in glomus cells between DBA/2J and A/J mice (Yamaguchi *et al.*, 2003). The carotid body of DBA/2J mice contain more glomus cells than that of the A/J mice, and more glomus cells in DBA/2J mice increase intracellular $Ca^{2+}$ in response to ACh than those in A/J mice.

Neurotransmitters play a critical role in chemotransmission of the carotid body by acting on chemoreceptor afferents. In addition, neurotransmitters contribute to the excitability of glomus cells not only by their immediate and

*Chemoreception*, Edited by Pequignot et al.
Kluwer Academic/Plenum Publishers, New York, 2003

direct action on their receptors, but also by their modulating effects on ion channel activities. For example, ACh modulates voltage-gated K (Kv) channels in cat glomus cells (Shirahata *et al.*, 2003). We hypothesized that Kv channel modulation by ACh may contribute to the differences in glomus cell excitability between DBA/2J and A/J mice.

## 2. MATERIALS AND METHODS

Experiments were performed in carotid bodies removed from DBA/2J and A/J strains of mice aged between 6 -10 weeks. Animals were deeply anesthetized with ketamine (100 mg/kg, i.p.) and sodium pentobarbital (50 mg/kg, i.p.). The carotid bodies were quickly harvested together with the carotid bifurcation and immersed in ice-cold and 5% $CO_2$/air-saturated modified Krebs solution (in mM: NaCl 118, KCl 4.7, $MgSO_4 \cdot 7H_2O$ 1.2, $KH_2PO_4$ 1.2, $CaCl_2$ 1.8, $NaHCO_3$ 25, and glucose 11.1, pH 7.4). Extra tissues were gently removed using a stereoscopic microscope. After incubation with Krebs solution at 37°C for 60 minutes, each tissue was placed in a recording chamber on the stage of an upright microscope (Axsoskop 2, Zeiss). The carotid body was perfused with Krebs solution containing 0.02% collagenase for 30 minutes to remove connective tissues covered the surface of the carotid body. Further, some connective tissues covering the cell membrane were dislodged by applying a jet of Krebs solution through a pipette with an orifice of ~5–10 μm. Glomus cells were visualized under an infrared differential interference (IR-DIC) video microscope with a water immersion objective lens (Figure 1). All experiments were performed while the carotid body was continuously perfused with Krebs solution at 37°C.

Tight-seal whole-cell recordings were made with a conventional patch pipette. The patch electrodes were pulled from a high lead glass (Corning 8161) using a puller (Sutter Instrument Co.). The patch electrodes which had resistances of 4~6 MΩ were filled with the internal solution (in mM): K gluconate 90, KCl 33, NaCl 10, $CaCl_2$ 1, HEPES 10, EGTA 10, MgATP 5, pH7.2 with KOH. Whole cell outward current was evoked by several voltage clamp pulses ranged from -80 mV to 60 mV. Pharmacological reagents were dissolved in Krebs solution and applied by perfusion. The currents were amplified and filtered at 2kHz with a low-pass Bessel filter using an Axopatch 200B patch-clamp amplifier (Axon Instruments). The signals were digitized by a Digidata 1320A (Axon

Instruments). A PC-based computer and pCLAMP8.0 (Axon Instruments) were used for acquisition and processing of data.

All data were reported as means ± SEM. To determine significant difference, Student's t test or ANOVA was used. Values were considered significantly different if $p < 0.05$.

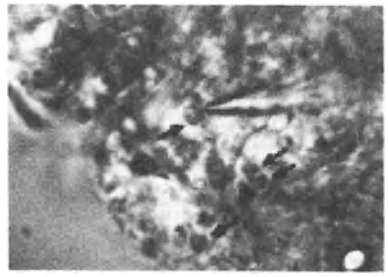

*Figure 1.* An image via an infrared CCD camera shows a part of the DBA/2J mouse carotid body. Glomus cells were relatively easily recognized (dark arrows). One glomus cell was patch clamped and voltage-gated outward current was recorded.

## 3. RESULTS

Slowly inactivated voltage-gated outward currents were readily observed in glomus cells of both strains. Amplitude of outward currents varied among cells. Minimum was 100 pA and maximum was 5000 pA. Current-voltage relationship indicated outward rectification with threshold of -30 mV. Potassium channel blockers 4-aminpyridine (4-AP, 1 mM) and iberiotoxin (Ibtx, 200 nM) significantly and reversibly attenuated outward current in glomus cells of both strains (Table 1). The combination of these blockers almost completely inhibited the outward current in both strains. These characteristics of Kv currents in glomus cells did not differ between the two strains of mice.

*Table 1.* Effects of Potassium Channel Blockers on Voltage-gated Outward Current (% Inhibition)

| Strains | 4-AP (1 mM) | Ibtx (200 nM) | 4-AP (1 mM) + Ibtx (200 nM) |
|---|---|---|---|
| DBA/2J | 70.0 ± 7.5 (n=24) | 32.2 ± 4.5 (n=12) | 93.4 ± 3.0 (n=10) |
| A/J | 70.0 ± 5.6 (n=15) | 30.8 ± 5.6 (n=13) | 89.9 ± 3.2 (n=12) |

The effect of ACh (100 μM) on Kv current in glomus cells was examined and found to be heterogeneous. In some glomus cells ACh reversibly attenuated K current (Figure 2A), but not in others (Figure 2B). Fifteen glomus cells were tested in DBA/2J mice, and 12 cells (80%) were responded to ACh (Figure 3A). However, only 3 glomus cells of 16 (19%) were responded in A/J mice (Figure 3B). In the responded glomus cells, the reduction of K current by ACh was 37.5 ± 5.0% in DBA/2J mice (n=12) and 36.5 ± 0.8% in A/J mice. These numbers were not significantly different.

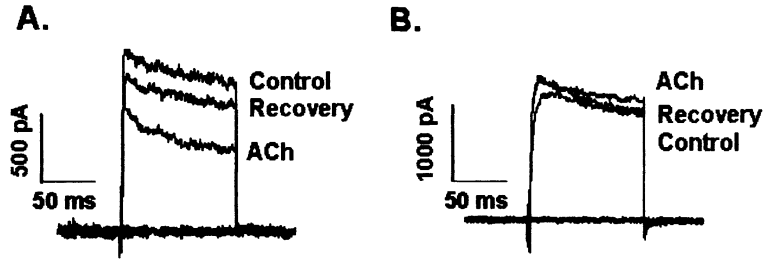


*Figure 2.* ACh heterogeneously modulates Kv current of glomus cells in both DBA/2J and A/J mice.

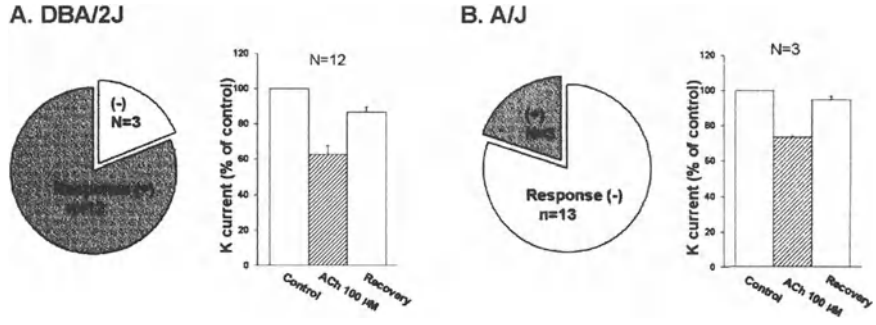


*Figure 3.* Differential effects of ACh 100 μM on Kv current of glomus cells in DBA/2J (left) and A/J (right) mice. More glomus cells in DBA/2J mice were influenced by ACh 100 μM.

## 4. DISCUSSION

In this study we have shown that (1) a new approach for employing patch clamp experiments in mouse glomus cells, (2) characteristics of Kv current in glomus cells of DBA/2J and A/J mice, and (3) differential effects of ACh on Kv current in glomus cells between DBA/2J and A/J mice.

Although we have used cultured mouse glomus cells for measuring intracellular calcium changes in our previous study (Yamaguchi *et al,* 2003), we chose to use an undissociated whole carotid body for patch clamp experiments in this study. Due to the small size of the carotid body, culturing mouse glomus cells is technically difficult. In this study we harvested the carotid body with major carotid arteries and visualized glomus cells with a water immersion objective lens and IR-DIC camera. The techniques simplified the procedures for identifying and approaching glomus cells.

General characteristics of Kv current were similar between DBA/2J and A/J strains. Judging from their kinetics and pharmacological responses, major components of Kv current in glomus cells in these two strains of mice appear to be a delayed rectifier, A-type channels, and large conductance calcium-activated K channels. These characteristics are similar to those in rabbit glomus cells, but somewhat different from those in rat and cat glomus cells (Shirahata & Sham. 1999).

The effect of ACh 100 μM on Kv current in DBA/2J glomus cells were similar to those in cat glomus cells (Shirahata *et al.,* 2003). Underlying mechanisms of this inhibition require further investigation. The responses of Kv current to ACh differed between DBA/2J and A/J strains. Inhibitory effect of ACh 100 μM was consistently found in glomus cells of DBA/2J mice (80%), but fewer cells (19%) responded in A/J mice. The results indicate that ACh differentially modulates Kv channels in glomus cells between DBA/2J and A/J strains of mice. ACh is released from glomus cells and the release increases during hypoxia (Fitzgerald et al, 1999; Shirahata *et al,* 1996). Released ACh would influence the excitability of glomus cells via several types of cholinergic receptors. Further, inhibitory effect of ACh on Kv current would prevent repolarization of glomus cells during hypoxia and maintain depolarization of glomus cells. The fact that the inhibition of K current by ACh is more prominent in DBA/2J glomus cells suggest that glomus cells in DBA/2J mice would be more excitable during hypoxia than those in A/J mice. This may be responsible, at least in part, for higher HVR in DBA/2J mice than that in A/J mice.

## ACKNOWLEDGEMENT

This study was supported by AHA 0255358N and NHLBI HL 61596.

## REFERENCES

Eisele J.H., Wuyam B., Savourey G., Eterradossi J., Bittel J.H., Benchetrit G., 1992, Individuality of breathing patterns during hypoxia and exercise. *J. Appl. Physiol.* 72: 2446-2453.

Fitzgerald R.S., Shirahata M., Wang H.Y., 1999, Acetylcholine release from cat carotid bodies. *Brain Res.* 841:53-61.

Kawakami Y., Yoshikawa T., Shida A., Asanuma Y., Murao M., 1982, Control of breathing in young twins. *J. Appl. Physiol.* 52: 537-542.

Nishimura M., Yamamoto M., Yoshioka A., Akiyama Y., Kishi F., Kawakami Y., 1991, Longitudinal analyses of respiratory chemosensitivity in normal subjects. *Am. Rev. Respir. Dis.* 143:1278-1281.

Shirahata M., Higashi T., Hirasawa S., Yamaguchi S., Fitzgerald R.S., Lande, B., 2003, Excitation of Glomus Cells : Interaction between Voltage-gated $K^+$ Channels and Cholinergic Receptors. In Lahiri, S., G. L. Semenza, and N. R. Prabhakar, eds. Oxygen Sensing: Responses and Adaptation to Hypoxia. New York, Marcel Dekker.

Shirahata, M., Ishizawa, Y., Igarashi A., Fitzgerald R.S., 1996, Release of acetylcholine from cultured cat and pig glomus cells. *Adv. Exp. Med. Biol.* 410:233-238.

Shirahata M. and Sham J.S.K., 1999, Roles of ion channels in carotid body chemotransmission of acute hypoxia. *Jpn. J. Physiol.* 49:213-228.

Tankersley C.G., Fitzgerald R.S., Kleeberger S.R., 1994, Differential control of ventilation among inbred strains of mice. *Am. J. Physiol.* 267: R1371-R1377.

Vizek M., Pickett C.K., Weil J.V., 1987, Interindividual variation in hypoxic ventiatory response: potential role of carotid body. *J. Appl. Physiol.* 63: 1884-1889.

Weil J.V., Bryne-Quinn E., Sodal I.E., Friesen W.O., Underhill B., Filley G.F., Grover R.F., 1970, Hypoxic ventilatory drive in normal man. *J. Clin. Invest.* 49: 1061-1072.

Yamaguchi S., Balbir A., Schofield B., Coram J., Tankersley C.G., Fitzgerald R.S., O'Donnell C.P., Shirahata M., 2003, Structural and functional differences of the carotid body between DBA/2J and A/J strains of mice. *J. Appl. Physiol.* : In press.

# Hypoxic Augmentation of Neuronal Nicotinic Acetylcholine Receptors and Carotid Body Function

MACHIKO SHIRAHATA, TOMOKO HIGASHI, JEFFREY A. MENDOZA, and SERABI HIRASAWA
*Departments of Environmental Health Sciences, Johns Hopkins Bloomberg School of Public Health, Baltimore, USA*

## 1. INTRODUCTION

It is generally accepted that neurotransmitters are involved in hypoxic chemotransmission of the carotid body. The release of neurotransmitters from the glomus cell, a putative chemoreceptor cell, appears to be triggered by an influx of calcium and subsequent increase in intracellular calcium ($[Ca^{2+}]i$). Several reports indicate that L-type and some other types of voltage-gated calcium channels are responsible for neurotranmitter release from glomus cells. Since these channels are activated by depolarization of the cell membrane, mechanisms of hypoxic depolarization of glomus cells has been a major focus of investigation (Shirahata and Sham, 1999).

In a previous study we found that cat glomus cells were gradually depolarized from –55 mV to –27 mV in response to hypoxia ($PO_2$ 25 mmHg) (Chou et al., 1996). However, the speed and the degree of depolarization may not be sufficient to activate voltage-gated $Ca^{2+}$ channels at mild hypoxia, where afferent nueral activity from the carotid body starts increasing. This increase in neural output assumes an increased release of excitatory neurotransmitter(s) preceded by an elevation in $[Ca^{2+}]i$. Therefore,

*Chemoreception*, Edited by Pequignot et al.
Kluwer Academic/Plenum Publishers, New York, 2003

we asked a question whether depolarization of glomus cells is prerequisite for the increase in $[Ca^{2+}]i$ and the following neurotransmitter release at the beginning of hypoxia.

$Ca^{2+}$ influx into the glomus cell can occur via nAChRs (Dasso et al, 1997; Shirahata et al, 1997). Several reports indicate that nicotine increases the release of catecholamines (Dinger et al., 1985; Gomez-nino et al., 1990; Obeso et al., 1997). As other nAChRs, nAChRs in glomus cells can be active at resting membrane potential (Higashi et al, in this book). Therefore, if nAChRs in glomus cells were activated at mild hypoxia, $[Ca^{2+}]i$ would increase before depolarization of the cell. In this study we hypothesized that mild hypoxia augments the activity of nAChRs.

## 2. MATERIALS AND METHODS AND RESULTS

### 2.1. The Effect of Mild Hypoxia on ACH Current

To test the hypothesis we used N1E-115 mouse neuroblastoma cells, which have been used to study effects of pharmacological agents on nAChRs (Oortgiesen et al., 1993) Since these cells do not synthesize ACh, they are desirable to study ACh-induced current. N1E-115 cells were plated on 25 mm glass coverslips, and cultured as described by Zwart et al (1994). Cells were used within 2 days after differentiation.

First, we confirmed the presence of α3, α4, and β2 subunits of nAChRs in N1E-115 cells. RT-PCR analysis showed the expression of mRNA for α3, α4, and β2 nAChR subunits. Further, positive immunoreactivity for α3, α4 and β2 subunits of nAChRs (dark grey) was seen in many N1E-115 cells (Fig. 1). The staining is not uniform among the cells, indicating the expression of nAChRs vary among individual cells.

For patch clamp experiments, a glass coverslip with cultured cells was placed in the recording chamber. The cells were continuously superfused with Krebs solution (2 ml/min). The composition of Krebs solution was (in mM): NaCl 118, KCl 4.7, $MgSO_4 \cdot 7H_2O$ 1.2, $KH_2PO_4$ 1.2, $NaHCO_3$ 25, EDTA 0.0016, and glucose 11.1, pH 7.4 equilibrated with 5% CO2/air or 5% $CO2/N_2$ at 37 °C. To avoid any interference derived from muscarinic receptor activation, atropine (1 μM) was included in Krebs solution. ACh was administered to a patched cell for 2 seconds using a Y tube method as described by Andoh et al.,1997).

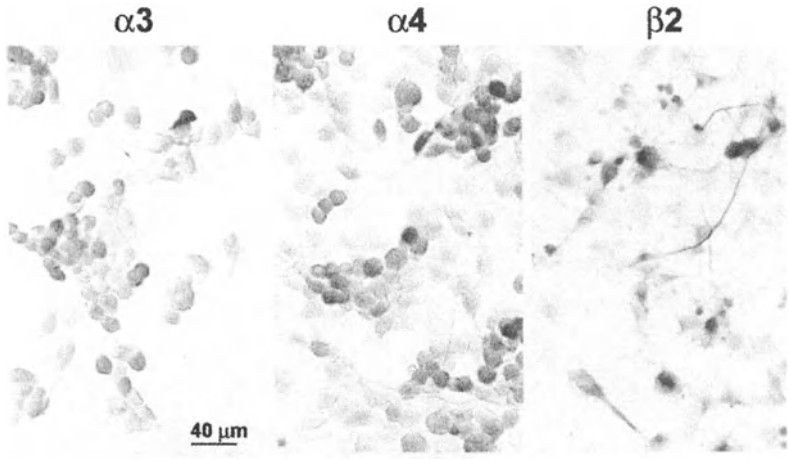


*Figure 1.* Immunocytochemical presentation of 3, 4, and 2 subunits of nAChRs in N1E-115 cells. Cultured cells were fixed with Zinc fixative at room temperature for 30 minutes. Endogenous peroxidase was quenched with 1% $H_2O_2$ in phosphate buffered saline. Nonspecific bindings and endogenous biotin were blocked with normal serum (1:70) including casein and with an avidin-biotin blocking kit (Vector), respectively. An appropriate primary antibody (anti-α3 nAChR, 1/2000, Sigma-RBI; anti-a4 nAChR, 1/1000, Covance; anti-β2 nAChR, 1/500, Covance) was applied overnight at room temperature. Subsequently, a biotinylated secondary antibody against rat IgG was applied for 1 hour at room temperature. A VECTASTAIN® *Elite* ABC (Vector) kit was used for peroxidase reaction, and SG (Vector) was used as a chromogen. The same class of IgG as each primary antibody was used as negative control, and no staining was observed (data not shown).

ACh (100 μM) administration evoked inward current in N1E-115 cells. When ACh was applied repeatedly with 5 min intervals during normoxia, ACh-induced current tended to decrease (desensitization; Fig. 2A). The peaks of the second (Challenge; normoxia) and the third (Control 2) ACh-induced currents were 52±9 % and 36±9 % of the first ACh-induced current (Control 1), respectively (n=18, mean±SEM; Fig. 2C). In the different set of experiments, after recording the first ACh-induced current (Control 1) the perfusate was changed from normoxic Krebs to hypoxic Krebs. When oxygen tension in the chamber reached to ~65 mmHg, which was monitored by an oxygen sensor (MI-730 oxygen Electrode, Microelectrodes), the second ACh-induced current was recorded. Desensitization was not observed. The mean peak currents by the second (Challenge; hypoxia) and the third (Control 2) ACh applications were 115±27 % and 108±34 % of the first ACh-induced current, respectively (n=6, mean ± SEM; Fig. 2C). These

values were significantly larger than those during normoxia (unpaired t test). The results suggest that mild hypoxia inhibits desensitization of ACh-induced current. It is also possible that desensitization may occur in some nAChRs, but simultaneously augmentation of activity may occur in some nAChRs.

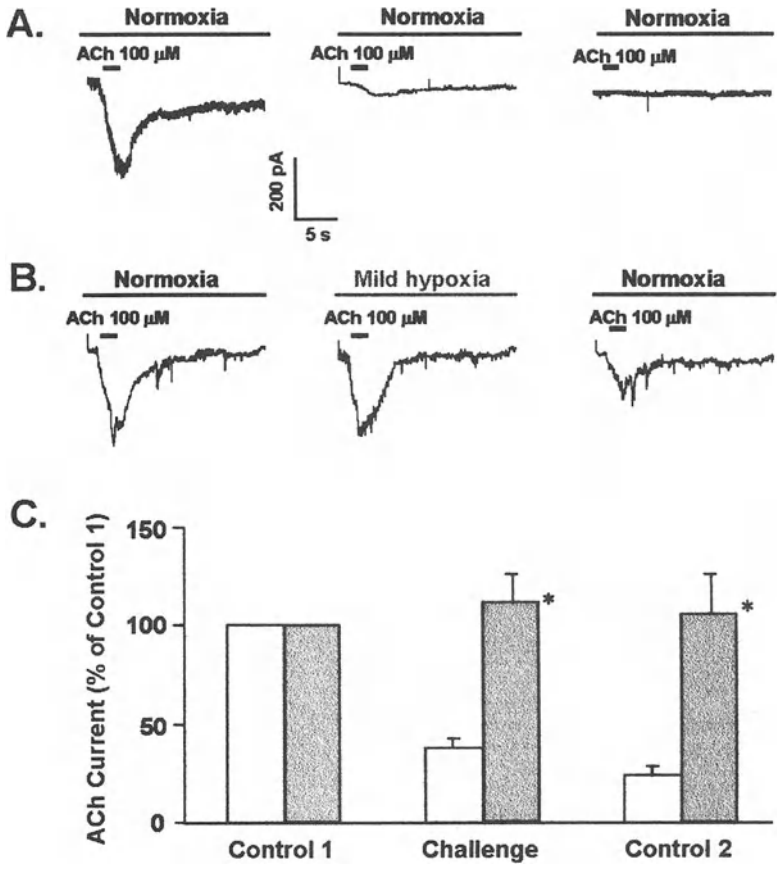


*Figure 2.* The effect of mild hypoxia on ACh-induced current in N1E115 cells. ACh-induced current was measured with a conventional whole cell configuration at -80 mV of holding potential. The patch electrodes with resistances of 4~6 MΩ were filled with the internal solution (in mM): CsF 40, CsCl 50, NaCl 10, $CaCl_2$ 1, HEPES 10, EGTA 10, MgATP 5, pH 7.2 with CsOH. **A.** ACh-induced current was recorded from the same cell with a repeated application of ACh at 5 minutes intervals during normoxia. **B.** The cell was exposed to mild hypoxia (~65 mmHg) during the second ACh application. Scales for the current and time were the same as A. **C.** Summary data of normoxia

challenge group (open bars; n=18) and hypoxia challenge group (shaded bars; n=6). *, significantly different from normoxic challenge group ($p<0.05$).

## 2.2. The Effect of Oxygen Tension on ACH-induced Carotid Body Excitation

Sensitivity of nAChR in the carotid body to oxygen tension was investigated in a whole animal preparation. Chemoreceptor neural output was measured from a whole carotid sinus nerve after barodenervation in an anesthetized and artificially ventilated cat as described previously (Ide et al., 1995). ACh administration to the carotid body increased carotid sinus nerve activity. A slight decrease in arterial oxygen tension from 114 to 84 mmHg did not change the baseline chemoreceptor neural activity, but it enhanced the ACh-induced increase in neural activity.

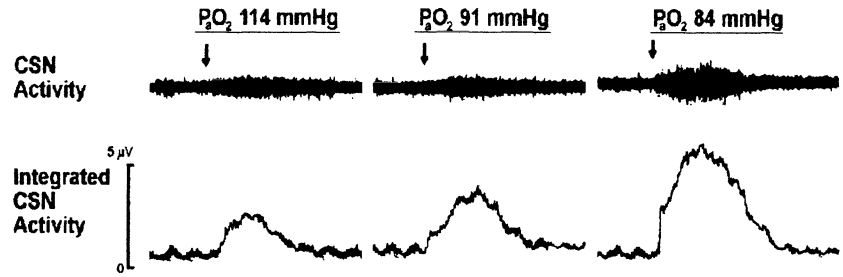


*Figure 3.* Oxygen tension influenced ACh-induced increase in carotid sinus nerve (CSN) activity. ACh (1 μg) was injected to the carotid body (indicated with arrows) via a catheter located near the carotid bifurcation. Arterial oxygen tension was reduced by changing inspired gas from an oxygen-enriched gas to air.

# 3. DISCUSSION

This study showed that mild hypoxia (~65 mmHg) modulated the activity of nAChRs in N1E-115 mouse neuroblastoma cells. Mild hypoxia appears to attenuate desensitization of the nAChR-mediated current or to enhance the current. The underlying mechanisms of this modulation are not known from this study. Hypoxia potentially influences redox states of nAChRs. Previous studies showed that reducing agents attenuated ACh-induced current (Amato et al., 1990; Tang and Aizenman, 1993). However, in these studies large doses of reducing agents were used. Hypoxic effects on nAChRs may

depend on different levels of redox states of nAChRs. This speculation was derived from following two reports. Wade et al (1998) have shown that hypoxia enhanced nAChR-mediated noradrenaline release from the sympathetic neuronal cell line. On the other hand, Lee et al., (1995) reported that anoxia inhibited ACh-binding to nAChRs in adrenal chromaffin cells. The possibility that moderate reduction of nAChRs may enhance the channel activity would be worth for further investigation.

Our study also suggest that the effect of ACh on carotid body neural output seems to be modulated by oxygen tension. It is possible that this effect is mediated by enhancement of nAChR activity in glomus cells and in afferent nerve endings. If the activity of nAChRs in glomus cells are enhanced during mild hypoxia, increased $Ca^{2+}$ influx via nAChRs would trigger release of neurotransmitters. Also, increased activity of nAChRs could depolarize glomus cells followed by activation of voltage-gated $Ca^{2+}$ channels and further release of neurotransmitters. If nAChRs in affeent nerve endings are activated by mild hypoxia, increased cation influx would lead to a greater excitatory postsynaptic potential and to trigger action potentials. Further studies are required to test whether enhanced nAChR activity could be one of the mechanisms of hypoxic increase in neural output of the carotid body.

## ACKNOWLEDGEMENT

This work was supported by NHLBI HL61596.

## REFERENCES

Amato, A., Connolly, C.N., Moss, S.J., Smart, T.G., 1990, Modulation of neuronal and recombinant GABAA receptors by redox reagents, *J. Physiol.* 517: 35-50.

Andoh, T., Furuya, R., Oka, K., Hattori, S., Watanabe, I., Kamiya, Y., Okumura, F., 1997, Differential effects of thiopental on neuronal nicotinic acetylcholine receptors and P2X purinergic receptors in PC12 cells, *Anesthesiology* 87: 1199-1209.

Chou, C.-L., Schofield, B., Sham, J.S.K., Shirahata, M., 1998, Electrophysiological and immunological demonstration of cell-type specific responses to hypoxia in the adult cat carotid body, 789:229-238.

Dasso, L.L., Buckler, K.J., Vaughan-Jones, R.D., 1997, Muscarinic and nicotinic receptors raise intracellular $Ca^{2+}$ levels in rat carotid body type I cells, *J. Physiol.* 498: 327-338.

Dinger, B., Gonzalez, C., Yoshizaki, K., Fidone, S., 1985, Localization and function of cat carotid body nicotinic receptors, *Brain Res.* 339: 295-304.

Gomez-Nino,A., Dinger,B., Gonzalez,C., Fidone,S.J., 1990, Differential stimulus coupling to dopamine and norepinephrine stores in rabbit carotid body type I cells, *Brain Res.* 525: 160-164.

Higashi, T., Yamaguchi, S., McIntosh, J.M., and Shirahata, M., 2003, Nicotinic acetylcholine receptor channels in cat chemoreceptor cells, *Adv. Exp. Med. Biol.*

Ide, T., Shirahata, M., Chou, C.L., Fitzgerald, R.S., 1995, Effects of a continuous infusion of dopamine on the ventilatory and carotid body responses to hypoxia in cats, *Clin. Exp. Pharmacol. Physiol.* 22: 658-664.

Lee, K., Ito, A., Koshimura, K., Ohue, T., Takagi, Y., Miwa, S., 1995, Differential effects of hypoxia on ligand binding properties of nicotinic and muscarinic acetylcholine receptors on cultured bovine adrenal chromaffin cells, *J. Neurochem.* 64: 874-882.

Oortgiesen, M., Leinders, T., Van Kleef, R.G., Vijverberg, H.P., 1993, Differential neurotoxicological effects of lead on voltage-dependent and receptor-operated ion channels, *Neurotoxicology* 14: 87-96.

Obeso, A., Gomez-Nino, M.A., Almaraz, L., Dinger, B., Fidone, S., Gonzalez, C., 1997, Evidence for two types of nicotinic receptors in the cat carotid body chemoreceptor cells, *Brain Res.* 754: 298-302.

Shirahata, M., Fitzgerald, R.S., Sham J.S.K., 1997, Acetylcholine increases intracellular calcium of arterial chemoreceptor cells of adult cats, *J. Neurophysiol.* 78: 2388-2395.

Shirahata, M., Sham, J.S.K., 1999, Roles of ion channels in carotid body chemotransmission of acute hypoxia, *Jpn. J. Physiol.* 49: 213-228.

Tang, L.H., Aizenman, E., 1993, The modulation of N-methyl-D-aspartate receptors by redox and alkylating reagents in rat cortical neurones in vitro, *J. Physiol.* 465: 303-323.

Wade, J.A., Vaughan, P.F., Peers, C., 1998, Hypoxia enhances [3H]noradrenaline release evoked by nicotinic receptor activation from the human neuroblastoma SH-SY5Y, *J. Neurochem.* 71: 1482-1489.

Zwart, R., Abraham, D., Oortgiesen, M., Vijverberg, H.P., 1994, Alpha 4 beta 2 subunit combination specific pharmacology of neuronal nicotinic acetylcholine receptors in N1E-115 neuroblastoma cells, *Brain Res.* 654: 312-318.

# Cholinergic Actions on Carotid Chemosensory System

PATRICIO ZAPATA, CAROLINA LARRAÍN, RICARDO FERNÁNDEZ and EDISON-PABLO REYES
*Laboratory of Neurobiology, Catholic University of Chile, Santiago, Chile*

## 1. INTRODUCTION

In simultaneous communications to the 15th International Congress of Physiological Sciences (Leningrad, 1935), Anichkov *et al.* and Heymans *et al.* reported that intracarotid injections of acetylcholine (ACh) provoke reflex hyperventilation in cats and dogs, respectively (see Zapata, 1997b). The first evidence that ACh increases the frequency of chemosensory discharge ($f_x$) of the carotid (sinus) nerve was provided by von Euler *et al.* (1941). The attention on ACh as a stimulant of the arterial chemoreceptors (carotid bodies (CBs) and aortic bodies) became greater when the glomus cells of the CB were shown to synthesize and store ACh, which was released in response to hypoxia or electrical stimulation (Eyzaguirre and Zapata, 1968b).

Since ACh is a vasodilating agent and the CB is extremely sensitive to changes in blood flow (see Zapata, 1997a), two approaches have been used to avoid the problem of its interference with its direct action on the chemoreceptor organ: injecting the cholinergic agonist nicotine instead of ACh in CB preparations *in situ*, or working with CBs superfused *in vitro* (Eyzaguirre's preparation).

All experiments here reported were performed on adult cats anaesthetized with pentobarbitone or in tissues obtained from these animals. The animals were euthanized by an overdose of pentobarbitone at the end of experiments.

*Chemoreception*, Edited by Pequignot et al.
Kluwer Academic/Plenum Publishers, New York, 2003

## 2. PREPARATIONS SUPERFUSED *IN VITRO*

Figure 1 shows the changes in $f_x$ obtained from the carotid nerve of CBs superfused *in vitro*. Injections of ACh into the superfusate of these preparations provoked reproducible increases in $f_x$. The left panel illustrates how the chemosensory excitation induced by ACh became very pronounced when eserine (cholinesterase inhibitor) had been added to the superfusing solution, and the disappearance of this potentiating effect after washing with eserine-free saline. The right panel shows the increases in $f_x$ evoked by two doses of ACh, their partial block during superfusion with mecamylamine and their recovery after washing this cholinergic antagonist. These observations indicate that the CB disposes of the enzymatic system for ACh destruction and that the receptors involved in ACh action are of the nicotinic type (nAChR). A full analysis of displacements of dose-response curves for ACh in the presence of anticholinesterases and cholinergic blockers has been presented by Eyzaguirre and Zapata (1968b). It must be noted that $f_x$ initially increased by the sole addition of eserine to the superfusate (Eyzaguirre & Zapata, 1968a).

*In vitro* superfusion of the petrosal ganglion, where the perikarya of carotid nerve chemosensory nerve fibres are located, allowed us to observe that topical applications of ACh and nicotine provoked dose-dependent increases in the frequency of antidromic discharges recorded from the carotid nerve, an action enhanced during superfusion with neostigmine (cholinesterase inhibitor) and blocked by mecamylamine (Alcayaga *et al.*, 1998). This indicates that the perikarya of carotid nerve fibres exhibit similar

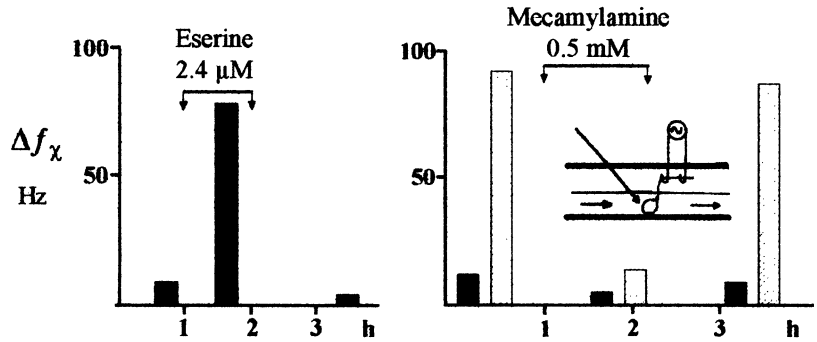


*Figure 1.* Cat's carotid bodies superfused *in vitro* with Locke's solution, equilibrated with 50% $O_2$ in $N_2$, at 35°C, flowing at 2.2 ml/min (left) and 1.2 ml/min (right). $\Delta f_x$, changes in frequency of chemosensory discharge above basal activity, in Hertz. Inset, preparation of CB bathed in flowing saline, with injections of acetylcholine chloride 100 µg (black bars) and 500 µg (hatched bars) given upstream and carotid nerve lifted into paraffin oil for recording.

responses to cholinergic agents than those of their nerve endings apposed to the glomus cells in the CB.

In a recent study, petrosal ganglion neurons from adult cats were dissociated and cultured for 7-12 days, after which intracellular recordings revealed that 67.4% of the neurons respond to ACh applications with action potentials or subthreshold depolarizations (Varas *et al.*, 2000). Since 387 petrosal ganglion neurons had been labelled by application of horse-radish peroxidase to the cut carotid nerve (Berger, 1980) and one of us had counted 2,296 sensory perikarya in this ganglion (cited in Eyzaguirre & Zapata, 1984), we can calculate that nearly 17% of the sensory neurons of the petrosal ganglion project to the carotid sinus and CB. Assuming that half of these neurons provide sensory innervation to the CB, there is a discrepancy between this percentage (8.5%) and the percentage of neurons responsive to ACh (67%). To solve this problem, another approach is necessary.

## 3. PREPARATIONS *IN SITU*

We also performed experiments in pentobarbitone-anaesthetized cats, in which the trachea was cannulated *per os* with a flexible tube connected to a Fleisch pneumotachograph #00 and volumetric pressure transducer to record ventilatory flow, which was integrated for reading tidal volume ($V_T$), and derived to a tachograph to record instantaneous respiratory frequency ($f_R$).

Application of nicotine to the surface of the CB evoked transient hyperventilation of the animal, which disappeared after section of the ipsilateral carotid nerve, demonstrating that it is due to reflex hyperventilation originated from excitation of CB sensory nerve endings (Fernández *et al.*, 2002). This is illustrated in Figure 2. However, application of ACh to the desheated stump of the central end of the carotid nerve does not result in reflex hyperventilation.

Furthermore, after surgical exposure of petrosal ganglion (by trepanation of the tympanic bulla, opening of the jugular foramen and decapsulation of the ganglion), direct application of nicotine to the ganglion does not result in reflex hyperventilation. But ventilation is transiently enhanced by applying KCl to the exposed petrosal ganglion (Figure 2).

In another series of experiments, in which the petrosal ganglion was carefully exposed without damaging its peripheral connections, we recorded the electrical activity from the carotid nerve. Here again, topical application of nicotine and ACh to the petrosal ganglion did not elicit antidromic action potentials in the carotid nerve, while this was obtained when applying KCl to the exposed surface of the ganglion (unpublished observations).

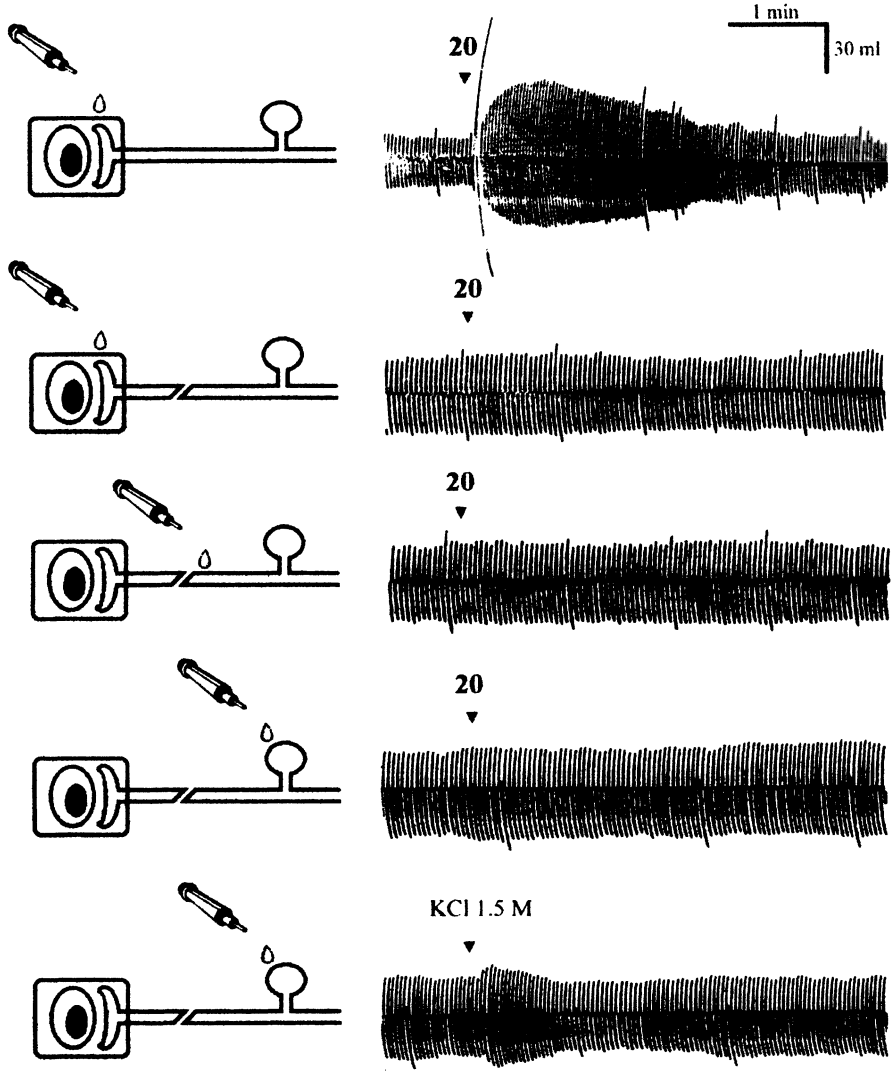


*Figure 2.* Polygraphic recordings of tidal volume (inspirations upward) in anaesthetized cats. Nicotine tartrate 20 μg applied to surface of carotid body before (1st recording) and after section of carotid nerve (2nd), to central stump of cut carotid nerve (3rd) and to exposed surface of petrosal ganglion (4th). For comparison, 10 μl of KCl 1.5 M applied to ganglion (5th).

The two series of experiments referred to above indicate that the perikarya of petrosal ganglion neurons *in situ* are not responsive to topical application of nicotinic cholinergic agonists.

We have also given nicotine injections intracarotidally, through a cannula inserted retrogradely into the superior thyroid artery. With the ipsilateral

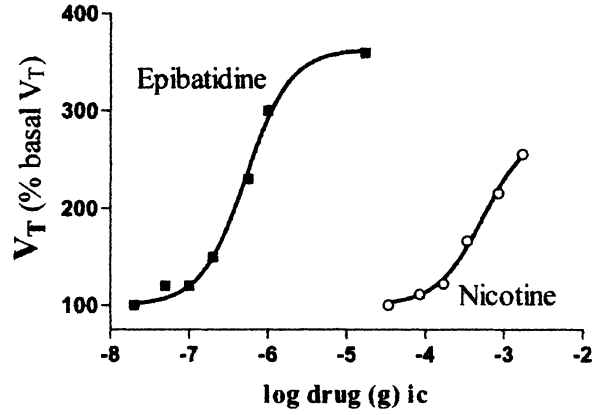


*Figure 3.* Reflex changes in tidal volume elicited by intracarotid injections of epibatidine tartrate and nicotine tartrate in one anaesthetized cat.

carotid nerve intact, this results in transient increases in $V_T$ that are dose-dependent, as illustrated in Figure 3. We also gave epibatidine, a selective agonist for neuronal nAChRs (NnAChRs). Intracarotid injections of epibatidine also result in increases in $V_T$, which are also dose-dependent. As shown in the figure, the sensitivity to epibatidine is nearly three orders of magnitude larger than that to nicotine. Larger doses of ACh were required to induce hyperventilation, but this may be due to its rapid destruction by cholinesterases. Anyhow, the transient hyperventilation elicited by these nicotinic cholinergic agonist is abolished after cutting the ipsilateral carotid nerve, thus demonstrating its reflex nature and origin from the CB.

For a comparison between the effectiveness of epibatidine and nicotine, we have also recorded the impulse activity from the peripheral section of the carotid nerve. Figure 4 shows the increase in $f_x$ provoked by an intracarotid injection of nicotine. Applying to the same preparation a nearly three orders of magnitude lower dose of epibatidine resulted in a more pronounced and prolonged increase in chemosensory activity.

Figure 5 illustrates an experiment in which one carotid nerve has been cut to record the electrical activity from its peripheral end, and the contralateral carotid nerve has been left intact as an input to medullary respiratory centres. It may be observed that increasing doses of nicotine given systemically (i.v.) provoked dose-dependent and temporally correlated increases in $f_x$ in one carotid nerve and in $V_T$, presumably contributed by the other carotid nerve. The brief apnoeas preceding the hyperventilation elicited by the larger doses of nicotine will be commented below.

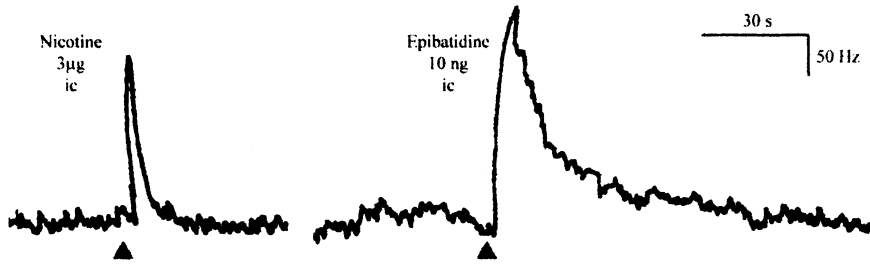


*Figure 4.* Polygraphic display (curvilinear tracings) of changes in frequency of chemosensory discharges ($\Delta f_x$) recorded from one carotid nerve in response to intracarotid injections of nicotine tartrate and epibatidine tartrate in one anaesthetized cat.

A recent paper from our laboratory (Fernández *et al.*, 2002) has been concerned with the ventilatory effects observed in the animal *in toto* in response to i.v. injections of nicotine. Transient hyperventilation is evoked by the lower doses of nicotine, increasing in magnitude dose-dependently, but interrupted by initial apnoeas when higher doses were given.

Hyperventilation along the full series of nicotine doses was the only effect observed after bilateral section of the vagus nerves, but was entirely reversed after bilateral section of the carotid and aortic nerves. On the contrary, only depressed ventilation was observed in animals in which the carotid and aortic nerves were initially cut, disappearing after the subsequent section of the vagus nerves. Thus, the enhanced ventilation produced by nicotine injections is derived from stimulation of carotid and aortic bodies, while the depressed ventilation originates from stimulation of vagal lung afferents.

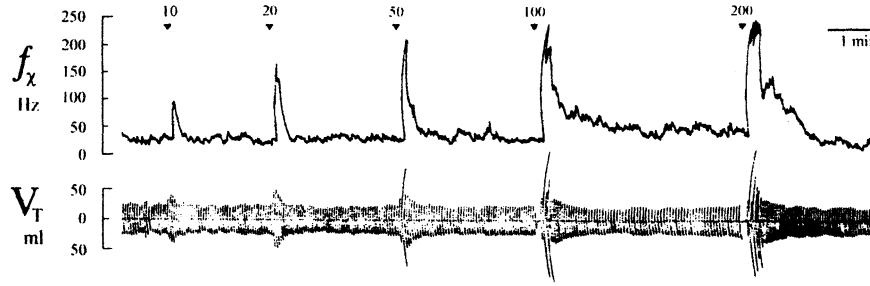


*Figure 5.* Simultaneous polygraphic recordings of frequency of carotid chemosensory discharges ($f_x$) and tidal volume ($V_T$) in one anaesthetized cat. Increasing doses (in μg/kg body weight) of nicotine tartrate given intravenously.

When considering the full series of observations on cholinergic actions on the chemoreceptive system here reported, it may be concluded that, in spite of the presence of NnAChRs in the perikarya of chemosensory neurons, the systemic application of nicotinic cholinergic agents only induces effects from the stimulation of those NnAChRs located in their peripheral endings.

## ACKNOWLEDGEMENTS

Work supported by grant 1010951 from FONDECYT. R Fernández and E-P Reyes are PhD Candidates with fellowships from CONICYT and DIPUC, respectively.

## REFERENCES

Alcayaga, J., Iturriaga, R., Varas, R., Arroyo, J., Zapata, P., 1998, Selective activation of carotid nerve fibers by acetylcholine applied to the cat petrosal ganglion *in vitro*. Brain Res. 786: 47-54

Berger, A.J., 1980, The distribution of the cat's carotid nerve afferent and efferent cell bodies using the horseradish peroxidase technique. Brain Res. 190: 309-320

Eyzaguirre, C., Zapata, P., 1968a, Pharmacology of pH effects on carotid body chemoreceptors *in vitro*. J. Physiol., Lond. 195: 557-588

Eyzaguirre, C., Zapata, P., 1968b, The release of acetylcholine from carotid body tissues. Further study on the effects of acetylcholine and cholinergic blocking agents on the chemosensory discharge. J. Physiol., Lond. 195: 589-607

Eyzaguirre, C., Zapata, P., 1984, Perspectives in carotid body research. J. Appl. Physiol., 57: 931-957

Fernández, R., Larraín, C., Zapata, P., 2002, Acute ventilatory and circulatory reactions evoked by nicotine: are they excitatory or depressant? Respir. Physiol. Neurobiol. 133: 173-182

Varas, R., Alcayaga, J., Zapata, P., 2000, Acetylcholine sensitivity in sensory neurons dissociated from the cat petrosal ganglion. Brain Res. 662: 201-205

Von Euler U.S., Liljestrand, G., Zotterman, Y., 1941, Über den Reizmechanismus der Chemorezeptoren im Glomus Caroticum. Acta Physiol. Scand. 1: 383-385

Zapata, P., 1997a, Chemosensory activity in the carotid nerve: Effects of physiological variables. In: *The Carotid Body Chemoreceptors* (C. González, ed.). Springer-Verlag, Berlin, pp 97-117

Zapata, P., 1997b, Chemosensory activity in the carotid nerve: Effects of pharmacological agents. In: *The Carotid Body Chemoreceptors* (C. González, ed.), Springer-Verlag, Berlin, pp. 119-146

# Nicotinic Acetylcholine Receptor Channels in Cat Chemoreceptor Cells

TOMOKO HIGASHI[1], SHIGEKI YAMAGUCHI[1], J. MICHAEL MCINTOSH[2], and MACHIKO SHIRAHATA[1]

*[1]Department of Environmental Health Sciences, Johns Hopkins Bloomberg School of Public Health, Baltimore, USA; [2]Department of Biology and Psychiatry, University of Utah, Salt Lake City, USA*

## 1. INTRODUCTION

Neurotransmitters are likely to play a key role for hypoxic chemotransmission in the carotid body. Among several neurotransmitters, ACh appears to be a major excitatory neurotransmitter in the cat carotid body (Fitzgerald, 2000). ACh may act directly on the afferent nerve endings and generates action potentials (Hayashida et al., 1980; Zhong & Nurse, 1997). Alternatively, ACh may work through nicotinic ACh receptors (nAChRs) in the carotid body chemosensory cells, glomus cells, and modulate the release of neurotransmitters (Fidone et al., 1990). Our recent data have shown the presence of α3, α4, β2 and β4, but not α7, subunits of nAChRs in the cat glomus cells (Hirasawa et al., in this book; Shirahata et al., 1998). Nicotinic AChRs belong to ligand-gated ion channels, that are composed of five receptor subunits. Their subunit compositions categorize nAChRs into three receptor types: (1) muscle type nAChRs, (2) heteromeric type neuronal nAChRs that consist of α subunits (α2-6) and β subunits (β2-4), and (3) homomeric type neuronal nAChRs that consist of only α subunits (α7-9). Their stoichiometry and their electrophysiological characteristics depend on the subunit compositions

*Chemoreception*, Edited by Pequignot et al.
Kluwer Academic/Plenum Publishers, New York, 2003

(McGehee & Role, 1995; Lindstrom et al., 1996). Since neuronal nAChR channels are permeable to $Ca^{2+}$ and $Na^{+}$ ions, their activation could significantly influence the excitability and function of glomus cells. In this study we examined electrophysiological and pharmacological characteristics of nAChRs in glomus cells and infer their role in the excitability of glomus cells.

## 2. CHARACTERISTICS OF NICOTINIC ACH RECEPTORS IN CAT GLOMUS CELLS

Patch clamp experiments were performed in cultured cat glomus cells. During experiments cells were continuously superfused with Krebs solution equilibrated with 5% $CO_2$/air. All experiments were performed at 37 °C. Cholinergic agents were applied via a puff pipette which was closely located to a patched cell. An application of ACh elicited relatively slowly activated and slowly inactivated inward current. A small but recognizable current was observed with 1 pM of ACh. The EC50 of ACh for the inward current (estimated by SigmaPlot) was 9 nM, and EC95 was 132 μM. We also tested several doses of nicotine (1-100 μM), and found that nicotine induces similar current to ACh in cat glomus cells.

To test Voltage-dependency of ACh-induced current, ACh (1 μM) was applied for 2 seconds to the patched cell at different holding potentials. We found that current voltage relationship had strong inward rectification with little apparent macroscopic current at the membrane potentials of –20 mV or less (Fig. 1)

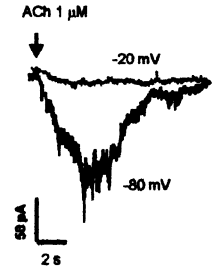


***Figure 1.*** Voltage-dependency of nAChR-mediated inward current. Conventional patch clamp techniques with a whole cell configuration were applied. The composition of bath solution is (in mM): NaCl 118, KCl 4.7, $MgSO_4 \cdot 7H_2O$ 1.2, $KH_2PO_4$ 1.2, $CaCl_2$ 1.8, $NaHCO_3$ 25, and glucose 11.1, pH 7.4 with 5%$CO_2$/air. The composition of the internal solution is (in mM): CsF 40, CsCl 50, NaCl 10, $CaCl_2$ 1, HEPES 10, EGTA 10, MgATP 5 pH 7.2 with CsOH. The currents were recorded from the same cell. Membrane potential was held at –80 or –20 mV and ACh (1 μM) was applied via a puff pipette for 2 seconds.

Pharmacological properties of nAChRs in cultured cat glomus cell were studied using competitive antagonists for nAChRs. Alpha-conotoxin MII is a specific antagonist for α3β2 nAChRs (Cartier *et al.*, 1996) and α6-containing nAChRs (Kuryatov *et al.*, 2000). 20 nM of α-conotoxin MII, which was included in Krebs for 4-5 min before the application of ACh, significantly inhibited the ACh-induced currents to 39 % of control (n= 6). 100 nM of α-conotoxin MII further decreased ACh-induced current to 9 % of control (n=2). DHβE is known to inhibit several types of nAChRs and low IC50 values were seen for α3β2, α4β2, and α4β4 nAChRs (Harvey et al., 1996; Chavez-Noriega *et al.*, 1997). ACh-induced inward currents in cultured cat glomus cells were sensitive to DHβE, and statistically significant inhibition was observed at 1 nM DHβE (37 % of control, n=6). 10 nM of DHβE almost completely inhibited current (n=1). Hexamethonium (300 μM), a nonspecific antagonist for neuronal nAChRs, significantly reduced ACh-induced inward currents in cultured cat glomus cells to 9 % of control (n=5).

## 3. EFFECTS OF NICOTINIC ACH RECEPTOR ACTIVATION ON GLOMUS CELL FUNCTION

Activation of nAChR causes influx of cations (Albuquerque et al., 1995; McGehee & Role, 1995). In cat glomus cells two major functional changes occurred. First, nicotinic agonists applied to resting glomus cells during normoxia depolarized the cells. ACh (1 mM) or nicotine (100 μM) were applied to 4 glomus cells, and their membrane potentials changed from -47 ±7 to -19±9 mV (mean±SEM; after crrection of junctional potential). Second, intracellular $Ca^{2+}$ ($[Ca^{2+}]i$) increased significantly by ACh (Figure 2A), as seen in our previous study (Shirahata et al., 1997). An application of DHβE (10 nM) significantly attenuated ACh-induced $[Ca^{2+}]i$ increase. Hexamethonium (300 μM) also significantly reduced ACh-induced $[Ca^{2+}]i$ increase.

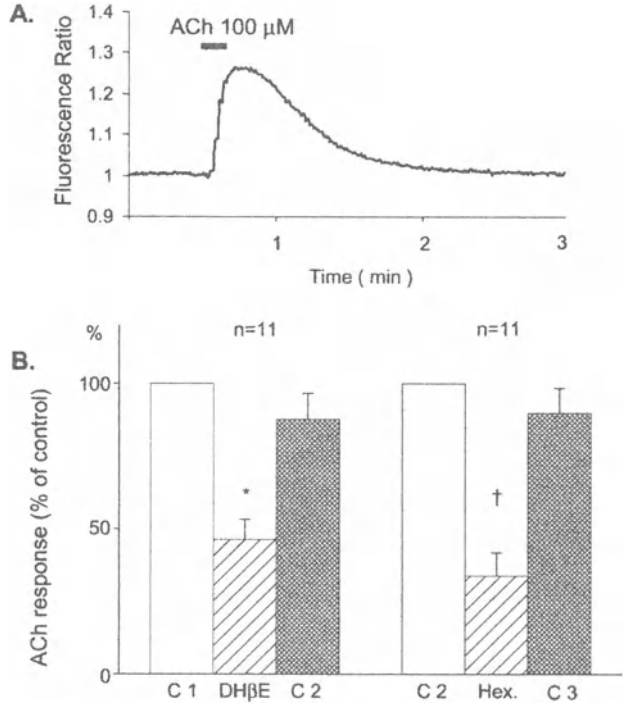


*Figure 2.* **A.** ACh (100 μM) increased intracellular $Ca^{2+}$ in cultured glomus cells. Intracellular $Ca^{2+}$ of clusterd cells was estimated from the ratio of two fluorescence emmision signals using Indo-1 (Shirahata et al, 1997). Cells were continually superfused with Krebs solution and ACh was applied via a puff pipette for 15 seconds. **B.** ACh-induced increase in intracellular $Ca^{2+}$ was partially inhibited by DHβE (10 nM). Hexamethonium (300 μM) also inhibited $Ca^{2+}$ response to ACh in cultured cat glomus cells. The fluorescence ratio of control 2 was smaller than control 1 due to photo bleaching. The same was true with the fluorescence ratio between control 2 and 3. Data are reported as mean ± SEM. (n=11). *, significantly different from control 1 & 2; †, significantly different form control 2 & 3. The response with DHβE and that with hexamethonium were not statistically different.

## 4. DISCUSSION

Electrophysiological experiments revealed features of nAChRs in cultured cat glomus cells, which, in some degree, resemble those of rat glomus cells (Wyatt & Peers, 1993). Our pharmacological experiments using α-conotoxin MII, DHβE, and hexamethonium further characterized these receptors. The data indicate that ACh-induced current in cat glomus cells is most likely via neuronal nAChRs which contain α3, α4 and β2 subunits. However, extremely high affinity of nAChRs for ACh suggests that other subunits may be also involved.

These characteristics of nAChRs in cat glomus cells together with high affinity for ACh seems to be important for glomus cell function. Because of the high affinity of nAChRs in glomus cells for ACh, even a small increase in ACh during hypoxia could strongly influence the function of glomus cells. During hypoxia, two major changes could happen in glomus cells by activation of nAChRs: depolarization and increase in $[Ca^{2+}]i$. In this study we reported that ACh depolarized glomus cells. Depolarization of glomus cells would activate voltage-gated $Ca^{2+}$ channels and increase $[Ca^{2+}]i$. An increase in $[Ca^{2+}]i$ would also occur via nAChRs. $[Ca^{2+}]i$ measurement in this study, in addition to previous reports ( Dasso et al., 1997; Shirahata et al., 1997), confirmed that activation of nAChRs in glomus cells increased $[Ca^{2+}]i$. An increase in $[Ca^{2+}]i$ would promote the release of ACh and other neurotransmitters. Thus, it appears that interaction of ACh and nAChRs in glomus cells consists a positive feedback loop. However, the system seems to be self-controlled. Due to a strong rectification of ACh-induced current, influx of cations ($Na^+$ and $Ca^{2+}$) via nAChRs differ with the membrane potential of glomus cells. Once glomus cells are depolarized, the influx of cations would become smaller and at positive membrane potential few cations would move via nAChRs. Therefore, it is likely that activation of nAChRs plays an important role in excitation of glomus cells at the early stage of hypoxia.

## ACKNOWLEDGEMENTS

The authors are grateful to Drs. James SK Sham, Itaru Watanabe, and Tomio Andoh for their suggestions and technical support. This work was supprted by HL61596 and MH53631.

## REFERENCES

Albuquerque E.X., Pereira E.F., Castro N.G., Alkondon M., Reinhardt S., Schroder H., and Maelicke A. (1995) Nicotinic receptor function in the mammalian central nervous system. *Ann N Y Acad Sci* 757, 48-72.

Cartier G.E., Yoshikami D., Gray W.R., Luo S., Olivera B.M., and McIntosh J.M. (1996) A new alpha-conotoxin which targets alpha3beta2 nicotinic acetylcholine receptors. *J Biol Chem* 271, 7522-7528.

Chavez-Noriega L.E., Crona J.H., Washburn M.S., Urrutia A., Elliott K.J., and Johnson E.C. (1997) Pharmacological characterization of recombinant human neuronal nicotinic acetylcholine receptors h alpha 2 beta 2, h alpha 2 beta 4, h alpha 3 beta 2, h alpha 3 beta 4, h alpha 4 beta 2, h alpha 4 beta 4 and h alpha 7 expressed in Xenopus oocytes. *J Pharmacol Exp Ther.* 280, 346-356.

Dasso L.L.T., Buckler K.J., and Vaughan-Jones R.D. (1997) Muscarinic and nicotinic receptors raise intracellular $Ca^{2+}$ levels in rat carotid body type I cells. *J Physiol (Lond)* 498, 327-338.

Fidone S.J., Gonzalez C., Obeso A., Gomez-Nino A., and Dinger B. (1990) Biogenic amine and neuropeptide transmitters in carotid body chemotransmission: experimental findings and perspectives. In Hypoxia: The adaptaions (ed. Sutton J.R., Coates G., and Remmers J.E.), pp. 116-126. B.C.Deker, Inc., Tronto.

Fitzgerald R.S. (2000) Oxygen and carotid body chemotransduction: the cholinergic hypothesis - a brief history and new evaluation. *Respir Physiol* 120, 89-104.

Harvey S.C., Maddox F.N., and Luetje C.W. (1996) Multiple determinants of dihydro-beta-erythroidine sensitivity on rat neuronal nicotinic receptor alpha subunits. *J Neurochem.* 67, 1953-1959

Hayashida Y., Koyano H., and Eyzaguirre C. (1980) An intracellular study of chemosensory fibers and endings. *J Neurophysiol* 44, 1077-1088.

Hirasawa, S., Mendoza, J.A., Jacoby ,D.B., Kobayashi, C, Fitzgerald, R.S., Schofield, B., Chandrasagaran, S., and Shirahata, M. (2003) Divers cholinergic receptors in the cat chemosensory unit. *Adv. Exp. Med. Biol.*

Kuryatov A., Olale F., Cooper J., Choi C., and Lindstrom J. (2000) Human alpha6 AChR subtypes: subunit composition, assembly, and pharmacological responses. *Neuropharmacology* 39, 2570-2590.

Lindstrom J., Anand R., Gerzanich V., Peng X., Wang F., and Wells G. (1996) Structure and function of neuronal nicotinic acetylcholine receptors. *Prog Brain Res* 109, 125-137.

McGehee D.S. and Role L.W. (1995) Physiological diversity of nicotinic acetylcholine receptors expressed by vertebrate neurons. *Annu Rev Physiol* 57, 521-546.

Shirahata M., Fitzgerald R.S., and Sham J.S.K. (1997) Acetylcholine increases intracellular calcium of arterial chemoreceptor cells of adult cats. *J Neurophysiol* 78, 2388-2395.

Shirahata M., Ishizawa Y., Rudisill M., Schofield B., and Fitzgerald R.S. (1998) Presence of nicotinic acetylcholine receptors in cat carotid body afferent system. *Brain Res* 814, 213-217.

Wyatt C.N. and Peers C. (1993) Nicotinic acetylcholine receptors in isolated type I cells of the neonatal rat carotid body. *Neuroscience* 54, 275-281.

Zhong H. and Nurse C.A. (1997) Nicotinic acetylcholine sensitivity of rat petrosal sensory neurons in dissociated cell culture. *Brain Res* 766, 153-161.

# Hypoxia Does Not Uniformly Facilitate the Release of Multiple Transmitters from the Carotid Body

DONG-KYU KIM, BETH A. SUMMERS, NANDURI R. PRABHAKAR, AND GANESH K. KUMAR*
*School of Medicine, Case Western Reserve University, Cleveland, OH, USA.*

## 1 INTRODUCTION

Studies from diverse species have established that type I cell, the putative oxygen sensing element of the carotid body (CB), expresses a variety of conventional neurotransmitters like acetylcholine (ACh), dopamine (DA), and neuropeptides and unconventional neurotransmitters like NO and CO [for recent reviews see, (Prabhakar 2000; Kumar and Prabhakar 2002)]. An essential step in the initiation of the sensory response of the CB to hypoxia involves the release of one or more of neurotransmitters from type I cells onto apposed sensory nerve endings (Prabhakar 2000). From direct measurement of neurotransmitter release, it has been shown that hypoxia facilitates the release of both DA (Fidone *et al.* 1982; Bairam *et al.* 1996; Chen *et al.* 2000), and substance P (Kim *et al.* 2001) in the rabbit CB. On the other hand, hypoxia facilitates ACh release in the cat CB (Fitzgerald *et al.* 1999). However, it has not yet been determined by simultaneous monitoring of several transmitters whether hypoxia in a given species evokes the release of multiple or only a subset of transmitters in the CB.

*Chemoreception*, Edited by Pequignot et al.
Kluwer Academic/Plenum Publishers, New York, 2003

In this report, we examined whether hypoxia induces the release of both ACh and DA in the rabbit CB in a coordinated manner. ACh and DA release in response to hypoxia were simultaneously monitored using sensitive methods involving HPLC combined with immobilized enzyme reactor column (IMER) and electrochemical detection (ECD).

# 2 MATERIALS AND METHODS

## 2.1 Isolation of carotid bodies

Animal experimental protocols were approved by the Case Western Reserve University Institutional Animal Care and Use Committee and are in agreement with the National Institutes of Health guide for the care and use of laboratory animals. Adult male New Zealand White rabbits (weighing 2.0-2.5 kg) were purchased from Charles River Laboratories (Wilmington, MA, USA). Animals were anaesthetized and the bifurcations at the common carotid arteries were rapidly excised. CBs were placed in ice-cold, oxygenated, $Ca^{2+}/Mg^{2+}$ free, modified Krebs-Ringer bicarbonate (KRB) solution containing 1mM isoOMPA (an inhibitor of non-specific cholinesterase) and 300 μM neostigmine (an inhibitor of acetylcholinesterase) until further analysis of neurotransmitter release.

## 2.2 Determination of ACh and DA

ACh was measured using HPLC coupled with an IMER column containing acetylcholinesterase and choline oxidase. ACh was separated from choline (Ch) by reverse phase microbore column and converted enzymatically to Ch and then to $H_2O_2$ by the sequential actions of enzymes immobilized in the IMER column. The amount of $H_2O_2$ formed in the IMER column serves as measure of ACh and was determined using an ECD and peroxidase-coated glassy carbon electrode with an oxidation potential of 100 mV versus Ag/AgCl. ACh was separated by isocratic elution with a mobile phase containing 30 mM $NaH_2PO_4$, pH 8.5 and bactericide, Kathon (5ml/L) at a flow rate of 130 μl/min. The elution profiles were recorded and analyzed using a Hitachi D-2500 Chromato-Integrator. ACh and Ch were eluted at ~13 and ~18 min, respectively with a detection limit of 80 femtomoles each.

Dopamine was separated on a Prodigy C-18 reverse-phase column by isocratic elution with a mobile phase consisting of 7 % (V/V) methanol, 0.1 M sodium acetate, 0.0125 M sodium citrate, 0.1 mM disodium EDTA and

0.215 mM sodium octyl sulfate, at pH 4.5. DA was eluted at ~9 min with a detection limit of 250 femtomoles.

The concentrations of ACh and DA were derived from a standard curve correlating their concentrations to the corresponding integrated peak size and/or current. The release of ACh and DA in the medium was expressed as femtomoles per min per CB.

## 2.3 Measurement of content of neurotransmitters and metabolites

For the determination of tissue contents of ACh, Ch, and DA, CBs were sonicated in 300 µl of medium containing 0.1 N $HClO_4$ and 0.25 mM disodium EDTA 3 times for 30 sec at 4°C. The homogenates were centrifuged at 12,000 x g for 15 min at 4°C and the clear supernatant was analyzed by HPLC-ECD as described above. For ACh analysis, 2 parts of the samples were first neutralized with 1 part of 0.1 N $Na_3PO_4$, pH 10.0 and then subjected to HPLC-ECD analysis.

## 2.4 Release studies with isolated carotid bodies

In each experiment, freshly isolated CBs from two rabbits were pre-incubated in oxygenated (95% $O_2$ + 5% $CO_2$) KRB medium containing the following (in mM: NaCl, 135; KCl, 5; $CaCl_2$, 1.8; $MgCl_2$, 1; Glucose, 11 and $NaHCO_3$, 22, pH 7.4) and 30 µM neostigmine for up to 60 min to stabilize the basal release of neurotransmitters.

In experiments assessing the effect of hypoxia on the release of ACh and DA, CBs were incubated sequentially in medium equilibrated with the following gas mixtures for the duration indicated: hyperoxia (95% $O_2$ + 5% $CO_2$, ~690mmHg) for 30 min (*basal*), hypoxia (1% $O_2$ + 5% $CO_2$ in $N_2$, ~11mmHg) for 30 min (*stimulus*), and hyperoxia for 30 min (*recovery to basal level*) with constant mixing.

During incubation, the medium was constantly mixed using a gentle stream of corresponding gas mixture. The $pO_2$, $pCO_2$ and pH of the medium were measured using a blood gas analyzer (Radiometer ABL 5, Copenhagen). The medium was immediately collected at the end of each gas challenges and aliquots (20 µl) of the medium were analyzed for the concentration of ACh and DA using HPLC-ECD methods as described above.

## 2.5 Data analysis

All values were presented as means ± SEM. Statistical significance was evaluated by a paired t-test or one-way ANOVA for repeated measures. $p$ values < 0.05 were considered significant.

# 3 RESULTS

## 3.1 Effects of hypoxia on ACh and DA release

The tissue concentration of ACh in the rabbit CB was 5.6 ± 1.3 picomoles per CB and was similar to the level reported in cat CB (Fidone *et al.* 1976). The basal release of ACh, during hyperoxia, was 5.88 ± 0.51 femtomoles/min/CB and hypoxia inhibited ACh release by 68% ($p<0.01$; n = 4). Upon re-oxygenation, ACh release promptly returned to near basal level suggesting that the observed inhibition is not due to slow deterioration of the tissue.

The tissue content of DA was 66.7 ± 3.1 pmoles per CB. The basal release of DA, during normoxia, was 67.4 ± 8.4 femtomoles/min/CB. In sharp contrast to ACh, there was a 6-fold increase in DA release by hypoxia compared to the basal, hyperoxic release ($p<0.01$; n = 4), consistent with findings reported previously in this species (Fidone *et al.* 1982; Bairam *et al.* 1996). The above results suggest that hypoxia inhibits ACh release whereas it augments DA release in rabbit CB.

# 4 DISCUSSION

In this investigation, we have monitored the release of ACh as well as DA from rabbit CB in response to a given hypoxic stimulus and showed that hypoxia facilitates DA but not ACh release from the CB. Our finding that hypoxia inhibits ACh release from the rabbit CB is in contrast to the previous report in cats wherein hypoxia facilitated ACh release (Fitzgerald *et al.* 1999). It is likely that the effect of hypoxia on ACh release from CB is species-dependent. Support for such a notion stems from the observations that ACh inhibited carotid body activity in rabbits whereas it increased the sensory discharge in the cat CB (Monti-Bloch and Eyzaguirre 1980). Nonetheless, our results are consistent with the hypoxia-induced gradual decline in ACh release from the myenteric plexus of guinea pig ileum (Larson and Martins 1981) and the inhibition of ACh release by hypoxia in

the whole brain and synaptosomal preparations (Gibson and Peterson 1982; Sanchez-Prieto *et al.* 1987; Chleide and Ishikawa 1990).

How does hypoxia facilitate the release of DA but not ACh in the rabbit CB? If ACh and DA are stored in the same vesicles in type I cells of the CB, then external stimuli would be expected to facilitate the release of both transmitters coordinately. From immunoelectron microscopic analyses of PC12 cells using antibodies specific to dopaminergic and cholinergic vesicles, it has been shown that ACh and DA are stored in distinct vesicles (Liu *et al.* 1994). It seems, therefore, plausible to suggest that ACh and DA are stored in distinct vesicles in the CB as they are in PC12 cells. If this is proven to be true, then the differential release of DA over ACh by hypoxia may arise from selective mobilization of dopaminergic but not cholinergic vesicles. However, it remains to be determined whether ACh and DA in the CB are individually stored in small synaptic-like vesicles and large-dense core vesicles, respectively.

## CONCLUSION

In summary, our finding that hypoxia inhibits ACh release from the rabbit CB suggest that ACh may not contribute to the *initiation* of the sensory response to hypoxia but may involve in the *modulation* of the hypoxic response of the rabbit CB.

## ACKNOWLEDGEMENTS

This study was supported by the National Heart, Lung, and Blood Institute grants HL-46462 and HL-25830.

## REFERENCES

Bairam A., Basson H., Marchal F., Cottet-Emard J. M., Pequignot J. M., Hascoet J. M. and Lahiri S. (1996) Effects of hypoxia on carotid body dopamine content and release in developing rabbits. J. Appl. Physiol. 80, 20-24.

Chen J., He L., Dinger B. and Fidone S. (2000) Stimulus-specific signaling pathways in rabbit carotid body chemoreceptors. Neuroscience 95, 283-291.

Chleide E. and Ishikawa K. (1990) Hypoxia-induced decrease of brain acetylcholine release detected by microdialysis. Neuroreport 1, 197-199.

Fidone S., Gonzalez C. and Yoshizaki K. (1982) Effects of low oxygen on the release of dopamine from the rabbit carotid body in vitro. J. Physiol. 333, 93-110.

Fidone S. J., Weintraub S. T. and Stavinoha W. B. (1976) Acetylcholine content of normal and denervated cat carotid bodies measured by pyrolysis gas chromatography/mass fragmentometry. J. Neurochem. 26, 1047-1049.

Fitzgerald R. S., Shirahata M. and Wang H. Y. (1999) Acetylcholine release from cat carotid bodies. Brain Res. 841, 53-61.

Gibson G. E. and Peterson C. (1982) Decreases in the release of acetylcholine in vitro with low oxygen. Bio.Chem. Pharmacol. 31, 111-115.

Kim D. K., Oh E. K., Summers B. A., Prabhakar N. R. and Kumar G. K. (2001) Release of substance P by low oxygen in the rabbit carotid body: evidence for the involvement of calcium channels. Brain Res. 892, 359-369.

Kumar G. K. and Prabhakar N. R. (2002) Multiple roles of neurotransmitters in the carotid body: involvement in sensory transmission and adaptation to hypoxia, in Oxygen Sensing: Responses and Adaptation to Hypoxia (Lahiri S., Prabharkar, N.R., and Semenza, G., ed.). Marcel Dekker, New York., in press.

Larson R. E. and Martins H. R. (1981) Early effect of glucose and oxygen deprivation on the spontaneous acetylcholine release from the myenteric plexus of the guinea pig ileum. Can. J. Physiol. Pharmacol. 59, 555-561.

Liu Y., Schweitzer E. S., Nirenberg M. J., Pickel V. M., Evans C. J. and Edwards R. H. (1994) Preferential localization of a vesicular monoamine transporter to dense core vesicles in PC12 cells. J. Cell. Biol. 127, 1419-1433.

Monti-Bloch L. and Eyzaguirre C. (1980) A comparative physiological and pharmacological study of cat and rabbit carotid body chemoreceptors. Brain Res. 193, 449-470.

Prabhakar N. R. (2000) Oxygen sensing by the carotid body chemoreceptors. J. Appl. Physiol. 88, 2287-2295.

Sanchez-Prieto J., Harvey S. A. and Clark J. B. (1987) Effects of in vitro anoxia and low pH on acetylcholine release by rat brain synaptosomes. J. Neurochem. 48, 1278-1284.

# Expression and Function of Presynaptic Neurotransmitter Receptors in the Chemoafferent Pathway of the Rat Carotid Body

IAN M. FEARON, MIN ZHANG, CATHY VOLLMER and COLIN A. NURSE.
*Department of Biology, McMaster University, 1280 Main St. West, Hamilton, ON L8S 4K1, Canada.*

## 1. INTRODUCTION

Hypoxic chemotransmission in the carotid body (CB) is mediated by the release of neurotransmitters (NTs) from type I cells onto adjacent sensory (petrosal) nerve endings (Gonzalez *et al.*, 1994; Urena *et al.*, 1994). In the rat, there is strong evidence of a role for the co-release of fast-acting neurotransmitters, including acetylcholine (ACh) and ATP (Zhang *et al.*, 2000), in chemosensory signalling. In contrast, little is known about the roles of NTs in mediating autoreceptor feedback mechanisms which are thought to play a role in modulating chemoreceptor output from the CB. Here, we present evidence for the involvement of two distinct NTs, γ-aminobutyric acid (GABA) and serotonin (5-HT), in mediating autoreceptor feedback onto type I cells during hypoxia. Although their actions are directly opposite, activation of receptors for either transmitter appears to regulate the activity of $O_2$-sensitive $K^+$ channels, such as the background $K^+$ channel Kcnk3 (Buckler *et al.*, 2000). 5-HT receptor activation also regulates the activity of the $O_2$-sensitive large-conductance $Ca^{2+}$-activated $K^+$ channel (Peers, 1990). These results demonstrate the roles of NTs in regulating secretion from type I cells, by converging signals from different sources onto the same $K^+$ channels involved in $O_2$ sensing and control of the receptor potential.

*Chemoreception*, Edited by Pequignot et al.
Kluwer Academic/Plenum Publishers, New York, 2003

# 2. MATERIALS AND METHODS

## 2.1. Cell culture

Preparation of co-cultures, or separate cultures of dissociated type I cell clusters or petrosal neurons (PNs), has been described previously (Zhong *et al.*, 1997). Cultures were grown at 37 °C in a humidified atmosphere of 95 % air:5 % $CO_2$ in F-12 nutrient medium (Gibco) supplemented with 10 % v/v foetal bovine serum (Gibco), 80 $UI^{-1}$ insulin (Sigma), 0.6 % (w/v) glucose, 2mM L-glutamine and 1 % penicillin-streptomycin (Gibco). Electrophysiological recordings were made 2-4 days after cells were plated in the case of separate cultures, and after 3-5 days in co-cultures.

## 2.2. Current-clamp recording

Procedures for recording responses from co-cultured PNs and type I cell clusters have been described elsewhere (Zhong *et al.*, 1997). Hypoxia ($Po_2$ ~5 mmHg) was generated by bubbling nitrogen into the extracellular perfusate.

## 2.3. Voltage-clamp measurement of $K^+$ and $Ca^{2+}$ currents

Culture dishes were mounted on the stage of a Zeiss Axiovert S100 microscope and perfused at the rate of 4 ml $min^{-1}$. Whole-cell patch-clamp recordings of $K^+$ (Fearon *et al.*, 2002) and $Ca^{2+}$ (Fearon *et al.*, 1997) currents were made as described previously. For perforated-patch recordings, EGTA and $Na_2ATP$ were omitted from the pipette solution and nystatin was included at a concentration of 300 μg/ml.

## 2.4. Drug solutions

Baclofen, 5-aminovaleric acid, hydroxysaclofen, H-89, PTX, anandamide and ketanserin were obtained from Sigma. Anandamide was used under license from Health Canada.

## 2.5. Immunofluorescence

Procedures for obtaining isolated CB sections have been described previously (Prasad *et al.*, 2001). Sections were incubated overnight at 4 °C in the primary antisera. Primary antibodies were: (i) guinea pig anti-rat $GABA_{B(1)}$ (1:500 dilution; Chemicon), (ii) guinea pig anti-rat $GABA_{B(2)}$ (1:500; Chemicon), and (iii) mouse anti-rat $5\text{-}HT_{2a}$ (1:16; Pharmingen). Secondary antibodies were either FITC-conjugated goat anti-guinea pig IgG (1:20 dilution; Jackson Immunoresearch Laboratories) or goat anti-mouse IgG (1:50 dilution; Cappel). Secondary antibodies were diluted in PBS containing 1 % BSA, 10 % normal goat serum and 0.3 % Triton X-100.

Samples were covered with Vectashield Mounting Medium (Vector Laboratories) before viewing under epi-fluorescence with a Zeiss IM35 or S16 microscope equipped with fluorescein and rhodamine filter sets.

# 3. RESULTS

## 3.1. $GABA_B$ receptors linked to Kcnk3 modulate hypoxic chemotransmission

When type I cells were exposed to hypoxia, membrane depolarisation due to inhibition of plasmalemmal $K^+$ channels could be seen under current-clamp (e.g. Figure 1A, *left*). In the presence of hydroxysaclofen (OHS; Figure 1A, *centre*) or 5-aminovaleric acid (5-AVA; not shown), selective inhibitors of $GABA_B$ receptors, the degree of depolarisation of the presynaptic cells was enhanced. This effect caused an increased release of NTs from the type I cells during hypoxia, since a similar effect was seen when recording the membrane potential of a postsynaptic petrosal neuron juxtaposed to a type I cluster in co-culture (Figure 1B). Enhancement of presynaptic depolarisation was mediated through a process involving activation of PKA since the effects of OHS were abolished by the selective PKA inhibitor, H-89 (50 μM). Furthermore, the effect of OHS was mediated via activation of the inhibitory G-protein, $G_i$, since its effects were abolished when cells were pre-treated for 24h in 500 ng/ml pertussis toxin (PTX).

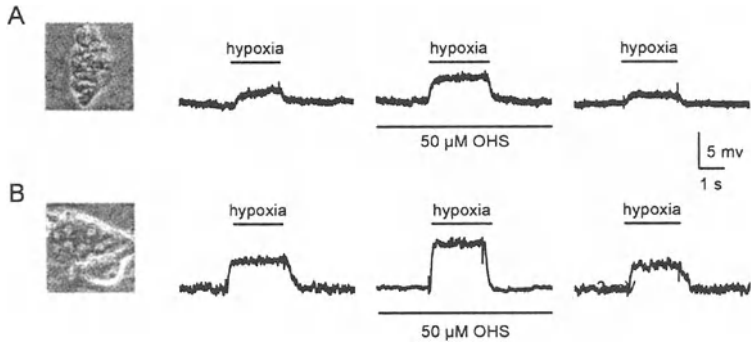


*Figure 1.* $GABA_B$ receptor blockade enhances hypoxic depolarisation in presynaptic type I cells (**A**), enhancing synaptic signalling onto postsynaptic petrosal neurons in co-culture (**B**). This effect is mediated by $G_i$-coupled activation of PKA (see text for details).

$GABA_B$ receptors regulate several types of $K^+$ conductance in the CNS (Bowery and Enna, 2000). To examine such regulation in the CB, we made voltage-clamp recordings from type I cells in isolated clusters. During

perforated patch recordings, to preserve cytoplasmic integrity, and with asymmetrical $K^+$ solutions, the $GABA_B$ receptor agonist baclofen (50 μM) enhanced outward $K^+$ current. For example, at a test potential of +30 mV, $K^+$ current amplitudes were increased by 14.0 ± 2.8 % in the presence of baclofen. The baclofen-sensitive current reversed at -78.7 ± 2.5 mV, close to the predicted $K^+$ equilibrium potential (-83 mV). Under symmetrical $K^+$ conditions, the baclofen-sensitive (difference) current was voltage-independent and reversed at –4.8 ± 1.9 mV (Figure 2A), close to the Nernst equilibrium potential for $K^+$ ions (0 mV) under these conditions. Enhancement of this background current by baclofen was abolished in the presence of 5 mM $Ba^{2+}$ (e.g. Figure 2B) and 10 μM anandamide (not shown), blockers of Kcnk3 (Buckler *et al.*, 2000; Maingret *et al.*, 2001). We propose that baclofen activates the $K^+$-selective background current Kcnk3 in type I cells.

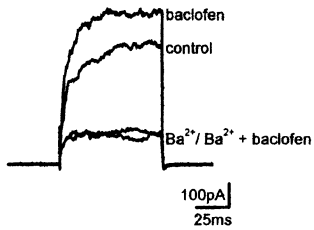


*Figure 2.* When recording from a type I cell, outward $K^+$ current amplitude (evoked by a step depolarisation to +60 mV) was enhanced by 50 μM baclofen. This effect was abolished in the presence of 5 mM $Ba^{2+}$, an inhibitor of background $K^+$ channels.

In previous studies, $GABA_B$ receptor activation caused inhibition of presynaptic neuronal voltage-gated $Ca^{2+}$ channels (Bowery & Enna, 2000). Under voltage-clamp, 50 μM baclofen was without effect on $Ca^{2+}$ currents. Mean $Ca^{2+}$ current induced by a step depolarisation to +10 mV from a holding potential of –80 mV was -38.2 ± 6.8 pA under control conditions and -41.8 ± 8.5 pA in the presence of 50 μM.

## 3.2. 5-HT and autoreceptor feedback inhibition of presynaptic hypoxic depolarisation

Previous studies have suggested a role for 5-HT in mediating and regulating CB synaptic transmission. Here, we examined the actions of 5-HT at presynaptic receptors located on isolated rat type I cells. Presynaptic depolarisation due to hypoxia was attenuated in the presence of the selective $5\text{-HT}_2$ receptor blocker, ketanserin (Figure 3). This attenuation was abolished in the presence of the specific PKC inhibitor, NPC 15437 (not shown). The magnitude of the depolarisation of postsynaptic neurons in co-culture with type I cells, which is determined by the amount of NT released, was also suppressed in the presence of ketanserin (not shown).

These data suggest that presynaptic 5-$HT_2$ receptor activation modulates the release of transmitters from type I cells via modulation of PKC.

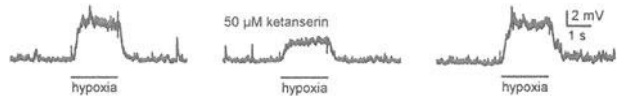


*Figure 3.* Current-clamp recordings made from a type I cell in an isolated cluster. The cell depolarised in response to hypoxia (5 mmHg, indicated), and this depolarisation was reversibly blunted in the presence of 50 μM ketanserin.

To investigate the mechanisms underlying the modulation of the presynaptic receptor potential by 5-HT, we performed voltage-clamp experiments and examined the effects of 5-HT on $K^+$ currents in type I cells. As shown in Figure 4, 5-HT (50 μM) caused a marked reduction in whole-cell $K^+$ current in these cells. Suppression was also observed in nominally $Ca^{2+}$-free solution, and the magnitude of the effects was reduced compared to that seen in the presence of extracellular $Ca^{2+}$. Since the suppression of $K^+$ current in normal $Ca^{2+}$ was similar to that caused by $Ca^{2+}$-free solution plus 5-HT in $Ca^{2+}$-free solution, we conclude that both $Ca^{2+}$-dependent and -independent $K^+$ currents are inhibited by 5-HT in type I cells.

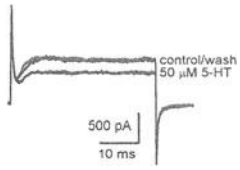


*Figure 4.* 5-HT inhibits whole-cell $K^+$ current in rat carotid body type I cells. Shown are evoked currents under control conditions, in the presence of 50 μM 5-HT, and following washout.

## 3.3 Expression of $GABA_B$ and 5-$HT_{2a}$ receptors in type I cells

The autoreceptor mechanisms described above, which we propose control NT output from type I cells, require the presence of receptors for the NTs on these cells. To test this possibility *in situ*, sections through the rat CB were immunostained using specific antibodies raised against $GABA_{B(1)}$ and $GABA_{B(2)}$ receptor subunits, and 5-$HT_{2a}$ receptors. Positive immunoreactivity was confined to regions corresponding to type I clusters (Figure 5). No staining was observed when sections were exposed to the secondary antibody without prior exposure to the primary antibody (not shown).

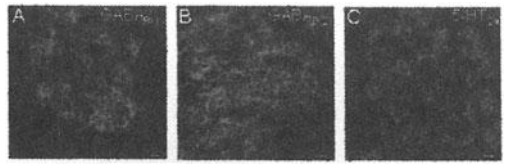


*Figure 5.* Expression of **(A)** $GABA_{B(1)}$, **(B)** $GABA_{B(2)}$ and **(C)** $5\text{-}HT_{2a}$ receptor subunits in the rat CB. Sections were immunostained using specific primary antibodies (see Methods). The pattern of staining strongly suggests these proteins are localised to clusters of type I cells.

## 4. DISCUSSION

Although not yet fully characterised, roles for several NTs in mediating synaptic signalling between presynaptic type I cells and postsynaptic PNs in the CB have been described. In contrast, less is known concerning NTs and their actions on the presynaptic type I cells in controlling release. Here, we present evidence for the involvement of two NTs, GABA and 5-HT, in regulating NT output from type I cells during hypoxia. In the case of GABA, it appears that $GABA_B$ receptor activation attenuates NT release since $GABA_B$ receptor blockers enhance synaptic transmission. The mechanism of this effect is one of receptor activation coupling to the inhibitory G-protein Gi to reduce PKA activity and regulate transmitter release. In support of this, enhancement of synaptic transmission by $GABA_B$ receptor antagonists is blocked by inhibitors of both PKA and $G_i$ function (Figure 1). The effector linked to the $GABA_B$ receptor is Kcnk3, since the effects of the $GABA_B$ receptor agonist baclofen on the voltage-independent $K^+$ current in type I cells was abolished in the presence of anandamide (Figure 2), a selective blocker of this channel (Maingret *et al.*, 2001). Since current through Kcnk3 is inhibited by stimulation of the cAMP-dependent protein kinase (Lopes *et al.*, 2000), we propose that $GABA_B$ receptor activation inhibits $G_i$, inhibiting PKA and activating Kcnk3. This gives rise to a hyperpolarisation which effectively blunts the depolarising receptor potential due to hypoxia.

In contrast to the effects of GABA, we demonstrate that 5-HT is involved in enhancing the release of transmitters from type I cells during hypoxia, in a mechanism involving presynaptic $5\text{-}HT_2$ receptors and activation of PKC. Although the effector through which the presynaptic effects of 5-HT are mediated is not fully elucidated, we can conclude that it is regulating both $Ca^{2+}$-dependent and –independent $K^+$ channels. Given the knowledge of $K^+$ channels involved in rat type I cell function, it is plausible that 5-HT is acting via the BK channel (Peers, 1990) and Kcnk3 (Buckler *et al.*, 2001). Indeed, it is recognised that Kcnk3 is modulated by PKC (Lopes *et al.*, 2000). It is interesting therefore to speculate that the actions of both GABA and 5-HT are mediated, at least in part, via an effect on Kcnk3. This raises

the possibility of the convergence of two distinct neuromodulatory mechanisms, as well as hypoxia (Buckler *et al.*, 2000) and possibly other chemostimulatory influences (Barbe *et al.*, 2002), onto the same $K^+$ channel to fine-tune NT release from type I cells.

Both $GABA_B$ and 5-$HT_2$ receptors are known to regulate the activity of neuronal voltage-gated $Ca^{2+}$ channels. However, in type I cells, the $GABA_B$ receptor agonist baclofen was without effect on $Ca^{2+}$ channel currents. Similarly, 5-HT was without effect on $Ca^{2+}$ currents in type I cells (e Silva & Lewis, 1995). Therefore, modulation of NT release is not due to regulation of $Ca^{2+}$ influx through these channels.

To summarise, here we present evidence that two NTs which are released from type I cells during hypoxia act back at presynaptic sites to modulate the further release of transmitters. The full implications of these autoregulatory feedback mechanisms, and their roles in the function and development of the mammalian CB, remain to be determined.

## ACKNOWLEDGEMENTS

Supported by a Wellcome Trust International Prize Travelling Research Fellowship (Ref: 06154) to I.M.F. and by a grant from the Canadian Institutes for Health Research (MOP 12037) to C.A.N.

## REFERENCES

Barbe C et al. (2002). *J. Physiol.*, 543, 933-945.
Bowery N, Enna SJ (2000). *J. Pharmacol. Exp. Ther.*, 2, 2-7.
Buckler KJ, Williams BA, Honore E (2000). *J. Physiol.*, 525, 135-142.
E Silva M, Lewis DL (1995). *J. Physiol.* 489, 689-699.
Fearon IM et al. (1997). *J. Physiol.*, 500, 551-556.
Fearon IM et al. (2002). *J. Physiol*, 545, 807-818.
Gonzalez C et al. (1994). *Phys. Rev.*, 74, 829-898.
Lopes CMB, et al. (2000) *J. Biol. Chem.*, 275, 16969-16978.
Maingret F et al. (2001) *EMBO J.*, 20, 47-54.
Peers C (1990). *Neurosci. Lett.*, 119, 253-256.
Prasad M et al. (2001). *J. Physiol.*, 537, 667-677.
Urena J et al. (1994). *Proc. Natl. Acad. Sci. U.S.A.*, 91, 10208-10211.
Zhang M et al.(2000). *J. Physiol.*, 525, 143-158.
Zhong HJ, Zhang M, Nurse CA (1997). *J. Physiol.*, 503, 599-612.

# Adenosine-Acetylcholine Interactions at the Rat Carotid Body

SÍLVIA V. CONDE and EMÍLIA C. MONTEIRO
*Department of Pharmacology Faculty of Medical Sciences, New University of Lisbon, Campo Mártires da Pátria, 130, 1169-056 Lisboa, Portugal*

## 1. INTRODUCTION

Excitatory effects on carotid body (CB) chemotransduction have been described for adenosine and acetylcholine (ACh). The importance of the excitatory effects of exogenous (Monteiro and Ribeiro, 1987) and endogenous adenosine (Monteiro and Ribeiro, 1989) observed *in vivo* in the rat is supported by the increase in adenosine concentrations during hypoxia (Conde and Monteiro, 2001). In response to hypoxia, the CB also releases ACh (Fitzgerald *et al.*, 1999) that activates nicotinic receptors (Shirahata *et al.*, 1997). ACh and nicotine increase $[Ca^{2+}]$ in type I cells via activation of nicotinic receptors (Dasso *et al.*, 1997) and induce the release of several neurotransmitters at the CB, e.g. catecholamines (Obeso *et al.*, 1997). In the present work we tested the hypothesis that ACh can induce the release of adenosine from rat carotid body by a mechanism that involves the activation of nicotinic receptors.

## 2. METHODS

The present work was carried out in *Wistar* rats (200-300 g) anaesthetized with sodium pentobarbital (60 mg/kg ip., Sigma). The rats were tracheostomised and breathed spontaneously during surgical procedure. The carotid bodies were removed *in situ,* under a Nikon SMZ-2B dissection scope and placed in 500 µl of ice-cold $95\%O_2 + 5\%CO_2$ equilibrated medium containing different drugs in accordance with the protocol used. The incubation medium (MI) was composed by (mM): NaCl 116; $NaHCO_3$ 24; KCl 5; $CaCl_2$ 2; $MgCl_2$ 1.1; HEPES 10; glucose 5.5; pH 7.42. After the

*Chemoreception*, Edited by Pequignot et al.
Kluwer Academic/Plenum Publishers, New York, 2003

removal of the CBs, the animals were sacrificed by an intracardiac injection of a lethal dose of pentobarbital in accordance with the European Union directives (Portuguese law nº 1005/92 and 1131/97). After 30 min of pre-incubation in hyperoxia (95%$O_2$ + 5%$CO_2$) at 37ºC, the CBs were submitted to a period of 10 min in normoxia (20%$O_2$ + 5%$CO_2$) or hypoxia (10%$O_2$ + 5%$CO_2$) in a medium containing erythro-9-(2-hydroxy-3-nonyl)adenine (EHNA, 2.5 μM, Sigma), inhibitor of adenosine deamination. The effect of nicotinic agonists on the release of adenosine from rat CBs was assessed in normoxia. Nicotinic agonists (i.e. ACh (Sigma), dimethylphenylpiperazinium (DMPP, Sigma) and nicotine (Sigma)) were included only in the incubation period to avoid nicotinic desensitisation. In the experiments with ACh the CBs were incubated in the presence of physostigmine an inhibitor of AChesterases. The effects of nicotinic antagonists, (d-tubocurarine, mecamylamine and di-hydro-β-erythroidine (DHβE) (all from Sigma), on the release of adenosine were assessed in hypoxia and were included in the pre-incubation period to assure an adequate diffusion of the drug and the blockade of nicotinic receptors. After the incubation period, nucleotides were extracted from the MI following the protocol described by Cunha *et al.* (Cunha *et al.*, 1994). An aliquot of the supernatant was kept at –20ºC until subsequent analysis by a reverse phase HPLC method with isocratic elution. The mobile phase was a solution of $KH_2PO_4$ 100 mM with 15% of methanol, pH 6.5 with a flux of 1.75 ml/min. The data are presented as means ± SEM values. The significance between the means was calculated by the unpaired Student's *t* test. Values of $P<0.05$ were considered to represent significant differences.

## 3. RESULTS

The effect of two nicotinic agonists, ACh and DMPP on adenosine concentrations released from intact rat CBs during normoxia are shown in Figure 1. Adenosine basal concentrations released from CBs during 10 min of normoxia, were 210.3 ± 20.83 nM/CB (n = 5). The incubation of the CBs with 30 μM of ACh in the presence of physostigmine (300 μM) caused only a slight and not statistical significant increase to 237.9 ± 30.66 nM of adenosine per CB (n = 5). However, when the incubation period of the CBs with ACh (30 μM) increased from 10 min to 30 min a 34% enhancement in adenosine concentrations was obtained when compared with basal concentrations of adenosine released during 30 min. DMPP (3-100 μM) caused a concentration-dependent increase in the amount of adenosine released by the CBs. The maximal concentrations of adenosine (290.8±18.6 nM/CB) were obtained with 100 μM of DMPP but in a concentration of

30μM it already caused a significant statistical increase of 28% in the release of adenosine (see Fig. 1).

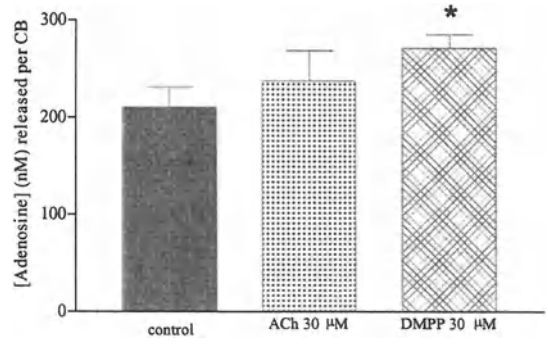


*Figure 1.* Effects of acetylcholine (ACh) and dimethylphenylpiperazinium (DMPP) on the release of adenosine from rat carotid bodies. Experiments with ACh were performed in the presence of 300 μM physiostigmine. DMPP (30 μM) increased by 28 % adenosine concentrations released from carotid bodies. Data are means ± S.E.M; n = 5 for control values and for adenosine released in the presence of ACh and n = 6 for adenosine values obtained in the presence of DMPP. * $P < 0,05$

The effect of nicotinic antagonists was assessed in hypoxia (10%$O_2$), in order to have a physiological stimulation of the chemoreceptor cells. Figure 2 shows a dose-response curve for two nicotinic receptor antagonists, d-tubocurarine and mecamylamine on the release of adenosine. The responses are expressed as percentage of effect under the adenosine values obtained from rat CBs during hypoxia. At the lowest concentration tested (100 nM), d-tubocurarine inhibits by 23.33 % the release of adenosine from rat CBs. The maximal response, which corresponds to a 52.25 % of inhibition was obtained with 200 μM of d-tubocurarine. The concentration that produces 30% of inhibition in the adenosine concentrations released by the CB ($IC_{30}$) was 223.9 nM. Mecamylamine at a concentration of 10 nM (lower concentration tested) induces a decrease of 17.9% in the adenosine levels released from CBs (Fig. 2). The maximal response corresponds to an inhibition of 45.1% in the adenosine concentrations and it was obtained with 100 μM of mecamylamine. The concentration that produces 30% of inhibition ($IC_{30}$) was 99.3 nM. These results suggest that mecamylamine is more potent than d-tubocurarine in inhibiting adenosine release from CB, being d-tubocurarine more efficient in the production of this inhibition (Figure 2).

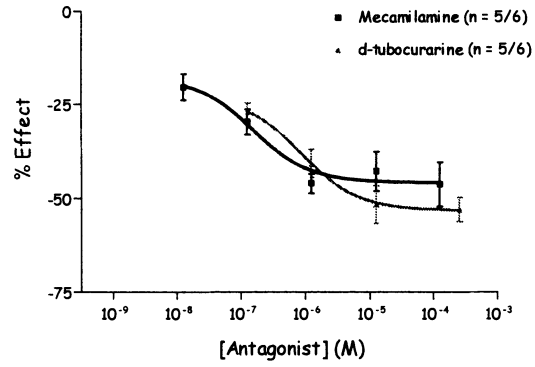


*Figure 2.* Log dose-response curve for the effects of d-tubocurarine and mecamylamine on the release of adenosine from rat carotid bodies. The responses are expressed as percentage of effect under the adenosine values released from rat carotid bodies in hypoxia (0% effect = 303.9±10.69 nM/CB). The $IC_{30}$ was 223.9 nM for d-tubocurarine and 99.3 nM for mecamylamine. The maximal effect was 52.25 ± 3.11 for d-tubocurarine and 45.1 ± 2.98 for mecamylamine. Data are means ± S.E.M..

Figure 3 shows the effect of another nicotinic receptor antagonist, DHβE on the release of adenosine elicited by hypoxia. DHβE was used in a concentration (1 μM) 10 times higher than that produces 80% of inhibition in $Ca^{++}$ currents in HEK293 cells (Sabey *et al.*, 1999). At the concentration studied (1 μM) it was observed a significantly decrease of 71% in the adenosine concentrations, to a value of 88.64 ± 6.94 nM/CB caused by DHβE. The order of potency of nicotinic antagonists obtained was: DHβE>mecamylamine>d-tubocurarine being compatible with the presence of two types of nicotinic receptors subunits, α2β2 and α4β4.

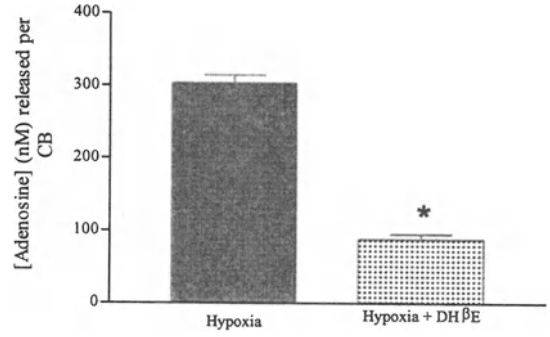


*Figure 3.* Effect of di-hydro-β-erythroidine (DHβE, 1μM) on the release of adenosine elicited by 10 min of hypoxia (10 % $O_2$). Data represents means ± S.E.M.; n = 5 for hypoxia and n = 4 for hypoxia plus DHβE. * $P < 0.001$

To distinguish between these two types of nicotinic receptors the effects of nicotine (0.1-100 nM) were also tested in the CBs during normoxia. The $EC_{25}$ and Emax values obtained from the concentration-response curves for the nicotinic agonists, DMPP and nicotine are represented in Table 1. The drug concentration that produces 25% of increase in the adenosine concentrations released from CB was 34.83μM for DMPP and 0.97 nM for nicotine and the maximal effects observed were 29.59% for DMPP and 72.31% for nicotine. From these results it is apparent that nicotine was more potent and efficient than DMPP in stimulating the release of adenosine from CBs.

*Table 1* – Mean ± SEM values for $EC_{25}$ and Emax obtained from concentration response curves for the nicotinic receptors agonists, dimethylphenylpiperazinium (DMPP) and nicotine.

| **Agonist** | **$EC_{25}$** | **Emax** (% effect) |
|---|---|---|
| DMPP (n = 4/5) | 34.83 μM | 29.59 ± 7.2 |
| Nicotine (n = 3) | 0.97 nM | 72.31 ± 9.19 |

# 4. DISCUSSION

This study demonstrated that ACh induces the release of adenosine from rat CBs by a mechanism that involves the activation of nicotinic receptors. We also showed that activation of nicotinic receptors contributes to the previously described (Conde and Monteiro, 2001) stimulatory effect of hypoxia on the release of adenosine in the carotid body. The pharmacological characterization of the nicotinic receptors that stimulate adenosine release at the rat CB is compatible with an α4β4 nicotinic receptor subtype.

The main conclusion was based on the observations that during normoxia DMPP, a nicotinic receptor agonist, induced the release of adenosine from rat CBs and that nicotinic receptor antagonists inhibited the release of this nucleoside elicited by hypoxia. This effect of DMPP on the release of adenosine was mimicked by ACh when CBs were incubated during longer periods (30 min). The reduced potency of ACh when compared with that of DMPP can be explained by the presence of a high concentration of physostigmine in the ACh experiments. It was shown that this acethylcolinesterase-inhibiting drug is a competitive ligand of ACh on α4-containing nicotinic ACh receptors (Zwart *et al.*, 2000). In other preparations, namely the neuromuscular junction DMPP enhances ACh release by activating nicotinic autoreceptors of the rat motor nerve endings

(Correia-de-Sá and Ribeiro, 1994). It was also shown that DMPP increases cathecolamine output in the rat adrenal gland (Nagayama et al., 1999). We can postulate that the effect of DMPP on the release of adenosine from the CB can be due to activation of nicotinic receptors predominantly located in the chemoreceptor cells, and thereby modulating the release of adenosine and probably other neurotransmitters.

The finding that mecamylamine and d-tubocurarine inhibited by approximately 50% the release of adenosine from CBs elicited by hypoxia suggests that the release of adenosine induced by hypoxia does not depend exclusively of nicotinic activation. It is well known in different preparations that adenosine modulates, stimulates or inhibits ACh release (Sebastião and Ribeiro, 2000) but no evidences were provided concerning the opposite effect. Since ATP is co-released with ACh at the CB (Zhang et al., 2000) and type I cells possess nicotinic autoreceptors, we can speculate that the fraction of adenosine released in response to nicotinic activation could be that originated from ATP degradation. Approximately 40% of the adenosine released during moderate (10%) hypoxia is coming from ATP (Conde and Monteiro, 2002) and also about 50% is blocked by nicotinic antagonism. In contrast, mecamylamine causes a complete blockade of catecholamines release (Obeso *et al.*, 1997) at the rabbit CB. The differences between the degree of inhibition induced by nicotinic antagonists on catecholamines and adenosine release at the CB can also be explained assuming that the release of these mediators depends on the presence of different nicotinic receptor subunits.

The rank order of potency found for the inhibitory effects of nicotinic antagonists on adenosine release from the CB was DHβE>mecamylamine>d-tubocurarine which could be compatible with the activation of α2β2 or α4β4 nicotinic receptors subunits (Alexander *et al.*, 2001). The distinction between these two nicotinic receptors subtype is made according to the relative potency of nicotine and DMPP (Alexander *et al.*, 2001). In the present work, nicotine was about 13 times more potent that DMPP, suggesting that ACh induces the release of adenosine from rat CB by a mechanism that involves α4β4 nicotinic receptors. These results are in agreement with the location of α4 subunits in CB type I cells shown by immunohistochemical techniques (Ishizawa *et al.*, 1996) and with the absence of α2 nicotinic subunits transcription in total CB RNA (Cohen *et al.*, 2002).

In conclusion, the present data show that activation of α4β4 nicotinic receptor subunits contributes to the release of adenosine/ATP from the CB in response to hypoxia.

# REFERENCES


Alexander, S.P.H., Mathie, A. and Peters, J.A., 2001. *TIPS Nomenclature Supplement*, 20th Edition, 1-12.

Cohen, G., Han, Z.Y., Grailhe, R., Gallego, J., Gaultier, C., Changeux, J.P. and Lagercrantz, H, 2002. β2 nicotinic acetylcholine receptor subunit modulates protective responses to stress: A receptor basis for sleep-disordered breathing after nicotine exposure, *PNAS*, 99:13272-13277.

Conde, S.V. and Monteiro, E.C, 2001. Hypoxia and extracellular pathway of adenosine production. *Eur. J. Biochem.*, 268:67.

Conde, S.V. and Monteiro, E.C, 2002. Origin of adenosine released by the rat carotid body. XVth ISAC Symposium. Lyon (France).

Correia-de-Sá, P. and Ribeiro, J.A., 1994, Potentiation by tonic $A_{2a}$-adenosine receptor activation of CGRP-facilitated [$^3$H]- ACh release from rat motor nerve endings, Br.J.Pharmacol., 111: 582-588

Cunha, R.A., Milusheva, E., Vizi, E.S., Ribeiro, J.A. and Sebastião, A.M., 1994. Excitatory and inhibitory effects of A1 and A2 adenosine receptor activation on the electrically evoked [$^3$H] acetylcholine release from different areas of the rat hippocampus. *J. Neurochem.*, 63:207-214.

Dasso, L.L.T., Buckler, K.J. and Vaughan-Jones, R.D., 1997. Muscarinic and nicotinic receptors raise intracellular $Ca^{2+}$ levels in rat carotid body type I cells, *J. Physiol.*, 498:327-338.

Fitzgerald, R.S., Shirahata, M. and Wang, H-Y., 1999. Acetylcholine release from cat carotid bodies, Brain Res., 841:53-61.

Ishizawa, Y., Fitzgerald, R.S., Shirahata, M. and Schofield, B., 1996. Localization of nicotinic acetylcholine receptors in cat carotid body and petrosal ganglion. *Adv. Exp. Med. Biol.*, 410:253-256.

Monteiro, E.C. and Ribeiro, J.A., 1987. Ventilatory effects of adenosine mediated by carotid chemoreceptors in the rat. *Naunyn-Schmiedeberg's Arch. Pharmacol.*, 335:143–148.

Monteiro, E.C. and Ribeiro, J.A., 1989. Adenosine deaminase and adenosine uptake inhibitors facilitate ventilation in rats. *Naunyn-Schmiedeberg's Arch. Pharmacol.*, 340:230-238.

Nagayama, T., Matsumoto, T., Kuwakubo, F., Fukushima, Y., Yoshida, M., Suzuki-Kusaba, M., Hisa, H., Kimura, T. and Satoh, S., 1999, role of calcium channels in catecholamine secretion in the rat adrenal gland, *J. Physiol.*, 520: 503-512

Obeso, A., Gómez-Nino, M.A., Almaraz, L., Dinger, B., Fidone, S. and González, C., 1997. Evidence for two types of nicotinic receptors in the cat carotid body chemoreceptor cells, *Brain Res.*, 754:298-302.

Sabey, K., Paradiso, K., Zhang J. and Henry Steinbach, J., 1999. Ligand binding and activation of rat nicotinic α4β2 receptors stably expressed in HEK293 cells, *Mol. Pharmacol.*, 55:58-66.

Sebastião, A.M. and Ribeiro, J.A., 2000, Fine-tuning neuromodulation by adenosine, *TIPS*, 21: 341-346

Shirahata, M., Fitzgerald, R.S. and Sham, J.S.K., 1997. Acetylcholine increases intracellular calcium of arterial chemoreceptor cells of adult cats, *J. Neurophysiol*, 78:2388-2395.

Zhang, M., Zhong, H., Vollmer, C. and Nurse, C.A., 2000, Co-release of ATP and ACh mediates hypoxic signaling at rat carotid body chemoreceptors. *J. Physiol.*, 525: 143-158

Zwart, R., van Kleef, R.G.D.M., Gotti, C., Smulders C.J.G.M. and Vijverberg, H.P.M., 2000. Competitive potentiation of acetylcholine effects on neuronal nicotinic receptors by acethylcholinesterase-inhibiting drugs, *J.Neurochem.*, 75:2492-2500.

# Diverse Cholinergic Receptors in the Cat Carotid Chemosensory Unit

SERABI HIRASAWA[1], JEFFREY A. MENDOZA[1], DAVID B. JACOBY[1,2], CHIYOKO KOBAYASHI[3], ROBERT S. FITZGERALD[1,2], BRIAN SCHOFIELD[1], SRINIVASAN CHANDRASEGARAN[1], and MACHIKO SHIRAHATA[1]

*Departments of Environmental Health Sciences[1] and Medicine[2], The Johns Hopkins Medical Institutions, Baltimore, USA; Group of Evolutionary Regeneration Biology[3], RIKEN Center for Developmental Biology, Kobe, Japan*

## 1. INTRODUCTION

Decades of studies have shown the presence of neurotransmitters in the glomus cell, the putative chemosensory cell, and the involvement of neurotransmitters in carotid body chemotransmission (Gonzalez et al., 1994). We have been proposing that ACh is a major excitatory neurotransmitter in the cat carotid body (Fitzgerald, 2000). ACh fulfills most of criteria as an excitatory neurotransmitter in the carotid body. Regarding the presence of cholinergic receptors, our immunohistological study has shown that α7 subunits of nicotinic ACh receptors (nAChRs) locate at chemoreceptor nerve endings (Shirahata et al, 1998), and that α4 and β2 subunits of nAChRs in glomus cells (Ishizawa et al, 1994). Expression or localization of other subunits of nAChRs or subtypes of muscarinic ACh receptors (mAChRs) has not yet been known. Neuronal nAChRs are ligand-gated cation channels. They are composed of two α (α2–6) and three β (β2–4) subunits, or of five α (α7–9) subunits. Among variable combinations, α3β4, α4β2, and α7 types appear to be the major nAChRs, and they are widely but distinctively expressed in the nervous system

*Chemoreception*, Edited by Pequignot et al.
Kluwer Academic/Plenum Publishers, New York, 2003

(Lukas et al, 1999). Muscarinic AChRs are pharmacologically and molecular biologically classified into 5 subtypes (M1-M5). They are distributed in the nervous system, smooth muscles and gland (Caulfield and Birdsall, 1998). The purpose of the current study is to investigate the gene expression of major cholinergic receptors and to localize the receptor proteins in the cat chemosensitive unit (the carotid body and the petrosal ganglion).

## 2. MATERIAL AND METHODS AND RESULTS

### 2.1 Neuronal Nicotinic ACH Receptors in the Cat Chemosensory Unit

Although homology was found among mammalian species in a particular cholinergic receptor subunit or subtype, DNA sequences encoding cat cholinergic receptors were not known. Therefore, we first determine the partial cDNA sequences for major nAChR subunits and mAChR subtypes. The superior cervical ganglia, the cerebral cortex and the heart were harvested from adult cats which were euthanized with ketamine (50 mg/kg, i.m.) and sodium pentobarbital (50-100 mg/kg, i.v.). Total RNA of these tissues was isolated using TRIzol following the manufacturer's protocol. Subsequently the samples were treated with RQI DNase I (Promega) to eliminate a possible genomic DNA contamination, and were purified with phenol chloroform extraction followed by ethanol precipitation. The purified RNA was reverse-transcribed to obtain first strand cDNA using random primers and Ready to Go You-Prime First Strand Beads (Amersham Phamacia Biosciences). Oligonucleotides for subsequent PCR reactions were designed to include the conserved regions of DNA sequences among human and rat cholinergic receptors obtained from GenBank. The PCR amplification was performed using Ready to Go PCR Beads (Amersham Pharmacia Biosciences). PCR products were separated by electrophoresis on 2 % agarose gel and cDNA was purified using QIAEX II Gel Extraction Kit (QIAGEN). The purified cDNA was cloned into plasmids using TA Cloning Kit for Sequencing (Invitrogen) following the manufacturer's protocol. The plasmids were transformed into the TOP10 chemically competent cell, and several appropriate colonies were selected and cultured separately. The plasmid DNA was extracted using QIAprep Spin miniprep Kit (QIAGEN). The purified plasmid DNA was sequenced at DNA Analyzing Facility at Johns

Hopkins Hospital. The obtained cDNA sequences and the deduced amino acid sequences were analyzed and identified by using BLASTN and BLASTP, NIH computer softwares.

The partial cDNA sequences encoding cat α3, α4, β2, and β4 subunits of nAChRs were determined. The cDNA sequences and deduced amino acid sequences are highly homologous to those of humans (>84% and >94%, respectively).

Subsequently, the total RNA was extracted from the carotid body and the petrosal ganglion followed by reverse transcription as described above. The sets of primers were designed within the determined sequences by using an on-line software, Primer3. The negative reaction control was total RNA as a template in PCR reaction, which detects a possible contamination of genomic DNA. The RT-PCR studies in the cat carotid body and petrosal ganglion revealed the expression of mRNA for α3, α4, β2 and β4 subunits. No band was detected in the negative reaction controls.

For localizing nAChR subunit proteins, immunohistochemistry was performed. The carotid body and the petrosal ganglion were fixed in zinc fixative, embedded in paraffin and sectioned at 4-5 μm. After deparaffinization, sections were heated in boiling 0.01M citric acid buffer (pH 8.0) for 5 min to retrieve the antigens (Shi, 1997). Endogenous peroxidase activity was quenched with 1% $H_2O_2$ in phosphate buffered saline (PBS). Endogenous biotin and non-specific bindings were blocked avidin-biotin with blocking kit (Vector) and normal goat serum (Vector, 1/70) including CAS Block™ (Zymed Laboratories), respectively. Tissues were incubated with appropriate primary antibodies (anti-α3 nAChR, 1/300, Sigma-RBI; anti-a4 nAChR, 1/1000, Covance; anti-β2 nAChR, 1/200; Covance; M1 mAChR, 1/20, Alamone Labs, M2 mAChR, 1/20, Alamone Labs) for 48-72 hrs at room temperature. Subsequently, a biotinylated anti-rat IgG (Vector, made in goat, 1/2000) was applied for 1 h at room temperature. VECTASTAIN® *Elite* ABC kit (Vector) was used for peroxidase reaction, and SG (Vector) was used as a chromogen. Between each step, tissues were washed three times in PBS for 5 min per wash. Purified IgG or antibodies preadsorbed with antigens, when available, were used as negative control.

Immunoreactivity against α3, α4 and β2 subunits of nAChRs was distributed in the cytoplasm of glomus cells (Fig. 1, left). In the section of the petrosal ganglion, the immunoreactivity against α3, α4 and β2 subunits of nAChRs was detected in the cell bodies of majority of neurons. Few nerve fibers in the petrosal ganglion were stained (Fig. 1, right). No staining was observed in negative controls.

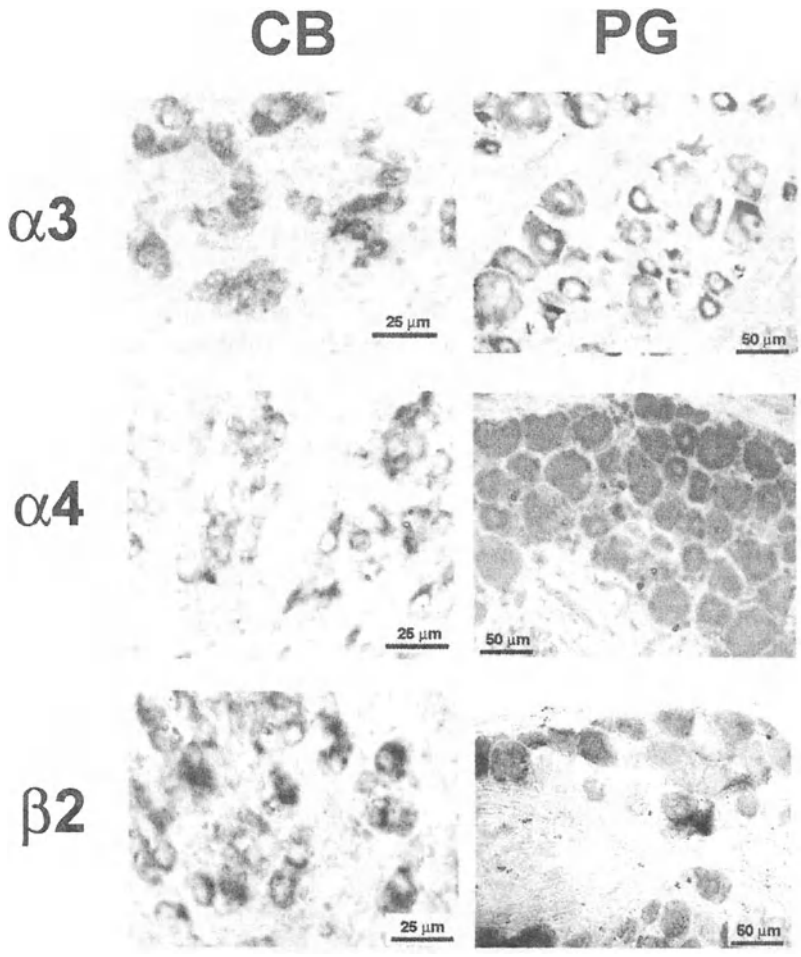


*Figure 1.* Positive immunoreactivity against α3, α4 and β2 subunits of nAChRs in the cat carotid body (CB) and the petrosal ganglion (PG). Positive stain was demonstrated in the carotid body by the dark gray ovoid shape about 10 μm in diameter. The lighter center is the large nucleus, a characteristic of glomus cells. In the petrosal ganglion, positive signals were mainly localized in the cell bodies.

## 2.2. Muscarinic ACH Receptors in the Cat Chemosensory Unit

The partial cDNA sequences encoding the third internal loop of cat M1, M2 and M3 mAChRs were determined as described above. The cDNA sequences and deduced amino acid sequences are highly homologous to those of humans (>90% and >91%, respectively). The RT-PCR studies in the cat carotid body and petrosal ganglion revealed the distinct bands of expected sizes for M1, M2, and M3 mAChRs.

Immunohistochemical studies showed that the immunoreactivity against M1 and M2 mAChRs was distributed in the cytoplasm of glomus cells and nerve fibers in the carotid body (Fig. 2, top). In the section of the petrosal ganglion, the immunoreactivity against M1 and M2 mAChRs was detected in the cell bodies of majority of neurons. Nerve fibers in the petrosal ganglion were also stained (Fig. 2, bottom). No staining was observed in negative control.

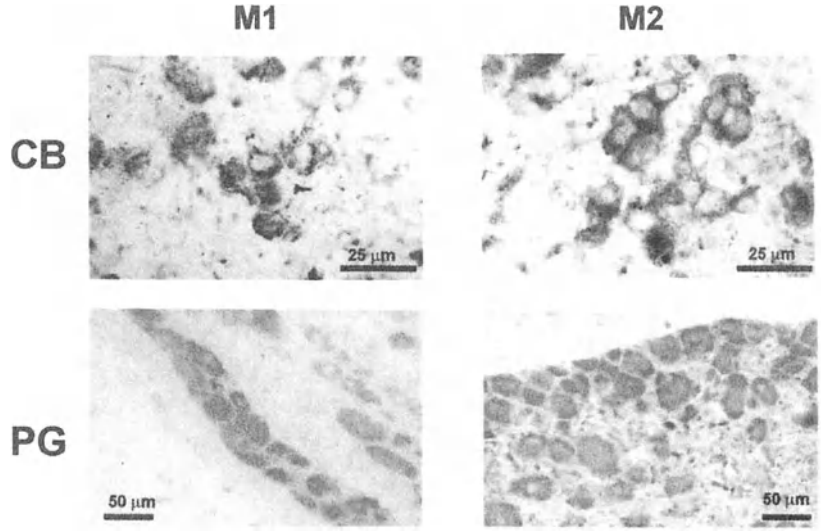


*Figure 2.* Positive immunoreactivity (dark gray) against M1 and M2 mAChRs in the cat carotid body (CB) and the petrosal ganglion (PG).

## 3. DISCUSSION

Previous pharmacological and radioligand binding studies suggest the presence of cholinergic receptors in the carotid body chemosensory unit (for a review, Fitzgerald 2000). The current study has clearly demonstrated that various types of nicotinic and muscarinic receptors are present in the cat carotid body and the petrosal ganglion.

Activation of nAChRs in glomus cells could influence the release of neurotransmitters. For example, it has been shown that nicotine increases the release of catecholamines from glomus cells in a calcium dependent manner (Fidone et al., 1990; Obeso et al., 1997). ACh application increases intracellular $Ca^{2+}$ in glomus cells (Dasso et al., 1997; Shirahata et al., 1997). Further, nAChRs appear actively involved in the generation of action potentials in chemoreceptor afferent neurons (Shirahata et al., 2000; Zhong and Nurse, 1997).

In mAChRs, odd-numbered receptors and even-numbered receptors are distinctively coupled to different G-protein subunits (Caulfield and Birdsall, 1998). Their modulatory effects in the release of catecholamines from the carotid body (Bairam et al., 2000: Wang and Fitzgerald, 2002) and in chemoreceptor neural responses to hypoxia (Fitzgerald, 2000) have been shown. Activation of mAChRs in rat glomus cells increases intracellular $Ca^{2+}$ (Dasso et al., 1997).

A complete picture of all the cholinergic receptors involved in chemotransmission processes is still lacking, but our data indicate that the glomus cells contain $\alpha 3$, $\alpha 4$, $\beta 2$ and $\beta 4$ subunits of nAChRs and M1, M2, and M3 mAChR subtypes. Chemosensory afferent fibers may contain all these subunits in addition to the previously reported $\alpha 7$ subunits of nAChRs and M1, M2, and M3 mAChRs. Several blockers and toxins, which are relatively selective for a particular type of nAChRs and mAChRs, are now available. Our data can help in choosing a proper antagonist when studying further the processes of carotid body chemotransmission.

## ACKNOWLEDGEMENTS

The study was supported by HL 61596 and HL50712.

# REFERENCES

Bairam A., Neji H., Marchal F., 2000, Cholinergic dopamine release from the in vitro rabbit carotid body. *J. Appl. Physiol.* 88:1737-1742.

Caulfield M.P., Birdsall N.J., 1998, International Union of Pharmacology. XVII. Classification of muscarinic acetylcholine receptors. *Pharmaco.l Rev.* 50:279-90

Dasso L.L., Buckler K.J., Vaughan-Jones R.D., 1997, Muscarinic and nicotinic receptors raise intracellular $Ca^{2+}$ levels in rat carotid body type I cells. *J. Physiol. (Lond)* 498: 327-338.

Fidone S.J., Gonzalez C., Obeso A., Gomez-Nino A., Dinger B., 1990, Biogenic amines and neuropeptide transmitters in carotid body chemotransmission: experimental findings and perspectives. In: Hypoxia: The adaptaions (Sutton JR, Coates G, Remmers JE, eds), pp 116-126. Toronto: B.C.Deker, Inc.

Fitzgerald R.S., 2000, Oxygen and carotid body chemotransduction: the cholinergic hypothesis - a brief history and new evaluation. *Respir. Physiol.* 120: 89-104.

Gonzalez C., Almaraz L., Obeso A., Rigual R., 1994, Carotid body chemoreceptors: from natural stimuli to sensory discharges. *Physiol. Rev.* 74: 829-898.

Ishizawa Y., Fitzgerald R.S., Shirahata M., Schofield B., 1996, Localization of nicotinic acetylcholine receptors in cat carotid body and petrosal ganglion. *Adv. Exp. Med. Biol.* 410: 253-256.

Lukas R.J., Changeux J.P., Le Novere N., Albuquerque E.X., Balfour D.J., Berg D.K., Bertrand D., Chiappinelli V.A., Clarke P.B., Collins A.C., Dani J.A.; Grady S.R., Kellar K.J., Lindstrom J.M., Marks M.J., Quik M., Taylor P.W., Wonnacott S., 1999, International Union of Pharmacology. XX. Current status of the nomenclature for nicotinic acetylcholine receptors and their subunits. *Pharmacol. Rev.* 51:397-401

Obeso A., Gomez-Nino M.A., Almaraz L., Dinger B., Fidone S., Gonzalez C., 1997, Evidence for two types of nicotinic receptors in the cat carotid body chemoreceptor cells. *Brain Res.* 754: 298-302.

Shi S.R., Cote R.J., Taylor C.R., 1997, Antigen retrieval immunohistochemistry: past, present, and future. *J. Histochem. Cytochem.* 45: 327-343.

Shirahata M., Fitzgerald R.S., Sham J.S., 1997 Acetylcholine increases intracellular calcium of arterial chemoreceptor cells of adult cats. *J. Neurophysiol.* 78: 2388-2395.

Shirahata M., Ishizawa Y., Rudisill M., Schofield B., Fitzgerald R.S., 1998, Presence of nicotinic acetylcholine receptors in cat carotid body afferent system. *Brain Res.* 814: 213-217.

Shirahata M., Ishizawa Y., Rudisill M., Sham J.S., Schofield B., Fitzgerald R.S., 2000, Acetylcholine sensitivity of cat petrosal ganglion neurons. *Adv. Exp. Med. Biol.* 475: 377-387.

Zhong H., Nurse C.A., 1997 Nicotinic acetylcholine sensitivity of rat petrosal sensory neurons in dissociated cell culture. *Brain Res.* 766: 153-161.

Wang H.Y., Fitzgerald R.S., 2002 Muscarinic modulation of hypoxia-induced release of catecholamines from the cat carotid body. *Brain Res.* 927:122-137.

# Carotid Chemosensory Neurons in the Petrosal Ganglia are Excited by ACh and ATP

[1,2]RODRIGO VARAS, [2]JULIO ALCAYAGA, and [1]RODRIGO ITURRIAGA
[1]*Lab. Neurobiología, Facultad Ciencias Biológicas, P. Universidad Católica de Chile and*
[2]*Lab. Fisiología Celular, Facultad de Ciencias, Universidad de Chile. Santiago, Chile.*

## 1. INTRODUCTION

Several molecules have been proposed as excitatory transmitters between carotid body (CB) glomus (type I) cells and petrosal ganglion (PG) neurons (Eyzaguirre and Zapata, 1984; Gonzalez *et al.*, 1994). Recently, experiments performed in the reconstituted rat CB chemosensory system (i.e. co-cultures of CB and petrosal-jugular cells) have suggested that both acetylcholine (ACh) and adenosine 5′-triphosphate (ATP) may act both as excitatory transmitters (Zhang *et al.*, 2000). However, this experimental design cannot preclude that non-carotid chemosensory (gustatory) or other (i.e. mechanosensory) neurons present in the PG may establish contact with glomus cells. Moreover, the response of cultured nodose neurons to an acidic challenge (a CB natural stimulus) change when glomus cells are present in culture, suggesting that the changes arise from synaptic and/or trophic interactions between glomus cells and nodose neurons (Alcayaga and Eyzaguirre, 1991). To circumvent this difficulty, we studied the effects of both ACh and ATP on identified cat PG chemosensory neurons, using an *in vitro* preparation, in which the PG remains connected to the carotid bifurcation and CB (Belmonte and Gallego, 1983). In addition, we studied the electrophysiological responses induced by ATP and ACh in dissociated PG neurons using whole-cell patch clamp techniques.

*Chemoreception*, Edited by Pequignot et al.
Kluwer Academic/Plenum Publishers, New York, 2003

## 2. METHODS

Adult cats of either sex (2.0-3.5 kg) were anaesthetized with sodium pentobarbitone (40 mg/kg, i.p). The carotid bifurcation containing the CB, the carotid sinus nerve (CSN) and the PG were removed from the cat and placed in ice-chilled, $Ca^{2+}$-$Mg^{2+}$-free modified Hanks' solution (mHBBS).

### 2.1. CB-PG Preparation

The preparation was dissected from surrounding tissue and transferred to a superfusion chamber with 2 compartments (1.5 ml each) communicated through a small channel. The carotid artery with the carotid sinus and CB was pinned to the bottom of one compartment and the PG to the other, while the CNS lied in the communicating channel filled with mineral oil to assess electrical isolation. Each compartment was superfused independently with Hanks' solution (in mM: NaCl 137, $CaCl_2$ 1.3, $MgSO_4$ 0.8, KCl 5.4, $KH_2PO_4$ 0.4, $Na_2HPO_4$ 0.3, D-glucose 5.6, HEPES 5 and $NaHCO_3$ 4.0) at pH 7,43 at 30°C and equilibrated with room air. The flow rate in both compartments was maintained at 1.2 ml/min with a pump controlling the input and output of the saline solution. The capsule of the PG was opened and the CSN was placed on a pair of platinum-iridium electrodes for electrical stimulation. The PG neurons were impaled under a microscope with glass pulled-microelectrodes (20-50 MΩ) filled with KCl 3M and connected to a conventional intracellular recordings system. In this study, neurons that respond with action potentials to CSN stimulation were included in the analysis. Carotid neurons were classified as chemosensory if their discharges increased in response of stop-flow and/or acidosis applied to the CB or as barosensory if their discharges increased in response to the mechanical deformation of the carotid sinus by a puff of Hank's solution.

### 2.2. Patch Clamp Recordings

The PGs were minced into 15-20 pieces, and enzymatically dissociated in mHBSS with 0.1% collagenase, 0.05% trypsin, 150 U/ml DNAse for 30-60 minutes. The dissociation, carried out under agitation at 38°C, was stopped by addition of 0.1 mg/ml soybean trypsin inhibitor and 10% fetal bovine serum. The cell suspension was centrifuged for 10 min at 2000 g and the pellet suspended in F-12 supplemented with 10% horse serum, 10% fetal bovine serum, 14 mM $NaHCO_3$ and nerve growth factor (15 ng/ml). The cells were plated into 35 mm Petri dishes coated with poly-L-lysine (0.1 mg/ml), and maintained at 38°C in water-saturated, 5% $CO_2$ in air atmosphere. The cultures -from 3 to 16 days- were placed in the stage of an inverted microscope and superfused (flow 1.2 ml/min) at room temperature

with modified Hanks' solution (in mM: NaCl 140, $CaCl_2$ 1.3, $MgSO_4$ 0.8, KCl 5.4, $KH_2PO_4$ 0.4, $Na_2HPO_4$ 0.3, D-glucose 5.6, HEPES 5 and $NaHCO_3$ 4) at pH 7,43 equilibrated with room air. The PG neurons were recorded with 1.5-mm O.D. borosilicate glass pulled- microelectrodes (1-2 MΩ) filled with an intracellular solution (in mM; KCl 135, NaCl 5, $CaCl_2$ 1, EGTA 10, HEPES 10, pH 7,2). Seal formation and membrane breakthrough (carried out in current-clamp mode) was monitored by observing the response to a 2-10 pA depolarizing current step during 50 ms. The resting membrane potential was measured in the current-clamp mode with no holding current. Voltage-clamp recordings were performed at a holding potential of –60 mV.

## 3. RESULTS

In the *in vitro* PG-CB preparation, intracellular recordings allow us to identify at least two types of PG neurons projecting through the CSN: i) neurons with humped somatic action potentials (hAP) that respond with one or few action potentials to long-lasting depolarization (39/49), and ii) neurons with action potential without a hump (non-hAP) that fire tonically during long-lasting depolarizing pulses (10/49). About 20% of each neuronal type corresponded to neurons with slow conducting axons (C-type neurons). 27/39 hAPs neurons were classified as chemosensory neurons because they responded to stop flow and acidic stimulation of the CB, but none of the remaining hAP neurons responded to carotid sinus mechanical stimulation The superfusion of Hank's with hexamethonium (10 μM) and suramin (100 μM) for 5 minutes reversibly suppressed the responses of the chemosensory neurons to stop flow (Fig. 1) and/or acidosis. Furthermore, somatic application of ACh and ATP to chemosensory neurons increased their frequency of discharge. Most of the non-hAP neurons responded to carotid sinus stimulation, but all were unresponsive to chemical stimulation or ACh, but ATP evoked a spiking activity in 4 of these neurons.

In cultured PG neurons, under voltage clamp, we found that ATP induced a concentration-dependent inward current that partly desensitized during 10s application pulses. The ATP-induced current had a threshold of 100 nM, and saturated at about 20 to 50 μM ($EC_{50}$ = 6.1 μM). This ATP-evoked current was mimicked by the P2X agonist α,β-methylene ATP ($EC_{50}$ = 7.2 μM) and reversibly blocked by suramin (50 μM). Similarly, ACh induced a fast inactivating inward current with a threshold between 10 and 50 μM that saturated about 1 to 5 mM ($EC_{50}$ = 182 μM). Fig. 2 shows the response of the same neuron to ACh and ATP. The ACh-evoked currents were mimicked by nicotine and reversibly blocked by hexamethonium (1 μM). From 57 neurons tested for ACh and ATP, 5 neurons (8.8%) responded to ACh only,

9 cells (15.8%) to ATP only, 34 neurons (59.6%) responded to both agents, while the remaining 9 neurons (15.8%) were unresponsive.

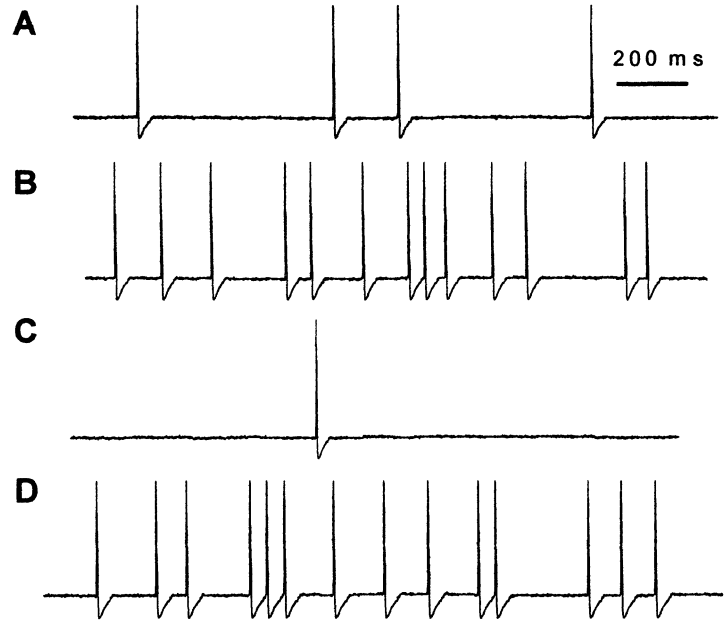


*Figure 1.* Effect of P2 and nACh receptor blockers on stop flow – induced activity in one hAP carotid neuron. **A,** Spontaneous activity of a hAP neuron in control condition. **B,** After 1 min of stop flow. **C,** After 1 min of stop flow following 5 min of superfusion with 100 μM suramin and 10 μM hexamethonium. **D,** After 1 min of stop flow following 10 minutes of washing out the drugs

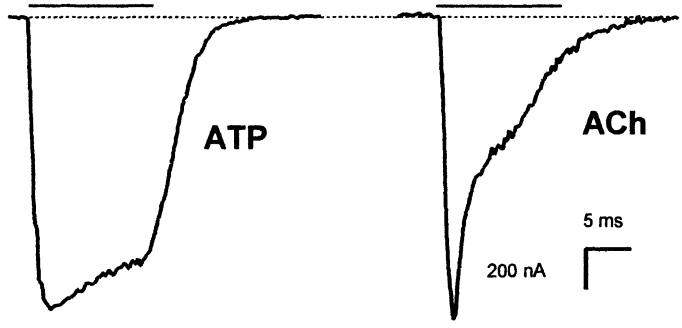


*Figure 2.* Whole cell currents evoked by ATP and ACh in the same neuron dissociated from the cat petrosal ganglion. A: Sustained inward current evoked during the 5 μM ATP pulse B: Fast inactivated inward current evoked by 500 μM ACh in the same neuron.

## 4. DISCUSSION

Present results confirm that cat PG neurons projecting to the CB are characterized by the presence of humped action potentials and phasic discharges in the soma, while the remaining neurons projecting through the carotid nerve present action potentials without a hump and tonic discharges (Belmonte and Gallego, 1983; Gallego, 1983). However, on both groups A-type and C-type neurons were present in our recordings. Our study shows that PG neurons projecting to the CB do not respond to mechanical stimulation of the carotid sinus, but are excited by stop flow and/or acidosis applied to the CB. These carotid chemosensory neurons also increased their frequency of discharge by somatic application of both ACh and ATP, indicating that the perikaryon of chemosensory neuron respond to both putative transmitters (See Alcayaga *et al.,* 1998; 2000). On the other hand, a combination of hexamethonium (10 μM) and suramin (100 μM) reversibly suppressed the responses evoked by stop flow or acidosis on carotid PG chemosensory neurons. In cultured cat PG neurons, ACh induces depolarization and spike generation (Varas *et al.,* 2000) and patch-clamp recordings have shown that ACh induces depolarization and inward currents in about 70% of rat (Zhong and Nurse, 1997) and 60% of cat PG neurons (Varas *et al.,* 2001), while ATP responses are mimicked and blocked by P2X agonists and antagonists, respectively.

Most cultured neurons of the cat CB showed a dose-dependent inward current in response to somatic application of ACh or ATP, with only 16% being insensitive to these transmitters. Moreover, both transmitters activated the vast majority of the responsive neurons. Similarly a high proportion of ACh responsive neurons have been described in cultures of the rat jugular-petrosal complex (Zhong and Nurse, 1997) and cat PG (Varas *et al.,* 2000). The ACh-induced responses appeared to be mediated by activation of nicotinic ACh receptors, as responses evoked in the cat whole PG (Alcayaga *et al.,* 1998) and in the rat jugular-petrosal complex neurons (Zhong and Nurse, 1997). The ATP-induced responses pharmacology suggests that responses depend on $P2X_{2,\ 3}$ receptors, as described in the rat jugular-petrosal complex neurons (Prasad *et al.,* 2001; Zhang *et al.,* 2000) and in the cat PG in vitro (Alcayaga *et al.,* 2000).

In the CB numerous molecules present in glomus cells, such as ACh, ATP, dopamine, and substance P have been postulated to be the excitatory transmitter in the CB (Gonzalez *et al.,* 1994). However, the identity of the excitatory transmitter between glomus cells and sensory afferent neurons is still debated. Our results support the idea that ACh and ATP are both excitatory transmitters in the cat CB and agree and extend previous observations (Zhong *et al.,* 2000). Recordings from rat petrosal-jugular neurons co-cultured with glomus cells often show spontaneous and hypoxia-

evoked excitatory postsynaptic responses. Hexamethonium (100 μM) or suramin (50 μM) alone only partially inhibited these responses, while application of both blocker almost eliminate all activity, suggesting that both ACh and ATP were released and mediate the excitatory hypoxic signaling between glomus cells and sensory neurons (Zhong *et al.*, 2000).

In summary, our data indicate that identified carotid chemosensory neurons in the PG respond to somatic application of both ACh and ATP. Moreover, the responses evoked by stop flow and acidosis in the CB can be blocked by nicotinic and purinergic blockers. Therefore, ACh and ATP appear to play an excitatory role in the cat CB.

## ACKNOWLEDGEMENT

Supported by grants FONDECYT 2010133 (RV) and DID ENL-02/15 (JA).

## REFERENCES

Alcayaga, J., and Eyzaguirre C. 1990, Electrophysiological evidence for the reconstitution of chemosensory units in co-cultures of carotid body and nodose ganglion neurons. *Brain Res.* 534, 324-328.

Alcayaga, J., Iturriaga, R., Varas, R., Arroyo, J., and Zapata, P. 1998, Selective activation of carotid nerve fibers by acethylcholine applied to the cat petrosal ganglion in vitro. *Brain Res.* 786, 47-54.

Alcayaga, J., Cerpa, V., Retamal, M., Arroyo, J., Iturriaga, R., and Zapata, P. 2000, Adenosine triphosphate-induced peripheral nerve discharges generated from the cat petrosal ganglion in vitro. *Neurosci. Lett.* 282, 185-188.

Belmonte, C., and Gallego R. 1983 Membrane properties of cat sensory neurons with chemoreceptor and baroreceptor endings. *J. Physiol. Lond.* 342, 603-614.

Eyzaguirre, C., and Zapata, P. 1984, Perspective in carotid body research. *J. Appl. Physiol.* 57, 931-957.

Gallego, R. 1983, The ionic basis of action potentials in petrosal ganglion cells of the cat. J. Physiol. Lond. 342, 591-602.

Gonzalez, C., Almaraz, L., Obeso, A., Rigual, R. (1994). Carotid body chemoreceptors: from natural stimuli to sensory discharges. Physiol. Rev. 74, 829-898.

Prasad, M., Fearon, I.M., Zhang, M., Laing, M., Vollmer, C., and Nurse, C.A. 2001, Expression of $P2X_2$ and $P2X_3$ receptor subunits in rat carotid body afferent neurons : role in chemosensory signalling. *J. Physiol. Lond.* 537, 667-677.

Varas, R., Alcayaga, J., and Zapata, P. 2000,. Acetylcholine sensitivity in dissociated neurons of the cat petrosal ganglion. *Brain Res.* 882, 201-205.

Varas, R., Iturriaga, R., Alcayaga, C., Cerpa, V., and Alcayaga, J. 2001, Current and voltage changes evoked by ACh and ATP in cat petrosal ganglion neurons. *Soc. Neurosci. Abstr.* 27, 288.12.

Zhong, H., and Nurse, C. 1997, Nicotinic acetylcholine sensitivity of rat petrosal sensory neurons in dissociated cell culture. *Brain Res.* 766, 153-161.

Zhang, M., Zhong, H., Vollmer, C., and Nurse, C. 2000, Co-release of ATP and ACh mediates hypoxic signalling at rat carotid body chemoreceptors. *J. Physiol. Lond.* 525, 143-158.

# The Use of NK-1 Receptor Null Mice to Assess the Significance of Substance P in the Carotid Body Function.

A.J. RICO, J. PRIETO-LLORET, D.F. DONNELLY, C. DE FELIPE*, CONSTANCIO GONZALEZ and R.RIGUAL.

*Depto. de Bioquímica y Biología Molecular y Fisiología/(IBGM). Universidad de Valladolid /(CSIC). Facultad de Medicina. Valladolid. *Instituto de Neurociencias, Universidad Miguel Hernández/CSIC, Alicante Spain*

## 1. INTRODUCTION: Update of the literature on Substance P and carotid body chemoreceptor function.

Substance P was discovered in 1931 by Euler and Gaddum as a chemically unidentified substance present in dry acetone-powder extracts of the intestine and biologically characterized by its ability to contract smooth muscle and to lower arterial blood pressure as a result of vasodilatation. Recognized the presence of the same active principle in extracts of brain and spinal cord, substance P was finally identified chemically as an undecapeptide by Chang and Leeman in 1970. Soon after, radioimmunoassays and immunohistochemical methods were available to accurately study the distribution of the peptide in different tissues (see Euler and Pernow, 1977).

The presence of substance P (SP) in the carotid body (CB) was established by the end of 1980 (see McDonald 1981; Fidone and Gonzalez 1986) on the basis of immunocytochemical studies, but discrepancies regarding the precise localization of the peptide were soon evident. Thus Cuello and McQueen (1980) found that, in addition to nerve fibers, around 20% of cat CB chemoreceptor cells were immunoreactive for SP, but Lundberg et al. (1979) and Wharton et al. (1980) reported that chemoreceptor cells in the same species were negative to SP, being the neuropeptide limited to the nerve fibers in the organ; the same findings were reported by Jacobowitz and Helke (1980) in the rat. Chen *et al.* (1986) found some immunopositive chemoreceptor cells in the cat but none in the rat. In an interesting study Scheibner et al., (1988) reported that chemoreceptor cells were negative to SP at birth, then acquired the neuropeptide

*Chemoreception*, Edited by Pequignot et al.
Kluwer Academic/Plenum Publishers, New York, 2003

during the first six weeks of postnatal life, with the immunopositivity decreasing thereafter; it was suggested that substance P might have been released from the nerve fibers and taken up by chemoreceptor cells. Prabhakar *et al.* (1989) working in the cat found that most chemoreceptor cells were immunoreactive to SP and neurokinin A. In humans, Smith et al. (1990) reported faint SP immunoreactivity of chemoreceptor cells in 16 out of 24 human CBs, but Kummer and Habeck (1991) only showed SP in nerve fibers. Wang *et al.* 1992, 1998) observed that over 70% of chemoreceptor cells in the cat were immunostained for SP, and that chronic hypoxia produced a marked decrease in the immunoreactivity to peptide. In the rabbit CB, Kusakabe *et al.* (1994) reported absence of immunoreactivity in chemoreceptor cells but the sensory innervation of the CB (fibers surrounding the parenchymal clusters) was rich in SP; comparable observations were made by Pizarro et al. (1995) in the goat CB. However, Kim *et al.* (2001) found that all or most rabbit CB chemoreceptor cells exhibit SP immunoreactivity, existing cells with strong and others with light reaction.

Using a different experimental approach, namely *in situ* hybridization techniques, Gauda *et al.,* (1996, 1998) have reported the absence of mRNA codifying for SP and neurokinin A (i.e, preprotachykinin A mRNA; Severini *et al.,* 2002) in chemoreceptor cells of the rat CB both in normoxic conditions and after a hypoxic exposure capable of increasing the transcription of the tyrosine hydroxylase gene. The same authors (Gauda *et al.,* 1998; see Gauda 2002) found that NK-1 receptor mRNA is absent in CB chemoreceptor cells, but it is present in a few petrosal ganglion neurons. Altogether the findings of Gauda and coworkers have led them to conclude that in the rat, SP cannot be considered an excitatory neurotransmitter between chemoreceptor cells and sensory nerve endings, because it is not made in chemoreceptor cells of this mammalian species; similarly SP can not modulate CB chemoreceptor function by acting presynapticaly on NK-1 receptors because the cells do not express the receptors. However, this does not imply that SP can not act on chemoreceptor cells because it can be released from the sensory nerve endings when they are activated and bind to nicotinic receptors to modulate their function (Mc Queen 1980; Clapham and Neher 1984; Livett and Marley 1993; Fitzgerald and Shirahata, 1994; Stafford *et al.,* 1998; Andoh *et al.,* 2001). In this regard the most common finding is that SP inhibits the effects of nicotine on CSN (Carotid Sinus Nerve) discharge (but see below). Consistent with that inhibitory role Fidone et al., (1990) showed that SP, at $10^{-6}$ M, greatly inhibited the release of catecholamines induced by nicotine in the cat CB.

The levels of SP have been reported for the cat, rabbit and human CBs. In the cat, Wharton *et al.*,(1980) and Prabhakar *et al.*,(1989) reported comparable

levels of 54 and 57 pmol/g tissue, and in the last paper was also found that the CB contains 85 pmol/g tissue of neurokinin A. In the rabbit CB, Hanson et al., (1986) found levels of ≈ 295 pmol/g tissue and more recently Kim *et al.* (2001) have reported lower values of ca. 48 pmol/g tissue. According to Hanson et al. (1986) SP levels in the rabbit CB decreased nearly 40% following hypoxic stimulation in vivo (5% $O_2$, 1 hour) and Kim *et al.* , (2001) reported a moderate increase in the release (basal x 2) during intense hypoxic stimulation in vitro. Interestingly enough the same laboratory (Prabhakar *et al.*, 1989) has previously reported a complex pattern of presumable release by hypoxia in the cat CB: neurokinin A levels were not affected by hypoxia, but were reduced by ≈ 60% after 1 hr of breathing 100% $O_2$ and SP levels increased three-fold after 1 hour of intense hypoxia in vivo but were not affected by 100% $O_2$ breathing. In the human CB the levels were smaller (16 pmol/g tissue; Heath et al.,1988), but the time elapsing between dead and tissue removal for analysis might explain the lower values.

Indirect evidence for SP release has been obtained by Prabhakar *et al.*, (1984, 1987, 1990, 1993, 1995), Cragg *et al.*, (1993, 1994) and De Sanctis *et al.*, (1994) by showing that substance P antagonists inhibit the CSN or the ventilatory response to hypoxic stimulation of the cat and rat CB. These experiments in fact would impinge on two relevant aspects of SP: 1) SP must be released, i.e., SP must be present in the extracellular milieu in order for the peptide (and non-peptide) inhibitors to interfere with its binding and action, and 2) endogenous SP must be excitatory at the chemoreceptor cell/sensory nerve ending complex because the interference with its action results in a decrease of the response to natural stimulation. Interestingly enough, in several studies of Prabhakar laboratory it has been found that SP antagonists reduce the response to hypoxa but not to hypercapnic stimuli, implying either that SP is not released in response to hypercapnic stimulus or that either SP or the antagonists are not active during hypercapnic stimulation. Similar conclusions can be attained from experiments in which inhibitors of neutral endopeptidase, which is responsible for SP degradation, increase the response to physiological stimuli in the cat (Kumar 1997; Kumar *et al.*, 2000) and mouse (Grassemann *et al.*, 1999).

Unfortunately other researchers did not confirm the inhibitory effects of SP antagonists. Thus, McQueen and Evrard (1990) showed that the DPDT-SP, a SP antagonist, was ineffective to alter the response to hypoxia whereas in Prabhakar *et al.* (1990) study it was able to abolish the response to hypoxia. In the same study Prabhakar et al. showed that the DPDT-SP did not alter the response to nicotine, implying that SP is not present in the extracellular milieu during nicotinic stimulation because exogenous substance P inhibits the response to nicotine (see Fitzgerald and Shirahata 1994; McQueen 1980); alternatively, it is possible that the antagonist is not effective to block the action of SP at the nicotinic receptor (Stafford *et al.*,

1998). Additionally, Pizarro *et al.* (1995) showed that the SP antagonist CP-96,345 increased the hypoxic ventilatory response in the goat; it should be mentioned that in this species SP depresses ventilation. We should also stress the marked difference in reported effectiveness of the SP antagonist CP-96,345 to alter CB chemoreceptor responses: in the cat, at a dose of 0.3-0.6 mg/Kg it inhibited by over 70% the CSN response to hypoxia (Prabhakar *et al.*, 1993); De Sanctis *et al.*, 1994) required doses of 10 mg/Kg to inhibit the hypoxic ventilatory response by 22% in the rat. Finally it should be mentioned that this non-peptide antagonist of SP is capable of inhibiting $Na^+$ and $Ca^{2+}$ channels (Caeser *et al.*, 1993; Schmidt *et al.*, 1992). To complete the picture, Monti-Bloch and Eyzaguirre (1985) found that SP in the cat CB in vitro increased basal activity at low concentrations ($<10^{-6}$ M) but was inhibitory at higher concentrations; at $10^{-6}$ M it inhibited the excitation produced by hypoxia and cyanide.

A final aspect that we should address in this introductory overview deals with the identity of SP (tachykinin) receptor(s) present in the CB and mediating the responses to this neuropeptide. By using antagonists, McQueen and Evrard (1990) and Prabhakar *et al.*, (1990) implied that SP excitation of CB chemoreceptors in the cat was probably mediated by NK-1 receptors. Soon after, Prabhakar *et al.* (1990) in a study in which the order of potency of different tachykinins was established, could conclude that NK-1 in fact was actually the receptor involved in the genesis of SP effects in the CB. The same conclusion was reached in studies with rat CB, where selective antagonists of NK-1 receptors abolished the response to injected SP and attenuated the response to hypoxia. Since chemoreceptor cells do not express NK-1 receptors (Gauda *et al.*, 1998; Gauda 2002) the actions of SP must be mediated by receptors located on the sensory nerve endings or by modulating the activity of nicotinic receptors located on chemoreceptor cells or sensory nerve endings. However, since SP is not synthesized in chemoreceptor cells (Gauda *et al.*, 1996, 1998), SP present in chemoreceptor cells must be taken up probably by endocytosis from the SP released from the sensory nerve endings; in this case SP would act as a false neurotransmitter to mediate its actions, although part of the actions of SP could be vascularly mediated (Monti-Bloch and Eyzaguirre, 1985).

In an attempt to clarify the possible significance of substance P in the chemoreception process we have designed the present study with mice lacking functional NK-1 receptors, which are known to mediate the actions of SP in the CB chemoreceptors in those species in which the tachykinin receptors have been characterized.

## 2. MATERIAL AND METHODS

We have used *in vitro* CB preparations from homozygous female mice of 6-8 weeks of age which NK-1 receptor gene has been disrupted at the first exon (see De Felipe *et al.*,1998) and genetically identical mice with intact NK-1 receptors as controls. The NK-1 null animals do not exhibit any special phenotype trait, and reproduce normally. After deep anesthesia with sodium pentobarbital (60 mg/Kg, i.p.) the animals were decapitated and the CB preparations consisting in the complex formed by the CB-CSN-glossopharyngeal nerve-petrosal ganglion were dissected free of surrounded tissue as previously described (Donnelly and Rigual, 2000). The preparations were transferred to a recording chamber and perfused with saline of different compositions and equilibrated at different $PO_2$ to record electrical activity extracellularly in the petrosal ganglion neurons with a ≈30 μm tip glass electrode and the release of catecholamines with a 5 μm tip carbon fiber placed inside the CB tissue (Rigual et al., 2000). A third electrode to measure de $PO_2$ in the superfusing saline equilibrated with the desired gas mixture was placed in the vicinity of the CB in the recording chamber. Acquisition and analysis of the data were computer assisted using WPI Datasponge software. Catecholamine levels in the CBs were measured as previously described (Vicario *et al.*, 2000).

## 3. RESULTS

Figure 1 shows sample records of $PO_2$, instantaneous CSN frequencies and a sample neurogram (part A) and $PO_2$ and carbon electrode responses (part B) obtained in CBs from wild type NK-1 (+/+) and a knock-out NK-1 (-/-) mice. No differences were noticeable in the difficulty to obtain the records nor in the responses recorded.

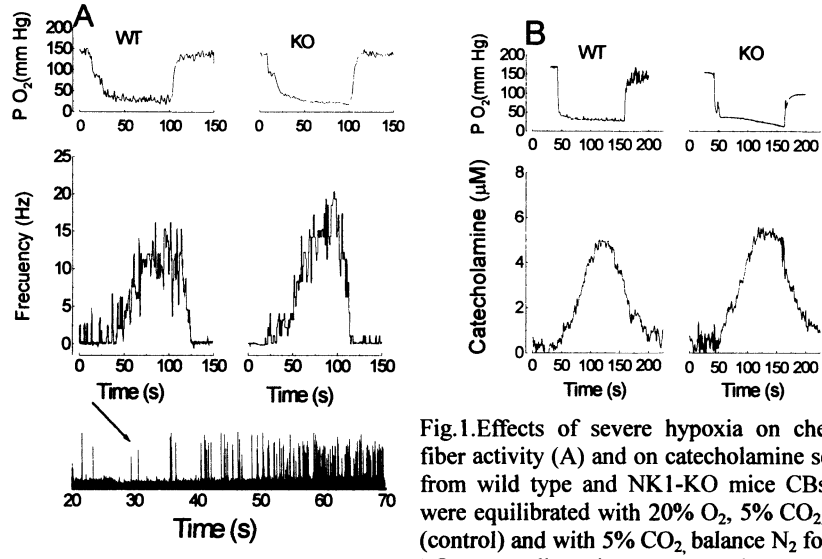


Fig.1.Effects of severe hypoxia on chemoreceptor fiber activity (A) and on catecholamine secretion (B) from wild type and NK1-KO mice CBs. Solurions were equilibrated with 20% $O_2$, 5% $CO_2$, balance $N_2$ (control) and with 5% $CO_2$, balance $N_2$ for (hypoxia). $PO_2$ recording is represented at the top. A poligraphic tracing of extracellular unit activity is also represented at the bottom.

Mean results from several experiments similar to that shown in Figure 1 are summarized in Table 1. The catecholamine content in the entire organ, as well as the peak intraglomic catecholamine concentration reached during hypoxic stimulation, was not different statistically between both groups of animals. Similarly, the basal activity and the peak responses obtained during hypoxic stimulation in the CSN were statistically identical. In other groups of experiments it the activity of the CSN was also assessed at a milder level of hypoxic stimulation, and no differences in the response were noticed, implying that there is not any shift in the threshold of the response.
As shown in Figure 1 there are not apparent differences between control and knock-out animals in the time courses of the changes in the CSN action potential frequency on switching the perfusion from normoxic to hypoxic solutions.

*Table 1.* Main findings in NK-1 receptors KO and in their control mice (means± SEM; in parenthesis is the sample size).

| | Wild type mice | NK-1(-/-) mice | Significance |
|---|---|---|---|
| Catecholamine content (pmole/CB) | DA 4.5 ± 0.4 (4)<br>NE 0.5 ± 0.07 (4) | DA 5.4 ± 0.7 (4)<br>NE 0.5 ± 0.04 (4) | n.s.<br>n.s. |
| Peak intraglomic catecholamine concentration (μM) at a $PO_2$ of ≈25 mmHg. | 4.3 ± 0.6 (9) | 4.9 ± 0.8 (13) | n.s. |
| Basal CSN activity (Hz) | 0.6 ± 0.2 (16) | 0.7 ± 0.2 (16) | n.s. |
| Peak CSN response to Hypoxia ($PO_2$ ≈25 mmHg ) | 19.8 ± 2.3 (8) | 21.5 ± 3.6 (8) | n.s. |

## 4. DISCUSSION

The present study shows that the elimination of the NK-1 receptor in mice by genetic manipulation of the animals does not alter the CB function in normal conditions nor does it alter the ability of the CB chemoreceptors to respond to hypoxia. The hypercapnic/acidotic stimuli were not studied in the present work because according to Prabhakar and coworkers (see Introduction) NK-1 antagonists do not mediate the CB responses to these stimuli. Since intraglomic NK-1 receptors would be located in the sensory fibers of the CSN, the present findings indicate that their absence does not modify the output of the CB chemoreceptors during normoxic and hypoxic conditions. Additionally, our data also show that the normality of the CB output at the CSN level is not the result of a compensatory mechanism at the

chemoreceptor cell level, because chemoreceptor cells from the NK-1 receptor null animals and control animals appear to behave identically in normoxic and hypoxic conditions and during non-specific stimulation with high external $K^+$ (Rigual *et al.*, 2002).

In conclusion, our study demonstrates a normal functionality of the CB chemoreceptors in mice lacking NK-1 receptors, and excluding possible interspecies variations and/or unrecognized compensatory mechanisms triggered by the absence of the NK-1 receptors, our findings do not support an all-important role for SP in the setting the CB chemoreceptor responses.

## ACKNOWLEDGEMENTS

Supported by Grants from the FIS (01/0728) and J. Castilla y León (VA46/00B) to R. Rigual, DGICYT (BFI2001-1713) to C. Gonzalez. And RED RESPIRA (FISS)

## REFERENCES

Andoh, T., Itoh, H., Watanabe, I., Sasaki, T., and Higashi, T., 2001, Mechanisms of modulation of neuronal nicotinic receptors by substance P and OAG. *Am. J. Physiol. Cell Physiol.* 281:1871-1880.

Caeser, M., Seabrook, G.R. and Kemp, J.A., 1993, Block of voltage-dependent sodium currents by the substance P receptor antagonist CP-96,345 in neurones cultured from rat cortex. *Br. J. Pharmacol.*109: 918-924.

Chang, M.M., and Leeman, S.E., 1970, Isolation of a sialogogic peptide from bovine hypothalamic tissue and its characterization as substance P.*J Biol. Chem.* 245:4784-4790.

Chen, I.I., Yates, R.D., and Hansen J.T., 1986, Substance P-like immunoreactivity in rat and cat carotid bodies: light and electron microscopic studies. *Histol. Histopathol.* 1:203-212.

Clapham, D.E., and Neher, E., 1984 Substance P reduces acetylcholine-induced currents in isolated bovine chromaffin cells.*J. Physiol.* 347:255-277.

Cragg, P.A., Kou, Y.R., and Prabhakar, N.R., 1993, Role of substance P in rat carotid body responses to hypoxia and capsaicin. *Adv. Exp. Med. Biol.* 337:265-270.

Cragg, P.A., Runold, M., Kou, Y.R., and Prabhakar, N.R., 1994, Tachykinin antagonists in carotid body responses to hypoxia and substance P in the rat. *Respir Physiol.* 95:295-310.

Cuello, A.C., and McQueen, D.S., 1980, Substance P: a carotid body peptide. *Neurosci.Lett.* 17:215-219.

De Felipe, C., Herrero, J.F., O'Brien, J.A., Palmer, J.A., Doyle, C.A., Smith, A.J., Laird, J.M., Belmonte, C., Cervero, F., and Hunt, S.P., 1998, Altered nociception, analgesia and aggression in mice lacking the receptor for substance P. *Nature.* 392:394-397.

De Sanctis, G.T., Green, F.H., Jiang, X., King, M., and Remmers, J.E., 1994, Ventilatory responses to hypoxia in rats pretreated with nonpeptide NK1 receptor antagonist CP-96,345. *J. Appl. Physiol.* 76:1528-1532.

Donnelly, D.F., and Rigual, R., 2000, Single-unit recordings of arterial chemoreceptors from mouse petrosal ganglia in vitro. *J. Appl. Physiol.* 88:1489-1495.

Euler, U. S., and Gaddum, J.H., 1931, An unidentified depressor substance in certain tissue extracts. *J Phisiol.* 72:74-87.

Euler, U.S., and Pernow, B., 1977, *Substance P Nobel Sympoium 37.* Raven Press, New York.

Fidone, S., and Gonzalez, C., 1986, Peripheral Chemoreceptors: Initiation and Control of Discharges. In *Handbook of Physiology. The Respiratory System II.* (A.P. Fishman eds.), Amer. Physiol. Soc. Bethesda, Maryland, pp. 247.

Fidone, S., Gonzalez, C., Obeso, A., Gomez Niño, A., and Dinger, B., 1990, Biogenic amine and neuropeptide transmitters in carotid body chemotransmission: Experimental Findings and Perspectives. In *Hypoxia* ( J.R. Sutton et al.eds.) B.C. Decker Inc., Toronto, pp. 116.

Fitzgerald, R.S., and Shirahata, M., 1994, Acetylcholine and carotid body excitation during hypoxia in the cat. *J. Appl Physiol.* 76:1566-1574.

Gauda, E.B., 2002, Gene expression in peripheral arterial chemoreceptors. *Microsc. Res. Tech.* 59:153-167.

Gauda, E.B., Bamford, O., and Gerfen, C.R., 1996, Developmental expression of tyrosine hydroxylase, D2-dopamine receptor and substance P genesin the carotid body of the rat. *Neuroscience.* 75:969-977.

Gauda, E.B., Bamford, O.S., and Northington, F.J., 1998, Lack of induction of substance P gene expression by hypoxia and absence of neurokinin 1-receptor mRNAs in the rat carotid body. *J Auton Nerv Syst.* 74:100-108.

Grasemann, H., Lu, B., Jiao, A., Boudreau, J., Gerard, N.P., and De Sanctis G.T., 1999, Targeted deletion of the neutral endopeptidase gene alters ventilatory responses to acute hypoxia in mice. *J. Appl Physiol.* 87:1266-1271.

Hanson, G., Jones, L., and Fidone, S., 1986, Physiological chemoreceptor stimulation decreases enkephalin and substance P in the carotid body. *Peptides* 7:767-769.

Heath D, Quinzanini M, Rodella A, Albertini A, Ferrari R, and Harris P., 1988, Immunoreactivity to various peptides in the human carotid body. *Res. Commun. Chem. Pathol. Pharmacol.*62:289-293.

Jacobowitz, D.M., and Helke, C.J., 1980, Localization of substance P immunoreactive nerves in the carotid body. *Brain Res. Bull.* 5:195-197.

Kim, D,K., Oh, E.K., Summers, B.A., Prabhakar, N.R, and Kumar, G.K., 2001, Release of substance P by low oxygen in the rabbit carotid body: evidence for the involvement of calcium channels. *Brain Res.* 892:359-369.

Kumar, G.K., 1997, Peptidases of the peripheral chemoreceptors: biochemical, immunological, in vitro hydrolytic studiesand electron microscopic analysis of neutral endopeptidase-like activity of the carotid body. *Brain Res.* 748:39-50.

Kumar, G.K., Kou, Y.R., Overholt, J.L., and Prabhakar, N.R., 2000, Involvement of substance P in neutral endopeptidase modulation of carotid body sensory responsesto hypoxia. *J. Appl. Physiol.* 88:195-202.

Kummer, W., and Habeck, J.O., 1991, Substance P- and calcitonin gene-related peptide-like immunoreactivities in the human carotid body studied at light and electron microscopical level. *Brain Res.* 554:286-92.

Kusakabe, T., Kawakami, T., Tanabe, Y., Fujii, S., and Takenaka, T., 1994, Distribution of substance P-containing and catecholaminergic nerve fibers in the rabbit carotid body: an immunohistochemical study in combination with catecholamine fluorescent histochemistry. *Arch. Histol. Cytol.* 57:193-9.

Livett, B.G., and Marley, P.D., 1993, Noncholinergic control of adrenal catecholamine secretion. *J. Anat.* 183:277-289.

Lundberg, J.M., Hokfelt, T., Fahrenkrug, J., Nilsson, G., and Terenius, L., 1979, Peptides in the cat carotid body (glomus caroticum): VIP-, enkephalin-, and substance P-like immunoreactivity. *Acta Physiol. Scand.* 107:279-81.

McDonald, D.M., 1981, Peripheral chemoreceptors: Structure-function rationships or the carotid body. In *Regulation of Breathing. Vol.17. Lung Biology in Health and Disease* (T.F. Hornbein and C. Lenfant, eds.), New York: Dekker, pp.1-29.

McQueen, D.S., 1980, Effects of substance P on carotid chemoreceptor activity in the cat. *J.Physiol.* 302:31-47.

McQueen, D.S. and Evrard Y., 1990, Use of selective antagonist for studying the role of putative transmitters in chemoreception. In *Arterial Chemoreception* (C. Eyzaguirre, S.J. Fidone, R.S. Fitzgerald, S. Lahiry and D.M. McDonald, eds.), Springer-Verlag, New York, pp.168-173.

Monti-Bloch, L., and Eyzaguirre, C., 1985, Effects of methionine-enkephalin and substance P on the chemosensory discharge of the cat carotid body. *Brain Res.* 338:297-307.

Pizarro, J., Ryan, M.L., Hedrick, M.S., Xue, D.H., Keith, I.M., and Bisgard, G.E., 1995, Intracarotid substance P infusion inhibits ventilation in the goat. *Respir. Physiol.* 101:11-22.

Prabhakar, N.R., Cao, H., Lowe, J.A. 3rd, and Snider, R.M., 1993, Selective inhibition of the carotid body sensory response to hypoxia by the substance P receptor antagonist CP-96,345. *Proc. Natl. Acad. Sci.* 90:10041-10045.

Prabhakar, N.R., Gauda, E., Kumar, G.K., and Kou, Y.R., 1995, Analysis of carotid chemoreceptor responses to substance P analogue in anaesthetized cats. *J. Auton. Nerv. Syst.* 52:43-50.

Prabhakar, N.R., Kou, Y.R, and Runold, M., 1990, Chemoreceptor responses to substance P, physalaemin and eledoisin: evidence for neurokinin-1 receptors in the cat carotid body.*Neurosci.Lett.* 120:183-186.

Prabhakar, N.R., Landis, S.C., Kumar, G.K., Mullikin-Kilpatrick, D., Cherniack, N.S., and Leeman, S., 1989, Substance P and neurokinin A in the cat carotid body: localization, exogenous effects and changes in content in response to arterial $PO_2$. *Brain Res.* 481:205-14.

Prabhakar, N.R., Mitra, J., and Cherniack N.S., 1987, Role of substance P in hypercapnic excitation of carotid chemoreceptors. *J Appl. Physiol.* 63:2418-2425.

Prabhakar, N.R., Runold, M., Yamamoto, Y., Lagercrantz, H., and von Euler, C., 1984, Effect of substance P antagonist on the hypoxia-induced carotid chemoreceptor activity. *Acta Physiol. Scand.* 121:301-303.

Rigual, R., Almaraz, L., Gonzalez, C. and Donnelly, D.F., 2000, Developmental changes in chemoreceptor nerve activity and catecholamine secretion in rabbit carotid body: possible role of Na+ and Ca+2 currents. *Pflugers Arch. – Eur. J. Physiol.* 439:463-470

Rigual, R., Rico, A.J., Prieto-Lloret, J., De Felipe, C., Gonzalez, C., and Donnelly, D.F., 2002, Chemoreceptor activity is normal in mice lacking the NK1 receptor..*Eur. J. Neurosci.* 16:2078-2084.

Scheibner, T., Read, D.J., and Sullivan, C.E., 1988, Distribution of substance P-immunoreactive structures in the developing cat carotid body. *Brain Res.* 453:72-78.

Schmidt, A.W., McLean S., and Heym, J., 1992, The substance P receptor antagonist CP-96,345 interacts with $Ca^{2+}$chanels. *Eur. J. Pharmacol.* 219: 491-492.

Severini C, Improta G, Falconieri-Erspamer G, Salvadori S, Erspamer V., 2002 The tachykinin peptide family.*Pharmacol. Rev.* 54:285-322.

Smith, P., Gosney, J., Heath, D., and Burnett, H., 1990, The occurrence and distribution of certain polypeptides within the human carotid body. *Cell Tissue Res.* 261:565-571.

Stafford GA, Oswald RE, Figl A, Cohen BN, Weiland G.A., 1998, Two domains of the beta subunit of neuronal nicotinic acetylcholine receptors contribute to the affinity of substance P.*J. Pharmacol. Exp. Ther.* 286:619-626.

Vicario, I., Rigual, R., Obeso, A., & González, C., 2000, Characterization of the synthesis and release of catecholamine in the rat carotid body in vitro. *Am. J. Physiol.* 278:490-495

Wang, Z.Z., Dinger, B., Fidone, S.J, and Stensaas, L.J., 1998, Changes in tyrosine hydroxylase and substance P immunoreactivity in the cat carotid body following chronic hypoxia and denervation. *Neuroscience.* 83:1273-1281.

Wang, Z.Z., Stensaas, L.J., Dinger, B., and Fidone, S.J., 1992, The co-existence of biogenic amines and neuropeptides in the type I cells of the cat carotid body. *Neuroscience.* 47:473-480.

Wharton, J., Polak, J.M., Pearse, A.G., McGregor, G.P., Bryant, M.G., Bloom, S.R., Emson, P.C., Bisgard, G.E, and Will, J.A., 1980, Enkephalin-, VIP- and substance P-like immunoreactivity in the carotid body. *Nature.* 284:269-271.

# Concomitant Effect of Acetylcholine and Dopamine on Carotid Chemosensory Activity in Catecholamine Depleted Cats

AIDA BAIRAM and YVES LAJEUNESSE
*Unité de recherche en périnatologie, Centre Hospitalier Universitaire de Québec, Hôpital Saint François d'Assise, Université Laval, Québec, PQ, Canada.*

## 1. INTRODUCTION

Carotid body chemotransduction mechanisms involve many neurotransmitters that are synthetized, stored, and released from the chemoreceptor cell. Acetylcholine (ACh) and dopamine (DA) are the main transmitters studied to date. It has been suggested that, at least in cats, ACh is an excitatory whereas DA is an inhibitory transmitter in the carotid body (as review see Eyzaguirre and Zapata, 1884; Fidone *et al.*, 1997; Fitzgerald, 2000). However, their role on chemosensory activity in response to hypoxia is still debated. Recently, in catecholamine-depleted cats where the storage and release of carotid body DA was greatly impeded by the use of ∝-methyl-paratyrosine and reserpine (Bairam and Marchal, in press), DA infusion was showed to inhibit the carotid sinus nerve chemosensory discharge rate (CSND) while ACh reversed the effect under basal condition. In response to hypoxia, DA slowed the initial increase of CSND whereas ACh accelerated it, while neither drug altered the steady-state chemosensory discharge under hypoxic conditions. One interpretation of these results was that DA infusion prevented the expression of ACh excitatory effect during hypoxia as it was infused before- and maintained throughout ACh administration. Using a similar model of adult cats pre-treated with ∝-methyl-paratyrosine and reserpine (Bairam and Marchal, in press), we investigated the effect of 1)

*Chemoreception*, Edited by Pequignot et al.
Kluwer Academic/Plenum Publishers, New York, 2003

ACh infusion on CSND response to different inspiratory oxygen concentrations ($FiO_2$) and 2) DA infusion while ACh is maintained. This protocol of drug administration should reveal the excitatory role of ACh on CSND under basal condition particularly in hypoxia. Indeed, the pre-treatment with ∝-methyl-paratyrosine and reserpine, which inhibits and depletes catecholamine synthesis and storage (Leitner and Roumy, 1986; Fitzgerald et al., 1983), should minimize the effects of endogenous release of DA on CSND.

## 2. MATERIALS AND METHODS

Studies were carried out in 7 adult cats aged 5-6 months. They received an i.p. injection of reserpine (5 mg/kg) 12h prior to the experiment and ∝-methyl-paratyrosine (250 mg/kg) every 2.5h throughout the experiment. The protocol was based on previous studies (Bairam and Marchal, in press). All details of the animal preparation, surgical procedure, technique for recording the discharge of a few chemosensory fibers of the carotid sinus nerve, and the apparatus used during experiments were similar to those described previously (Bairam and Marchal, in press). Anesthesia was induced with sodium pentobarbitone (35 mg/kg, i.p.) followed by maintenance dose of 3 - 5 mg/kg/min through a cannulated radial vein. Cats were ventilated artificially with a respiratory pump that the inspiratory gas mixture could be easily switched from 21% $O_2$ (air, normoxia) to 8% $O_2$ in $N_2$ (hypoxia) and to 100% $O_2$ (hyperoxia) (Bairam and Marchal, in press).

Experiment was started when both CSND rate and arterial blood pressure (ABP) were stable in normoxia. The control period was defined as the period before any drug infusion. Drug infusion was started while the cat was breathing air. ACh was then infused alone for 20 min (25 µg/kg/min) (Sigma/RBI, Oakville, Ontario, Ca) after which DA infusion was started throughout a separate vein and maintained concomitantly with Ach for an additional 20 min (5 µg/kg/min) (Intropin®, 200mg/5ml). The hypoxic response was evaluated by switching the $F_iO_2$ from air to hypoxia for 2-3 min and then to hyperoxia for 2-3 min in control period (i.e. before any drug infusion) and into 10 min of each of Ach and Ach + DA infusion.

The steady-state CSND and ABP were averaged over 1 min of stable recording in normoxia, hypoxia and hyperoxia. Also, CSND was averaged over the first 45 sec of exposure to hypoxia and the value was expressed as % of steady-state discharge and defined as initial CSND response to

hypoxia. Measurements of arterial blood gases (AVL 995) were obtained at steady-state of normoxia, hypoxia and hyperoxia, at control and during drug infusions.

Data are expressed as a mean ± SEM. Statistical analysis was performed using two-way-analysis of variance for repeated measurements (Stat View 4.5). A difference was considered as statistically significant at $p < 0.05$.

## 3. RESULTS

Measurements of pH, $PaO_2$, and $PaCO_2$ obtained at steady state during normoxia, hypoxia and hyperoxia are presented in Table 1. There was no difference of pH, $PaO_2$or $PaCO_2$ between control, ACh and ACh+ DA.

*Table 1.* Steady state arterial blood gases, pH, and arterial blood pressure at three $F_iO_2$ levels at control and during drug infusions.

| $FiO_2$ (%) | | Control | ACh | ACh+DA |
|---|---|---|---|---|
| 21 % | pH | 7.36 ± 0.01 | 7.37 ± 0.02 | 7.36 ± 0.01 |
| | $PaO_2$ (mmHg) | 106.8 ± 6.4 | 97.8 ± 4.2 | 96.8 ± 3.1 |
| | $PaCO_2$ (mmHg) | 34.9 ± 0.8 | 31.0 ± 1.8 | 34.7 ± 2.3 |
| | ABP (mmHg) | 93.9 ± 5.0 | 70.7 ± 2.2* | 67.1 ± 3.4* |
| 8 % | pH | 7.40 ± 0.01 | 7.40 ± 0.02 | 7.39 ± 0.02 |
| | $PaO_2$ (mmHg) | 31.8 ± 2.1 | 31.0 ± 0.8 | 30.4 ± 0.9 |
| | $PaCO_2$ (mmHg) | 30.0 ± 2.1 | 31.0 ± 1.9 | 33.5 ± 2.1 |
| | ABP (mmHg) | 79.8 ± 10.2 | 59.5 ± 2.8 | 56.9 ± 6.6* |
| 100 % | pH | 7.34 ± 0.01 | 7.36 ± 0.02 | 7.34 ± 0.01 |
| | $PaO_2$ (mmHg) | 539.0 ± 12.9 | 523.7 ± 30.1 | 493.5 ± 39.2 |
| | $PaCO_2$ (mmHg) | 38.6 ± 1.2 | 33.5 ± 1.7 | 34.4 ± 2.4 |
| | ABP (mmHg) | 104.3 ± 8.6 | 88.9 ± 2.1 | 86.1 ± 5.7 |

Values are mean ± sem for 7 cats. Acetylcholine (ACh); dopamine (DA); Arterial $PO_2$ ($PaO_2$); arterial $PCO_2$ ($PaCO_2$); arterial blood pressure (ABP). * $p > 0.05$ vs control.

Effects of ACh on CSND. The mean steady-state CSND of the 7 cats in normoxia, hyperoxia and hypoxia at control and during ACh infusion is presented in Fig 1 A and B. ACh increased CSND as compared with control in normoxia and hyperoxia (Fig. 1A, $p < 0.02$). Although ACh increased CSND in response to hypoxia, the difference was not significant compared with control (Fig. 1B), as also showed in the representative recording (Fig. 2).

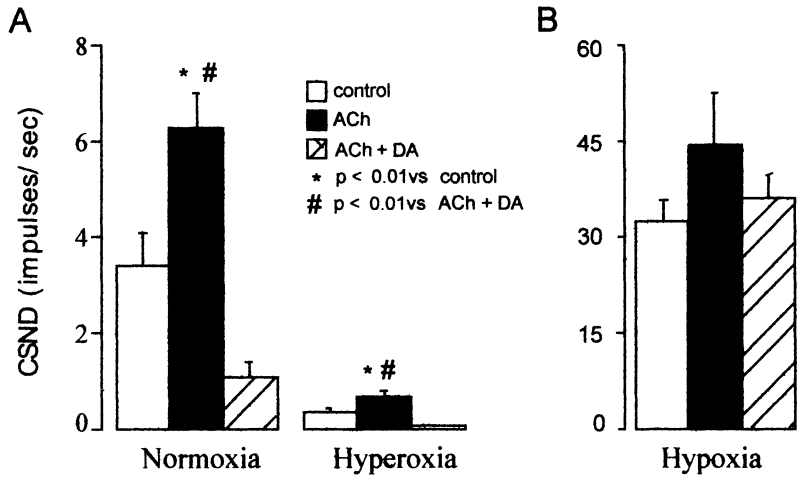


*Figure 1.* Steady-state carotid sinus nerve chemosensory response to drugs infusion. In normoxia and hyperoxia, acetylcholine (ACh) increases and dopamine (DA) decreases the carotid sinus nerve chemosensory discharge (CSND) compared with control (A). In hypoxia, CSND is not different among control, ACh and ACh + DA (B).

The initial increase of CSND in response to hypoxia was accelerated by ACh compared to control (50 ± 6% vs 38 ± 4%, $p < 0.01$) as illustrated in Fig. 2.

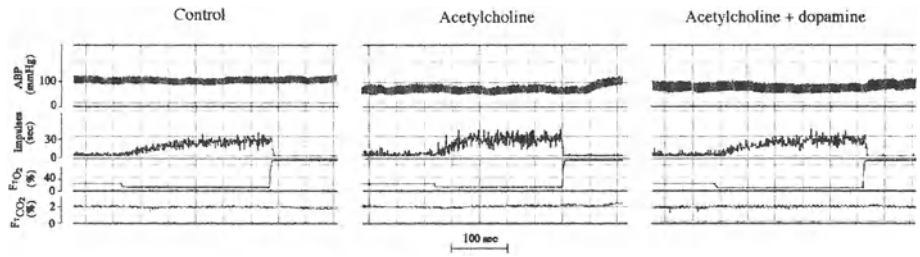


*Figure 2.* Representative recording of chemosensory response (CSND) to hypoxia at control, under acetylcholine (ACh) and acetylcholine + dopamine (DA) infusions. The CSND increases faster at the begining of the response to hypoxia with ACh compared to control and to ACh + DA. The steady-state CSND response to hypoxia is similar between control, ACh and ACh + DA. ABP : arterial blood pressure; $FtO_2$ and $FtCO_2$ : concentrations of $O_2$ and $CO_2$ in the tracheal gas.

Effects of ACh + DA on CSND. Addition of DA to the ongoing ACh infusion antagonized the excitatory effect of ACh and decreased CSND

in both normoxia and hyperoxia compared to control ($p < 0.02$) or to ACh alone ($p < 0.03$, Fig. 1A). In hypoxia, although DA decreased CSND to near control level, CSND was not significantly different compared with ACh alone (Fig. 1B and Fig. 2). The initial CSND increase in response to hypoxia was not significantly different compared to ACh or to control (46 ± 3%) (Fig. 2).

ABP changes by ACh and ACh+DA (Table 1). In normoxia, ACh decreased ABP below control ($p < 0.05$). This decreasing in ABP by ACh was maintained with the addition of DA ($p < 0.05$ vs control). In hypoxia, ABP was lower than control only when DA was added to ACh. ABP was not different between control and ACh or ACh+DA infusion in hyperoxia.

## 4. DISCUSSION

Our findings show that in ∝-methyl-paratyrosine and reserpine pre-treated cats, ACh increases CSND under basal condition. In response to hypoxia, ACh accelerates the initial increase of CSND without changing the steady-state chemosensory activity. DA antagonizes the excitatory effects of ACh in normoxia and hyperoxia and induces no change of steady-state chemosensory activity in hypoxia.

When ABP was reduced below control with ACh and with ACh+DA, CSND was respectively higher and lower than control in normoxia. Indeed, when ABP was not affected by drugs infusion in hyperoxia, CSND was increased with ACh and decreased with ACh+DA. In hypoxia, ABP was lower than control only with the addition of DA while CSND was similar to control, to ACh and to ACh+DA. It seems unlikely that ABP changes influenced CSND in this study. Mitchel and McCloskey (1974) showed that a small proportion of chemoreceptor fibers are affected by decreasing ABP below 50 mmHg and that drugs inducing haemodynamic changes did not significantly modify CSND in cats (Docherty and McQueen, 1979).

Reserpine and ∝-methyl-paratyrosine were used to reduce catecholamine stores and synthesis. Despite this treatment, control CSND could be recorded at the three $FiO_2$ as previously showed (Bairam and Marchal, in press), indicating that catecholamine is not mandatory to initiate the chemosensory activity. Recent studies proposed ACh as an excitatory transmitter in the carotid body (see for review Fitzgerald, 2000). In normoxia and hyperoxia, our results are consistent with such excitatory effect of ACh. They further indicate that ACh contribution to the initiation of the chemoreceptor activity may occur when carotid body catecholamine content

is largely depleted. In cat, many pharmacological studies suggested that ACh enhances the CSND response to hypoxia (see for review Eyzaguirre and Zapata, 1984; Fitzgerald, 2000). Although ACh failed to increase the steady state chemosensory response to hypoxia, it was found to accelerate the dynamic of this response suggesting that ACh plays a significant role in the initiation of the hypoxic response. The failure to demonstrate that ACh enhances steady-state CSND response to hypoxia may be related, at least in part, to the variability in the individual responses observed with ACh, as the CSND was only increased in 4/7 cats. Also, part of this discrepancy may be related to a differences in experimental model, in vivo (present study) vs isolated carotid body *in vivo* (see for review Fitzgerald, 2000) or *in vitro* (Iturriaga *et al.*, 2000). Finally, ACh stimulates both nicotinic and muscarinic receptors in the carotid body. Nicotinic receptor stimulation was repeatedly shown to increase CSND in cat whereas muscarinic receptor activation was suggested to control DA, ACh and/or other transmitters release from the carotid body (see for review Fitzgerald, 2000; Bairam *et al.*, 2000).

The interesting observation made here is that DA not only reversed the excitatory effect of ACh but induced a strong inhibitory effect as it decreased CSND below control level under basal condition of normoxia and hyperoxia. These results are in line with the known inhibitory effect of exogenously applied DA on CSND (Fidone *et al.*, 1997) but also indicate that endogenously released DA may modulates the chemosensory activity as previously suggested (Bairam and Marchal, in press) and controls the excitatory effect of ACh, in particular, at the beginning of exposure to hypoxia. The overall results suggest that an interaction between ACh and DA regulates the initiation of chemosensory response to hypoxia while the steady-state response may depend on other factors.

It is concluded that ACh increases CSND whereas DA antagonizes ACh excitatory effects and these are stimulus-dependent.

## ACKNOWLEDGEMENTS

This work was supported by the Téléthon de la recherche sur les maladies infantiles. A. B. is Research Scholar of the Research Center, HSFA. We thank Dr R. Kinkead for his valuable help reviewing the manuscript.

# REFERENCES

Bairam A., and Marchal F., Carotid sinus nerve chemosensory response to dopamine and acetylcholine in catecholamine depleted cats. *Respir. Physiol. Neurobiol.* In press.

Docherty, R.J., and McQueen S., 1979, The effects of acetylcholine and dopamine on carotid chemosensory activity in the rabbit. *J. Physiol.* 288, 411-423.

Eyzaguirre, C., and Zapata,P., 1984, Perspectives in carotid body research. *J. Appl. Physiol.* 57, 931-957.

Fidone, S.J., Gonzalez, C., Almaraz, L., Dinger B., 1997, Cellular mechanisms of peripheral chemoreceptor function. In: *The Lung*, vol. 2, Crystal, R.J., West, J.B., Barnes, P.J., and Weibel, E.R., (eds), Lippincott-Raven, Philadelphia, New York, pp 1725-1746.

Fitzgerald, R.S., 2000, Oxygen and carotid body chemotransduction: the cholinergic hypothesis - a brief history and new evaluation. *Respir. Physiol.* 120, 89-104.

Fitzgerald, R.S., Garger, P., Hauer, M.C., Raff, H., Fecheter, L., 1983, Effect of hypoxia and hypercapnia on catecholamine content in cat carotid body. *J. Appl. Physiol.* 54, 1408-1413.

Iturriaga, R., Alcayaga, J., Zapata, P., 2000, Lack of correlation between cholinergic-induced changes in chemosensory activity and dopamine release from the cat carotid body in vitro. *Brain Res.* 868, 380-385.

Leitner, L.M., and Roumy, M., 1986, Chemoreceptor response to hypoxia and hypercapnia in catecholamine depleted rabbit and cat carotid bodies in vitro. *Pflüger Arch.* 406, 419-423.

Mitchell, J.H., and McCloskey, D.I., 1974, Chemoreceptor responses to sympathetic stimulation and changes in blood pressure. *Respir. Physiol.* 20, 297-302.

# Contribution of Neural and Endothelial Isoforms of the Nitric Oxide Synthase to the Inhibitory Effects of NO on the Cat Carotid Body

VIVIANA VALDES, MATIAS MOSQUEIRA, and RODRIGO ITURRIAGA
*Laboratorio de Neurobiología, Facultad de Ciencias Biológicas, P. Universidad Católica de Chile,. Santiago 1, Chile.*

## 1. INTRODUCTION

Nitric oxide (NO) produced within the carotid body (CB) is an inhibitory modulator of hypoxic chemoreception (Chugh *et al.,* 1994; Wang et al., 1994, 1995; Iturriaga *et al.,* 1998). Administration of NO donors and NO gas to the cat CB reduces the chemosensory response to hypoxia (Chugh *et al.,* 1994; Iturriaga *et al.,* 1998; Iturriaga *et al.,* 2000b). Conversely, the inhibition of nitric oxide synthase (NOS) increases the frequency of carotid chemosensory discharges ($f_x$) in the cat CB *in situ* and *in vitro* (Wang *et al.,* 1994; Iturriaga *et al.,* 1998). It has been proposed that NO produce vasodilatation in the CB (Chugh *et al.,* 1994; Wang *et al.,* 1994; Lahiri and Buerk, 1998), retrograde inhibition of glomus cell's excitability (Wang *et al.,* 1994), inhibition of glomus cell's $Ca^{+2}$ channels activity (Summers *et al.,* 1999), modulation of petrosal ganglion neurons excitability (Alcayaga *et al.,* 1997), and inhibition of mitochondrial metabolism (Iturriaga *et al.,* 2000b). In the CB, the endothelial NOS (eNOS) is located in the endothelial cells and the neuronal (nNOS) in the sensory terminals of C fibers and parasympathetic neurons (Chugh *et al.,* 1994; Wang *et al.,* 1994, 1995).

The contribution of nNOS and eNOS isoforms to the production of NO in the CB has been assessed indirectly by testing the effect of the pharmacological and genetic suppression of these NOS isoforms activities

*Chemoreception*, Edited by Pequignot et al.
Kluwer Academic/Plenum Publishers, New York, 2003

on ventilatory responses induced by hypoxia and NaCN. Gozal et al. (1996) found that the specific nNOS inhibitor S-methyl-L-thiocitrulline did not modify rat ventilatory responses induced by NaCN, but the non-specific NOS inhibitor L-NAME significantly enhanced them. In contrast, Kline et al. (1998, 2000) using mutant mice deficient in nNOS and eNOS exhibited great respiratory responses to hypoxia and NaCN than wild type, while the hypoxic response was attenuated in mutant mice lacking eNOS compared with the wild type. But these studies measured the effects of NOS isoforms on ventilation, not on CB chemosensory discharges. Thus, we studied the effects of NO and the pharmacological inhibition of nNOS and eNOS on the cat CB chemosensory response to hypoxia, nicotine and NaCN. We compared the effects of the non-selective NOS inhibitor L-NAME, and the specific nNOS inhibitor 1-(2-trifluoromethylphenyl) imidazole (TRIM) on the chemosensory response to hypoxia, and to several doses of nicotine and NaCN. The experiments were performed using an in vitro preparation of the cat CB perfused at constant pressure (Iturriaga *et al.,* 2000a) to avoid cardiovascular and respiratory systemic effects produced by NO donor and NOS inhibitors.

## 2. METHODS

Experiments were performed on adult cats (2-4 kg) anesthetized with sodium pentobarbitone (40 mg/kg ip, followed by additional iv doses). The carotid bifurcation including the CB and the carotid sinus nerve was perfused *in vitro* with Tyrode, as previously described (Iturriaga *et al.,* 2000a). The carotid bifurcation was cannulated through the common carotid artery, excised and placed in a chamber. The CB was perfused with Tyrode at 38.5 ± 0.5°C and pH 7.40, equilibrated with 20% $N_2$ and 5% $CO_2$ and simultaneously superfused with Tyrode equilibrated with 95% $N_2$ and 5% $CO_2$. Chemosensory discharges were recorded from the carotid nerve placed on a pair of platinium electrodes lifted into mineral oil. The neural signals were preamplified, amplified, filtered and fed to an electronic amplitude discriminator. Selected chemosensory impulses were counted to assesses $f_x$ expressed in Hz. The $f_x$ signal was digitized with an analog-digital board DIGIDATA 1200 (Axon Instruments). Chemosensory responses were expressed as the summation of chemosensory discharges over baseline ($\Sigma f_x$). The sensitivity and reactivity of responses to nicotine (0.01-100μg) and NaCN (0.01-100μg) were studied before (control) and during the perfusion with Tyrode with L-NAME (1mM), or TRIM (100μM). Chemosensory responses to hypoxic perfusion ($PO_2$ ≈30 torr) were measured in the same CBs before (control) and during perfusion with Tyrode with TRIM (100μM) and with L-NAME (1mM) for 15 min. Data were expressed as means ± SE.

Responses were expressed as percentages of their maximal control response, which correspond to the maximal chemosensory discharge attained with the larger doses of nicotine and NaCN. Statistical differences between dose-response curves for all conditions were analyzed by two-way ANOVA with repeated measures, and pos hoc analyses were performed by the Bonferroni test. Difference for two samples was assessed with the Student's t-test.

# 3. RESULTS

## 3.1 Effects of L-NAME and TRIM on chemosensory responses induced by nicotine.

Perfusion with Tyrode with L-NAME (1mM) increased the chemosensory response ($\Sigma f_x$) to nicotine due to an increase in the duration of the responses. In contrast, TRIM did not increase $\Sigma f_x$ induced by the same doses of nicotine. Fig. 1 summarizes the effects of L-NAME and TRIM on the dose-response curves for nicotine in 6 CBs.

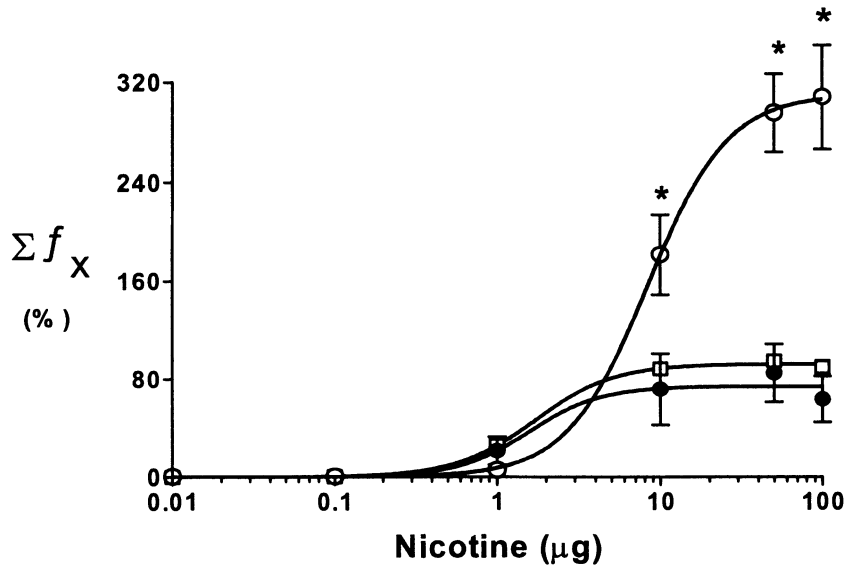


*Figure 1.* Comparison of the effects of L-NAME (○) and TRIM (●) on the control chemosensory dose-response curve (□) for nicotine. $\Sigma f_x$, Summation of carotid chemosensory discharge over baseline. *, $p < 0.01$ Bonferroni test after two-way ANOVA between L-NAME and TRIM to the control dose-response curve.

Nicotine produced a higher maximal response in the presence of L-NAME than TRIM (max$\Sigma f_x$ of 309.8 ± 26.7 vs. 74.2 ± 12.6%, $p < 0.05$) but both curves had similar $ED_{50}$ (8.2± 2 and 1.6 ± 0.6 μg for L-NAME and TRIM, respectively). The chemosensory responses induced by nicotine in doses equal or larger than 10μg were significantly higher ($p< 0.01$) in the presence of L-NAME. Thus, the blockade of both eNOS and nNOS with L-NAME produced a large increased in the reactivity of the dose-response curve induced by nicotine as compared to the blockade of nNOS alone.

## 3.2 Effects of L-NAME and TRIM on chemosensory responses induced by NaCN.

The chemosensory responses ($\Sigma f_x$) induced by NaCN in doses equal or larger than 1 μg were significantly higher ($p< 0.01$) in the presence of L-NAME than TRIM or control condition (Fig. 2). Multiple comparison with Bonferroni test indicated that the chemosensory responses induced with the doses lower than 10μg, were higher in the presence of L-NAME than in the presence of TRIM ($p < 0.01$). The $ED_{50}$ in the presence of TRIM and L-NAME were 54.3 ± 0.6 and 1.1 ± 0.6% μg, respectively ($p < 0.05$, t-test).

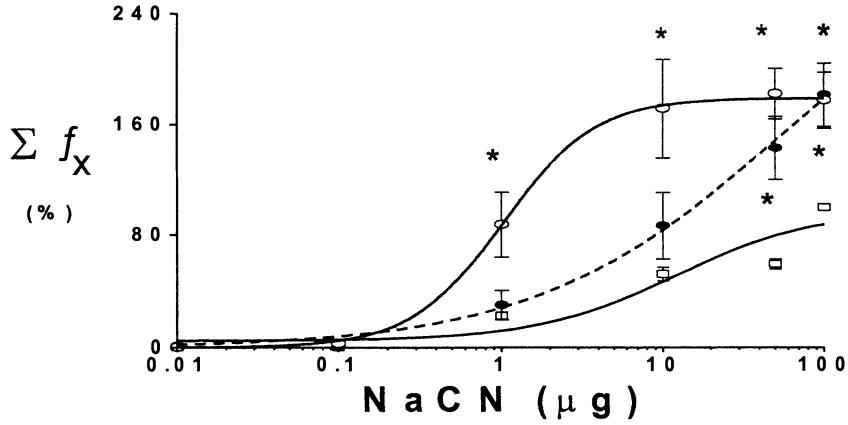


*Figure 2.* Comparison of effects of L-NAME (O) and TRIM (●) on the control chemosensory dose-response curve (□). $\Sigma f_x$, Summation of carotid chemosensory discharge over baseline. *, $p < 0.01$ Bonferroni test after two-way ANOVA, between L-NAME and TRIM to the control dose-response curve.

## 3.3 Effects of TRIM and L-NAME on the chemosensory response to hypoxia.

Fig. 3 summarizes the effects of L-NAME and TRIM on the response to hypoxic perfusion ($PO_2 \approx 30$ torr for 2 min) in 4 CBs. During perfusion with Tyrode containing L-NAME (1mM) the maximal hypoxic response increased. On the contrary, during perfusion with Tyrode with TRIM (100μM), the maximal chemosensory response to hypoxia was smaller –but not significantly different- than the control response. Multiple comparisons with the Bonferroni test after one-way ANOVA ($p < 0.01$) indicated that the chemosensory response to hypoxia was higher in the presence of L-NAME than in the presence of TRIM, or during control perfusion ($p < 0.05$). In fact, during control perfusion max$f_x$ was 344.5 ± 19 Hz, and in the presence of L-NAME and TRIM, max$f_x$ was 384 ± 23.1 vs. 325.8 ± 23.1 Hz, respectively ($p < 0.01$ by one-way ANOVA).

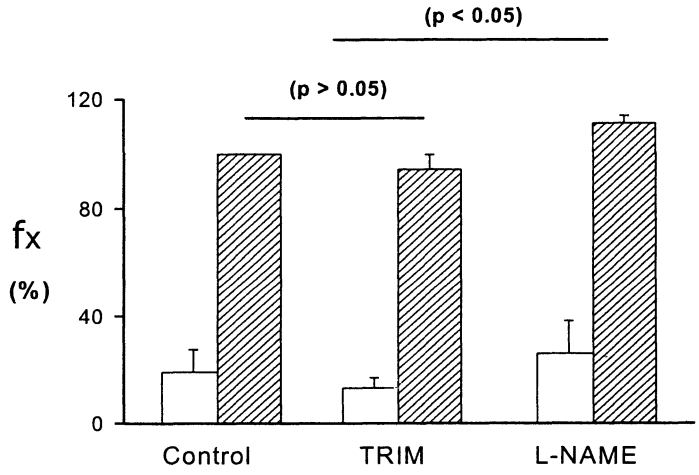


*Figure 3.* Summary of the effects of TRIM and L-NAME on chemosensory response to hypoxia in 4 CBs during control perfusion and after 10 min of perfusion with TRIM (100 μM) and after 10 min with L-NAME (1mM). $f_x$ carotid chemosensory frequency of discharges expressed as % of maximal control response. Empty bars, basal $f_x$ Hatched bars, max$f_x$. ($p < 0.05$, Bonferroni test after one-way ANOVA).

# 4 DISCUSSION

Kline et al. (1998) used mutant mice lacking nNOs to study the contribution of NO produced by nNOS in the control of ventilation. Mutant mice without nNOS showed greater ventilatory responses to hypoxia than wild-type controls. Kline et al. (1998) attributed part of this effect to an enhancement of CB chemosensory responsiveness, because the ventilatory responses to brief hyperoxia and to NaCN were pronounced in mutant mice. The response to hypercapnia was similar in both groups, indicating that hypoxic ventilatory responses were specifically augmented in mutant mice lacking nNOS. However, peripheral as well as central mechanisms dependent on nNOS may contribute to the enhanced respiratory responses to hypoxia observed in mutant mice by Kline *et al.* (1998; 2000).

Our results show that NO produced by nNOS within the cat CB partially inhibits chemosensory responses to NaCN. But the comparison of the effects produced by L-NAME (inhibition of nNOS and eNOS isoforms) with those effects produced by TRIM (inhibition of the nNOS) on the dose-response curves for nicotine and NaCN indicates a predominant contribution of the eNOS to the action of NO in the cat CB. Our data are in accordance with Gozal et al (1996), but disagree with results obtained by Kline et al (1998). However, it is possible that different contributions of eNOS and nNOS to the NO production in the mouse CB may explain the results of Kline et al. (1998; 2000). Present results clearly show that L-NAME enhanced the response to hypoxia, NaCN and nicotine resulting in an increase of discharges over baseline ($\Sigma f_x$). By contrast, TRIM enhances only the responses to high doses of NaCN, but not those to hypoxia and nicotine. These results indicate that both NOS isoforms may contribute to the NO effect in the CB, but eNOS is the major source for NO in the CB that maintains a tonic inhibitory effect upon chemoreceptor activity. However, we cannot conclude that all of the effects of NO produced by eNOS are vascularly mediated. It is plausible that NO produced by endothelial cells may diffuse and reach several targets in the CB such as glomus cells and the nerve endings.

# ACKNOWLEDGEMENTS

Work supported by grant FONDECYT 198-0965 and by the Office for Research and Graduate Studies (DIPUC) of the P. Universidad Católica de Chile.

# REFERENCES

Alcayaga J., Iturriaga R, Ramirez J, Readi R, Quezada C, and Salinas S. 1997, Cat carotid body chemosensory response to non-hypoxic stimuli are inhibited by sodium nitroprusside both *in situ* and *in vitro*. *Brain Res.* 767: 384-387.

Chugh DK, Katayama M, Mokashi A, Debout DE, Ray DK, and Lahiri S. 1994, Nitric oxide-related inhibition of carotid chemosensory nerve activity in the cat. *Resp. Physiol.* 97: 147-156.

Gozal D, Gozal E, Gozal YM, and Torres JE. 1996, Nitric oxide synthase isoforms and peripheral chemoreceptor stimulation in conscious rats. *Neuroreport* 26: 1145-1148.

Iturriaga R, Alcayaga J, and Rey S. 1998, Sodium nitroprusside blocks the cat carotid chemosensory inhibition induced by dopamine, but not that by hyperoxia. *Brain Res.* 799: 26-34.

Iturriaga R, Villanueva S, and Mosqueira M. 2000a, Dual effects of nitric oxide on cat carotid body chemoreception. *J.Appl. Physiol.* 89: 1005-1012.

Iturriaga R, Mosqueira M, and Villanueva S. 2000b, Effects of nitric oxide gas on carotid body chemosensory response to hypoxia. *Brain Res.* 855: 282-286.

Kline D, Yang T, Huang P, and Prabhakar NR. 1998, Altered response to hypoxia in mutant mice deficient in neuronal nitric oxide synthase *J.Physiol. Lond.*. 511: 273-287.

Kline D, Yang T, Huang P, Premkumar DR, Thomas AJ, and Prabhakar NR. 2000, Blunted respiratory responses to hypoxia in mutant mice deficient in nitric oxide synthase-3. *J. Appl. Physiol.* 88: 1496-1508.

Lahiri S, and Buerk DG. 1998, Vascular and metabolic effects of nitric oxide synthase inhibition evaluated by tissue $PO_2$ measurements in carotid body. *Adv. Exp. Med. Biol.* 454: 455-460.

Summers BA, Overholt JL, and Prabhakar, NR. 1999, Nitric oxide inhibits L-type $Ca^{2+}$ current in glomus cells of the rabbit carotid body via a cGMP-independent mechanism. . *Neurophysiol.* 81: 1449-1457.

Wang Z-Z, Stensaas LJ, Bredt DS, Dinger B, and Fidone SJ. 1994, Localization and actions of nitric oxide in the cat carotid body. *Neuroscience* 60: 275-286.

Wang Z-Z, Stensaas LJ, Dinger B, and Fidone SJ. 1995, Nitric oxide mediates chemoreceptor inhibition in the cat carotid body, *Neuroscience* 65; 217-229.

# Nitric Oxide and Calcium Binding Protein in Hypoxic Rat Carotid Body

[1]HIDEKI MATSUDA, [2]YOSHIAKI HAYASHIDA, and [3]TATSUMI KUSAKABE

*[1]Department of Otorhinolaryngology, Yokohama City University School of Medicine, Yokohama 236-0004, Japan; [2]Department of Systems Physiology, University of Occupational and Environmental Health, Kitakyushu 807-8555, Japan; [3]Department of Sport and Medical Science, Kokushikan University, Tokyo 206-8515, Japan;*

## 1. INTRODUCTION

The occurence and distribution of nitric oxide synthase (NOS)-containing nerve fibers have been demonstrated by means of NOS immunohistochemistry and NADPH-diaphorase (NADPH-d) histochemistry (Wang, *et al.*, 1993; Grimes, *et al.*, 1994; Höhler, *et al.*, 1994; Tanaka, *et al.*, 1994). Recently, we reported the distribution of NOS immunoreactive fibers in the chronically hypoxic rat carotid body (Kusakabe, *et al.*, 1998). The density of NOS fibers in the chronically hypoxic carotid body was significantly reduced. This finding suggests that altered nitrergic innervation of the chronically hypoxic carotid body is a feature of hypoxic adaptation.On the other hand, the first evidence for the presence of the calcium binding protein (spot 35-protein) in afferent nerve fibers in the rat carotid body has been shown by Kondo (1990). Recently, in the same hypoxic carotid body, we reported a similar reduction in the density per unit area of calbindin D-28k immunoreactive nerve fibers (Kusakabe *et al.*, 2000). Calbindin D-28k belongs to a family of calcium binding proteins, and plays important roles in the storage and transport of intracellular $Ca^{2+}$ (Baimbridge and Miller, 1982).

*Chemoreception*, Edited by Pequignot et al.
Kluwer Academic/Plenum Publishers, New York, 2003

In the present review, the distribution and abundance of NOS and calbindin D-28k immunoreactive fibers in the carotid body are compared in normoxic and chronically hypoxic rats (10% $O_2$ and 3.0-4.0% $CO_2$ for 3 months). In particular, a possible correlation of NOS and calbindin D-28k in the chemoreceptor mechanism is discussed.

## 2. CHANGES IN THE DISTRIBUTION OF NOS AND CALBINDIN D-28K IMMUNOREACTIVE NERVE FIBERS IN THE CHRONICALLY HYPOXIC RAT CAROTID BODY

In the normoxic carotid body, a large number of NOS-, and calbindin D-28k-immunoreactive nerve fibers were found around the small arteries and arterioles, and around and within clusters of chromogranin A (CGA) and tyrosine hydroxylase (TH) immunoreactive glomus cells in the carotid body (Figs. 1A, B, 2A, B). They appeared as thin processes with many varicositiess. When expressed by the density per unit area of the parenchyma in the normoxic carotid body, the mean density of varicosities in NOS fibers associated with the vasculature and with glomus cells was 14.77 ±2.36 and 8.87±2.06/$10^4$ $\mu m^2$, respectively. The density of NOS fibers associated with the blood vessels was about 1.7 (14.77/8.87) times higher than that with the glomus cells (Fig. 3) indicating that NOS fibers were predominantly distributed around the vasculature. In the same way, the mean density of varicosities in calbindin D-28k fibers associated with vasculature and with glomus cells was 2.71±0.63 and 5.18±1.01 /$10^4$ $\mu m^2$, respectively (Fig. 4).The density of calbindin D-28k fibers associated with the glomus cells was about 1.9 (5.18/2.71) times higher than that with the vasculature.

The chronically hypoxic carotid body was found to be enlarged several fold in comparison with the normoxic carotid body as previously reported.The enlarged carotid bodies contained many expanded blood vessels in a maze-like arrangement (Figs. 1C, 2C). Although the distribution pattern of NOS fibers in the chronically hypoxic carotid body was similar to that in the normoxic carotid body, the mean density of varicosities in NOS fibers associated with the vasculature and with the glomus cells was significantly ($p<0.01$) reduced from 14.77±2.36 to 6.38±1.44/$10^4$ $\mu m^2$, and from 8.87±2.06 to 2.07±0.77/$10^4$ $\mu m^2$, respectively (Fig. 3). This indicates that the ratio of NOS fibers around the blood vessels and glomus cells in the chronically hypoxic carotid body vs. that in the normoxic control carotid body was 0.43 (6.38/14.77) and 0.23 hypoxic carotid bodies

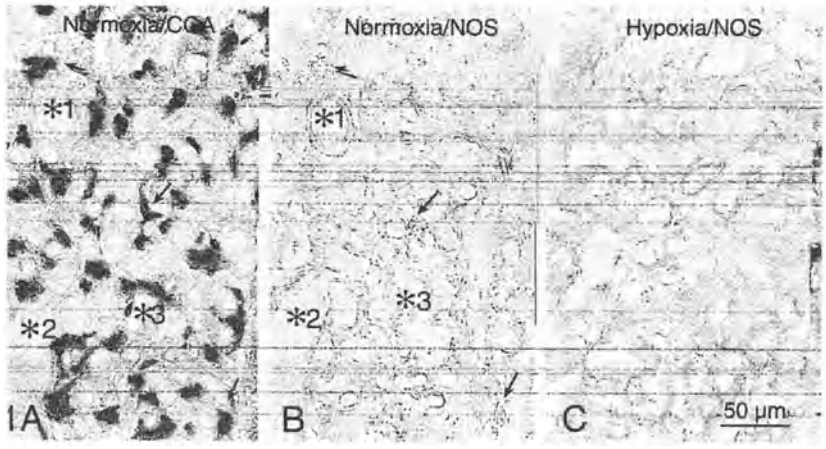


*Figure 1.* A and B are serial sections of a control normoxic carotid body stained with CGA (A) and NOS (B). Blood vessels (*1-3) in 1A correspond to those in 1B. The area of CGA-immunoreactive glomus cells (arrows in A) corresponds to that of NOS-immunoreactive fibers (arrows in B). A small number of NOS fibers (C) in a chronically hypoxic carotid body. Scale bar: 50µm. Reproduced from Kusakabe et al. (1998) with permission of the publisher.

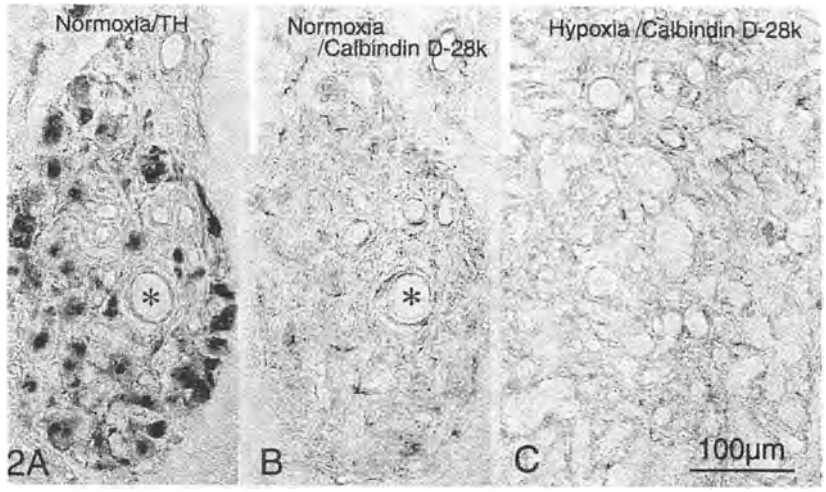


*Figure 2.* A and B are serial sections of a control normoxic carotid body stained with TH (A) and calbindin D-28k (B). Blood vessels (*) in 2A correspond to those in 2B. A small number of calbindin D-28k fibers (C) in a chronically hypoxic carotid body. Scale bar: 100µm. Reproduced from Kusakabe et al. (2000) with permission of the publisher.

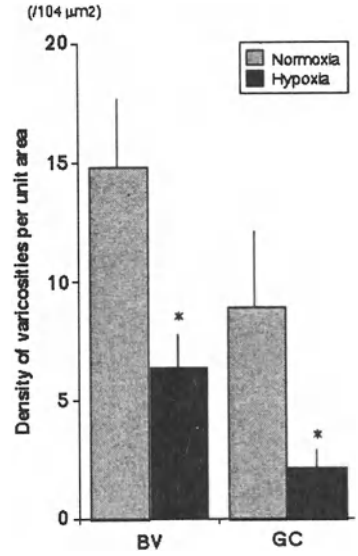


*Figure 3.* Histogram comparing the density of varicosities in NOS fibers per unit area associated with blood vessels (BV) and glomus cells (GC) in normoxic and chronically hypoxic carotid bodies. * $p<0.01$. Reproduced from Kusakabe et al. (1998) with permission of the publisher.

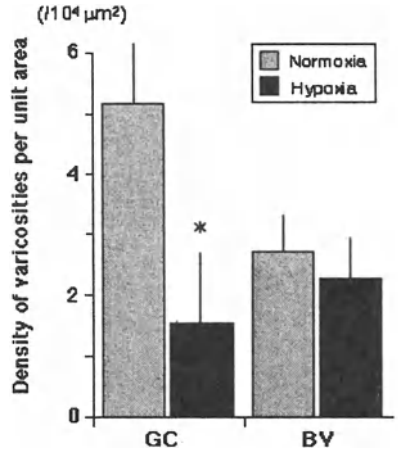


*Figure 4.* Histogram comparing the density of varicosities in calbindin D-28k fibers per unit area associated with glomus cells (GC) and blood vessels (BV) in normoxic and chronically hypoxic carotid bodies. * $p<0.005$. Reproduced from Kusakabe et al. (2000) with permission of the publisher.

In and around the normoxic and chronically carotid body some intrinsic NOS-immunoreactive neurons were found (2.07/8.87), respectively, but no NOS-immunoreactive glomus cells or vascular endothelium were observed. Although the distribution pattern of calbindin D-28k fibers in the chronically hypoxic carotid bodies was similar to that in the normoxic carotid bodies, the relative abundance of immunoreactive fibers was smaller than in the normoxic carotid bodies. The mean density of varicosities in calbindin D-28k fibers associated with the glomus cells was significantly ($p<0.005$) smaller from $5.18\pm1.01$ to $1.53\pm0.63/10^4$ $\mu m^2$ (Fig. 4). There was no significant decrease in the density of calbindin D-28k fibers associated with the vasculature in the normoxic and chronically hypoxic carotid bodies. The ratio of calbindin D-28k fibers associated with the glomus cells in the chronically hypoxic carotid bodies vs. those in the normoxic control carotid bodies was about 0.3 (1.53/5.18).

## 3. POSSIBLE CORRELATION OF CALBINDIN D-28K and NOS-CONTAINING FIBERS

The density of NOS and calbindin D-28k immunoreactive nerve fibers associated with the glomus cells in chronically hypoxic rat carotid bodies was significantly lower (23% and 30%, respectively) than in the normoxic control carotid bodies. Altered density of NOS and calbindin D-28k-containing fibers in the chronically hypoxic carotid body may be a feature of acclimatization during chronic hypoxic exposure. NOS immunoreactive nerve fibers originate in the glossopharyngeal petrosal ganglion (Wang et al., 1993). Many neurons in the petrosal ganglion showed the coexistence of calbindin D-28k and nicotinamide adenosine dinucleotide phosphate (NADPH) diaphorase, a histochemical marker for NOS (Ichikawa and Helke, 1996). This led us to suppose the coexistence of calbindin D-28k and NOS in the nerve fibers associated with the glomus cells in the carotid body although there is not yet direct evidence for this.

In the carotid body, it has been suggested that nitric oxide (NO) directly released from the axonal terminals of sensory C-fibers to adjacent glomus cells inhibits hypoxic activity in the normoxic carotid body through a cGMP second messenger system (Wang et al., 1993). On this basis, we have suggested that the chemosensory mechanisms in the chronically hypoxic carotid body may be involved in 'disinhibition' resulting from reduced NO synthesis (Kusakabe et al., 1998a). A similar reduction in the density of calbindin D-28k and NOS-containing fibers in the chronically hypoxic carotid body and the possibility of coexistence of these two substances may indicate an interaction of

these two substances during acclimatization to hypoxia. This shows that calbindin D-28k may be involved in NO release at terminals by modulating the calcium concentrations in. neurons. Actually, it has been suggested that centrifugal nerve activity in the axonal terminals of sensory C-fibers in the carotid body activates NOS via peripheral axon reflexes, which are involved in a $Ca^{2+}$-dependent mechanism (Wang, *et al.,* 1995). Therefore, the recent immunohistochemical observations on NOS and calbindin D-28k suggest a morphological basis for involvement of calcium binding protein in the neural pathway that modulates carotid body chemoreception.

## ACKNOWLEDGEMENTS

We are grateful to Ms. K. Haraguchi of the Department of Systems Physiology, University of Occupational and Environ-mental Health for hypoxic animal husbandry. This work was supported by grants-in aid 11670015 from the Ministry of Education, Science, Sports, and Culture, Japan.

## REFERENCES

Baimbridge, K.G., and Miller, J.J., 1982, Immunohistochemical localization of calcium-binding protein in the cerebellum, hippocampal formation and olfactory bulb of the rat. *Brain Res.* 245: 223-229.

Grimes, P.A., Mokashi, A., Stone, R.A., and Lahiri, S., 1994, Nitric oxide synthase in autonomic innervation of the cat carotid body. *J. Auton. Nerv. Syst.* 54: 80-86.

Höhler, B., Mayer, B., and Kummer, W., 1994, Nitric oxide synthase in the rat carotid body and carotid sinus. *Cell Tissue Res.* 276: 559-564.

Ichikawa, H., and Helke, C.J., 1996, Coexistence of calbindin D-28k and NADPH-diaphorase in vagal and glossopharyngeal sensory neurons of the rat. *Brain Res.* 735: 325-329.

Kondo, H., Yamamoto, M., and Goto, K., 1990, Immunohistochemical and in situ hybridization. Evidence for a calcium-binding protein in the sinus nerve. In: Arterial Chemoreception. (C. Eyzaguirre, S.J. Fidone, R.S. Fizgerald, S. Lahiri, and D.M. McDonald, eds). Springer-Verlag. New York. pp.24-30.

Kusakabe, T., Matsuda, H., Harada, H., Hayashida, Y., Gono, Y., Kawakami, T., and Takenaka, T., 1998, Changes in the distribution of nitric oxide synthase immunoreactive nerve fibers in the chronically hypoxic rat carotid body. *Brain Res.* 795: 292-296.

Kusakabe, T., Matsuda, H., Hirakawa, H., Hayashida, Y., Ichikawa, T., Kawakami, T., and Takenaka, T., 2000, Calbindin D-28k immunoreactive nerve fibers in the carotid body of normoxic and chronically hypoxic rats. *Histol. Histopathol.* 15: 1019-1025.

Tanaka, K., and Chiba, T., 1994, Nitric oxide synthase containing neurons in the carotid body and sinus of the guinea pig,. *Microscop. Res. Tech.* 29: 90-93.

Wang, X.J., Cheng, G.F., Dinger, B.G., and Fidone, S.J., 1989, Effects of hypoxia on cyclic nucleotide formation in rabbit carotid body in vitro. *Neurosci. Lett.* 105: 164-168.

Wang, Z.Z., Stensaas, L.J., Bredt, D.S., Dinger, B., and Fidone, S.J., 1994, Localization and action of nitric oxide in the cat carotid body. *Neuroscience* 60: 275-286.

# Carotid Body Nitric Oxide Activity in Spontaneously Diabetic BB Rat

GIUSEPPINA BIANCHI., MARISA CACCHIO., ARTESE L.°, FERRERO G.°, RAPINO CINZIA., GRILLI A.*, FELACO M.* and CAMILLO DI GIULIO

*Department of Biomedical Sciences, Centre of Excellence for Aging, * Dept. of Biomorphology and ° Odontostomatology "G. d'Annunzio" University. Chieti . Italy.*

## 1. INTRODUCTION

Carotid body (CB) is made up neuroepithelial tissue and it exhibits some characteristics which are similar to those of endocrine gland (Lawson, 1980; Paulding *et al.*, 2002). Oxygen chemosensitive mechanisms are present in the carotid body, but the site and precise mechanisms of chemotransduction are still unknown.

It is known that NO synthase (NOS) catalyses the reaction of L-arginine into L-citrulline. NO behaves as a biological messenger molecule implicated in many physiological functions involving homeostatic adaptation, and in CB it modulates chemosensory discharges (Di Giulio *et al.*, 2000, Prabhakar *et al.*, 2001).

Diabetes implicates a series of alterations in the homeostatic mechanisms (Felaco *et al.*, 2001). The phenomena which accompany diabetes have not all been elucidated. Diabetes is characterized by angiopathy, tissue hypoxia, reduction in ventilatory response to hypoxia and hypercapnia. Further, diabetes is accompanied by arteriosclerosis with remodelling of capillary network, reduction in organ blood flow, inducing a reduction in oxygen supply to CB. Thus diabetes very closely resembles a state of chronic hypoxia. Insulin is important for glucose transport, gene regulation, sodium reabsorption, cation pump activation, vasodilatation and NO release (Felaco *et al.*, 2000). Diabetic rats could be used as models for improving our knowledge on chemoreception. (Kowyama *et al.*, 2000)

*Chemoreception*, Edited by Pequignot et al.
Kluwer Academic/Plenum Publishers, New York, 2003

postulated that CB could play an important role in glucoregulation in vivo, and Pardal *et al.*, 2002) showed the low glucose sensing in CB.

The hypoxic ventilatory response is characterised by an increase in ventilatory frequencies, representing a homeostatic reaction to the peripheral oxygen requirements by cells (Lahiri *et al.*, 2002). In diabetic patients, the reduction in ventilatory response to hypoxia could be correlated with neuropathy of the afferent and efferent motor-sensitive fibres, with hyperglycemia that reduce nerve conductivity. We believe that chemoreceptors are somehow affected by diabetes since chemotransduction response is modified.

Our hypothesis is that in diabetes NOS expression in CB could be a trigger in the reduction of ventilatory response to hypoxia and hypercapnia. Such a reduction can be the result of an increased free radical production (Wickens, 2001) that could potentially damage cell membranes as well as oxidative enzymes, especially those containing sulfhydryl groups responsible for the oxygen sensitive mechanisms. In diabetes the blunted homeostatic reaction is related to the alteration in the receptor structure, that reduces chemosensory output. The oxygen–glucose uptake could interfere with pigment molecules in the plasma membrane or in the mitochondria, affecting the oxygen sensitive mechanisms also influenced by glucose level and APT formation.

For example, $O_2$ sensitivity is attenuated after prolonged exposure to 100% $O_2$ at 1 ATA (Lahiri *et al.*,1987). The same phenomenon can be observed during aging and diabetes. Animals exposed to high oxygen pressure produce free radicals in tissues, modifying mitochondria structure and function. During chronic hypoxia NOS activity increases, and nitric oxide inhibits chemosensory discharge. NOS increases in response to tissue hypoxia, so explaining the reduction in diabetic ventilatory response to hypoxia. If diabetes is correlated with aging due to free radical production and damage in both situations, then the correlation between diabetes and chronic hypoxia can be done in light of a decrease in blood $pO_2$ which is common to both conditions. Hypoxia induces hypertrophy of CB cells, activation of dopaminergic, nitrergic and peptidergic (Lahiri *et al.*, 1990; Prabhakar *et al.*, 2001; Kusakabe *et al.*, 1998), and the increase in NO would take part in the reduction of the ventilatory adaptation to hypoxia in diabetes.

## 2. METHODS

The distribution of nitric oxide (NOS) immunoreactive nerve fibers was compared between control rats and diabetic rats. Three groups of Wistar rats weighting 200-250 g were used, according to the guidelines of the

Declaration of Helsinki. One was kept in room air (21 % $O_2$) as a control group, the others was kept in a Plexiglas chamber for 12 days in chronic hypoxia (10-11 % inspired oxygen). Chamber temperature and $CO_2$ were kept in physiological ranges. Male Wistar rats and pre-diabetic male Bio Breeding Wistar (BB/W) rats were used in this study. The BB/W rats were obtained from the Animal Resources Division, Health Protection Branch, Ottawa, Ontario, Canada. The Wistar rats represent the non-diabetic control rats, while the BB/W rats were the diabetic animals. The BB/W rats develop signs of diabetes at approximately 85 days of age; this diabetes corresponds to a form of juvenile insulin-dependent type 1 diabetes mellitus, resembling human diabetes mellitus 1. The disease is characterized by insulitis of Langerhans islets. Urine tests for glucose and ketones gave positive results in the diabetic rats and not in the controls. Blood glucose level averaged 308 ± 102 mg/dL in the diabetic rats versus 76 ± 8 mg/dL in the controls. From the onset of diabetes, the BB/W rats were given a small dose of ultralente insulin with an insulin microinfusion device that released insulin daily for 1 month without exogenous insulin administration to prevent ketoacidosis. The microinfusion device was implanted by the supplier of rats.The rats were anaesthetized with Nembutal 40 mg/kg, i.p. and the CBs were dissected. Heme tetrahydrobiopterin, calmodulin, NADPH and flavins are required as cofacor together with the presence of oxygen. The presence of NADPH diaphorase able to detect this reaction was used since 1960. Diaphorase activity and immunohistochemistry for nitric oxide synthase (NOS) (Bredt *et al.*, 1990) were used to quantify the reaction from arginine to NO. Carotid body tissues were immersed over night in ice cold 4 % paraformaldehyde in 0.1 M phosphate buffered saline (PBS). Tissues were then rinsed in 15 % sucrose PBS (1 h) and stored at 4°C in 30 % sucrose PBS (2 h). Ten micrometer thick sections were cut using a cryomicrotome (Reichert-Jung Frigocut 2800), thaw-mounted onto microscope slides, fixed by immersion in acetone at 4°C for 5 min, and air-dried. Slides were stored at 4°C until used. For the immunohistochemical staining of NO synthase, slides were preincubated in PBS for 5 min and then with NOS1 of rat origin ( R.20- Santa Cruz Biotech, Inc) which was diluted 1:100 in PBS and applied for 30 min, at 37 °C. Slices were then washed twice in PBS for 5 min, and in Tris-HCl buffer, pH 7.6 for 10 min. A peroxidase-conjugated second antibody, goat antirabbit IgG, was added for 10 min, and slides were again washed in PBS. The peroxidase label was developed using diaminobenzidine (DAB) dissolved in imidazole buffer, pH 7.6 for 6-10 min , washed in tris-HCl buffer, and dehydrated. For histochemical staining of NADPH-diaphorase, slides were immersed for 30 min at 37 °C in 50 mM Tris-HCl, pH 8.0, 1 mM NADPH, 0.5 mM nitroblue tetrazolium (NBT), 0-2 % Triton X-100. The slides were briefly washed in PBS and dehydrated with a graded series of

ethyl alcohols. Slides from both staining procedures were mounted using Permount, cover-slipped and photographed through a Leitz Dialux microscope. CBs densitometric analyses were carried out randomly, using a Sony Video camera connected with a Quantimet 500 Plus (Leica) to determine the gray intensity levels.

## 3. RESULTS

Imunohistochemistry shows that NOS and NADPH-diaphorase are present in the carotid body (Fig.1, Fig 2). NOS and NADPH- diaphorase expression increase in diabetic rat CBs as compared to non diabetic. NOS diaphorase expression increases in the hypoxic rat CBs as compared to the non hypoxic group as shown in Fig.3.

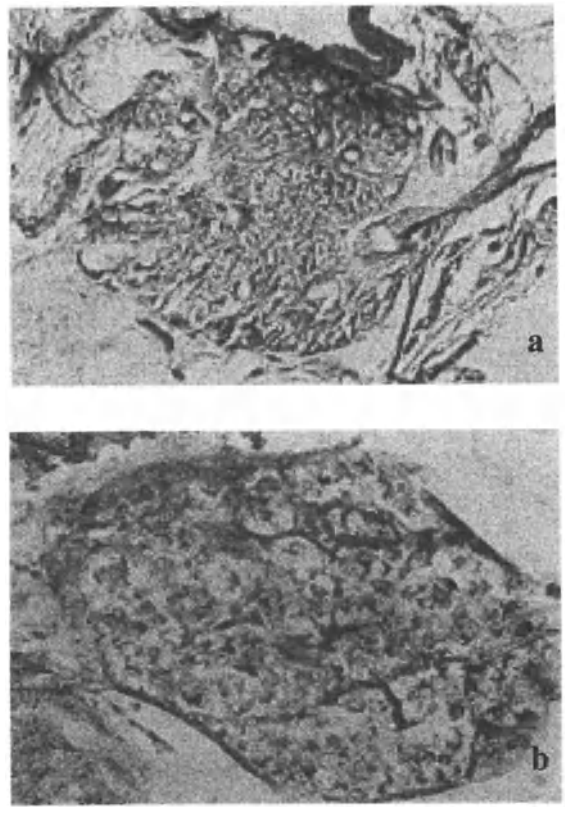


*Figure 1.* Immunohistochemical detection of NOS in CB non diabetic (a) and diabetic (b) rat (250x).

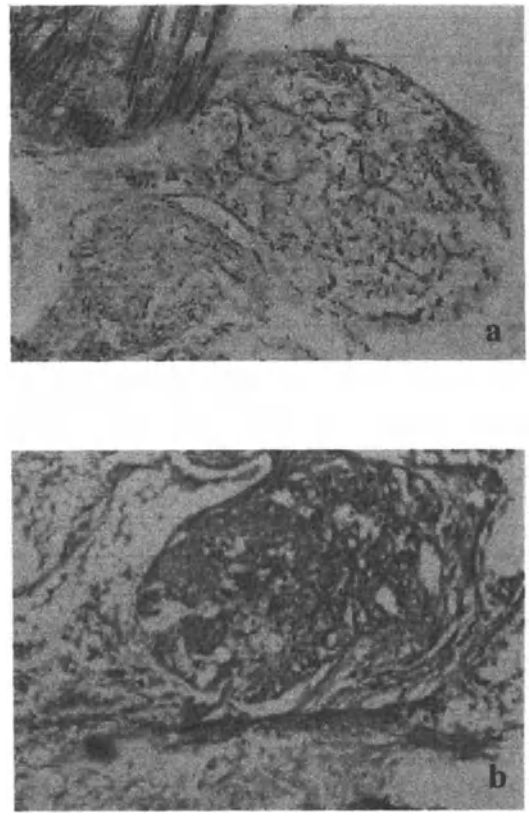


*Figure 2.* NADPH-diaphorase detection in CB normoxic (a) and diabetic (b) rat (250x).

## 4. DISCUSSION

Time course of NOS expression during chronic hypoxia depends on the level of hypoxia and on the time of real exposure to low levels of oxygen. The meaning of "chronic hypoxia" is controversial. Do we consider minutes, hours, days, months of exposure to hypoxia and do we consider intermittent hypoxia as a chronic stimulus? (Schmidt, 2002). Normally acute hypoxia inhibits enzyme activity, while in chronic hypoxia most enzymes such as tyrosine hydroxilase, NOS, VEGF are stimulated representing a homeostatic defence mechanism. Acute and chronic effects involve different pathways. NOS stimulation in CB diabetic BB rats can be correlated to a status of chronic hypoxia in other diabetic organs due to arteriosclerosis,

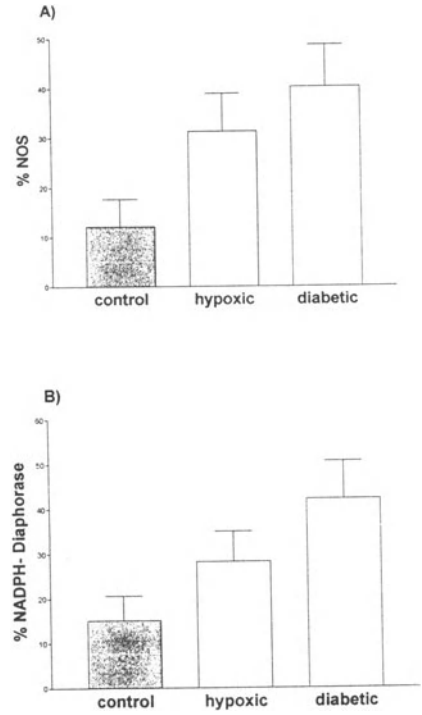


*Figure 3.* Carotid body NOS and NADPH-diaphorase expression

increase in extracellular matrix and other factors increasing the diffusion-distance between blood and mitochondria (Habeck et al., 1988). The alterations in mitochondria reflect the inability of CB diabetic mitochondria to use oxygen supply. The need of mitochondria activity for NOS expression might not be so important, but the interaction among tissue pH, $O_2$ and $CO_2$ reflects blood pH and the subsequent intracellular pH that affect all cell activities and their oxygen consumption. Glucose and insulin regulation influences aging through formation of cross links altering collagen elasticity. Therefore, oxygen –glucose uptake together with CB structural changes could represent the missing ring shared by diabetes and aging (Sohal *et al.*, 1990).

The increase in NOS could be responsible for the reduction in the ventilatory response in diabetes and in respiratory adaptations during chronic hypoxia. Insulin can reduce CB discharge through vasodilation and the resulting relative hyperoxia and the reduced oxygen sensitivity in diabetes can be linked to the inhibitory effect of NOS on the chemosensory discharge (Eringa *et al.*, 2002).

The assumption that the age related changes are more pronounced after hypoxia could be true also for diabetes. Indeed, aging like diabetes is a "stress" for CB structure and function, and the oxygen sensitive apparatus is less sensitive in diabetes. In a previous study we demonstrated that CB hyperoxia damage is more pronounced in young rats than in old rats, showing that the oxygen sensitive mechanisms decrease with age (Di Giulio et al., 1998). Moreover diabetic patients have a decrease in the maximum oxygen consumption just like the aged and people living at high altitude (Martinelli *et al.*, 1990, Cerretelli *et al.*,1996). Also the notion that diabetes does not induces CB hypertrophy after hypoxia is the demonstration that the hypertrophic potential is lower in diabetic CB. Actually, we do not know how and why in chronic hypoxia or in diabetes CB NOS is stimulated. Diabetic microangiopathy induces remodelling of capillary networks in several organs including CB, so one of the teleological ends could be the increase in blood flow to compensate for the reduction in oxygen supply.

In conclusion, diabetes could be useful in understanding the importance of insulin and glucose for the oxygen sensitive mechanisms. The oxygen sensitive mechanisms in diabetes could be less sensitive to hypoxia, and the free radical production can destroy the pigment molecules in plasma membrane or in the mitochondria. NOS increase and neuropeptide release are a reaction to the inability of CB to use the reduced oxygen supply. If we consider that during chronic hypoxia NO increases the level of cGMP showing an inhibitory effect on chemosensory discharge, the increase in NOS in diabetes may play an important role in ventilatory adaptation.

## REFERENCES

Bredt, D.S., Hwang, P.M., Snyder, S.H.,1990, Localization of nitric oxide synthase indicating a neuronal role for nitric oxide. *Nature* 347: 768.

Cerretelli, P., and Hoppeler, H.,1996, Morphological and metabolic response to chronic hypoxia: the muscle system. *Handbook of Physiology –Environment Physiology* 50: 1155-118.

Di Giulio, C., Di Muzio, M., Sabatino, G., Spoletini, L., Amicarelli, F., Di Ilio, C., and Modesti, A., 1998, Effect of chronic hyperoxia on young and old rat carotid body ultrastructure. *Exp Gerontol.* 33: 319-329.

Di Giulio, C., Grilli, A., Ciocca, I., Macrì, M.A., Daniele, F., Sabatino, G., Cacchio, M., Da Porto, R., Di Natale, F., and Felaco, M., 2000, Carotid body NO-CO interaction and chronic hypoxia. In *Oxygen sensing: Molecule to Man* (S. Lahiri, N.R. Prabhakar, R.E. Forster, eds.),Kluver Press, New York, pp. 685-690.

Eringa, E.C., Stehouwer, C.D., Merlijn, T., Wessterhof, N., Sipkema, P., 2002, Physiological concentrations of insulin induce endothelin-mediated vasoconstriction during inhibition of NOS or PI3-kinase in scheletal muscle arterioles. *Cardiovasc. Res.* 56: 464-71.

Felaco, M., Grilli, A., De Lutis, M.A., Patrono, A., Libertini, N., Taccardi, A., Di Napoli, P., Di Giulio, C., and Conti, P., 2001, e-NOS expression and localization in healthy and diabetic rat hearts. *Annals of Clinical and Laboratory Science* 31: 179-186.

Felaco, M., Grilli, A., Gorbunov, N., Di Napoli, P., De Lutis, M.A., Di Giulio, C., Taccardi, A., Barsotti, A., Barbacane, R., Reale, M., and Conti, P., 2000, Endothelial NOS expression and ischemia- reperfusion in isolated working rat heart from hypoxic and hyperoxic conditions. *Biochim and Biophys Acta.* 1542: 203-211.

Habeck, J.O., Huckstorf, C., and Behm, R., 1988, The paraganglia within the carotid bifurcation regions of young and old spontaneously hypertensive rats (SHR) after exposure to chronic hypobaric hypoxia. I. The carotid bodies. *Anat. Anz.* 165: 45-54.

Koyama, Y., Coker, R.H., Stone E.E., Lacy, D.B., Jabbour, K., Williams, P.E., 2000, Evidence that carotid bodies play an important role in glucoregulation in vivo. *Diabetes* 49: 1434-1442.

Kusakabe, T., Hayashida, Y., Matsuda, H., Gono, Y., Powell, F.L., Ellisman, M.H., Kawakami, T., Takenaka, T., 1998, Hypoxic adaptation of the peptidergic innervation in the rat carotid body. *Brain Res* 806: 165-74.

Lahiri, S., Mulligan, E., Andronikou, S., Shirahata, M., and Mokashi, A.,1987, Carotid body chemosensory function in prolonged normobaric hyperoxia in the cat. *J. Appl. Physiol.* 62: 1924-1931.

Lahiri, S., Mokashi, A., Di Giulio, C., Sherpa, A.K., Huang, W.X., and Data, P.G., 1990, Carotid body adaptation: Lesson from chronic stimuli. In *Hypoxia: The Adaptations* (J.R. Sutton, G. Coates, J.E. Remmers, and B.C. Dekker, eds.), Philadelphia, pp. 127-130.

Lahiri, S., Di Giulio, C., and Roy A., 2002, Lesson from chronic intermittent and sustained hypoxia. *Respir. Physiolo. and Neurobiol.* 130: 223-233.

Lawson, W., 1980, The neuroendocrine nature of the glomus cells: an experimental, ultrastructural and histochemical tissue culture study. *Laryngoscope* 90: 120-144.

Martinelli, M.R., Winterhalder, P.,Cerretelli, P.,Howald, H., and Hoppeler, H., 1990, Muscle lipofuscin content and satellite cell volume is increased after high altitude exposure in humans. *Experientia* 46: 672-676.

Pardal, R., Lopez-Barneo, J., 2002, Low glucose-sensing cells in the carotid body. *Nature Neurosci.* 583: 197-198.

Paulding, W.R., Schnell, P.O., Bauer, A.L., Striet, J.B., Nash, J.A., Kuznetsova, A.V., Czyzyk-Krzeska, M.F., 2002, Regulation of gene expression for neurotransmitter during adaptation to hypoxia in oxygen-sensitive neuroendocrine cells. *Microsc. Res. Tech.* 59: 178-197.

Prabhakar, N.R., Fields, R.D., Baker, T., Fletcher, E.C., 2001, Intermittent hypoxia: cell to system. *Am. Physiol. Lung Cell Mol. Physiol.* 281: 524-528.

Schmidt, W., 2002, Effect of Intermittent Exposure to High altitude on blood volume and erythropoietic activity. *High Altitude Medic. & Biol.* Vol.3: 167-176.

Sohal, R.S., Sohal, B.H., and Brunk, U.T., 1990, Relationship between antioxidant defences and longevity in different mammalian species. *Mech. Aging Dev.* 53(3): 217-227.

Wickens, A.P., 2001, Ageing and the free radical theory. *Respir. Physiol.* 128: 379-391.

# Contribution of Dopamine $D_2$ Receptors for the cAMP Levels at the Carotid Body

JOANA R. BATUCA, TERESA C. MONTEIRO and EMÍLIA C. MONTEIRO

*Department of Pharmacology Faculty of Medical Sciences, New University of Lisbon, Campo Mártires da Pátria, 130, 1169-056 Lisboa, Portugal*

## 1. INTRODUCTION

There is a general consensus that the effects of dopamine at the carotid body (CB) are mediated by activation of both $D_1$ and $D_2$ receptor subtypes (González *et al.*, 1994). $D_1$- and $D_2$-like receptors have been defined traditionally by their opposing effects on the enzyme adenylate cyclase (AC), with $D_1$–like ($D_1$ and $D_5$) receptors positively coupled to this enzyme, whereas $D_2$-like ($D_2$, $D_3$ and $D_4$) are either negatively coupled or uncoupled to this effector (Missale *et al.*, 1998). Excitatory effects of exogenous dopamine (1 and 10 μM) on cyclic adenosine 3',5'-monophosphate (cAMP) production have been described at the rabbit CB equilibrated with hyperoxia and attributed to the activation of $D_1$ receptors (Pérez-Garcia *et al.*, 1990; Almaraz *et al.*, 1991). The present work was undertaken to investigate the contribution of $D_2$ receptors to cAMP production at the rat CB in hyperoxia, normoxia and hypoxia.

## 2. METHODS

The experiments were performed in CBs isolated from adult *Wistar* rats (male and female) anaesthetized with sodium pentobarbitone (60mg/Kg i.p.), tracheostomized and breathing spontaneously. Under a dissecting scope the CBs were removed *in situ* from carotid bifurcation and pre-incubated, to allow recovery of the preparation, during 15min, at 37°C in a shaker bath in medium equilibrated with hyperoxia (95%$O_2$/5%$CO_2$). Medium composition

*Chemoreception*, Edited by Pequignot et al.
Kluwer Academic/Plenum Publishers, New York, 2003

described by Pérez-Garcia *et al.*, (1990) was (mM): NaCl 116; $NaHCO_3$ 24; KCl 5; $CaCl_2$ 2; $MgCl_2$ 1.1; HEPES 10; glucose 5.5 at pH 7.40. After the pre-incubation period the CBs were placed in fresh medium equilibrated with different gas mixtures and drugs: **Experiments in hyperoxia:** Pre-incubation in the presence of isobutylmethylxanthine (IBMX, 0.5 mM), a phosphodiesterase inhibitor. Incubation period of 30min at 37°C in medium equilibrated with 95%$O_2$/ 5%$CO_2$ containing IBMX 0.5 mM plus dopamine 3, 10, 100 and 300 μM. **Experiments in normoxia:** Pre-incubation in medium without drugs or in the presence of IBMX 0.5 mM alone or with forskolin (FSK, 3 μM) an activator of AC. Incubation period of 10min or 30min at 37°C in medium equilibrated with 20%$O_2$/5%$CO_2$/75%$N_2$ containing IBMX 0.5 mM alone or in the presence of FSK 3 μM, or FSK 3 μM plus dopamine 3, 10, 100 and 300 μM. **Experiments in hypoxia:** Pre-incubation in medium without drugs. Incubation period of 10min or 30min at 37°C in medium equilibrated with 10%$O_2$/5%$CO_2$/85%$N_2$ or 5%$O_2$/5%$CO_2$/90%$N_2$ containing IBMX 0.5 mM alone or in the presence of domperidone 0.5 nM, 10 nM and 1 μM.

**cAMP quantification** was assayed using two different methods radioimmunoassay (RIA, *TRK 432 Amersham*) as previously described (Monteiro *et al.*, 1996) or enzymeimmunoassay (EIA, *RPN 225 Amersham*). Due to the small size of the rat CB, 40–60 μg, cAMP values were expressed as pmol/CB.

## 2.1 Statistics

Data are expressed as means ± SEM values. The significance of the differences between the means was calculated by the unpaired *Student's t* test. Values of $P<0.05$ were considered to represent significant differences.

## 2.2 Drugs

Sodium pentobarbitone, IBMX, FSK and dopamine were from Sigma, domperidone from RBI and trichloroacetic acid and diethyl ether from Merck. All solutions were made in incubation medium, except FSK stock solution (20 mM) that was made in DMSO and domperidone stock solution (0.5 mM) that was made in HCl. The pH of solutions was readjusted to 7.40 with NaOH or HCl where necessary.

# 3. RESULTS

The cAMP values, determined by EIA, in CB basal conditions (normoxia without drugs) were 0.12 ± 0.02 pmol/CB (n=4) (Fig. 1). Phosphodiesterase inhibition obtained by incubation of the CBs with 0.5 mM IBMX for 10, 30 and 45min, increased cAMP levels in a time-dependent manner (Fig. 1). The

maximal value (1.53 + 0.36 pmol/CB, n=5) was obtained during 30min incubation, but no statistically significant differences were found between the results obtained with IBMX during 30 and 45min (Fig. 1).

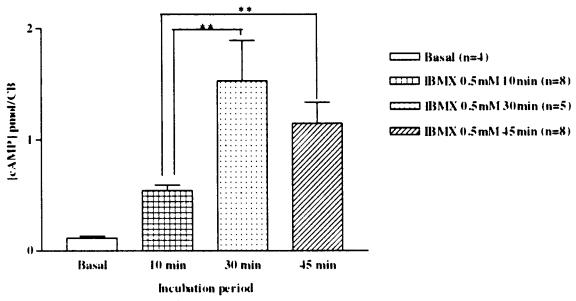


*Figure 1.* Effect of different incubation periods of IBMX on cAMP content at the rat CBs using EIA assay. Tissues were incubated in a solution without IBMX (basal) or containing IBMX 0.5 mM during 10, 30 and 45min (15 min pre-incubation period + 30min incubation period), equilibrated with normoxia. $^{**}P<0.01$.

Basal cAMP levels of the rat CB quantified by EIA and RIA, in the same experimental conditions (95%$O_2$/5%$CO_2$; IBMX 0.5 mM), were respectively 0.56 ± 0.16 pmol/CB (n=8) and 9.10 ± 0.83 pmol/CB (n=6).

To investigate the inhibitory effects of exogenous dopamine on cAMP production, CBs were pre-incubated with an activator of AC, FSK (3 μM). FSK increased cAMP production from 1.15 + 0.19 pmol/ CB, n=8 to 5.29 + 0.80 pmol/CB, n=3 (360% effect), (Fig.2).

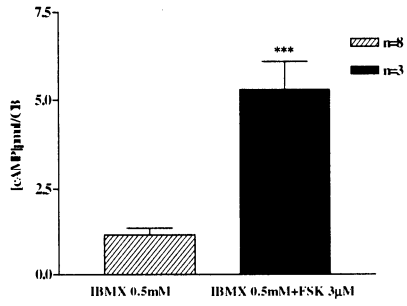


*Figure 2.* Effect of forskolin on cAMP content at the rat CBs using EIA assay. Tissues were incubated in a solution containing IBMX 0.5 mM alone, or IBMX 0.5 mM plus FSK 3 μM at normoxia. $^{***}P<0.0001$.

The effect of exogenous dopamine (3–300 μM) on cAMP production in CBs stimulated by FSK is shown in Fig. 3. In these CBs, incubated in hyperoxic conditions, dopamine caused a dose-dependent inhibitory effect on cAMP production induced by FSK. Although different basal cAMP values were quantified at the CB using RIA or EIA (56.75 ± 6.71 pmol/CB, n=4 for RIA and 5.29 ± 0.80 pmol/CB, n=3 for EIA), no differences were observed between the inhibitory effects of dopamine (300 μM) on cAMP quantified by the two methods.

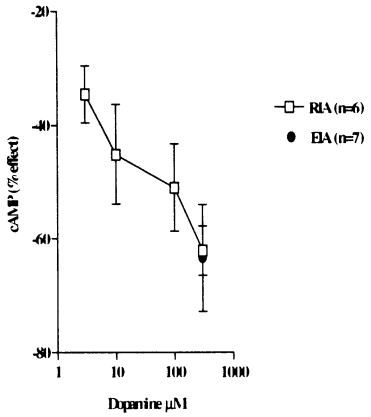


*Figure 3.* Effect of exogenous dopamine on cAMP content at the rat CBs previously stimulated by FSK, using two different methods: RIA and EIA. Tissues were incubated in a solution containing IBMX 0.5 mM plus FSK 3 µM and selected concentrations of dopamine (3, 10, 100 and 300 µM) at 95%$O_2$ (RIA), or 20%$O_2$ (EIA). 0% effect were 56.75 ± 6.71 pmol/CB (n=4) and 5.29 ± 0.80 pmol/CB (n=3) for RIA and EIA respectively.

The inhibitory effects of dopamine were not detected when FSK was added to the incubation medium simultaneously with dopamine instead of being added 15min before (Fig. 4, normoxia). When the effect of exogenous dopamine was investigated in the absence of prior stimulation of the CBs with normoxia or hyperoxia dose-dependent excitatory effects of exogenous dopamine (10 and 300 µM) on cAMP were observed (Fig. 4). However, the increases in cAMP caused by dopamine were more evident during normoxia (Fig. 4).

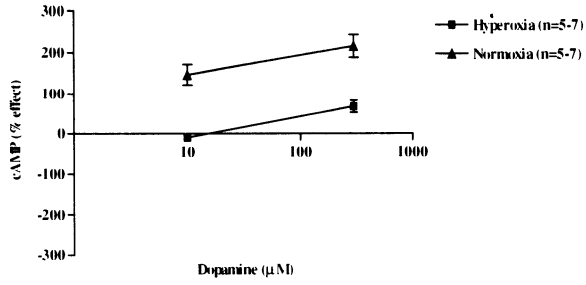


*Figure 4.* Effect of exogenous dopamine on cAMP content at the rat CBs in normoxia and hyperoxia. Tissues were incubated in a solution containing IBMX 0.5 mM and selected concentrations of dopamine (10 and 300 µM). 0% effect were 9.10 ± 0.83 pmol/CB (n=6) for hyperoxia RIA and 3.46 + 0.47 pmol/CB (n=4) for normoxia EIA.

To minimize the differences found in basal cAMP values (0% effect in Fig 4) quantified in hyperoxia and normoxia the results were expressed in % effect. In the experiments during normoxia, FSK was also present (added simultaneously to dopamine) in the incubation medium and cAMP values obtained with FSK alone were considered basal values and compared with those obtained with FSK plus dopamine (10 and 300 µM).

In another group of experiments, the effects of a dopamine $D_2$-receptor antagonist, domperidone, on cAMP content at the CBs were studied. In these experiments, the CBs were stimulated in hypoxic and normocapnic conditions, with two different $O_2$ concentrations, 10% and 5%. Domperidone was used in three different concentrations (0.5 nM, 10 nM and 1 µM). Dose-

response curves for the effects of domperidone on cAMP content are shown in Fig. 5.

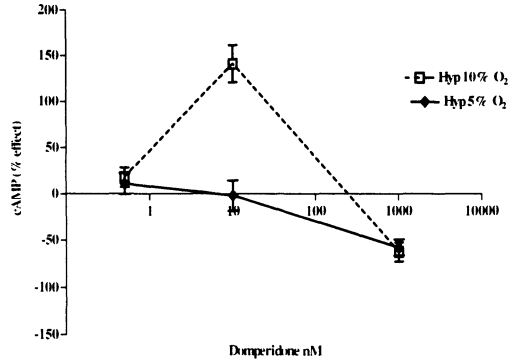


*Figure 5.* Effect of domperidone, on cAMP content at the rat CBs in different hypoxias, using EIA assay. Tissues were incubated for 10min in a solution containing IBMX 0.5 mM alone or with domperidone 0.5 nM, 10 nM and 1 μM equilibrated with hypoxia 10%$O_2$ (0 % effect 0.71 ± 0.18 pmol/CB, n=7) or hypoxia 5%$O_2$ (0 % effect 0.46 ± 0.05 pmol/CB, n=6).

Blockade of $D_2$ receptors with domperidone at a dose of 10 nM increased cAMP from 0.71 ± 0.18 pmol/CB (n=7) to 1.82 ± 0.15 pmol/CB in the CBs submitted to 10%$O_2$. This effect was not observed in the CBs submitted to 5%$O_2$. With higher concentrations of domperidone (1 μM) only inhibitory effects were observed during the two different intensities of hypoxia (Fig.5).

## 4. DISCUSSION

At the whole CB, during hyperoxia and normóxia, dopamine can inhibit cAMP production, probably by acting in $D_2$-receptors negatively coupled to AC. Blockade of these dopamine $D_2$–receptors increased cAMP at the CB during moderate hypoxia (10%$O_2$). However, during more intense hypoxia (5%$O_2$), the activation of $D_2$-receptors negatively coupled to cAMP production was not evident. Excitatory effects of dopamine on cAMP production were also observed. These excitatory effects were more pronounced in normoxia than in hyperoxia and were also present in hypoxia.

The cAMP values quantified by EIA in the rat CB do not support the existence of animal species differences because they were of the same magnitude of those described in the rabbit, 2–43 pmol/mg (Wang *et al.*, 1989; Pérez-Garcia *et al.*, 1990; Almaraz *et al.*, 1991 and Chen *et al.*, 1997) or the cat CBs, 7–13 pmol/mg (Delpiano and Acker, 1984) using RIA methodologies. The time–dependent effect of IBMX observed in our preparations contrasts with that reported by Pérez-Garcia *et al.* (1990) in the rabbit CB who found higher cAMP values during IBMX incubation of 10min than 30min. FSK was used in a concentration close to the $EC_{50}$ for cAMP in the rabbit CB (Pérez-Garcia *et al.*, 1990) in order to access both the

inhibitory effects of dopamine and the additive excitatory effects of dopamine on cAMP production.

The present results provide the first evidence concerning the second messenger triggered by activation of dopamine $D_2$–receptors at the CB. These results also strength the importance of the experimental conditions, namely CB previous stimulation, to demonstrate dopamine inhibitory effects. The present results do not exclude the coupling of dopamine receptors to other second messenger pathways at the CB. For instance, it has been show in many preparations that $D_2$–like receptors increase outward $K^+$ currents, leading to cell hyperpolarization (for a review see Missale *et al.*, 1998) the effects of dopamine on $PO_2$ sensitive $K^+$ current at the CB are not well established. Since only dopamine and domperidone were used in the present work the inhibitory effect on cAMP cannot be attributed exclusively to activation of dopamine $D_2$ receptors subtype: all dopamine $D_2$–like receptors ($D_2$, $D_3$ and $D_4$) could be involved. The presence in the CB, of dopamine $D_1$-receptors positively coupled to AC, previously demonstrated by Almaraz *et al.*, (1991), was also confirmed in the present work.

Hypoxia releases dopamine from chemoreceptor cells and the amount of dopamine is dependent on the intensity of hypoxic stimulus (González *et al.*, 1994). It is well accepted that low doses of dopamine depress carotid sinus nerve (CSN) activity and high doses cause excitatory effects, commonly preceded by depression in CSN activity (Zapata, 1997). The importance and physiological significance of these different effects is not clear and have been discussed in terms of differences of dopamine receptors localization within the CB. In the present work it was shown that dopamine $D_2$ inhibitory receptors apparently are not functional during hypoxia 5%$O_2$. Dopamine excitatory effects on cAMP were more evident in 20%$O_2$ than in 95%$O_2$ and also detected in hypoxia (5% and 10%$O_2$). Used in a dose of 1 μM domperidone is not a specific blocker for $D_2$ receptors. Its $K_i$ for $D_2$ receptors in rat striatum is 0.9 nM and doses of 1 μM can block also $D_1$ and adrenoceptors (Leysen *et al.*, 1977). This lack of specificity agrees with the blockade of excitatory effects observed in the present work during hypoxia 5% and 10%$O_2$. Domperidone concentrations between 1 nM to 10 μM were also used in other CB preparations (Bairam *et al.*, 2000). Based in these preliminary results we postulated the hypothesis that the equilibrium between dopamine $D_1$ and $D_2$ receptor activation or dopamine excitatory and inhibitory effects could be dependent of $O_2$ concentrations.

Basal cAMP production at the CB is modified by different $O_2$ tensions (Pérez-Garcia *et al.*, 1990) and by adenosine receptor agonists and antagonists (Monteiro *et al.*, 1996; Chen *et al.*, 1997). Interactions between adenosine and dopamine have been described in many preparations namely

at the CB (Monteiro and Ribeiro, 2000) and can also be involved in dopamine different contribution to cAMP production at the CB.

It is concluded that at the CB, dopamine can act on both $D_2$-receptors negatively coupled to AC or on $D_1$-receptors positively coupled to cAMP production. It is proposed that preferential activation of each subtype of receptors is dependent on $O_2$ levels, being $D_2$-receptors activation inversely related to the intensity of hypoxic stimulus.

## ACKNOWLEDGEMENTS

The authors are grateful to Mrs. Eunice Matos Silva for her skilful technical assistance, to the Department of Microbiology and "Centro de Malária e Doenças Tropicais" for samples lyophilisation, and to the Department of Biochemistry for lending the spectrophotometric plate reader and washer.

## REFERENCES

Almaraz, L., Pérez-García, M.T. and González, C., 1991. Presence of $D_1$ receptors in the rabbit carotid body. *Neuroscience Letters*, 132:259-262.

Bairam, A., Néji, H., De-Grandpré, P. and Carrol, J.L., 2000. Autoreceptor mechanism regulating carotid body dopamine release from adult and 10 – day – old rabbits. *Respiration Physiology*, 120:27-34.

Chen, J., Dinger, B. and Fidone, S.J., 1997. cAMP production in rabbit carotid body: role of adenosine. *J.Appl. Physiol.* 82: 1771-1775.

Delpiano, M.A. e Acker, H., 1984. $O_2$ chemoreception of the cat carotid body *in vitro*. In: *Oxygen Transport to Tissue* (D.W. Lubbers et al, eds), Plenum Publishing Corporation, pp 705-717.

González, C., Almaraz, L., Obeso A. and Rigual, R., 1994. Carotid body chemoreceptors: from natural stimuli to sensory discharges. *Physiological Reviews*, 74:829.

Leysen J.E., Tollenaere J.P., Koch M.H.J. and Laduron P.M., 1977. Differentiation of opiate and neuroleptic receptor binding in rat brain. *Eur. J. Pharmacol.* 43 :253-267.

Missale, C., Nash, S.R., Robinson, S.W., Jaber, M. and Caron, M.G., 1998. Dopamine receptors: from structure to function. *Physiological Reviews*, 78:189-225.

Monteiro, E.C., Vera-Cruz, P., Monteiro, T.C. and Silva and Sousa, M.A., 1996. Adenosine increases the cAMP content of the rat carotid body *in vitro*. In: *Frontiers in Arterial Chemoreception*. (P. Zapata et al, eds), Plenum, New York, pp 299-303.

Monteiro, E.C. and Ribeiro, J.A., 2000. Adenosine-dopamine interaction and ventilation mediated through carotid body chemoreceptors. In: *Oxygen Sensing: Molecule to Man*. (S. Lahiri et al., eds), Kluwer Academic/Plenum Publishers, pp 671-684.

Pérez-García, M.T., Almaraz, L. and González, C., 1990. Effects of different types of stimulation on cyclic AMP content in the rabbit carotid body: functional significance. *Journal of Neurochemistry*, 55:1287-1293.

Wang, W.J., Cheng, G.F., Dinger, B.G. and Fidone, S.J., 1989. Effects of hypoxia on cyclic nucleotide formation in rabbit carotid body in vitro. *Neuroscience Letters*, 105:164-168.

Zapata P., 1997. Chemosensory activity in the carotid nerve : effects of pharmacological agents. In: *The Carotid Body Chemoreceptors* (C. González, ed), Springer-Verlag, pp 119-146.

# Chemosensitivity of Medullary Respiratory Neurones

## *A role for ionotropic P2X and $GABA_A$ receptors*

ALEXANDER V. GOURINE, and K. MICHAEL SPYER
*Department of Physiology, Royal Free and University College London Medical School, London NW3 2PF, UK*

## 1. INTRODUCTION

Under normal physiological conditions blood and brain $pO_2$ and $pCO_2$ are maintained at constant levels by the neural activity that controls breathing. Central respiratory drive is highly sensitive to changes in arterial $pCO_2$, so that even a small increases in $pCO_2$ in arterial blood evokes a rapid increase in minute ventilation. Levels of $CO_2$ are monitored by the peripheral chemoreceptors located within the carotid bodies, and in some species in the aortic bodies, and by the central chemoreceptors within the medulla oblongata (Daly, 1997; Nattie, 1999, 2001). The ventilatory response to hypercapnia is largely preserved in experimental animals after denervation of the carotid and aortic bodies and according to the estimate of Heeringa *et al.* (1979) up to 80% of the $CO_2$-evoked response is mediated by the action of $CO_2$ at the brainstem chemosensitive sites.

The ventrolateral surface of the medulla (VLM) is believed to function as a primary central chemoreceptive area (Loeschcke, 1982; Ballantyne and Scheid, 2000), although other regions of the brainstem such as the rostral part of the ventral respiratory group, the medullary raphe nuclei, the nucleus tractus solitarii (NTS), the locus coeruleus (LC) and others have been reported to be chemoreceptive (Nattie, 1999, 2001). It is suggested that neurones within these areas function as chemoreceptors (Ballantyne and Scheid, 2000, 2001). Whilst the mechanisms responsible for this chemosensitivity remains largely unknown, it is clear that changes in $[H^+]$,

*Chemoreception*, Edited by Pequignot et al.
Kluwer Academic/Plenum Publishers, New York, 2003

that follow changes in $pCO_2$ represents the adequate stimulus for central chemosensitive neurones (Cherniack, 1993; Ritucci *et al.*, 1998). The VLM also contains a network of respiratory neurones responsible for generation of the respiratory rhythm as well as premotor neurones responsible for transmitting this rhythm to spinal motoneurons controlling the diaphragm and intercostal muscles (Richter, 1982; Richter *et al.*, 1992; McCrimmon *et al.*, 2000; Richter and Spyer, 2001). There is growing evidence that some VLM neurones with respiratory-related activity are intrinsically sensitive to the changes in $[H^+]$ that follow changes in arterial $pCO_2$ (Kawai *et al.*, 1996; Ballantyne and Scheid, 2000). This brief review describes potential mechanisms of chemosensitivity of these VLM respiratory neurones involving ionotropic P2X and $GABA_A$ receptors.

## 2. CHEMOSENSITIVITY OF VLM RESPIRATORY NEURONES: A ROLE FOR P2X RECEPTORS?

### 2.1 P2X Receptors are Sensitive to Changes in Extracellular $[H^+]$

P2X receptors are ATP-gated non-selective cation channels permeable to $Na^+$, $K^+$ and $Ca^{2+}$ ions (Ralevic and Burnstock, 1998). Seven P2X receptor subunits ($P2X_{1-7}$) have been cloned and characterised in terms of agonist/antagonist selectivity (Buell *et al.*, 1996; Ralevic and Burnstock, 1998). An intriguing feature of the P2X receptors is that their sensitivity to ATP is modulated by extracellular pH. In HEK293 cells transfected with $P2X_1$, $P2X_3$ and $P2X_4$ subunits the currents evoked by ATP are reduced by acidification of the extracellular environment (Stoop *et al.*, 1997). Conversely, in HEK293 cells and in *Xenopus* oocytes transfected with $P2X_2$ subunit, the currents induced by ATP application are potentiated by lowering the external pH (King *et al.*, 1996; Stoop *et al.*, 1997; Wildman *et al.*, 1997). These data suggested that if VLM respiratory neurones possess P2X receptors their chemosensitivity may be due to changes in sensitivity of P2X receptors to ATP evoked by shifts in local $[H^+]$.

### 2.2 P2X Receptors and Hypercapnia-Evoked Changes in Respiration

Recent data obtained in this laboratory indicate that this indeed may be the case (Spyer and Thomas, 2000). In anaesthetised and artificially ventilated rats the P2 receptor antagonist suramin attenuates the respiratory

responses to changes in arterial $pCO_2$ when microinjected into the VLM (Thomas *et al.*, 1999). Furthermore, microionophoretic application of P2 receptor antagonists suramin or pyridoxal-5'-phosphate-6-azophenyl-2',4'-disulphonic acid (PPADS) completely blocks hypercapnia-evoked increases in the activity of pre-inspiratory and inspiratory VLM neurones (Thomas and Spyer, 2000). Interestingly, although post-inspiratory and expiratory neurones were excited by increasing levels of inspired $CO_2$, and also by ionophoretically applied ATP, the $CO_2$-evoked effects were unaffected by P2 receptor blockade (Thomas and Spyer, 2000). At a first glance these data indicate that certain P2X receptors localised within the VLM are involved in mediating respiratory response evoked by an increase in the level of the inspired $CO_2$, and also that ATP acting on these receptors is responsible for the increases in activity of medullary pre-inspiratory and inspiratory neurones during hypercapnia. However, the involvement of purinergic transmission in the central mechanisms of respiratory control appears to be more complex.

## 2.3 Tonic Influence of ATP on VLM Respiratory Network

Bilateral microinjection of P2 receptor antagonist suramin into the VLM of anaesthetised and artificially ventilated rat not only resulted in attenuation of the respiratory response to hypercapnia, but also significantly reduced resting (i.e. during normocapnia) phrenic nerve discharge, in some cases causing complete cessation of the central respiratory drive (Thomas *et al.*, 1999). Similarly, it was found that ionophoretic application of P2 antagonists suramin or PPADS not only blocks hypercapnia-evoked increases in the activity of pre-inspiratory and inspiratory VLM neurones, but also reduces baseline firing in a significant proportion of these neurones (Thomas and Spyer, 2000). These data indicate that even during normocapnia, the VLM respiratory network and within it pre-inspiratory and inspiratory neurones are likely to be under tonic excitatory influence of ATP mediated by certain P2 receptors. Therefore, it remains unclear whether the effects of P2 receptor blockade on hypercapnia-evoked ventilatory (VLM neuronal) responses are merely due to a general suppression of central inspiratory drive or are due to a reduced efficacy of chemosensitivity. To obtain further evidence in support of the latter we determined the extent of P2X receptor expression among the VLM respiratory neurones.

## 2.4 $P2X_2$ Receptor Subunit Expression in VLM Respiratory Neurones

Expression of $P2X_1$, $P2X_2$, $P2X_5$ and $P2X_6$ receptor subunits has been demonstrated in the VLM (Kanjhan *et al.*, 1999; Yao *et al.*, 2000; Thomas *et al.*, 2001). However, although, sensitivity of virtually all subtypes of P2X receptors to ATP is modulated by the external pH, homomeric $P2X_2$ receptors are unique in terms of their sensitivity to extracellular pH within the physiological range (King *et al.*, 1997; Wildman *et al.*, 1997). Even mild acidification (a decrease in pH from 7.45 to 7.10) increases by 2-3 fold the amplitude of the inward ATP-evoked currents at recombinant $P2X_2$ receptors (Wildman *et al.*, 1997). In addition, ATP currents evoked at heteromeric $P2X_{2/6}$ and $P2X_{1/2}$ receptors are also modulated by external pH (King *et al.*, 2000; Brown *et al.*, 2002), indicating that $P2X_2$ subunit is essential for the high sensitivity of the P2X receptors to $[H^+]$ changes in the extracellular environment. Therefore, we suggested that if P2X receptors mediate hypercapnia-induced changes in the activity of VLM respiratory neurones, these neurones are likely to express $P2X_2$ receptor subunit.

Indeed, $P2X_2$ subunit has been found to be expressed in the VLM as well as in the other chemoreceptive sites of the brainstem, including LC, NTS and the raphe nuclei (Kanjhan *et al.*, 1999; Yao *et al.*, 2000). However, in a recent study only a relatively small proportion of VLM neurones that display rhythmic respiratory-related activity expressed $P2X_2$ receptor subunit. In anaesthetised and artificially ventilated rats VLM respiratory neurones were labelled with Neurobiotin using the juxtacellular method (Pinault, 1996). Less then 20% (2 out of 11) of juxtacellularly labelled neurones with inspiratory-related discharge (pre-inspiratory and inspiratory) and 50% (6 out of 12) of labelled expiratory neurones were found to be immunoreactive for the $P2X_2$ receptor subunit (Gourine, Atkinson, Deuchars and Spyer, unpublished observations).

## 2.5 Plausible Neuronal Mechanisms

These data correlate well with the results of our electrophysiological experiments aimed to evaluate the effect of ionophoretic application of ATP on the activity of medullary respiratory neurones. In anaesthetised and artificially ventilated rats ATP increases activity of only ~30% of neurones with inspiratory-related discharge (Gourine and Spyer, unpublished observations). This proportion is similar to the proportion of VLM pre-inspiratory and inspiratory neurones found to express $P2X_2$ receptor subunit. This proportion of VLM neurones with inspiratory-related discharge that express $P2X_2$ subunit or are excited by ionophoretic application of ATP is

significantly smaller than the proportion of these cells that are excited during hypercapnia. Hypercapnia increased the activity of 85% of inspiratory and 66% of pre-inspiratory VLM neurones and in all cases excitation of these neurones during hypercapnia was reduced or abolished by microionophoretic application of the P2 receptor antagonists suramin or PPADS (Thomas and Spyer, 2000).

A possible explanation for this apparent discrepancy is that P2X receptors may be expressed by VLM neurones that are activated during hypercapnia and provide excitatory drive to the pre-inspiratory and inspiratory neurones. If this is correct, then the VLM neurones with inspiratory-related discharge may not need to express P2X receptors to exhibit chemosensitivity. Sensitivity to changes in $[H^+]$ may be a property of other VLM neurones which may or may not have respiratory-related modulation of their activity (similar to NTS "chemosensitive" neurones that fire tonically, without any rhythmic relation to the phrenic nerve bursts [for review, see Sapru, 1996]). The effect of P2 receptor blockers on hypercapnia-induced increases in activity of VLM pre-inspiratory and inspiratory neurones could be explained by their action on the adjacent chemosensitive elements that express $P2X_2$ receptor subunits and provide excitatory drive to these inspiratory neurones. The absence of an ATP evoked increase in VLM inspiratory neuronal discharge may be a consequence of a diminished sensitivity of these P2X receptors in conditions of normocapnia (i.e. at pH values close to 7.4).

It is also possible that VLM neurones with inspiratory-related discharge are inherently chemosensitive and their sensitivity to changes in $pCO_2/[H^+]$ is mediated either by P2X receptors that do not contain $P2X_2$ receptor subunits or by metabotropic P2Y receptors. Alternatively, it is conceivable that during hypercapnia changes in the presynaptic P2X receptor function may be responsible for $CO_2$-evoked excitation of VLM neurones. This possibility is supported by the results of Deuchars *et al.* (2001) who demonstrated that $P2X_7$ receptors are present in presynaptic excitatory terminals in the medulla oblongata. If this is the case, then the diminished sensitivity of these receptors to ATP during normocapnia can also explain why a relatively small proportion of these neurones respond to the ionophoretic application of ATP.

Finally, our latest data suggest that sensitivity of P2X receptors to changes in extracellular $[H^+]$ may not be responsible for chemosensitivity of the brainstem neurones at all. In anaesthetised and artificially ventilated rats by means of amperometric enzymatic biosensors we were able to demonstrate in real time that hypercapnia induces a marked increase in concentration of ATP on the ventral surface of the medulla, and that this increase coincides exactly with the increase in amplitude of the phrenic

nerve bursts (Gourine, Llaudet, Dale and Spyer, unpublished observations). Therefore, it is possible that during hypercapnia an increase in $[ATP]_e$ is responsible for the overall augmentation of the central respiratory output. These data are in accord with previous results demonstrating a reduction of the resting phrenic nerve discharge following bilateral microinjection of the P2 receptor antagonist suramin (Thomas *et et.*, 1999). Thus, the hypercapnia-induced increase in ATP concentration in the extracellular fluid in the VLM, rather than an increase in sensitivity of certain P2 receptors to ATP, may underline the involvement of purinergic signalling in the mechanisms of central chemosensitivity.

## 2.6 Conflicting Data

There are data, that are difficult on a first glance to reconcile with the hypothesis that ATP has a major role as a mediator of central $CO_2$ chemoreception. If ATP at the VLM were to have such a role it would be expected that an increase in ventilation would be evoked during normocapnia when ATP is injected into the VLM. Instead, ATP has been shown to induce an immediate and profound expiratory apnoea when microinjected into the rostral VLM (Thomas *et al.*, 2001).

This can be reconciled with our demonstration that $P2X_2$ receptor subunit immunoreactivity is confined predominantly to the population of the VLM expiratory neurones (50% of VLM expiratory neurones appear to express $P2X_2$ receptor subunit; Gourine, Atkinson, Deuchars and Spyer, unpublished observations). Secondly, expiratory neurones in the rostral VLM are significantly more sensitive to ATP, compared to the pre-inspiratory and inspiratory neurones (microionophoretic application of ATP increases activity of ~80% of studied expiratory neurones; Gourine and Spyer, unpublished observations). Therefore, the combination of these results suggest that apnoea evoked by ATP microinjected into the restricted area of rostral VLM is due to P2X-receptor mediated increase in activity of expiratory neurones, which are the most abundant type of respiratory neurones in this area of the brainstem. Taking into the account the limitations of agonist injections for functional studies we conclude that these results provide further evidence that ATP is an important regulator of the activity of VLM expiratory neurones, but do not rule out the hypothesis of the ATP role as a mediator of central $CO_2$ chemoreception.

# 3. CHEMOSENSITIVITY OF VLM RESPIRATORY NEURONES: A ROLE FOR $GABA_A$ RECEPTORS?

## 3.1 $GABA_A$ Receptors are Sensitive to Changes in Extracellular $[H^+]$

The fact that $GABA_A$ receptor function can be significantly influenced by changes in the external $[H^+]$ indicated potential involvement of these ionotropic receptors in the mechanisms of $CO_2$ chemosensitivity of the brainstem neurones. Several studies have demonstrated that lowering external pH can enhance (Gallagher *et al.*, 1983; Robello *et al.*, 1994; Pasternack *et al.*, 1996) or reduce (Smart, 1992; Pasternack *et al.*, 1996; Huang and Dillon, 1999] GABA-activated responses on $GABA_A$ receptors. Krishek *et al.* (1996) have demonstrated that the subunit composition of recombinant $GABA_A$ receptors significantly affects their sensitivities to $H^+$. These data indicate that if VLM respiratory neurones possess $GABA_A$ receptors then the mechanism of their $pCO_2/H^+$-chemosensitivity may involve acidification-induced changes in sensitivity of these $GABA_A$ receptors to GABA.

## 3.2 A Role For $GABA_A$ Receptors in the Mechanisms of pH-Sensitivity of VLM Inspiratory Neurones

Indeed, there is evidence that the pattern of distribution and density of chemosensitive neurones in the VLM is similar to those of neurones containing GABA (Miura *et al.*, 1998) and that chemosensitive neurones in the VLM express $GABA_A$ receptors (Kanazawa *et al.*, 1998). There is also evidence that VLM respiratory neurones and, in particular, inspiratory neurones are under tonic GABA-induced inhibition mediated by $GABA_A$ receptors (Haji *et al.*, 1992; Schmid *et al.*, 1996; Dogas *et al.*, 1998; Yajima and Hayashi, 1999).

Recent data obtained in our laboratory provide further evidence supporting a role for $GABA_A$ receptors in the mechanisms of pH-sensitivity of VLM inspiratory neurones. In experiments in anaesthetised and artificially ventilated rats we have compared the effect of $GABA_A$ receptor blockade (application of bicuculline methiodide [BMI]) and that of hypercapnia on the discharge of the VLM inspiratory neurones as well as the effects of $GABA_A$ receptor blockade on the firing of these neurones during normo- and hypercapnia (Gourine and Spyer, 2001). Ionophoretic application of BMI evoked an increase in the resting firing rates of all recorded VLM inspiratory neurones (n=22), confirming that these neurones

are under tonic GABA-ergic inhibition mediated by $GABA_A$ receptors. The BMI-induced increase in discharge of VLM inspiratory neurones was not affected by kynurenic acid - a broad spectrum excitatory amino acid receptor antagonist, indicating that the effect of BMI directly results from its action on post-synaptic $GABA_A$ receptors. Interestingly, during hypercapnia, changes in the discharge pattern (i.e. an increase in the discharge frequency during the neurone's normally active phase) and firing frequency of the VLM inspiratory neurones were virtually identical to those, evoked by ionophoretic application of BMI (10 mM, 20 nA) in conditions of normocapnia. Similarities in the effects of $GABA_A$ receptor blockade and that of hypercapnia on the discharge pattern of the VLM inspiratory neurones, as well as the lack of a BMI (20 nA) effect on their discharge during hypercapnia support the hypothesis that partial withdrawal of a tonic $GABA_A$ receptor-mediated inhibition contributes to the $CO_2$-evoked increase in activity of these neurones.

## 3.3 Recruitment

It appears that the VLM also contains a population of electrically silent neurones which display rhythmic respiratory-related electrical activity during $GABA_A$ receptor blockade (application of BMI) and hypercapnia (Gourine and Spyer, 2001). Interestingly, neurones that were induced to fire by BMI but did not show respiratory-related activity were not affected by an increase in inspired $CO_2$. Furthermore, some of these silent neurones that show respiratory-related activity during both BMI application and hypercapnia were also induced to fire by microionophoretic application of ATP (Gourine and Spyer, unpublished observations). The question which remains open is whether the population of electrically silent neurones which display rhythmic respiratory-related activity during $GABA_A$ receptor blockade and hypercapnia represent a "pool" of neurones that are recruited during hypercapnia and contribute to the increase in amplitude of the phrenic nerve bursts.

From these studies we conclude that hypercapnia-evoked activation of VLM inspiratory neurones may involve a withdrawal in part of a tonic $GABA_A$ receptor-mediated inhibition and this disinhibition may play a role in the hypercapnia-induced overall increase in ventilatory activity. Since this mechanism of $CO_2$-evoked increase in activity of VLM respiratory neurones requires intact synaptic transmission, it is supported by the early evidence that in conditions of synaptic blockade neurones in slices from the ventral medullary surface lose their sensitivity to changes in $[H^+]$ (Fukuda and Loeschcke, 1977, 1979).

# 4. DISCUSSION

In this brief overview we have mentioned and discussed in detail the data suggesting that pH sensitivity of ionotropic receptors P2X and $GABA_A$ may underline $CO_2$ chemosensitivity of the medullary respiratory neurones. However, there are several issues that complicate studies on brainstem chemosensitive neurones, and the involvement of ionotropic receptors in the chemosensory mechanism also requires consideration.

## 4.1 Brainstem Chemosensitive Neurones

It is likely that many CNS neurones are sensitive to changes in extracellular $[H^+]$. As yet there are no quantitative criteria to distinguish general neuronal sensitivity to pH from specific chemosensory function. If certain localised areas of the brainstem have evolved to function as chemoreceptors we expect to find that certain neurones in these areas would possess a unique sensitivity to $pCO_2/H^+$, which is much higher compared to that of the other central neurones. Second, even if the existence of such neurones within central chemosensitive sites is documented we have to have firm criteria to discriminate between chemosensitive neurones that provide input to the respiratory network (respiratory chemosensitive) from these that do not (non-respiratory chemosensitive). As suggested by Ballantyne and Scheid (2000) "one approach to looking for connections between chemosensitive neurones and the neurones controlling ventilation is to use the respiratory rhythm itself as an indication of connectivity, and to ask whether neurones showing this rhythm are also chemosensitive". This is exactly the approach we used in our studies to investigate the role of P2X and $GABA_A$ receptors in the mechanisms of chemosensitivity of the medullary respiratory neurones.

There is, however, a possibility that some intrinsically chemosensitive neurones may be overlooked by this approach. Although, there is evidence obtained in the brainstem-spinal cord preparation of the neonatal rat that some VLM neurones that display rhythmic respiratory-related activity are inherently sensitive to changes in $pCO_2/[H^+]$ (Kawai *et al.*, 1996), at present we do not know whether in the adult chemosensitivity is also a property of VLM neurones which may not have any respiratory-related modulation of their activity. As discussed above in relation to the role of P2X receptors in central chemosensitivity, it is possible that some tonic VLM neurones can function as chemosensors, detect changes in local $[H^+]$ and provide excitatory input to the VLM respiratory network.

## 4.2 Ionotropic Receptors Sensitive to Changes in $[H^+]$

As described already there is significant evidence that P2X receptor sensitivity to ATP as well as $GABA_A$ receptor sensitivity to GABA are modulated by the external pH. The fact that both P2X and $GABA_A$ receptor functions are altered by acidification of the extracellular environment indicates potential involvement of these ionotropic receptors in the mechanisms of $H^+$ chemosensitivity of the brainstem respiratory neurones. However, direct extrapolation from these data on the complex situations *in vivo* could be both misleading and naïve since in the majority of studies P2X and $GABA_A$ receptors show pH-sensitivity outside the range of physiological changes in pH (eg. at pH 5.4), and (or) experiments on the expressed receptors are done at room temperature (eg. at 18-20°C). Although, these studies are useful in terms of characterisation of the receptor function, they are not physiologically relevant since in the living brain under non-pathological conditions pH rarely decreases below 7.2-7.0 and the temperature (in most mammalian species) is maintained within a narrow range of 37-38°C. Hence, our recent data that indicate that there is a hypercapnia-induced increase in ATP concentration in the extracellular fluid in the VLM, rather than the increase in sensitivity of certain P2X receptors to ATP, may underline the involvement of purinergic signalling in the mechanisms of central chemosensitivity.

## 4.3 Conclusion

In this report the evidence indicating that both P2X and $GABA_A$ receptors play an important role in central $CO_2$ chemoreception and are involved in mediation of ventilatory response to hypercapnia has been reviewed and discussed in detail. Although, $CO_2$-evoked alterations in P2X and $GABA_A$ receptor function are not solely responsible for hypercapnia-induced changes in the activity of VLM chemosensitive neurones, we conclude that modifications of ATP-excitatory and GABA-inhibitory inputs are essential features of the chemosensory control of respiratory activity.

## ACKNOWLEDGEMENTS

The experimental work described was supported by the Biotechnology and Biological Sciences Research Council (UK). We thank Professor N. Dale and Dr. G. Ackland for critical reviews of the manuscript.

# REFERENCES

Ballantyne, D., and Scheid, P., 2000, Mammalian brainstem chemosensitive neurones: linking them to respiration in vitro. *J. Physiol.* 525: 567-577.

Ballantyne, D., and Scheid, P., 2001, Central chemosensitivity of respiration: a brief overview. *Respir. Physiol.* 129: 5-12.

Brown, S.G., Townsend-Nicholson, A., Jacobson, K.A., Burnstock, G., and King, B.F., 2002, Heteromultimeric $P2X_{1/2}$ receptors show a novel sensitivity to extracellular pH. *J. Pharmacol. Exp. Ther.* 300: 673-680.

Buell, G., Collo, G., and Rassendren, F., 1996, P2X receptors: an emerging channel family. *Eur. J. Neurosci.* 8: 2221-2228.

Cherniack, N.S., 1993, Physiological roles of central chemoreceptors. In *Respiratory control – Central and Peripheral Mechanisms* (D.F. Speck, M.S. Dekin, W.R. Revellette and D.T. Frazier, eds.), University of Kentucky, pp.138-146.

Daly, M.DeB., 1997, Peripheral arterial chemoreception and respiratory-cardiovascular integration. In *Monograph for the Physiological Society.* Oxford University Press, Oxford.

Deuchars, S.A., Atkinson, L., Brooke, R.E., Musa, H., Milligan, C.J., Batten, T.F., Buckley, N.J., Parson, S.H., and Deuchars, J., 2001, Neuronal $P2X_7$ receptors are targeted to presynaptic terminals in the central and peripheral nervous systems. *J. Neurosci.* 21: 7143-7152.

Dogas, Z., Krolo, M., Stuth, E.A., Tonkovic-Capin, M., Hopp, F.A., McCrimmon, D.R., and Zuperku, E.J., 1998, Differential effects of $GABA_A$ receptor antagonists in the control of respiratory neuronal discharge patterns. *J. Neurophysiol.* 80: 2368-2377.

Fukuda, Y., and Loeschcke, H.H., 1977, Effect of $H^+$ on spontaneous neuronal activity in the surface layer of the rat medulla oblongata *in vitro*. *Pflugers Arch.* 371: 125-134.

Fukuda, Y., and Loeschcke, H.H., 1979, A cholinergic mechanism involved in the neuronal excitation by $H^+$ in the respiratory chemosensitive structures of the ventral medulla oblongata of rats *in vitro*. *Pflugers Arch.* 379: 125-135.

Gallagher, J.P., Nakamura, J., and Shinnick-Gallagher, P., 1983, The effects of temperature, pH and Cl-pump inhibitors on GABA responses recorded from cat dorsal root ganglia. *Brain Res.* 267: 249-259.

Gourine, A.V., and Spyer, K.M., 2001, Chemosensitivity of medullary inspiratory neurones: A role for $GABA_A$ receptors? *Neuroreport* 12: 3395-3400.

Haji, A., Takeda, R., and Remmers, J.E., 1992, Evidence that glycine and GABA mediate postsynaptic inhibition of bulbar respiratory neurons in the cat. *J. Appl. Physiol.* 73: 2333-2342.

Heeringa, J., Berkenbosch, A., de Goede, J., and Olievier, C.N., 1979, Relative contribution of central and peripheral chemoreceptors to the ventilatory response to $CO_2$ during hyperoxia. *Respir. Physiol.* 37: 365-379.

Huang, R.Q., and Dillon, G.H., 1999, Effect of extracellular pH on GABA-activated current in rat recombinant receptors and thin hypothalamic slices. *J. Neurophysiol.* 82: 1233-1243.

Kanazawa, M., Sugama, S., Okada, J., and Miura, M., 1998, Pharmacological properties of the $CO_2/H^+$-sensitive area in the ventral medullary surface assessed by the effects of chemical stimulation on respiration. *J. Auton. Nerv. Syst.* 72: 24-33.

Kanjhan, R., Housley, G.D., Burton, L.D., Christie, D.L., Kippenberger, A., Thorne, P.R., Luo, L., and Ryan, A.F., 1999, Distribution of the $P2X_2$ receptor subunit of the ATP-gated ion channels in the rat central nervous system. *J. Comp. Neurol.* 407: 11-32.

Kawai, A., Ballantyne, D., Muckenhoff, K., and Scheid, P., 1996, Chemosensitive medullary neurones in the brainstem-spinal cord preparation of the neonatal rat. *J. Physiol.* 492: 277-292.

King, B.F., Townsend-Nicholson, A., Wildman, S.S., Thomas, T., Spyer, K.M., and Burnstock, G., 2000, Coexpression of rat $P2X_2$ and $P2X_6$ subunits in *Xenopus* oocytes. *J. Neurosci.* 20: 4871-4877.

King, B.F., Wildman, S.S., Ziganshina, L.E., Pintor, J., and Burnstock, G., 1997, Effects of extracellular pH on agonism and antagonism at a recombinant $P2X_2$ receptor. *Br. J. Pharmacol.* 121: 1445-1453.

King, B.F., Ziganshina, L.E., Pintor, J., and Burnstock, G., 1996, Full sensitivity of $P2X_2$ purinoceptor to ATP revealed by changing extracellular pH. *Br. J. Pharmacol.* 117: 1371-1373.

Krishek, B.J., Amato, A., Connolly, C.N., Moss, S.J., and Smart, T.G., 1996, Proton sensitivity of the $GABA_A$ receptor is associated with the receptor subunit composition. *J. Physiol.* 492: 431-443.

Loeschcke, H.H., 1982, Central chemosensitivity and the reaction theory. *J. Physiol.* 332: 1-24.

McCrimmon, D.R., Ramirez, J.M., Alford, S., and Zuperku, E.J., 2000, Unraveling the mechanism for respiratory rhythm generation. *Bioessays* 22: 6-9.

Miura, M., Okada, J., and Kanazawa, M., 1998, Topology and immunohistochemistry of proton-sensitive neurons in the ventral medullary surface of rats. *Brain Res.* 780: 34-45.

Nattie, E., 1999, $CO_2$, brainstem chemoreceptors and breathing. *Prog. Neurobiol.* 59: 299-331.

Nattie, E., 2001, Central chemosensitivity, sleep, and wakefulness. *Respir. Physiol.* 129: 257-268.

Pasternack, M., Smirnov, S., and Kaila, K., 1996, Proton modulation of functionally distinct $GABA_A$ receptors in acutely isolated pyramidal neurons of rat hippocampus. *Neuropharmacology* 35: 1279-1288.

Pinault, D., 1996, A novel single-cell staining procedure performed in vivo under electrophysiological control: morpho-functional features of juxtacellularly labeled thalamic cells and other central neurons with biocytin or Neurobiotin. *J. Neurosci. Methods* 65: 113-136.

Ralevic, V., and Burnstock, G., 1998, Receptors for purines and pyrimidines. *Pharmacol. Rev.* 50: 413-492.

Richter, D.W., 1982, Generation and maintenance of the respiratory rhythm. *J. Exp. Biol.* 100: 93-107.

Richter, D.W., Ballanyi, K., and Schwarzacher, S., 1992, Mechanisms of respiratory rhythm generation. *Curr. Opin. Neurobiol.* 2: 788-793.

Richter, D.W., and Spyer, K.M., 2001, Studying rhythmogenesis of breathing: comparison of *in vivo* and *in vitro* models. *Trends Neurosci.* 24: 464-472.

Ritucci, N.A., Chambers-Kersh, L., Dean, J.B., and Putnam, R.W., 1998, Intracellular pH regulation in neurons from chemosensitive and nonchemosensitive areas of the medulla. *Am. J. Physiol.* 275: R1152-R1163.

Robello, M., Baldelli, P., and Cupello, A., 1994, Modulation by extracellular pH of the activity of $GABA_A$ receptors on rat cerebellum granule cells. *Neuroscience* 61: 833-837.

Sapru, H.N., 1996, Carotid chemoreflex. Neural pathways and transmitters. *Adv. Exp. Med. Biol.* 410: 357-364.

Schmid, K., Foutz, A.S., and Denavit-Saubie, M., 1996, Inhibitions mediated by glycine and $GABA_A$ receptors shape the discharge pattern of bulbar respiratory neurons. *Brain Res.* 710: 150-160.

Smart, T.G., 1992, A novel modulatory binding site for zinc on the $GABA_A$ receptor complex in cultured rat neurones. *J. Physiol.* 447: 587-625.

Spyer, K.M., and Thomas, T., 2000., Sensing arterial $CO_2$ levels: a role for medullary P2X receptors. *J. Auton. Nerv. Syst.* 81: 228-235.

Stoop, R., Surprenant, A., and North, R.A., 1997, Different sensitivities to pH of ATP-induced currents at four cloned P2X receptors. *J. Neurophysiol.* 78: 1837-1840.

Thomas, T., Ralevic, V., Bardini, M., Burnstock, G., and Spyer, K.M., 2001, Evidence for the involvement of purinergic signalling in the control of respiration. *Neuroscience* 107: 481-490.

Thomas, T., Ralevic, V., Gadd, C.A., and Spyer, K.M., 1999, Central $CO_2$ chemoreception: a mechanism involving P2 purinoceptors localized in the ventrolateral medulla of the anaesthetized rat. *J. Physiol.* 517: 899-905.

Thomas, T., and Spyer, K.M., 2000, ATP as a mediator of mammalian central $CO_2$ chemoreception. *J. Physiol.* 523: 441-447.

Wildman, S.S., King, B.F., and Burnstock, G., 1997, Potentiation of ATP-responses at a recombinant $P2X_2$ receptor by neurotransmitters and related substances. *Br. J. Pharmacol.* 120: 221-224.

Yajima, Y., and Hayashi, Y., 1999, Ambiguous respiratory neurons are modulated by $GABA_A$ receptor-mediated inhibition. *Neuroscience* 90: 249-257.

Yao, S.T., Barden, J.A., Finkelstein, D.I., Bennett, M.R., and Lawrence, A.J., 2000, Comparative study on the distribution patterns of $P2X_1$-$P2X_6$ receptor immunoreactivity in the brainstem of the rat and the common marmoset (*Callithrix jacchus*): association with catecholamine cell groups. *J. Comp. Neurol.* 427: 485-507.

# Effects of Controller Dynamics on Simulations of Irregular and Periodic Breathing

GUY LONGOBARDO, CARLO J. EVANGELISTI, AND NEIL S. CHERNIACK
*(Department of Medicine, UDMNJ, Newark, NJ)*

## 1. INTRODUCTION

It is now clear that irregularities and instabilities in ventilation can result from the fact that there is feedback in the respiratory control system. This largely accounts for various forms of periodic breathing including Cheyne-Stokes respiration, central apneas during non-REM sleep, and the transient apneas that sometimes occur even in awake healthy people after periods of voluntary hyperventilation or with hypoxia.It is even possible that obstructive sleep apneas in part occur by differences in the effects of feedback on chest wall compared to upper airway muscles. These disturbances in breathing can be reproduced by feedback models of chemical control and often can be caused experimentally by interventions and system changes suggested by the mathematical models. However there remain instances, as in the apneas that appear in REM sleep or in premature infants that are difficult to explain simply by feedback problems.

In current models aiming at simulating periodic breathing, the respiratory controller as shown in Figure 2 is treated as a black box, which generates respiratory patterns as sine waves of airflow (Longobardo *et al.*, 2002). The relationship between frequency and tidal volume is expressed by one or more linear equations. Although the complexities of respiratory generation have been appreciated for years, only relatively recently has the construction of mathematical models of the respiratory pattern generation been attempted. Moreover quite recently it has been recognized that the production of the respiratory pattern may involve pacemaker neurons as well as mutually inhibitory networks of inspiratory and expiratory neurons (Butera *et al.*, 1999).

*Chemoreception*, Edited by Pequignot et al.
Kluwer Academic/Plenum Publishers, New York, 2003

But the effects of these newer concepts on breathing when included in feedback models of respiratory regulation have not been studied.

In this paper we have examined the effect of more realistic models of respiratory pattern generation in the respiratory controller on the simulation of periodic breathing. We have tested the effects on post-hyperventilation breathing of including in our previously published neuro-chemical model of the regulation of breathing various models of the respiratory pattern generator. We also have hypothesized a mechanism for respiratory control during REM Sleep.

## 2. RESULTS

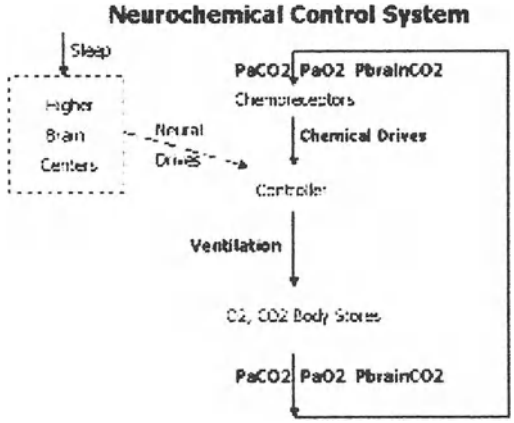


*Figure 1* is a block diagram of the Neurochemical Control System. The chemical inputs,PaCO2, PbrainCO2, and PaO2 are joined by neural inputs that modulate alertness arising for example from higher brain centers. Through the controller these inputs determine the ventilation that is required to bring the system into equi-librium. Ventilation drives the respiratory muscles and the lungs, and changes body gasses. The gas values are fed back to the controller, which again adjusts the ventilation.

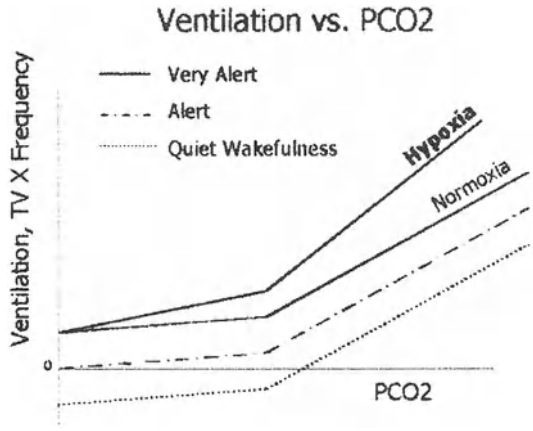


*Figure 2* shows the controller for the present neurochemical control system. It has no dynamics. The ventilatory demand varies linearly with CO2, with low response at sub-normal PCO2 values, and greater response at normal and hypercapnic levels. As alertness factors decrease, the ventilation threshold for the chemical controller is lowered, so that at a given PCO2 the possibility for apneas increases.

## 2.1 Description of Models of Respiratory Pattern Generation

We studied in detail two models of Respiratory Pattern Generation (RPG), the Matsugu/Duffin/ Poon model (1998), and the Botros/Bruce (1990) models. These RPG models predict neuron membrane potential which we related to phrenic nerve activity, and then linearly to Tidal Volume and Frequency. These models are based on the oscillations that result from the interactions of a system of mutually inhibiting neurons. They do not require pacemakers to oscillate, but since pacemakers may have an impact on the membrane potential of these circuits we also studied the impact of pacemaker neurons, and noise on ventilation. These RPG's were then inserted into the neurochemical feedback model as part of the controller. In order to test the ventilatory response following hyperventilation we drove arterial PCO2 down to 19 mm Hg by hyperventilation with 37% O2. There are already experimental data available against which these results may be compared. (Meah and Gardner, 1994, Longobardo, *et al.*, 2002).

### 2.1.1 Matsugu Model

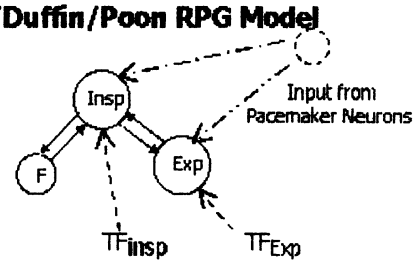


$$dX_i/dt=-(1/T_i)*X_i-\Sigma W_{ij}*S(X_j)+(1/T_i)*R_i+TFi+\text{Pacemakers}$$

where $TF_{insp}$ and $TF_{exp}$ = Chemical and Neural Tonic Forces

*Figure3* shows the Matsugu model.It is a minimal" model, with two neurons,an Inspiratory, and an Expiratory. A"virtual interneuron" is added to provide the adaptation function which seems to be present in the Inspiratory Neuron, a self-limiting ability which, as firing increases leads to lessening of activity. The equations are first-order differential equations, with the neuron Time Constant Ti, and the mutually inhibiting terms Wij*S (Xj).

External inputs are TFi, the tonic forces that represent chemical and neural inputs, and Pacemakers, which represent respiratory pacemakers or other extraneous inputs from external systems. These latter can be periodic or random, and enter mathematically at the same point as TFi and Pacemakers. The frequency response of this model is limited, both in magnitude and range and required entrainment by pacemakers to yield the frequency vs. ventilation observed in humans. (This is also true of the Botros Model described later, but to a more limited extent.) For frequency to rise with increasing ventilation the Matsugu model also requires the assumption of a differential response to tonic forces by the Inspiratory and Expiratory neuron in order to have frequency variation.

### 2.1.2 Botros Model

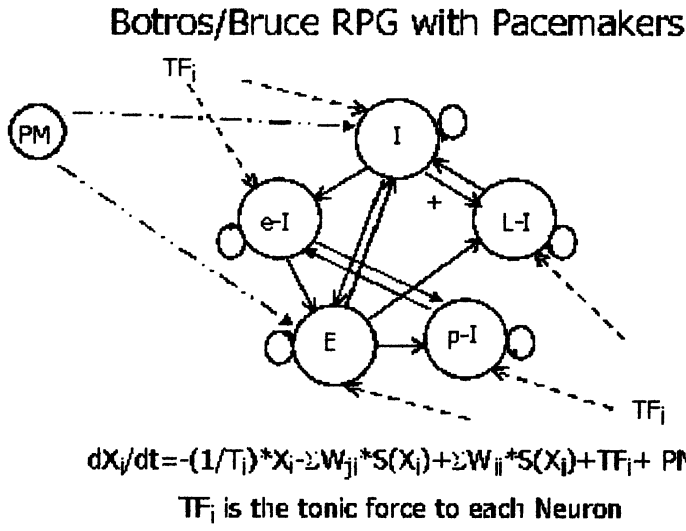


*Figure 4* shows the Botros/Bruce Model, which uses five neuronal groups. Three represent inspiratory neurons, I, Inspiratory, L-I, Late Inspiratory, e-I, early Inspiratory. Two represent expiratory neurons, p-I, post-Inspiratory, and E, Expiratory. The equations for each neuron are mathematically of the same form as the Matsugu model. However the Bruce model is more stable in its response to changing inputs, and shows less variation in ventilation in the steady state. The responses of the neurons to tonic forces are in constant proportion as the tonic force is varied.

## 2.2 Simulations

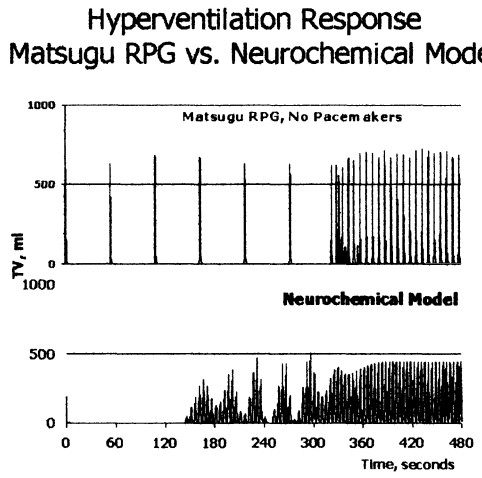


*Figure 5* compares the post-hyperventilation response of the neurochemical model with the Matsugu RPG in the controller (in the top panel) to the response of the model with the original "black box" controller of the earlierneurochemical model in the bottom panel (Longobardo et al., 2002). In this implementation, the Matsugu model has a natural frequency of one breath/minute at near zero ventilation, which causes the spikes in ventilation during the first minutes after hyperventilation. In human experiments, this period is usually an apneic period of varying duration a without the occurrence of intervening large breaths, which the "black box" neurochemical model simulates well. Note also that the recovery and equilibrium response are highly irregular.

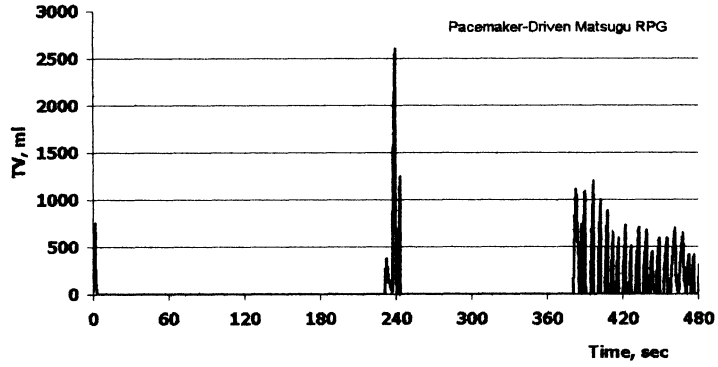


*In Figure 6* pacemakers *were* included in the Matsugu model to yield experimentally observed frequency ventilation relationships. Pacemaker frequency and amplitude increased with tonic force, so that the pacemakers entrained the RPG at higher frequencies, while at normal ventilation and below the pacemaker and the RPG interacted with each other. Inclusion of the pacemakers as an integral part of the oscillating system stabilized the response Even so stabilized, the response of the Matsugu model is typified by long apneas and abnormally irregular ventilation.

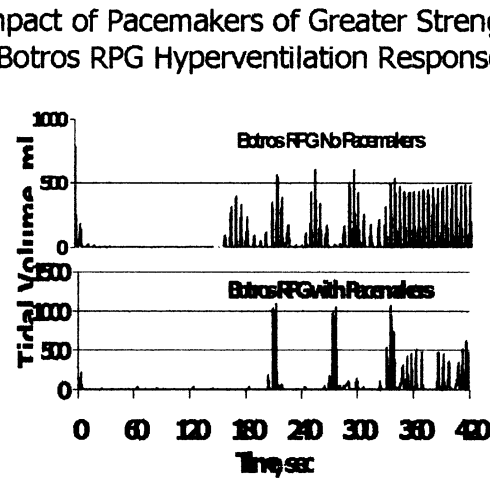


*Figure 7*, in the upper panel shows the response of the Botros model (without a pacemaker disturbance) to the hyperventilation disturbance. Frequency and tidal volume are clearly less regular in the post-hyperventilation period than in the neurochemical model and that both expiratory prolongations and apneas occur. However the dynamics of the changes ventilatory level in both models are rather similar. The addition of a pacemaker of sufficient strength, shown in the lower panel increases the initial apneic period by about a minute, causes additional significant apneic periods and bursts of large amplitude, and delays equilibrium. The frequency used for the pacemakers in this case was 1 cycle/minute. The essential features of the response depend on the pacemaker frequency and amplitude. As the disturbing pacemaker amplitude and frequency are reduced the response becomes less erratic and more like the response without the pacemaker input.

## 2.3 REM Sleep

The effects on the chemical controller produced by Non-REM sleep have been represented by an increase in the threshold needed for ventilation as shown in Figure 2 and Figure 8 (Longobardo *et al.*, 2002). REM sleep can be characterized as a state in which neural drives are high, but arising internally rather than from the environment, and chemical drives are rather low (Orem et al., 2000), and thus the movement of the CO2 response curve to the right as shown in Figure 8.

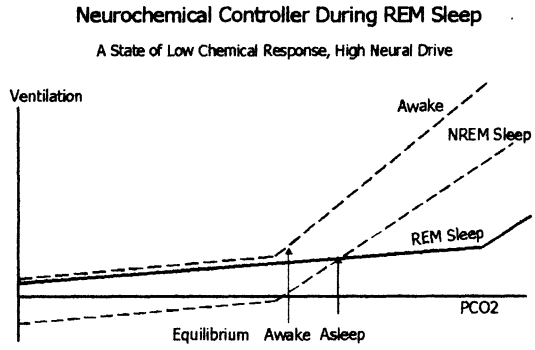


***Figure 8***

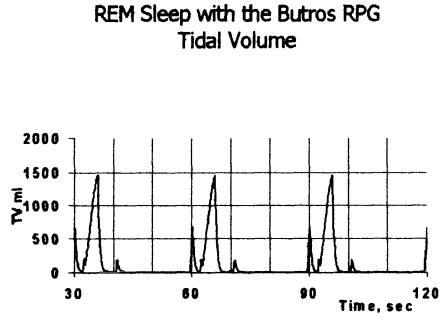


*Figure 9*

With the controller characteristic shown in Figure 8, of low chemical drive and high neural drive, a periodic sinusoidal input to the neuronal circuit produced the regular pattern of hyperventilation and apnea shown in Figure 9. A random non-periodic input provides a similar of periods of hyperventilation and apnea but they do not occur as regularly. These inputs could result from pacemaker activity or oscillatory changes in respiratory excitation occurring from activity in other physiological systems, e.g. baroreceptors.

## 3. DISCUSSION

Models of the feed back control of breathing have included chemoreceptors and more recently the effects of arousal but have treated the respiratory controller as a featureless black box and ignored the increasing volume of data on the neuronal basis of respiratory rhythm generation. On the other hand, models of the respiratory pattern generator in the past have attempted to duplicate the firing patterns of different types of medullary respiratory neurons but these patterns were not been related to actual levels of ventilation or their impact on ventilatory control assessed. When the controller was represented by networks of mutually inhibitory and excitatory inspiratory and expiratory neurons and included in the model of the neurochemical control of breathing, the essential features of the response to hyperventilation were not changed very much though it became possible to distinguish absent neuronal activity from expiratory prolongations. In the Botros model as in the neurochemical model with the black box controller, post-hyperventilation continued to be characterized by a period of apnea followed by alternating, relatively smooth cycles of increasing and diminishing amplitude in the level of ventilation, until equilibrium is reached. The Matsugu model could not produce results that were realistic when subjected to hyperventilation.

Both models have quite a narrow frequency response, and have a peak frequency, which depends on the distribution of neurochemical drives to inspiratory and expiratory groups of neurons. As ventilation increases, frequency reaches a peak and then diminishes, almost the reverse of what is seen during hypercapnia in humans where tidal volume plateaus but frequency continues to rise with rising values of ventilation.

There is evidence that pacemaker cells contribute to respiratory pattern generation in immature and perhaps even in adult animals and humans. Models of ion fluxes and membrane potential changes in populations of putative pacemaker neurons have been developed which allow these neurons to fire in tonic, bursting or beating manners. (Butera *et al.*, 1999). These properties of

pacemaker neurons have not been previously related to ventilation levels or tidal volume/ frequency patterns. The addition of regular sinusoidal inputs, representing pacemaker cells causes a much more irregular appearance of apneas. Similar results occur when inputs are not sinusoidal or occur irregularly. While we have called these sinusoidal inputs "pacemaker", they could just as well represent input impinging on the respiratory neurons from the internal or external environment or reflexly. In the Matsugu model examined in this study, pacemaker like activity was needed to simulate the full frequency response observed usually in humans breathing over a subnormal to above normal levels of ventilation. For the Botros model it is possible to increase the frequency in hypercapnia varying the time constants in the neuronal circuit inversely with PCO2. This produces a plateau in tidal volume as frequency continued to rise with rising values of ventilation.

We have begun to use these models to explore their usefulness in simulations of breathing in REM sleep. We have tentatively hypothesized that REM sleep is a state in which chemical drives are relatively suppressed but neural activity is high and noisy and have been encouraged by our initial results showing irregular and periodic breathing during REM sleep even without a disturbance that might cause irregular ventilation because of feedback control.

## REFERENCES

Butera, R.J., Jr., Rinzel, J., Smith, J.C., 1999. Models of Respiratory Rhythm Generation in the Pre-Botzinger Complex. I. Bursting pacemaker Neurons. *J. Neurophysiol*: 81:398-415.

Botros, S. M., Bruce, E. N., 1990, Neural Network Implementation of a three-Phase Model of Respiratory Rhythm Generation. *Biol. Cybern.* 63:143-153.

Longobardo, G., Evangelisti, C., N.S. Cherniack, 2002, Effects of neural drives on breathing in the awake state in humans, *Respir. Physiol.* 129: 317-333.

Matsugu, M., Duffin, J., Poon, C-S., 1998. Entrainment, Instability, Quasi-periodicity, and Chaos in a Compound Neural Oscillator. *J. Comp. Neurosciences*:5, 35-50.

Meah, M.S., Gardner, W. N., 1994. Post-Hyperventialtion Apnea in Conscious Humans. *J. Physiol.* 477 (3), 527-538.

Orem, J., Lovering, A. T., Dunin-Barkowski, W., Vidruk, E. H., 2000
Endogenous excitatory drive to the respiratory system in rapid eye movement sleep in cats. *J.Physiol.*527,2: 365-376.

# $CO_2/H^+$ Signal Transduction and Central Ventilatory Control

HOMAYOUN KAZEMI
*Pulmonary & Critical Care Unit Massachusetts General Hospital and Harvard Medical School Boston, Massachusetts 02114, U.S.A.*

## 1. INTRODUCTION

For over a century it has been known that $CO_2$ has profound effects on the level of ventilation and that minute ventilation is exquisitely sensitive to changes in partial pressure of $CO_2$ ($PCO_2$). It is also known that effects of $CO_2$ on ventilation are primarily through changes in hydrogen ion concentration $[H^+]$ in the brain. Several areas of chemosensitivity have been identified in the midbrain, particularly on the ventral surface of the medulla (VMS) that are essential in generating the neural output in response to changes in $[H^+]$ (Schlaefke et al, 1970; Burton and Kazemi, 2000; Kazemi and Johnson 2002). How the $CO_2/H^+$ signal is transduced centrally has been the subject of great interest and suggestions have included (i) $H^+$ receptors, (ii) $H^+$ gradient across neural membranes, (iii) altering ion channels and (iv) neurotransmitter release or activation.

*Chemoreception*, Edited by Pequignot et al.
Kluwer Academic/Plenum Publishers, New York, 2003

This paper presents data from different experimental and clinical conditions to suggest that the neurotransmitter acetylcholine is essential in the $CO_2/H^+$ signal transduction and that central rhythmogenesis is cholinergic dependent.

## 2. EXPERIMENTAL DATA

Studies to be reported in this section have been performed in our laboratories over the past 10-12 years and several aspects have already been reported in the literature. Relevant findings for this communication will be presented below.

### 2.1 Cholinergic systems and respiratory output in response to acidosis

In lightly anesthetized dogs it was demonstrated that perfusing the ventricular-cisternal system with acidic CSF increased ventilation by 40% when the CSF pH was reduced by 0.4 pH (Burton et al, 1989). This response occurred when the infusing fluids' pH was reduced by increasing $PCO_2$ (respiratory acidosis) or by keeping $PCO_2$ constant and reducing bicarbonate (metabolic acidosis). The increase in ventilation in response to CSF acidosis was totally blocked with simultaneous infusion of the muscarinic antagonist atropine (Burton et al, 1989). In other studies, we showed that acetylcholine perfusion increased ventilation and atropine perfusion decreased ventilation. The increase in $[H^+]$ lessens the activity of the enzyme cholinesterase, which degrades acetylcholine, allowing the excitatory neurotransmitter to increase its duration and intensity of action (Burton et al, 1997).

### 2.2 Assessment of cholinergic system in brain-spinal cord preparation of the neonatal rat.

Synthesis, vesicle formation, release and receptor binding of acetylcholine was studied in a brain stem-spinal cord preparation in the neonatal rat. The brain slice was perfused in a special solution where specific inhibitors of the biochemical steps in the cascade from acetylcholine generation to receptor binding were used and neural discharge from $C_1$-$C_4$ were recorded. The neural output in a dose-dependent manner was reduced in every instant, indicating the importance of the integrity of the cholinergic system in generating the

respiratory neural output under normal acid-base conditions as well as in acidosis (Burton et al 1994, 1995).

Using microinjection technique and an inhibitor of acetylcholine release, OH-citrate, and we mapped the VMS in the brain-spinal cord preparation where cholinergic inhibition led to cessation of neuronal firing. Figure 1 is the summary data from multiple injections at different sites on the VMS. The dark circles indicate inhibition of neural discharge and open circles where no effect was noted. Areas of cholinergic inhibition demonstrate an angiocentric distribution, suggesting that the chemoreceptors are in close proximity of vessels. Multiple injections at different depth, showed that the greatest inhibition of neural discharge was at 200μ below the ventral surface of the medulla.

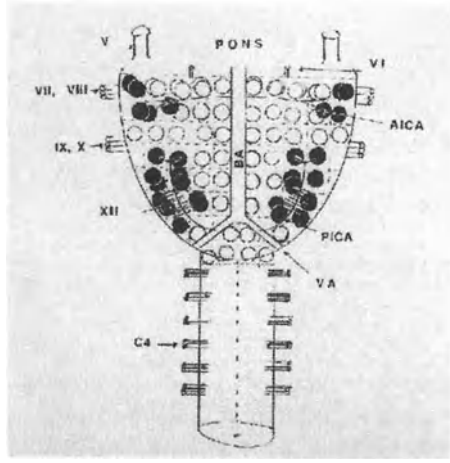


*Figure 1.* A diagram of the isolated brainstem and cervical cord with ventral surface up. Cranial nerves are labeled with Roman numerals. The 4th cervical spinal rootlet (C-4) is noted. Vertebral artery (VA), posterior inferior cerebellar artery (PICA), basilar artery (BA) and anterior inferior cerebellar artery (AICA) are shown. A grid with 0.5 mm squares is superimposed on the medulla. The circles represent a summary of 91 microinjection sites explored in 18 isolated brainstems. Open circles represent sites of no responses and closed circles represent sites of positive, depressive responses.
(Reprinted with permission, *Brain Research*, 1995)

## 2.3. Genetics of central respiratory drive

Acetylcholine is formed by combing acetyl-CO A (generated from the Kreb cycle) with choline. The essential enzyme in this reaction is cholineactelyl transferase (CHAT) viz:

Acetyl-CoA- + Choline → Acetylcholine.
↑
CHAT

The gene for CHAT was identified in the early 1990s – and resides on chromosome 10-q 11.2 (the ret gene) (Viegas-Pequignot et al, 1991; Strauss et al, 1991). Using a knock out mouse model for ret gene, we studied the hypoxic and hypercapnic ventilatory responses in the first day of life in the offspring of heterozygote mice for ret gene (Ret +/-).

None of the offspring had a ventilatory response to hypoxia. Not unexpected since the hypoxic response matures during second and third days of life. The ret negative animal (Ret -/-) had essentially no ventilatory response to inhaled $CO_2$ (8%). The wild type (Ret +/+) increased ventilation by 3-4 fold in response to $CO_2$ breathing and the heterozygotes (Ret +/-) had about 1-1.5 fold increase in ventilation with $CO_2$ breathing (Burton et al, 1997).

## 3. DISCUSSIONS AND CLINICAL RELEVANCE

The experimental data reviewed above and studies from other laboratories (Fukuda and Loeschcke 1979; Nattie et al, 1989; Kawai et al, 1996) show that an intact cholinergic system in the CNS is essential in the ventilatory response to $CO_2$. The $CO_2/H^+$ signal is transducted through acetylcholine and furthermore central neural respiratory drive has a significant cholernigc component and without it there is hypoventilation, $CO_2$ retention and early death.

Disordered breathing, hypoventilation and diminished sensitivity to $CO_2$ are present in many clinical states and are often apparent early in life and can be fatal. Neuropathological studies in sudden infant death syndrome (SIDS) victims have shown abnormalities in the arcuate nucleus and in expression of muscarinic receptors (Filiano and Kinney, 1992). The same abnormalities have also been reported in central congenital hypoventilation syndrome (CCHS) (Folgering et al, 1979)

Familial factors are important in both CCHS and SIDS and they may overlap between the two syndromes. In another congenital disease affecting the parasympathetic system, Hirschsprung's disease, there is a 20% incidence of congenital hypoventilation. In CCHS patients some 50% have Hirschsprung's disease (Croaker et al, 1998). All these clinical entities underline the importance of the cholinergic system in central drive of ventilation and the fact that hypoventilation and $CO_2$ retention result in poorly developed or malfunctioning parasympathetic system.

The conditions cited above usually affect infants and children; however, a genetic expression of this biological abnormality may be the basis of hypoventilation and hypercapnia in the adult population with various forms of lung disease.

## ACKNOWLEDGEMENTS

Most of the work from our laboratory has been supported by grants from the National Institutes of Health (NIH) and the Shoolman Fund of the Pulmonary & Critical Care Unit. I am most grateful to my colleague, Melvin D. Burton, M.D., for his work in the laboratory on the cholinergic system and to Kathleen Sweeney Laing for her secretarial assistance.

## REFERENCES

Burton MD, Johnson DC, Kazemi H, 1989, CSF acidosis augments ventilation through cholinergic mechanisms. *J Appl Physiol* 66:2565-2572.

Burton MD, Nouri K, Baichoo S, Samuels-Toyloy N, Kazemi H, 1994, Ventilatory output and acetylcholine perturbations in release and muscarinic receptor activation. *J Appl Physiol* 77:2275-2284.

Burton MD, Nouri M, Kazemi H, 1995, Acetylcholine and central respiratory control: perturbations of acetylcholine synthesis in the isolated brainstem of the neonatal rat. *Brain Res* 670:39-47.

Burton MD, Kawasrima A, Bryaer JA, Kazemi H, Shannon DC, Schuchardt A, Constantini F, Pachnis V, Kinane TB, 1997, Ret proto-oncogene is important for the development of respiratory $CO_2$ sensitivity. *J Auton Nerv Syst* 63:137-143.

Burton MD, Johnson DC, Kazemi H, 1997, The central respiratory effects of acetylcholine vary with CSF pH. *J Autonomic Nerv Syst* 62:27-32.

Burton MD, Kazemi H, 2000, Neurotransmitters in central respiratory control. *Respir Physiol* 122:111-121.

Croaker GD, Shi E, Simpson E. Cartmill T, Cass DT, 1998, Congenital central hypoventilation syndrome and Hirschsprung's disease. *Arch Dis Child* 78:316-322.

Filiano JJ, Kinney HC, 1992, Arcuate nucleus hypoplasia in the sudden infant death syndrome. *J Neuropathol Exp Neurol* 51:393-403.

Folgering H, Kuyper F, Kille JF, 1979, Primary alveolar hypoventilation in an infant without external arcuate nucleus. *Bull European Pathophysiol Respir* 15:659-665,

Fukuda Y, Loeschcke HH, 1979, Cholinergic mechanism involved in neuronal excitation by $H^+$ in rats *in vitro*. *Pflugers Arch* 379:125-135.

Kawai A, Ballantyne D, Muckenhoff K, Scheid P, 1996, Chemosensitive medullary neurons in the brainstem-spinal cord preparation of the neonatal rat. *J Physiol London* 70:1-7.

Kazemi H, Johnson DC, 2002, Respiration. In: *Encyclopedia of the Human Brain.* (VS Ramachandran, Editor) Academic Press, San Diego, 4:209-216.

Nattie EE, Wood J, Mega A, Goritski W, 1989, Rostral ventrolateral medulla muscarinic receptor involvement in central ventilatory chemosensitivity. *J Appl Physiol* 66:1462-1470.

Schlaefke ME, See WR, Loeschcke JJ, 1970, Ventilatory response to alterations of $H^+$ ions concentration in small areas of the ventral medullary surface. *Physiol* 10:198-212.

Strauss WL, Kemper RR, Jayakar P, Kong CF, Hersh LB, Hilt DC, Rabin M, 1991, Human choline acetyltransferase gene maps to region 10q11-q22.2 by *in situ* hybridization. *Genomics* 9:396-398.

Viegas-Pequignot E, Berrard S, Brice A, Apiou F, Mallet J, 1991, Localization of a 900-bp-long fragment of the human choline acetyltransferase gene to 10q11.2 by nonradioactive *in situ* hybridization. *Genomics* 9:210-212.

# Differential Expression of Intracellular Acidosis in Rat Brainstem Regions in Response to Hypercapnic Ventilation

JOSEPH C. LAMANNA*, MAXWELL NEAL*, KUI XU* and MUSA A. HAXHIU**

**Department of Anatomy, Case Western Reserve University, 10900 Euclid Ave., Cleveland, OH, USA; **Department of Pediatrics, Rainbow Babies and Children's Hospitals, 11100 Euclid Ave., Cleveland, OH, and Department of Physiology and Biophysics, Howard University, Washington, D.C., USA*

## 1. INTRODUCTION

Over the last 40 years, intensive research has been performed on localization of chemosensory cells. These studies have established the primary importance of the ventral medullary chemosensitive areas, located just beneath the surface of the ventrolateral aspect of the medulla oblongata (Mitchell *et al.*, 1963; Schläfke and Loeschcke.,1967., Loeschcke *et al.*,1970), and the presence of chemosensitive neurons in regions outside of these putative chemosensory regions (Coates *et al.*, 1993).

Furthermore, it has been shown that the central chemosensory cells in the brainstem reticular formation and suprapontine regions are neurotransmitter-specific containing neurons. These cell groups include monoaminergic nuclei (Haxhiu *et al.*, 2001) that are components of neuronal networks involved in the regulation of diverse functions, including behavioral control.

Alterations in the partial pressure of carbon dioxide ($pCO_2$) can lead to pH changes in the brain. Recent studies indicate that an increase in intracellular [$H^+$] concentration participates in hypercapnia-induced stimulation of the medullary chemosensory neurons (Ballantyne and Scheid, 2000; Dean *et al,*. 2001; Nattie, 1999; Putnam 2001; Wang *et al.*, 2002). Hence, we hypothesized that hypercapnia would preferentially induce intracellular acidification of chemosensory neurons, and the grade of acidification could proximate the sensitivity and location of chemosensory regions.

*Chemoreception*, Edited by Pequignot et al.
Kluwer Academic/Plenum Publishers, New York, 2003

We tested our hypothesis using the pH-sensitive neutral red histophotometry. This method has been used to visualize intracellular pH (pHi) in ischemic (Hoxworth *et al.,* 1999; LaManna *et al.,* 1992) and hypoxic (LaManna *et al.,* 1996) brain tissue.

Analyses of intracellular pH from digital photographs of serial brainstem coronal sections showed that hypercapnia induces a prominent intracellular acidification in neurons within putative chemosensitive regions of the ventral aspect of medulla oblongata. In contrast, minimal or no changes occur in neurons within the nucleus tractus solitarius. These findings suggest that brainstem neurons differentially regulate intracellular pH during hypercapnic stress.

## 2. METHODS

### 2.1. Animal preparation

Anesthetized rats (250-450g) were cannulated and infused with 3 mL of 2% Neutral Red over 30 minutes. After 20 minutes of infusion rats were intubated and ventilated with either room air or a mixture of 7% $CO_2$, 21% $O_2$, 71% $N_2$. Rat brains were then funnel frozen *in situ* after 15 minutes of ventilation. Brains were removed in a glove box kept at or below -25° C, then mounted in a cryotome maintained at -25° C.

### 2.2. pHi analysis

Dyed brainstem sections together with undyed brain sections (as a spectrophotometric blank) were photographed with a digital camera. Two grayscale images were taken for each section, one through a 550 nm band pass filter and one through a 450 nm filter. These two wavelengths correspond to the peak absorption of the acid (550 nm) and base (450 nm) forms of neutral red. Pixels from the images were then converted into optical density (OD) values of the acid and base present in the tissue. The ratio of acid OD to base OD was converted into pHi using a previously published calibration curve (LaManna and McCracken, 1986), after checking standards for consistency :pHi = -1.3(550 OD/ 450 OD) + 10.5

To aid in localization, coronal sections were collected from each brain, corresponding to the digital photograph, and sectioning and stained with cresyl violet. Noesys (Fortner Research) software was used to create 3-D reconstructed pHi maps of hypercapnic and sham brainstems.

# 3. RESULTS

## 3.1. Induction of Hypercapnia

Animals ventilated with the hypercapnic gas mixture had, as expected, significantly higher $pCO_2$ blood gas levels, but $pO_2$ levels were not significantly changed (Fig.1).

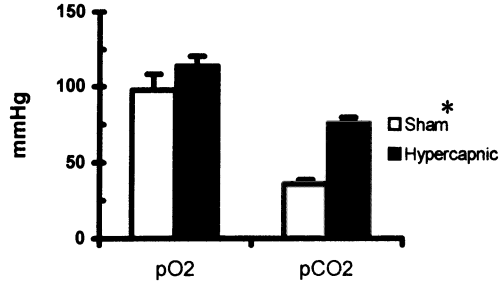


*Figure 1.* Blood gas levels of sham and hypercapnic rats taken within 2 minutes prior to funnel freezing onset. Asterisk indicates a significant difference between sham and hypercapnic animals ($p<0.05$).

## 3.2. pHi analysis on Coronal sections

Serial coronal brainstem sections from sham and hypercapnic animals were produced and examined for regional differences in pHi (Fig. 2).

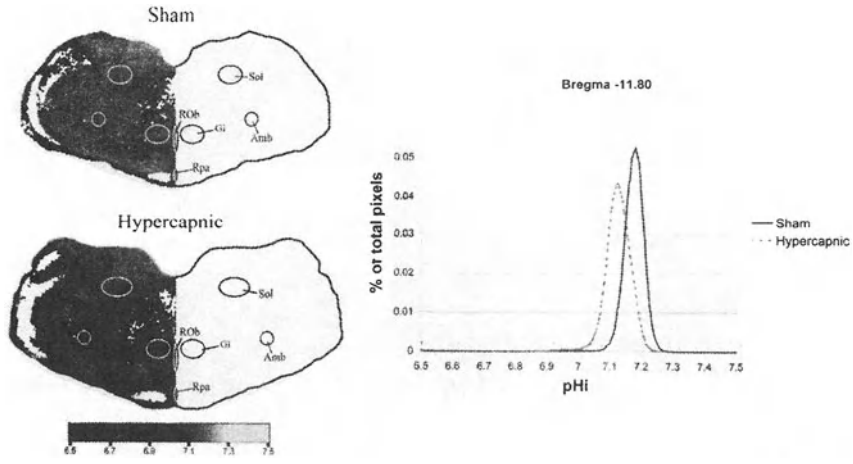


*Figure 2.* pHi greyscale sections from bregma –11.80 and corresponding pHi histogram. White matter is shown in white on the greyscale images and was not included in the histogram data. Abbreviations: Amb: Nucleus Ambiguous, Gi: Gigantocellular Reticular Nucleus, RPa: Raphe Pallidus Nucleus, ROb: Raphe Obscurus Nucleus, Sol: Solitary Tract and Nucleus.

## 3.3. Analysis of Specific Nuclei

Sections stained with cresyl violet were used as a guide to locate relevant brainstem nuclei on the pseudocolor images for further analysis and comparisons of pHi.

*Table 1.* Brainstem nuclei pHi. * indicates a significant difference between sham and hypercapnic animals ($p<0.05$)

| | Sham (n=3) | Hypercapnic (n=3) |
|---|---|---|
| Rostral Nucleus Ambiguus Region | 7.20 ± 0.02 | 7.14 ± 0.02 * |
| Nucleus Tractus Solitarius | 7.20 ± 0.02 | 7.17 ± 0.01 |
| Raphe Pallidus | 7.16 ± 0.03 | 7.08 ± 0.04 * |
| Raphe Obscuris | 7.17 ± 0.01 | 7.10 ± 0.05 |
| Gigantocellular Reticular Nucleus | 7.17 ± 0.01 | 7.12 ± 0.02 * |
| Inferior Olivary Nucleus | 7.20 ± 0.02 | 7.15 ± 0.01 * |

## 3.4. 3-D Models

Serial pseudocolor pHi images were aligned to create 3-D models of sham and hypercapnic brainstem pHi (Fig. 3). Two different pH ranges are shown below.

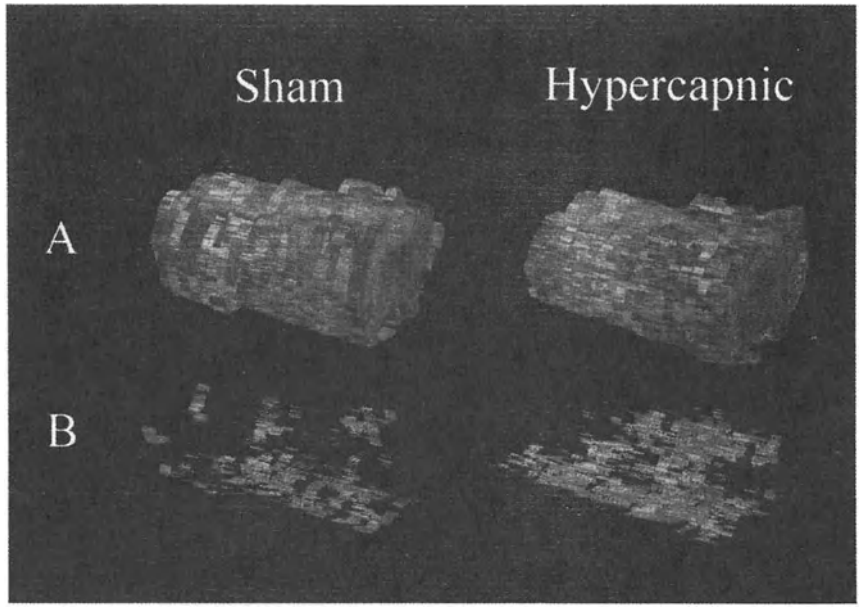


*Figure 3.* A: 3-D reconstructions of sham and hypercapnic brainstem pHi; Bregma –14.08 to –9.30 mm, 6.9 <pHi< 7.5. B: 3-D reconstructions of sham and hypercapnic brainstems cropped to show more acidified areas only; Bregma –14.08 to –9.30 mm, 7.035 <pHi< 7.065.

## 4. DISCUSSION

In the present study we have quantified changes in intracellular pH in medullary neurons induced by hypercapnia. The results indicate that neurons within putative chemosensory regions of the ventral aspect of medulla oblongata, including medullary raphe neurons, respond to breathing of hypercapnic gas mixture with prominent intracellular acidosis, while a decrease in intracellular pH in neurons of the nucleus tractus solitarius is insignificant or completely absent ((Fig. 3, B). These results correlate with previous studies on

distribution of medullary chemosensory cells activated by hypercapnia (Belegu *et al.*, 1998; Coates *et al.*, 1993) and support the physiological findings that chemosensitivity is partly due to changes in intracellular pH and neurons within chemosensitive regions of ventral medulla differentially regulate intracellular pH compare to neurons in other medullary regions (Wang *et al.*, 2002; Nattie, 1999), including those located within the nucleus tractus solitarius.

## 5. SUMMARY AND CONCLUSIONS

We determined the regional intracellular pH (pHi) of rat brainstem in response to hypercapnia. Neutral red spectrophotometry was used to characterize changes in intracellular pH along the dorsal and ventral aspects of the medulla oblongata. Male Wistar rats (250-350 g) were infused with 3 ml of 2% Neutral Red over the course of 30 minutes. After 20 minutes of infusion, the rats were ventilated with either 7% $CO_2$, 21% $O_2$ in $N_2$ or room air for 15 minutes. Our data indicate that hypercapnia induces prominent intracellular acidification in neurons within putative chemosensitive regions of the ventral aspect of medulla oblongata. On the contrary, minimal or no changes were observed in neurons within the nucleus tractus solitarius. These findings suggest that brainstem neurons differentially regulate intracellular pH during hypercapnic stress.

## REFERENCES

Ballantyne, D., and Scheid, P., 2000, Mammalian brainstem chemosensitive neurones: linking them to respiration in vitro. *J.Physiol* 525 Pt 3: 567-577.

Belegu, R., Hadziefendic, S., Dreshaj, I.A., Haxhiu, M.A., and Martin, R.J., 1999, $CO_2$ induced c-fos expression in medullary neurons during early development. *Respir. Physiol.* 117: 13-28.

Coates, E.L., Li, A., and Nattie, E.E., 1993, Widespread sites of brainstem ventilatory chemoreceptors. *J. Appl. Physiol.* 75: 5-14.

Dean, J.B., Kinkade, E.A., and Putnam, R.W., 2001, Cell-cell coupling in $CO_2/H^+$-excited neurons in brainstem slices. *Respir.Physiol* 129: 83-100.

Haxhiu, M.A., Tolentino-Silva, F., Pete, G., Kc, P., and Mack, S.O., 2001, Monoaminergic neurons, chemosensation and arousal. *Respir Physiol.* 129: 191-209.

Hoxworth, J., Xu, K., Yinong, Z., Lust, W.D., and LaManna, J.C., 1999, Cerebral metabolic profile, selective neuron loss, and survival of acute and chronic hyperglycemic rats following cardiac arrest and resuscitation. *Brain Research* 821: 467-479.

LaManna, J.C., and McCracken, K., 1984, The use of neutral red as an intracellular pH indicator in rat brain cortex in vivo. *Anal. Biochem.* 142: 117-125.

LaManna, J., Haxhiu, M., Kutina-Nelson, K., Pundik, S., Erokwu, B., Yeh, E., Lust, W., and Cherniack, N., 1996, Decreased energy metabolism in brainstem during central respiratory depression in response to hypoxia. *J. Appl. Physiol.* 81: 1772-1777.

LaManna, J., Griffith, J., Cordisco, B., Lin, C., and Lust, W., 1992, Intracellular pH in rat brain in vivo and in brain slices. *Can. J. Physiol. Pharmacol.* 70: S269-277.

Loeschcke, H.H., De Lattre, J., Schläfke, M.E., and Trouth, C.O., 1970, Effects on respiration and circulation of electrically stimulating the ventral surface of the medulla oblongata. *Respir. Physiol.* 10, 184-197.

Mitchell, R.A., Loeschcke, H.H., Massion, W.H., and Severinghaus, J.W., 1963, Respiratory responses mediated through superficial chemosensitive areas on the medulla. *J. Appl. Physiol.* 18, 523-533.

Nattie, E., 1999, Brainstem chemoreceptors and breathing. 1999, *Prog. Neurobiol.* 59: 299-331.

Putnam, R.W., 2001, Intracellular pH regulation of neurons in chemosensitive and nonchemosensitive areas of brain slices. *Respir.Physiol* 129 : 37-56, 2001.

Schläfke, M.E., and Loeschcke, H.H., 1967, Lokalisation eines an der regulation von Atmung und Kreislauf beteiligten Gebietes an der ventralen Oberfläche der Medulla oblongata durch Kälteblockade. *Pflügers Arch.* 297: 201-220.

Wang, W., Bradley, S.R., Richerson, G.B., 2002, Quantification of the response of rat medullary raphe neurones to independent changes in pH(o) and P(CO2). *J Physiol.* 540 (Pt 3): 951-70.

# Tentative Role of the $Na^+/H^+$ Exchanger Type 3 in Central Chemosensitivity of Respiration

HEIDRUN KIWULL-SCHÖNE*, MARTIN WIEMANN**, STILLA FREDE**, DIETER BINGMANN**, and PETER KIWULL*

**Department of Physiology, Ruhr-University, D-44780 Bochum and **Department of Physiology, University GH Essen, D-45122 Essen, Germany*

## 1. INTRODUCTION

*In vitro* studies by Wiemann et al. (1999, 2001) have shown cultured $CO_2/H^+$ sensitive neurons from the ventrolateral medulla oblongata of newborn rats to enhance their bioelectric activity upon intracellular acidification induced by selective inhibition of the $Na^+/H^+$ exchanger type 3 (NHE-3). Recently, Kiwull-Schöne et al. (2001) demonstrated the presence of NHE-3 mRNA in the adult rabbit brainstem, and likewise found NHE-3 immunoreactive neurons in brainstem areas, which have prevalence for central chemosensitivity. The same study revealed that NHE-3 inhibition by the brain-permeant substance S8218 (Aventis Pharma) also significantly modified the central respiratory $CO_2$-response of rabbits *in vivo*.

We now compare the respiratory effects of NHE-3 inhibition before and during acute hypercapnia with those during prolonged $CO_2$-retention, a situation often being met with chronic obstructive pulmonary disease (COPD). In this context, the question arose, whether prolonged respiratory acidosis would raise the rate of brainstem NHE-3 and/or NHE-3 prevalence in chemosensitive areas.

*Chemoreception*, Edited by Pequignot et al.
Kluwer Academic/Plenum Publishers, New York, 2003

## 2. METHODS

Experiments were performed in 20 male rabbits (mean weight ±SEM: 3.2 0.1 kg). Experimental setup and protocol are the same as described by Kiwull-Schöne et al. (2001).

Seven untreated controls from this former study and seven rabbits exposed to elevated inspiratory $CO_2$ fractions of 0.06 for 72 hours were compared for the effects of NHE-3 inhibition with S8218 on the respiratory $CO_2$- response. Another six control rabbits and five of the chronic hypercapnic animals were sacrificed at the end of experiments, to quickly remove and snap freeze the medulla oblongata (ca. 5 mm rostral to 5 mm caudal from the obex) to study the expression of NHE-3 by RT-PCR (for details see Kiwull-Schöne *et al.,* 2001), GAPDH being used as an internal reference marker. Arterial blood-gases and acid-base conditions were determined under different experimental steady state conditions as well as before anaesthesia (Radiometer, Denmark). For general anaesthesia an initial dose of about 65 mg/kg sodium pentobarbital was given, followed by continuous infusion of about 7.5 mg/kg/h. Respiratory $CO_2$-responses were assessed during artificial ventilation after vagotomy and muscle relaxation by Alloferin$^{(R)}$ (Hoffmann-La Roche, Germany). Phrenic nerve compound potentials were recorded by a bipolar silver electrode and pre-amplifier (WPI, USA), the signal being rectified and leakage-integrated with a time constant of 140 ms. Tidal phrenic nerve amplitude (IPNA) and respiratory rate ($f_R$) were estimated from the integrated recordings (Fig. 1), whereby IPNA was normalized to the maximum arbitrary value obtained in each animal (Kiwull- Schöne *et al.,* 2001). Phrenic minute activity was calculated as IPNA $f_R$.

Generally, the animals inhaled $O_2$-enriched air to maintain arterial $PO_2$ values in the range of 20 kPa. The $CO_2$-response of IPNA $f_R$ activity was tested at different steady-state levels of $PaCO_2$ up to 6-7 kPa above the individual apneic threshold value. Effects of NHE-3 inhibition were studied after intravenous application of the brain-permeant substance S8218 (Aventis Pharma, Germany). Drug infusion was started at high rates of 1ml/min (1 mg/ml saline) for 20 min, followed by lower rates of 0.1 ml/min to reach cumulative doses of about 10 mg $kg^{-1}$ and to maintain constant plasma levels in the range of 0.3 g/ml (about $10^{-6}$ M).

Statistical differences between means (±SEM) under control conditions and during NHE-3 inhibition were analysed by paired-samples t-tests, whereas group means on treatment with prolonged hypercapnia and those of controls were compared by independent-samples t-tests at a significance level of $P_D < 0.05$ (SPSS 11.0 for Windows, SPSS Inc., USA).

## 3. RESULTS

The mean apneic threshold $PaCO_2$, estimated by mechanical hyperventilation until phasic phrenic nerve activity ceased (Fig. 1), ranged about 3.1 kPa in the control group (Fig. 2) and was higher ( at about 3.5 kPa) in the chronic hypercapnic group. NHE-3 inhibition by intravenous application of the brain-permeant substance S8218 lowered these values on an average by 0.45 ±0.11 kPa and by 0.39 ±0.10 kPa, respectively, the inhibitory effect not being significantly different between groups (Fig. 3A).

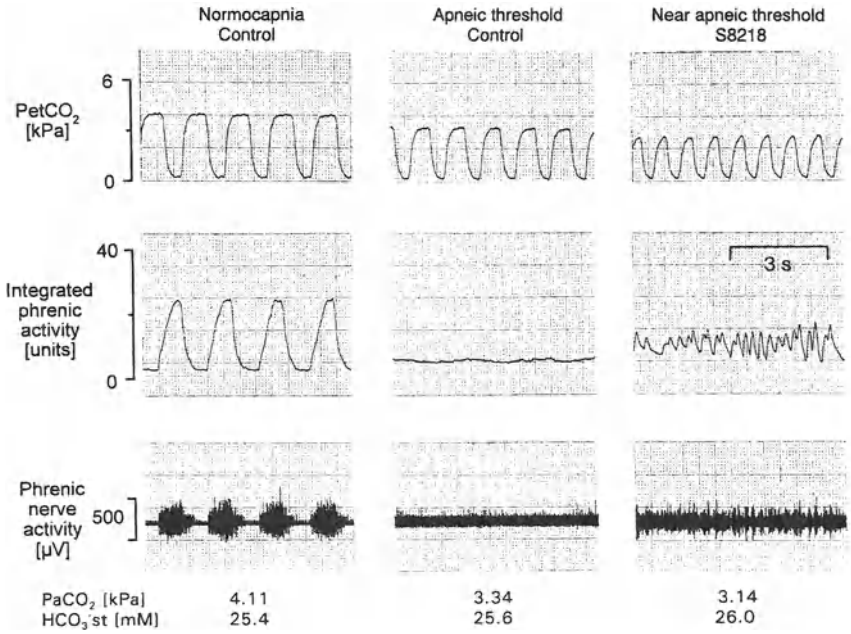


*Figure 1.* Effect of NHE-3 inhibition on apneic threshold $PCO_2$. From top to bottom: Endtidal $PCO_2$ ($PetCO_2$), integrated phrenic nerve activity (IPNA) and phrenic nerve compound potential. Male rabbit from the control group, 4.15 kg, vagotomized, carotid chemodenervated and hyperventilated to apnea. Stronger hyperventilation upon NHE-3 inhibition, with much lower values of endtidal and arterial $PCO_2$ than under control conditions, does not completely abolish rhythmic nerve discharge, but rather elicits irregular oscillations (in about half of the observations).

Due to non-linearity, quantification of $CO_2$-responses was attempted by exponential curve fitting (Fig. 2), responses being fully characterized by $x_0$ (the apneic threshold $PaCO_2$), $y_{max}$ (the maximum response) and $x_{0.5}$ (the above threshold rise in $PaCO_2$ necessary to reach the half-maximum response). Chronic hypercapnia due to the rise in $x_0$ (see above) led to a right-ward shift of the $CO_2$-response curves with no change in $y_{max}$ (not shown). Application of S8218 - besides equally lowering $x_0$ in both groups - did enhance $y_{max}$ in all individuals of the control group by an average of about 45 % (Fig. 2), but only in 4 rabbits of the chronic hypercapnic group, so that the average change of $y_{max}$ was smaller although not significantly different from control (Fig. 3B).

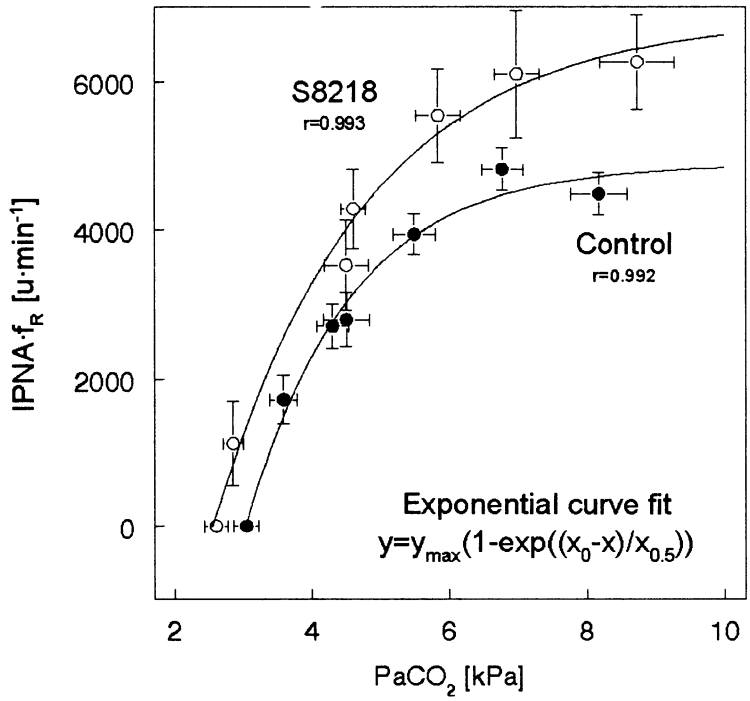


*Figure 2.* Effect of NHE-3 inhibition on average central respiratory $CO_2$-responses. Integrated phrenic minute activity (IPNA $f_R$) as function of arterial $PCO_2$ before (closed circles) and after (open circles) application of S8218. Means ±SEM of 7 vagotomized and mechanically ventilated rabbits are data from Kiwull-Schne et al. (2001). Non-linearity of central respiratory $CO_2$-responses is illustrated by highly correlated exponential curve fits.

Similarly, levels of NHE-3 mRNA within the brainstem were not significantly changed: The ratio of NHE-3/GAPDA normalized to the maximum ratio revealed 66.2 ±11.1% for the control condition and 49.4 ±8.3% after three days on chronic hypercapnia, with no significant difference between groups (Fig. 3C). However, NHE-3/GAPDH was significantly correlated with the spontaneous arterial $PCO_2$ determined during wakefulness before any treatment (unpublished data).

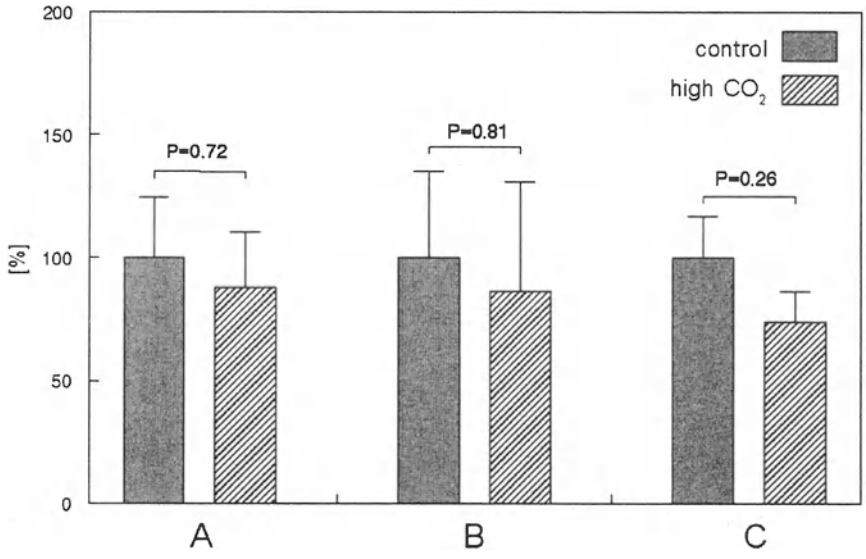


*Figure 3.* The missing role of chronic hypercapnia for NHE-3-inhibition by S8218 and for brainstem NHE-3 expression. Values are means ±SEM from 5-7 rabbits, either untreated controls or those underlying an inspiratory $CO_2$ load for 72 hours. Control mean values are normalized to 100%.

(A) Change in apneic threshold $PaCO_2$ by S8218.

(B) Change in maximum respiratory $CO_2$ response by S8218.

(C) NHE-3/GAPDH ratio in the brainstem.

Chronic hypercapnia fails to significantly influence pharmacological NHE-3 inhibition as well as brainstem NHE-3 prevalence

Our results clearly show that the central respiratory system can be activated by NHE-3 inhibition *in vivo*. Assuming that NHE-3 at medullary chemosensitive neurons is blocked by S8218, impaired neuronal acid extrusion is to be expected. There is now growing evidence for intracellular pH ($pH_i$) as the adequate signal to elicit central respiratory $CO_2$-responses. This view is supported by direct $pH_i$ measurements *in vitro* and *in vivo*, either in neonatal-rat brainstem slices (Ritucci et al., 1997, 1998) or orgonotypic cultured neurons (Wiemann et al., 1998, 1999, 2001) or in whole brains of humans (Lassen, 1990) and animals (Nattie et al., 2002). The concomitant extracellular acidification during hypercapnia is thought to maintain the characteristically constant $pH_i$ in $CO_2$ sensing neurons by slowing the $Na^+/H^+$ antiporter (Ritucci et al., 1998), most probably being the subtype NHE-3 (Wiemann, pers. comm.).

We studied respiratory $CO_2$ responses without feedback control in mechanically ventilated rabbits, in which inhibition of NHE-3 has been shown to elicit a $CO_2$-mimetic drive in the control group (Kiwull-Schne et al. 2001). Now, from non-linear regression analysis this inhibitory effect can be addressed as being approximately additive, since roughly the same additional respiratory drive by S8218 arose in the low (threshold) and the high (maximum) range of $PaCO_2$ (Fig. 2). Comparing normal and chronic hypercapnic animals on 6% inspired $CO_2$ for 72 hours, the higher apneic threshold $PaCO_2$ after chronic hypercapnia may be ascribed to the increment in buffer-base, most likely due to enhanced renal bicarbonate reabsorption, which has been shown for rabbits on 10% $CO_2$ for 56 hours to be caused by increased rates of the Na/H antiporter in proximal tubules (Krapf, 1989). We discerned a rightward-shift of the $CO_2$ responses by chronic hypercapnia with no difference in the maximum $CO_2$ response, quite in agreement with the lacking change in $CO_2$-sensitivity in spontaneously breathing rabbits (Kiwull-Schne and Kiwull, 1987) and rats (Kondo et al., 2000) on prolonged exposure to high $CO_2$. After chronic hypercapnia, NHE-3 inhibition by the brain permeant substance S8218 lowered the apneic threshold $PaCO_2$ to nearly the same extent as in controls and remained effective to restore the threshold $PaCO_2$ to the normal range. Thus, NHE-3 inhibition appears useful to counteract the risk for central apnea, both under normal blood-gas conditions and with prolonged $CO_2$ retention as a model of COPD. In this context, clinical observations suggest an increased $Na^+/H^+$ antiporter activity to be a marker for patients predisposed to obstructive sleep apnea (Tepel et al., 2000).

Similarly to the negligible impairment by chronic hypercapnia of the pharmacological NHE-3 inhibitory effects on acute $CO_2$ responses (Fig. 3 A, B) also brainstem NHE-3 mRNA expression (Fig. 3C) remained unaffected, at least after 3 days on 6% $CO_2$.

However, higher occurrence of NHE-3 in the brainstem was accompanied by higher spontaneous $PaCO_2$ values during wakefulness, implying that NHE-3 expression in central chemosensitive neurons influences base-line respiratory drive. Since NHE-3 prevalence in chemosensitive areas was not affected by external factors like chronic respiratory acidosis, it may be a significant intrinsic factor for determining the set point of the respiratory $CO_2$ response.

## REFERENCES

Kiwull-Schne, H., Kiwull, P., 1987, The significance of chemical control mechanisms for the adaptation of pulmonary ventilation to prolonged hypercapnia. *Atemw. Lungenkrkh.* 13: 346-350.

Kiwull-Schne, H., Wiemann, M., Frede, St., Bingmann, D., Wirth, K.J., Heinelt, U., Lang, H.-J., Kiwull, P., 2001, A novel inhibitor of the $Na^+/H^+$ exchanger type 3 activates the central respiratory $CO_2$ response and lowers the apneic threshold. *Am. J. Resp. Crit. Care Med.* 164: 1303-1311.

Kondo, T., Kumagai, M., Ohta, Y., Bishop, B., 2000, Ventilatory responses to hypercapnia and hypoxia following chronic hypercapnia in the rat. *Respir. Physiol.* 122: 35-43.

Krapf, R., 1989, Mechanisms of adaptation to chronic respiratory acidosis in the rabbit proximal tubule. *J. Clin. Invest.* 83: 890-896.

Lassen, N.A., 1990, Is central chemoreceptor sensitive to intracellular rather than extracellular pH? Clin. Physiol. 10: 311-319.

Nattie, E., Li, A., Meyerand, E., Dunn, J.F., 2002, Ventral medulla $pH_i$ measured in vivo by $^{31}P$ NMR is not regulated during hypercapnia in anesthetized rat. *Respir. Physiol. & Neurobiol.* 130: 139-149.

Ritucci, N.A., Dean, J.B., Putnam, R.W., 1997, Intracellular pH response to hypercapnia neurons from chemosensitive areas of the medulla. *Am. J. Physiol.* 273: R433-R441.

Ritucci, N.A., Chambers-Kersh, L., Dean, J.B., Putnam, R.W., 1998, Intracellular pH regulation in neurons from chemosensitive and nonchemosensitive areas of the medulla. *Am. J. Physiol.* 275: R1152-R1163.

Tepel, M., Sanner, B.M., van der Giet, M., Zidek, W., 2000, Increased sodium-proton antiporter activity in patients with obstructive sleep apnoea. *J. Sleep Res.* 9: 285-291.

Wiemann, M., Bingmann, D., 2001, Ventrolateral neurons of medullary organotypic cultures: intracellular pH regulation and bioelectric activity. *Respir. Physiol.* 129: 57-70.

Wiemann, M., Baker, R.E., Bonnet, U., Bingmann, D., 1998, $CO_2$-sensitive medullary neurons: activation by intracellular acidification. *NeuroReport* 9: 167-170.

Wiemann, M., Schwark, J.-R., Bonnet, U., Jansen, H.W., Grinstein, S., Baker, R.E., Lang, H.-J., Wirth, K., Bingmann, D., 1999, Selective inhibition of the $Na^+/H^+$ exchanger type 3 activates $CO_2/H^+$-sensitive medullary neurones. *Pflügers Arch.* 438: 255-262.

# Effect of Losartan Microinjections into the NTS on the Cardiovascular Components of Chemically Evoked Reflexes in a Rabbit Model of Acute Heart Ischemia

L.B.ROSÁRIO, ISABEL ROCHA and LUIS SILVA-CARVALHO*
*Instituto de Fisiologia da Faculdade de Medicina da Universidade de Lisboa. Av. Prof. Egas Moniz, 1649-028 Lisbon, Portugal*

## Abstract

In the acute phase of myocardial infarction (MI) there are modifications of the autonomic outflow with an increase in the sympathetic tone and changes in cardiovascular reflexes. Activation of angiotensin AT1 receptors in the nucleus tractus solitarii (NTS) inhibits the baroreceptor and enhances the carotid chemoreflex. In this study, we investigated the role of NTS-AT1 receptors on the cardiovascular reflex responses evoked on stimulation of carotid chemoreflex and cardiac chemosensitive fibres in the acute phase of MI. We also test the hypothesis that changes in cardiovascular responses to activation of carotid chemo and cardiac chemosensitive reflexes are secondary to changes in haemodynamic conditions due to infarction or to the activation of nociceptors of the heart. Rabbits were anaesthetised, paralysed and artificially ventilated. Carotid chemoreceptors and cardiac chemosensitive fibres were stimulated with lobeline and ATP, respectively. Arterial blood pressure, electrocardiogram and heart rate were monitored. A craneotomy was made to expose the caudal portions of the medulla and a multibarreled glass microelectrode was inserted in order to allow the identification of NTS and the microinjection of losartan (an angiotensin AT1 receptor antagonist). The heart was exposed by a midline thoracotomy and cardiac ischemia was produced by ligating the left descending coronary artery. The carotid chemoreflex and cardiac chemosensitive reflexes were evoked before and following the coronary ligation. The effect of losartan injection into the NTS on these reflexes was also assessed. In control experiments reflexes were assessed before and after the administration of capsaicin and procainamide. Results show that the activation of carotid chemoreflex elicited a greater increase of blood pressure and bradycardia after MI and than this was partially reversed by losartan microinjection after MI. Also the stimulation of cardiac chemosensitive fibres evoked a larger decrease on blood pressure and heart rate after MI and these were also partially reversed by losartan. The same enhancement of cardiovascular carotid chemo and cardiac chemosensitive receptors was observed after administration of capsaicin on the ventricular surface but not after procainamide. In conclusion, this study strongly suggests that, at NTS level, angiotensin AT1 receptors are involved in the modifications of autonomic outflow observed in the acute phase of MI.

*Chemoreception*, Edited by Pequignot et al.
Kluwer Academic/Plenum Publishers, New York, 2003

# 1. INTRODUCTION

After acute myocardial infarction (MI) an imbalance of the sympathetic / parasympathetic output is observed (Baron and Lesh, 1996) provoking a state of sympathetic activation (Zhang *et al.*, 1999) which has been implicated in the sudden death that could follow MI (Baron and Lesh, 1996). A depression of the baroreceptor reflex occurs (Schwartz *et al.*, 1988). Recently we observed an increase in the cardiovascular component of the carotid chemoreflex and cardiac chemosensitive reflexes (Rocha *et al.*, in submission). The changes observed in the cardiovascular component of these reflexes can be due to changes in haemodynamic conditions observed after MI. As an alternative the changes could be due to a central mechanism, the activation of nociceptors during heart ischemia acting at central level of integration of reflexes at the NTS (nucleus tractus solitarii) level. At this level Paton and Kasparov (1999, 2000) showed an inhibition of the baroreceptor reflex and an increase of the chemoreceptor reflex after the microinjection of angiotensin II into the caudal NTS, an area involved in integration of cardiovascular reflexes.

In the present study, we test the hypothesis that MI induced effects on the sympathetic / parasympathetic balance is mediated by angiotensin acting on AT1 receptors at NTS level. If proven the enhancement of the carotid chemoreflex and cardiac chemosensitive reflexes observed after MI could be reversed at least in part by the microinjection of losartan into the NTS. We also test the hypothesis of those effects being due to stimulation of nociceptors and not to changes in baseline conditions.

# 2. METHODS

### Methods 1: Effect of losartan

Experiments were performed in 6 New Zealand white rabbits (3-3,5kg) of both sexes, anaesthetised with sodium pentobarbitone (40mg/kg, I.V.) supplemented as necessary with IV bolus injections. An adequate level of anaesthesia was maintained by ensuring the absence of a withdrawal reflex before neuromuscular blockade and alterations of blood pressure and heart rate to a noxious stimulation after blockade. The femoral vein and artery were cannulated for intravenous drug administration and blood pressure recording, respectively. The trachea was cannulated low in the neck and the animal was ventilated with $O_2$-enriched air applied after neuromuscular blockade with pancuronium bromide (Pavulon; 4mg/kg/h) using a positive

pressure ventilator (Harvard Apparatus Ltd). Ventilation was regulated to maintain end-tidal $CO_2$ between 4,5 and 5%. A positive end-respiratory pressure of 2 cm of water was applied to the system after thoracotomy. Rectal temperature was kept at 36.5°-38°C by a servo controlled heating blanket (Harvard Apparatus Ltd). The left carotid bifurcation was identified and the tip of a catheter was placed within the left carotid sinus by retrograde cannulation of a branch of the left external carotid artery. A catheter introduced through the right common carotid artery was retrogradelly advanced to the origin of the left aorta allowing the injection of drugs into the coronary arteries. The positioning of the tip of this catheter was controlled by X-Ray image (Phillips BV300). The electrocardiogram (ECG) was recorded (Lectromed) from four surface-electrodes applied to the limbs and instantaneous heart rate derived (Lectromed ratemeter 5250). The urinary bladder was cannulated and drained. A thoracotomy was made to expose the heart and the pericardium was opened. The left descendent coronary artery was identified and a silk thread reference was placed between the superior 2/3 and the inferior 1/3. The animal was then placed in a stereotaxic frame to expose the caudal medulla. In this condition the carotid chemoreceptors and the chemosensitive cardiac receptors were stimulated. The reference thread around the descending coronary artery was tied and 30 minutes were allowed for the stabilization of the preparation. The chemo-tests were then repeated. The nucleus tractus solitarii (NTS) was identified and a four barrelled glass microelectrode (tip diameter 40-60μm) was inserted into the left NTS using either stereotaxic co-ordinates (5) or surface landmarks. The barrels of the microelectrode were filled with Wood's metal for electrical stimulation (50Hz, 1ms, 50μA), losartan in artificial CSF (20μM, pH=7.4±0.1), CSF and the last barrel was filled with pontamine sky blue dye (2%) in sodium acetate (1M) in order to mark the sites of microinjection. Losartan was microinjected, and all the tests were repeated again after stabilization of BP and HR.

***Cardiac chemosensitive and carotid chemoreceptors stimulation***

Stimulation of the carotid body chemoreceptors was performed by injection of lobeline (20μg/kg, pH=7.4±0.1) into the left carotid sinus (Heymans and Neil, 1958). Chemosensitive cardiac receptors were stimulated using an ATP injection (0.1ml; 20mM, pH=7.4±0.1) (McQueen *et al.*, 1998). Cardiac chemosensitive receptors were stimulated before and 30 minutes following the ligation of the anterior descending coronary artery. At the end of the experiment the animals were killed with an overdose of anaesthetic.

**Methods 2: Effect of capsaicin**

These experiments were performed in another 6 New Zealand white rabbits (3.1-3.4 kg), of both sexes. A protocol similar to the one described in methods 1 was used until thoracotomy. The pericardium was opened. The reflexes were tested and 0.5 ml of 0.5mg/ml solution of capsaicin was administered on the surface of the left ventricle. After stabilization of blood pressure and heart rate reflexes assessement was repeated.

**Methods 3: Effect of procainamide**

Experiments were made in another 6 New Zealand white rabbits (3.0-3.6 kg) of both sexes. A protocol similar to Methods 2 was used. Instead of capsaicin, procainamide was administered in a bolus of 0.5ml of 100mg/ml solution.

**Drugs**

All drugs were dissolved in artificial cerebrospinal fluid (CSF). The drugs and their sources were ATP (adenosine 5′-triphosphate, disodium salt, Sigma Chemical Co.), lobeline (Sigma Chemical Co).

**Histology**

The sites where losartan was microinjected were marked by the microinjection of pontamine sky blue dye. The brainstem was removed and fixed overnight in paraformaldehyde 2%. The medulla was sectioned transversely (60μm) and stained with neutral red. The microinjection sites were confirmed microscopically with the use of the Meessen and Olszewski rabbit atlas (1949) (Fig1).

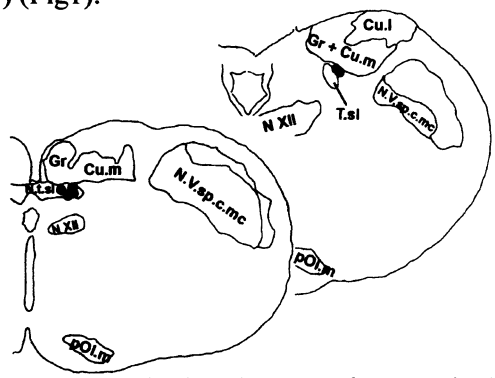


*Figure 1.* Drawing showing the microinjection sites of losartan in the NTS (n=5). Cu.m: nucleus cuneatus medialis; Gr: nucleus gracilis; N.t.sl: nucleus tractus solitarii; N.V.sp.c.mc: nucleus tractus spinalis trigemini caudalis; N.XII: nucleus nervi hypoglossi; pOl.m: nucleus paraolivaris medialis

**Data analysis**

All recorded variables were digitised (Instrutech VR100B, Digitimer Ltd.) and recorded on videotape. Off-line analysis was made using a computer A/D system with data capture and analysis software (CED1401, Spike2). For statistical analysis the paired *t*-test was used and differences were considered significant where $p<0.05$.

All data are expressed as mean±SEM. For the variables recorded, baseline values were taken 5s before the beginning of the stimulation. These values were compared with the peak of the response evoked by the stimulation.

# 3. RESULTS

## 3.1. Effect of losartan

After stabilization of the preparation, values of systolic blood pressure (BPs), diastolic arterial blood pressure (BPd) and heart rate (HR) were 120±1.5 mmHg, 93±1.2 mmHg and 229±2.2 bpm. Intracarotid injection of lobeline evoked an increase in mean arterial blood pressure (mBP) of 25±1.4mmHg and a decrease in HR of 14±1.4 bpm. Injection of ATP at the origin of the aorta evoked a decrease in mBP of 39±2.2 mmHg and a decrease in HR of 16±1.5 bpm (Figs.2 and 3). Thirty minutes after the ligation of the descending coronary artery values of BPs, BPd and HR were 111 ±1.6 mmHg, 85±1.3 mmHg and 233± 2.2 bpm, respectively. Carotid chemoreceptor stimulation evoked a rise of 32±1.9 mmHg in BPm and a decrease of 32±2.4 bpm significantly different from control situation ($n=6$; $p<0.01$; $n=6$, $p<0.01$). The activation of cardiac chemosensitive reflexes evoked a decrease in mBP of 50±1.5 mmHg and of 25±1.7 bpm in HR, values that are significantly different from those observed in basal conditions ($n=6$, $p<0.01$; $n=6$, $p<0.01$) (Figs. 2 and 3). After microinjection of losartan into the NTS, resting values of cardiovascular variables were BPs 108±2.5 mmHg, BPd 81±1.6 mmHg and HR 231±2.6 bpm. Carotid chemoreflex evoked an increase in BPm of 28±0.9 mmHg and a decrease on HR of 21±1.6 bpm different from those observed after MI ($n=6$, $p<0.01$; $n=6$, $p<0.01$) and under basal conditions ($n=6$, $p<0.01$; $n=6$, $p<0.01$). Activation of chemosensitive receptors in the heart evoked a decrease in mBP of 41±2.5 mmHg and in HR of 20±1.4 bpm different from MI ($n=6$, $p<0.01$; $n=6$, $p<0.01$) and basal conditions (Figs. 2 and 3). These data show, for both types of receptors, that losartan microinjection reversed the magnitude of the chemically evoked responses but not to the level under basal conditions.

## 3.2 Effects of capsaicin

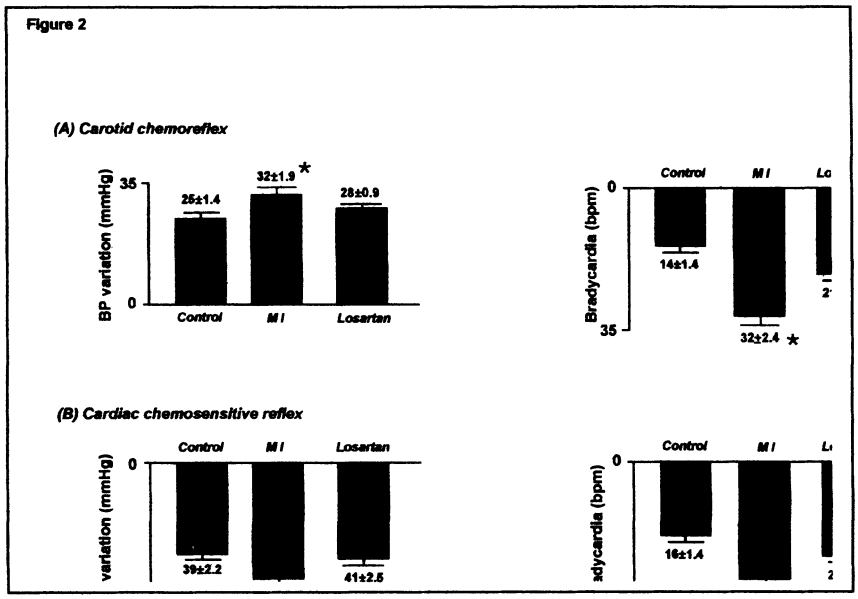


*Figure 2.* Effect of carotid chemoreflex (A) and cardiac chemosensitive reflex (B) evoked on basal conditions (open chest and pericardium), after myocardial infarction (MI) and microinjection of losartan. (BP, blood pressure; HR, heart rate). * highly significant, $p<0.001$

Control values for these experiments for BPs, BPd, mBP and HR were 118±0.9mmHg, 92±0.9 mmHg, 101±0.8mmHg and 229± 1.3 bpm, respectively. The effect of carotid body stimulation on BP was represented by an increase in mBP of 23±0.9mmHg. After capsaicin and stabilization of the preparation the values of BPs, BPd, mBP and HR were 128 ± 2.4mmHg, 97±1.8 mmHg, 107±1.3mmHg and 241± 1.4 bpm, respectively. The carotid chemoreflex stimulation provoked larger increases in pressure of 28±0.6 mmHg, significantly larger than that observed in basal conditions ($p<0.001$).

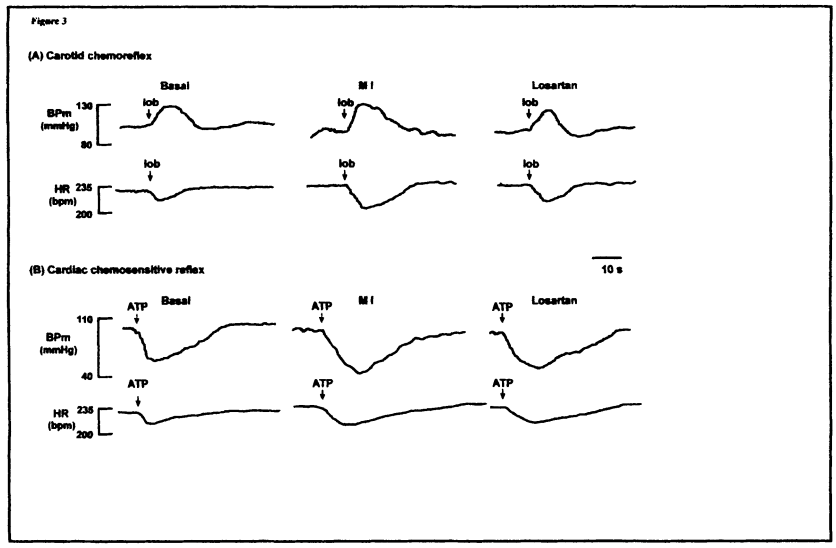


*Figure 3.* Effect of myocardial infarction on the reflex cardiovascular evoked responses and the reversal of the effect by the microinjection of losartan into the NTS

### 3.3 Effect of procainamide

Control values for BPs, BPd, mBP and HR were 117 ±0.9 mmHg, 90±0.9 mmHg, 99±0.8 mmHg and 228± 2.3 bpm, respectively. In this condition, the effect of carotid body stimulation on blood pressure was an increase of 24 ±1.1mmHg. After procainamide and stabilization of the preparation, the new haemodynamic values for BPs, BPd, mBP and HR were 108±1.5 mmHg, 82±1.4mm Hg, 91±1.1mmHg and 255±1.6 bpm, respectively, significantly different from control values. In this situation, the chemoreflex evoked and increase in pressure of 23±1.5 mmHg not significantly different from baseline values (p=0.56, NS).

## DISCUSSION

The present data confirm our previous observations (Rocha *et al.*, in submission) that after acute myocardial infarction an increase in the efficacy of chemical evoked reflexes is observed. This coincides with a decrease in the baroreflex (Schwartz *et al.*, 1988). The observed changes are not the result of haemodynamic modifications provoked by heart ischemia since procainamide that provokes a decrease in cardiac contractility (Sugiyama *et al.*, 1999) evokes a similar decrease in pressure to the one observed in MI without changing the efficacy of the carotid chemoreflex. An excitation of

cardio-nociceptors seems to be involved since the direct stimulation of nociceptors with capsaicin provokes a similar pattern of modification of the reflexes that MI with opposite changes in haemodynamic baseline conditions. The observed changes are reversed partially by the microinjection of losartan into the NTS. The blockade of AT1 receptors in NTS prevents the effect of the microinjection of angiotensin in the same area that consist on an enhancement of inhibitory synaptic transmission in some cells and an excitation of others, an effect mediated by the release of substance P (Kasparov and Paton, 1999). These effects mediated at NTS are related with an inhibition of the baroreceptor reflex and the facilitation of the carotid chemoreflex (Paton and Kasparov, 1999).

Angiotensin actions on AT1 receptors on the NTS can thus modulate in opposite direction, baroreceptor and non-baroreceptor neuronal pathways. An inhibition of the baroreflex (Paton and Kasparov, 2000) and an enhancement of the chemosensitive reflexes - seen in our experimental conditions- occur similar to those described elsewhere, an effect partially prevented by the blockade of AT1 receptors into the NTS. The results thus suggest that after MI a neuronal network involving AT1 receptors at the NTS level is activated. The origin of the angiotensin involved in this activation has not been directly demonstrated. However, angiotensin (at least in the rat) exists in HDA cells (Lind *et al.,* 1985) and HDA is able to modulate cardiovascular reflexes acting on NTS level (Jordan, 1990; Silva-Carvalho *et al.,* 1995). HDA is activated by nociceptive stimulation at the heart level. The possibility thus exists, further supported by the present results that activation of HDA after MI acts on NTS neurons facilitating chemosensitive reflexes and inhibiting baroreflexes. The reversion of the effect of MI on the reflexes was not total with losartan application. As microinjections were performed only on one side at NTS level this could explain the lack of a complete reversion. However, the possibility exists that a different mechanism, not involving angiotensin II or independent of the NTS, is responsible, in part, for the observed changes in reflexes.

The effect that we observed with losartan microinjection into the NTS relate to changes occurring immediately (up to 30 minutes) after MI and do not allow us to suggest a therapeutic beneficially effect of AT1 blockade in the controlling of autonomic dysfunction after MI. More long-term observation on the sensitivity of these reflexes is necessary. However, our results strongly suggest that after MI, AT1 receptors at the NTS level are involved in the reflex modification of the autonomic output.

## ACKNOWLEDGEMENTS

The authors are specially grateful to Professor K.Michael Spyer for his support and help in reviewing this manuscript.

## REFERENCES

Baron, HV, Lesh, MD (1996). Autonomic nervous system and sudden death. J *Am. Coll. Cardiol.*, 27: 1053-60

Heymans C, Neil, E (1958). The effect of drugs on the chemoreceptors. In: *Reflexogenic Areas of the Cardiovascular System. Churchill*, London, pp 192

Jordan, D (1990). Autonomic changes in afective behavior. In: "*Central Regulation of Autonomic Function*". Ed.: A.D.Loewy and K.M.Spyer, Oxford University Press

Kasparov, S, Paton, JFR (1999). Differential effects of angiotensin II in the nucleus tractus solitarius-II- Plausible neuronal mechanisms. *J.Physiol.*, 521: 227-238

Lind, RW, Swanson, LW, Ganten, D (1985). Organization of angiotensin II immunoreactive cells and fibres in the rat central nervous system. An immunohistochemical study. *Neuroendocrinol.*, 40: 2-24

McQueen, MS, Bond, SM, Moores, C, Chesssell, I, Humphrey, PP, Dowd, E. (1998) Activation of P2X receptors for adenosine triphosphate evokes cardiorespiratory reflexes in the anaesthetised rats. *J. Physiol*, 507 (3):843-55

Meessen, H, Olszewski, J (1949) Cytoarchitektonischer *Atlas des Rautenhirns des Kaninchens, S. Krager*

Paton, JFR, Kasparov, S (1999). Differential effects of angiotensin II on cardiovascular reflexes mediated by nucleus tractus solitarius-a microinjection study. *J.Physiol.*, 521: 213-225

Paton, JFR, Kasparov, S (2000). Sensory channel specific modulation in the nucleus of the solitary tract. *J.Aut.Nerv.Syst.*, 80: 117-129

Rocha, I, Rosário, LB, Oliveira, EI, Barros, MA, Silva-Carvalho, L Changes in arterial and cardiac chemosensitive reflexes after acute heart ischemia in the anaesthetized rabbit. Submitted

Schwartz PJ, Zaza A, Pala M, Locati E, Beria G, Zanchetti A (1988) Baroreflex sensitivity and its evolution during the first year after myocardial infarction. *J; Am. Coll; Cardiol* 12(3): 629-636

Silva-Carvalho, L, Dawid-Milner, MS, Spyer, KM (1995). The pattern of excitatory inputs to the nucleus tractus solitarii evoked on stimulation in the hypothalamic defence area in the cat. *J.Physiol.*, 487.3: 727-737

Sugiyama, A, Takehana, S, Kimura, R, Hashimoto, K (1999) Negative chronotropic and inoytropic effects of class I antiarrhythmic drugs assessed in isolated canine blood-perfused sinoatrial node and pappilary muscle preparations. *Heart Vessels*, 14(2): 96-103

Zhang W, Huang BS, Leenen FH (1999) Brain renin-angiotensin system and sympathetic hyperactivity in rats after myocardial infarction. *A. J. Physiol.* 276(5/2): H1608-H1615

# Effects of Acute Hypoxic Conditions on Extracellular Excitatory Amino Acids and Dopamine in the Striatum of Freely-moving Rats

SANDRINE PARROT[*], JEAN-MARIE COTTET-EMARD[#], VALERIE SAUVINET[*], JEAN-MARC PEQUIGNOT[§], and LUC DENOROY[*]

[*]*Laboratoire de Neuropharmacologie et Neurochimie, INSERM U512, Université Claude Bernard, Lyon, France,* [#]*Laboratoire de Physiologie de l'Environnement, UA-6451, Université Claude Bernard, Lyon, France,* [§]*Laboratoire de Physiologie des Régulations Métaboliques Cellulaires et Moléculaires, CNRS UMR 5123, Université Claude Bernard, Lyon, France*

## 1. INTRODUCTION

Experimental in vitro or in vivo studies have shown that striatum is specially vulnerable to hypoxia. In this brain area, deep hypoxic episodes, as those encountered in ischemia/anoxia, lead to a neuronal loss (Banasiak *et al.*, 2000; Tuor *et al.*, 2001) which is thought to be linked to an enhanced release of neurotransmitters, mainly dopamine (DA) and glutamate (Glu) (Globus *et al.*, 1995; Kunimatsu *et al.*, 1999; Nakajima *et al.*, 1996; Szatkowski and Attwell, 1994; Wang *et al.*, 1995). However, tolerable hypoxaemic hypoxia can also affect striatum. This type of hypoxia occurs in environmental oxygen concentration ($FiO_2$) of 10-12% or even lower, e.g. during life in altitude or in several pathological states such as respiratory insufficiency. Although tolerable hypoxic exposure does not lead to apparent alterations in energy metabolism of the brain (Duffy *et al.*, 1975; Norberg and Siesjö, 1975) and does not induce any neuronal loss (Miyamoto and Auer, 2000), it produces behavioral disturbances in animals (Brown and Engel, 1973; Speiser *et al.*, 1990), which may be linked to alterations in striatal neurotransmission. Indeed, in vivo extracellular DA concentration is increased by tolerable hypoxia in the striatum of freely-moving adult rats

*Chemoreception*, Edited by Pequignot et al.
Kluwer Academic/Plenum Publishers, New York, 2003

(Akiyama *et al.*, 1991) or rat pups (Nakajima *et al.*, 1996). In contrast to DA, alterations in excitatory amino acid neurotransmission during tolerable hypoxia are poorly documented. Although Glu concentration has been reported to be increased in striatal tissue from rat pups (Krajnc *et al.*, 1996), in vivo studies performed on ventilated anaesthetised animals failed to show any change in extracellular Glu during acute tolerable hypoxia (Kunimatsu *et al.*, 1999; Pastuszko, 1994). However, these latter studies could have missed changes since anaesthetics can influence extracellular Glu (Rozza *et al.*, 2000; Shiraishi *et al.*, 1997). Moreover, these former data give only partial information on amino acid neurotransmission, since the extracellular concentration of Asp, the second excitatory amino acid which may exhibit different alterations than Glu in some pathophysiological conditions (Abarca and Bustos, 1999), was not monitored.

Insofar as the neurochemical consequences of acute tolerable hypoxia are less known than those of ischemia/anoxia, the effects of tolerable hypoxia on both excitatory amino acids and DA were studied. Along this line, striatal extracellular levels of both Glu and Asp, as well as DA and its metabolites 3,4-dihydroxyphenyl acetic acid (DOPAC) and homovanillic acid (HVA) were monitored in awake rats, by brain microdialysis, during tolerable hypoxaemic hypoxia ($FiO_2$ 10%) or during local histotoxic anoxia/ischemia induced by sodium cyanide/2-desoxiglucose for comparison. In such an *in vivo* unanaesthetized preparation, simultaneous monitoring of excitatory amino acids and catecholamines shows differential changes in extracellular neurotransmitters according to the type of hypoxia.

## 2. EXTRACELLULAR CONCENTRATION OF STRIATUM NEUROTRANSMITTERS DURING TOLERABLE HYPOXIA

In order to assess that animals perceived acute systemic hypoxia, we checked whether they exhibited the physiological hyperventilation response to hypoxic hypoxia. For that purpose, three parameters of ventilation (respiratory frequency, $F_R$; tidal volume, $V_T$ and minute ventilation, $V_e$) were monitored during the first 15 minutes of hypoxic exposure. Ventilation responses to acute hypoxic hypoxia (10% $O_2$) are shown in Table 1. Briefly, $V_e$, $F_R$ and $V_T$ were significantly higher during 10% $O_2$ hypoxia.

The extracellular concentrations of Glu and Asp in the striatum of awake rats were not affected by the 1-hour 10% $O_2$ hypoxia, as compared to control values (data not shown).

*Table 1.* Acute hypoxic ventilatory response of awake rats during microdialysis experiment.

| Hypoxia | Respiratory frequency ($F_R$) (breaths / min) | Tidal volume ($V_T$) (ml) | Minute ventilation (Ve) (ml/min) |
|---|---|---|---|
| 10 % $O_2$ hypoxia | | | |
| normoxia period | 101.8 ± 5.9 | 2.4 ± 0.4 | 238.4 ± 32.3 |
| hypoxia ($5^{th}$ min) | 138.6 ± 5.1* | 3.5 ± 0.4* | 473.7 ± 44.1* |
| hypoxia ($15^{th}$ min) | 161.5 ± 6.0* | 2.8 ± 0.2 | 447.9 ± 37.8* |
| Histotoxic hypoxia | | | |
| normoxia period | 97.4 ± 3.2 | 1.9 ± 0.1 | 183.1 ± 16.4 |
| anoxia period | 90.8 ± 3.7 | 2.1 ± 0.4 | 183.6 ± 27.9 |

$F_R$, $V_T$ and $V_e$ were measured during the normoxic period preceding the hypoxic exposure after the onset of 10% $O_2$ hypoxia (n = 7) or after the administration of NaCN and 2-DG by reverse dialysis (n = 6). *p < 0.05 as compared to normoxia (ANOVA, followed by Fisher PLSD test).

The extracellular concentrations of DA, DOPAC and HVA in the striatum of freely-moving rats before, during and after 1 hour 10% $O_2$ hypoxia are shown in Fig. 1. During the hypoxic exposure, DA concentration increased progressively to reach +185 % of control values at the end of hypoxia ($p < 0.01$). When normoxia was restored, DA levels returned to baseline within 15 minutes. In contrast to DA, DOPAC concentration decreased significantly (–46%, $p < 0.05$) as compared to normoxic controls; in addition, the lowering in DOPAC was delayed as compared to the increase in DA. On the other hand, extracellular HVA level was unaltered. In normoxic animals, one can notice a fall in DA, DOPAC and HVA extracellular concentrations occurring from the $6^{th}$ dialysate, which may be related to circadian variations in extracellular concentrations of monoamines and metabolites (Paulson and Robinson, 1996).

## 3. EXTRACELLULAR CONCENTRATION OF STRIATUM NEUROTRANSMITTERS DURING LOCAL ANOXIA/AGLYCEMIA

In contrast to systemic hypoxic exposure, administration of 2 mM sodium cyanide (NaCN)/10 mM 2-desoxiglucose (2-DG) by reverse dialysis did not modify $V_e$, $V_T$ and $F_R$ as compared to control values (Table 1).

As shown in Fig. 2, the extracellular concentrations of Glu and Asp were markedly increased in the striatum during the 1-hour local histotoxic anoxia/aglycemia (Glu : +980%, $p<0.01$ ; Asp : +1068%, $p<0.01$). This effect lasted the 15 minutes following the end of NaCN/2-DG application.

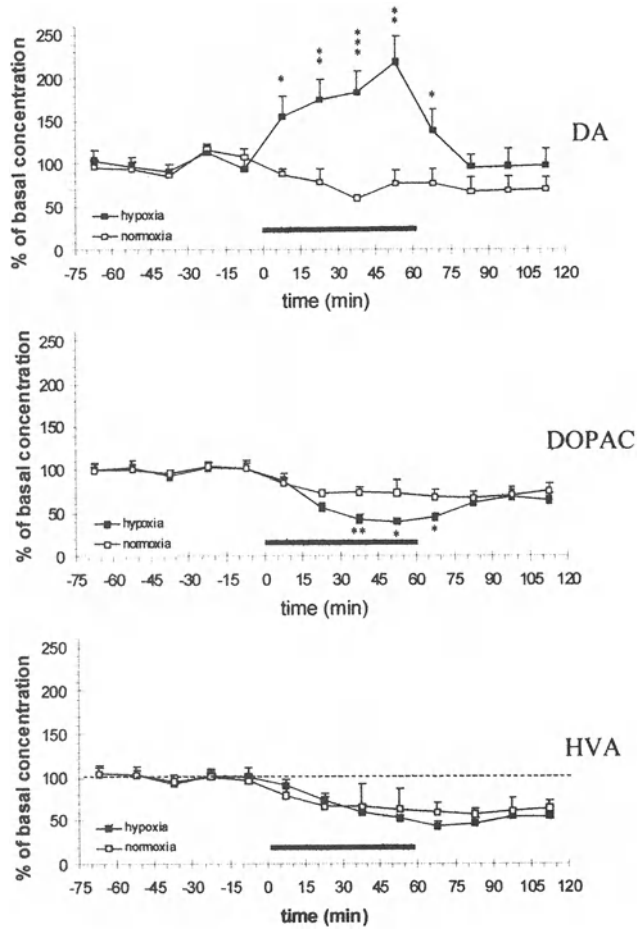


*Figure 1.* Effects of 10% $O_2$ hypoxia on 15-min microdialysate DA (top), DOPAC (middle) and HVA (bottom) levels from striatum of freely-moving rats. Full symbols represent experiments with normoxic conditions, open circles those with hypoxic conditions. Hypoxia was lasting 1 h (black line). The changes in DA, DOPAC and HVA levels are expressed as percent (mean ± SEM) of baseline levels: 2.39 ± 0.37 nM, 1262.1 ± 139.7 nM and 831.7 ± 112.8 nM respectively (n = 12). *p<0.05, **p<0.01, ***p<0.001, ANOVA followed by Fisher PSLD test.

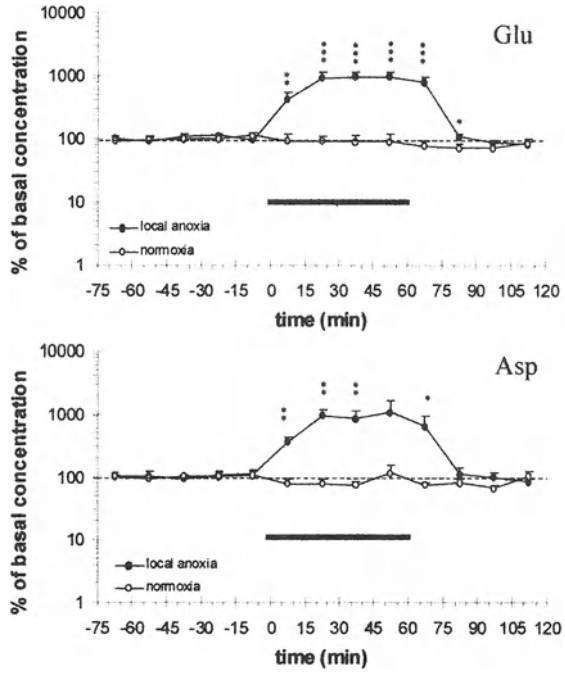


*Figure 2.* Effects of histotoxic anoxia/aglycemia on 15-min microdialysate Glu (top) and Asp (bottom) levels (logarithmic scale) from striatum of freely-moving rats. Full symbols represent experiments with normoxic conditions, open circles those with hypoxic conditions. Local anoxia/aglycemia was induced by administrating 2 mM NaCN/10 mM 2-DG by reverse dialysis (black line).The changes in Glu and Asp levels are expressed as percent (mean ± SEM) of baseline levels: 0.93 ± 0.20 µM and 50.8 ± 11.5 nM respectively (n = 10). *p<0.05, **p<0.01, ***p<0.001, ANOVA followed by Fisher PSLD test.

The extracellular concentrations of DA, DOPAC and HVA before, during and after 1-hour local histotoxic anoxia/aglycemia are shown in Fig. 3. During the first 15 minutes of the NaCN/2-DG administration by reverse dialysis, extracellular DA concentration exhibited a huge increase when compared to control animals (+13335 %, i.e., 143-fold, $p < 0.01$). Thereafter, DA concentration was lowered over the hypoxic period, although remaining significantly higher than in controls. A smaller increase in extracellular DOPAC concentration (+41 % as compared to controls ; $p<0.05$) occurred at the beginning of NaCN/2-DG application; thereafter DOPAC level returned to control value. In contrast, extracellular HVA concentrations was decreased during the local histotoxic anoxia/aglycemia (–30 % as compared to controls ; $p<0.01$).

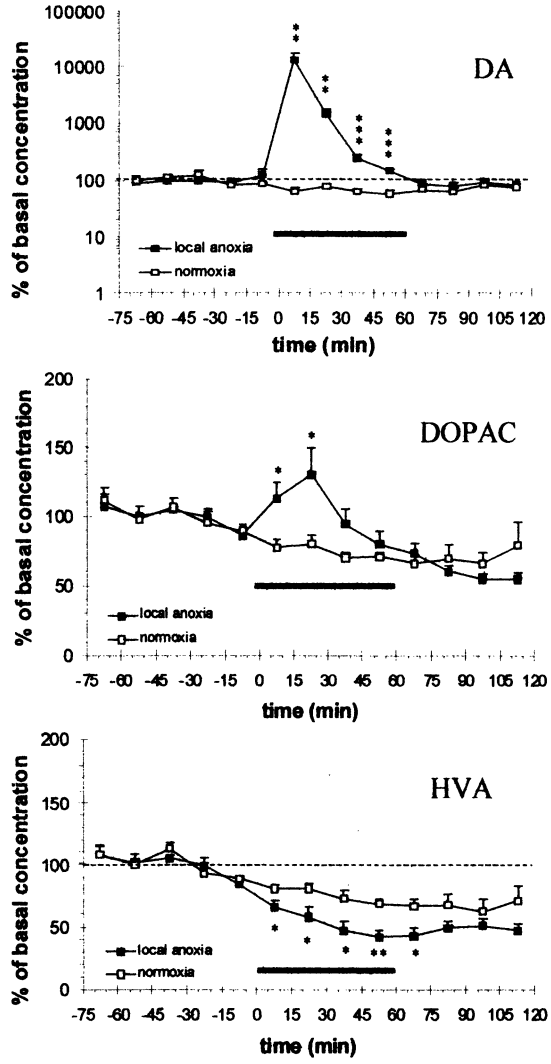


*Figure 3.* Effects of histotoxic anoxia/aglycemia on 15-min microdialysate DA (top, logarithmic scale), DOPAC (middle) and HVA (bottom) levels from striatum of freely-moving rats. Full symbols represent experiments with normoxic conditions, open circles those with hypoxic conditions. Hypoxia was lasting 1 h (black line). The changes in DA, DOPAC and HVA levels are expressed as percent (mean ± SEM) of baseline levels: 1.99 ± 0.41 nM, 613.6 ± 43.5 nM and 522.9 ± 36.9 nM respectively (n = 5). *p < 0.05, ANOVA followed by Fisher PSLD test.

# 4. DISCUSSION

## 4.1 Tolerable hypoxia does not affect extracellular Glu and Asp, whereas anoxia/aglycemia does

The present study shows that a 1-hour tolerable hypoxaemic hypoxia failed to affect the extracellular level of Glu and Asp in the striatum. This result is in accordance with former works showing that hypoxia of similar degree does not affect extracellular Glu in the striatum of rats (Kunimatsu *et al.*, 1999) or piglets (Pastuszko, 1994). In contrast to earlier works carried out on ventilated anaesthetised animals, the present study, performed on awake rats exhibiting the physiological ventilatory response to hypoxia, clearly shows that tolerable hypoxia does not affect extracellular Glu and Asp concentrations.

Contrary to tolerable hypoxia, the intra-striatal administration of NaCN and 2-DG by reverse dialysis, mimicking anoxia and hypoglycaemia occurring in ischemia (Vornov *et al.*, 1994), induced a very large increase in extracellular Glu and Asp. The changes obtained here are in accordance with the well known enhancement of extracellular striatal Glu during an ischemic episode. However, previous studies described alterations only in anaesthetised rats (Kunimatsu *et al.*, 1999). Now, the present study clearly shows that a local ischemia-like episode leads to a large enhancement in extracellular Glu and Asp in freely moving rats.

This latter effect should be due to Glu/Asp transporters reversal, as previously reported for other models of anoxia or ischemia (Szatkowski and Attwell, 1994). One explanation is that cyanide ions and desoxiglucose induced a fall in ATP leading to an inhibition of the plasma membrane $Na^+$-$K^+$ ATPase. The disruption of the ionic gradient across plasma membranes provokes a reversal of the Glu/Asp uptake systems located in both neurons and glial cells and to a non-vesicular release of Glu and Asp. The sustained massive enhancement in extracellular Glu and Asp suggests that the stores of both amino acids are not depleted during the anoxia/aglycemia and is consistent with the idea that the Glu and Asp synthesis may not be impaired, as suggested from in vitro studies (Huang and Hertz, 1994).

## 4.2 Tolerable hypoxia, as well as anoxia/aglycemia, affect extracellular DA

The present work shows that a 1-hour tolerable hypoxaemic hypoxia induced a small increase in extracellular DA concentration and a delayed decrease in extracellular DOPAC. The HVA concentration was unaltered.

Several hypotheses can be raised to explain those effects. At first, a slowered DA catabolism, as suggested by the decrease in DOPAC, is unlikely to explain the higher extracellular DA level. Indeed, if the MAO activity had been lowered because of a lack of available oxygen as suggested by Trouvin *et al.* (1986), the fall in DOPAC would have not been delayed as compared to the increase in DA. Besides, the extracellular concentration of 5-HIAA, a serotonin metabolite formed under the action of the same MAO as DOPAC remained unaltered under our experimental conditions (data not shown), suggesting also that an inhibition of MAO activity should not be lowered under our conditions of hypoxia.

Second, as suggested by previous studies carried out on ventilated anaesthetised animals (Kuo *et al.*, 1998; Wang *et al.*, 1995), the increase in DA may result from presynaptic mechanisms facilitating DA release from striatal dopaminergic terminals and involving N-methyl-D-aspartate (NMDA) receptors. Finally, two other assumptions to explain the effects of hypoxia may consider a higher activity of nigro-striatal dopaminergic fibers leading to an enhanced DA release, or a partial slowering of the DA uptake system leading to a higher extracellular DA level (Akiyama *et al.*, 1991).

In contrast to tolerable hypoxia, the local anoxia/aglycemia induced a huge increase in extracellular DA concentration occurring at the beginning of the NaCN/2-DG perfusion. This change is likely to result from a reversal of the DA uptake system under anoxic/aglycemic conditions, (Globus *et al.*, 1995; al., Nakajima *et al.*, 1996; Wang *et al.*, 1995). Since this huge efflux of DA mainly occurred at the onset of local anoxia/aglycemia, it did not seem to be linked with an increased DA synthesis aimed to replenish transmitter stores, in agreement with earlier studies reporting lowered tyrosine hydroxylase activity during acute deep hypoxia (Davis and Carlsson, 1973). However, the present anoxic/aglycemic insult did not induce a total depletion of striatal DA, since the extracellular DA returned to basal level as soon as the end of the NaCN/2-DG administration.

On the other hand, the small transient increase in extracellular DOPAC, may correspond to an enhanced cytoplasmic level of DA which is metabolised to DOPAC by intracellular MAO. The high cytoplasmic level of DA may result from the inhibition of the vesicular uptake of DA due to the fall in ATP induced by the anoxia/aglycemia condition. However, the discrepancy between the efflux of DA and the small increase in DOPAC may be partly explained by an increased clearance of produced DOPAC from blood, since brain endothelial cells are particularly sensitive to histotoxic anoxic insult (Ahlemeyer *et al.*, 1977).

## 5. CONCLUSION AND PERSPECTIVES

In summary, the present study, performed on awake rats, provides evidence that hypoxia-induced increases in extracellular striatal Glu and Asp only occur during deep hypoxic conditions, which are linked to a fall in energy status. In contrast, increases in extracellular DA occur in tolerable hypoxia and in anoxia/aglycemia, but exhibit different magnitudes and time courses according to the type of hypoxia.

The differences in neurochemical effects of tolerable hypoxaemic hypoxia and local anoxia/aglycemia described here, may also reflect the differences in the response of the organism to a systemic or to a local hypoxia. Indeed, the peripheral chemoreceptors were stimulated only during the hypoxaemic hypoxia, as showed by hyperventilation. Further anatomical and physiological studies will state a link between carotid body chemoreceptors and basal ganglia, as suggested by previous works. Indeed, the hypoxia-induced changes in striatal indolamines depend on the integrity of the carotid sinus nerve (Poncet *et al.*, 1998) and patients with Parkinson's disease may exhibit altered ventilatory response to hypoxia (Serebrovskaya *et al.*, 1998).

## TECHNICAL NOTES

Animals. Male Sprague Dawley rats (270-300 g, IFFA CREDO, France) were anaesthetised with chloral hydrate (400 mg/kg/i.p.). A canula-guide (CMA12, CMA, Sweden) was implanted above the right striatum at the following coordinates relative to bregma: anterior 0 mm, lateral 3.5 mm, ventral 2 mm below the brain surface according to the atlas of Paxinos and Watson (1998). Canula-guides were secured with screws and dental cement. After surgery, rats were housed in individual cages with food and water ad libitum in a light and temperature controlled room. From the $7^{th}$ to the $12^{th}$ post-operative days, animals were progressively habituated to the experimentation chamber. The microdialysis experiment was performed 14 days after canula-guide implantation.

Microdialysis experiment. Concentric microdialysis probes were constructed from regenerated cellulose dialysis tubing (3 mm active dialysis length), fused-silica capillary tubing and flat probe holders (Harvard, USA). Parts were assembled in order to implant the probes in canulae-guides at 6.5 mm below the brain surface (Parrot, 2000). The probes were perfused at 1 µl/min with artificial cerebrospinal fluid (aCSF, 145.0 mM NaCl, 2.70 mM KCl, 1.0 mM $MgCl_2$, 1.20 mM $CaCl_2$, 0.45 mM $NaH_2PO_4$, 2.33 mM $Na_2HPO_4$, pH = 7.4). Three hours after probe implantation, collection of 15 min microdialysates was initiated.

Application of hypoxia. Hypoxaemic hypoxia was induced by lowering $O_2$ concentration in the experiment chamber with 10% $O_2$ in nitrogen. Histotoxic anoxia/aglycemia was induced in situ by administrating 2 mM NaCN and 10 mM 2-DG by reverse dialysis. Both hypoxia were applied for 1 h.

Ventilation response to acute hypoxia. Resting ventilation and ventilation response to acute hypoxia were measured simultaneously to microdialysates collection using a barometric plethysmograph (Roux et al., 2000). For that purpose, rats were placed in a plethysmographic chamber (volume 4 L) for simultaneous collection of microdialysates and ventilation monitoring (for further details, see Parrot, 2000).

Analytical procedures. After collection, each microdialysate was split in two fractions: 10 µl were used for monoamines and metabolites analysis, while 5 µl were used for Glu and Asp determination. After addition of 2 µl of a conservative medium [acetic acid 1.6 M, EDTA 4.8 mM and bisulfite sodium 2.4 mM] containing 30 pg of epinine as an internal standard, samples were analysed for monoamines and metabolites contents using a high-performance liquid chromatography with electrochemical detection (HPLC-ED) system. It consisted of a Lichrospher 100RP18-ec (250×3 mm) column (Merck, Germany). The working potentials were E1: 300mV and E2: 780 mV. The phase mobile was composed of 500 mM acetic acid, 50 mM sodium acetate, 30 mM citric acid, 1 mM EDTA, 1.7 mM sodium heptane sulfonate and 6% methanol and was pumped at a flow rate of 0.55 ml/min. The injection volume was 8 µl.

Samples for amino acid analysis were derivatized by the fluorogene naphthalene-2,3-dicarboxaldehyde and sodium cyanide; an internal standard (a-aminoadipic acid) was also added at this step (Bert *et al.*, 1996). Derivatized samples were analysed for amino acid contents using an automatic capillary electrophoresis P/ACE™ MDQ system (Beckman, USA) equipped with a LIF detector (Picometrics, France). The excitation was performed by a He-Cd laser (Liconix, USA) at a wavelength of 442 nm. Separations were carried out with a 50 cm × 50 mm i.d. fused-silica capillary (effective length: 40 cm), a 75 mM sodium borate pH 9.20 ± 0.02 as running buffer, applied voltage of 25 kV, hydrodynamic injection of the sample (10 s, 0.2 psi, followed by 5 s of 0.1 M $H_3PO_4$, 0.2 psi).

Data analysis. At the end of each experiment, rats were sacrificed in order to verify the placement of the probe. Data are given as mean ± SEM. Differences between hypoxic and control experiments were tested using ANOVA and post-hoc comparisons by Fisher PLSD test. The level of significance was set at $p<0.05$ for all comparisons.

## ACKNOWLEDGEMENTS

The work was supported by the Université Claude Bernard Lyon I, the Institut National de la Santé et de la Recherche Médicale (INSERM U512), the Centre National de la Recherche Scientifique (CNRS UMR 5123 and PICS Bolivie 917) and the Ministère de la Jeunesse, de l'Education Nationale et de la Recherche (MJENR). S.P. held a doctoral fellowship from MJENR.

# REFERENCES

Abarca, J., and Bustos, G., 1999, Differential regulation of glutamate, aspartate and gamma-amino-butyrate release by N-methyl-D-aspartate receptors in rat striatum after partial and extensive lesions to the nigro-striatal dopamine pathway. *Neurochem. Int.* 35: 19-33.

Ahlemeyer, B., Brust, P., and Johannsen, B., 1977, Different response of cerebral and non-cerebral endothelial cells to cytotoxic hypoxia. *Neurochem. Int.* 31: 39-44.

Akiyama, Y., Koshimura, K., Ohue, T., Lee, K., Miwa, S., Yamagata, S., and Kikuchi, H., 1991, Effets of hypoxia on the activity of the dopaminergic neuron system in the rat striatum as studied by in vivo brain microdialysis. *J. Neurochem.* 57: 997-1002.

Banasiak, K.J., Xia, Y., and Haddad, G.G., 2000, Mechanisms underlying hypoxia-induced neuronal apoptosis. *Prog. Neurobiol.* 62: 215-249.

Bert, L., Robert, F., Denoroy, L., Stoppini, L., and Renaud, B., 1996, Enhanced temporal resolution for the microdialysis monitoring of catecholamines and excitatory amino acids using capillary electrophoresis with laser-induced fluorescence detection. Analytical developments and in vitro validations. *J. Chromatogr. A* 755: 99-111.

Brown, R., and Engel, J., 1973, Evidence for catecholamine involvement in the suppression of locomotor activity due to hypoxia. *J. Pharm. Pharmacol.* 25: 815-819.

Davis, J.N., and Carlsson, A., 1973, The effect of hypoxia on monoamine synthesis, levels and metabolism in rat brain. *J. Neurochem.* 21: 783-790.

Duffy, T.E., Nelson, S.R., and Lowry, O.H., 1972, Cerebral carbohydrate metabolism during acute hypoxia and recovery. *J. Neurochem.* 19: 959-977.

Globus, M.Y.T., Busto, R., Dietrich, W.D., Martinez, E., Valdes I., and Ginsberg, M.D., 1995, Effect of ischemia on the in vivo release of striatal dopamine, glutamate, and gamma-aminobutyric acid studied by intracerebral microdialysis. *J. Neurochem.* 51: 1455-1464.

Huang, R., and Hertz, L., 1994, Effect of anoxia on glutamate formation from glutamine in cultured neurons: dependence on neuronal subtype. *Brain Res.* 660: 129-137.

Krajnc, D., Neff, N.H., and Hadjiconstantinou, M., 1996, Glutamate, glutamine and glutamine synthetase in the neonatal rat brain following hypoxia. *Brain Res.* 707: 134-137.

Kuo, M.F., Song, D., Murphy, S., Papadopoulos, MD., Wilson, D.F., and Pastuszko, A., 1998, Excitatory amino acid receptor antagonists decrease hypoxia induced increase in extracellular dopamine in striatum of newborn piglets. *Neurochem. Int.* 32: 281-289.

Kunimatsu, T., Asai, S., Kanematsu, K., Zhao, H., Kohno, T., Misaki, T., and Ishikawa, K., 1999, Transient in vivo membrane depolarization and glutamate release before anoxic depolarization in rat striatum. *Brain Res.* 831: 272-282.

Miyamoto, O., and Auer, R.N., 2000, Hypoxia, hyperoxia, ischemia and brain necrosis. *Neurology* 54: 362-371.

Nakajima, W., Ishida, A., and Takada, G., 1996, Effect of anoxia on striatal monoamine metabolism in immature rat brain compared with that of hypoxia: an in vivo microdialysis study. *Brain Res.* 740: 316-322.

Norberg, K., and Siesjö, B.K., 1975, Cerebral energy metabolism in hypoxic hypoxia. I. Pattern of activation of glycolysis, a reevaluation. *Brain Res.* 86: 31-44.

Parrot, S., 2000, PhD Thesis, *Intérêts et limites de la microdialyse intracérébrale couplée à l'électrophorèse capillaire pour l'étude des acides aminés excitateurs cérébraux.* Université Claude Bernard Lyon I.

Pastuszko, A., 1994, Metabolic responses of the dopaminergic system during hypoxia in newborn brain. *Biochem. Med. Metab. Biol.* 51: 1-15.

Paulson, P.E., and Robinson, T.E., 1996, Regional differences in the effects of amphetamine withdrawal on dopamine dynamics in the striatum. Analysis of circadian patterns using automated on-line microdialysis. *Neuropsychopharmacology* 14: 325-337.

Paxinos, G., and Watson, C., 1998, *The rat brain in stereotaxic coordinates, 4th Edition.* Academic Press, Sydney.

Poncet, L., Denoroy, L., Dalmaz, Y., and Pequignot, J.M., 1998, Effects of carotid sinus nerve transection on changes in neuropeptide Y and indolamines induced by long-term hypoxia in rats. *Pflügers Arch.* 437: 130-138.

Roux, J.C., Peyronnet, J., Pascual, O., Dalmaz, Y., and Pequignot, J.M., 2000, Ventilatory and central neurochemical reorganisation of $O_2$ chemoreflex after carotid sinus nerve transection in rat. *J. Physiol.* 522: 493-501.

Rozza, A., Masoero, E., Favalli, L., Lanza, E., Govoni, S., Rizzo, V., and Montalbetti, L., 2000, Influence of different anaesthetics on extracellular aminoacids in rat brain. *J. Neurosci. Methods* 101: 165-169.

Serebrovskaya, T., Karaban, I., Mankovskaya, I., Bernardi, L., Passino, C., and Appenzeller, O., 1998, Hypoxic ventilatory responses and gas exchange in patients with Parkinson's disease. *Respiration* 65: 28-33.

Shiraishi, M., Kamiyama, Y., Huttemeier, P.C., and Benveniste, H., 1997, Extracellular glutamate and dopamine measured by microdialysis in the rat striatum during blockade of synaptic transmission in anesthetized and awake rats. *Brain Res.* 759: 221-227.

Speiser, Z., Amitzi-Zonder, J., Ashkenazi, R., Gitter, S., and Cohen, S., 1990, Central catecholaminergic dysfunction and behavioural disorders following hypoxia in adult rats. *Behav. Brain Res.* 37: 19-27.

Szatkowski, M., and Attwell, D., 1994, Triggering and execution of neuronal death in brain ischaemia: two phases of glutamate release by different mechanisms. *Trends Neurosci.* 17: 359-365.

Trouvin, J.H., Prioux-Guyonneau, M., Cohen, Y., and Jacquot, C., 1986, Rat brain monoamine metabolism and hypobaric hypoxia: a new approach. *Gen. Pharmacol.* 17: 69-73.

Tuor, U.I., Hudzik, T.J., Malisza, K., Sydserff, S., Kozlowski, P., and Del Bigio, M.R., 2001, Long-term deficits following cerebral hypoxia-ischemia in four-week-old rats: correspondence between behavioral, histological, and magnetic resonance imaging assessments. *Exp. Neurol.* 167: 272-281.

Vornov, J.J., Tasker, R.C., and Coyle, J.T., 1994, Delayed protection by MK-801 and tetrodotoxin in a rat organotypic hippocampal culture model of ischemia. *Stroke* 25: 457-464.

Wang, Y., Chiou, A.L., Yang, S.T., and Lin, J.C., 1995, Ketamine antagonizes hypoxia-induced dopamine release in rat striatum. *Brain Res.* 693: 233-245.

# Activity of Dorsal Medullary Respiratory Neurons in Awake Rats

F.P. MARTIAL[*], M.DUNLEAVY[*], J.F.X. JONES[#], P. NOLAN[#], R.G. O'REGAN[#], W. MCNICHOLAS[§] and A. BRADFORD[*]

*[*]Department of Physiology, Royal College of Surgeons in Ireland, [#]Department of Human Anatomy and Physiology, NUID, [§]Respiratory Sleep Laboratory, St. Vincent's University Hospital, NUID, Ireland*

## 1. INTRODUCTION

Sleep disordered breathing (SDB) is a major clinical disorder affecting 2-4% of the middle-aged [Young *et al.*, 1993] and is a major public health problem [Phillipson, 1993]. It is characterized by multiple episodes of collapse of the upper airway (UA) during inspiration when the negative pressure in the UA is not adequately counteracted by contraction of UA dilator muscles (obstructive sleep apnoea, OSA) or more rarely by episodic central hypopnoea or apnoea i.e. reduced neural drive to the respiratory muscles [Deegan and McNicholas, 1995]. This results in sleep fragmentation and asphyxia and is associated with hypersomnolence, impaired cognitive function and increased risk of pulmonary and systemic hypertension, congestive heart failure, cardiac arrhythmias, myocardial infarction, stroke and vehicular accidents [Deegan and McNicholas, 1995; Peter *et al.*, 1995]. OSA is caused by collapse of the UA during sleep because of a reduction in tone of the UA muscles that dilate and stabilize the UA during inspiration [Remmers *et al.*, 1978]. However, the cause of the reduction in UA muscle tone occurring in OSA is not known but there is evidence suggesting that it is due to a withdrawal of serotonergic or noradrenergic facilitation of the hypoglossal motor nucleus (XIIn), in the dorsal medulla, that contains the motoneurons to the UA muscles (see Horner, 2000, for review). An

*Chemoreception*, Edited by Pequignot et al.
Kluwer Academic/Plenum Publishers, New York, 2003

understanding of the activity of this nucleus is fundamental to understanding the cause of OSA and opens the possibility of pharmacological intervention to treat or prevent OSA [Horner, 2000]. There is some evidence implicating alterations in this central control of respiration in the pathophysiology of SDB [Horner, 1996; Pack, 1995] and histochemical brainstem abnormalities have been identified in patients who have died of sleep apnoea [Sullivan *et al.*, 1990]. The XIIn receives crucial inputs from other central areas involved in the integration of responses to chemoreceptors and mechanoreceptors, such as the nucleus tractus solitarius (NTS) [Ono *et al.*, 1994; Peever *et al.*, 2002]. However, little is known about the premotor inputs to the XIIn. During apnoeas, there is systemic hypoxia and hypercapnia and the UA muscle responses to systemic hypoxia and hypercapnia play a crucial role in the prevention of apnoea during sleep normally [Parisi et al., 1987; Brouillette and Thach, 1980; Gleeson et al., 1989; Bowes et al., 1981] and in the termination of apnoeic events in SDB [Parisi et al., 1987; Gleeson et al., 1989].

The rat has been shown to be a good model of human ventilatory control [Olson and Dempsey, 1978]. However, anaesthesia has profound effects on ventilatory control [Hwang *et al.*, 1983]. Therefore, in this study, we wish to characterize respiratory-related activity in the dorsal medulla in conscious rats and to measure the responses to acute hypoxia, hypercapnia and asphyxia.

## 2. METHOD

Six male Wistar rats, weighing 320 ± 40 g (mean ± s.d.) were used in these experiments. On the day of surgery, animals were anaesthetized (pentobarbitone 60mg/kg IP) and placed in a stereotaxic frame. Body temperature was monitored and maintained at 37°C. Two thin tungsten wires, crimped in a gold-plated connector 1.0-1.2 mm apart, were advanced stereotaxically through an occipital craniotomy to the NTS and XIIn according to Paxinos rat brain coordinates [Paxinos and Watson, 1986]. Neuronal activity was continously monitored and the depth of the electrode tip was determined by detection of a spontaneous breathing-related activity or by a response to 9% $CO_2$ on one or both electrodes. The electrodes were then sealed on the skull and animals allowed to recover for 48 h. Neuronal activity in the brainstem could then be recorded for several days (10 ± 4 days, mean ± s.d.).

On recording days, animals are placed in a restraining body plethysmograph and challenged with hypoxia (10% $O_2$ in $N_2$), hypercapnia (9% $CO_2$ in air) and asphyxia (10% $O_2$ , 3% $CO_2$in $N_2$).

For each challenge, recordings of the neuronal activity were made for 1 minute before, for 5 minutes during, and for 4 minutes after the challenge and breathing was also recorded with a pneumotachograph placed in the wall of the plethysmograph.

Simultaneous multiunit extracellular recordings of neurons in the dorsal medulla were recorded to measure their responses to respiratory stimuli. The signal from each electrode was processed off-line by dedicated software (Spike 2, Cambridge Electronic Design) to sort out the different neurons. Cross-correlations of the neuronal responses were computed for every possible pair of ipsi-laterally or contra-laterally recorded neurons. A positive cross-correlation indicates an increase in the firing rate of a neuron shortly before or after the occurrence of a spike in the other neuron, whereas a negative cross-correlation indicates a decrease of the firing rate. Respiratory frequency, tidal volume and ventilation were computed from the respiration recordings. Animals were killed by pentobarbitone overdose IP and the brain was removed and stored in 10% formalin for later histological verification of electrode placement.

# 3. RESULTS

## 3.1 Neuronal responses

In 46 recording sessions, 31 different neurons, identified by their spike amplitude and shape, were recorded from 10 electrodes. 4 types of responses to respiratory challenges were observed which were classified as follows:

- no response (0) : non-rhythmic activity unaffected by the challenges
- respiratory activity (R) : rhythmic activity matching the respiratory rhythm
- positive response (E) : tonic non-rhythmic activity increased during at least one of the challenges
- negative response (I) : tonic non-rhythmic activity decreased during at least one of the challenges

*Post mortem* slicing of the brains showed that 4 electrodes (14 cells) were in the XIIn area and 6 (17 cells) in the NTS area. Respiratory activity was recorded in 18 control recordings (7 in the NTS area, 11 in the XIIn area). Among these neurons, 17 discharged during inspiration and 1 during expiration (in the NTS area). Sixteen recordings showed respiratory activity during hypoxia, 9 in the NTS area, 7 in the XIIn area, 19 during asphyxia, 11 in the NTS area, 8 in the XIIn area and 14 during hypercapnia, 6 in the NTS area, 8 in the XIIn area. None of these distributions differed significantly from the control.

During hypoxia, 37 type E responses, 27 in the NTS area and 10 in the XIIn area, and 17 type I cells, 6 in the NTS area and 11 in the XIIn area, were recorded. The proportions of the 2 types in these areas were significantly different ($\chi^2$, $P<0.01$).
During asphyxia, 21 type E cells, 16 in the NTS area and 5 in the XIIn area, and 12 type I cells, 7 in the NTS area and 5 in the XIIn area, were recorded. During hypercapnia, 18 type E cells, 11 in the NTS area and 7 in the XIIn area, and 23 type I cells, 16 in the NTS area and 7 in the XIIn area, were recorded. There were no significant differences between the proportions of type E and I cells in these two conditions. Table 1 shows all the responses recorded.

| responses type | Hypoxia | | Asphyxia | | Hypercapnia | |
|---|---|---|---|---|---|---|
| | NTS area | XIIn area | NTS area | XIIn area | NTS area | XIIn area |
| 0 | 39 | 27 | 45 | 27 | 48 | 30 |
| R | 9 | 7 | 11 | 8 | 6 | 8 |
| E | 27 | 10 | 16 | 5 | 11 | 7 |
| I | 6 | 11 | 7 | 5 | 16 | 7 |
| total | 81 | 55 | 79 | 45 | 81 | 52 |

*Table 1* : Proportions of the 4 response types (total number of recordings = 136)

The proportions of E and I responses in the XIIn area were identical for the 3 challenges. In the NTS area, these porportions did not significantly change between hypoxia and asphyxia, although both differed significantly from the E/I ratio observed in response to hypercapnia ($\chi^2$, $P<0.05$).

Excitatory responses to hypoxia and asphyxia lasted for the duration of the challenge and activity returned to baseline in less than 2 minutes after the offset. The response to hypercapnia showed an initial burst of higher activity for the first minute, and a rebound of increased activity at the offset of the challenge before returning to baseline. Inhibitory responses to asphyxia and hypercapnia lasted for the duration of the challenge and activity returned to baseline in less than 2 minutes after the offset. The response to hypoxia showed a rebound of high activity for several minutes after the offset of the challenge. Figure 1 shows the evolution of the mean frequency of neuronal discharges for each minute of recording.

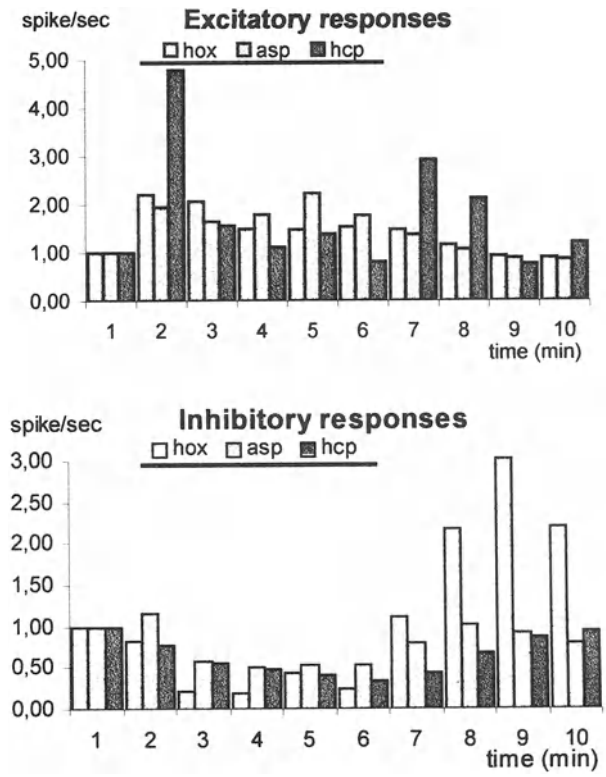


*Figure 1* : Normalized average activity per minute of type E and I responses (hox = hypoxia ; asp = asphyxia ; hcp = hypercapnia, 1.00 = baseline activity recorded during the first minute, bar indicates period of challenge)

## 3.2 Neuron cross-correlations

One hundred and fifty two of the 346 pairs of recordings (72/160 ipsi-lateral and 80/186 contra-lateral) were studied for cross-correlation. Forty three pairs of R-type neurons (19 ipsi-lateral, 24 contra-lateral) firing during inspiration showed simultaneous activity of the two neurons. Among the 109 pairs of type E and I neurons, 36 showed significant cross-correlation in control recordings, 52 during hypoxia, 56 during asphyxia and 51 during hypercapnia. Table 2 shows all the cross-correlations observed.

| respiratory cell pairs | | ctrl | hox | asp | hcp |
|---|---|---|---|---|---|
| ipsi | NTS | 9 | 3 | 6 | 5 |
| | XII | 10 | 9 | 9 | 10 |
| | | 19 | 12 | 15 | 15 |
| contra | NTS-NTS | 6 | 2 | 6 | 0 |
| | XII-XII | 12 | 12 | 12 | 12 |
| | NTS-XII | 6 | 1 | 1 | 6 |
| | | 24 | 15 | 19 | 18 |

| E and I cell type pairs | | ctrl | hox | asp | hcp |
|---|---|---|---|---|---|
| ipsi | NTS | 24 | 15 | 11 | 23 |
| | XII | 29 | 27 | 23 | 24 |
| | | 53 | 42 | 34 | 47 |
| contra | NTS-NTS | 17 | 13 | 8 | 17 |
| | XII-XII | 24 | 20 | 24 | 24 |
| | NTS-XII | 15 | 15 | 3 | 15 |
| | | 56 | 48 | 35 | 56 |

*Table 2* : Numbers of cross-correlations observed.

Cross-correlations computation showed that negative cross-correlations appeared mostly ipsi-lateral and were not affected by any challenge. Positive cross-correlations were observed mainly in contra-lateral recordings, and their proportion significantly increased during asphyxic stimulation ($\chi^2$, $P<0.05$). Figure 2 shows the percentages of positive and negative cross-correlations in ipsi- and contra-lateral pairs.

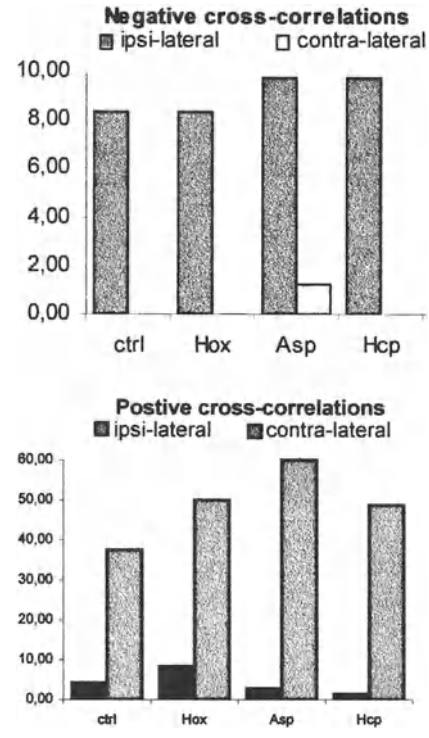


*Figure 2:* Percentages of ipsi- and contra- lateral cross-correlations

# 4. DISCUSSION

Most physiological studies on central regulation of respiration have been performed on anaesthetized animals. However, the effect of anaesthesia on ventilatory control is significant [Olson and Dempsey, 1978] and can affect respiratory related activity in the dorsal medulla [Hwang *et al.*, 1983]. We thus chose to record neuronal activity with a pair of electrodes on either side of the dorsal medulla of conscious spontaneously breathing rats. We concentrated on two medullary locations : the NTS, the major sensory relay nucleus of the vagus nerve and the hypoglossal nucleus (the twelfth cranial nerve). We identified two main types of cells involved in respiratory control :

- rhythmic cells, closely matching the breathing rhythm,
- tonically firing cells (i.e. without respiratory rhythm) reacting to the variation of inspired gas composition.

Previous *in vitro* studies have shown that some non-rhythmic medullary neurons are chemosensitive with respect to $O_2$ and/or $CO_2$, and that these neurons can be excited or inhibited in response to changes in gas concentration [Dean *et al.*, 1990; Okada *et al.*, 1993; Nolan and Waldrop, 1996]. We found that over prolonged recording periods, although the proportion of total responses (excitatory + inhibitory) to hypoxia did not differ significantly between the two areas, the NTS had a significantly greater proportion of excitatory responses compared with the XIIn. It was also observed that, in the NTS, the relative proportion of inhibitory and excitatory responses to hypercapnia differed significantly from that same proportion of responses to hypoxia or asphyxia.

Spike correlation studies showed that inhibitory interconnections between cells were mostly found ipsi-laterally and were stable, not being altered in number by hypoxia and/or hypercapnia. These correlations are likely to be due to intrinsic interconnections. In contrast, positive cross-correlations were found between contra-lateral cells and increased by asphyxia. This increase in the positive contra-lateral cross-correlations, strongly suggests a recruitment and synchronization of cell activity in response to a asphyxia, either through common activation by external drive, or through excitatory cross-connections. Previous reports have demonstrated bilateral neuron synchronization in the ventral respiratory group [Tian and Duffin, 1997; Shen *et al.*, 2002]. Our results suggest that the same kind of mechanism exists in the dorsal group and that presumably both sides of the rat's dorsal medulla are more powerfully integrated during this challenge.

## ACKNOWLEDGEMENTS

This work was supported by a Marie Curie Fellowship of the European Community Programme IHP under contract number HPMD-CT-2000-00041

## REFERENCES

Bowes, G., Townsend, E.R., Bromley, S.M., Kozar, L.F., Phillipson, E.A., 1981, Role of the carotid body and of afferent vagal stimuli in the arousal response to airway occlusion in sleeping dogs. *Am. Rev. Respir. Dis.* 123(6):644-647.

Brouillette, R.T., Thach, B.T., 1980, Control of genioglossus muscle inspiratory activity. *J. Appl. Physiol.* 49(5):801-808.

Dean J.B., Bayliss, D.A., Erickson, J.T., Lawing, W.L., Millhorn, D.E., 1990, Depolarization and stimulation of neurons in nucleus tractus solitarii by carbon dioxide does not require chemical synaptic input. *Neurosci.* 36(1):207-216.

Deegan, P.C, McNicholas, W.T., 1995, Pathophysiology of obstructive sleep apnoea. *Eur. Respir. J.* 8(7):1161-1178.

Gleeson, K., Zwillich, C.W., White, D.P., 1989, Chemosensitivity and the ventilatory response to airflow obstruction during sleep. *J. Appl. Physiol.* 67(4):1630-16377.

Horner, R.L., 2000, Impact of brainstem sleep mechanisms on pharyngeal motor control. *Respir. Physiol.* 119(2-3):113-121.

Horner, R.L., 1996, Motor control of the pharyngeal musculature and implications for the pathogenesis of obstructive sleep apnea. *Sleep* 19(10):827-853.

Hwang, J.C., St John, W.M., Bartlett, D. Jr., 1983, Respiratory-related hypoglossal nerve activity: influence of anesthetics. *J. Appl. Physiol.* 55(3):785-792.

Nolan, P.C., Waldrop, T.G., 1996, In vitro responses of VLM neurons to hypoxia after normobaric hypoxic acclimatization. *Respir. Physiol.* 105(1-2):23-33.

Okada, Y., Muckenhoff, K., Scheid, P., 1993, Hypercapnia and medullary neurons in the isolated brain stem-spinal cord of the rat. *Respir. Physiol.* 93(3):327-336.

Olson, E..B., Dempsey, J.A., 1978, Rat as a model for humanlike ventilatory adaptation to chronic hypoxia. *J. Appl. Physiol.* 44(5):763-769.

Ono, T., Ishiwata, Y.., Inaba, N., Kuroda, T., Nakamura, Y., 1994, Hypoglossal premotor neurons with rhythmical inspiratory-related activity in the cat: localization and projection to the phrenic nucleus. *Exp. Brain Res.* 98(1):1-12.

Pack, A.I., 1995, *In Regulation of Breathing* (J.A. Dempsey and A.I. Pack eds), Dekker Press, N.Y.

Parisi, R.A., Croce, S.A., Edelman, N.H., Santiago, T.V., 1987, Obstructive sleep apnea following bilateral carotid body resection. *Chest* 91(6):922-924.

Paxinos, G., Watson, C., 1986, The rat brain in stereotaxic coordinates. Tokyo: Academic Press.

Peever, J.H., Shen, L., Duffin, J., 2002, Respiratory pre-motor control of hypoglossal motoneurons in the rat. *Neurosci.* 110(4):711-722.

Peter, J.H., Koehler, U., Grote, L., Podszus, T., 1995, Manifestations and consequences of obstructive sleep apnoea. *Eur. Respir. J.* 8: 1572-1583.

Phillipson, E.A., 1993, Sleep apnea--a major public health problem. *N. Engl. J. Med.* 328(17):1271-1273.

Remmers, J.E., deGroot, W.J., Sauerland, E.K., Anch, A.M., 1978, Pathogenesis of upper airway occlusion during sleep. *J. Appl. Physiol.* 44: 931-938.

Shen, L., Peever, J.H., Duffin, J., 2002, Bilateral coordination of inspiratory neurones in the rat. *Pflugers Arch.* 443(5-6):829-835.

Sullivan, C..E., Parker, S. et al., 1990, *In Sleep and Respiration*, Wiley-Liss, Inc., pp. 325-336.

Tian, G.F., Duffin, J., 1997, Synchronization of ventral-group, bulbospinal inspiratory neurons in the decerebrate rat. *Exp. Brain Res.* 117(3):479-487.

Young, T., Palta, M., Dempsey, J., Skatrud, J., Weber, S., Badr, S., 1993, The occurrence of sleep-disordered breathing among middle-aged adults. *N. Engl. J. Med.* 29:328(17):1230-1235.

# Cardiovascular and Respiratory Responses to Heme Oxygenase Inhibition in Conscious Rats

HARUHISA HIRAKAWA[*], SHIGERU OIKAWA[*], VERNON S. BISHOP[#], and YOSHIAKI HAYASHIDA[*]

[*]*Department of Systems Physiology, University of Occupational and Environmental Health, Japan, Kitakyushu, Fukuoka, Japan;* [#]*Department of Physiology, University of Texas Health Science Center at San Antonio, San Antonio, TX, USA*

## 1. INTRODUCTION

Many studies have indicated that endogenous carbon monoxide (CO) generated by the heme oxygenase (HO) system plays a physiological role as a second messenger (Maines, 1997). Although it has been suggested that the HO inhibitor-induced pressor response is mediated by the autonomic nervous system (Johnson *et al.*, 1995), no direct evidence has been demonstrated by neural recordings. Furthermore, a recent study found that CO appears to modulate carotid body sensory activity (Prabhakar *et al.*, 1995). However, the effect of HO inhibitor on tonic ventilatory regulation in conscious animals has not been examined. Accordingly, the main purpose of this study was to examine the respiratory response and the role of the autonomic nervous system in regulation of the cardiovascular response to the administration of zinc deuteroporphyrin 2, 4-bis glycol (ZnDPBG), an inhibitor of HO activity, in conscious rats. To assess the contribution of peripheral chemoreceptors (carotid and aortic bodies) to these responses, we also examined the effect of HO inhibition on respiration and the cardiovascular system in arterial chemo-denervated rats.

*Chemoreception*, Edited by Pequignot et al.
Kluwer Academic/Plenum Publishers, New York, 2003

# 2. MATERIALS AND METHODS

This study was performed in accordance with the guidelines specified for institutional animal care and approved by the ethics committee for animal care and experimentation, University of Occupational and Environmental Health, Japan.

## 2.1 Surgical Procedures

### 2.1.1 Peripheral Chemo-denervation

Carotid body lesion was performed using the method of Verna *et al.* (1975). Rats were premedicated with atropine (0.5 mg/kg, ip) and anesthetized with sodium pentobarbital (50mg/kg, ip). After a midline incision on the ventral region of the neck, the carotid bifurcation was exposed and the common carotid artery was clamped. The carotid body region was locally frozen by applying a metal rod that had been previously immersed in liquid nitrogen. A few minutes after the freezing, the circulation was restored by releasing the clamp. To eliminate the afferent input from aortic chemoreceptors, then, the superior laryngeal nerve was sectioned at its junction with the vagus nerve. These procedures were performed bilaterally at least 3months before the experiment, since it has been reported that regeneration of the carotid sinus nerve was complete after 3 months (Verna *et al.*, 1975). At the end of the experiment, the rats were perfused with heparinized phosphate buffer, prepared for histological examination and confirmed that the carotid body was destructed by freezing.

### 2.1.2 Implantation of Catheters and Electrode

Under sodium pentobarbital anesthesia (50 mg/kg, ip), polyethylene catheters were inserted into the abdominal aorta from the right femoral artery to measure arterial blood pressure (ABP) and into the inferior vena cava from the right femoral vein to administer drugs. A silicone catheter was placed within the intraperitoneal space through a midline abdominal incision to administer ZnDPBG. The electrode for renal sympathetic nerve recording was implanted as described previously (Hirakawa *et al.*, 1997). All of the catheters and electrodes were routed subcutaneously to exit at the nape. After all of the surgical procedures, antibiotics were administered for 2 days. The rats were allowed at least 4 days to recover from the surgery.

## 2.2 Recording Procedure

The electronic signals representing mean arterial blood pressure (MAP), heart rate (HR), and integrated renal sympathetic nerve activity (RSNA) were fed into an analog-to-digital converter (MacLab/8, ADInstruments, USA). We extracted the respiration waveform from ABP by using a narrower band-pass filter (E-3291A, NF Electric Instruments, Japan) (Hirakawa *et al.*, 1997).

## 2.3 Experimental Protocols

All experiments were carried out in conscious freely moving rats. ZnDPBG was dissolved (15 μmol/mL) in $Na_2CO_3$ (50 nmol/L) immediately before use. We examined the effect of the systemic administration of ZnDPBG on MAP, HR, RSNA, and respiratory responses in intact rats and peripheral chemo-denervated rats. After 30 min to collect control data, rats were given an intraperitoneal injection of ZnDPBG (45 μmol/kg) or vehicle alone (50 nmol/L $Na_2CO_3$). MAP, HR, RSNA, and the respiration waveform were recorded continuously for the control period and for 2 h after the administration of ZnDPBG.

## 2.4 Blood Sampling

Arterial blood (0.08ml) was sampled to assess blood gases and arterial pH during the control period and at 2h after the administration of ZnDPBG. Arterial blood gas analysis was performed using a gas analyzer (ABL-520, Radiometer, Denmark).

## 3. RESULTS

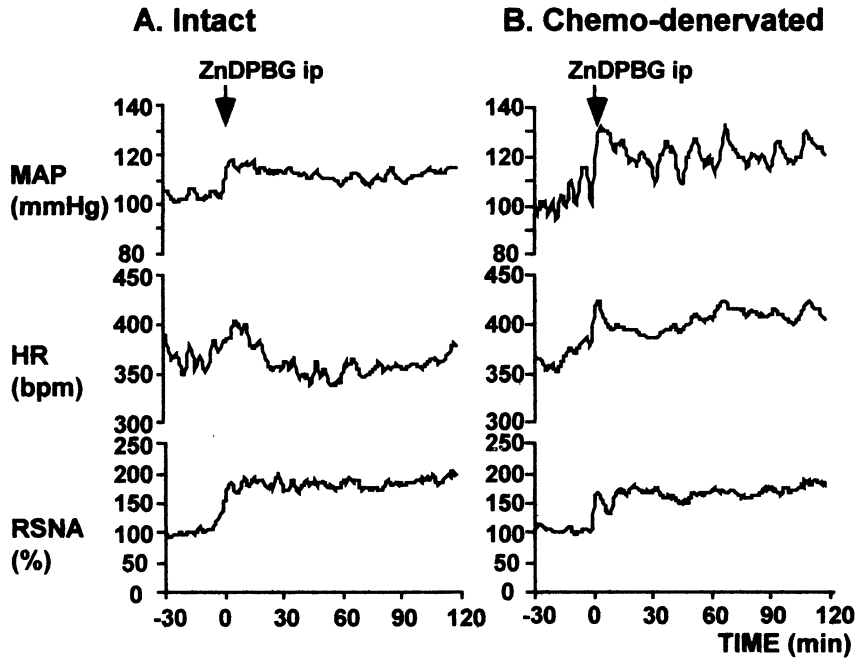


Figure 1. Effect of zinc deuteroporphyrin 2, 4-bis glycol (ZnDPBG) on mean arterial blood pressure (MAP), heart rate (HR), and renal sympathetic nerve activity (RSNA) in intact (A) and peripheral chemo-denervated rats (B).

### 3.1 Effects of ZnDPBG on Respiration and Arterial Blood Gases

In intact rats, ZnDPBG reduced the respiratory rate from 72.0 ± 4.3 to 60.8 ± 2.5 breaths/min, but did not affect $PaO_2$ (95.8 ± 1.0 mmHg vs. 96.8 ± 0.9 mmHg), $PaCO_2$ (38.3 ± 2.1 mmHg vs. 37.9 ± 1.4 mmHg), or pH (7.488 ± 0.008 vs. 7.497 ± 0.006).

On the other hand, in peripheral chemo-denervated rats, ZnDPBG induced no changes in the respiratory rate (72.7 ± 5.6 breaths/min vs. 71.9 ± 2.4 breaths/min), $PaO_2$ (98.4 ± 1.1 mmHg vs. 100.5 ± 1.9 mmHg), $PaCO_2$ (40.2 ± 2.3 mmHg vs. 41.8 ± 2.0 mmHg), and pH (7.476 ± 0.002 vs. 7.495 ± 0.001).

## 3.2 Effects of ZnDPBG on MAP, HR, and RSNA in Intact Rats

Average values of MAP, HR, and RSNA before and after the injection of ZnDPBG are shown in Fig. 1A. The mean values for the 30-min control period and the last 30 min of the experimental period are shown in Table 1. ZnDPBG increased MAP from 102.6 ± 1.1 mmHg to 110.8 ± 0.2 mmHg and RSNA from 100 % to 182.9 ± 29.7 %, but did not affect HR.

## 3.3 Effects of ZnDPBG on MAP, HR, and RSNA in Peripheral Chemo-denervated Rats

The effects of ZnDPBG on MAP, HR, and RSNA are shown in Fig. 1B and Table 1. ZnDPBG induced increases in MAP (from 102.5 ± 0.3 mmHg to 120.8 ± 2.6 mmHg), HR (from 364.9 ± 17.3 bpm to 408.7 ± 10.8 bpm), and RSNA (from100 % to 167.8 ± 43.0 %). There were no differences in mean values of MAP and HR between intact and chemo-denervated rats during the control period.

*Table 1.* MAP, HR, and RSNA in intact and peripheral chemo-denervated rats before and after the administration of ZnDPBG

| | MAP, mmHg | HR, beats/min | RSNA, % |
|---|---|---|---|
| *Intact* | | | |
| Control | 102.6±1.1 | 366.0±13.5 | 100 |
| ZnDPBG | 110.8±0.2 | 357.2±14.2 | 182.9±29.7 |
| *Chemo-denervated* | | | |
| Control | 102.5±0.3 | 364.9±17.3 | 100 |
| ZnDPBG | 120.8±2.6 | 408.7±10.8 | 167.8±43.0 |

Values are means ± SE of mean arterial blood pressure (MAP), heart rate (HR), and renal sympathetic nerve activity (RSNA) before and after the administration of zinc deuteroporphyrin 2, 4-bis glycol (ZnDPBG) in intact and peripheral chemo-denervated rats.

# 4. DISCUSSION

The major findings of the present study are

1) inhibition of the HO-mediated conversion of heme to CO by ZnDPBG induced a decrease in the respiratory rate in intact rats but not in chemo-denervated rats,

2) in intact rats, ZnDPBG increased MAP and RSNA, but did not affect HR, and 3) in peripheral chemo-denervated rats, ZnDPBG increased MAP, HR, and RSNA.

In the present study, the administration of ZnDPBG reduced the respiratory rate, whereas arterial pH, $PaCO_2$, and $PaO_2$ showed no differences before and after ZnDPBG treatment, suggesting that ZnDPBG caused an increase in tidal volume in intact rats. It is likely that this depression of respiratory rate induced by ZnDPBG is mediated via its action on carotid and/or aortic body chemoreceptors, since the destruction of carotid body and aortic denervation abolished this respiratory response.

It has been suggested that ZnDPBG induced an increase in BP via autonomic function, since autonomic ganglionic or α1-adrenoreceptor blockade abolished this pressor effect (Johnson et al., 1995). The present study demonstrated that HO inhibition significantly increased MAP and RSNA in intact and chemo-denervated rats, and that the increases in MAP paralleled those in RSNA. These results indicate that the pressor response to HO inhibition was mainly due to activation of the sympathetic nervous system. Furthermore, there was no difference in the increase in RSNA between intact and chemo-denervated rats. The finding that peripheral chemo-denervation did not attenuate the sympatho-excitatory response to ZnDPBG suggests that this sympatho-excitation may be due to the inhibition of CO formation in the central nervous system.

## REFERENCES

Hirakawa, H., Nakamura, T., and Hayashida, Y., 1997, Effect of carbon dioxide on autonomic cardiovascular responses to systemic hypoxia in conscious rats. *Am. J. Physiol.* 273 (42): R747-R754.

Johnson, R. A., Laversa, M., Askari, B., Abraham, N. G., and Nasjletti, A., 1995, A heme oxygenase product, presumably carbon monoxide, mediates a vasopressor function in rats. *Hypertension* 25: 166-169.

Maines, M. D., 1997, The heme oxygenase system: a regulator of second messenger gases. *Annu. Rev. Pharmacol. Toxicol.* 37: 517-554.

Prabhakar, N. R., Dinerman, J. L., Agani, F. H., and Snyder, S. H., 1995, Carbon monoxide: A role in carotid body chemoreception. *Proc. Natl. Acad. Sci.* 92: 1994-1997.

Verna, A., Roumy, M., and Leitner, L.-M., 1975, Loss of chemoreceptive properties of the rabbit carotid body after destruction of the glomus cells. *Brain Res.* 100: 13-23.

# Peripheral Chemoreceptor Input to Cardiac Vagal Preganglionic Neurones in the Anaesthetised Rat

DEIRDRE M.O'LEARY and JAMES F.X. JONES.
*Department ofHuman Anatomy and Physiology, University College Dubin, Earlsfort Terrace, Dublin 2, Irleand.*

## 1. INTRODUCTION

There is anatomical evidence that there are two main populations of preganglionic neurones that project to the cardiac vagal branch in several species including rat, cat and dog. One population originates in the ventrolateral nucleus ambiguus (NA), and comprises neurones with small myelinated axons (B-fibres) (McAllen and Spyer, 1978). The other group originates in the dorsal vagal motor nucleus (DVMN) and comprises mainly of slowly conducting, unmyelinated axons (C- fibres) (Ford *et al.*, 1990). The B-fibre group has been shown to display a powerful respiratory-related component to their activity (McAllen and Spyer, 1978), whereas it has been reported that the majority of C-fibre vagal efferents located in the DVMN show no modulation in phase with respiration (Jones *et al.*, 1998).

A study of the modulation of cardioinhibitory reflexes by central respiratory drive (Daly, 1991) had shown that the heart rate response to chemoreceptor stimulation is powerfully modulated by central respiratory rhythm. Since there are two populations of cardiac vagal preganglionic neurons in the brainstem (B-and C-fibre neurones), and the B-fibre group exhibits respiratory rhythm, it led us to the hypothesis that chemoreceptor input selectively activates the B-fibre group alone.

*Chemoreception*, Edited by Pequignot et al.
Kluwer Academic/Plenum Publishers, New York, 2003

## 2. METHODS

Eleven adult male Wistar rats weighing 233-332 g (302.4 ± 36.8; mean ± S.D.) were anaesthetised with urethane (1.5 g $kg^{-1}$ i.p.). In all animals, temperature was measured with a rectal thermometer and maintained at 37° using a Harvard homeothermic blanket system. The left femoral vein was cannulated for administering supplemental anaesthesia, fluids and drugs, and the left femoral artery was cannulated for recording arterial blood pressure (BP). BP was measured with a Statham P23Db transducer (Statham Ltd., Puerto Rico). A cervical tracheotomy was performed and the trachea cannulated just below the larynx. The animals were artificially ventilated with humidified $O_2$ enriched air at a frequency of 60/min and a tidal volume of 2 ml (Harvard rodent ventilator, model 683). The level of anaesthesia was assessed by the absence of a withdrawal reflex and cardiovascular response to paw pinch. The chest was opened in the midsternal line and an expiratory pressure of 1-3 cm $H_2O$ was applied to prevent complete collapse of the lungs. A cannula was inserted into the right jugular vein to allow administration of drugs directly into the right atrium.

The cardiac branch of the right vagus was identified by its anatomical position. Once identified, the vagus and the cardiac branch were cut and transposed to a 2-chambered Perspex bath placed adjacent to the extrathoracic trachea. Collagenase (1 mg $ml^{-1}$, Sigma; C7657; 1280-1330 units of activity per mg) was dissolved in HEPES buffered Tyrode solution and left in the bath for 5 min to facilitate the stripping of the epineurium. Once stripped, the whole nerve was placed on a bipolar electrode, constructed from silver wire (250 μm in diameter), in the first chamber of the bath. The signal recorded from this bipolar electrode was used to construct a spike-triggered average (STA) and a moving time average (MTA), or was integrated to act as an index of central respiration. The nerve was held in position on the bipolar electrode with a mixture of paraffin oil and petroleum jelly in approximately equal volumes. The second chamber of the bath was filled with HEPES buffered Tyrode solution and a glass suction electrode (WPI; PG61150-4, internal diameter 10-50 μm) was used to record single efferent activity from the cardiac branch. At the end of each experiment, the animal was killed with an overdose of pentobarbitone sodium.

The fibre signal was digitised using an analogue to digital converter (1401 Interface, Cambridge Electronic Design (CED)), and analysed using spike recognition software (Spike2, CED), which allowed discrimination of individual spikes from a mixed signal. Only discriminated units with a distinctive height and shapes, measured over a period of 2-3 ms in duration, were included for analysis (Figure 1).

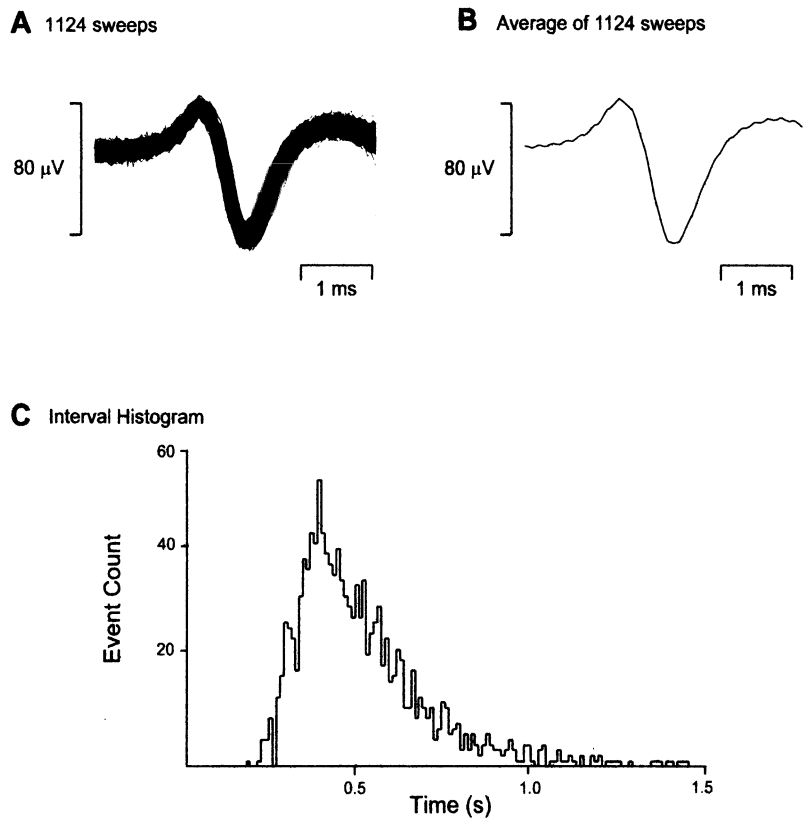


*Figure 1*: Spike Discrimination

**A:** Superimposition of 1124 sweeps, demonstrating the effectiveness of the spike discrimination.

**B:** Average spike shape compiled from 1124 sweeps

**C:** Interval histogram for this unit constructed off-line with Spike2 software.

All units were analysed off-line using post-stimulus time histograms (PSTH) of neural activity against respiration and heart rate (Figure 2). Conduction velocity of the recorded units was calculated with reference to latencies of the STAs of the electrical activity of the whole ipsilateral vagus. Once the conduction velocities were calculated, the units could be classified as B-fibres (conduction velocity 3-15 m $s^{-1}$) or C-fibres (conduction velocity <2 m $s^{-1}$). For a large number of units, STAs could not be generated; therefore conduction velocities could not be calculated. These units were termed unclassified.

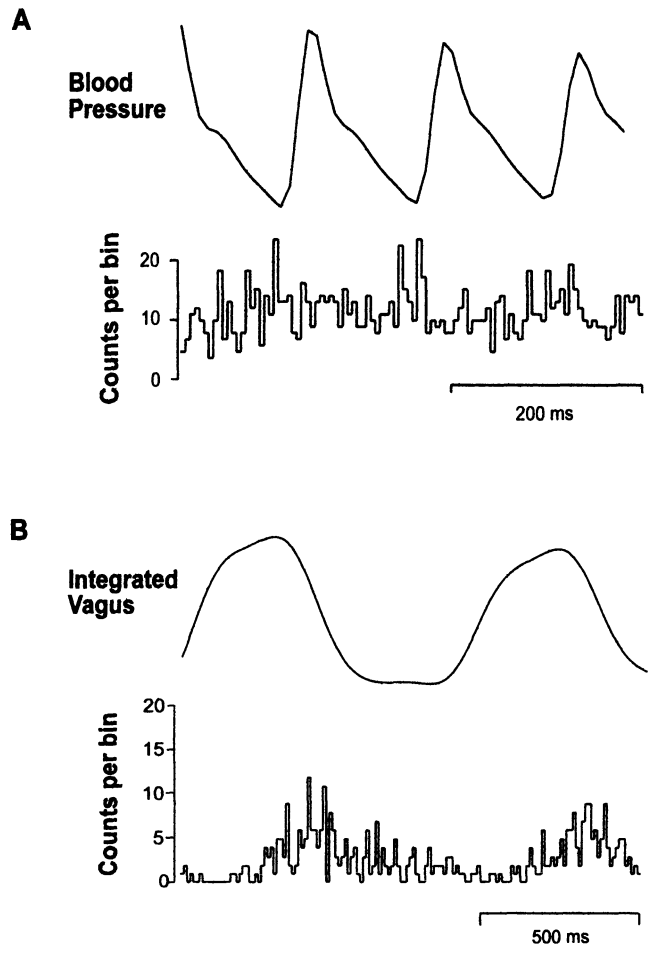


*Figure 2*: Post Stimulus Time Histograms (PSTH)
**A:** The top trace is an average of the femoral arterial blood pressure signal (1287 sweeps). A PSTH of the unit activity is shown beneath. No relationship to the blood pressure signal is seen.
**B:** The top trace is an averaged integrated neurogram of whole cervical vagus electrical activity (120 sweeps). This serves as an index of central respiratory activity. A PSTH for the unit against respiration shows post-inspiratory activity.

Sodium cyanide was administered via the cannula in the right jugular vein and the response of each discriminated unit was recorded. To eliminate the possibility that the unit was responding to the rise in blood pressure caused by cyanide, we also monitored the response of the unit to the vasoconstrictor, methoxamine (20 µl bolus, 1 mg $ml^{-1}$).

# 3. RESULTS

One hundred and thirty five cardiac units were recorded. Of these, only 29 were successfully classified using spike triggered averaging. STA showed that 14 of these axons were unmyelinated C-fibres (conduction velocity <2 $ms^{-1}$) and 15 were myelinated B-fibres (conduction velocity 3-15 $ms^{-1}$). A typical response to cyanide can be seen in Figure 3. In this figure, an increase in the firing frequency of the unit can be clearly seen. The response to methoxamine for this unit was also tested (not shown). Methoxamine produced a rise in blood pressure similar to that seen following administration of cyanide, without increased firing frequency of the unit. None of the units that responded to cyanide were excited by injections of methoxamine, indicating that the excitatory action of cyanide was due to a chemoreflex rather than a baroreflex.

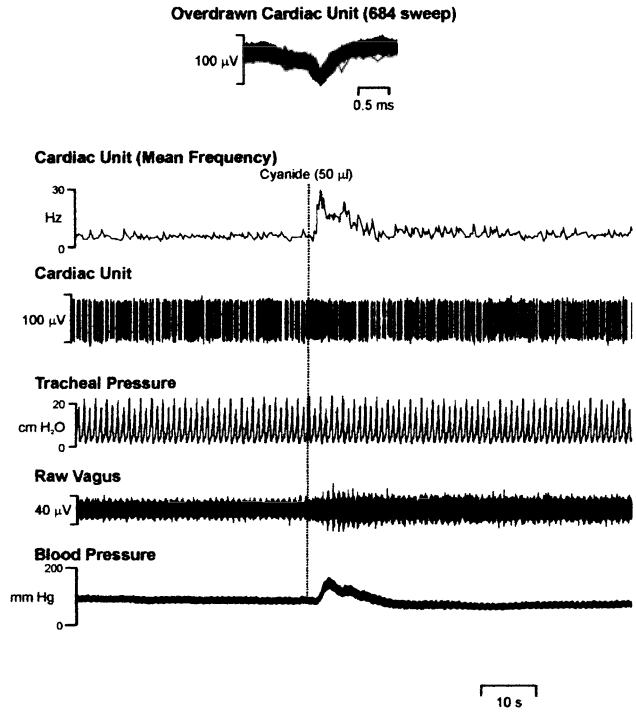


*Figure 3*: Response to Cyanide
The upper trace shows the shape of the cardiac unit and all the superimposed sweeps for that unit on a short time scale. Below this is the firing frequency of the unit, the individual recorded cardiac spikes, the tracheal pressure, the raw vagal signal and the blood pressure, recorded before and after administration of cyanide. The time of administration of cyanide is indicated by the dotted line.

An increase in activity in response to cyanide was recorded in 8/15 B-fibres (53%; 5-58%) and 4/14 C-fibres (29%; 26-79%) (mean and exact 95% confidence limits for the binomial distribution). Therefore we could not reject the "null hypothesis" that B- and C-fibres are equally likely to respond to cyanide injections.

## 4. DISCUSSION

We have described an effective method of measuring the conduction velocities of single cardiac vagal units and have successfully identified both B- and C-fibres in the cardiac vagal branch of the rat. B-and C-fibres were found to have an equal prevalence. Both of these fibre types were found to be equally likely to be excited by injections of cyanide. Therefore, we can reject the hypothesis that chemoreceptor input selectively activates cardiac vagal preganglionic B-fibres alone. Furthermore, the population of cardiac vagal preganglionic neurones in the rat was found to be more diverse than expected. Six different subtypes were discriminated on the basis of conduction velocity and respiratory modulation of discharge. We recorded tonic, inspiratory and expiratory B-fibres, and tonic, inspiratory and expiratory C-fibres. The physiological significance of this diversity of fibre type is still to be elucidated.

## ACKNOWLEDGEMENTS

The authors gratefully acknowledge the generous support of the Wellcome Trust, UK.

## REFERENCES

Daly, M. de Burgh, 1991, Some reflex cardioinhibitory responses in the cat and their modulation by central inspiratory neuronal activity. *J. Physiol.* 439, 559-577.

Ford, T.W., Bennett, J.A., Kidd, C. and McWilliam, P.N., 1990, Neurones in the dorsal motor vagal nucleus of the cat with non-myelinated axons projecting to the heart and lungs. *Exp.l Physiol.* 75, 459-473.

Jones, J.F.X., Wang, Y. and Jordan, D., 1998, Activity of C fibre cardiac vagal efferents in anaesthetised cats and rats. *J. Physiol.* 507, 869-880.

McAllen, R.M. and Spyer, K.M., 1978, Two types of vagal preganglionic motoneurones projecting to the heart and lungs. *J. Physiol.* 439, 365-374.

# Hypoxic Remodelling of $Ca^{2+}$ Homeostasis in Rat Type I Cortical Astrocytes

[1]CHRIS PEERS, [1]IAN F. SMITH, [1]JOHN P. BOYLE and [2]HUGH A. PEARSON

*[1]Institute for Cardiovascular Research, and [2]School of Biomedical Sciences, Worsley Medical and Dental Building, University of Leeds, Leeds LS2 9JT, UK.*

## 1. INTRODUCTION

Higher brain functions are susceptible to damage through exposure to the prolonged hypoxia of ischemia or chronic cardiorespiratory disease (Incalzi *et al.*, 1993; Kogure and Cato, 1993). Indeed, there is a well-documented increased incidence of dementias in patients who have previously suffered prolonged hypoxic or ischemic episodes arising as a consequence of cardiovascular dysfunction such as stroke or arrhythmia (Tatemichi *et al.*, 1994; Moroney *et al.*, 1996).

Many non-neuronal cell types (particularly astrocytes) contribute to intercellular signalling in the central nervous system at several levels (Verkhratsky *et al.*, 1998). Astrocytes and other glia are in intimate contact with neurones and have projections that are located at neuronal synapses (Ventura and Harris, 1999). Indeed, chemical synapses and gap-junction connections between astrocytes and neurones have been identified (Bergles *et al.*, 2000). Activation of astrocytes by neuronal transmitters has been reported at levels of transmitter concentrations found adjacent to synaptic clefts (Kang *et al.*, 1998). Astrocytic activation is usually manifest as a rise of intracellular $Ca^{2+}$ concentration ($[Ca^{2+}]_i$) due to release of $Ca^{2+}$ from internal stores as well as $Ca^{2+}$ uptake from the extracellular space (Deitmer *et al.*, 1998; Grosche *et al.*, 1999).

This fundamental initial response correlates with neuronal synaptic activity, and a rise of $[Ca^{2+}]_i$ in one astrocyte can initiate $Ca^{2+}$ waves that

*Chemoreception*, Edited by Pequignot et al.
Kluwer Academic/Plenum Publishers, New York, 2003

propagate across significant distances via adjacent astrocytes (Araque *et al.*, 2001).

Here, we have examined how intracellular $Ca^{2+}$ stores are modulated by prolonged hypoxia. Hypoxia is a key feature of numerous cardiorespiratory diseases associated with disturbance of higher brain functions (see above).

## 2. METHODS

### 2.1 Cell culture and chronic hypoxia

To obtain astrocytes, cerebral cortices were removed from 6-8 day old Wistar rat pups and placed immediately in ice-cold buffer solution, minced, and digested 0.25μg/ml trypsin and 0.5μg/ml DNase I at 37°C. The tissue was then pelleted, and the pellet triturated with a Pasteur pipette. The cell suspension was taken and centrifuged at 1300 rpm for 90s before resuspension into 60 ml of Eagle's minimal essential culture medium (10% FCS and 1% penicillin-streptomycin). The cell suspension was then aliquoted onto glass coverslips in 6- and 24-well tissue culture plates. Cells were then kept in a humidified incubator at 37°C (95% air; 5% $CO_2$). Four to six hours following plating, cells were washed with fresh media to remove non-adhered cells. This resulted in a culture of primarily type I cortical astrocytes (as confirmed by positive immunostaining with an anti-GFAP antibody). Culture medium was exchanged every 3-4 days and cells were grown in culture for up to 14 days. All recordings were made from cells between days 5-12.

Cells exposed to chronic hypoxia were sub-cultured in the same way as control cells but 24h prior to experimentation were transferred to a humidified incubator equilibrated with 2.5% $O_2$, 5% $CO_2$ balanced with $N_2$. Following exposure to hypoxia, cells were kept in room air for no longer than 1h while microfluorimetric recordings took place.

### 2.2 Microfluorimetric recordings

To measure cytosolic $[Ca^{2+}]$, glass coverslips with cells were incubated in 2 ml of control solution containing 4μM Fura-2AM for 1h at 21°C-24°C in the dark, as previously described (24). Perfusate was nominally $Ca^{2+}$-free: NaCl 135mM, KCl 5mM, $MgSO_4$ 1.2mM, Hepes 5mM, EGTA 1mM and glucose 10mM (pH 7.4, osmolarity adjusted to 300mOsm with sucrose, 21-24°C). Fragments of coverslips were transferred to a 80μl recording chamber on the stage of an inverted microscope, and continuously perfused (1-2 ml/min). $[Ca^{2+}]_i$ was determined using an Openlab System. Excitation (at wavelengths 340 nm and 380 nm) was provided using a Xenon arc lamp.

Emission was collected through the objective and a 510 nm filter (40nm band width). Digital images were sampled at 14-bit resolution by an intensified CCD camera and ratios of resulting images produced every 4s. Regions of interest were used to restrict data collection to individual cells. Drugs and agonists were applied to cells as indicated. All experiments were conducted at room temperature (21-24°C).

## 3. RESULTS AND DISCUSSION

Application of bradykinin (BK; 100nM) to cells perfused with $Ca^{2+}$-free solution evoked transient rises of $[Ca^{2+}]_i$ due to liberation of $Ca^{2+}$ from endoplasmic reticulum stores (Figure 1). Responses evoked in chronically hypoxic astrocytes were significantly greater (e.g. Figure 1), despite the $EC_{50}$ values for BK being similar in the two cell groups (not shown). This finding suggested either that chronic hypoxia increased the size of the mobilizable intracellular $Ca^{2+}$ pool, or that $Ca^{2+}$ buffering / extrusion was disturbed by chronic hypoxia. To investigate the role of $Na^{+}$ / $Ca^{2+}$ exchange (NCX) in BK-evoked responses, BK was applied during perfusion with a solution which was $Na^{+}$-free (replaced with equimolar NMDG). In control cells, BK-evoked responses were significantly enhanced (e.g. Figure 1) indicating that NCX played a significant role in $Ca^{2+}$ extrusion in astrocytes. By contrast, $Na^{+}$ removal was without effect in chronically hypoxic astrocytes (e.g. Figure 1), suggesting that hypoxia somehow caused an inhibition of NCX.

Previous studies have shown that dysfunction of mitochondria can disturb NCX (Opuni and Reeves, 2000), and so a role for mitochondria in the enhanced BK-evoked rises of $[Ca^{2+}]_i$ seen following chronic hypoxia was investigated. Results are summarized in Figure 2. In control cells, application of 10μM FCCP with 2.5 μg/ml oligomycin evoked a modest, transient rise of $[Ca^{2+}]_i$.

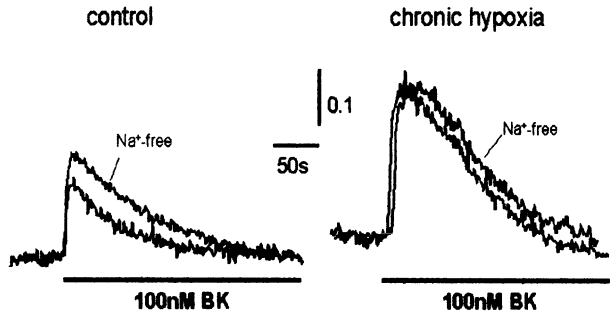


*Figure 1.* Chronic hypoxia inhibits plasmalemmal $Na^+$ / $Ca^{2+}$ exchange.

Example rises of $[Ca^{2+}]_i$ evoked by application of 100nM BK for the period indicated by the horizontal bars in control (left) and chronically hypoxic (right) type I cortical astrocytes. In each case, the perfusate was $Ca^{2+}$-free and either contained $Na^+$, or $Na^+$ was replaced with NMDG ($Na^+$-free, as indicated). Scale bars apply to both traces (the vertical calibration bar is in ratio units).

Subsequent application of BK in the continued presence of mitochondrial inhibition evoked responses which were much larger than seen without mitochondrial inhibition. For chronically hypoxic cells, responses differed in two respects. Firstly, FCCP and oligomycin evoked greater responses than were seen in control cells (Figure 2). Secondly, subsequent BK-evoked responses were no greater than those observed in the absence of mitochondrial inhibition. It is noteworthy that the BK-evoked responses seen in control cells during mitochondrial inhibition were of a magnitude comparable to those seen in chronically hypoxic astrocytes.

These studies suggest that chronic hypoxia exerts dramatic effects on $Ca^{2+}$ homeostasis in type I cortical astrocytes. Clearly, NCX appears to be inhibited in hypoxic cells, whereas it contributes significantly to shaping the rise of $[Ca^{2+}]_i$ following liberation of $Ca^{2+}$ from the endoplasmic reticulum. Secondly, chronic hypoxia appears to cause excessive $Ca^{2+}$ loading of mitochondria, since FCCP / oligomycin treatment evoked greater responses than were seen in controls (Figure 2). Interestingly, mitochondrial inhibition greatly enhanced BK-evoked responses seen in control cells, whereas those observed in chronically hypoxic cells were unaffected. This indicates that in control cells, $Ca^{2+}$ uptake by mitochondria is a significant factor in cellular buffering of cytosolic rises of $[Ca^{2+}]$. Furthermore, hypoxic loading of mitochondria by $Ca^{2+}$ prevents them from acting as a $Ca^{2+}$ buffer, and so BK-evoked responses appear larger since $Ca^{2+}$ uptake by mitochondria is inhibited.

This, together with the inhibition of $Ca^{2+}$ extrusion via NCX, accounts for

the larger $[Ca^{2+}]_i$ rises seen on application of BK to chronically hypoxic cells.

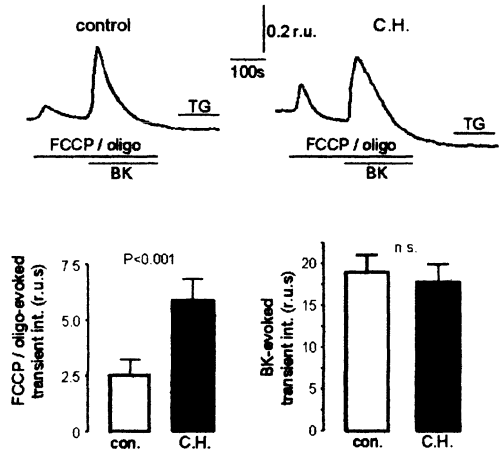


*Figure 2.* Chronic hypoxia enhances mitochondrial $Ca^{2+}$ content

Example rises of $[Ca^{2+}]_i$ evoked by application of 10μM FCCP together with 2.5 μg/ml oligomycin, and in the additional presence of 100nM BK. Following washout, cells were exposed to 1μM thapsigargin (TG). Drug applications were for the periods indicated by the horizontal bars in control (left) and chronically hypoxic (C.H., right) astrocytes. In each case, the perfusate was $Ca^{2+}$-free, and scale bars apply to both traces. The vertical calibration bar is in ratio units (r.u.).

(B) Bar graph indicating mean integrals (with s.e.m. bars) of the transient rise of $[Ca^{2+}]_i$ evoked by FCCP and oligomycin (left), and by BK in the continued presence of FCCP and oligomycin (right). Data are taken from control cells (open bars) and chronically hypoxic cells (hatched bars). Statistical difference between control and C.H. cells is indicated by *P* value shown. (n=4-6 experiments in each case, from each of which at least 3 cells were measured).

The present findings indicate that chronic hypoxia causes dramatic remodelling of $Ca^{2+}$ homeostasis in type I cortical astrocytes. Such effects are likely to be of physiological significance following periods of prolonged hypoxia, and may contribute to the damage of higher brain functions associated with hypoxic episodes such as stroke.

## ACKNOWLEDGEMENTS

This work was supported by the Medical Research council and the Wellcome Trust.

# REFERENCES

Araque, A., Carmignoto, G., and Haydon, P. G., 2001, Dynamic signaling between astrocytes and neurons. *Annu.Rev.Physiol.* 63: 795-813.

Bergles, D. E., Roberts, J. D., Somogyi, P., and Jahr, C. E., 2000, Glutamatergic synapses on oligodendrocyte precursor cells in the hippocampus. *Nature* 405: 187-191.

Deitmer, J. W., Verkhratsky, A. J., and Lohr, C., 1998, Calcium signalling in glial cells. *Cell Calcium* 24: 405-416.

Grosche, J., Matyash, V., Moller, T., Verkhratsky, A., Reichenbach, A., and Kettenmann, H., 1999, Microdomains for neuron-glia interaction: parallel fiber signaling to Bergmann glial cells. *Nat.Neurosci.* 2: 139-143.

Incalzi, R. A., Gemma, A., Marra, C., Muzzolon, R., Capparella, O., and Carbonin, P., 1993, Chronic obstructive pulmonary disease. An original model of cognitive decline. *Am.Rev.Respir.Dis.* 148: 418-424.

Kang, J., Jiang, L., Goldman, S. A., and Nedergaard, M., 1998, Astrocyte-mediated potentiation of inhibitory synaptic transmission. *Nat.Neurosci.* 1: 683-692.

Kogure, K. and Kato, H., 1993, Altered gene expression in cerebral ischemia. *Stroke* 24: 2121-2127.

Moroney, J. T., Bagiella, E., Desmond, D. W., Paik, M. C., Stern, Y., and Tatemichi, T. K., 1996, Risk factors for incident dementia after stroke. Role of hypoxic and ischemic disorders. *Stroke* 27: 1283-1289.

Opuni, K. and Reeves, J. P., 2000, Feedback inhibition of sodium/calcium exchange by mitochondrial calcium accumulation. *J.Biol.Chem.* 275: 21549-21554.

Tatemichi, T. K., Paik, M., Bagiella, E., Desmond, D. W., Stern, Y., Sano, M., Hauser, W. A., and Mayeux, R., 1994, Risk of dementia after stroke in a hospitalized cohort: results of a longitudinal study. *Neurology* 44: 1885-1891.

Ventura, R. and Harris, K. M., 1999, Three-dimensional relationships between hippocampal synapses and astrocytes. *J.Neurosci.* 19: 6897-6906.

Verkhratsky, A., Orkand, R. K., and Kettenmann, H., 1998, Glial calcium: homeostasis and signaling function. *Physiol.Rev.* 78: 99-141.

# Effect of $CO_2$ on Cardiovascular Regulation in Conscious Rats

SHIGERU OIKAWA[*], HARUHISA HIRAKAWA[*], TATSUMI KUSAKABE[#], and YOSHIAKI HAYASHIDA[*]

[*]*Department of Systems Physiology, University of Occupational and Environmental Health, Fukuoka, Japan;* [#]*Department of Sport and Medical Science, Kokushikan University, Tokyo, Japan*

## 1. INTRODUCTION

Carbon dioxide is known to have a significant effect on the cardiovascular and respiratory systems mainly by an action within the central nervous system (CNS), possibly on chemosensitive neurons on the surface of the medulla (Somers *et al.*, 1989). $CO_2$ is also known to activate peripheral chemoreceptors. There are many reports on cardiovascular responses to hypercapnia in various experimental settings (Marshall, 1986, Rose *et al.*, 1983, Somers *et al.*, 1989, Walker, 1987). Although most studies indicated an increase in arterial blood pressure (ABP) during hypercapnia, the results of heart rate (HR) response were conflicting. We have previously reported that hypercapnia elicited cardiovascular changes due to an increase in sympathetic nerve activity (SNA) by the direct effect of $CO_2$ on CNS and a simultaneous increase in parasympathetic nerve activity via an activation of peripheral chemoreceptors during hypoxia (Hirakawa *et al.*, 1997). However, there is only a little information regarding a role of peripheral chemoreceptors in autonomic regulation of the cardiovascular system during hypercapnia without an interaction of hypoxia. In this study, we examined autonomic nervous activity and cardiovascular responses in intact and chemo-denervated conscious rats during normoxic hypercapnia.

*Chemoreception*, Edited by Pequignot et al.
Kluwer Academic/Plenum Publishers, New York, 2003

## 2. MATERIALS AND METHODS

This study was performed in accordance with the guidelines specified for the institutional animal care and approved by the ethics committee of animal care and experimentation, University of Occupational and Environmental Health, Japan.

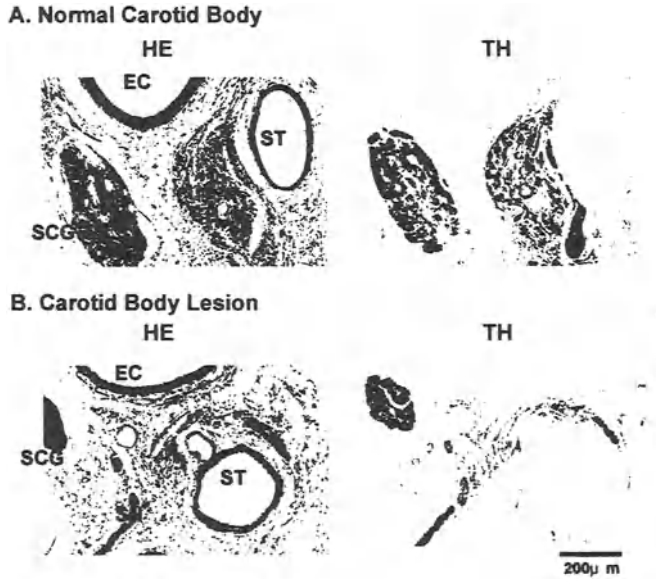


*Figure 1.* A: Sections of carotid bifurcation from an intact rat. B: Sections of carotid bifurcation from a rat that received carotid body lesion by freezing 3 months previously. HE, hematoxylin-eosin; TH, tyrosine hydroxylase antiserum; CB, carotid body; EC, external carotid artery; SCG, superior cervical ganglion; SN, sinus nerve; ST, superior thyroid artery.

### 1.1 Surgical Procedures

The experiments were performed in male Wistar rats, weighing between 300 and 600 g, and were divided into three groups: intact, carotid bodies lesioned and aortic nerves sectioned (CBAN), and aortic nerves sectioned (AN) rats.

### 1.1.1 Peripheral Chemo-denervation

Rats were premedicated with atropine (0.5 mg/kg, i.p.) and anesthetized with sodium pentobarbital (50 mg/kg). After a midline incision on the ventral region of the neck, the carotid bifurcation was exposed and the common carotid artery was clamped. The carotid body region was locally frozen by applying a metal rod that had been previously immersed in liquid nitrogen in accordance with the procedure of Verna *et al.* (1975). A few minutes after the freezing, the circulation was restored by releasing the clamp. To eliminate afferent input from aortic receptors, the superior laryngeal nerve was sectioned at its junction of the vagus nerve. These procedures were performed bilaterally at least 3 months before the experiment, since it has been reported that regeneration of the carotid sinus nerve was complete after 3 months (Verna *et al.*, 1975). At the end of the experiment, the rats were perfused with heparinized phosphate buffer, prepared for histological examination and confirmed that the carotid body was destructed by freezing as shown Figure 1.

### 1.1.2 Implantation of Catheters and Electrodes

Under sodium pentobarbital anesthesia (50 mg/kg, i.p.), polyethylene catheters were inserted into the abdominal aorta from the right femoral artery to measure ABP, and into the inferior vena cava from the right femoral vein to administer drugs. The electrodes for recording of renal sympathetic nerve activity (RSNA) was implanted as described previously (Hirakawa *et al.*, 1997). All the catheters and the electrodes were routed subcutaneously to exit at the nape. After all surgeries were completed, antibiotics were administered for 2 days. The rats were allowed at least 4 days of recovery from the surgery.

## 1.2 Data Recording

The electronic signals of ABP, HR, and RSNA were fed into an analog-to-digital converter (MacLab/8, ADInstruments, U.S.A.) and displayed on a computer. We extracted the respiration wave from ABP by using a bandpass filter (E-3291A, NF Electric Instruments, Japan) (Hirakawa *et al.* 1997).

## 1.3 Experimental Protocols

More than 4 days after implantation of the electrodes and catheters, each rat was placed in an airtight acrylic chamber (40 L), where the rat was allowed free movement. Control measurements for 20 min commenced when stable ABP, HR, and RSNA were observed. After the control measurement, air was replaced by a hypercapnic gas mixture (6% $CO_2$) for 20 min. To avoid hyperoxia due to tachypnea, $O_2$ concentration in the box was reduced to about 16%. The flow of air, $N_2$, and $CO_2$ was regulated (total 20 L/min) by a multi-flowmeter, and the $O_2$ and $CO_2$ concentration within the chamber were continuously monitored with a gas analyzer (Respina IH 26, San-ei, Japan). The hypercapnic gas mixture was then replaced by air for a recovery period of 20 min. The temperature within the chamber was maintained at 25 ℃.

Arterial blood samples were taken during control and exposure periods, and analyzed for pH and gas tension by a gas analyzer (ABL-520, Radiometer, Denmark).

## 2. RESULTS

*Table 1.* Arterial blood pH, $PCO_2$, $PO_2$ respiratory rate during control and hypercapnic periods

| | pH | $PCO_2$ (mmHg) | $PO_2$ (mmHg) | Resp rate (breaths/min) |
|---|---|---|---|---|
| **Intact rats** | | | | |
| Control | 7.47 | 39.4 | 97.9 | 79.5 |
| Hypercapnia | 7.36 | 54.0 | 94.1 | 126.5 |
| **CBAN rats** | | | | |
| Control | 7.47 | 38.9 | 95.9 | 81.0 |
| Hypercapnia | 7.33 | 55.7 | 99.8 | 122.0 |
| **AN rats** | | | | |
| Control | 7.48 | 44.3 | 90.6 | 78.5 |
| Hypercapnia | 7.38 | 59.5 | 85.8 | 126.0 |

CBAN, carotid body lesioned and aortic nerve sectioned; AN, aortic nerve sectioned.

There were no differences in pH, $PaCO_2$, $PaO_2$, and respiratory rate (RR) during control among the three groups. Hypercapnic exposure induced a decrease in pH, increases in $PaCO_2$, RR and no change in $PaO_2$. There were also

no differences in pH, $PaCO_2$, $PaO_2$, and RR during hypercapnic exposure among the three groups as shown in Table 1.

Figure 2 shows autonomic cardiovascular responses to hypercapnic exposure in intact (A), CBAN (B), and AN (C) rats. In intact rats, hypercapnia induced increases in mean ABP (MABP) from 105.8 to 112.3 mmHg, and RSNA from 100 to 116 %, and a decrease in HR from 363.1 to 322.5 beats/min. In CBAN rats, hypercapnia induced increases in MABP from 101.2 to 117.1 mmHg, and RSNA 100 to 121.6 %, and no significant change in HR (372.8 vs. 375.4 beats/min). In AN rats, hypercapnia induced increases in MABP from 97.4 to 102.9 mmHg, and RSNA from 100 to 119.3 %, and no significant change in HR (372.6 vs. 376.7 beats/min).

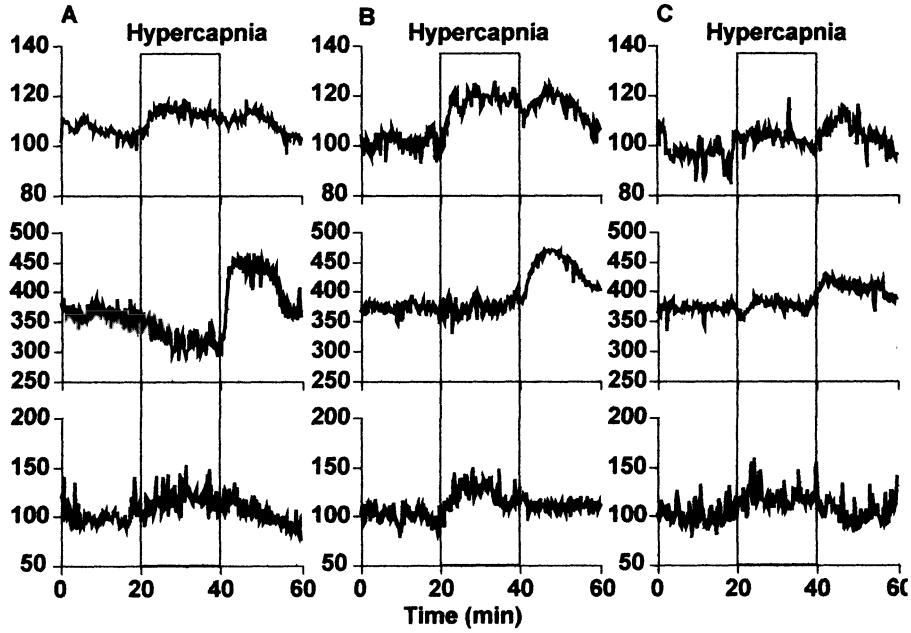


*Figure 2.* Autonomic cardiovascular responses to hypercapnic exposure in intact (A), carotid body lesioned and aortic nerve sectioned (B), aortic nerve sectioned (C) rats

## 3. DISCUSSION

In the present study, hypercapnia induced an increase in both ABP and RSNA in intact rats. Although it has been suggested that hypercapnia has a direct vasoconstricting effect on blood vessels (Fukuda *et al.*, 1989), our result indicates that activation of the sympathetic nervous system played an important role in elevated ABP during hypercapnia. Furthermore, the increases in ABP and RSNA during hypercapnia were also observed in peripheral chemo-denervated rats. These results suggested that these pressor responses were mainly due to the sympatho-excitatory effect of hypercapnia via its action within the central nervous system. Our findings are in agreement with a previous study that superfusion of hypercapnic acid over ventral surface induced a sympatho-excitation (Lioy *et al.*, 1981).

In spite of an increase in RSNA, HR decreased during hypercapnia in intact rats. This result suggests that hypercapnia also activates the parasympathetic nervous system. Moreover, hypercapnia-induced bradycardia was not observed in rats that had their aortic nerves sectioned and with or without carotid bodies, suggesting that afferent input through aortic nerves played an important role in bradycardia observed during hypercapnia in intact rats. It is doubtful that augmented respiration modulated HR, since there were no differences in respiratory responses between intact and chemo-denervated rats. Bradycardia induced by hypercapnia was also not likely due to its direct action on the heart, since HR did not decrease during hypercapnia in chemo-denervated rats. Taken these findings together, bradycardia observed during hypercapnia may be due to an activation of the parasympathetic nervous systems via aortic nerves.

## REFERENCES

Fukuda, Y., Sato, A., Suzuki, A., and Trzebski, A., 1989, Autonomic nerve and cardiovascular responses to changing blood oxygen and carbon dioxide levels in the rat. *J. Auton. Nerv. Syst.*, 28: 61-74.

Hirakawa, H., Nakamura, T., Hayashida, Y., 1997, Effect of carbon dioxide on autonomic cardiovascular responses to systemic hypoxia in conscious rats. *Am. J. Physiol.* 273 (Regulatory Integrative Comp. physiol. 42): R 747-R 754.

Lioy, F., Hanna, B. D., Polosa, C., 1981, Cardiovascular control by medullary surface chemoreceptor. *J. Auton. Nerv. Syst.* 3, 1-7.

Marshall, J. M., 1986, Modulation of the centrally-evoked visceral alerting / defence response by changes in CSF pH at the ventral surface of the medulla oblongata and by systemic hypercapnia. *Pflugers Arch.* 407, 46-54.

Rose, C. E. Jr., Althaus, A. J., Kaiser, D. L., Miller, E. D., Carey, R. M., 1983, Acute hypoxemia and hypercapnia: increase in plasma catecholamines in conscious dogs. *Am. J. Physiol.* 245 ( Heart Circ. Physiol. 14): H924-H929.

Somers, V. K., Mark, A. L., Zavala, D. C., Abboud, F. M., 1989, Contrasting effects of hypoxia and hypercapnia on ventilation and sympathetic activity in humans. *Am. J. Physiol.* 67 (5), 2101-2106.

Verna, A., Roumy, M., Leitner, L.-M., 1975, Loss of chemoreceptive properties of the rabbit carotid body after destruction of the glomus cells. Brain Res. 100, 13 – 23.

Walker, B. R., 1987, Cardiovascular effect of V1- vasopressinergic antagonism during acute hypercapnia in the conscious rats. *Am. J. Physiol.* 252 (Regulatory Integrative Comp. Physiol. 21): R127- R133.

# A6 Noradrenergic Cell Group Modulates the Hypoxic Ventilatory Response

CHRISTOPHE SOULAGE, DAVID PERRIN, JEAN-MARIE COTTET-EMARD, and JEAN-MARC PEQUIGNOT
*Laboratoire de Physiologie Intégrative, Cellulaire et Moléculaire, UMR CNRS 5123 Laboratoire de Physiologie de l'Environnement, EA 645*
*Faculté de Médecine Grange Blanche, 8 avenue Rockefeller, 69373 Lyon cedex 08*

## 1. INTRODUCTION

A6 noradrenergic cell groups or locus coeruleus (LC) are a pair of nuclei located in the peri-ventricular grey-matter of the rostral pons (Dalhström & Fuxe, 1964). A6 possesses a high concentration of noradrenergic perikarya accounting for nearly 45 % of the whole brain noradrenergic cell bodies. It extensively projects in the brain and provides noradrenergic innervation to many brain areas and to the spinal cord (Fritschy & Grzanna, 1990). Kaehler et al. (1999) demonstrate an activation of A6 cell group under hypoxia. Indeed, LC neurones exhibit an increased firing rate (Elam et al., 1981, Guyenet et al., 1993) and an immediate early gene induction (c-fos) under exposure to systemic hypoxia (Breen et al., 1996). Several studies (Li et al, 1992, Guyenet et al, 1993) strongly suggest that A6 is involved in central modulation of breathing, however its role in the ventilatory response to hypoxia remains to be defined. The aim of the present study was to define in adult rat the contribution of the LC noradrenergic neurons for the establishment of the ventilatory response to short-term hypoxia. Hence, we developped a selective lesion of the LC noradrenergic component using 6-hydroxydopamine (6-OHDA). The ventilatory effect of this

*Chemoreception*, Edited by Pequignot et al.
Kluwer Academic/Plenum Publishers, New York, 2003

lesion was tested in awake and unrestained animals by analyzing the hypoxic ventilatory response using whole body plethysmography.

## 2. METHODS

**2.1. Animals and surgical procedures** Male Sprague Dawley OFA rats, weighing 220-250g, were anesthetized with pentobarbital sodium (35-$mg.kg^{-1}$ ip.). The animal was held solidly in a stereotaxic frame. Head skin was incised and a hole was drilled in the occipital bone at LC coordinates. The injection needle (o.d. 0.4 mm) was placed 0.8-mm posterior to lambda, 1.2-mm lateral from midline and 7.3-mm below dura matter according to Paxinos & Watson (1986). 6-OHDA (SIGMA, Saint Quentin, France) was dissolved extemporaneously in artificial cerebrospinal fluid (aCSF) containing 0.1% ascorbic acid. A 1-µL bolus containing 3.25-µg of 6-OHDA was injected unilaterally at a flow rate of $0.125\text{-}\mu L.min^{-1}$. The sham-operated group underwent the same surgical procedure but only received 1-µL of vehicle.

**2.2. Ventilatory measurements** Ventilation was measured in awake unrestrained rats 15 days after surgery using a home made whole-body plethysmograph as described by Bartlett & Tenney (1970). Temperature, $O_2$ and $CO_2$ levels inside the chamber were constantly monitored. Rat was left 45 min in the chamber to acclimate. When it was quiet, the pressure fluctuations related to breathing were recorded with a differential pressure transducer (Celesco, CA, USA). Minute ventilation ($V_E$), tidal volume ($V_T$) and respiratory frequency ($f$), were calculated from a breath-by-breath computer analysis of the spirogram. Ventilation was measured in normoxic conditions and during 1-min of normobaric hypoxia, achieved by flushing the plethysmograph with a gas mixture containing 10% $O_2$ balance $N_2$.

**2.3. Histology.** A colorimetric method (Glenner et al., 1957), based on the reduction of nitroblue tetrazolium by monoamine oxidases (MAO) present in catecholaminergic neurons, was used to quantify the locus coeruleus lesion. One day after the ventilatory measurements were completed, rats were sacrificed by decapitation, brains were rapidly removed and frozen in -45°C isopentane. The frozen brains were cut into serial coronal slices of 60-µm thickness and mounted on gelatine-coated slides. After drying at room temperature, slides were incubated at 37°C in a bath containing tryptamine, nitroblue tetrazolium and

$Na_2SO_4$ in phosphate buffer as described by Glenner et al. Slides were washed twice in phosphate buffer and mounted. Sections were imaged and digitalized using a CCD camera mounted on a dissecting microscope. The positively stained surfaces were quantitated from slides containing locus coeruleus using a Leica Q500IW PC computer equipped with Q Win V2.0 software (Leica Imaging System Ltd, Cambridge, UK).

**2.4. Data analysis** Results are presented as the mean ± SEM. Ventilations were compared between sham-operated and 6-OHDA lesioned groups using U-Mann & Whitney test. Injection side and contralateral side of the brains were compared on histological slices using Wilcoxon test for paired data. Differences were considered as significant when $P < 0.05$.

## 3. RESULTS

**3.1. Lesion analysis** Fifteen days after surgery, the mean body weights of the 6-OHDA-treated rats did not significantly differ from that of sham-operated rats (356 ± 19 g vs. 354 ± 15 g). Unilateral injection of-3.25-µg 6-OHDA resulted in a marked decrease (-81%) in monoamine oxidase (MAO) positive areas corresponding to LC relative to the controlateral intact side (Table 1).

Table 1. Locus coeruleus MAO positively stained areas (arbitrary unit)

| | Intact side | Injection side | Change | |
|---|---|---|---|---|
| Vehicle | 329 ± 25 | 299 ± 24 | -9% | n.s. |
| 6-OHDA | 348 ± 18 | 60 ± 7 | -81% | $P < 0.001$ |

*Table 1* Estimation of LC surface area in sham-operated and 6-OHDA treated rats. Results are expressed as mean ± SEM. Note that injection of the vehicle alone, containing 0.1% of ascorbic acid, failed to alter LC area.

**3.2. Ventilatory consequences** Resting ventilation : Under basal condition (room air, 21% $O_2$), no differences in minute ventilation, tidal volume or frequency were detected between sham-operated and 6-OHDA treated animals (Figure 1).

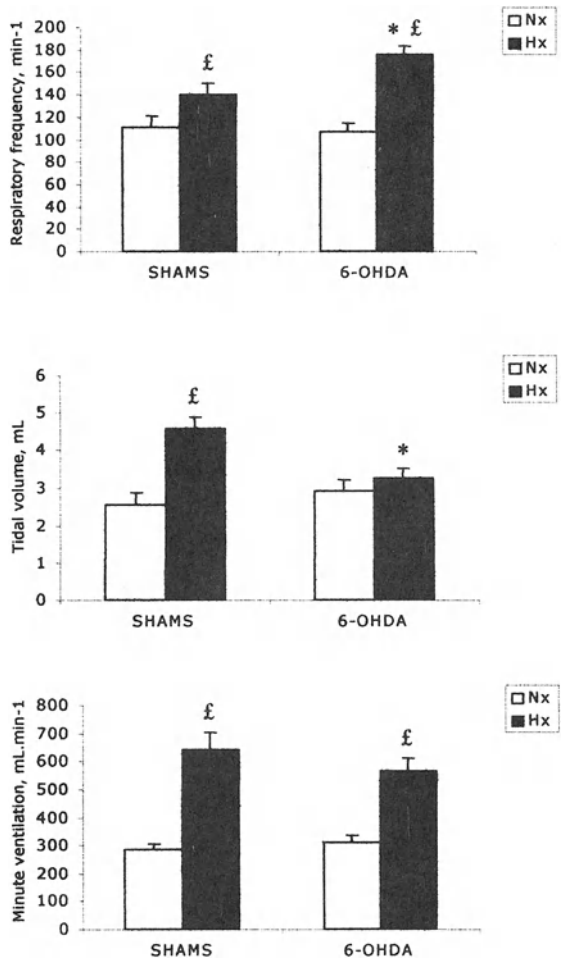


*Figure 1.* Effect of a unilateral lesion of A6 noradrenergic cell group on ventilation of adult rats. Measurement were done in normoxia (Nx, open bar) and under 1 minute of 10% O2 hypoxia (Hx, solid bar). N = 7 in each group. £ significant difference between normoxia and hypoxia. * significant difference between sham-operated and 6-OHDA treated rats.

Hypoxic ventilatory response: Animals were considered to have a significant response to hypoxia if minute ventilation measured under hypoxia significantly differed from basal resting minute ventilation. According to this criterion, both groups exhibited a significant ventilatory response to hypoxia. The lesion suppressed the increase of $V_T$ observed under hypoxia (6-OHDA vs Shams: +11% vs. +79%, $P< 0.001$). This blunted response in VT is however compensated by an enlarged response in frequency ($176 \pm 8$ min $^{-1}$ vs. $140 \pm 10$ min$^{-1}$, $P < 0.01$). The minute ventilation under hypoxia did not significantly differ between the two groups (Figure 1).

## 4. DISCUSSION

Unilateral injection of 3.25-µg of 6-OHDA resulted in a marked decrease of MAO positively stained area whereas vehicle alone (aCSF, 0.1% ascorbic acid) had no effect. The Glenner's staining is based on the reduction of nitroblue tetrazolium by monoamine oxydases (MAO), the main catecholamine-degrading enzymes, present in every catecholaminergic neurones. In the LC, Hida & Araï, (1998) demonstrate that virtually all MAO positive elements are also tyrosine hydroxylase (TH)-immunoreactive (i.e. noradrenergic neurones). Moreover, all the MAO activity is localized within noradrenergic neurones and no MAO activity is found in any TH-negative neurones (Araï et al, 1998). Thus, the profound decrease in MAO positive LC area indicates a marked loss of noradrenergic neurones in the A6 area.

The unilateral lesion failed to alter the ventilation in normoxia indicating that the A6 noradrenergic neurones do not play a key role under basal conditions. A6 do not seem to exert a modulatory influence on ventilation in normoxia. Under hypoxia, the main feature of the 6-OHDA treated animals is a blunted response in tidal volume compared to the sham operated ones. However, minute ventilation level remains unchanged since this weak response in $V_T$ is compensated by a significant increase in $f$. It is particularly noticeable that such a mechanism of "balance" between $f$ and $V_T$ has already been described. Indeed, Roux et al (2000) observed that bilateral carotid sinus nerve transection leads to a blunted response in $f$ under hypoxia compensated by an enlargement of $V_T$.

This increased response in $V_T$ is associated with a neurochemical reorganization of the chemoreflex pathway and especially an increase in TH

activity in A6 cell groups. Taken together, these results strongly suggest that separated mechanisms are acting in the regulation of $V_T$ and $f$ and that under hypoxia these two components of the ventilatory response are well controlled. A6 noradrenergic neurones seem involved in the regulation of the tidal volume component of the hypoxic ventilatory response.Accordingly, $V_T$ is classically thought to be a relative direct index of the output of the brainstem control system to the respiratory motoneurones (Clark and Von Euler, 1972).

Our study provides evidence that the A6 noradrenergic cell group participates in the ventilatory response to hypoxia, however the mechanisms involved remain to be defined. The major respiratory groups namely the ventral respiratory group (VRG), the dorsal respiratory group (DRG) and the pontine respiratory group (PRG) are in close association with some important catecholaminergic cell groups (respectively A1C1, A2C2, and A7). Although the respiratory neurons are not catecholaminergic (Pilowsky *et al*, 1993), they possess adrenoceptors (Champagnat *et al.*, 1979) and then could undergo a catocholaminergic influence. Since A6 noradrenergic neurons establish reciprocal connections with these respiratory areas, it could modulate the hypoxic ventilatory response through an action on these groups. Furthermore, Dobbins and Feldman (1994) also described a direct projection of locus coeruleus on respiratory premotoneurones. Then the A6 neurones could directly affect the recruitment of phrenic motoneurones and then modulate the respiratory depth under hypoxia.

In summary, the present data indicate that if A6 noradrenergic cell group does not seem to play a leading role in breathing modulation in normoxia, it participates to the ventilatory response to hypoxia through a control of the tidal volume.

## ACKNOWLEDGEMENTS

This work was supported by CNRS (UMR CNRS 5123) and Université Claude Bernard- Lyon I. C. Soulage held a fellowship from the French Ministère de la Recherche et de la Technologie. D. Perrin is recipient of fellowships from the Région Rhône-Alpes (grant "Programme Emergence").

# REFERENCES

Arai R, Horiike K, Hasegawa Y. (1998) Dopamine-degrading activity of monoamine oxidase in locus coeruleus and dorsal raphe nucleus neurons. A histochemical study in the rat. *Neurosci. Lett.* Jun 26;250(1):41-4.

Bartlett, D., Tenney, S.M. (1970). Control of breathing in experimental anemia. *Respir.Physiol.*10: 384-395.

Breen S, Rees S, Walker D. (1997) Identification of brainstem neurons responding to hypoxia in fetal and newborn sheep. *Brain Res.* Feb 14;748(1-2):107-21.

Champagnat J, Denavit-Saubie M, Henry JL, Leviel V. (1979) ~ echolaminergic depressant effects on bulbar respiratory mechanisms. *Brain Res.* Jan 5;160(1 -68.

Clark FJ, von Euler C. (1972) On the regulation of depth and of breathing. *J. Physiol.* (London) Apr;222(2):267-95

Dahlstrom A, Fuxe K. (1964) Localization of monoamines in the lov rain stem. *Experientia.* Jul 15;20(7):398-9.

Dobbins EG, Feldman JL. (1994) Brainstem network controlling descending drive to phrenic motoneurons in rat. *J. Comp. Neurol.* Sep 1;347(1):64-86.

Elam M, Yao T, Thoren P, Svensson, TH, (1981) Hypercapnia and hypoxia: chemoreceptor-mediated control of locus coeruleus neurons and splanchnic, sympathetic nerves. *Brain Res.* Oct 19;222(2):373-81.

Fritschy, J.M., et Grzanna, R. (1990). Distribution of locus coeruleus axons within the rat brainstem demonstrated by Phaseolus vulgaris leucoagglutinin anterograd tracing in combination with dopamine-β-hydroxylase immunofluorescence. *J. Comp. Neurol.* 293: 616-631.

Glenner, G.G., Burtner, H.J., & Brown, G.W. (1957). The histochemical demonstration of monoamine oxidase activity by tetrazolium salts. *J. Histochem. Cytochem.* 5:, 591-600.

Guyenet PG, Koshiya N, Huangfu D, Verberne AJ, Riley TA. (1993) Central respiratory control of A5 and A6 pontine noradrenergic neurons. *Am. J. Physiol.* Jun; 264(6 Pt 2):R1035-44

Hida T, Arai R. (1998) Monoamine oxidase activity in noradrenaline neurons of the locus coeruleus of the rat. A double-labeling histochemical study. .*Brain Res.* Dec 14;814(1-2):209-12.

Kaehler, S.T., Singewald, N., & Philippu, A. (1999). The release of catecholamines in hypothalamus and locus coeruleus is modulated by peripheral chemoreceptors. *Naunyn Schmiedebergs Arch. Pharmacol.* 360(4): 428-434.

Li, X.Y., Xia, B.L., & Huang, C.J., (1992). Effects of injection of L-glutamate into the locus coeruleus complex area on the respiration. *J. Tongji Med. Univ.* 12(4):, 205-8.

Paxinos, G., et Watson, C. (Eds.), (1986). The rat brain in stereotaxic coordinates, *Academic Press,* San Diego, CA.

Pilowsky PM, Jiang C, Lipski J. (1990) An intracellular study of respiratory neurons in the rostral ventrolateral medulla of the rat and their relationship to catecholamine-containing neurons. *J. Comp. Neurol.* Nov 22;301(4):604-17.

Roux, J.C., Peyronnet, J., Pascual, O., Dalmaz, Y., & Pequignot, J.M. (2000). Ventilatory and central neurochemical reorganisation of $O_2$ chemoreflex after carotid sinus nerve transection in rat. *J. Physiol. (London)* 522(3):, 493-501.

# Ventilatory Chemosensory Drive in Cats, Rats and Guinea-pigs

RICARDO FERNÁNDEZ, IVETTE ARRIAGADA, ANA-MARÍA GARRIDO, CAROLINA LARRAÍN and PATRICIO ZAPATA
*Laboratory of Neurobiology, Catholic University of Chile, Santiago, Chile.*

## 1. CHEMOSENSORY DRIVE IN NORMOXIA

Comroe and Schmidt (1938) proposed that decreasing $P_aO_2$ is the effective stimulus for arterial chemoreceptors (aortic and carotid bodies), but they considered that these peripheral chemoreceptors could not play a role in the ventilatory control in normoxia. Nevertheless, electrophysiological recordings from the carotid (sinus) nerves showed chemoreceptor activity at normoxic $P_aO_2$, which became feeble or absent when the animal was made hyperoxic by breathing pure oxygen (Landgren and Zotterman, 1951; Åstrand, 1954).

The peripheral chemosensory drive may be considered as the tonic reflex enhancement of ventilation originated from the arterial chemoreceptors, and superimposed upon centrally generated ventilatory output. As proposed by Dejours (1957), the magnitude of chemosensory drive under steady-state conditions may be assessed by the decrease in ventilation resulting from the withdrawal of reflex influence from peripheral chemoreceptors provoked by inhalation of 100% $O_2$. That such phenomenon resulted from the withdrawal of a reflex from the arterial chemoreceptors was shown by its suppression after interruption of carotid and aortic nerves (Bouverot *et al.*, 1965).

*Chemoreception*, Edited by Pequignot et al.
Kluwer Academic/Plenum Publishers, New York, 2003

In normoxic humans at rest, the oxygen test reduces ventilation by about 10% after a delay of 10 s, but if subjects have been breathing hypoxic mixtures, the inhalation of pure $O_2$ produces a considerably larger fall in ventilation (Dejours, 1962).

We performed experiments in 10 mongrel cats, 5 Guinea-pigs and 6 Sprague-Dawley rats, all males, anaesthetized with sodium pentobarbitone 40, 50 and 60 mg/kg i.p., respectively, with supplementary doses given i.v. to maintain a light level of surgical anaesthesia (stage III, plane 2). With animals placed in supine position, body temperature was maintained at about 38°C with a regulated heating pad. Experiments were performed at a mean barometric pressure of 745 Torr, at which animals were born and grown. Animals breathed spontaneously through a tracheal tube introduced *per os* and connected to a Fleisch pneumotachograph of proportionate size (models 00, 000 and 0000) and a differential pressure transducer for measuring ventilatory flow, which was converted into tidal volume ($V_T$) through an integrator, and also derived to a tachograph to obtain instantaneous respiratory frequency ($f_R$). Because of the larger resistance of inner tubings to the flow of $O_2$ compared to $N_2$, the pneumotachographs were calibrated for flows of different mixtures of these two gases, and the values of $V_T$ reported in this paper are corrected to eliminate this misreading. The inspired fraction of oxygen ($F_IO_2$), resulting from mixtures of variables flows of pure $O_2$ and $N_2$ delivered from tanks, was determined by a paramagnetic analyser. Arterial blood pressure was recorded from a cannula inserted into a femoral artery and connected to a pressure transducer. Recordings were displayed in polygraph and stored on digital video tapes for later analyses.

Basal ventilation in each of these animals was very uniform in amplitude and rate (Table I). The differences in values of $V_T$ and $f_R$ between different specimens and species prompted us to express ventilatory changes as

*Table 1.* Ventilatory changes evoked by 5-10 s hyperoxic test on normoxic background.

| | Cats (n=19) | | Rats (n=11) | | Guinea-pigs (n=6) | |
|---|---|---|---|---|---|---|
| $F_IO_2$ | 0.20 | 1.00 | 0.20 | 1.00 | 0.20 | 1.00 |
| $V_T$ (ml) | 29.8 ± 2.4 | 21.5 ± 1.8[b] | 2.3 ± 0.1 | 2.3 ± 0.1 | 3.8 ± 0.7 | 2.9 ±0.5[a] |
| $f_R$ ($min^{-1}$) | 17.5 ± 0.6 | 15.0 ±0.5[b] | 99.9 ± 4.6 | 85.8 ± 4.7[b] | 60.5 ± 7.4 | 54.0 ±6.9[a] |

n = number of manoeuvres. Means ± SEM's. Paired Student's *t* tests: $P<0.01^a$, $<0.001^b$

percentages of the corresponding preceding basal levels. Statistical differences between ventilatory parameters in different conditions were ascertained by paired Student's *t*–tests and ANOVA with Dunnett's Multiple Comparison Test, and considered significant when $P<0.05$.

In cats, suddenly changing $F_IO_2$ from 0.20 to 1.00 for 5-10 s produced consistently well defined decreases in $V_T$, the fall in $V_T$ reaching its nadir (to 72% of basal level) between 3 to 5 cycles, followed by 14% decrease in $f_R$ (Figure 1). In rats, this brief hyperoxic test evoked a significant decrease in $f_R$ (to 86% of basal level), with no significant changes in $V_T$. In Guinea-pigs, hyperoxia evoked a decrease in $V_T$ (to 76% of basal level), followed by 11% decrease in $f_R$ (Figure 1). Absolute ventilatory values reached on exposure to oxygen are given in Table I.

Animals were also subjected to changes in $F_IO_2$ from 0.20 (normoxic state) to 1.00 (hyperoxic state) for 1 min. Figure 2 illustrates that hyperoxia decreases both $V_T$ and $f_R$ in cats, $f_R$ in rats and results in minimal changes in Guinea-pigs. It has previously been reported (Cragg and Schwenke, 1996) that Guinea-pigs do not hypoventilate when subjected to $O_2$ tests, suggesting that their arterial chemoreceptors do not drive ventilation in normoxia. This has been interpreted as a genotypic adaptation to the high altitude at which their ancestors used to live.

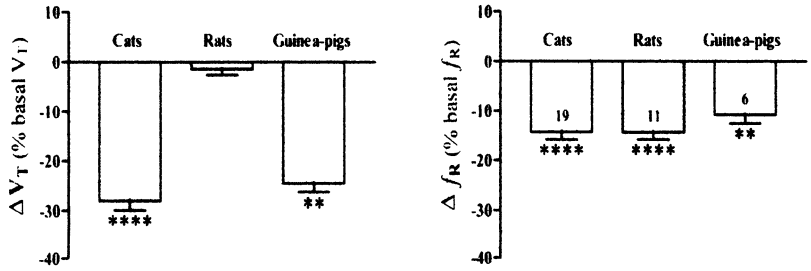


*Figure 1.* Ventilatory changes evoked by 5-10 s hyperoxic tests on normoxic background. Values, Means ± SEM's expressed as percentages of basal levels. Within parentheses, number of manoeuvres. Paired Student's *t* tests: P<0.01**, <0.001****.

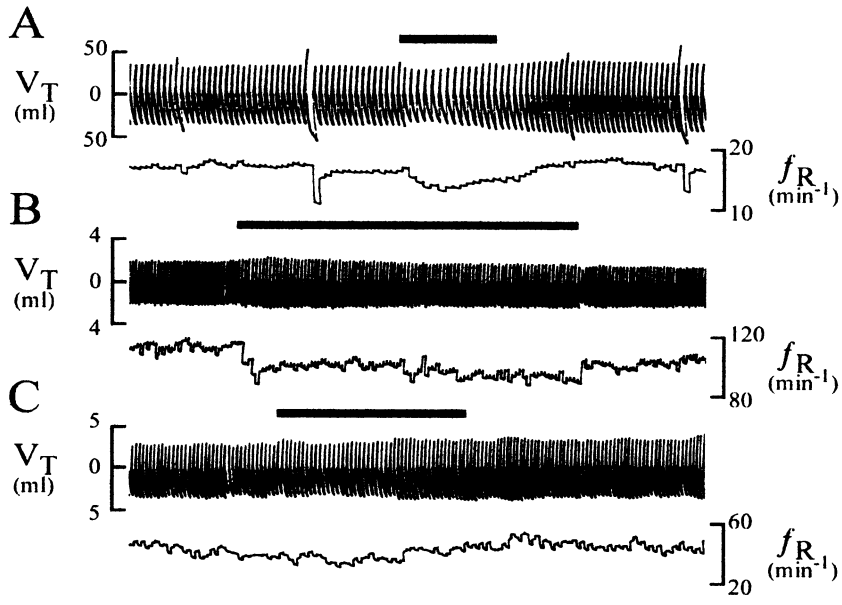


*Figure 2.* Polygraphic recording of changes in tidal volume (inspirations upward) and instantaneous respiratory frequency evoked by 1 min hyperoxia (horizontal bars) in a cat (A), a rat (B), and a Guinea-pig (C).

## 2. CHEMOSENSORY DRIVE IN HYPOXIA

Trying to establish a steady-state in hypoxic conditions, animals were subjected to breathing of gas mixtures enriched in $N_2$ to reduce $F_IO_2$ to 0.15, 0.10, 0.075, 0.05 and 0.025 for 1 min, after which $F_IO_2$ was quickly shifted to 1.0 by giving pure oxygen, which was maintained for the following minute.

In cats, hypoxic challenges produced marked increases in $V_T$, with many evoked gasps, and secondarily a moderate tachypnoea. The degree of increased ventilation was related to the degree of applied hypoxia (Figure 3A). Subsequent hyperoxia decreased $V_T$ proportionally to the degree of hyperventilation reached during the hypoxic challenge. Furthermore, decreases in $f_R$ were also proportional to the decreasing levels of preceding $F_IO_2$. Both, $V_T$ and $f_R$ decreases induced by hyperoxia were larger than those observed in control condition (from normoxia to hyperoxia). When breathing was shifted from $F_IO_2$ 0.05 to 1.0, the cats fell in apnoea, lasting from 40 to 60 s.

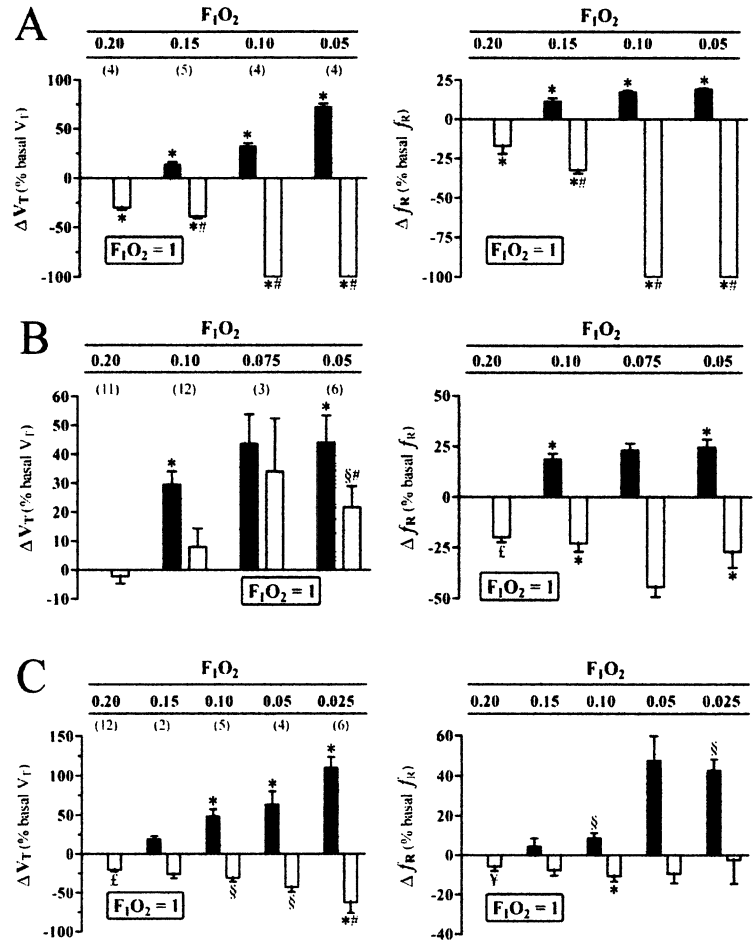


*Figure 3.* Ventilatory changes induced by 1 min hyperoxia preceded by normoxia (control response) or by 1 min of different levels of hypoxia in cats (A), rats (B) and Guinea-pigs (C). Values, Means ± SEM's expressed as percentages of basal levels. Within parentheses, number of manouvres. Paired Student's *t* tests *vs* normoxic level: $P<0.05^{¥}$, $<0.001^{£}$. ANOVA *vs* normoxic level: $P< 0.05^{§}$, $<0.001^{*}$; *vs* hyperoxia on normoxic background: $P<0.001^{\#}$.

In rats the picture was different. One minute of breathing different hypoxic mixtures evoked a progressive increase in $f_R$, and a moderate increase in $V_T$, with evoked gasps. Turning to hyperoxia for the following 60 s evoked larger

decrease in $f_R$ than those observed in control condition (Figure 3B), with no significant changes in $V_T$.

In Guinea-pigs, switching from normoxia to different levels of hypoxia evoked progressive increases in $V_T$, with no consistent changes in $f_R$. Subsequent hyperoxia reduced $V_T$ (Figure 3C). However, only when hyperoxia was preceded by extreme hypoxia ($F_IO_2$ = 0.025), a larger decrease in $V_T$ than that observed in control conditions (normoxia followed by hyperoxia) was observed. The only significant changes in $f_R$ were observed in control response and when hyperoxia was preceded by 10% $O_2$.

Observations on Guinea-pigs presented above are not coincident with a previous report (Cragg and Schwenke.,1996) on hypoxic-evoked hyperventilation unmodified by carotid bodies denervation by bilateral sectioning of the glossopharyngeal nerves, and interpreted as insensitivity of their carotid bodies to hypoxia. The ventilatory depression evoked by hyperoxia interrupting hypoxic exposure suggests that the arterial chemoreceptors do indeed drive ventilation under this condition.

In summary, the chemosensory drive in normoxia -assessed by hyperoxic tests- is stronger in cats than in rats and in Guinea-pigs. During hypoxia-induced hyperventilation, the chemosensory drive became so enhanced in cats that its withdrawal by hyperoxia could lead to apnoea; this means that hypoxia-evoked hyperventilation had resulted in pronounced hypocapnia and depression of central chemoreceptors and medullary respiratory centres. The enhancement of chemosensory drive in hypoxic conditions was less pronounced in rats and Guinea-pigs. Furthermore, while ventilatory changes in response to either hyperoxia or hypoxia mainly consist in changes in $V_T$ in both cats and Guinea-pigs, those observed in rats are mostly expressed by changes in $f_R$, meaning different strategies of respiratory responsiveness in these animals. This is consistent with observations of pronounced $V_T$ enhancements or depressions exhibited by cats in response to NaCN and dopamine injections, respectively (Eugenín *et al.*, 1989; Zapata and Zuazo, 1980), in contrast to the more pronounced changes in $f_R$ observed in rats in response to these drugs (Cárdenas and Zapata, 1981, 1983).

## ACKNOWLEDGEMENTS

Work supported by grant 1010951 from FONDECYT. R Fernández is PhD Candidate with a fellowship from CONICYT. I Arriagada and A-M Garrido were medical students.

## REFERENCES

Åstrand, P.O., 1954, A study of chemoreceptor activity in animals exposed to prolonged hypoxia. *Acta Physiol. Scand.* 30: 335-342.

Bouverot, P., Flandrois, R., Puccinelli, R., Dejours, P., 1965, Étude du rôle des chémorécepteurs artériels dans la régulation de la respiration pulmonaire chez le chien éveillé. *Arch. Intl. Pharmacodyn.* Thér. 157: 253-271.

Cárdenas, H., Zapata, P., 1981, Dopamine-induced ventilatory depression in the rat, mediated by carotid nerve afferents. *Neurosci. Lett.* 24: 29-33.

Cárdenas, H., Zapata, P., 1983, Ventilatory reflexes originated from carotid and extra-carotid chemoreceptors in rats. *Am. J. Physiol.* 244: R119-R125.

Comroe, J.H. Jr., Schmidt, C.F., 1938, The part played by reflexes from the carotid body in the chemical regulation of respiration in the dog. *Am. J. Physiol.* 121: 75-97.

Cragg, P.A., Schwenke, D.O., 1996, Role of carotid bodies in the Guinea-pig. *Adv. Exp. Med. Biol.* 410: 377-381.

Dejours, P., 1957, Intérêt méthodologique de l'étude d'un organisme vivant à la phase de rupture d'un équilibre physiologique. *Compt. Rend. Acad. Sci., Paris*, 245: 1946-1948.

Dejours, P., 1962, Chemoreflexes in breathing. *Physiol. Rev.* 42: 335-358.

Eugenín, J., Larraín, C., Zapata, P., 1989, Correlative contribution of carotid and aortic afferences to the ventilatory chemosensory drive in steady-state normoxia and to the ventilatory chemoreflexes induced by transient hypoxia. *Arch. Biol. Med. Exp.* 22: 395-408.

Landgren, S., Zotterman, Y., 1951, The recording of chemoceptive spike activity in dogs. *Acta Physiol. Scand.* 22: 79-82.

Zapata, P., Zuazo, A., 1980, Respiratory effects of dopamine-induced inhibition of chemosensory inflow. *Respir. Physiol.* 40: 79-92.

# Deletion of Tachykinin NK1 Receptor Gene in Mice does not Alter Respiratory Network Maturation but Alters Respiratory Responses to Hypoxia.

GERARD HILAIRE*, HENRI BURNET*, KRZYSZTOF PTAK[$], MICHAEL SIEWEKE[£], BRUNO BLANCHI[£], CARMEN DE FELIPE[#], STEPHEN HUNT[%] and ROGER MONTEAU[$]

**GERM - CNRS, 280 Bd St. Marguerite, 13009 Marseille, France; [$] UMR 6153 CNRS-INRA, Faculté St Jérôme, 13397 Marseille, France; [£] CIML, CNRS - INSERM, Campus Luminy, 13288 Marseille, France; [#] Instituto de Neurosciencias, San Juan de Alicante, Spain; [%] Dpt of Anatomy and Developmental Biology, University College, London, UK*

## 1. INTRODUCTION

The aim of this study was to shed some light on the role of Substance P (SP) and its neurokinin $NK_1$ receptors ($NK_1R$) in respiratory network maturation and function. On the one hand, as SP is detected early during development (Tsuchida *et al.*, 1990; Beresford et al., 1992; Taoka *et al.*, 1996; St John *et al.*, 1997), SP is assumed to play a role in the early organization of the CNS (Quirion and Dam, 1986) and therefore in that of the respiratory network. On the other hand, compelling evidence exists that activation of $NK_1R$ affects ventilation. First, $NK_1R$ are expressed within the pre-Bötzinger complex, a region containing putative rhythm generating neurons (Gray *et al.*, 1999; Wang *et al.*, 2001) and $NK_1R$ activation increases respiratory activity (Hedner et al., 1984; Chen et al., 1990; Yamamoto *et al.*, 1992; Monteau *et al.*, 1996; Ptak *et al.*, 1999, 2000a, b) whereas destruction of $NK_1R$-positive cells alters breathing (Gray et al., 2001). Second, SP may be implicated in the central transmission of the inputs from the carotid bodies (CB) which detect peripheral hypoxia since SP is contained in CB afferent nerves (Liebstein *et al.*, 1985; Lindefors *et al.*, 1986) and in fiber terminals within the nucleus tractus solitarius (Lipski *et al.*, 1977; Mantyh *et al.*, 1989). SP concentration increases within the nucleus tractus solitarius during hypoxia, but not after CB denervation (Srinivasan *et al.*, 1991). Furthermore, lack of the SP degradation enzyme increases SP concentration within nucleus tractus solitarius and enhances the respiratory response to hypoxia (Grasemann *et al.*, 1999).

*Chemoreception*, Edited by Pequignot et al.
Kluwer Academic/Plenum Publishers, New York, 2003

To determine the role of $NK_1R$, we compared the respiratory activity of maturing mice and their responses to hypoxia in wild type($NK_1^{+/+}$) and mutant ($NK_1^{-/-}$) mice which do not express $NK_1R$ (De Felipe *et al.*, 1998).
Results show that $NK_1R$ are involved in the adult respiratory response to hypoxia but they do not support a significant role for $NK_1R$ in the prenatal maturation of the respiratory network and in its responses to hypoxia at birth.

## 2. RESULTS

### 2.1 Perinatal Expression of $NK_1$ Receptors in $NK_1^{+/+}$ Mice

At gestational day 18, i.e. about 2 days before birth, immunohistochemistry in $NK_1^{+/+}$mice revealed $NK_1R$ in the medial raphe areas, in the phrenic motor nucleus and in medullary respiratory-related areas (Bianchi *et al.*, 1995; Monteau and Hilaire, 1991; Hilaire and Duron, 1999) such as the nucleus tractus solitarius, the reticular formation and the nucleus ambiguus regions (Fig. 1A), and the rostral ventrolateral medulla (Fig. 1B). In neonates, $NK_1R$ were found in the same areas but no $NK_1$ immunoreactivity was observed in fetuses or in neonates of the $NK_1^{-/-}$ strain.

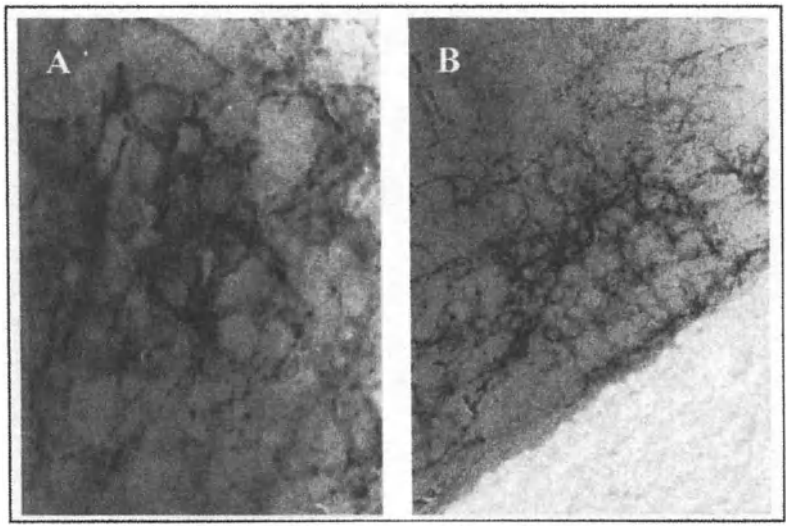


*Figure 1*: Immunohistochemical detection of $NK_1R$ in E18 fetuses of $NK_1^{+/+}$mice showing $NK_1R$ expression in the regions of the nucleus ambiguus (A) and the pre-Bötzinger complex (B).

## 2.2 *In vitro* Respiratory Activity in $NK_1^{+/+}$ and $NK_1^{-/-}$ Neonates

In vitro brainstem-spinal cord preparations were used to analyze the rhythmic phrenic bursts (PBs) produced by the isolated respiratory network of control and mutant neonates (Fig. 2A). Neither the mean frequency of the PBs (10.6 ± 1.5 vs. 9 ± 2.1 cycle.min$^{-1}$, for 10 control and 11 $NK_1^{-/-}$ mice, respectively), nor their duration, nor their individual variability differed between the two strains.

Applying exogenous SP (100 nM; 5 min) to seven $NK_1^{+/+}$ preparations significantly increased the mean PB frequency by 48 ± 13 % and the PB amplitude by 35 ± 8 % whereas SP had no significant effects in eleven $NK_1^{-/-}$ preparations. This reveals that no adaptive process implicating $NK_2$ or $NK_3$ receptors developed during the prenatal period to compensate for the lack of $NK_1R$ in $NK_1^{-/-}$ mice. In addition, applying the $NK_1R$ antagonist GR 82334 to $NK_1^{+/+}$ preparations (100 nM; 20 min., n=5) to block any effects of endogenous SP did not significantly alter the PB occurrence, suggesting that, despite the responses to exogenous SP, no endogenous SP was modulating the respiratory network.

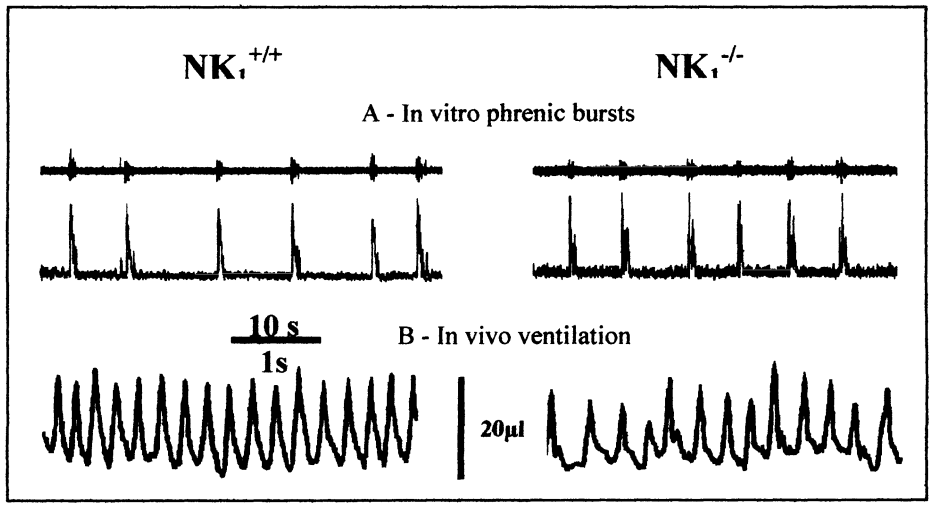


*Figure 2:* Neither the *in vitro* phrenic bursts produced by the isolated respiratory network (in A, upper and lower traces, raw and integrated phrenic activity, respectively) nor the *in vivo* ventilation (in B) differed between $NK_1^{+/+}$ and $NK_1^{-/-}$ neonates (left and right parts, respectively).

## 2.3 *In vivo* Ventilation of Neonatal, Young and Adult $NK_1^{+/+}$ and $NK_1^{-/-}$ Mice

At P5, plethysmography recordings of ventilation of non-anaesthetized neonates (Fig. 2B) failed to reveal significant differences in mean respiratory frequency (Rf, 213 ± 17 vs. 190 ± 15 cycle.min$^{-1}$), tidal volume ($V_T$, 21 ± 3 vs. 24 ± 7 µl) and minute ventilation ($V_E$, 4.4 ± .6 vs. 4.5 ± 1.5 ml.min$^{-1}$) between $NK_1^{+/+}$ and $NK_1^{-/-}$ mice. At P12-P14, in slightly anaesthetized young mice, the resting $V_T$ (80 ± 7 vs. 83 ± 9 µl, control and $NK_1^{-/-}$ mice, respectively) and $V_E$ (7.9 ± .8 vs. 7.9 ± .9 ml.min$^{-1}$) were significantly increased when compared to P5 but no inter-strain significant differences were again observed. Finally at P24-P28, slightly anaesthetized adult mice showed further increased $V_T$ (170 ± 15 vs. 150 ± 11 µl, ns) and $V_E$ (25 ± 3 vs. 20 ± 3 ml.min$^{-1}$) but again no inter-strain differences.

## 2.4 Respiratory responses to hypoxia in $NK_1^{+/+}$ and $NK_1^{-/-}$ mice

Replacing room air (21% $O_2$) by a hypoxic mixture (10% $O_2$) for short 3 min periods in $NK_1^{+/+}$ and $NK_1^{-/-}$ neonates slightly increased the Rf (+11 ± 6 % vs. +41 ± 14 % of control Rf in $NK_1^{+/+}$ and $NK_1^{-/-}$ mice, respectively) and the $V_T$ (+53 ± 16 % vs. +18 ± 9 %), leading to a significant increase in $V_E$ in both strains (44 ± 13 vs. 62 ± 13 %). Thus, hypoxia already facilitated mouse ventilation at P5 and the response was not affected by $NK_1R$ deficiency.

At P12-P14, all the breathing parameters increased under hypoxia (Rf, +20 ± 7 vs. +12 ± 5 % of control; $V_T$, +52 ± 11 vs. +28 ± 6 % in $NK_1^{+/+}$ and $NK_1^{-/-}$ mice respectively), leading to a significant increase in $V_E$ in both strains (180 ± 15 vs. 151 ± 10 %; Fig. 6). Although the mean increases in Rf, $V_T$ and $V_E$ were smaller in $NK_1^{-/-}$ than in $NK_1^{+/+}$ mice, the inter-strain differences were not significant.

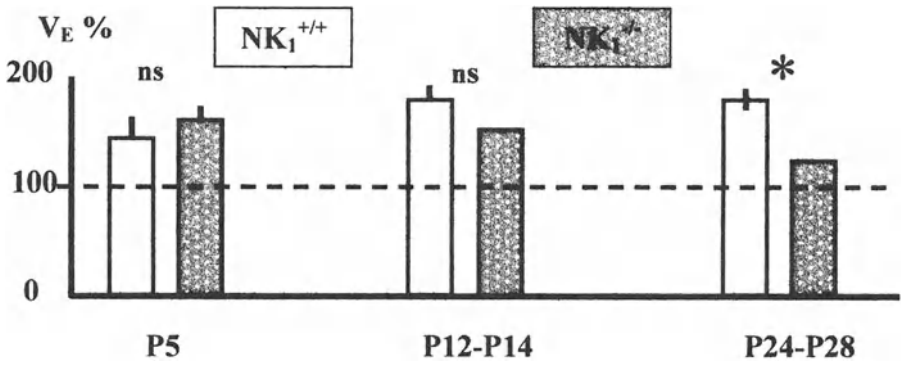


*Figure 3:* Changes in minute ventilation ($V_E$ %, expressed in % of control value under normoxia) induced by 3 min hypoxic challenge (10 % $O_2$) in $NK_1^{+/+}$ and $NK_1^{-/-}$ mice at different ages (P5, P12-P14 and P24-P28). Hypoxia significantly increased $V_E$ at all ages in both strains but a significant difference between $NK_1^{+/+}$ and $NK_1^{-/-}$ mice occurred at P24-P28 (*); ns: non significant interstrain difference.

At P24-P28, the hypoxic challenge revealed significant inter-strain differences in the $V_E$ of slightly anaesthetized adult mice; hypoxia significantly increased the mean $V_T$ in both strains (133 ± 5 vs. 120 ± 5%) but the Rf only in $NK_1^{+/+}$ mice (+36 ± 9 vs. +7 ± 5 %). Thus, the resulting increases in $V_E$ were significantly larger in $NK_1^{+/+}$ (+80 ± 10 %) than in $NK_1^{-/-}$ (+23 ± 6 %) adult mice.

## 3. DISCUSSION – CONCLUSION

Comparison of respiratory activity recorded *in vivo* and *in vitro* in neonatal $NK_1^{+/+}$ and $NK_1^{-/-}$ mice shows that the respiratory network can develop and produce normal respiratory rhythm in the absence of $NK_1R$. However, the $NK_1R$ contributes significantly to the facilitation of ventilation by hypoxia in adults.

Both *in vivo* and *in vitro*, the respiratory network of $NK_1^{+/+}$ and $NK_1^{-/-}$ neonates produces virtually indistinguishable rhythmic activity, with similar Rf,

$V_T$, $V_E$ as well as PB bursts frequency. Thus, despite the early expression of $NK_1R$ during development (Tsuchida *et al.*, 1990; Beresford *et al.*, 1992; Taoka *et al.*, 1996; St John *et al.*, 1997), these receptors are not required for the prenatal development of the respiratory network and for rhythm generation. Neurons expressing $NK_1R$ in the pre-Bötzinger Complex are assumed to play a key role in neonatal respiratory rhythmogenesis (Smith *et al.* 2001). Our results clearly indicate that the cells expressing $NK_1R$ may be crucial but not the $NK_1R$ itself.

The general concept is accepted that blood hypoxia is detected by the peripheral CB which activate the central respiratory network and that both SP and its $NK_1R$ are implicated in this regulation. We show herein that $NK_1R$ deficit does not alter the respiratory response to hypoxia in P5 neonates and in young mice, although the $V_E$ facilitation is slightly but insignificantly weaker in $NK_1^{-/-}$ mice. For adults however, the difference reaches the significant level, with a larger response to hypoxia in $NK_1^{+/+}$ than $NK_1^{-/-}$ mice. Thus, it is likely that the contribution of $NK_1R$ to breathing facilitation by short-lasting hypoxia follows a developmental process: the regulation is independent of $NK_1R$ at birth, but clearly dependent on $NK_1R$ during adulthood.

During adulthood, the weakness of the respiratory response to hypoxia in $NK_1^{-/-}$ mice may originate at different levels: i) the detection of hypoxia by the CB, ii) the transmission of peripheral hypoxic inputs at the level of the nucleus tractus solitarius, and/or iii) the response in respiratory frequency by the rhythmogenic system of the pre-Bötzinger Complex. In $NK_1^{+/+}$ and $NK_1^{-/-}$ adult mice, as the response of CB to hypoxia is similar (see Donnelly *et al.*, Chemoreceptor activity in $NK_1^{-/-}$ mice, this issue) and as hypoxia similarly increases $V_T$ but increased Rf only in $NK_1^{+/+}$ adult mice (present results), a working hypothesis is that deficiency in hypoxic regulation of the $NK_1^{-/-}$ adult mice originates from the lack of $NK_1R$ in the pre-Bötzinger Complex.

To conclude, $NK_1R$ do not play a key role in the prenatal maturation of the respiratory network, in the neonatal respiratory rhythmogenesis, or in its regulation by short-lasting hypoxia at birth. However, they contribute to the breathing facilitation by hypoxia during adulthood.

## REFERENCES

Beresford, I.J.M., Ireland, S.J., Stables, J. & Hagan, R.M. (1992) Ontogeny and characterization of [125I]Bolton Hunter-eledoisin binding sites in rat spinal cord by quantitative autoradiography. *Neuroscience*, 46, 225-32. OK

Bianchi, A.L., Denavit-Saubie, M. & Champagnat, J. (1995) Central control of breathing in mammals : neuronal circuitry, membrane properties, and neurotransmitters. *Physio.l Rev.*, 75, 1-45.

Chen, Z., Hedner, J. & Hedner, T. (1990) Local effects of substance P on respiratory regulation in the rat medulla oblongata. *J. Appl. Physiol.*, 68, 693-699. OK

De Felipe, C., Herrero, J.F., O'Brien, J.A., Palmer, J.A., Doyle, C.A., Smith, A.J., Laird, M.A., Belmonte, C., Cervero, F. & Hunt, S.P. (1998) Altered nociception, analgesia and aggression in mice lacking the receptor for substance P. *Nature*, 392, 394-397. OK

De Sanctis, G.T., Green, F.H., Jiang, X., King, M. & Remmers, J.E. (1994) Ventilatory response to hypoxia in rats pretreated with nonpeptide NK1 receptor antagonist CP-96,345. *J. Appl. Physiol.*, 76, 1528-1532.

Grasemann, H., Lu, B., Jiao, A., Boudreau, J., Gérard, N.P. & De Sanctis, G.T. (1999) Targeted deletion of the neutral endopeptidase gene alters ventilatory response to acute hypoxia in mice. *J. Appl. Physiol.*, 87, 1266-1271.

Gray, P.A., Rekling, J.C., Bocchiaro, C.M. & Feldman, J.L. (1999) Modulation of respiratory frequency by peptidergic input to rhythmogenic neurons in the pre-Bötzinger complex. *Science*, 286, 1566-1568.

Gray, P.A., Janczewski, W.A., Mellen, N., McCrimmon, D.R. & Feldman, J.L. (2001) Normal breathing requires pre-Bötzinger complex neurokinin-1 receptor-expressing neurons. *Nat. Neurosci.*, 4, 927-930.

Hedner, J., Hedner, T., Wessberg, P. & Jonason, J. (1984) Interaction of substance P with the respiratory control system in the rat. *J. Pharm. Exp. Ther.*, 228, 196-201.

Hilaire, G. & Duron, B. (1999) Maturation of the mammalian respiratory system. *Physiol. Rev.*, 79, 325-360.

Koshiya, N. & Smith, J.C. (1999) Neuronal pacemaker for breathing visualized in vitro. *Nature*, 400, 360-363.

Liebstein, A.G., Dermietzel, R., Willenberg, I.M. & Pauschert, R. (1985) Mapping of differents neuropeptides in the lower brainstem of the rat with special reference to the ventral surface. *J. Autonom. Nerv. Syst.*, 14, 299-313.

Lindefors, N., Yamamoto, Y., Pantaleo, T., Lagercrantz, H., Brodin, E. & Ungerstedt, U. (1986) *In vivo* release of substance P in the nucleus tractus solitarii increases during hypoxia. *Neurosci. Lett.*, 69, 94-97.

Lipski, J., McAllen, R.M. & Spyer, K.M.. (1977) The carotid chemoreceptor input to the

respiratory neurones of the nucleus of tractus solitarus. *J. Physiol.*, 269, 797-810.

Mantyh, P.W., Gates, T., Mantyh, C.R. & Maggio, J.E. (1989) Autoradiographic localization and characterization of tachykinin receptor binding sites in the rat brain and peripheral tissues. *J. Neurosci.*, 9, 258-279.

Monteau, R. & Hilaire, G. (1991) Spinal respiratory motoneurons. *Prog. Neurobiol.*, 37, 83-144.

Monteau, R., Ptak, K., Broquère, N. & Hilaire, G. (1996) Tachykinins and central respiratory activity: an *in vitro* study on the newborn rat. *Eur. J. Pharmacol.*, 314, 41-50.

Ptak, K., Di Pasquale, E. & Monteau, R. (1999) Substance P and central respiratory activity: a comparative *in vitro* study on foetal and newborn rats. *Dev. Brain Res.*, 114, 217-227.

Ptak, K., Konrad, M., Di Pasquale, E., Tell, F., Hilaire, G. & Monteau, R. (2000a) Cellular and synaptic effect of substance P on neonatal phrenic motoneurones. *Eur. J. Neurosci.*, 12:1-13.

Ptak, K., Hunt, S.P. & Monteau, R. (2000b) Substance P and central respiratory activity: a comparative *in vitro* study in $NK_1$ receptor knockout and wild-type mice. *Eur. J. Physiol.*, 440, 446-451.

Quirion, R. & Dam, T.V. (1986) Ontogeny of substance P receptor binding sites in rat brain. *J. Neurosci.*, 6, 2187-2199.

Smith, J.C., Ellenberger, H.H., Ballanyi, K., Richter, D.W. & Feldman, J.L. (1991) PreBötzinger complex: a brain stem region that may generate respiratory rhythm in mammals. *Science*, 254, 726-729.

Srinivasan, M., Goiny, M., Pantaleo, T., Lagercrantz, H., Brodin, E., Runold, M. & Yamamoto, Y. (1991) Enhanced *in vivo* release of substance P in the nucleus tractus solitarii during hypoxia in the rabbit: role of peripheral inputs. *Brain Res.*, 546, 211-216.

St John, P.A., Ludwig, C.P. & Lai, J. (1997) Substance P receptor expression and cellular responses to substance P in prenatal rat spinal cord cells. *J. Recept. Signal Transduct. Res.*, 17, 569-583.

Taoka, M., Song, S.Y., Kubota, M., Minegishi, A., Yamakuni, T. & Konishi, S. (1996) Increased level of neurokinin-1 tachykinin receptor gene expression during early postnatal development of rat brain. *Neuroscience*, 74, 845-853.

Tsuchida, K., Shigemoto, R., Yokota, Y. & Nakanishi, S. (1990) Tissue distribution and quantitation of the mRNAs for three rat tachykinin receptors. *Eur. J. Biochem.*, 193, 751-757.

Wang, H., Stornetta, R.L., Rosin, D.L., Guyenet, P.G. (2001) Neurokinin-1 receptor-immunoactive neurons of the ventral respiratory group in the rat. *J. Comp. Neurol.*, 434, 128-146.

Yamamoto, Y., Onimaru, H. & Homma, I. (1992) Effect of substance P on respiratory rhythm and pre-inspiratory neurons in the ventrolateral structure of rostral medulla oblongata: an *in vivo* study. *Brain Res.*, 599, 272-276.

# Autonomic Ganglion Cells : Likely Source of Acetylcholine in the Rat Carotid Body

ESTELLE B. GAUDA*, REED COOPER and SHEREÉ M. JOHNSON[+]
*Department of Pediatrics, Johns Hopkins Medical Institutions, 600 N. Wolfe Street, Baltimore, Maryland, USA 21287; [+]Department of Physiology and Biophysics, College of Medicine, Howard University 520 "W" Street, N.W., Washington, DC 20059*

## 1. INTRODUCTION

Peripheral arterial chemoreceptors are essential to respiratory and cardiac homeostasis. Although the components of these chemoreceptors lie within a tiny structure, the carotid body, the physiological affects resulting from activation of the peripheral arterial chemoreceptors have profound effects on arousal responses and cardiorespiratory responses to hypoxia and asphyxia (Gonzalez *et al.*, 1994). In response to hypoxia, hypercapnia and acidosis the glomus cell within the arterial chemoreceptor depolarizes; intracellular calcium levels rises, and neurotransmitters are released. These neurotransmitters bind to autoreceptors on the glomus cell and postsynaptic receptors on the carotid sinus nerve. Binding of neurotransmitters to autoreceptors on glomus cells regulates further neurotransmitter release, while binding to postsynaptic receptors on chemoafferent nerve fibers results in electrical output through the carotid sinus nerve (for reviews, see Gonzalez *et al.*, 1994 ; Prabhakar 1994).

Many putative inhibitory and excitatory transmitter systems are involved in chemotransmission. Dopamine is the most abundant neurotransmitter in the carotid body, and is synthesized in the glomus cells (Verna 1997). It has been measured in homogenates of the carotid body; tyrosine hydroxylase (TH), the rate-limiting enzyme for catecholamine synthesis, immunoreactivity and mRNA have been localized to glomus cells in all animals studied to date,( for review see

*Chemoreception*, Edited by Pequignot et al.
Kluwer Academic/Plenum Publishers, New York, 2003

Gauda 2002). Dopamine inhibits chemotransmission (Bee and Pallot 1995; Iturriaga, *et al.*, 1994) (Janssen ., 1998; Tomares, *et al.*, 1994) through binding to inhibitory $D_2$-dopamine autoreceptors and postsynaptic receptors (Dinger *et al.*, 1981). Acetylcholine (ACh) has also been detected in homogenates of the carotid body of many mammalian species, and physiological and pharmacological experiments suggest that ACh might have an excitatory role in arterial chemoreception (Hellstrom 1977; Eyzaguirre *et al.*, 1965; Fitzgerald, *et al.*,2000) Even though ACh was the first substance proposed as a neurotransmitter involved in hypoxic chemosensitivity (Schweitzer 1938), the source of ACh within the carotid body is still the subject of major debate (Fitzgerald 2000); (Gauda 2002). We, thus, used in situ hybridization histochemistry (ISHH) to determine the source of mRNAs encoding choline acetyltransferase (ChAT) the rate-limiting enzyme for ACh synthesis and vesicular acetylcholine transferase (VAChT), the protein that transports ACh from the cytoplasm to synaptic vesicles.

## 2. METHODS

Tissues were removed from rat pups born on postnatal days 4 and 14 (n=7, each age) who were born spontaneously to time-dated Sprague-Dawley rats. All animals were briefly anesthetized with 3% methoxyflurane and decapitated. The bifurcation of the carotid artery with the carotid body and the nodose, petrosal, jugular (NG/PG/JG) and superior cervical ganglia, were quickly removed *en bloc*, placed in embedding media (Triangle Biomedical Sciences, Durham N.C.), and quick frozen on dry ice.The tissues were stored at $-70^0$ C until further processing for ISHH.

### 2.1 ISHH.

Tissue blocs were cut in 12μm sections on a cryostat. Sections were thaw-mounted onto gelatin-chrome, alum-subbed slides. Slide-mounted sections were then fixed in 4% paraformaldehyde, acetylated in fresh 0.25% acetic anhydride in 0.1 M triethanolamine, dehydrated in ascending series of alcohols, delipidated in chloroform, and then rehydrated in a descending series of alcohols. Slides were air dried and then stored at $-20^0$ C.

Since multiple splice variants are known to exist for both ChAT and VAChT, we used clones the contained the entire coding region of the rat ChAT (Ishii *et al.*, 1990) and VAChT (Bejanin *et al.*, 1994) genes. (These clones were kindly provided by Dr. Hidemi Misawa, Tokyo Metropolitan Institute for

Neuroscience, Tokyo, Japan). The cDNAs were subsequently subcloned into a Bluescript (Stratagene) plasmid to allow for *in vitro* transcription to generate sense and antisense ribonucleotide probes. Specificity of the sense and antisense digoxigenin labeled ribonucleotide probes have been well characterized and presented by (Ichikawa *et al.,* 1997); Ishii *et al.*, 1990). In our experiments, probes were labeled with $^{35}$S-UTP to increase the sensitivity of the probe to detect very low concentrations of mRNA in the tissue sections. Labeled probes (1.2-1.5 x $10^6$ dpm) were added to 100 µl of hybridization buffer (50% formamide, 600 mM NaCl, 300 mM NaCl, 20 mM Tris-HCl, pH 7.5, 1 mM EDTA, 10% dextran sulfate, 1X Denhardt's solution, 100 µg/ml salmon sperm DNA, 250 µg/ml yeast total RNA (Type XI), 250 µg/ml yeast tRNA, and 100 mM dithiothreitol) and then applied to slides containing 8-10 sections per slide. Prior to hybridization the sections were treated with Proteinase K (2.5 µg/ml; Fisher Biotech, Fairlawn, NJ), for 5 mins and then rinsed in phosphate buffered saline (PBS). Hybridization was performed at 55$^0$C overnight. The slides were then washed in 1X SSC (0.15 M sodium choloride/0.015 M sodium citrate, pH 7.2) at room temperature. After treatment with RNAase A (20 mg/ml), slides were washed at 60$^0$C in 0.2XSSC, rinsed in deionized water and air dried. Slides were then dipped in Kodak photographic emulsion, dried and exposed in the dark at -20$^0$C for 8-10 weeks. After exposure, the slides were thawed, developed with Dektol (Kodak, NY), fixed in Kodak Fixer, rinsed and counterstained with thionin and coverslips applied with Permount.

To verify the specificity of the ribonucleotide probes by ISHH, rat coronal brain sections (Bregma 0.70, Paxinos and Watson) were hybridized, exposed and developed simultaneously with the experimental slides. Uniformly these control slides demonstrated the known patterns of expression in striatopallidal neurons for ChAT and VAChT mRNA and protein (Ichikawa *et al.,* 1997 ; Ishi, et al., 1990; Hohmann and Herkenham, 2000). In addition, the pattern of ChAT and VAChT gene expression differed for the carotid body, (NG/PG/JG) and superior cervical ganglia, further demonstrating probe specificity.

## 2.2 Data analysis

Comparisons were made between slides processed, hybridized, exposed and developed in parallel. For this report, qualitative assessment of the presence or absence of silver grains over cells in the carotid body and ganglia in addition to isolated autonomic ganglia in the nerve fibers and on the periphery of the carotid body was performed. In addition, tissue sections were visually inspected for

intensity of the silver grains and reported as less or greater between the two age groups.

## 3. RESULTS

The regional distribution of the hybridization signal for ChAT and VAChT were qualitatively the same in animals at 4 and 14 postnatal day as shown in Figure 1A and B. The signal intensity, however, was greater for VAChT than ChAT mRNA in both groups of animals in all tissues that the genes were expressed. Other than the isolated clusters of silver grains on the perimeter of the carotid body, we did not detect ChAT or VAChT mRNA expression in the carotid body of any of the tissue sections in either age group (Figures1A,B and 2A,B). ChAT and VAChT mRNA expression was commonly seen within nerve fibers throughout the tissue sections Figures 1 and 3. As seen in figure 3A,B and C, VAChT mRNA is expressed within isolated autonomic ganglion cells along the carotid sinus nerve as it approaches the carotid body and the 9$^{th}$ cranial nerve as it exists the petrosal ganglion, Figure 3C and D.

ChAT and VAChT mRNA expression was also seen in the petrosal ganglion in both age groups. VAChT mRNA expression was greater than ChAT in both groups, and the intensity of the silver grains for VAChT mRNA was greater in 4 versus 14 day animals (Figure 2B,C) (quantitative not shown). Lastly, VAChT mRNA expression was seen in few isolated cells within the superior cervical ganglion (Figure 4).

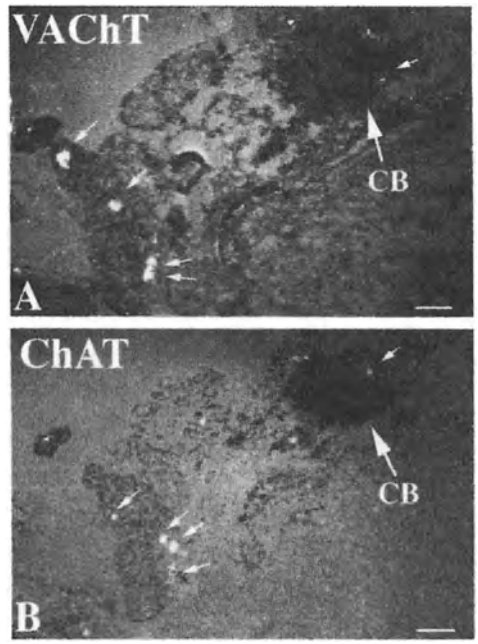


*Figure 1.* Expression of (A) VAChT and (B) ChAT mRNAs in nerve fibers and on the periphery of the carotid body (CB) in 12μm serial sections. VAChT and ChAT mRNA expression is represented by clusters of small white dots (arrows). The relative distribution of VAChT and ChAT mRNAs are the same in the serial sections of a 14 day old animal.

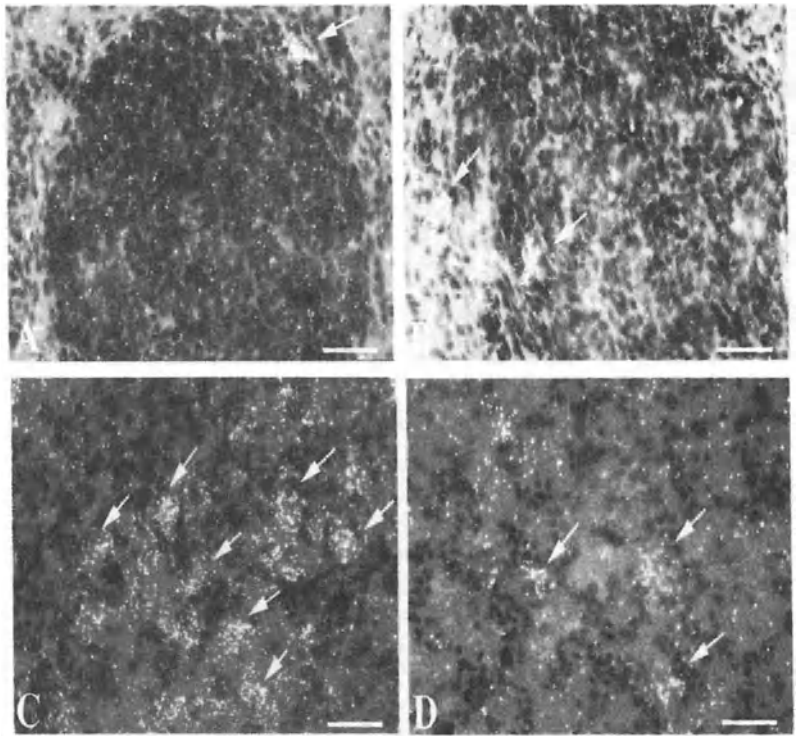


*Figure 2* .Expression of VAChT mRNA on the periphery of the carotid body (A,B) and within the perikarya of the petrosal ganglion (C,D) in 4 (A,C) and 14 (B,D) day old animals. Clusters of silver grains (white dots) represent mRNA expression (arrows) which is more abundant in the perikarya of the petrosal ganglion in the 4 day (C) than in the 14 day old animal. Scale bar is 50 μm.

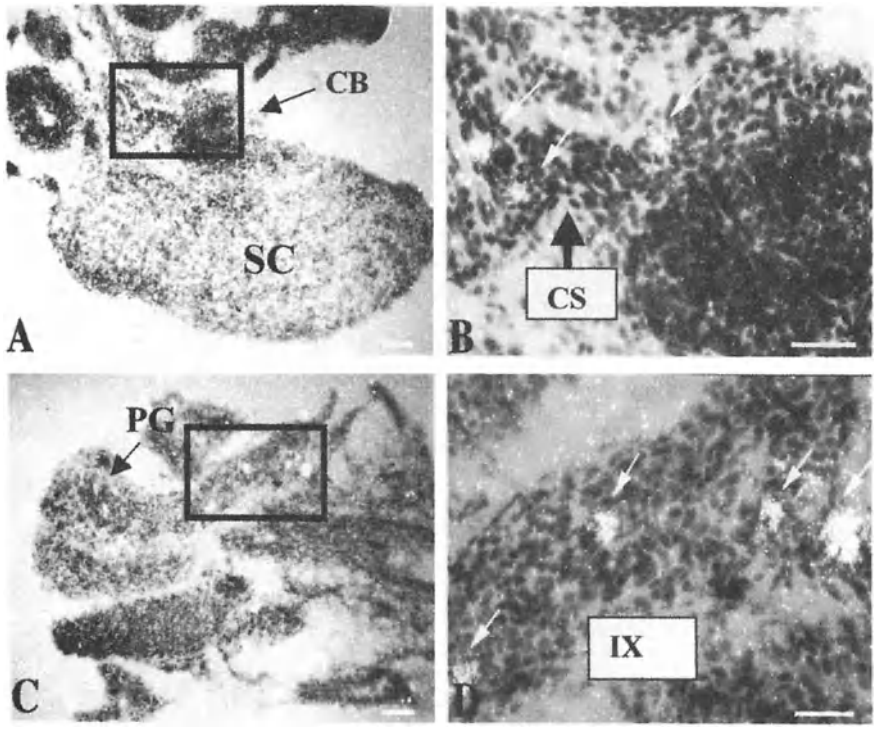


*Figure 3.* Expression of VAChT mRNAs in the carotid sinus nerve (A,B) and along the 9th cranial nerve (C,D) in a 4 day old rat. Clusters of silver grains (white dots, arrows) represent mRNA expression. B and D are high power views of insert in A and B. SCG is superior cervical ganglion, CB is carotid body, PG is petrosal ganglion, CSN is carotid sinus nerve and IX is 9th cranial nerve. Scale bar is 50 μm.

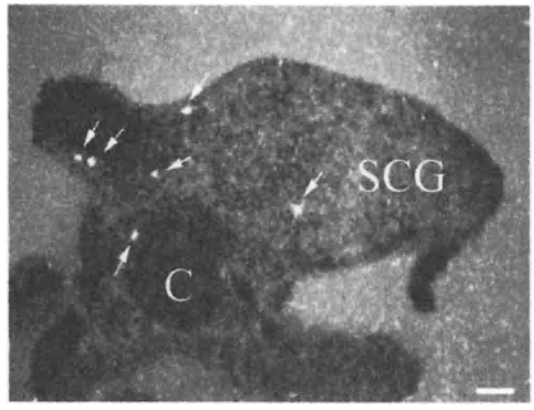


*Figure 4.* VAChT mRNA expression in superior cervical ganglion in the newborn rat. Clusters of silver grains (white dots, arrows) represent mRNA expression in minimal cells within the superior cervical ganglion (SCG). Scale bar is 50 μm.

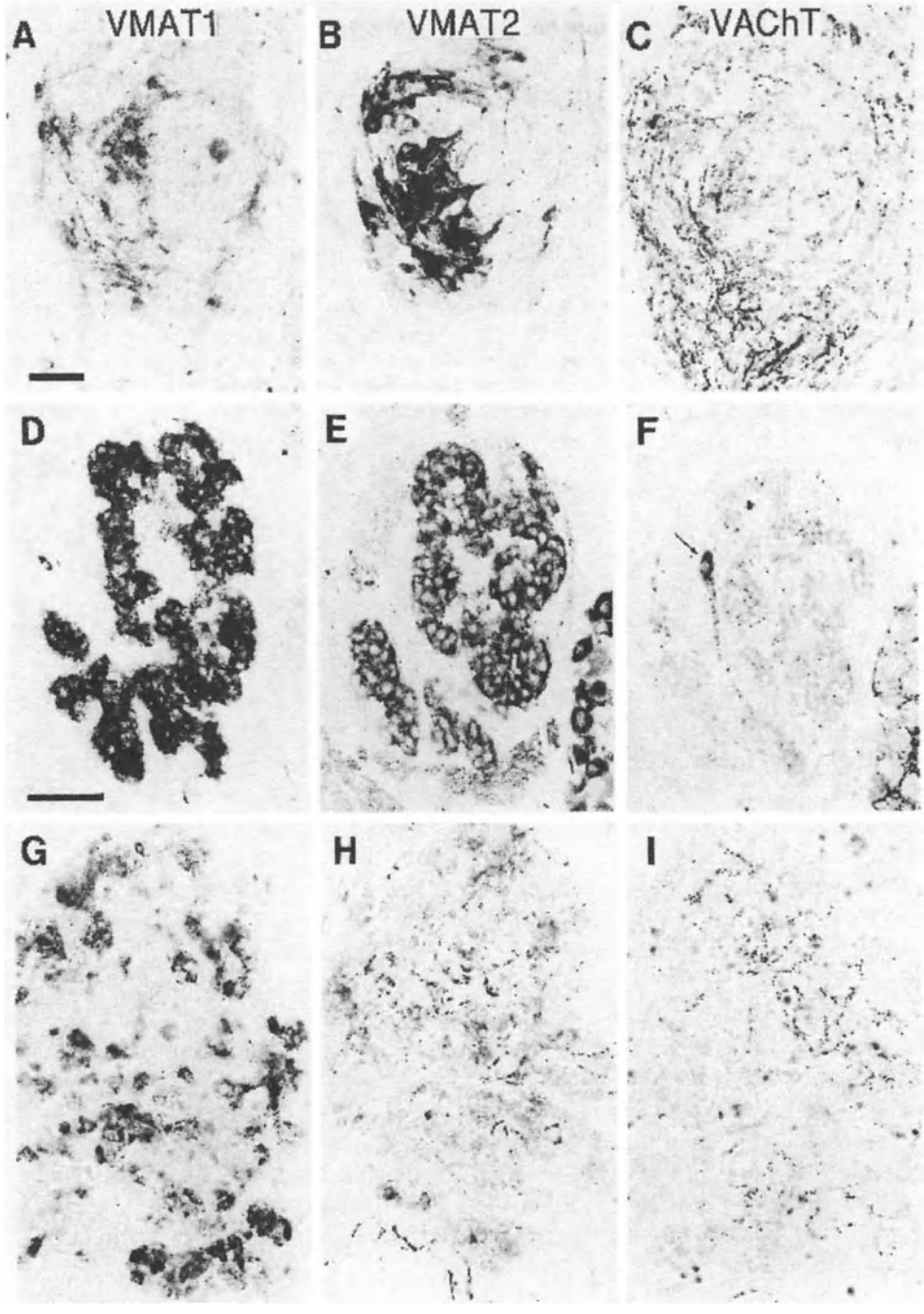
A
VMAT1
B
VMAT2
C
VAChT
D
E
F
G
H
I

*Figure 5.* VMAT1, VMAT2 and VAChT immunoreactivity in the carotid body, E16 to adult. VMAT1 (A), VMAT2 (B), and VAChT (C) immunoreactivity in E16 carotid body. VMAT1 and VMAT2 are expressed in cells of the carotid body at E16, with levels of VMAT2 being much higher than VMAT1. VAChT immunoreactivity is present in fibers which innervate the cells of the carotid body. VMAT1, VMAT2 and VAChT immunoreactivity in the P6 carotid body. At P6, relative expression of VMAT1 and VMAT2 has changed, with VMAT1 levels higher than VMAT2. Note the superior cervical ganglion (SCG) on bottom right in panels D-F, adjacent to carotid body, with ganglionic cells strongly positive for VMAT2. Note also preganglionic VAChT-positive fibers both in the carotid body and in the SCG. The arrow in F points to a VAChT positive ganglion cell at the margin of the carotid body. VMAT1 (G), VMAT2 (H) and VAChT(I) immunoreactivity in adult carotid body. In the carotid body of adult rats, difference in the relative intensity of staining for VMAT1 and VMAT2 has become pronounced. VAChT staining persists in fibers inside the carotid body. Note also varicose fibers on blood vessels in (H), which stain for VMAT2. Bar in (A) = 25 μm and applies to panels A-C; bar in D= 50 μm and applies to panels D-I. (reprinted with permission from Schütz, B., Schäfer, M. K.-H., Eiden L.E., and Eberhard Weihe. Vesicular amine transporter expression and isoform selection in developing brain, peripheral nervous system and gut. Developmental Brain Research 1998:106 181-204.)

## 4. DISCUSSION

Using ISHH with radioactive ribonucleotide probes, we have demonstrated that the definitive markers for cholinergic cells and neurons, ChAT and VAChT mRNAs, are not expressed in glomus cells of the rat carotid body but are expressed in autonomic ganglion cells on the periphery of the carotid body, in nerve fibers innervating the carotid body, and in petrosal ganglion cells. Although not quantitatively presented in this preliminary report, we also observed that 1) the level of expression of VAChT mRNA in petrosal ganglion neurons decreased with increasing maturation from 4 to 14 postnatal days, and 2) hypoxic exposure ($10\%O_2$) for 4 hours did not induce ChAT or VAChT mRNA expression in the carotid body or increase its expression in the petrosal ganglion cell bodies in either age group (data not shown).

ACh content has been measured in the homogenates of the cat carotid body (Eyzaguirre *et al.*, 1965; Fidone *et al.*, 1976). In response to hypoxia, ACh is released from the adult carotid body *in vitro* (Fitzgerald *et al.*, 1999). Although ACh content and release can be measured in multicellular tissues, localization of cells and neurons that synthesize ACh has been more difficult. ChAT enzymatic activity is a marker of cholinergic neurons. However, ChAT is difficult to detect in tissues; it exist in small amounts and is an unstable enzyme and is also measured in homogenates of tissues. Thus, localization of the protein and mRNA for both VAChT and ChAT by immunohistochemistry or ISHH, respectively, has become the methods of chose for identification of cholinergic

neurons (Oda 1999). Expression of both genes and proteins are required for the acquisition and the maintenance of the cholinergic phenotype (Rand and Russell. 1984); (Weihe *et al.,* 1998) ChAT and VAChT proteins are synthesized in the perikaryon of cholinergic neurons, however the proteins can be transported to distal neuronal processes and varicosities (Barbosa *et al.*, 2002); Frizell et al., 1970). Because the carotid body is a small, compact and multicellular, it is difficult to discern immunoreactivity of varicosities surrounding glomus cells from that of immunoreactivity within glomus cell using light microscopy. We, thus, used ISHH which allowed us to unequivocally determine specific cellular location of ChAT and VAChT mRNAs within the peripheral arterial chemoreceptors.

VAChT and ChAT genes are unique; both genes share a common gene locus, with the first intron of the ChAT gene containing the open reading frame encoding VAChT [for review see (Oda 1999)]. In addition, multiple splice variants exist for both genes yet, a single form of ChAT and VAChT is translated in rodents (Oda 1999). The cDNAs that were used in our study to generate full-length ribonucleotide probes contained the base sequence for the entire open reading frame for both ChAT and VAChT genes. Thus, the probes should have hybridized with all known splice variants of the ChAT and VAChT mRNAs that have been so far identified. We think that it is highly unlikely that the glomus cells within the carotid body would contain a unique and different unidentified splice variant of these two genes that would differ from the mRNAs detected in immediately adjacent autonomic ganglion cells and within the perikarya of the petrosal ganglion. We cannot, however, exclude the possibility that the level of gene expression within the glomus cells was below the level of detection. Yet, our findings corroborate those of Schütz *et al* (1998) who demonstrated with immunohistochemistry that nerve fibers within the rat carotid body and adjacent autonomic ganglion cells were immunoreactive for VAChT and not glomus cells within the carotid body. The most intense immunostaining for VAChT was observed during embryonic development with a reduction in intensity of the immunoreactivity with postnatal maturation (Schütz *et al.,* 1998). Although glomus cells were not immunoreactive for VChAT, glomus cells were intensely immunoreactive for vesicular monamine transporters VMAT1 and VMAT2 (transporter for catecholamines)( Figure 5).

In summary, ACh is present in the carotid body of several animal species. In an attempt to better characterize the source of ACh within the carotid body, we exploited the specificity of ISHH to detect mRNAs for ChAT and VAChT. Our data strongly support that the source of ACh detected in homogenates of the rat carotid body is not from glomus cells but more likely from autonomic ganglion

cells or neuronal varicosities within the carotid body. Detailed description of the histology of autonomic ganglion cells in peripheral arterial chemoreceptors has been provided by McDonald et al (McDonald 1983). We speculate that our findings can be extrapolated to other mammalian species, specifically the cat, since autonomic ganglia detected in nerve and on the periphery of the carotid body has also been extensively described by De Castro in 1926 (see (McDonald 1983) for this species. Although our data *do not support that ACh is synthesized and released from glomus* cells, the extensive cholinergic innervation and presence of nicotinic and muscarinic acetylcholine receptors within the carotid body (for review see (Fitzgerald 2000), suggest that ACh is likely involved in modulation of hypoxic chemosensitivity by a mechanisms that has not to date been elucidated.

## ACKNOWLEDGEMENTS

We would like to thank Dr. Gabrielle McLemore for her careful critique of the manuscript. This work was supported by NIH, RO1DA13940.

## REFERENCES

Barbosa, J. Jr., Ferreira, L.T., Martins-Silva, C., Santos, M.S., Torres, G.E., Caron, M.G., Gomez, M.V., Ferguson, S.S., Prado, M.A., and Prado, V.F., 2002, Trafficking of the vesicular acetylcholine transporter in SN56 cells: a dynamin-sensitive step and interaction with the AP-2 adaptor complex. *J.Neurochem. 82:* 1221-1228.

Bee, D., and Pallot, D.J., 1995, Acute hypoxic ventilation, carotid body cell division, and dopamine content during early hypoxia in rats. *J Appl Physiol 79:* 1504-1511.

Bejanin, S., Cervini, R., Mallet, J., and Berrard, S., 1994, A unique gene organization for two cholinergic markers, choline acetyltransferase and a putative vesicular transporter of acetylcholine. *J.Biol.Chem. 269:* 21944-21947.

Dinger, B., Gonzalez, C., Yoshizaki, K., and Fidone, S.J., 1981, [3H] Spiroperidol binding in normal and denervated carotid bodies. *Neuroscience Letters 21:* 51-55.

Eyzaguirre, C., Koyano, H., and Taylor, J.R., 1965, Presence of acetylcholine and transmitter release from carotid body chemoreceptors. *J.Physiol 178:* 463-476.

Fidone, S.J., Weintraub, S.T., and Stavinoha, W.B., 1976, Acetylcholine content of normal and denervated cat carotid bodies measured by pyrolysis gas chromatography/mass fragmentometry. *J.Neurochem. 26:* 1047-1049.

Fitzgerald, R.S., 2000, Oxygen and carotid body chemotransduction: the cholinergic hypothesis - a brief history and new evaluation. *Respir.Physiol 120:* 89-104.

Fitzgerald, R.S., Shirahata, M., and Wang, H.Y., 1999, Acetylcholine release from cat carotid bodies. *Brain Res. 841:* 53-61.

Fitzgerald, R.S., Shirahata, M., and Wang, H.Y., 2000, Acetylcholine is released from in vitro cat carotid bodies during hypoxic stimulation. *Advances in Experimental Medecine and Biology 475:* 485-494.

Frizell, M., Hasselgren, P.O., and Sjostrand, J., 1970, Axoplasmic transport of acetylcholinesterase and choline acetyltransferase in the vagus and hypoglossal nerve of the rabbit. *Exp.Brain Res. 10:* 526-531.

Gauda, E.B., 2002, Gene expression in peripheral arterial chemoreceptors. *Microsc.Res.Tech. 59:* 153-167.

Gonzalez, C., Dinger, B.G., and Fidone, S.J., 1994, Mechanisms of carotid body chemoreception. In *Regulation of Breathing* (J. A. Dempsey & A. I. Pack, eds.), Marcel Dekker, Inc., pp. 391-470.

Hellstrom, S., 1977, Putative neurotransmitters in the carotid body mass-fragmentographic studies. *Adv.in Biochem.Psychopharmacol. 16:* 257-263.

Hohmann, A.G., and Herkenham , M., 2000, Localization of cannabinoid CB(1) receptor mRNA in neuronal subpopulations of rat striatum: a double-label in situ hybridization study. *Synapse 37:* 71-80.

Ichikawa, T., Ajiki, K., Matsuura, J., and Misawa, H., 1997, Localization of two cholinergic markers, choline acetyltransferase and vesicular acetylcholine transporter in the central nervous system of the rat: in situ hybridization histochemistry and immunohistochemistry. *J. Chem.Neuroanat. 13:* 23-39.

Ishii, K., Oda, Y., Ichikawa, T., and Deguchi, T., 1990, Complementary DNA's for choline acetyltransferase from spinal cords of rat and mouse: nucleotide sequences, expression in mammalian cells, and in situ hybridization. *Molecular Brain Research 7:* 151-159.

Iturriaga, R., Larraine, C., and Zappata, P., 1994, Effects of dopaminergic blockade upon carotid chemosensory activity and its hypoxic-induced excitation. *Brain Res 66B:* 145-154.

Janssen, P.L., O'Halloran, K.D., Pizarro, J., Dwinell, M.R., and Bisgard, G.E., 1998, Carotid body dopaminergic mechanisms are functional after acclimatization to hypoxia in goats. *Respir.Physiol 111:* 25-32.

McDonald, D.M., 1983, Morphology of the rat carotid sinus nerve. I. Course, connections, dimensions and ultrastructure. *J.Neurocytol. 12:* 345-372.

Oda, Y., 1999, Choline acetyltransferase: the structure, distribution and pathologic changes in the central nervous system. *Pathol.Int. 49:* 921-937.

Prabhakar, N.R., 1994, Neurotransmitters in the carotid body. *Adv. Exp. Med. Biol. 360:* 57-69.

Rand, J.B., and Russell, R.L., 1984, Choline acetyltransferase-deficient mutants of the nematode Caenorhabditis elegans. *Genetics 106:* 227-248.

Schütz, Schäfer, M.K., Eiden, L.E., and Weihe, E., 1998, Vesicular amine transporter expression and isoform selection in developing brain, peripheral nervous system and gut. *Brain Res.Dev.Brain Res. 106:* 181-204.

Schweitzer A., 1938, Action of prostigmin and acetycholine on respiration. *Quart J Exp Physiol 28:* 33-47.

Tomares, S. M., Bamford, O.S., Sterni, L.M., Fitzgerald, R.S., and Carroll, J.L., 1994, Effects of domperidone on neonatal and adult carotid chemoreceptors in the cat. *J.Appl.Physiol 77:* 1274-1280.

Verna , A., 1997, The Mammalian Carotid Body: Morphological Data. In *The Carotid Body Chemoreceptors* (C. Gonzalez, ed.), Landes Bioscience Austin, Texas, U.S.A., pp. 1-29.

Weihe, E., Schäfer, M.K., Schütz, B., Anlauf, M., Depboylu, C., Brett, C., Chen, L., and Eiden, L.E., 1998, From the cholinergic gene locus to the cholinergic neuron. *J.Physiol Paris 92:* 385-388.

# Effects of Perinatal Hyperoxia on Carotid Body Chemoreceptor Activity *in Vitro*

PRIETO-LLORET J, CACERES AI, RIGUAL R, OBESO ANA, ROCHER A, BUSTAMANTE R, CASTAÑEDA J*, LÓPEZ-LÓPEZ JR, PEREZ-GARCIA T, AGAPITO T and GONZÁLEZ CONSTANCIO.

*Dept. de Bioquímica y Biología Molecular y Fisiología/(IBGM). Universidad de Valladolid /(CSIC). Facultad de Medicina. Valladolid. Spain. *Intensive Care Unit. University Hospital of Valladolid. Valladolid. Spain.*

## 1. INTRODUCTION

The arterial carotid body (CB) chemoreceptors are highly vascularized sensory organs located in the proximity of the carotid artery bifurcation and formed by clusters of parenchymal cells. The cell clusters are penetrated by sensory fibers of the carotid sinus nerve (CSN) which form synapses with the parenchymal chemoreceptor cells. Functionally, the CBs are the origin of a regulatory loop devoted to restore $O_2$ availability in situations of hypoxia (Richalet, 1997). To achieve this function chemoreceptor cells detect blood $PO_2$, being activated by hypoxia. Hypoxia increases the rate of the release of neurotransmitters from the cells augmenting the action potential frequency in the CSN; this increased activity stimulates the brainstem regulators of respiration and hyperventilation and increased arterial blood $PO_2$ ensue (Gonzalez et al., 1994).

The functional maturation of the CB chemoreceptors and of the neuronal circuits responsible for the hypoxic hyperventilation is, as in other sensory systems (e.g., visual system, Hubel and Wiesel, 1977), greatly modified by the specific stimulation in the perinatal period. In fetal or neonatal animals the CSN sensory fibers only become activated at $PO_2$ of ≈20-25 mmHg, but in the postnatal period, associated to the increase in arterial $PO_2$ of the extrauterine life, there is a resetting of the threshold to 70-75 mmHg for hypoxic response in the CSN (and for hypoxic hyperventilation; Donnelly, 1997). This resetting of the hypoxic responses is also noticeable at the level of $Ca^{2+}$ rise (Washicko *et al.*, 1999) and catecholamines (CA) release (Rigual *et al.*, 2000) produced by hypoxia. However in animals born and reared in a hypoxic ambience mimicking the intrauterine life the resetting of the hypoxic threshold does not occur (Eden and Hanson, 1987; Sterni *et al.*, 1999). Perinatal hyperoxia has also profound

*Chemoreception*, Edited by Pequignot et al.
Kluwer Academic/Plenum Publishers, New York, 2003

effects in the CB function: exposure of rats to hyperoxia (30-60% $O_2$) the last week of intrauterine life and the initial 15-30 days of postnatal life produces a permanent reduction in the CSN response to respond to hypoxia with normal or impaired hypoxic hyperventilation and a hypoplasia of the CB (Eden and Hanson, 1986; Ling *et al.*, 1996, 1997a,b; Erickson *et al.*, 1998; Fuller *et al.*, 2001, 2002). The functional deficit seems to be located in the CB itself, as electrical stimulation of the central stump of the sectioned CSN elicits an increase in phrenic activity identical than in control animals (Ling *et al.*, 1997a).

The aim of the present study was to determine the responsiveness of chemoreceptor cells to hypoxia, as measured by the release of CA (Fidone *et al.*, 1982), and to correlate this response with that elicited in the action frequency of the CSN in rats perinatally exposed to a hyperoxic atmosphere.

## 2. MATERIAL AND METHODS

**2.1 General.** The experiments were performed in Sprague-Dawley rats of both sexes born and reared in the atmospheres shown in Figure 1. Mothers of experimental animals were individually caged and kept with their litters in a hyperoxic atmosphere (Figure 1A) achieved by continuously flushing a glass chamber with the desired gas mixture. The composition of the gas mixture was verified at the outlet of the chamber where a continuous gas flow was maintained to secure washing out of $CO_2$, heat and vapor water; temperature was stable at 22-25 °C. The chamber was opened every 4 days to clean the animals and to replace food and water. Control animals were maintained in a normal atmosphere as shown in Figure 1B.

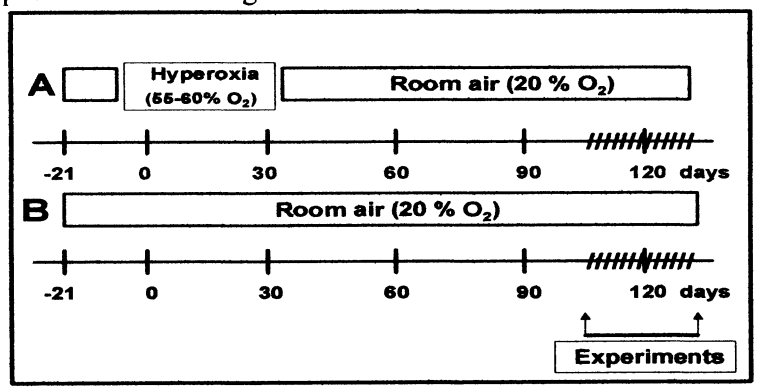


*Figure 1.* Schema showing the time course of the treatment of the animals used for the experiments. A, experimental animals. B, control animals.

**2.2. Surgical procedures.** Rats were anesthetized with $Na^+$-pentobarbital (60mg/kg, i.p.) and after an incision in the anterior midline of the neck the carotid arteries were dissected past the carotid bifurcation. A block of tissue including the carotid bifurcation and the glossopharyngeal nerve was removed and placed in a lucite chamber filled with ice-cold/100% $O_2$-equilibrated Tyrode (in mM: 140 NaCl, 5 KCl, 2 $CaCl_2$, 1 $MgCl_2$, 10 HEPES and 5 glucose) to dissect free of surrounding tissue the CB attached to the CSN until its entrance in the glossopharyngeal nerve. After a mild controlled digestion (collagenase I, 1 mg/ml; trypsin, 0.1 mg/ml; 10 min; 37 °C), the preparation was transferred to a perfusion chamber mounted on the stage of an inverted microscope and superfused with bicarbonate/$CO_2$-buffered saline (in mM: 120 NaCl, 3 KCl, 2 $CaCl_2$, 1 $Na_2HPO_4$, 1 $MgSO_4$, 24 $NaHCO_3$ and 10 glucose) at 35°C. During the entire experimental procedure all measures were taken to ensure the animals did not suffer distress at any time. The protocols were approved by the Institutional Animal Care and Use Committee of the University of Valladolid.

**2.3. Recording of the activity in the CSN.** Single or pauci fiber recordings were made with a suction electrode in small filaments dissected from the CSN. The pipette potential was amplified 1000x (Neurolog Digitimer, Hertfordshire, England), displayed on an oscilloscope and stored on computer (Datasponge, WPI, Berlin). Electrical activity was identified as chemoreceptor based on the spontaneous generation of action potentials at irregular intervals and confirmed by an increase in activity on switching the normoxic perfusate (20% $O_2$/5% $CO_2$, balance $N_2$) to an intensely hypoxic one equilibrated with 0% $O_2$, 5% $CO_2$, balance $N_2$. Neural activity was converted to logic pulses which were summed each second and converted to a voltage proportional to the sum. Chamber $PO_2$ was recorded with an electrode polarized to –0.8V against a Ag-AgCl ground electrode, and stored on the computer along with raw nerve signal.

**2.4. Measurement of CA secretion.** Free tissue CA were measured using a carbon fiber electrode inserted into the CB tissue as previously described (Rigual et al., 2000). The electrode was a 5μm carbon fiber insulated (but the tip) with a polyethylene tube (ProCFE, Dagan Instruments, Minneapolis, MN). The electrode was attached to an EI-400 potentiostat (Ensman, Bloomington,IN) with the potential fixed at +200mV, which is above the oxidation potential for dopamine. Calibration was performed by exposing the electrode to superfusates containing 0-5 μM dopamine.

**2.5. Data analysis and statistics.** The activity of the CSN fibers and the levels of free tissue catecholamine were measured in normoxia and in hypoxia. Electrical activity in CSN was determined as the difference between peak hypoxic activity and baseline activity measured prior to the presentation of the stimulus. The correspondent deltas (peak - basal activity) was normalized to 100% in control animals, and in the chronically hyperoxic animals expressed as the correspondent percentage. The release of CA was similarly evaluated. Data were compared using Student's unpaired t-test. Significance level was established at $p<0.05$.

## 3. RESULTS

Figure 2 shows sample records of CSN activity and release of CA in preparations obtained from control (A and C) and from hyperoxic animals (B and D) during superfusion with normoxic and hypoxic solutions. Figures 2A and 2 B show histograms of the instantaneous frequency in the CSN in response to

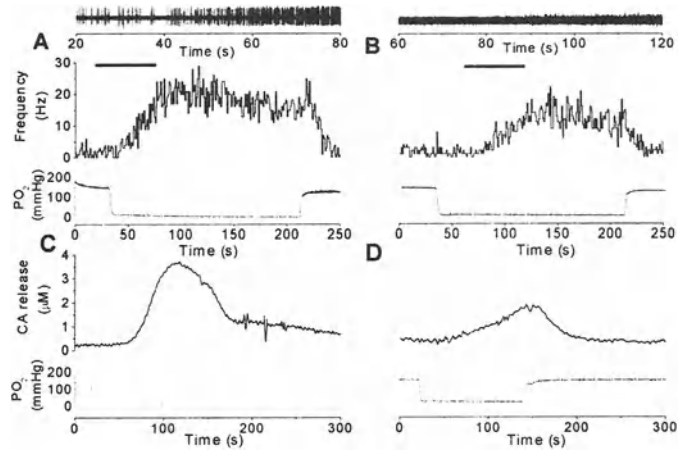


*Figure 2.* Sample records of CSN responses to hypoxia in a CB/CSN preparation obtained from a control (A) and a hyperoxic animal (B) with the correspondent neurograms shown at their top. In (C) and (D) are shown CA release responses to hypoxia in a CBs obtained, respectively from a control and a hyperoxic animal.

a decrease in the $PO_2$ of the perfusing solution. From these recordings it is evident that with a comparable level of basal activity, the hypoxic response is stronger in the preparation obtained from the control (A) than from the

hyperoxic animal (B); it is also evident that the onset of the response is faster in the control than in the hyperoxic preparation. On top of the histograms are presented sample neurograms recorded during the periods marked by the horizontal bars in A and B; these neurograms are shown to substantiate that the recordings of neural activity in the CSN obtained from hyperoxic animals is more difficult than in the preparations from control animals, an observation that correlates with the previously described degeneration of chemosensory fibers in the CSN after even only one week of perinatal hyperoxia (Erickson et al., 1998). Figures 2C and 2D show voltammograms for CA obtained in CB preparations from a control (C) and a hyperoxic (D) rat; the CA release response is nearly double in the CB obtained from control than from the hyperoxic animal.

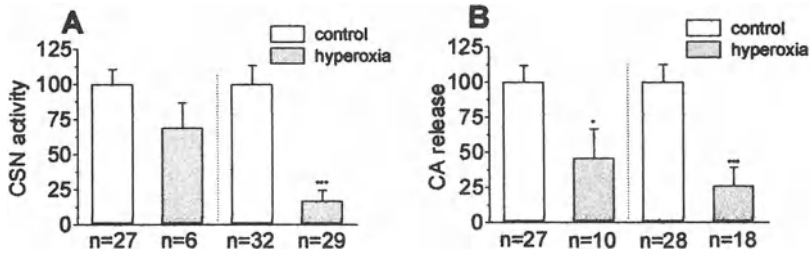


**Figure 3.** *Comparison of the CSN and the CA release responses to intense hypoxia in preparations from control and from hyperoxic animals.*

Figure 3A and 3B show, respectively, mean CSN and CA release responses to hypoxia in preparations from control and hyperoxic animals. When we consider the successful preparations, i.e., those in which we were able to record action potentials in the CSN (n = 27 and 6 in control and hyperoxic animals, respectively), the responses in the hyperoxic group represented 69.4 ± 17.5% of the control responses (100.0 ± 10.7%) and the differences were not statistically significant. However, when we include all the preparations (32 controls, 27 responders + 5 non-responders; 29 hyperoxic, 6 responders + 23 non-responders) the mean response in the hyperoxic group represented only 17.0 ± 7.5% of that found in the control group (100.0 ± 13.1) and the differences were highly significant ($p < 0.001$). The difference observed between control and hyperoxic animals computed in the latter manner is nearly identical to that found by Ling et al. (1997) for an asphyctic test. The mean results obtained in the release of CA calculated in the same manner show a difference in the response

that is already significant when comparing the responder preparations (100.0 ± 11.8% (n = 27; control) *vs,* 46.0 ± 20.4% (n= 10; hyperoxic) ($p < 0.05$), and becomes highly significant when all the preparations in each group are included (100.0 ± 12.3% (n = 28) in controls *vs,* 26.5 ± 12.8% (n = 18) in hyperoxic animals; $p < 0.001$).

## 4. DISCUSSION

The present results confirm previous findings by showing that altering the ambient $PO_2$ (i.e., the level of stimulation of the CB) in the perinatal period alters profoundly the functionality of the CB chemoreceptors. Interestingly enough, in the case of the CB chemoreceptors the alteration affects the sensory organ itself while in the visual system, for example, the retina seems to function normally after perinatal visual deprivation, being alterations in the central connectivity of visual pathways the responsible for the loss of functionality of the visual system (Hubel and Wiesel, 1977). Our findings confirm and extend previous data of the group of Wisconsin (e.g. Ling et al., 1997b). Thus, it is evident that as an entire population the rats born and reared for the first month of age in a hyperoxic atmosphere exhibit a hypoxic response at the level of the CSN activity that is significantly smaller, representing only about 17% of that seen in the control group. However, if the data on the electrical activity of the CSN are further analyzed they evidence that the perinatal hyperoxic treatment produces different degrees of functional damage in the different members of the population in spite of an identical perinatal treatment. Some animals, represented by the responder group (i.e., 6 out of 29 animals or 21%), exhibit an attenuated response to hypoxia but sensory units in their CB-CSN are functional, while most of the animals (23 out of 29) are non-responders. The quality of an animal as non-responder, seems to be due to two different reasons: truly non-responder animals and animals in which we were unable of registering the action potentials in the CSN; there are no means to decide which percentage of the non-responders belong to each category.

Comparable results were obtained when recording the release of CA. However considering the significantly greater percentage of responder animals (10 out of 18; i.e., 55%) in comparison with the data on the electrical activity in the CSN (21%) it would appear that, in spite of the reduced size of the CB in the hyperoxic animals (Erickson et al., 1998), the sensitivity and the easiness of the voltammetric technique are responsible for the difference. This interpretation seems to be supported by a smaller number of failures in the recording of the

release of CA (3.5%) than the CSN response (15.6%) in control animals. When considering the entire group, the comparable level of reduction of the postsynaptic (i.e., action potential frequency in the CSN) and of the presynaptic response (i.e., the release of CA from chemoreceptor cells) would indicate that communication between chemoreceptor cells and the nerve endings of the CSN (i.e., the synaptic transmission between the two elements) is not altered. It would appear that either the level of the neurotransmitters in chemoreceptor cells, or the ability of the cells themselves to detect hypoxia or the mechanisms coupling the detection of hypoxia to the exocytotic machinery have been permanently altered by the perinatal hyperoxic treatment, but further experiments are needed to decide among these possibilities.

## ACKNOWLEDGEMENTS

Supported by Grant from the FISs (01/0728) to R. Rigual, DGICYT Grants BFI2001-1713 to C Gonzalez and BFI2001-1691 to JR Lopez-Lopez and RED RESPIRA (FISS).

## REFERENCES

Donnelly, DF. (1997) Function of the carotid body intra-utero and in the postnatal period. In: *The Carotid Body Chemoreceptors*, edited by C. Gonzalez. Heidelberg, Germany. Springer-Verlag pp. 193-202.

Eden, GJ and Hanson, MA (1986). Effects of hyperoxia from birth on the carotid chemoreceptor and ventilatory responses of rats to acute hypoxia. *J. Physiol.* 374: 24P.

Eden, GJ, and Hanson, MA. (1987). Effects of chronic hypoxia from birth on ventilatory response to acute hypoxia in the newborn rat. *J. Physiol.* 392: 11-19.

Erickson JT, Mayer, C, Jawa, A, Olson EB, Jr, Vidruk, EH, Mitchell, GS and Katz, DM. (1998). Chemoafferent degeneration and carotid body hypoplasia following chronic hyperoxia in newborn rats. *J. Physiol.* 509: 519-526.

Fidone S, Gonzalez C, Yoshizaki K. (1982). Effects of low oxygen on the release of dopamine from the rabbit carotid body in vitro. *J Physiol.* 333:93-110.

Fuller DD, Bavis RW, Vidruk EH, Wang ZY, Olson EB Jr, Bisgard GE, Mitchell GS. (2002) Life-long impairment of hypoxic phrenic responses in rats following 1 month of developmental hyperoxia. *J Physiol.* 538:947-955.

Fuller DD, Wang ZY, Ling L, Olson EB, Bisgard GE, Mitchell GS. (2001) Induced recovery of hypoxic phrenic responses in adult rats exposed to hyperoxia for the first month of life. *J Physiol.* 536:917-926.

Gonzalez, C, Almaraz, L, Obeso, A and Rigual, R. (1994) Carotid body chemoreceptors: from natural stimuli to sensory discharges. *Physiol. Rev.* 74:829-898.

Hubel DH, Wiesel TN. (1977) Ferrier lecture. Functional architecture of macaque monkey visual cortex. *Proc R Soc Lond B Biol Sci.* 198:1-59.

Ling, L, Olson, EB, Vidruk, EH and Mitchell, GS. (1996) Attenuation of the hypoxic ventilatory response in adult rats following one month of perinatal hyperoxia. *J. Physiol.* 495: 561-571.

Ling L, Olson EB Jr, Vidruk EH, Mitchell GS. (1997a). Integrated phrenic responses to carotid afferent stimulation in adult rats following perinatal hyperoxia. *J Physiol.* 500: 787-796.

Ling, L, Olson, EB, Vidruk, EH and Mitchell, GS. (1997b) Developmental plasticity of the hypoxic ventilatory response. *Respiration Physiol.* 110: 261-268.

Richalet JP (1997) Oxygen sensors in the organism: examples of regulation under altitude hypoxia in mammals. *Comp. Biochem. Physiol. A Physiol.* 118: 9-14.

Rigual R, Almaraz L, Gonzalez C, and Donnelly DF (2000). Developmental changes in chemoreceptor nerve activity and catecholamine secretion in rabbit carotid body: possible role of $Na^+$ and $Ca^{2+}$ currents. *Pflügers Arch. Eur. J. Physiol.* 439: 463-470.

Sterni LM, Bamford OS, Wasicko MJ, Carroll JL. (1999). Chronic hypoxia abolished the postnatal increase in carotid body type I cell sensitivity to hypoxia. *Am. J. Physiol.* 277: L645-L652, 1999.

Washicko MJ, Sterni, LM, Bamford OS, Montrose SM and Carroll JL (1999). Resetting of postnatal maturation of oxygen chemosensitivity in rat carotid chemoreceptor cells. *J. Physiol.* 514: 493-503.

# Prenatal Hypoxia and Early Postnatal Maturation of the Chemoafferent Pathway

JULIE PEYRONNET, JEAN-CHRISTOPHE ROUX, DAVID PERRIN, JEAN-MARC PEQUIGNOT, HUGO LAGERCRANTZ*and YVETTE DALMAZ

*Laboratoire de Physiologie des Régulations Métaboliques, Cellulaires et Moléculaires, UMR CNRS 5123, Faculté de Médecine, 8 avenue Rockefeller, 69 373 Lyon cedex 08, France, *Department of Woman and Child Health, Karolinska Institute, S 171766 Stockholm, Sweden*

## 1. INTRODUCTION

Perinatal hypoxia can cause various short-term, long-term or life-spanning sequelae. Early postnatal hypoxic exposure within the first days of life after birth induces adverse and long-term effects on postnatal growth (Soulier *et al.* 1997; Peyronnet *et al.* 2000), neurobehavioural development (Nyakas *et al.* 1996), breathing and ventilatory response to hypoxia (Okubo et Mortola, 1988; Hertzberg *et al.* 1992; Peyronnet *et al.* 2000) and development of central catecholaminergic areas involved in respiratory control (Seidler & Slotkin, 1990; Soulier *et al.* 1997; Peyronnet *et al.* 2000). Postnatal breathing onset and respiratory control are dependent on the peripheral chemoreceptors. Chemosensitivity is low in the foetus and resets to a higher $O_2$ level within a couple of days after birth. However, the peripheral chemoreceptors and their integrative ventilatory response are not mature at birth and are susceptible to be modulated by changes in environmental oxygen occurring during the early postnatal period. In fact, prolonged hypoxic exposure from birth increases the basal activity of the carotid bodies (Hertzberg *et al.* 1992; Soulier *et al.* 1997), delays the onset of the chemoreflex response to hypoxia (Eden & Hanson, 1987; Hertzberg *et al.* 1992) and elicits hyperventilation in adults (Okubo & Mortola, 1988). The nature of these disturbances depends on the duration and severity of hypoxia, as well as the gestational age of the foetus at the time of the insult.

The present study examines the effects of prenatal hypoxia lasting 2 weeks in the rat, from embryonic day 5 (E5) to embryonic day 20 (E20), on the early postnatal maturation of the chemoafferent pathway both neurochemically and functionally, from birth to 9 weeks of postnatal age. In the first protocol, we focused on the neurochemical activity of the carotid bodies, and in a second protocol we investigated the impact of the neurochemical disturbances on physiological function, *i.e.* on ventilation.

*Chemoreception*, Edited by Pequignot et al.
Kluwer Academic/Plenum Publishers, New York, 2003

The physiological impact of these neurochemical alterations was evaluated on resting ventilation and on integrated ventilatory response to chemoreceptor stimulation *i.e.* to acute postnatal hypoxia. The ventilatory response to hypoxia was used to determine the degree of functional integrity of the chemoafferent pathway.

## 2. METHODS

Prenatal hypoxia was performed as following. Twenty pregnant rats (SpragueDawley, IFFA Credo, l'Arbresle, France) were placed from E5 to E20 in a normobaric Plexiglass chamber supplied with a gas mixture consisting of 10% $O_2$—90% $N_2$ and maintained at 10 ± 0· 5% $O_2$. They had free access to food and water. The $CO_2$ expired by the rats was eliminated by circulating the gas mixture from the chamber through soda lime and never exceeded 0· 1 %. Metabolic water contained in expiratory gases was trapped continuously into a chilled glass tank. The temperature inside the chamber was set at 26 ± 1 °C.On gestational day E20 , pregnant rats were removed from the hypoxic chamber (10% $O_2$) and were housed individually under normoxia (21% $O_2$) in a climatised room at 26 ± 1 °C with a 12 h light—dark cycle. They were allowed free access to food and water. At birth, in normoxia, pups were mixed and redistributed randomly to nursing dams. These hypoxic offspring were considered as the hypoxic group (Hypo). A normoxic group of 20 pregnant rats (pregnancy in normoxia giving normoxic offspring) was treated similarly. These normoxic offspring were considered as the control group (Cont). The experiments were performed using only male pups in order to avoid neurochemical and ventilatory gender differences (Porter, 1986; Mortola & Saiki, 1996). To ensure a common nutritional status among the various litters, each nursing group contained 10-12 pups.

Ventilation was measured in awaked unrestrained rats, at birth, 3 days, 7 days, 21 days and 68 days after birth using barometric plethysmographs described by Bartlett & Tenney (1970). Temperature, $O_2$ and $CO_2$ levels inside the animal chamber were continuously monitored. The inlet and outlet tubes of the animal chamber were closed and pressure fluctuations related to breathing were recorded with a differential pressure transducer (Celesco, California). When the rat was quiet, minute ventilation was calculated from breath-by-breath by computer analysis of the spirogram and was expressed in ml $min^{-1}$. Resting ventilation was first recorded under normoxic conditions (21% $O_2$). The hypoxic ventilatory response was performed after one, 4, 7 and 10 minutes of 10% $O_2$. HVR is calculated as the difference between normoxic and hypoxic values. TH activity can be used as a marker of the rate of catecholamine synthesis. *In vivo* TH activity was estimated by measuring L-DOPA accumulation after inhibition of L-amino acid

decarboxylase by NSD 1015 (3-hydroxybenzylhydrazine dichloride: Sigma) (Carlsson *et al* 1972). NSD 1015 was injected intraperitoneally (100 mg $kg^{-1}$ of body weight) 10 min before sacrifice. TH activity was expressed in picomoles of L-DOPA formed in 10 min and per pair of carotid body.

All experiments were carried out according to the ethical principles laid down by the French (Ministère de l'Agriculture) and EU Council Directives for care of laboratory animals (No. 02889).

## 3. RESULTS

### Resting ventilation

Prenatal hypoxia elicited basal hyperventilation ($V_E$) until P21 (P0: +30%, P3: +40%, P7: +35%, P21: +71% compare to Cont). No more changes were observed in the adult group.

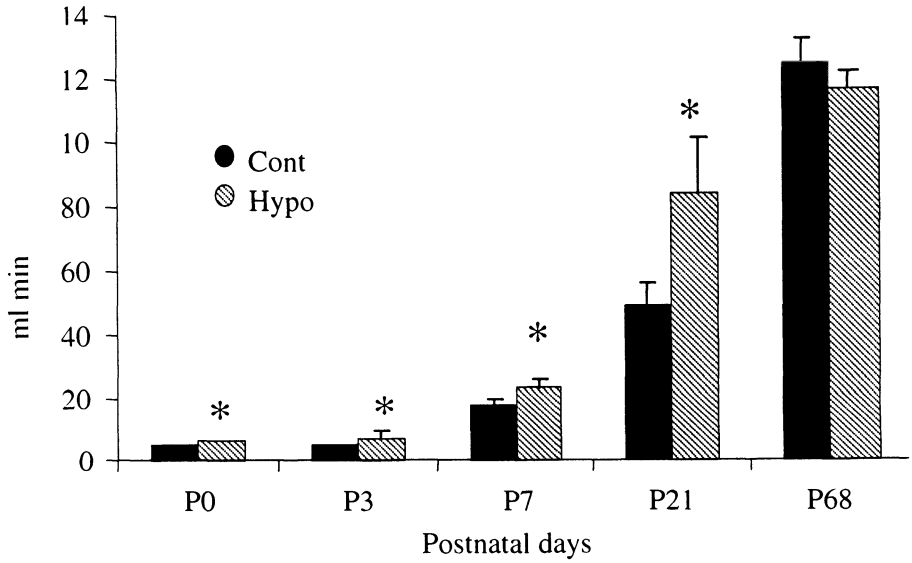


*Figure 1.* Effects of a prenatal hypoxia on resting ventilation (21% $O_2$) at birth (P0), 3, 7, 21 and 68 days after birth. Each bar represents the mean ± s.e.m. of minute ventilation in ml.min in the Hypo group of rats (grey bar) and in the Cont group of rats (black bar). In each different group of age and group of rats, the number of animal was at least 7. * represents a significant difference between the Hypo and the Cont group with $p<0,005$. The resting ventilation was significantly increased until 3 weeks of age in the Hypo group.

## Hypoxic Ventilatory Response

In the 1-week-old group of rats only the Cont group showed a significant increase of the $V_E$ at one minute (+41% compare to the resting data) and the response to hypoxia was biphasic. It returned to baseline levels at the end of 1 min of hypoxia (figure 2). In the 1week-old-rats of the Hypo group, hypoxia failed to alter significantly the minute ventilation. At 3 weeks of age the $V_E$ significantly increased in both group and the amplitude of response was higher in the Hypo group than in the Cont group, respectively +73% and +63%. In the 9-week-old group of rats ventilation was enhanced at the same rate in both groups. After 7 minutes of hypoxia the Hypo group showed smaller amplitude of response (+67% at 7 min and +58% at 10 min) compared to the Cont group response (+88% at 7 min and +95% at 10 min).

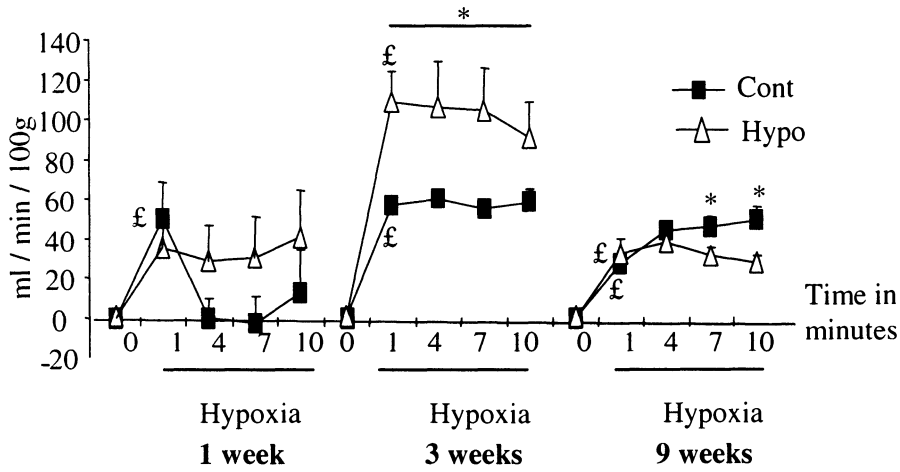


*Figure 2.* Effect of prenatal hypoxia on the amplitude of the hypoxic ventilatory response to 10% $O_2$ hypoxia of 1, 3 and 9-week-old rats. This graph represents the means ± s.e.m. of the differences between resting values and the data obtained during the hypoxic test, after 1, 4, 7 and 10 min of hypoxic exposure, and therefore represents the response amplitude. Open triangles represent data obtained from the prenatal hypoxic off spring (Hypo) and filled squares represent data obtained from the control group of rats (Cont). In each graph: the left panel represents 1-week-old rats, the middle panel 3-week-old rats and the right panel 9-week-old rats. £P < 0· 05, significant difference between 1 min of hypoxia and normoxia; *P < 0· 05, significant difference between Cont and Hypo group.

### Neurochemical maturation

In the carotid bodies of Cont pups, the TH activity was high at birth (P0) and decreased markedly the first postnatal weeks (P3, -57%; P7, -61%) (Table 1). Thereafter (P14), TH activity increased to reach again the birth level. This developmental pattern is consistent with previous results showing at birth a drop of the dopamine turnover rate and TH mRNA in the CB (Hertzberg et al, 1990; Holgert et al 1995). The prenatal hypoxic treatment amplified the decrease of TH activity measured in the carotid bodies (P3 -25%; P7 -41% compare to the age-matched Cont group). However in oldest rats, the effects of prenatal hypoxia are reversed, with a TH activity strongly activated in the carotid bodies (+95% compare to the age-matched Cont group).

| % of variation compare to the values at birth | 3 days | 7 days | 14 days | 21 days | 68 days |
|---|---|---|---|---|---|
| Cont | -57 | -61 | -2 | -39 | -23 |
| Hypo | -75 | -82 | -14 | -40 | 17 |
| Cont/Hypo | $P<0.05$ | $P<0.05$ | $P<0.05$ | *n.s.* | $P<0.05$ |

*Table 1.* Percentages of variation of Tyrosine Hydroxylase activity in the carotid bodies at 3, 7, 14, 21 and 68 days after birth compare to the birth level. $P < 0{\cdot}05$, significant difference between Cont and Hypo group. We observed an enhanced decrease of TH activity in the Hypo group until 14 days. When pups became adults, we still observed a slit decrease of TH activity compare to birth levels in the Cont group. Inversely, in the Hypo group TH activity was increased and significantly different from the Cont group.

## 4. DISCUSSION

*Effect of a prenatal hypoxia on ventilation*

Carotid Bodies afferents provide a tonic excitatory input to medullary respiratory neurons and are necessary to stabilize the rhythmic respiration during neonatal periods (Hofer, 1986; Forster et al., 2000). In the present study we show that Hypo rats display greater resting ventilation from birth until P21. This result could result from an increase of the peripheral inputs but also be due to an impairment of the central integration sites. Our data support at least, neurochemical impairment at the carotid body level. However, we cannot rule out central disturbances since prenatal hypoxia is known to compromise the cellular development and synaptogenesis in the brain (Slotkin et al, 1986).

Measuring the response to sustained hypoxia provides information about the time-dependent components, which determine the overall ventilatory response, *i.e.,* the initial step reflects the carotid body chemosensitivity and central processing, whilst the second phase of the response reflects the integration of peripheral chemosensory inputs and subsequent central adaptative events.

The 1-week-old pups of the Cont group exhibited a biphasic hypoxic ventilatory response. The ventilatory response to hypoxia changes with maturation, and is characteristically biphasic during the first days of postnatal life (Lahiri *et al.* 1978; Eden & Hanson, 1987; Fung et al, 1996) and can be recorded until 5, 7 or 14 days of postnatal age when exposed to hypoxic mixtures of 15%, 12% or 8% $O_2$ respectively. This is thought to reflect first the stimulatory effect of hypoxia acting via the carotid chemoreceptors (Lahiri *et al.* 1978), and second a depressant effect arising from inhibitory mechanisms of brainstem origin (Nolan & Waldrop, 1996; Waites *et al.* 1996). Catecholaminergic neurones located in the ventral (A5) and dorsal pons (A6) are strongly involved in this depression phase (Errchidi et al, 1990, Okada et al, 1998). Indeed, catecholamines acting at α2-receptors appear particularly relevant (Bissonnette 2000). Biphasic response to hypoxia is then not an "all or nothing" phenomenon, and the pattern of hypoxic ventilatory response is dependent on maturational processes (Eden & Hanson, 1987). In contrast, 1-week-old rats exposed to hypoxia during gestation did not exhibit an initial increase in ventilation in response to 10% $O_2$. In the Hypo rats, the reduced catecholamine activity in carotid bodies might contribute to the absence of hypoxic response thus suggesting that these rats were less sensitive than the controls. In rats, the functional development of carotid bodies continues for up to 2 weeks after birth and this process of maturation has been previously reported to be altered by early postnatal hypoxia (Hertzberg *et al.* 1992). The present study indicates that prenatal hypoxia also altered the functional development of carotid bodies. In humans, the negative effects of hypoxia on carotid body sensitivity have been described in chronically hypoxic adults and children, and in persons born at a high altitude, all of whom develop long-lasting insensitivity to acute hypoxia (Lahiri *et al* 2000).

At 3 weeks of age, the Hypo as well as the Cont group responded to hypoxia with a sustained increase in ventilation from the first minute of exposure. The response of the Hypo group was amplified compared to the response of the matched-age Cont group. By 9 weeks of age, the differences between hypoxic ventilatory response of the control and the treated rats had largely disappeared. These results are consistent with those of Ling and collaborators (Ling *et al.* 1996, 1998), who reported that the functional impairment of the ventilatory and phrenic responses of rats to hypoxia

following perinatal hyperoxia was attenuated with advancing age, and was virtually eliminated by 15 months of age.

*Tyrosine hydroxylase activity in the carotid body*

Carotid body in the fetus is active and well adapted to the low $O_2$ tension *in utero*. At birth, suddenly exposed to relative high $O_2$ level, carotid bodies changes their setting of sensitivity. In this system, dopamine is mainly considered as an inhibitory neuromodulator and a correlation between the increase of the carotid body sensitivity to hypoxia and the decrease of dopamine release has been proposed during this perinatal transition (Hertzberg et al, 1990; Holgert et al 1995).

Prenatal hypoxia acts on the development of TH activity exhibiting a time dependent effect. The prenatal stress is especially characterized during the first postnatal week, by a gradual down-regulation followed in oldest rats by an up-regulation. TH catalyzes the rate-limiting step in the biosynthesis of the catecholamines, which require molecular oxygen to participate to the enzymatic reaction (Kumer *et* Vrana, 1996). To explain the effect of prenatal hypoxia on the TH activity, one suggestion is that the difference between the fetal and the postnatal oxygen tension could be higher in Hypo than in Cont pups and then be responsible of an adjustment of the TH metabolism. The gene that encodes TH is regulated by oxygen tension and the level of transcription and the RNA stability are both regulated during low $O_2$ conditions (Kumer *et* Vrana, 1996).

In human, fetal hypoxia might result from several pathophysiological situations including maternal anemia, hypertension, and smoking or reduced oxygen inhalation in high altitude. Such environment has been described to be one of the major pathological factors inducing neuronal cell injury, neurodegeneration and cell death (Vakas *et al*, 1996). The present study demonstrates that prenatal hypoxia impairs the early postnatal development of the functional and neurochemical carotid chemoafferent pathway with a catecholamine-dependent mechanism. For instance, in sudden infant death syndrome, the catecholamine content appears strongly increased in the CB (Perrin *et al*, 1984) while before the death these children exhibited abnormal ventilation (Gordon *et al*, 1984; Schechtman *et al*, 1990). Then, prenatal hypoxic model appears particularly relevant in order to better understand the neurochemical pathogenesis of this developmental disorder.

## REFERENCES

Bartlett, D., Jr. and Tenney, S. M. (1970) Control of breathing in experimental anemia. *Respir Physiol* 10, 384-95.

Bissonnette, J. M. (2000) Mechanisms regulating hypoxic respiratory depression during fetal and postnatal life. *Am J Physiol Regul Integr Comp Physiol* 278, R1391-400.

Carlsson, A., Davis, J. N., Kehr, W., Lindqvist, M. and Atack, C. V. (1972) Simultaneous measurement of tyrosine and tryptophan hydroxylase activities in brain in vivo using an inhibitor of the aromatic amino acid decarboxylase. *Naunyn Schmiedebergs Arch Pharmacol* 275, 153-68.

Eden, G. J. and Hanson, M. A. (1987) Effects of chronic hypoxia from birth on the ventilatory response to acute hypoxia in the newborn rat. *J Physiol* 392, 11-9.

Errchidi, S., Hilaire, G. and Monteau, R. (1990) Permanent release of noradrenaline modulates respiratory frequency in the newborn rat: an in vitro study. *J Physiol* 429, 497-510.

Forster, H. V., Pan, L. G., Lowry, T. F., Serra, A., Wenninger, J. and Martino, P. (2000) Important role of carotid chemoreceptor afferents in control of breathing of adult and neonatal mammals. *Respir Physiol* 119, 199-208.

Fung, M. L., Wang, W., Darnall, R. A. and St John, W. M. (1996) Characterization of ventilatory responses to hypoxia in neonatal rats. *Respir Physiol* 103, 57-66.

Gordon, D., Cohen, R. J., Kelly, D., Akselrod, S. and Shannon, D. C. (1984) Sudden infant death syndrome: abnormalities in short term fluctuations in heart rate and respiratory activity. *Pediatr Res* 18, 921-6.

Hertzberg, T., Hellstrom, S., Holgert, H., Lagercrantz, H. and Pequignot, J. M. (1992) Ventilatory response to hyperoxia in newborn rats born in hypoxia-- possible relationship to carotid body dopamine. *J Physiol* 456, 645-54.

Hertzberg, T., Hellstrom, S., Lagercrantz, H. and Pequignot, J. M. (1990) Development of the arterial chemoreflex and turnover of carotid body catecholamines in the newborn rat. *J Physiol* 425, 211-25.

Hofer, M. A. (1986) Role of carotid sinus and aortic nerves in respiratory control of infant rats. *Am J Physiol* 251, R811-7.

Holgert, H., Hokfelt, T., Hertzberg, T. and Lagercrantz, H. (1995) Functional and developmental studies of the peripheral arterial chemoreceptors in rat: effects of nicotine and possible relation to sudden infant death syndrome. *Proc Natl Acad Sci U S A* 92, 7575-9.

Kumer, S. C. and Vrana, K. E. (1996) Intricate regulation of tyrosine hydroxylase activity and gene expression. *J Neurochem* 67, 443-62.

Lahiri, S., Brody, J. S., Motoyama, E. K. and Velasquez, T. M. (1978) Regulation of breathing in newborns at high altitude. *J Appl Physiol* 44, 673-8.

Lahiri, S., Rozanov, C. and Cherniack, N. S. (2000) Altered structure and function of the carotid body at high altitude and associated chemoreflexes. *High Alt Med Biol* 1, 63-74.

Ling, L., Olson, E. B., Jr., Vidruk, E. H. and Mitchell, G. S. (1996) Attenuation of the hypoxic ventilatory response in adult rats following one month of perinatal hyperoxia. *J Physiol* 495, 561-71.

Ling, L., Olson, E. B., Jr., Vidruk, E. H. and Mitchell, G. S. (1998) Slow recovery of impaired phrenic responses to hypoxia following perinatal hyperoxia in rats. *J Physiol* 511, 599-603.

Mortola, J. P. and Saiki, C. (1996) Ventilatory response to hypoxia in rats: gender differences. *Respir Physiol* 106, 21-34.

Nolan, P. C. and Waldrop, T. G. (1996) Ventrolateral medullary neurons show age-dependent depolarizations to hypoxia in vitro. *Brain Res Dev Brain Res* 91, 111-20.

Nyakas, C., Buwalda, B. and Luiten, P. G. (1996) Hypoxia and brain development. *Prog Neurobiol* 49, 1-51.

Okada, Y., Kawai, A., Muckenhoff, K. and Scheid, P. (1998) Role of the pons in hypoxic respiratory depression in the neonatal rat. *Respir Physiol* 111, 55-63.

Okubo, S. and Mortola, J. P. (1988) Long-term respiratory effects of neonatal hypoxia in the rat. *J Appl Physiol* 64, 952-8.

Perrin, D. G., Cutz, E., Becker, L. E., Bryan, A. C., Madapallimatum, A. and Sole, M. J. (1984) Sudden infant death syndrome: increased carotid-body dopamine and noradrenaline content. *Lancet* 2, 535-7.

Peyronnet, J., Roux, J. C., Geloen, A., Tang, L. Q., Pequignot, J. M., Lagercrantz, H. and Dalmaz, Y. (2000) Prenatal hypoxia impairs the postnatal development of neural and functional chemoafferent pathway in rat. *J Physiol* 524 Pt 2, 525-37.

Porter, J. C. (1986) Relationship of age, sex, and reproductive status to the quantity of tyrosine hydroxylase in the median eminence and superior cervical ganglion of the rat. *Endocrinology* 118, 1426-32.

Schechtman, V. L., Harper, R. M., Kluge, K. A., Wilson, A. J. and Southall, D. P. (1990) Correlations between cardiorespiratory measures in normal infants and victims of sudden infant death syndrome. *Sleep* 13, 304-17.

Seidler, F. J. and Slotkin, T. A. (1990) Effects of acute hypoxia on neonatal rat brain: regionally selective, long-term alterations in catecholamine levels and turnover. *Brain Res Bull* 24, 157-61.

Slotkin, T. A., Cowdery, T. S., Orband, L., Pachman, S. and Whitmore, W. L. (1986) Effects of neonatal hypoxia on brain development in the rat: immediate and long-term biochemical alterations in discrete regions. *Brain Res* 374, 63-74.

Soulier, V., Dalmaz, Y., Cottet-Emard, J. M., Lagercrantz, H. and Pequignot, J. M. (1997) Long-term influence of neonatal hypoxia on catecholamine activity in carotid bodies and brainstem cell groups of the rat. *J Physiol* 498, 523-30.

Waites, B. A., Ackland, G. L., Noble, R. and Hanson, M. A. (1996) Red nucleus lesions abolish the biphasic respiratory response to isocapnic hypoxia in decerebrate young rabbits. *J Physiol* 495, 217-25.

# pH Sensitivity of Spinal Cord Rhythm in Fetal Mice in *Vitro*

JAIME EUGENÍN, ESTIBALIZ AMPUERO, CLAUDIA D. INFANTE, EVELYN SILVA, and ISABEL LLONA
*Laboratory of Neural Systems, Department of Biology, Universidad de Santiago de Chile, Casilla 40, Correo 33, Santiago, Chile*

## 1. INTRODUCTION

The spinal respiratory rhythm generator is a neural network localized at the segments C4-C6 able to produce synchronous long lasting rhythmic bursts of action potentials on both phrenic nerves (Dubayle and Viala, 1996). As other spinal cord rhythms, the spinal respiratory rhythm can be induced in curarized rabbits after cervical transection by administration of nialamide-DOPA (Viala and Freton, 1983). This spinal rhythm can also be induced in the *in vitro* brainstem-spinal cord preparation from newborn rat or mouse by deep diethyl ether anaesthesia, or bath administration of glutamic acid, N-methyl-D-aspartic acid, amphetamine, 5-hydroxytryptophan, or high potassium concentration (Dubayle and Viala, 1998). It has been shown that the spinal respiratory rhythm recorded from neonatal rat brainstem-spinal cord preparation is sensitive to $H^+$ and $CO_2$ (Dubayle and Viala, 1998). However, in most of the experiments the extent to what this chemosensitive response depends directly on the spinal respiratory generator was undefined, because chemical stimulation or the pharmacological inductors affect also the activity of the medullary respiratory pattern generator and both, the medullary and spinal respiratory oscillators, are coupled (Dubayle and Viala, 1996). Uncoupling of these generators by spinal

*Chemoreception*, Edited by Pequignot et al.
Kluwer Academic/Plenum Publishers, New York, 2003

transection at C2 segment caused the disappearance of the spinal respiratory rhythm in most of the neonatal preparations (Dubayle and Viala, 1998).

In the fetal rat brainstem-spinal cord preparation spontaneous spinal respiratory rhythm can be observed either preceding to or coexisting with the medullary respiratory rhythm (Di Pasquale et al., 1992, Greer et al., 1992). Thus, early fetal stages may be suitable to investigate the isolated responses to changes in pH of the spinal respiratory generator. Our aim was to study the pH sensitivity of spontaneous spinal respiratory rhythm recorded from cervical ventral roots in the isolated CNS from fetal mice before the appearance of the medullary respiratory activity.

## 2. METHODS

Experiments were carried out in accordance with the Institute for Laboratory Animal Research (ILAR) Guide for the Care and Use of Laboratory Animals and approved by the Bioethics committee of the Universidad de Santiago de Chile. Timed-pregnant CF1 mice were anaesthetized with ketamine (80 mg Kg-1 i.p.) and xylazine (10 mg Kg-1 i.p.) and maintained at 37 °C. After fetal mice were delivered by C-section, the mother was sacrificed by anesthetic overdose. Fetuses were immediately immersed in artificial cerebrospinal fluid (aCSF) containing (mM): NaCl, 125.0; KCl, 5.0; $NaHCO_3$, 24.0; $KH_2PO_4 \times H_2O$, 1.25; $CaCl_2$, 0.8; $MgSO_4.7H_2O$, 1.25 at 4 C. The medium was supplemented with D-glucose to a final concentration of 30 mM and equilibrated with $O_2$:$CO_2$ = 95%: 5%, (pH 7.37-7.40). The CNS was removed, and decerebrated through a pontomesencephalic transection, transferred to a recording chamber of 1 ml in volume, and superfused with warmed aCSF at 25 °C. Spontaneous spinal cord activity from C4-C6 ventral roots was recorded with suction microelectrodes connected to a differential amplifier, integrated, displayed, and analyzed with AD data acquisition system (Digipack 1200 A, Axon Instruments). The pH of the brainstem superfusion medium (7.0, 7.4) was selectively changed by gassing aCSF in presence of different final concentrations of bicarbonate (9 and 26 mM, respectively). The tip of a micro-combination pH electrode (Orion Research Inc.) was placed into the recording chamber and connected to a pH/ion amplifier (A-M Systems) to record the pH of the superfusion medium. Amplitude of fictive respiration was estimated from the peak value of the integrated ventral root activity. Respiratory frequency was measured from 3-6 minutes of recording in steady-state conditions inmediately before, during, and after acidification of the medium. Non-parametric statistic for paired samples (Wilcoxon signed-rank test) was performed using a significance level $p < 0.05$.

## 3. RESULTS

Spontaneous spinal activity could be recorded from E14 fetuses. This activity consisted in rhythmic bursts of action potentials 3-40 s of duration, appearing at a frequency about 0.5 $min^{-1}$ (Figure 1). The integration of the burst of action potentials described different shapes. In some cases a fast ascending phase is followed by a slow descending phase (Figure 1). In other cases, the ascending phase is very slow (not illustrated). In about half of the preparations, the spinal respiratory activity coexisted with medullary respiratory-like activity very similar to that described in neonates (Infante and Eugenin, 2000).

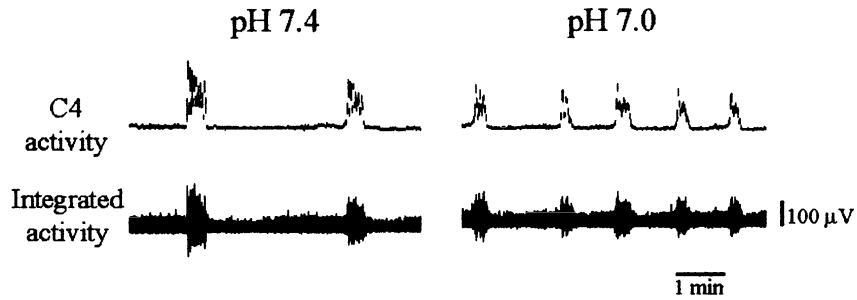


*Figure 1.* Effect of acidification of the superfusion medium upon the spontaneous activity recorded from C4 ventral root in the brainstem-spinal cord preparation of E14 fetus.

Switching the pH of the bath superfusion from 7.4 to 7.0 increased the frequency to 212% and decreased the amplitude to 65% of the low frequency spinal cord rhythm (Figure 1 and 2). This pattern of response to pH was observed before and after transection of the spinal cord at the level of C1.

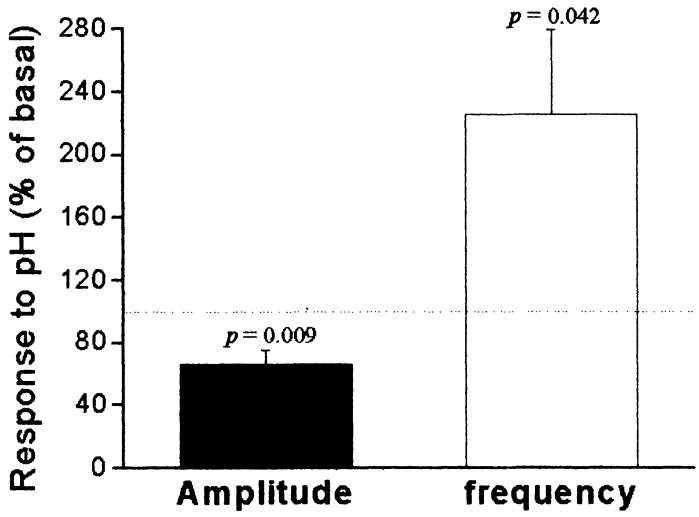


*Figure 2.* Effects of acidification of the medium upon the amplitude and frequency of the spontaneous C4 activity recorded from brainstem-spinal cord preparation of E14 fetuses. Bars and vertical lines are means ± S.E.M, respectively. Statistical significance p was obtained using Wilcoxon signed-rank test (n=9 from 3 litters).

## 4. DISCUSSION

The present results show that low frequency and long duration spinal rhythm recorded in vitro in the E14 fetal mouse is modulated by chemical input. Two observations strongly suggest that this spinal rhythm generator is itself sensitive to changes of pH: i) The pH effect occurred in absence of a medullary respiratory rhythm, which allows to exclude any indirect effect due to coupling, and; ii) The rhythm was also pH-sensitive after cervical transection preserving the same pattern of response.

Previous work in the brainstem preparation from rat fetus was focussed in the evaluation of $CO_2$ sensitivity of the (medullary) respiratory-like rhythm (Di Pasquale et al., 1992). Perfusion with $CO_2$ free medium decreased the frequency of the (medullary) respiratory-like rhythm in E20, but not in E17 fetal rats. Differences may be related to interspecies differences and the use of different

kinds of chemical stimuli. Interspecies differences between newborn mouse and rat have been demonstrated for the noradrenergic in vitro regulations on respiration (Viemari and Hilaire, 2002). Several reports suggest that $CO_2$ and $H^+$ have access to different brainstem structures, which could explain differences in the pattern of respiratory responses to both stimuli.

Finally, that the pattern of response to pH of the embryonic spinal cord rhythm is similar to that observed for the respiratory-like rhythm in newborn mice (Infante and Eugenin, 2000), suggests that common mechanisms are involved in their chemical modulations.

## ACKNOWLEDGEMENTS

This work was supported by grant FONDECYT 1010242.

## REFERENCES

Di Pasquale, E., Monteau, R. and Hilaire, G. 1992, In vitro study of central respiratory-like activity of the fetal rat. Ex. *Brain Res 89:* 459-464.

Dubayle, D. and Viala, D. 1996, Interactions between medullary and spinal respiratory rhythm generators in the in vitro brainstem spinal cord preparation from newborn rats. Exp *Brain Res* 109: 1-8.

Dubayle, D. and Viala, D. 1996, Localization of the spinal respiratory rhythm generator by an in vitro electrophysiological approach. N*euroreport* 7: 1175-80.

Dubayle, D. and Viala, D. 1998, Effects of $CO_2$ and pH on the spinal respiratory rhythm generator in vitro. *Brain Res Bull* 45: 83-7.

Greer, J.J., Smith, J.C. and Feldman, J.L. 1992, Respiratory and locomotor patterns generated in the fetal rat brain stem-spinal cord in vitro. *J. Neurophysiol.* 67: 996-999.

Infante, C.D. and
Eugenin, J. 2000, pH sensitivity in the isolated Cns of newborn mouse. *Adv Exp Med Biol* 475: 785-8.

Viala, D. and Freton, E. 1983, Evidence for respiratory and locomotor pattern generators in the rabbit cervico-thoracic cord and for their interactions. Exp. *Brain Res.* 49: 247-256.

Viemari, J. and Hilaire, G. 2002, Noradrenergic receptors and in vitro respiratory rhythm: possible interspecies differences between mouse and rat neonates. *Neurosci. Lett.* 294: 149-153.

# Time Dependent Regulation of Dopamine $D_1$- and $D_2$-Receptor Gene Expression in the Carotid Body of Developing Rabbits by Hypoxia

AIDA BAIRAM*, YVES LAJEUNESSE*, VINCENT JOSEPH*, and YVES LABELLE#.

**Unité de recherche en périnatologie, # Unité de recherche en génétique humaine et moléculaire, Centre de Recherche, Hôpital Saint François d'Assise, Université Laval, Québec, P.Q., Canada.*

## 1. INTRODUCTION

In the central nervous system, activation of dopamine (DA) receptors (R) by their substrate, DA, modulates the regulation of genes encoding DA Rs themselves (Sidhu *et al.*, 1999; Missale *et al.*, 1998; Gerfen *et al.*, 1990). These effects were shown to be: 1) tissue and region specific, 2) dependent on physiological function of activated DA Rs, and, 3) due to the synergistic effect of stimulation of DA $D_1$ and $D_2$ Rs types (Missale *et al.*, 1998; Gerfen *et al.*, 1990).

Hypoxia increases DA release from the carotid body (CB). And, this release depends on the duration and the intensity of exposure to hypoxia (Fidone *et al.*, 1997), and on age (Bairam *et al.*, 1996b; Donnelly and Doyle, 2000). Since the CB contains both DA R types, $D_1$ and $D_2$, (Almaraz *et al.*, 1991; Fidone *et al.*, 1997; Bairam *et al.*, 1996a, 1998), we determined whether the duration of exposure to hypoxia modulates DA $D_1$- and $D_2$-R mRNA expression levels. Also, because the CB DA $D_2$-R mRNA level increases with age (Bairam *et al.*, 1996a), the pattern of changes of DA $D_1$- and $D_2$-R mRNA levels in response to hypoxia was evaluated in developing rabbits. Using RT-PCR analysis, we showed that 6 and 24 h exposure to 8% $O_2$ down-regulated DA $D_1$- and $D_2$-R mRNA expression levels. This

*Chemoreception*, Edited by Pequignot et al.
Kluwer Academic/Plenum Publishers, New York, 2003

modulation is dependent on exposure duration for the $D_1$-R only. And, the pattern of hypoxia-modulated $D_1$- and $D_2$-R RNA levels is age dependent. This work represents a small part of a more exhaustive study (Bairam *et al.*, in revision)

## 2. MATERIALS AND METHODS

### 2.1. Animals and Organs Collection

Three groups of 1 (n=105), 25 days old (n=75) and adult New Zeland rabbits (5-6 months old; n=45) were studied. Rabbits were housed in a hypoxic chamber and exposed to 8% $O_2$ in $N_2$ for 6 or 24 h. The chamber $O_2$ and $CO_2$ (less than 0.3%) concentrations were continuously monitored. Control animals for each age group underwent similar management but were exposed to normoxia (21% $O_2$) for 24h.

CBs were collected, frozen immediately and pooled depending on age, $O_2$ concentration and time exposure, and stored at –80°C for further analyses. Animal preparation, surgery, and CBs collection were similar to that described previously (Bairam *et al.*, 1996a; 1998). Briefly, each rabbit was anesthetized with a mixture of ketamine (50 mg/kg) and xylazine (10 mg/kg) injected i.p. for newborns and i.m. for adults, rapidly tracheotomized and artificially ventilated with the same $O_2$ concentration that it received in the chamber. The striatum was also collected, pooled in the same manner as for the CB, and analyzed since it is rich in DA $D_1$- and $D_2$-R.

### 2.2. $D_1$ and $D_2$ R mRNA Amplification

RNA preparation. Frozen CBs were homogenized and total RNA was extracted using the RNeasy Qiagen kit (Qiagen, Hilden, Germany) and DNA eliminated using RNase-Free DNase (Qiagen, Hilden, Germany) following the procedure described by the manufacturer. RNA was quantified by both UV spectrophotomery and after staining with ethidium bromide and comparison of the staining intensities with that of the 28 and 18S ribosomal RNA marker (Pharmacia, Uppsala, Sweden) used at different known concentrations.

RT-PCR reaction. DA $D_1$- and $D_2$-R mRNAs target sequences were amplified by RT-PCR with specific oligonucleotides primers based on GeneBank data for rabbit and rat, respectively (gb Y 10662; gb M 36831).

These primers were: $D_1$ forward, 5'-CTCTTGGTGGCT GTCTTGGTCAT- 3' (residues 95-117) and reverse, 5' - CAGGGAAGAGGAAATGGAATACG-3' (residues 462-484); $D_2$ forward, 5'AAGCGCCGAGTTACTGTCATGAT-3' (residues 572-594) and reverse, 5'GACAATGGAGGTATAGACCACAAAGGC-3' (residues 689-715).

The $D_2$ primers amplify a common segment for short and long $D_2$-R isoforms. The reverse primers were also used for reverse transcription. The RT-PCR reaction was performed as described (Bairam et al., 1996a; 1998). Briefly, the specific first strand cDNA synthesis for either the $D_1$- or the $D_2$-R mRNA was generated using 0.1 µg of total RNA. For the $D_1$-R segment, the PCR reaction was 32 cycles each composed of 30 sec at 94°C; 30 sec at 60°C; 1 min at 72°C, followed by a final extension step for 7 min at 72°C. For the $D_2$-R segment, the PCR reaction was 33 cycles each composed of 30 sec at 94°C; 30 sec at 66°C; 1 min at 72°C, followed by a final extension step for 7 min at 72°C. RT-PCR was performed in triplicate using three RNA preparations.

Hybridization and l abeling. The PCR products were separated by electophoresis on 1.6% agarose gels in Tris-borate-EDTA buffer (TBE), transferred overnight by capillarity in 0.4 N NaOH onto Biodyne B membranes. Membranes were then pre-hybridized and hybridized overnight at 42°C with $^{32}$P-labeled internal probes (5 X $10^5$ cpm/ml) which were: 5'-GTCTCGTCCAGGGAAGTGGCATTCC-3' (405-429) and 5'-TTGTTGAGTCCGAAGAGCAGTGGG-3' (631-654) for the $D_1$- and $D_2$-R, respectively. Membranes were washed stringently then exposed to X-ray film (Kodak BIOMAX MR). The hybridization signal was quantified by densitometry using Image Analyser Software program, Quantity One 4.2 (Bio-Rad, Mississauga, Ontario, Canada). Signals were detected as bands of 390 bp the $D_1$- and of 144 bp for the $D_2$-R segment, as expected from the cDNA sequence data.

## 2.3. Data Analysis

The $D_1$- and $D_2$-R transcript levels obtained in hypoxia after 6 or 24h exposure were evaluated in difference with normoxia (control) which was assigned the arbitrary unit of 1 and results were then expressed as % changes from control. Levels obtained were compared between conditions but not between ages. Statistical analysis used ANOVA for multiple factors and differences with $P < 0.05$ were considered significant.

# 3. RESULTS

An example of amplified products of the CB and striatum $D_1$-and $D_2$-R mRNA at all ages studied under control condition (i.e., normoxia) is showed in Figure 1 A&B. Both $D_1$- and $D_2$-R mRNAs were detected in the CB and striatum at 1, 25 days old and adult rabbits.

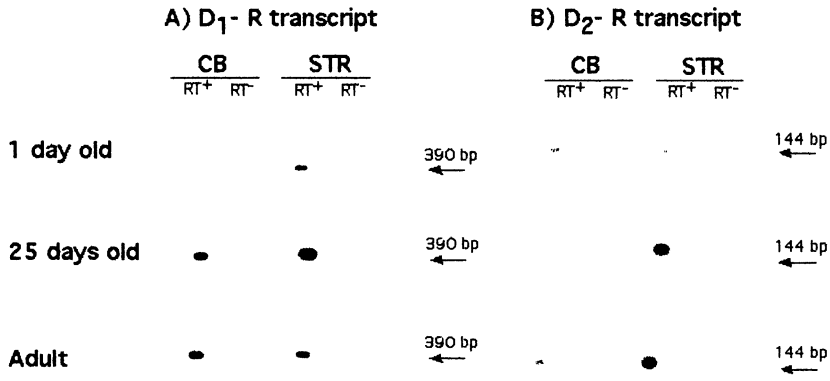


*Figure 1.* RT-PCR - amplification of DA $D_1$- and $D_2$- receptor mRNA in the carotid body (CB) and striatum (STR) of control (normoxia) rabbits. In the carotid body and the striatum, signals for the DA $D_1$- and $D_2$-R mRNA were obtained at expected sizes at each of age studied when the amplification reaction was run with RT (+) but not without RT (-).

## 3.1. Effects of Hypoxia on CB DA $D_1$-R Transcript Level (Table 1).

At 1 day old, 6 or 24h exposure to 8% $O_2$ decreased the $D_1$-R transcript level compared with control ($p < 0.01$). However, its level after 24h exposure was lower than after 6h exposure ($p < 0.01$). In 25 days old, hypoxia decreased the $D_1$-R transcript level as compared with control ($p < 0.01$) to the same extent after 6 and 24h exposure. In adults, hypoxia also decreased the $D_1$-R transcript level compared with control ($p < 0.01$) and the level after 24h was lower than after 6h exposure, as was observed in 1 day old. Although the general pattern was a decrease in $D_1$-R transcript level by hypoxia at any age studied, this decrease was 2-3 fold lower in adult compared with 1 and 25 days old.

## 3.2. Effects of Hypoxia on CB DA $D_2$-R Transcript Level (Table 1).

In all ages studied, hypoxia significantly decreased the $D_2$-R transcript level compared with control ($p < 0.01$). This decrease was comparable after 6 and 24h exposure, and was about 2 fold more in adult than in 1 and 25 days old rabbit. Similarly to DA $D_1$-R mRNA decrease by hypoxia, the $D_2$-R mRNA decrease was also age dependent.

In the striatum, neither $D_1$-nor $D_2$-R mRNA levels were modified by hypoxia (data not shown).

*Table 1.* Dopamine $D_1$- and $D_2$-R transcript levels in developing rabbit carotid body

| | DA $D_1$-R mRNA transcript level % change from control (normoxia) | | DA $D_2$-R mRNA transcript level % change from control (normoxia) | |
|---|---|---|---|---|
| | Hypoxia ($F_iO_2$=8%) | | Hypoxia ($F_iO_2$=8%) | |
| Age | 6h | 24h | 6h | 24h |
| 1 day | - 16.0 ± 1.9* | - 39.6 ± 1.8*+ | - 22.2 ± 3.9* | - 23.1 ± 2.9* |
| 25 days | - 32.5 ± 1.5* | - 23.3 ± 4.6* | - 19.6 ± 1.3* | - 20.3 ± 1.2* |
| adult | - 47.5 ± 7.2* | - 64.9 ± 4.5*+ | - 40.6 ± 8.5* | - 44.9 ± 8.4* |

Values are mean ± sem. * $p < 0.01$ vs control; + $p < 0.01$ vs 6h

# 4. DISCUSSION

Our results show that hypoxia down regulated both CB DA $D_1$- and $D_2$-R mRNA and this down-regulation is 2-3 fold more in adult than in young rabbits. However, the exposure duration to hypoxia affected $D_1$- but not $D_2$-R mRNA expression levels.

Athough the results obtained in control CB were in line with previous observations (Bairam *et al.*, 1996a; 1998), they further added new information as they showed that the CB of 1 and 25 days old rabbits contains the $D_1$-R mRNA as in adults (Bairam et al; 1998). Hence, the CB of newborn and adult rabbits contains both DA R mRNAs. Exposure to hypoxia for 24 – 48h significantly decreases CB $D_2$-R mRNA expression level (Huey and Powell, 2000). The present study added more information and showed that both DA R mRNAs in the CB are down regulated by hypoxia in newborns as well as in adults. Different mechanisms may be involved in this regulation phenomenon. Hypoxia induces a sustained increase of DA release from the CB (Fidone *et al.*, 1997). As with the central nervous system (Sidhu *et al.*,

1999; Missale *et al.*, 1998; Gerfen *et al.*, 1990), it might be possible that DA release from the chemoreceptor cells regulated the expression levels of $D_1$- and $D_2$-R mRNA. Since hypoxia down-regulated the CB DA $D_1$- and $D_2$-R transcripts levels 2 –3 fold more in adult than pups rabbits, an age related mechanism may also be involved in hypoxia-induced decrease in DA receptor mRNA levels. This age-related mechanism might be due to the fact that the sensitivity of the type I cells to $O_2$ and/or the sensitivity of DA receptors towards their substrate, DA, is/are more mature in adult than in pup rabbits. In fact, the $D_2$-autoreceptors that control negatively DA release from the CB are less functional in pup than in adult rabbits (Bairam et al., 2000). Finally, hypoxia induced time-dependent changes in $D_1$-R mRNA expression levels only. It is suggested that 6h exposure to hypoxia was sufficient to produce maximal effects on $D_2$-R RNA expression levels while longer duration may be necessary for the $D_1$-R. It is still to be examined if the level observed after 24h exposure is maximal for the $D_1$-R. Further studies are needed to determine whether the hypoxia-induced decrease in CB DA receptor transcript levels is due to reduced gene transcription or to change in mRNA stability.

DA at the CB level may be involved in the ventilatory adaptation to hypoxia. It is tempting to suggest that the effect of DA on chemoreceptor function may not be due to activation of $D_2$-R alone, at least, in response to short term (6 and 24h) exposure to hypoxia as both CB $D_1$- and $D_2$-R mRNAs are modulated by hypoxia.

## ACKNOWLEDGEMENTS

We are grateful to Pierre De-Grandpré for his excellent technical assistance building the hypoxia room. A. B. and V.J. are Research Scholar of the Research Center, HSFA and Téléthon de la recherche sur les maladies infantiles. Y. L. is Research Scholar of the FRSQ. This study was supported by a grant from the Association Pulmonaire de Québec.

## REFERENCES

Almaraz, L., Perez-Garcia, M. T., and Gonzalez, C., 1991, Presence of D1 receptors in the rabbit carotid body. *Neurosci. Lett.* 132:259-262.

Bairam, A., Dauphin, C., Rousseau, F., and Khandjian, EK., 1996a, Expression of dopamine D2 receptor mRNA isoforms at the peripheral chemoreflex afferent pathway in developing rabbits. *Am. J. Respir. Cell. Mol. Biol.* 15: 374-381.

Bairam, A., Marchal, F., Cottet-Emard, J.M., Basson, H., Pequignot, J. M., Hascoet, J. M., and Lahiri, S., 1996b, Effects of hypoxia on carotid body dopamine content and release in developing rabbits. *J.Appl. Physiol.* 80: 20-24.

Bairam, A., Frenette, J., Dauphin, C., Carroll, J.L., and Khandjian, E.W., 1998, Expression of dopamine D1-receptor mRNA in the carotid body of adult rabbits, cats and rats. *Neurosci. Res.* 31: 147-154.

Bairam, A., Néji, H., De-Grandpré, P., and Carroll, J.L., 2000, Autoreceptor mechanism regulating carotid body dopamine release from adult and 10-day-old rabbits. *Respir Physiol.* 120: 27-34.

Bairam, A., Carroll, J., Labelle, Y., Khandjian, E.W., Differential changes in dopamine $D_2$- and $D_1$-receptor mRNA levels induced by hypoxia in the arterial chemoreflex pathay organs in one day old and adult rabbits. *Biol. Neonate* (in revision).

Donnelly, D.F., and Doyle, T.P., 1994, Developmental changes in hypoxia-induced catecholamines release from rat carotid body, in vitro. *J. Physiol.* 475, 267-275.

Fidone, S. J., Gonzalez, C., Almaraz, L., and Dinger B., 1997, Cellular mechanisms of peripheral chemoreceptor function. In: *The Lung*, vol. 2, (Crystal, R.J., West, J.B., Barnes, P.J. and Weibel, E.R. eds.), Lippincott-Raven, Philadelphia, New York, pp. 1725-1746.

Gerfen, C.R., Engber, T.M., Mahan, L.C., Susel, Z., Chase, T.N., Monsma, F.J., and Sibley, D.R., 1990, D1 and D2 dopamine receptor-regulated gene expression of striatonigral and striatopallidal neurons. *Neuroscience* 250: 1429-1432.

Huey, K.A., and Powell, F.L., 2000, Time-dependent changes in dopamine $D_2$-receptor mRNA in the arterial chemoreflex pathway with chronic hypoxia. *Mol. Brain Res.* 75: 264-270.

Missale, C., Russel Nash, S., Robinson, S.W., Jaber, M., and Caron, M.G., 1998. Dopamine receptors: from structure to function. *Physiological Rev.* 78: 189-225.

Sidhu, A., Olde, B., Humblot, N., Kimura, K., and Gardner, N., 1999, Regulation of human D1 dopamine receptor function and gene expression in SK-N-MC neuroblastoma cells. *Neuroscience*, 91: 537-547.

# Ventilatory Response to $CO_2$ in New born Mouse

MARÍA CRISTINA ORDENES, JAIME EUGENÍN and ISABEL LLONA
*Laboratory of Neural Systems, Department of Biology, Faculty of Chemistry and Biology, University of Santiago, Casilla 40 Correo 33, Santiago CHILE.*

## 1. INTRODUCTION

Mice are an increasingly important model system to study respiratory control, mainly due to the use of transgenic approaches (Katz and Balkowiec, 1997; Aizenfisz et al., 2002) and the ability to produce in vitro preparations where respiratory rhythm can be studied (Hilaire and Duron, 1999; Eugenín et al., 2001). A number of factors may alter the magnitude of the ventilatory response to the $CO_2$ such as age (Coates and Silvis, 1999; Matsuoka and Mortola, 1995), anesthesia, genetic differences in sensibility to $CO_2$ (Tankersley *et al.*, 2002) or circadian pattern. Therefore we studied the evolution of the ventilatory response to $CO_2$ during the first week of life, when important changes in the respiratory system of mice and rats occurs (Paton *et al.*, 1994).

Moderate hypoxia and hypercapnia are potent stimulants which evoke a marked hyperventilation that results from a reinforcement of the activity of the medullary neuronal network responsible for the generation and maintenance of the basic respiratory rhythm. Multiple signals are received, processed, and transmitted by way of the nucleus tractus solitarius (NTS) to provide peripheral and central information to respiratory related networks. The NTS is a region harboring neurons that respond to $CO_2$ stimulation via postsynaptic activation as well as neurons having putative chemosensory function (Haxhiu *et al.*, 1996; Nattie, 2000). Thus, we expected to find activation of the NTS in newborn mice that respond to hypercapnia.

*Chemoreception*, Edited by Pequignot et al.
Kluwer Academic/Plenum Publishers, New York, 2003

The goals of this study were to characterize in intact, unanesthetized mice developmental changes in breathing pattern during the first postnatal week and to determine whether the hypercapnic ventilatory response in mice is accompanied by activation of NTS

## 2. MATERIALS AND METHODS

*Animals.* Newborn CF-1 mouse of both sexes ranging in age from postnatal day 0 (day of birth, P0) to 7 (P7) were studied. All procedures were performed in accordance with the European Communities Council Directive of 24 november 1986 (86/609/EEC) regarding the care and use of animals for experimental procedures and approved by the Bioethics Committee of the Universidad de Santiago de Chile.

*Measurement of lung ventilation.* Baseline ventilatory parameters and responses to hypercapnia were measured in unanesthetized mice using head out whole-body plethysmography. After acclimatization for 10 min, $CO_2$ (10% $CO_2$, 21% $O_2$ balanced with $N_2$) was delivered during 30 minutes. The tests were performed 10 a.m and 1 p.m at constant temperature of 30°C. For each $CO_2$ exposure, the respiratory parameters: Tidal volume ($V_T$), respiratory frequency ($f_R$) and minute ventilation (Ve) for 10 respiratory cycles were analyzed. Significance ($p< 0.05$) was determined using Wilcoxon Sign-Rank test.

*Immunohistochemistry.* Two hours after the end of a 15 min $CO_2$ stimulation or control period, mice were anaesthetised with ether and transcardially perfused with phosphate-buffered saline (PBS) followed by 4% paraformaldehyde-0.1% picric acid in PBS. Brainstem coronal sections (30 μm) from control and $CO_2$ stimulated animals were processed free floating simultaneously. After blocking in 5% normal goat serum in PBS, sections were incubated with anti c-Fos antibody (Ab-5, Calbiochem, USA), for 24 h, and processed using the avidin-biotin immunoperoxidase method with a commercial kit (ABC Elite Kit, Vector Laboratories, USA). Fos immunopositive nuclei of the NTS at the level of the area postrema (-7.31 to -7.61 from Bregma; Paxinos and Franklin, 1997) were counted using NIH Image software.

## 3. RESULTS

Baseline $V_T$ and $f_R$ increased during the first week of life. When normalized by weight, $V_T$ was lower at P2 and P7 than at P0 ($7.6 \pm 4.4$ μl/g; n= 12). The $f_R$ normalized by weight was significantly higher at P1 and P2 than at P0 ($47.7 \pm 14.7$ $min^{-1}$/g: n= 12) Ventilation (Ve) was higher at P1 and P4 when compared to P0. Figure 1 shows the ventilatory response to

$CO_2$ stimulation. The respiratory parameters $V_T$, $f_R$ and Ve are expressed as percentage of basal values before the stimulus. The increase in Ve reflected changes in $V_T$. However, at P0 hypercapnia produced also an increase in $f_R$.

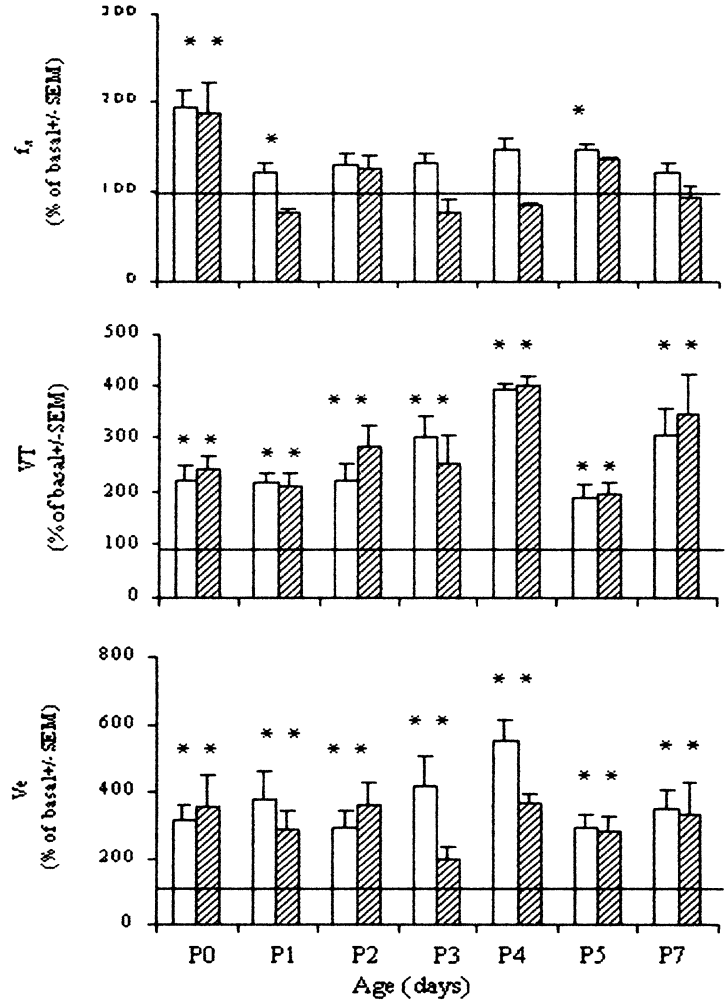


*Figure 1.* Response to 10% $CO_2$ stimulation during the first postnatal week. $CO_2$ was delivered for 30 min and respiratory parameters ($V_T$, $f_R$, Ve) were recorded 10 min prior to (Basal: horizontal line), 1 min immediately after (empty bar), and the last 10 min (hatched bar) of the $CO_2$ stimulation period. The asterisks show values significantly different ($p<0.05$) from basal. Number of animals: P0 (9), P1(6), P2 (5), P3 (5), P4 (4), P5 (4), P7 (7).

The increase in Ve is maintained during the period of $CO_2$ challenge at all ages studied other than P4, where Ve could not be sustained during the 30 minutes of stimulation. The $CO_2$ stimulation produced an increase in the Fos expression at the level of the NTS as shown in figure 2. The number of

labeled cells increased (x 2) after 15 minutes of $CO_2$ stimulation (average of 7 animals).

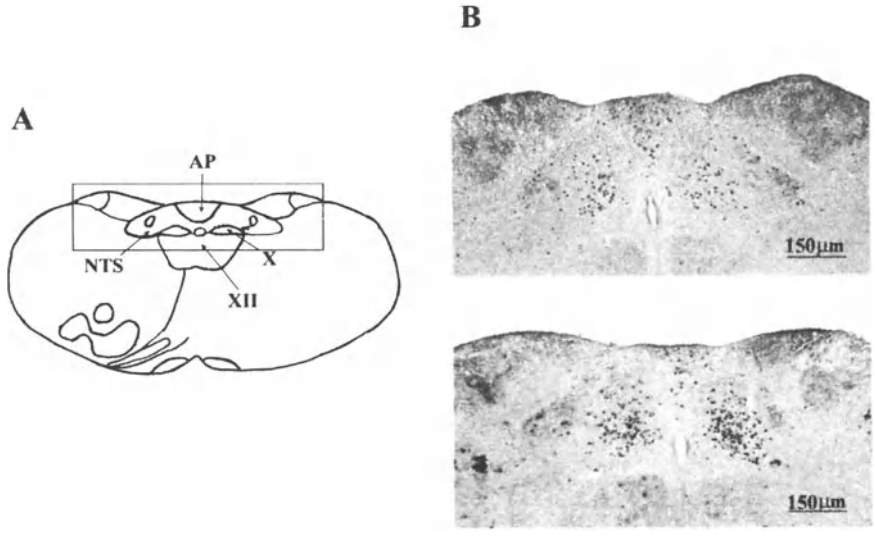


***Figure 2***. A) Neuroanatomical location of the mouse brainstem depicts the NTS. Brainstem sections obtained from this region were analyzed for FOS expression using immunohistochemistry techniques (See details in Methods). B) Photomicrograph showing FOS expression from control (upper) and $CO_2$ stimulated (lower) P0 mice.

## 4. DISCUSSION

This is the first report on the breathing pattern for the CF-1 mice strain at early postnatal life. A general feature of breathing pattern data in neonatal mice is their variability (Jacquin *et al.*, 1996). Although methodological differences will account for some of the variability, genetic differences between strains will also contribute (Tankersley *et al.*, 1994). Thus, it is necessary to establish the profile of the breathing pattern for different mouse strains taking into account the increasing interest in understanding respiratory deficits of transgenic mice (Erickson *et al.*, 1996) and the role of these deficits in the inability of many transgenic animals to survive beyond one or two days (Funk *et al.*, 1997; Jacquin *et al.*, 1996). The pattern of $CO_2$

response in the CF-1 mice is characterized by an increase in minute ventilation mainly sustained on changes in $V_T$. However, at the day of birth the change in Ve is also supported by changes in $f_R$. This pattern of response is different from the Swiss IOPS mice recently described by Renolleau *et al.* (2001) and young rats (Stunden *et al.*, 2001), where the rise in Ve produced by increasing inspired $CO_2$, is associated with an increase in $V_T$ but not in $f_R$. The difference may be ascribed to a different $CO_2$ sensitivity. Recently, Tankersley *et al.* (2002) demonstrated that genetic determinants confer variation between inbred mouse strains with respect to the magnitude and pattern of ventilation during hypercapnic challenge.

An attractive and widely accepted tool to map multisynaptic neuronal pathways is Fos immunohistochemistry. Using this approach we were able to show an increase in the Fos expression in the NTS with a $CO_2$ stimulation of only 15 minutes. In previous studies larger periods were always used. With larger stimulation periods it is possible that Fos expression is the result not only of the respiratory effect but secondary to metabolic changes. Wickström *et al.*, (1999) did not find increased expression of Fos in NTS after one hour 12% $CO_2$ stimulation. They used newborn rats and found mainly increase in the VMS and could not confirm earlier reports on other extra VMs $CO_2$ sensitive areas, like NTS described in the adult (Sato *et al.,* 1992, Teppema *et al.*, 1997). In summary, we characterized the ventilatory response to $CO_2$ in neonatal CF-1 mice. The mechanism underlying the changes in $V_T$ and $f_R$ in response to $CO_2$, remains to be investigated. Our results showed that the activation of NTS is part of the events involved in this response as early as the day of birth.

## ACKNOWLEDGMENTS

This work was supported by grants FONDECYT # 1000025 and DICYT-USACH # 020043ILR.

## REFERENCES

Aizenfisz, S., Dauger, S., Durand, E., Vardon, G., Levacher, B., Simonneau, M., Pachnis, V., Gaultier, C., and Gallego, J., 2002, Ventilatory responses to hypercapnia and hypoxia in heterozygous c-ret newborn mice. Respir. Physiol. Neurobiol. 131: 213-222.

Coates, E.L., and Silvis, M.L., 1999, Age-related changes in the ventilatory response to inspired $CO_2$ in neonatal rats. Res. Physiol. 118: 173-179.

Erickson, J.T., Conover, J.C., Borday, V., Champagnat J., Barbacid M., Yancopoulos, G., Katz, D.M. 1996, Mice lacking brain-derived neurotrophic factor exhibit visceral sensory neuron losses distinct from mice lacking NT4 and display a severe developmental deficit in control of breathing. J. Neursci. 16: 5361-5371.

Eugenin, J., Llona, I., Infante, C., Ampuero, E., 2001, In vitro approach to the chemical drive of breathing. Biol. Res. 34: 117-122.

Franklin, K.B.J. and Paxinos, G., 1997, The mouse brain in stereotaxic coordinates. Academic Press Inc., USA.

Funk, G.D., Johnson, S.M., Smith, J.C., Dong, X.W., Lai, J., Feldman, J.L., 1997, Functional respiratory rhythmgenerating network in neonatal mice lacking NMDAR1 gene. J. Neurophysiol. 78: 1414-1420.

Haxhiu, M.A., Yung, K., Erokwu, B., Cherniak, N.S., 1996, $CO_2$ -induced expression of c-fos expression in the CNS catecholaminergic neurons. Res. Physiol. 105: 35-45.

Hilaire, G. and Duron, B., 1999, Maturation of the mammalian respiratory system. Physiol. Rev. 79: 325-359.

Jacquin, T.D., Borday, V., Schneider-Maunoury, S., Topilko, P., Ghilini, G., Kato, F., Charnay, P., Champagnat, J., 1996, Reorganization of pontine rhythmogenic neuronal networks in Krox-20 knockout mice. Neuron 17: 747-758.

Katz, D.M., and Balkowiec, A., 1997, New insight into the ontogeny of breathing from genetically engineered mice. Curr. Opin. Pulm. Med. 3: 433-439.

Matsuoka, T., and Mortola, J.P., 1995, Effects of hypoxia and hypercapnia on the Hering-Breuer reflex of the concious newborn rat. J. Appl. Physiol. 78: 5-11.

Nattie, E., 2000, Multiples sites for central chemoreception: their roles in response sensitivity and in sleep and wakefulness. Res. Physiol. 122: 223-235.

Paton, J., Ramirez, J.M., Richter, D.W., 1994, Mechanism of respiratory rhythm generation changes profoundly during early life in mice and rats. Neurosci. Lett. 170: 167-170.

Renolleau, S., Dauger, S., Autret, F., Vardon G., Gaultier C., Gallego, J., 2001, Maturation of baseline breathing and hypercapnic and hypoxic ventilatory responses in newborn mice. Am. J. Physiol. Regulatory Integrative Comp. Physiol. 281: R1746-R1753.

Robison, D.M., Kwok, H., Adams B.M., Peebles, K.C., Funk, G.D., 2000 Development of the ventilatory response to hypoxia in Swiss CD-1 mice. J. Appl. Physiol. 88: 1907-1914.

Sato, M., Severinghaus, J.W., Basbaum, A., 1992, Medullary $CO_2$ -chemoreceptor neuron identification by c-fos immunocytochemistry. J. Appl. Physiol. 73: 96-100.

Stunden, C.E., Filosa, J.A., García, A.J., Dean, J.B., Putman, R.W., 2001. Development of in vivo ventilatory and single chemosensitive neuron responses to hypercapnia in rats. Resp. Physiol. 127: 135-155.

Tankersley, C.G., Haxhiu, M.A., Gauda, E.B., 2002, Differential $CO_2$ -induced c-fos gene expression in the nucleus tractus solitarii of inbred mouse strains. J. Appl. Physiol. 92: 1277-1284

Tankersley, C.G., Fitzgerald, R.S., Kleeberger, S.R., 1994, Differential control of ventilation among inbred strains of mice. Am. J. Physiol. Regulatory Integrative Comp. Physiol. 267: R1371-R1377.

Teppema, L.J., Veening, J-G., Kranenburg, A., Dahan, A., Berkenbosch, A., Olievier, C., 1997, Expression of c-fos in the rat brainstem after exposure to hypoxia and to normoxic and hyperoxic hypercapnia. J. Comp. Neurol. 388: 169-190.

Wickström, H.R., Holgert, H. Hökfelt, T., Lagercrantz, H., 1999. Birth-related expression of c-fos, c-jun and substance P mRNAs in the rat brainstem and pia mater: possible relationship to changes in central chemosensitivity. Dev. Brain Res. 112: 255-266.

# Long-term effects of Neonatal Cryoanesthesia on Hypoxic Ventilatory Response in Weanling Rats Depend on Neonatal Testosterone

JOSEPH VINCENT, SOLIZ JORGE, and PEQUIGNOT JEAN-MARC
*CRSFA, CHUQ, dpt pediatrics, University Laval, Quebec, Canada; University Irchel Zurich, Switzerland and Lab physiology, Université Claude Bernard UMR CNRS 5123, Lyon, France.*

## 1. INTRODUCTION

Among the factors known to interact with the developmental plasticity of the respiratory controller network, gender and perinatal testosterone secretion have recently been described to influence the ventilatory response to acute or chronic hypoxia before puberty (Mortola *et al.*, 1996; Joseph *et al.*, 1999; Joseph *et al.*, 2000). In the present experiments, we used cryoanesthesia as a tool to perform neonatal gonadectomy to address the hypothesis that endogenous neonatal testosterone secretion in male pups could affect the hypoxic ventilatory response (HVR – 10 % $O_2$) in weanling (20-22 day-old) male rats. We selected weaning as an age of fully mature HVR (Joseph *et al.*, 2000), while rats are still sexually immature, thus allowing to discard any effect related to endogenous secretion of adult testes (Tatsumi *et al.*, 1994). Our findings show that cryoanesthesia by itself produces a marked decrease of HVR in weanling rats, and this effect was dependent on the neonatal testosterone secretion. Because the cryoanesthesia approach is in many ways similar to surgical processes used for arterial switch operation in human neonates (performed under cardiopulmonary bypass, cardiocirculatory arrest and deep hypothermia), our findings may be potentially relevant for long term outcomes of infants submitted to this surgical procedure.

*Chemoreception*, Edited by Pequignot et al.
Kluwer Academic/Plenum Publishers, New York, 2003

## 2. HVR IN WEANLING MALE RATS AFTER CRYONESTHESIA: INTERACTION WITH NEONATAL TESTOSTERONE

Newborn male pups were deeply anesthetized by immersion in melting ice for 5 minutes then placed on a chilled metal plate for surgery (5 minutes). This procedure (also called cryoanesthesia) results in reversible cardiac and respiratory arrest and is highly recommended for surgical procedure in newborn rats (Danneman *et al.*, 1997). Following cryoanesthesia the animals were placed under a heating lamp for auto-resuscitation (none of the animals died following surgery). Pups were then returned to their mothers within one hour following the onset of anesthesia and left undisturbed until weaning. A subset of rats (n=6) was used to assess the effect of cryoanesthesia (cryo) by comparing their HVR with intact male rats (n=7). Another group was gonadectomized during cryoanesthesia (Cryo gdx - n=8) and some of these gonadectomized rats received an injection of testosterone (1 mg, sc) following surgery (Cryo gdxT - n=8). There were no significant effects of neonatal treatment on body weight in weanling rats (figure 1 p=0.14 - ANOVA). Cryoanesthesia by itself resulted in decreased HVR in weanling rats (figure 2 – upper panels) owing to a marked reduction of the tidal volume response. Gonadectomy was able to reverse the effect of cyoanesthesia (figure 1 - lower panels), and this effect was suppressed if gonadectomized animals received testosterone.

*Figure 1:* Body weight (g) of intact weanling rats or following neonatal cryoanesthesia with or without testosterone injection. All values are means ± sem. No significant effects of neonatal treatment appeared after ANOVA analysis (p=0.14).

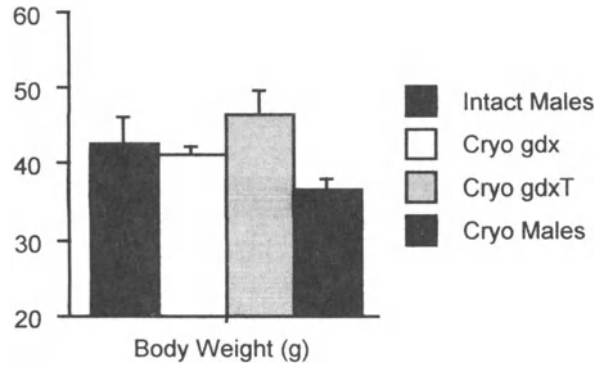

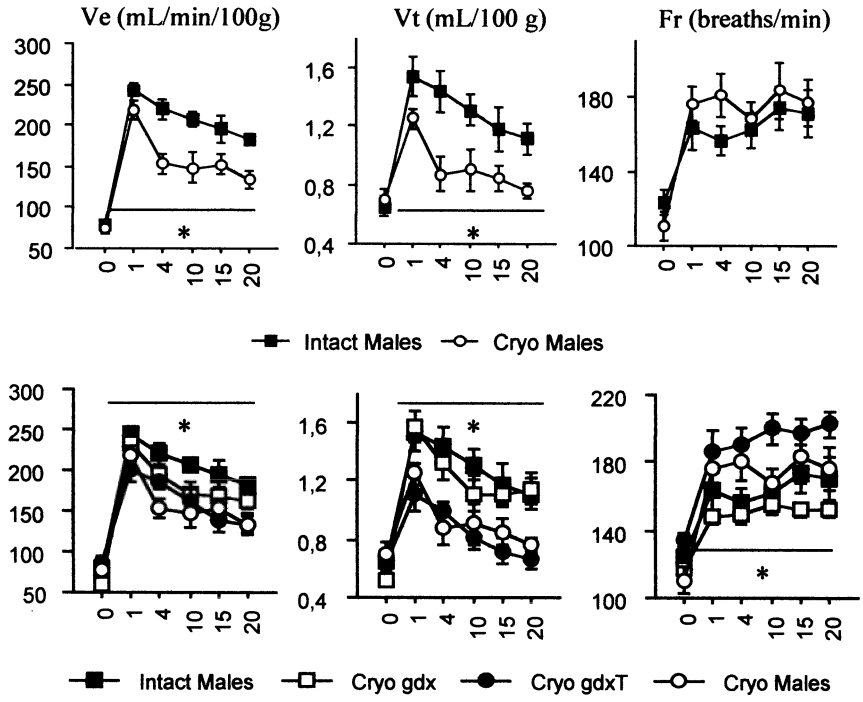


*Figure 2:* Minute ventilation (Ve), tidal volume (Vt) and respiratory frequency (Fr) measured in intact weanling males and following neonatal cryoanesthesia (upper panels) or following cryonasthesia and gonadectomy with or without testosterone injection (lower panels). All measurements have been done in 20-22 day-old rat pups by whole body plethysmography during an acute exposure to hypoxia (minutes in hypoxia are shown on x axis). All values are means ± sem. * indicates a significant ($p<0.05$) group effect after 2-way ANOVA.

## 3. DISCUSSION

The present data show that cryoanesthesia induces a marked decrease of HVR in weanling rats. Additionally, there was a clear interaction between the neonatal testosterone secretion and the effect of neonatal cryoanesthesia. Cryoanesthesia is currently viewed as a method of choice for neonatal surgery (Danneman *et al.*,1997). One of the interesting effects of cryonaesthesia is that it produces a cardiorespiratory arrest and deep hypothermia. This pattern is very close to what is used in neonatal cardiac surgery which is performed under continuous low flow cardiopulmonary bypass, combined with cardiocirculatory arrest in deep hypothermia. Although required for heavy cardiac surgery in newborn, recent studies have

reported long-term behavioral and motor coordination defects in infants that have been submitted to this surgery as neonates (Bellinger *et al.*, 1999; Hovels-Gurich *et al.*, 2002). By using an animal model that is almost similar, the present data show that alterations of the respiratory control system may also appear and that these effects are dependent on the neonatal testosterone surge known to occur in newborn mammals (MacLusky *et al.*, 1981). The site(s) of hormonal interaction remain to be determined, but are likely to involve changes in multiple targets including the carotid bodies, central respiratory areas and/or peripheral effectors of the chemoreflex pathway.

## ACKNOWLEDGEMENTS

Funded by Centre National de la Recherche Scientifique (France), Fondation de la Recherche pour les Maladies Infantiles (Quebec, Canada) Association Pulmonaire du Quebec (Quebec, Canada) and Chaire de périnatalogie Jeanne et Jean-Louis Lévesque (Québec, Canada).

## REFERENCES

Bellinger, D.C., Wypij, D., Kuban, K.C., Rappaport, L.A., Hickey, P.R., Wernovsky, G., Jonas, R.A. and Newburger, J.W., 1999, Developmental and neurological status of children at 4 years of age after heart surgery with hypothermic circulatory arrest or low-flow cardiopulmonary bypass. *Circulation* 100(5): 526-532.

Danneman, P.J. and Mandrell, T.D., 1997, Evaluation of five agents/methods for anesthesia of neonatal rats. *Lab Anim Sci* 47(4): 386-395.

Hovels-Gurich, H.H., Konrad, K., Wiesner, M., Minkenberg, R., Herpertz-Dahlmann, B., Messmer, B.J. and Von Bernuth, G., 2002, Long term behavioural outcome after neonatal arterial switch operation for transposition of the great arteries. *Arch Dis Child* 87(6): 506-510.

Joseph, V., Soliz, J., Pequignot, J., Sempore, B., Cottet-Emard, J.M., Dalmaz, Y., Favier, R., Spielvogel, H. and Pequignot, J.M., 2000, Gender differentiation of the chemoreflex during growth at high altitude: functional and neurochemical studies. *Am J Physiol, Regulatory Integrative and Comparative Physiology* 278(4): R806-R816.

Joseph, V., Soliz, J., Pequignot, J.M., Favier, R. and Spielvogel, H., 1999, Gender-related differences in the control of breathing in prepubertal high altitude rats: effect of the neonatal testosterone secretion. *Adv Exp Med Biol* 474: 393.

MacLusky, N.J. and Naftolin, F., 1981, Sexual differentiation of the central nervous system. *Science* 211: 1294- 1303.

Mortola, J.P. and Saiki, C., 1996, Ventilatory response to hypoxia in rats: gender differences. *Respir Physiol* 106: 21-34.

Tatsumi, K., Hannhart, B., Pickett, C.K., Weil, J.V. and Moore, L.G., 1994, Effects of testosterone on hypoxic ventilatory and carotid body neural responsiveness. *Am J Respir Crit Care Med* 149(5): 1248-1253.

# Systemic and Cellular Responses to Intermittent Hypoxia: Evidence for Oxidative Stress and Mitochondrial Dysfunction

YINGJIE PENG, GUOXIANG YUAN, JEFFREY L. OVERHOLT, GANESH K. KUMAR, AND NANDURI R. PRABHAKAR*
*School of Medicine, Case Western Reserve University, Cleveland, OH, USA.*

## 1. INTRODUCTION

Episodic hypoxia is associated with recurrent apnea syndromes (central or obstructive apneas). Epidemiological studies have shown good correlation between apneas and hypertension, myocardial infarctions and abnormalities in ventilatory control system (Nieto et al., 2000). Studies on experimental animal models have demonstrated that hypoxia, rather than hypercapnia, is the primary stimulus that is responsible for developing cardiovascular abnormalities (see Fletcher, 2001 for ref).

Studies on human subjects with obstructive and central apneas led to the idea that recurrent apneas lead to altered carotid body function, which in turn contributes to development of hypertension (Narkiewicz *et al.*, 1999). In experimental animals, denervation of carotid bodies prevents development of hypertension resulting from chronic intermittent hypoxia (CIH; Fletcher, 2001). Although these studies suggest that CIH leads to altered carotid body function, there are no studies demonstrating the effects of CIH on carotid body sensory activity. Therefore, *one objective* of the present study was to examine the effects of CIH on carotid body sensory activity.

*Chemoreception*, Edited by Pequignot et al.
Kluwer Academic/Plenum Publishers, New York, 2003

It is being increasingly recognized that altered gene expression and the resulting *de novo* protein synthesis are critical for adaptations of physiological systems during chronic hypoxia (see Prabhakar, 2001 for ref). Whether intermittent hypoxia also alters gene expression, and if so by what mechanisms has not been yet explored. The *second objective* of the present study was to assess the effects of intermittent hypoxia on gene expression and to elucidate the possible mechanism(s).

# 2. MATERIALS AND METHODS

## 2.1 Experiments on Carotid Body Sensory Activity

Experiments were performed on adult, male rats (Sprague-Dawley, 250-350 g). Animals were subjected to 10 days of intermittent hypoxia for 8h/day. This was accomplished by placing awake, unrestrained animals in a specialized chamber wherein inspired oxygen levels were alternated between 15s of hypoxia (5% $O_2$) and 5min of 21% $O_2$ (9 episodes/h). The duration of gases was controlled by timed solenoid valves. Animals were subjected to intermittent hypoxia between 9:00 AM and 5:00 PM. Parallel experiments were performed on animals exposed to alternating cycles of 21% $O_2$ that served as controls. Following exposure to either intermittent hypoxia or to normoxia, animals were anesthetized with urethane (1.2 g/kg; i.p.). A femoral artery and vein were cannulated for measurements of arterial blood pressure and for systemic administration of fluids, respectively. Animals were paralyzed with pancuronium bromide (2.5mg/kg/h; i.v.) and mechanically ventilated with a respirator connected to tracheal cannula. Carotid body sensory activity was recorded as described previously (Gragg *et al.*, 1994). Body temperature of the animals was maintained at 38 ± 1°C by means of heating pad. Arterial blood samples were collected for measurements of $pO_2$, $pCO_2$, and pH.

## 2.2 Experiments with cell cultures

PC12 cells were grown in Dulbecco's Modified Eagle's medium (DMEM) supplemented with 10% horse serum, 5% fetal bovine serum (FBS), 100 U/ml penicillin and 100 μg/ml streptomycin. All experiments were performed in serum free medium. Cell cultures were exposed to alternating cycles of hypoxia (1% $O_2$; 15s) and normoxia (21% $O_2$; 4min) in a humidified Lucite chamber at 37°C. The durations of hypoxia and

normoxia were adjusted by timed solenoid valves. $O_2$ levels in the tissue culture medium and in the chamber were monitored by an oxygen electrode (Lazar) and $O_2$ analyzer (Beckman LB2), respectively, and recorded on a strip chart recorder. Total cellular RNA was isolated by Rneasy mini kit method (Qiagen) following manufacturers protocol. *c-fos* and β-actin mRNAs were analyzed by northern blot analysis as described previously (Premkumar *et al.*, 2000). Changes in mRNAs were quantified by optical density measurements.

# 3. RESULTS

## 3.1 CIH-induces long-term facilitation (LTF) of carotid body sensory activity

The effect of acute repetitive hypoxia (10 episodes of 15s 12% $O_2$ interspersed with 5 min hyperoxia) on the carotid body sensory activity was examined in naïve and CIH conditioned rats. In naïve animals, sensory activity increased with each hypoxic episode, returned to baseline after terminating each hypoxic challenge and remained at this level for 60 min. Whereas to a given hypoxic challenge, carotid body sensory response was greater in CIH conditioned rats ($P<0.01$). More importantly, baseline activity progressively increased with each successive hypoxic challenge and this increase in baseline activity persisted for 60 min after terminating the acute hypoxic challenges. On average, baseline activity increased by 250% of pre-hypoxic levels. This persistent elevation in baseline sensory activity will be referred to as long-term facilitation (LTF) of sensory activity. The LTF in sensory activity is not due to changes in blood pressure or blood gases, as these variables were comparable between baseline and the post-hypoxic period ($P> 0.05$). In sharp contrast, exposing animals to a comparable, cumulative duration of sustained hypoxia (4h, which is equivalent to 10 days of CIH) did not induce LTF in carotid body activity in any of the six animals studied.

Recently, it has been suggested that episodic hypoxia represents a form of oxidative stress and reactive oxygen species (ROS) play an important role in pathophysiological changes resulting from recurrent hypoxia (Prabhakar, 2002). The following experiments were performed to test whether ROS are involved in CIH-induced LTF. Aconitase enzyme activity was monitored in carotid bodies to test whether CIH increases generation of $O_2^{\bullet-}$. Increased $O_2^{\bullet-}$ production should inhibit aconitase activity. Aconitase activity was decreased by 83% in carotid bodies from CIH-conditioned animals

indicating increased generation of $O_2^{\bullet-}$. To test the functional significance of $O_2^{\bullet-}$, rats were treated with a stable superoxide dismutase (SOD) mimetic (MnTMPyP; 5 mg/ kg/day; I.P), a potent scavenger of $O_2^{\bullet-}$, or vehicle (saline; n =6 each) before subjecting them to CIH conditioning. LTF was markedly attenuated in SOD mimetic treated animals ($P<0.01$; ANOVA). This increased production of $O_2^{\bullet-}$ may arise from mitochondria. Analysis of mitochondrial electron transport chain revealed significant decreases in complex I activity in carotid bodies from CIH-conditioned animals.

### 3.2 Intermittent Hypoxia induces *c-fos* proto-oncogene expression in cell cultures and involves ROS-dependent mechanisms

We examined the effects of recurrent hypoxia on *c-fos* gene expression as a read out of cellular response and explored the involvement of ROS. *c-fos* mRNA and *c-fos* promoter activity (–356 to +109 fragment of the *c-fos* promoter linked to luciferase) were examined in pheochromocytoma (PC12) cells exposed to normoxia or to intermittent hypoxia (IH). IH paradigm consisted of 15s of 1% $O_2$ followed by 4min of 21%$O_2$. *c-fos* mRNA as well as promoter activities were significantly elevated in cells exposed to IH (3.0- 3.5 fold, $P<0.01$, n =5). Pre-treatment of cells with SOD mimetic (MnTMPyP; 25μM), a potent scavenger of $O_2^{\bullet-}$, completely prevented *c-fos* mRNA and promoter activation by IH. Aconitase enzyme activity (an index of $O_2^{\bullet-}$) decreased by 78% in IH exposed cells, suggesting increased generation of $O_2^{\bullet-}$. The effects of IH on *c-fos* expression were associated with marked decrease in mitochondrial complex I, but not complex III activities.

## 4. DISCUSSION

The present results demonstrate that IH profoundly influences carotid body function in intact animals and induces gene expression in cell cultures. More importantly, our data indicates that for a given duration of hypoxia IH is more potent than sustained hypoxia in eliciting systemic cellular responses.

In intact animals CIH conditioning induced ROS-dependent plasticity in the carotid body manifested as LTF in the sensory activity. More importantly, comparable, cumulative duration of sustained hypoxia was unable to elicit LTF. These observations suggest that induction of LTF is unique to IH. The fact that IH-induced LTF is prevented by SOD mimetic suggests that ROS play an important role in inducing LTF. Marked

inhibition of aconitase activity in CIH-conditioned carotid bodies further support the idea that IH indeed increases ROS generation in the chemoreceptor tissue. Further, our data suggests that mitochondria are one important source of ROS generation during IH. What might be the functional significance of LTF in the sensory activity? Recurrent apnea patients exhibit increased sympathetic activity and elevated blood pressure even in daytime when there are no apneas. Our finding that CIH induces LTF may be of relevance to elevated blood pressure and sustained sympathetic activation seen in sleep apnea patients. It is likely that LTF in carotid body sensory reflexly triggers sympathetic activation, which in turn contributes to elevated blood pressures. Such a possibility is supported by the observations that recurrent apnea patients, who experience repetitive hypoxia, no longer develop hypertension after removal of carotid bodies (see Prabhakar, 2001 for ref), and denervation of the carotid bodies prevents elevations in sympathetic nerve activity in CIH conditioned rats (see Fletcher, 2001 for ref).

It is clear from our data that IH stimulates *c-fos* proto-oncogene expression in cell cultures. These findings are consistent with an early study reporting increased c-Fos protein expression in central nervous system of CIH-conditioned rats (Greenberg *et al.*, 1999) Our data further demonstrate that *c-fos* stimulation by recurrent hypoxia requires transcriptional activation. More importantly, our results demonstrate that for a given duration of hypoxia, IH is more potent in activating *c-fos* than sustained hypoxia. What makes the recurrent more effective than sustained hypoxia? The feature that distinguishes recurrent from sustained hypoxia is the periodic normoxic episodes. By analogy, recurrent hypoxia resembles ischemia-reperfusion. Since reperfusion results in increased generation of ROS (Ambrosio *et al.*, 1995) and ROS stimulate gene expression (see Dröge, 2002 for ref), we reasoned that the effects of recurrent hypoxia are mediated by ROS. A role for ROS in IH-induced *c-fos* activation is supported by the findings that: a) SOD mimetic prevents IH-induced *c-fos* expression; and b) aconitase activity is decreased in IH-exposed cells. We further identified mitochondrial complex I as one important source of increased $O_2^{\cdot-}$ generation during IH. What might be the physiological significance of *c-fos* induction by recurrent hypoxia? *c-fos* contributes to the formation of the AP-1 transcription factor complex. AP-1 regulates several downstream genes including tyrosine hydroxylase (TH) that encodes the rate-limiting enzyme in catecholamine synthesis (see Prabhakar, 2001 for ref). Catecholamine levels are elevated in patients with recurrent apneas (see Prabhakar, 2001 for ref). Therefore, it is possible that *c-fos* contributes to elevated blood pressures by activating the AP-1 complex leading to increased TH production and catecholamine synthesis.

## CONCLUSION

In summary, our results from intact animals and cell cultures demonstrate that intermittent hypoxia represents a form of oxidative stress involving increased generation of $O_2^{\cdot-}$. Further, we found that the mitochondria are one important source of ROS generation during IH.

## ACKNOWLEDGEMENTS

The work reported in this communication is supported by grants from National Institute of Health, Heart, Lung and Blood (HL-25830; HL-66448).

## REFERENCES

Ambrosio, G., Tritto, I., and Chiariello, M., 1995, The role of oxygen free radicals in preconditioning. *J.Mol.Cell Cardiol.* 27: 1035-1039.

Cragg, P.A., Runold, M., Kou, Y.R., and Prabhakar, N.R., 1994, Tachykinin antagonists in carotid body responses to hypoxia and substance P in the rat. *Respir Physiol.* 95(3):295-310.

Dröge, W., 2002, Free radicals in the physiological control of cell function. *Physiol. Rev.* 82(1): 47-95.

Fletcher, E.C., 2001, Physiological consequences of intermittent hypoxia: systemic blood pressure. *J Appl.Physiol* 90: 1600-1605.

Greenberg, H.E., Sica, A., Scarf, S.M., and Ruggiero, D.A., 1999, Expression of c-Fos in the rat brainstem after chronic intermittent hypoxia. *Brain Res.* 816: 638-645.

Narkiewicz, K., van de Borne, P.J., Pesek, C.A., Dyken, M.E., Montano, N., and Somers, V.K., 1999, Selective potentiation of peripheral chemoreflex sensitivity in obstructive sleep apnea. *Circulation.* 99(9):1183-1189.

Nieto, F.J., Young, T.B., Lind, B.K., Sahahar, E., Samet, J.M., Redline, S., D' Agostino, R.B., Newman, A.B., Lebowitz, M.D., Pickering, T.G., 2000, Association of sleep disordered breathing, sleep apnea, and hypertension in a large community based study. *JAMA* 283:1829-1836.

Prabhakar, N.R., 2001, Oxygen sensing during intermittent hypoxia: cellular and molecular mechanisms. *J. Appl.Physiol.* 90: 1986-1994.

Prabhakar, N.R., 2002, Sleep apneas: an oxidative stress? *Am.J.Respir.Crit.Care Med.* 859-860.

Premkumar, D.R.D., Mishra, R.R., Overholt, J.L., Simonson, M.S., Cherniack, N.S., Prabhakar, N.R., 2000, L-type $Ca^{2+}$ channel activation regulates induction of c-fos transcription by hypoxia. *J.Appl. Physiol.* 88:1898-1906.

# Effects of Hypobaric Hypoxia on the Intercellular Coupling of Glomus Cells

R.G. JIANG and CARLOS EYZAGUIRRE
*Department of Physiology, University of Utah School of Medicine, Salt Lake City, UT, USA*

## 1. INTRODUCTION

Prolonged exposure to a hypobaric medium induces profound effects on the carotid body, as reported in many studies. Among these we remark hyperplasia and hypertrophy of glomus cells, increased transmitter secretion and an increase in connexin Cx43 linking coupled glomus cells (Poncet *et al.*, 1996; Wang and Bisgard, 2002; Chen *et al.*, 2002). Thus, the number of gap junctions between glomus cells appeared to be more numerous in animals chronically exposed to hypobaric conditions.

The purpose of this study was to compare the functional behavior of gap junctions in animals exposed to a normal environment (about 640 Torr in Salt Lake City) and in those that had been kept at 380 Torr for 3 weeks in a hypobaric chamber.

*Chemoreception*, Edited by Pequignot et al.
Kluwer Academic/Plenum Publishers, New York, 2003

# 2. METHODS

## 2.1 Electrical recordings

Carotid bodies were excised from Sprague-Dawley rats (both male and female) weighing 60-200 g anesthetized with intraperitoneal injections of sodium pentobarbital (50 mg/kg). The organs were placed in a lucite chamber through which flowed a physiological solution equilibrated with 100% $O_2$. The $pO_2$ of the saline was 300 Torr at pH 7.43.

The preparations were mounted on the stage of an inverted microscope and viewed with phase-contrast or Hoffmann optics. For stimulation and recording, two microelectrodes filled with 3M KCl (tip resistance 20-40 MΩ), with a tip separation of 10-15 μm, were mounted on one micromanipulator and lowered into the tissue for intracellular penetration of adjoining glomus cells. The electrodes were connected to independent amplifiers that allowed current delivery to the cells, and the recording of voltages produced in the cells. The behavior of intercellular junctions is independent of the membrane potentials (Ems) of the cells within physiological parameters. Under current clamping (or voltage recordings), a pulse delivered to Cell 1 elicited a voltage drop ($V_1$) in this cell. In coupled cells, voltages were also detected in coupled Cell 2 because a voltage drop occurred across the intercellular junction ($\Delta Vj$). Consequently, the electrode lodged in Cell 2 registered $E_2$, which was smaller than $V_1$. The degree of coupling was established as the coupling coefficient ($K_c$) equal to $E_2/V_1$.

## 2.2 Morphological identification

The carotid bodies were cut into 100-150 μm slices and kept on ice before using. The slices were then immersed in a lucite chamber filled with physiological solution, bubbled with 100% $O_2$ and kept at 30-32°C. The chamber was mounted on the stage of the inverted microscope.

Glomus cells were identified by immuno fluorescence staining for TH. Tissues were fixed in 4% paraformaldehyde for 15-18 h at 4°C or 1 h at room temperature. After washing with TBST (50 mM Tris-HCl, 150 mM NaCl, 0.3% Triton X-100, pH 7.6), the tissue was treated with 2% goat serum in TBST for 1 h at room temperature. Then, the tissues were incubated in the primary antibody, which was rabbit anti-tyrosine hydroxylase (CHEMOCON), for 15-18 h at 4°C. This antibody was diluted 1:500 in TBST plus 2% goat serum. The secondary

antibody was Texas Red goat anti-rabbit IgG (Vector Laboratories), diluted 1:100 in 50 mM TBS (Tris-HCl and 150 mM NaCl, pH 7.6). Tissues were incubated in the secondary antibody for 30 min at room temperature and washed with TBS before being covered with Vectashield placed on a cover glass slip.

To identify stimulated and recorded cells we used electrodes made from two-barrel borosilicate glass tubing with filaments (WPI). One barrel was filled with 3 M KCl (2-10 MΩ) for stimulation and recording. For microejections, the other barrel was filled with 5% Lucifer Yellow (Lucifer Yellow CH, Lithium salt, Molecular Probes) in 150 mM LiCl. When the double-barrel microelectrode was inserted into a cell, dye ejection was accomplished with 100 ms negative current pulses (1-50 nA) delivered through the dye-filled barrel and applied for 1-5 min at 100 ms intervals. After dye ejection the tissue was fixed.

Tissues thus prepared were examined with a confocal microscope (Zeiss LSM 510). Images were acquired in the green and red channels by Argon and HeNe lasers and viewed as series of optical sections of from 0.8 to 4 μm. All images were processed with LSM 5 Examiner and Adobe PhotoDeluxe. It was possible to independently examine the green (LY) and red (TH) images, or to superimpose them.

## 3. RESULTS

Fig. 1 shows superimposed confocal images of carotid body glomera. The darker background (stained for TH) shows light rings of cytoplasm (red in the original) surrounding unstained and dark nuclei. In the middle we see brightly stained glomus cells after ejecting Lucifer Yellow into one of them. It is apparent that LY did not stay only in the injected cell, but the dye spread to adjoining glomus cells indicating coupling between them. This phenomenon occurred in carotid bodies from normal and hypobaric animals. However, at this point we have not conducted quantitative imaging studies to see if there are differences between carotid bodies extracted from normal and hypobaric animals.

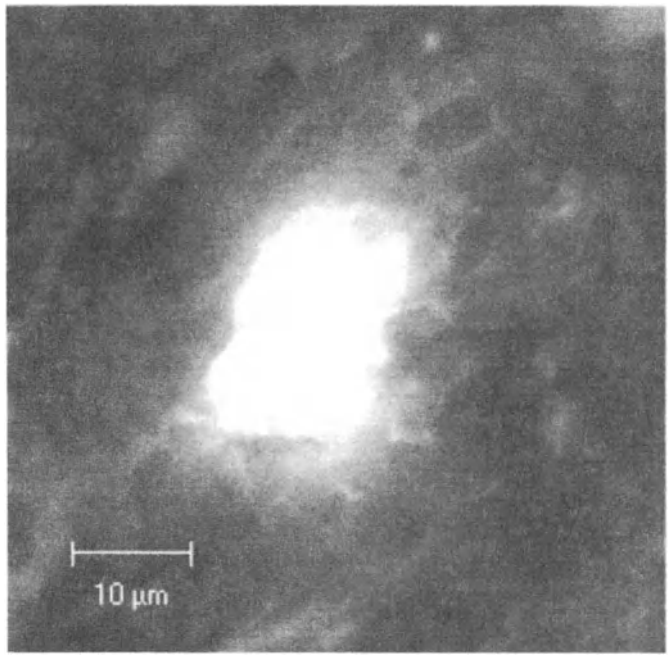


*Figure 1.* Superimposed confocal images of rat carotid body double stained for tyrosine hydroxylase (TH) and Lucifer Yellow (LY). The background (TH) shows light rings of cytoplasm (red in original) surrounding dark and unstained nuclei. Ejection of LY into one glomus cell brightly stains several glomus cells, showing dye coupling.

In another series of experiments we tested whether there were differences in electric coupling between glomus cells in carotid bodies of rats exposed to a normal environment and those of rats exposed to hypobaric conditions for three weeks. Fig. 2 shows the results.

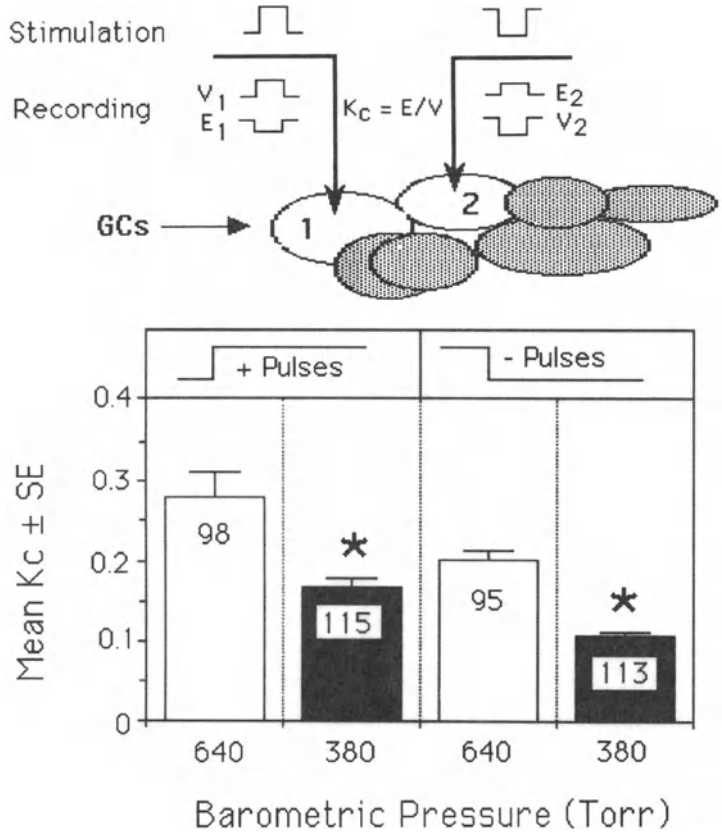


*Figure 2.* Upper part. Schematic diagram showing stimulating and recording conditions. Lower part. Left block (open column) mean $K_c$ obtained from 98 coupled pairs from normal animals. Black column, mean $K_c$ of 115 cell pairs from 3-week hypobaric animals. Right block, similar results obtained by application of negative pulses to 95 glomus cell pairs from normal animals and 113 cell pairs from 3-week hypobaric animals. Left asterisk, $p > 0.05$. Right asterisk, $p > 0.0002$ (Kolmogorov-Smirnov test).

The upper part of the illustration is a schematic diagram showing the stimulating and recording conditions. Two coupled glomus cells (C1 and C2) were impaled with microelectrodes. Positive pulses applied to Cell 1 elicited a voltage drop in this cell ($V_1$) and a smaller deflection ($E_2$) in Cell 2. Negative pulses applied to Cell 2 induced a voltage drop ($V_2$) in this cell and a smaller negative voltage drop ($E_1$) in Cell 1. The relation E/V is $K_c$ or the coupling coefficient.

The lower part of the figure (left block) shows that $K_c$ for positive pulses ($E_2/V_1$) was significantly lower in carotid bodies from hypobaric animals (black column) than from organs removed from normal animals (open column). Something similar happens to $K_c$ obtained during the application of negative pulses (right block). However, negative pulses were significantly more depressed in carotid bodies obtained from hypobaric animals.

## 4. CONCLUSIONS

Our results clearly indicate that chronic hypobaric conditions (3 weeks) reduce coupling between glomus cells of the rat carotid body. This happens despite the fact that these conditions significantly increase the number of gap junctions between glomus cells (Chen *et al.* 2002).

This apparent discrepancy could be explained because hypobaric glomus cells contain and secrete more chemicals than cells in normobaric rat (Jackson and Nurse, 1997). Increased secretion under hypobaric circumstances may be produced by increased intracellular calcium in glomus cells (Hempleman, 1996). and, high calcium tends to uncouple glomus cells (Abudara and Eyzaguirre, 1996). Thus, it seems that many of the extra junctions either are non functional or have been closed during the secretory process. The latter is not unusual since secretion in many glands is accompanied by intercellular uncoupling. In the carotid body, we have suggested that active or secreting glomus cells tend to uncouple, whereas they tend to be more tightly coupled when they are recharging (Eyzaguirre and Abudara, 1999).

## ACKNOWLEDGEMENTS

This work was supported by NIH grant NS 07938.

## REFERENCES

Abudara, V., and Eyzaguirre, C., 1996, Effects of calcium on the electric coupling of carotid body glomus cells. *Brain Res.* 725: 125-131.

Chen, J., He, L., Dinger, B., Stensaas L., and Fidone, S., 2002, Chronic hypoxia upregulates connexin43 expression in rat carotid body and petrosal ganglion. *J. Appl Physiol.* 92: 1480-1486.

Eyzaguirre, C., and Abudara, V., 1999, Carotid body glomus cells: chemical secretion and transmission (modulation?) across cell-nerve ending junctions. *Resp. Physiol.*, 115: 135-149.

Hempleman, S.C., 1996, Increased calcium current in carotid body glomus cells following in vivo acclimatization to chronic hypoxia. *J. Neurophysiol.* 76: 1880-1886.

Jackson, A., and Nurse, C., 1997, Dopaminergic properties of cultured rat carotid body chemoreceptors grown in normoxic and hypoxic environments. *J. Neurochem.* 69: 645-654.

Poncet, L, Denoroy, L., Dalmaz, Y., Pequignot, J.M., and Jouvet, M., 1996, Alteration in central and peripheral substance P- and neuropeptide Y-like immunoreactivity after chronic hypoxia in the rat. *Brain Res.* 733: 64-72.

Wang, Z.Y., and Bisgard, G.E., 2002, Chronic hypoxia-induced morphological and neurochemical changes in the carotid body. *Microsc. Res.* Tech. 59: 168-177.

# Oxygen Sensing by Human Recombinant Large Conductance,Calcium-activated Potassium Channels

## *Regulation by chronic hypoxia*

[1]PAUL J KEMP, [1]MATTHEW E HARTNESS and [2]CHRIS PEERS
*[1]School of Biomedical Sciences and [2]Institute for Cardiovascular Research, Worsley Medical and Dental Building, University of Leeds, Leeds LS2 9JT, UK.*

## 1. INTRODUCTION

Individuals suffering from a variety of cardiorespiratory diseases which are characterised by sustained or intermittent chronic hypoxia - such as chronic obstructive pulmonary disease, sleep apnoea, emphysema, congestive heart failure and stroke – often undergo pathological adaptation of tissue responses to acute hypoxia. Such a notion is supported experimentally by observations in chemosensing tissues such as the pulmonary vasculature, where voltage-gated $K^+$ channel expression is selectively suppressed in chronic hypoxia (Smirnov *et al.*, 1994) and carotid body, where chronic hypoxia both *in vitro* (Stea *et al.*, 1992; Stea *et al.*, 1995), and *in vivo* (Wyatt *et al.*, 1995; Eden & Hanson, 1987a; Eden & Hanson, 1987b) has been shown to modulate the acute cellular and whole-body hypoxic responses. Thus, it seems likely that remodelling of ion channel functional activity by sustained or intermittent episodes of hypoxia may underlie the responses to certain pathologies such as pulmonary hypertension (for recent reviews see Prabhakar, 2001; Prabhakar, 2002; Lanfranchi & Somers, 2001) in addition to the well documented adaptation to high altitude (Monge & Leon-Velarde, 1991).

MaxiK channels are expressed in many of the tissues affected by chronic hypoxia where they may well represent the main acute hypoxia-inhibitable $K^+$ conductance. This being the case, a central theme in adaptative responses in such tissues during pathological process characterised by chronic hypoxia may be long-term regulation of maxiK expression, activity, or both (*i.e* functional remodelling of the acute hypoxic response by chronic hypoxia). To investigate this possibility we have employed HEK293 cells stably co-

*Chemoreception*, Edited by Pequignot et al.
Kluwer Academic/Plenum Publishers, New York, 2003

expressing the human α/β-maxiK subunits (which are sensitive to acute hypoxia, Lewis *et al.*, 2002) to study the effect of long-term, severe hypoxia on channel functional expression using a combination of electrophysiological and biochemical approaches.

## 2. METHODS

### 2.1 Cell culture and chronic hypoxia

Human embryonic kidney 293 (HEK 293) cells which express human brain αβ maxiK channels (Ahring *et al.*, 1997) were maintained in Earle's minimal essential medium (containing L-glutamine) supplemented with 10 % fetal calf serum, 1% antibiotic antimycotic, 1% non-essential amino acids and 0.2% Gentamycin in a humidified incubator gassed with 5% $CO_2$/95% air. Cells were passaged every 7 days in a ratio of 1:25 using $Ca^{2+}$- and $Mg^{2+}$-free phosphate-buffered saline. The co-expressed α- (KCNMA1, Genbank U11717) and β- (KCNMB1, Genbank U42600) subunits were under control of two separate promoters. For the experiments described herein, cells were cultured for up to 3 days on glass coverslips at 37°C in water-saturated environments of either 2.5% $O_2$/5% $CO_2$/92.5% $N_2$ ($pO_2$ ~ 18mmHg – "Chronic Hypoxia") or 21% $O_2$/5% $CO_2$/74% $N_2$ ($pO_2$ ~ 143 mmHg – "Normoxia"). In some cases, cells were also cultured in the presence of 5 $\mu g.ml^{-1}$ actinomycin D or 10 μM cyclohexamide for the 72 h experimental period.

### 2.2 Patch-clamp recording

Cells were transferred to a continuously perfused ($5ml.min^{-1}$) recording chamber mounted on the stage of an inverted microscope. For the whole-cell recordings, pipette solution was $K^+$-rich and contained (in mM): 10 NaCl, 117 KCl, 2 $MgSO_4$, 10 HEPES, 2 $Na_2ATP$ with $Ca^{2+}$ buffered to 4 nM, 27 nM, 300 nM, and 3 μM using EGTA and $CaCl_2$ in appropriate ratios, pH 7.2. Bath solution was $Na^+$-rich and contained (in mM): 135 NaCl, 5 KCl, 1.2 $MgCl_2$, 5 HEPES, 2.5 $CaCl_2$, 10 D-glucose, pH 7.4. Following successful transition to the whole-cell recording mode, capacitance transients were compensated and measured. To evoke whole cell currents, two voltage protocols (Vh = -70mV, 0.1 Hz) were used: 1) *standard ramp*, voltage ramps from -100 mV to +60 mV, (1 s, 0.1 Hz); 2) *time series*, single increment to +60 mV (50 ms). Solutions which were employed to produce *acute* hypoxia were bubbled with $N_{2(g)}$ for at least 30 min, prior to perfusion of cells; this produced no shift in pH. $pO_2$ was measured (at the cell) using a polarized carbon fibre electrode (Mojet *et al.*, 1997) to be 25-40 mmHg. Normoxic

solutions were equilibrated with room air. All $K^+$ currents were recorded at a bath temperature (22 ± 0.5 °C). Current recordings were made using an Axopatch 200B amplifier and Digidata 1320 A/D interface.

## 2.3 Immunoblotting

The expression of maxiK α- and β-subunits was measured by immunoblotting of crude cell extracts taken from confluent cell layers as follows. The confluent cell layer was rinsed twice with divalent cation-free PBS and removed by scraping in SDS-PAGE sample buffer (1 ml per 75 $cm^2$ flask, without 2-mercaptoethanol and bromophenol blue) and lysate boiled for 10 min. A sample (100 µl) was taken for protein assay and replaced with 100 µl of 2-mercaptoethanol and 10 µl bromophenol blue (saturated). This was boiled for a further 10 min and equal protein amounts were analysed by SDS-PAGE. Proteins were transferred to polyvinylidene difluoride membrane at a constant voltage of 30 V overnight and immunoblotted with maxiK channel α antibody (diluted 1:250) or crude antisera raised against residues 58-75 of rat BK β1 subunit (diluted 1:6000). In some experiments the antibody was preadsorbed with this sequence using 2 µg of peptide per 1 µl of undiluted antibody for 1 h at room temperature. After thorough washing of membranes, immunolabelled proteins were detected using enhanced chemiluminescence and maxiK subunit expression was quantified by densitometry.

## 2.4 Immunocytochemistry

Cells on coverslips were washed twice with PBS and fixed for 5 min. (10% formalin at 37°C). The remaining procedures were carried out at room temperature. Cells were washed three times in PBS and then incubated in PBS containing 1mM sodium azide and 5% normal goat serum for 3 h. Cells were then incubated overnight in 1:160 dilution of maxiK β1 subunit (see above). After thorough washing with PBS, the cells were permeabilised by incubation with 0.5% Triton X-100 for 15 min., washed 3 times in PBS and then blocked for a further 3 h. Cells were then incubated overnight in maxi K channel α antibody (Transduction Laboratories, Lexington, KY, US) diluted 1:250 and/or crude antisera raised against residues 58-75 of rat BK β1 subunit (Biochem Pharm, Innsbruck, Austria) at a dilution of 1:6000. Following washing, cells were incubated in Cy3-labeled anti-rabbit antiserum and FITC-labeled antimouse antiserum for 3 h. prior to mounting and viewing with a laser confocal microscope. For controls, primary antibodies were omitted which resulted in no specific fluorescent staining in all cases.

# 3 RESULTS AND DISCUSSION

At all levels of $[Ca^{2+}]_i$, chronic hypoxia caused an increase in whole cell current density. For example, over the physiologically important $[Ca^{2+}]_i$ range (27 nM - 300 nM), chronic hypoxia evoked a large and significant augmentation in current density from 56.0 ± 7.1 (n = 10) to 108.3 ± 14.9 $pA.pF^{-1}$ (n = 7) and 137.1 ± 30.4 (n = 9) to 285 ± 68.9 $pA.pF^{-1}$ (n = 6), respectively. The time-course of the regulatory effect was relatively slow with significant up-regulation by chronic hypoxia not apparent until at least 24 hours into the experimental exposure.

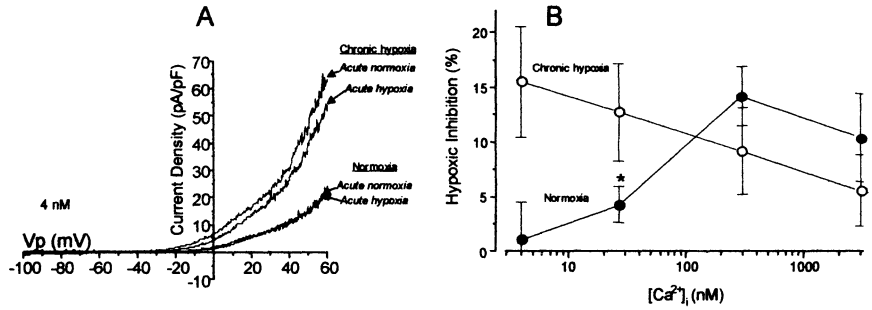


*Figure 1. Chronic hypoxic modulation of whole cell current.*
(A) Current density-voltage relationships before and during acute hypoxia in exemplar cells following 3d culture in either normoxia (Normoxia) or chronic hypoxic (Chronic hypoxia) with $[Ca^{2+}]_i$ buffered to 4 nM during the electrophysiological experiment shown. (B) Mean effects of $[Ca^{2+}]_i$ on the acute hypoxic sensitivity of recombinant $maxiK^+$ in normoxic (closed symbols, n = 5-14) and chronic hypoxia (open symbols, n = 5-9).

Figure 1A shows exemplar currents from normoxic and chronically hypoxic cells before and during *acute* hypoxia ($[Ca^{2+}]_i$ = 4nM). Consistent with data from excised patches, whole-cell current recorded from cells cultured for 72 hr in normoxia showed a $[Ca^{2+}]_i$-dependent sensitivity to acute hypoxia (Figure 1B). Although this effect of *acute* hypoxia on whole currents was qualitatively similar to that demonstrated in inside-out patches, the sensitivity of the system was shifted towards lower, more physiologically pertinent $[Ca^{2+}]_i$; *i.e.* whole cell currents were inhibited maximally at 300nM $[Ca^{2+}]_i$ (see Figure 1B) whereas currents from inside-out patches were inhibited maximally at $[Ca^{2+}]_i$ greater than 1 μM (Lewis *et al.*, 2002). Thus, in normoxic cells with low $[Ca^{2+}]_i$, the maxiK whole cell current demonstrated little or no acute hypoxic sensitivity ( 1.1 ± 3.4 % inhibition, n =8 - Figure 1A and B) but increased as $[Ca^{2+}]_i$ rose (Figure 1B).

In complete contrast chronic hypoxia dramatically changed this pattern of $Ca^{2+}$ sensitivity of the acute hypoxic response such that channel inhibition was enabled even at very low $[Ca^{2+}]_i$ (15.5 ± 5.0 % inhibition, n = 8 - Figure 1A and B).

In order to investigate the molecular nature of the functional change in acute hypoxic sensitivity evoked by chronic perturbation of ambient $pO_2$, we studied the effect of chronic hypoxia on maxiK α- and β-subunit expression using western blotting and immunocytochemistry. Using the α-subunit antibody, a major band of the expected size was detected (125 kDa - Figure 2A). Chronic hypoxia did not change the expression of this subunit (Figure 2C). Two bands were detected with the β-subunit (Figure 2B, left panel). The higher molecular weight band was of approximately 35 kDa, consistent

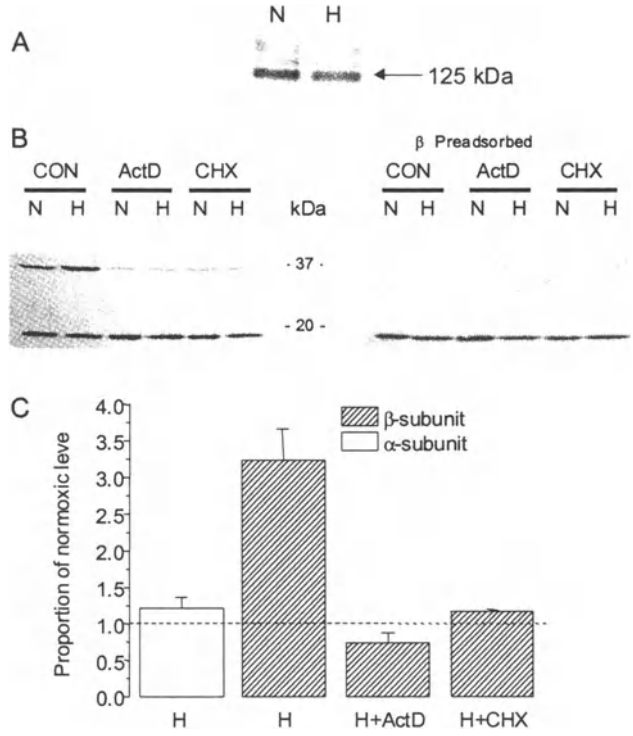


*Figure 2. Regulation of subunit expression by chronic hypoxia.*
Western blotting was carried out with a monoclonal antibody to the α subunit (A), polyclonal antiserum to the β-subunit (*B, left panel*) antiserum to the β-subunit following pre-adsorption (*B, right panel*). Cells were treated with 5 $\mu g.ml^{-1}$ actinomycin D (*ActD*) or 10 μM cyclohexamide (*CHX*) for 72 h. prior to preparation of cell lysates, as indicated. Representative immunoblots are shown from four separate experiments. (C) mean normalised expression levels of maxiK α- and β- subunits present in the chronic hypoxic cells under each condition.

with a previous report of heavy glycosylation of this protein which always appears as a band of molecular weight in excess of 30 kDa on SDS-PAGE gels (Garcia-Calvo *et al.*, 1994). This upper band disappeared following the preadsorption step (Figure 2B, right panel) Chronic hypoxia significantly increased β-subunit expression by 3.24 ± 0.42 fold (Figure 2C, n = 6) and this dramatic increase by chronic hypoxia was completely inhibited by the addition of 5 $\mu g.\mu l^{-1}$ actinomycin D or 10 μM cyclohexamide to the cells for the chronic hypoxia culture period (Figure 2B and C),

Selective up-regulation of β-subunit expression in response to chronic hypoxia was confirmed by laser confocal immunocytochemistry. In the normoxic cells (Figure 3A, inset), the α subunit staining (green) was localised mainly at the periphery of the cells consistent with a plasma membrane location. Some intracellular staining was also detected presumably due to ongoing trafficking of the α subunit. In the cells cultured in chronic hypoxia, the α-subunit staining was also concentrated at the plasma membrane and the intensity of the staining was similar to that seen in the normoxic cells. Staining for the β-subunit staining (red) demonstrated a different pattern. Although some β-subunit immunoreactivity was also located at the plasma membrane in normoxia (Figure 3A, inset), the staining was less intense than that of α-subunit and the sub-cellular localization was more diffuse, suggesting a major component of intracellular storage. Chronic hypoxia generally increased β-subunit staining and the overlaid images (Figure 3B, inset) suggest increased co-localisation of the α and β subunits (yellow). The functional correlate of transcriptional blockade with actinomycin D is shown in Figure 3. Consistent with the earlier set of experiments, cells cultured in normoxic conditions (27nM $[Ca^{2+}]_i$) the absence of actinomycin D (vehicle control normoxia – Figure 3A and E) showed little or no acute hypoxic inhibition whilst chronic hypoxia elicited the expected increase in current density and enabled acute hypoxic inhibition (vehicle control chronic hypoxia – Figure 3B, and E). Actinomycin D induced a mild diminution of current density (Figure 3C and E).

However, and in complete contrast to the untreated cells, the presence of actinomycin D during chronic hypoxia resulted in full suppression of the usual chronic hypoxia-evoked increase in current density and blocked the ability of chronic hypoxia to up-regulate acute hypoxic inhibition (Figure 3D and E).

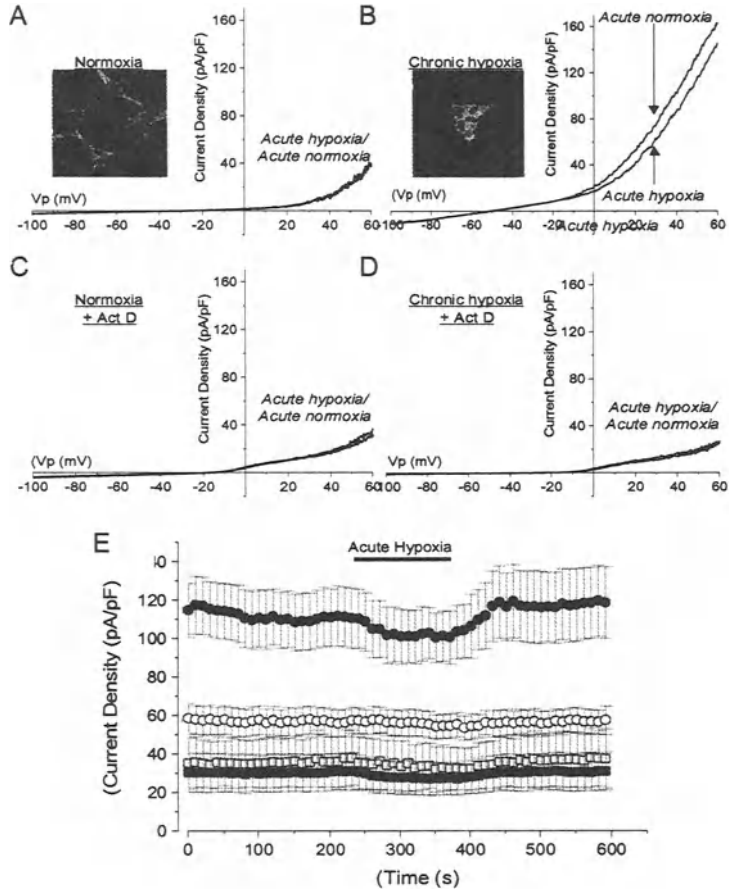


*Figure 3. Effect of Actinomycin D treatment on chronic hypoxic regulation.* Current density-voltage derived from the voltage ramp protocols recorded before and during acute hypoxia untreated normoxic (A) and chronically hypoxic (B) cells and in normoxic (C) and chronically hypoxic (D) cells treated with 5 μg/ml actinomycin D for 72h, as indicated ($[Ca^{2+}]_i$ = 27 nM). (E) Mean time-series' from normoxic cells (open symbols) and chronic hypoxic cells (closed symbols) either untreated (circles) or treated with actinomycin D (squares). Application of hypoxic perfusate is indicated by horizontal bar. Insets show co-localization of α-subunit and β-subunit in cells treated with normoxia (A, inset) or chronic hypoxia (B, inset).

Furthermore, chronic hypoxia completely failed to increase current density or modulate acute hypoxic sensitivity in a separate HEK293 cell line stably expressing only the α-subunit of the maxiK channel complex (98.7 ± 15.2 $pA.pF^{-1}$ following 72h in normoxia versus 94 2 ± 12.3 $pA.pF^{-1}$ following 72h in hypoxia; n = 5 for both).

Our findings demonstrate directly that the human α/β maxiK channel heteromer is an $O_2$-sensitive $K^+$ channel and support strongly the notion that hypoxic inhibition of this channel occurs primarily via a reduction in $Ca^{2+}$-sensitivity with an additional, minor reduction in unitary conductance. Furthermore, the idea that chronic hypoxia exerts a dramatic influence on maxiK channel functional expression is evidenced by the observations that severe, prolonged hypoxia evokes increased $K^+$ current density, altered $Ca^{2+}$-sensitivity of acute $O_2$ regulation, dynamic and differential up-regulation of the β-subunit, and augmented co-localization of the α- and β–subunits in the plasma membrane.

Funded by The Wellcome Trust and The British Heart Foundation.

## REFERENCES

Ahring, P. K., Strobaek, D., Christophersen, P., Olesen, S. P., & Johansen, T. E., 1997, Stable expression of the human large-conductance $Ca^{2+}$-activated $K^+$ channel alpha- and beta-subunits in HEK293 cells. *FEBS Lett.* 415, 67-70.

Eden, G. J. & Hanson, M. A., 1987a, Effects of chronic hypoxia from birth on the ventilatory response to acute hypoxia in the newborn rat. *J.Physiol.* 392, 11-19.

Eden, G. J. & Hanson, M. A., 1987b, Maturation of the respiratory response to acute hypoxia in the newborn rat. *J.Physiol.* 392, 1-9.

Garcia-Calvo, M., Knaus, H. G., Garcia, M. L., Kaczorowski, G. J., & Kempner, E. S., 1994, Functional unit size of the charybdotoxin receptor in smooth muscle. *Proc.Natl.Acad.Sci.USA* 91, 4718-4722.

Lanfranchi, P. & Somers, V. K., 2001, Obstructive sleep apnea and vascular disease. *Respir.Res.* 2, 315-319.

Lewis, A., Ashford, M. L. J. Ashford, C. Peers & P. J. Kemp, 2002, Hypoxia inhibits human recombinant maxi $K^+$ channels by a mechanism which is membrane delimited and $Ca^{2+}$-sensitive. *J. Physiol.* 540, 771-780.

Mojet, M. H., Mills, E., & Duchen, M. R., 1997, Hypoxia-induced catecholamine secretion in isolated newborn rat adrenal chromaffin cells is mimicked by inhibition of mitochondrial respiration. *J.Physiol.* 504, 175-189.

Monge, C. & Leon-Velarde, F., 1991, Physiological adaptation to high altitude: oxygen transport in mammals and birds. *Physiol.Rev.* 71, 1135-1172.

Prabhakar, N. R., 2001, Oxygen sensing during intermittent hypoxia: cellular and molecular mechanisms. *J.Appl.Physiol.* 90, 1986-1994.

Prabhakar, N. R., 2002, Sleep apneas: an oxidative stress? *Am.J.Respir.Crit.Care Med.* 165, 859-860.

Smirnov, S. V., Robertson, T. P., Ward, J. P. T., & Aarsonson, P. I., 1994, Chronic hypoxia is associated with reduced delayed rectifier $K^+$ current in rat pulmonary artery muscle cells.

*Am.J.Physiol.* 266, H365-H370.

Stea, A., Jackson, A., Macintyre, L., & Nurse, C. A., 1995, Long-term modulation of inward currents in O2 chemoreceptors by chronic hypoxia and cyclic AMP in vitro. *Journal Of Neuroscience* 15, 2192-2202.

Stea, A., Jackson, A., & Nurse, C. A., 1992, Hypoxia and $N_6$, $O_2$'-dibutyryladenosine 3',5'-cyclic monophosphate, but not nerve growth factor, induce $Na^+$ channels and hypertrophy in chromaffin-like arterial chemoreceptors. *Proc.Natl.Acad.Sci.USA* 89, 9469-9473.

Wyatt, C. N., Wright, C., Bee, D., & Peers, C., 1995, $O_2$-sensitive $K^+$ currents in carotid-body chemoreceptor cells from normoxic and chronically hypoxic rats and their roles in hypoxic chemotransduction. *Proc.Natl.Acad.Sci.USA* 92, 295-299.

# Altered Expression of Vascular Endothelial Growth Factor and FLK-1 Receptor in Chronically Hypoxic Rat Carotid Body

J. CHEN, BRUCE DINGER, R. JYUNG*, L. STENSAAS and SALVATORE FIDONE

*Department of Physiology University of Utah School of Medicine; *Massachusetts Eye and Ear Infirmary & Harvard Medical School*

## 1. INTRODUCTION

The mammalian carotid body maintains a high level of chemoreceptor output and provides support for increased ventilatory drive over an extended period in animals chronically exposed to a low $O_2$ environment (i.e., chronic hypoxia, CH; Bisgard, 2000). Important features of carotid body adaptation to CH include hypertrophy and hyperplasia of $O_2$-sensitive type I cells, and marked dilation of surrounding microvascular elements (McGregor *et al.*, 1984; Laidler & Kay, 1975). Although little is known about the cellular mechanisms which mediate these remarkable morphological changes (Pequignot *et al.*, 1987; Bisgard, 2000), similar $O_2$-sensitive changes occur in the lung and heart where CH elicits constriction and thickening of vessel walls in the pulmonary circuit and hypertrophy of the right ventricle, resulting in pulmonary hypertension (Rabinovitch *et al.*, 1979).

The present study examines the hypothesis that up-regulation of an angiogenic peptide, vascular endothelial growth factor (VEGF), and its Flk-1 (fetal liver kinase) receptor, a transmembrane tyrosine kinase (Thomas, 1996; Ferrara, 1999), mediates CH induced microvascular remodeling in the carotid body. Up-regulation of this growth factor is predicted to precede, or co-occur with the active phase of vascular remodeling, and Flk-1 should likewise be expressed by carotid body vascular endothelial cells. Previous studies have

*Chemoreception*, Edited by Pequignot et al.
Kluwer Academic/Plenum Publishers, New York, 2003

shown that vascular changes in the rat carotid body are fully developed by 14 days of CH (Pequignot & Hellstrom, 1983). Therefore the present study focuses on morphometric assessments and immunocytochemical analysis of VEGF and Flk-1-receptor expression in the carotid body in animals exposed to hypobaric hypoxia (380 Torr; equivalent to 5500 m) for 0, 3,7 and 14 days.

## 2. MATERIALS AND METHODS

### 2.1 Animals and Exposure to Hypobaric Hypoxia

All procedures involving animals were approved by the University of Utah Institutional Animal Care and Use Committee. Adult male albino rats (180-200g) were housed in standard rodent cages with 24 hr access to pellet food and water and placed in a hypobaric chamber where pressures were reduced over 12-24 hours from ambient (~640 Torr at Salt Lake City, 1400 m) to 380 Torr, equivalent to 5500m, where it was maintained. The chamber was opened every 2 days to replenish food and water. Age-matched control male rats were similarly housed outside the chamber.

### 2.2 Histology and Morphometry

Four groups of 2 rats exposed to 0, 3, 7, or 14 days of hypobaric hypoxia were anesthetized with Ketamine (10 mg/kg, i.m.) plus Xylazine (0.9 mg/kg, i.m.) and fixed by intracardiac perfusion with phosphate buffered (pH 7.4) 1% glutaraldehyde plus 1% paraformaldehyde. Carotid bodies were removed and post-fixed for 2 hr in osmium tetroxide, dehydrated in ethanol, and embedded in Epon. Semi-thin (0.5-1.0 μm) sections from 3 levels in each carotid body were mounted on clean glass slides and stained with methylene blue. Images of 3-5 sections through midportions of the carotid body were analyzed using NIH ImageTool, version 2.0. Vessel volume density was calculated based on the fractional area within the carotid body capsule occupied by the lumen of blood vessels, in accord with stereological principles described by Weibel (1979). Data were analyzed using ANOVA and compared with Bonferroni post-tests.

### 2.3 Immunocytochemical localization of VEGF and Flk-1 Receptor Protein.

Four groups of rats exposed to 0 (n = 7), 3 (n = 2), 7 (n = 2), or 14 (n = 7) days of hypobaric hypoxia were anesthetized as above and perfused intracardially with ice-cold 4% paraformaldehyde in 0.1 M phosphate-buffered saline (PBS). Carotid bodies were removed, immersed in the same fixative (1 hour), rinsed in 15% sucrose/PBS (2 hours), and stored at 4 $^{0}$C in 30% sucrose/PBS (overnight).

Cryostat sections (6 μm) thaw-mounted onto gelatin subbed slides were exposed to avidin-biotin preblocking reagents (20 min, Vector), incubated at 4 $^{0}$C overnight in primary antibody (anti-VEGF, rabbit polyclonal, 1:4000; anti-Flk-1-receptor protein, rabbit polyclonal, 1:4000 to 1:16,000; Santa Cruz Biotechnology, Inc.) in PBS containing 0.3% Triton X-100. Sections were then rinsed in PBS, incubated in biotinylated goat anti-rabbit IgG (2 hours; Vector), rinsed (20 min), incubated in avidin-biotinylated horseradish peroxidase complex (2 hours, Vector elite kit), and treated with 3',3'-diaminobenzidine tetrahydrochloride and hydrogen peroxide. In randomly selected control sections the primary antibody was replaced with normal rabbit serum; no specific immunoreactivity was found in these specimens.

# 3. RESULTS

## 3.1 Effect of Chronic Hypoxia on Carotid Body Morphology

In the normal carotid body (fig. 1A), parenhymal cell lobules predominate and are comprised of groups of ovoid type I cells and terminal sensory axon enlargements enveloped by type II cells. The surrounding connective tissue contains a network of small arteries, veins and fenestrated sinusoids whose diameter ranges between 4 and 20 μm in normal animals (McDonald, 1983).

Following exposure to hypoxia for 3 days, blood vessels contained larger, darker endothelial cells which protruded into the lumen and type I cells had enlarged nuclei with a large nucleolus (arrows fig. 1B). Mitotic type I cells were observed sporadically (not shown). No mitotic figures were observed in specimens from animals exposed to CH for 7 or 14 days.

Marked enlargement of blood vessels was apparent throughout the carotid body following 7 days of CH (fig. 1C). Endothelial cells with large, dark nuclei protruded into the lumen of the thin-walled, irregularly-shaped sinusoidal vessels. Enlarged parenchymal cell lobules were slightly distorted by the adjacent vessels and contained large, round type I cells.

A greatly enlarged loose connective tissue stroma surrounded the exceedingly large (up to 100 μm), thin-walled sinusoids at day 14 (fig. 1D). Endothelial cells (vertical arrows) were made conspicuous by a prominent nucleus which frequently protruded into the vessel lumen. The extensive vascular remodeling involved further distortion of parenchymal cells which appeared drawn out into elongated aggregates of flat rather than round type I cells (horizontal arrows). Individual chemosensory type I cells were abnormally large and contained a large nucleus and prominent nucleolus resembling the nucleus of nerve cells.

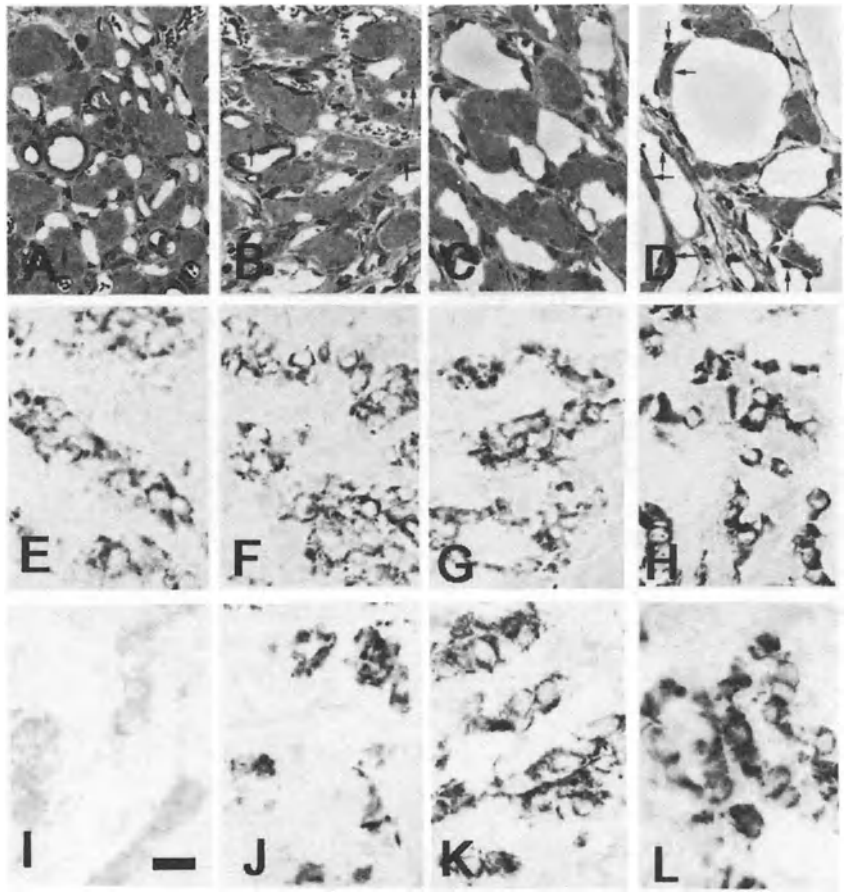


*Figure 1.* **(A-D)** CH-induced tissue remodeling in rat carotid body. **(A)** Normal; lobules of type I and type II cells situated in a dense connective tissue stroma penetrated by a complex network of small blood vessels. **(B)** Following 3 days of hypoxia changes in the vasculature are minimal, but most type I cells are enlarged with enlarged nucleus and central nucleolus (small arrows). **(C)** Vascular dilation is evident following 7 days of CH. Chemosensory lobules retain intimate apposition to the expanding blood vessels. **(D)** At 14 days elongate lobules (horizontal arrows) remain attached to the hyper-dilated blood vessels. Darkly staining endothelial cells commonly protrude into the lumen of dilated sinusoids (vertical arrows). **(E-H)** VEGF immunocytochemistry in rat carotid body. **(E)** In normal carotid body VEGF is expressed in the cytoplasm of most oxygen-sensitive type I cells, whose ovoid nuclei are unstained. The intensity of VEGF immunostaining is elevated following 3 days of CH **(F)**, and further increases are evident after 7 **(G)** and 14 **(H)** days of CH. **(I-L)** Flk-1 receptor is undetectable or is present at low levels in normal carotid body **(I)**. Expression of Flk-1 is evident in some type I cells after 3 days of hypoxia **(J)**, and increasingly higher levels of the receptor protein appear following 7 **(K)** and 14 **(L)** days of CH. Bar = 20 μm.

Morphometric data presented in Table 1 quantify the effects of CH on blood vessel morphology involving the center of the carotid body. The incidence of blood vessel profiles was not significantly altered following exposure to CH for 3, 7, or 14 days (n = 3 or 4). In contrast, the volume of the lumen of blood vessels increased steadily, and was nearly 3-fold greater than normal after 14 days of CH ($p<0.001$). Moreover, the mean lumen area of individual vessels was elevated 2.4-, 3.9- and 16-fold at 3, 7 and 14 days of CH, respectively ($p<0.001$).

*Table 1.* Effect of Chronic Hypoxia on Carotid Body Blood Vessel Morphology

| Chronic Hypoxia (days) | Vessels/ Section | Volume Density (%) | Mean Vessel Area $(\mu m)^2$ |
|---|---|---|---|
| 0 | 96.8 ± 14.0 | 15.2 ± 1.8 | 117.9 ± 26.1 |
| 3 | 128.0 ± 6.9 | 22.0 ± 6.9 | 288.4 ± 84.5 |
| 7 | 74.7 ± 20.7 | 28.6 ± 5.9 | 458.8 ± 103.5 |
| 14 | 82.7 ± 14.5 | 44.4 ± 3.3** | 1873.2 ± 260*** |

Values are means ± standard error. ** and *** indicate $p<0.01$ and $p<0.001$, respectively, compared to 0 days exposure.

## 3.2 Effect of Chronic Hypoxia on VEGF and Flk-1 Expression

In the normal carotid body, VEGF immunostaining occurred in a majority of type I chemosensory cells whose staining intensity varied from medium to dark (fig. 1E). The present preparations are not suitable for assessing immunostaining involving the sustentacular Schwann cells ensheathing the type I cells. VEGF immunoreactivity also occurred in a few smooth muscle cells in arteries at the surface of the carotid body. Other tissue elements, including vascular endothelial cells, nerves, and cells in the connective tissue stroma were immunonegative for VEGF, but sinuous immunopositive cell processes were occasionally found which could not be identified as to cell type. Exposure to CH for 3 or 7 days (fig. 1F and 1G) resulted in a moderate elevation of VEGF reaction product intensity; however, 14 days of CH (fig. 1H) produced a striking enhancement, with high levels of reaction product present in virtually all type I cells. Exposure to hypoxia did not elicit detectable VEGF expression in other cell types in the carotid body.

Immunocytochemical studies of Flk-1 receptor expression in the carotid body likewise reveal progressive hypoxia-induced up-regulation (fig. 1I-L). In the normal carotid body, Flk-1 immunoreactivity was either low or not detectable (fig. 1I). However, after only 3 days of CH (fig. 1J), numerous type I cells immunopositive for Flk-1 were present, and a progressive increase in the intensity and incidence of immunopositive cells followed 7-day exposure to CH (fig. 1K). CH for 14 days elicited a marked increase in the overall intensity of immunostaining of virtually all type I cells (fig. 1L). As with VEGF immunostaining, it was not possible to ascertain the precise status of sustentacular Schwann cells with respect to the expression of Flk-1 receptor protein. The prominent vascular endothelial cells lining the enlarged sinusoids within the carotid body were immunonegative for Flk-1 in both normal or CH preparations. However, positive immunostaining for Flk-1 was observed in a few cells of large blood vessels outside the carotid body.

## 4. DISCUSSION

In agreement with previous studies (Pequignot *et* Hellstrom, 1983; McGregor *et al.*, 1984; Laidler *et* Kay, 1975), our morphological data indicate that CH induces rapid remodeling of the carotid body. It is of particular interest that these major readjustments are preceded by up-regulation of VEGF and its Flk-1 receptor in the hypertrophic type I cells. This is consistent with previous studies which have shown VEGF mRNA expression to be rapidly and reversibly induced by exposure to low oxygen in a variety of cells (Minchenko *et al.*, 1994; Ladoux & Frelin, 1993; Tuder *et al.*, 1995; Christou *et al.*, 1998). The VEGF gene is known to contain a regulatory region binding hypoxia-inducible-factor-1 (HIF-1) upstream from the transcription initiation site (Forsythe *et al.*, 1996). Although Flk-1 expression is similarly up-regulated, an HIF-1 binding site has not as yet been found in the promoter region of this gene.

In contrast to the pulmonary circuit where CH elicits thickening and narrowing of arteries, carotid body small sinusoidal vessels are the principal elements enlarged and distended following sustained hypoxia, while arteries are normal. These changes appear to be due primarily to hypertrophy of the fenestrated endothelial cells during the enlargement of the thin-walled vessels. Since the incidence of such sinusoids does not increase in CH preparations, our quantitative morphological data indicate a minor role for angiogenesis in the remodeling process. Similar changes have recently been reported in collateral vessels after femoral artery occlusion, where a role for VEGF in the vascular adjustment was not supported (Deindl *et al.*, 2001).

The fact that Flk-1 expression was restricted to the chemosensory cell lobules indicates that type I (and perhaps type II) cells are the primary site of both VEGF secretion and VEGF action in the hypoxic carotid body. Flk-1 expression has been identified in proliferating Schwann cells of regenerating peripheral nerve (Sondell *et al.*, 1999) which are similar to type II cells in the carotid body. Since the initial elevation of Flk-1 receptor at day 3 of CH correlates with the appearance of conspicuous mitotic cells it is not only consistent with paracrine involvement of VEGF and its Flk-1 receptor in proliferation of type I cells, but may also involve type II cells in the response to CH.

A poorly understood aspect of CH-induced tissue remodeling is the combination of hypertrophy and rearrangement of chemosensory elements within lobules of the carotid body. Such "flattened" sheets of type I and type II cells between expanded sinusoidal vessels are never observed in chemosensory tissue from normal animals. Recent studies showing that cultured vascular smooth muscle cells and breast carcinoma cells expressing Flk-1 receptors migrate on fibronectin substrates following exposure to VEGF-165 (Price *et al.*, 2001; Ishida *et al.*, 2001) suggest the possible involvement of VEGF and Flk-1 receptor in the rearrangement of carotid body chemosensory cells following prolonged exposure to hypoxia.

In summary, the current data are not consonant with the hypothesis that VEGF and its Flk-1 receptor mediate CH-induced vascular expansion in carotid body. However, VEGF and Flk-1 receptor up-regulation in the chemosensory tissue occurs coincident with hyperplasia of type I cells, and the dynamic reshaping of chemosensory cell lobules. VEGF may therefore participate in the growth of type I cells, and their associated spatial readjustments. Because type I cells initiate hypoxic chemotransduction, our findings suggest the additional possibility that the autocrine and paracrine effects of VEGF may influence important physiological adjustments elicited by sustained exposure to hypoxia.

**ACKNOWLEDGEMENTS** Supported by USPHS Grants NS 12636 and NS 07938.

## REFERENCES

Bisgard,G.E., 2000, Carotid body mechanisms in acclimatization to hypoxia. *Resp. Physiol.* 121: 237-246.

Christou, H., Yoshida, A., Arthur, V., Morita, T., and Kourembanas, S., 1998, Increased vascular endothelial growth factor production in the lungs of rats with hypoxia-induced pulmonary hypertension. *Am. J. Respir. Cell. Mol. Biol.* 18(6): 768-776.

Deindl, E., Buschmann, I., Hoefer, I.E., Podzuweit, T., Boengler, K., Vogel, S., van Royen, N., Fernandez, B., and Schaper, W., 2001, Role of ischemia and of hypoxia-inducible genes in arteriogenesis after femoral artery occlusion in the rabbit. *Circ. Res.* 89: 779-786.

Ferrara, N., 1999, Role of vascular endothelial growth factor in the regulation of angiogenesis. *Kidney Int'l* 56: 794-814.

Forsythe, J.A., Jiang, B.-H., Iyer, N.V., Agani, F., Leung, S.W., Koos, R.D., and Semenza, G.L., 1996, Activation of vascular endothelial growth factor gene transcription by hypoxia-inducible factor 1. *Molec. Cell. Biol.* 16(9): 4604-4613.

Ishida, A., Murray, J., Saito, Y., Kanthou, C., Benzakour, O., Shibuya, M., and Wijelath, E.S., 2001, Expression of vascular endothelial growth factor receptors in smooth muscle cells. *J. Cell. Physiol.* 188: 359-368.

Ladoux, A., and Frelin, C., 1993, Hypoxia is a strong inducer of vascular endothelial growth factor mRNA expression in the heart. *Biochem. Biophys. Res. Comm.* 195(2): 1005-1010.

Laidler, P., and Kay, J.M., 1975, A quantitative morphological study of the carotid bodies of rats living at a simulated altitude of 4300 meters. *J. Path.* 117: 183-191.

Laidler, P., and Kay, J.M., 1978, A quantitative study of some ultrastructural features of the type I cells in the carotid bodies of rats living at a simulated altitude of 4300 meters. *J. Neurocytol.* 7: 183-192.

McDonald, D.M., 1983, A morphometric analysis of blood vessels and perivascular nerves in the rat carotid body. *J. Neurocytol.* 12: 155-199.

McGregor, K.H., Gil, J., and Lahiri, S., 1984, A morphometric study of the carotid body in chronically hypoxic rats. *J. Appl. Physiol.: Respirat. Environ. Exercise Physiol.* 57: 1430-1438.

Minchenko, A., Bauer, T., Salceda, S., and Caro, J., 1994, Hypoxic stimulation of vascular endothelial growth factor expression *in vitro* and *in vivo*. *Lab. Invest.* 71(3): 374-379.

Pequignot, J.-M., Hellstrom, S., and Johansson, C., 1987, DL-propranolol inhibits the vascular changes in the rat carotid body induced by long-term hypoxia. *Virchows Arch. A* 411: 331-336.

Pequignot, J.M., and Hellstrom, S., 1983, Intact and sympathectomized carotid bodies of long-term hypoxic rats. *Virchows Arch.* 400: 235-243.

Price, D.J., Miralem, T., Jiang, S., Steinberg, R., and Avraham, N., 2001, Role of vascular endothelial growth factor in the stimulation of cellular invasion and signaling of breast cancer cells. *Cell Growth & Differentiation* 12: 128-138.

Rabinovitch, M., Gamble, W., Nadas, A.S., Miettinen, O.S., and Reid, L., 1979, Rat pulmonary circulation after chronic hypoxia: hemodynamic and structural features. *Am. J. Physiol.* 236(6): H818-H827.

Sondell, M., Lundborg, G., and Kanje, M., 1999, Vascular endothelial growth factor stimulates Schwann cell invasion and neovascularization of acellular nerve grafts. *Brain Res.* 846: 219-228.

Thomas, K.A., 1996, Vascular endothelial growth factor, a potent and selective angiogenic agent. *J. Biol. Chem.* 271(2): 603-606.

Tuder, R.M., Flook, B.E., and Voelkel, N.F., 1995, Increased gene expression for VEGF and the VEGF receptors KDR/Flk and Flt in lungs exposed to acute or to chronic hypoxia. *J. Clin. Invest.* 95: 1798-1807.

Weibel, E.R., 1979, *Serological Methods*. Academic Press:London, New York.

# Role of HIF-1 in Physiological Adaptation of the Carotid Body during Chronic Hypoxia

*MAN-LUNG FUNG, and GEORGE L. TIPOE
*Departments of *Physiology and Anatomy, University of Hong Kong, Faculty of Medicine Building, 21 Sassoon Road, Pokfulam, Hong Kong, China*

## 1. INTRODUCTION

Chemoreceptors in the carotid body (CB) increase intracellular calcium and afferent nerve discharge in hypoxia and, thus, play an important role in the regulation of cardiorespiratory responses to hypoxia (see Gonzalez *et al.* 1994 for review). Also, the CB plays a central role in the ventilatory acclimatization to hypoxia involving an initial rapid increase in ventilation followed by a progressive hyperventilation during hours and weeks of hypoxic exposure (see Bisgard, 2000; Lahiri *et al.* 2001 for reviews). It is well known that the CB enlarges in human and animals living at high altitude or exposed to chronic hypoxia. The enlargement may be due to an increased vasculature, cellular hypertrophy and hyperplasia of the glomus cells in the CB (Dhillon *et al.* 1984; McGregor *et al.* 1984; Bee *et al.* 1986).

Recently a surge of new evidence suggests that a heterodimeric transcriptional factor directly induced by severe tissue or cellular hypoxia, namely hypoxia-inducible factor-1 (HIF-1) is a key controller for the transcriptional regulation of the gene expression of a spectrum of proteins for the cellular response to hypoxia (see Semenza, 2001 for review). These proteins such as endothelin-1 (ET-1), inducible nitric oxide synthase (iNOS) and vascular endothelial growth factor (VEGF) play important physiological roles in the control of vascular tone and angiogenesis. In the CB, chronic hypoxemia induces remodeling of the vasculature; stimulates proliferation of the glomus cells, i.e. the chemosensitive cells, and changes their excitability and sensitivity to the chemical signals. In addition, HIF-1-targeted genes are expressed in the CB, indicating a role of HIF-1 and its modulation of the target gene expression in chronic hypoxemia. Hence the aims of the study

*Chemoreception*, Edited by Pequignot et al.
Kluwer Academic/Plenum Publishers, New York, 2003

are to examine the role of HIF-1 in the anatomical, functional and molecular changes of the CB during chronic hypoxemia. This may provide hints on the molecular regulation and its functional significance related to the ventilatory acclimatization of the hypoxic response at high altitude and the development of pathophysiological events during chronic hypoxemia in diseases.

## 2. METHODS

The experimental protocol for this study was approved by the Committee on the Use of Live Animals in Teaching and Research of The University of Hong Kong. Sprague-Dawley rats (120-150 g) were randomly divided into normoxic control and chronically hypoxic (CH) group. While the control was maintained in room air, CH rats were kept in a 300-liter acrylic chamber for normobaric hypoxia in the same room and had free access to water and chow. The oxygen fraction inside the chamber was kept at 10±0.5% and was established by a mixture of room air and nitrogen which was regulated by an oxygen analyser (Vacumetrics Inc., CA, USA). Carbon dioxide was absorbed by soda lime granules and excess humidity was removed by a desiccator. The chamber was opened twice a week for an hour to clean the cages and replenish food and water. The rats were exposed to hypoxia for 4 weeks and were immediately used in experiments after taken out of the chamber.

Following deep anesthesia with halothane, the rat was decapitated and the carotid bifurcation was excised rapidly. The CB was carefully dissected free from the bifurcation in chilled rat Ringer's solution oxygenated with 95% $O_2$ and 5% $CO_2$. The CB was then incubated in a tissue bath with collagenase and protease in oxygenated Ringer's for 30 min.

For electrophysiology, ex-vivo CB was held in the recording chamber at 35±1 °C, and superfused with oxygenated Ringer's solution in a flow rate of 2 ml/min. Single or pauci-fiber activities of the sinus nerve were recorded extracellularly with a suction electrode. The signal was amplified, filtered, monitored, digitized and stored for off-line analysis. Acute hypoxia was induced by switching the perfusate to Ringer's solution gassed with 95% $N_2$ and 5% $CO_2$.

Intracellular calcium was measured in fura-2 loaded glomus cells freshly dissociated from rat CBs by spectrofluorimetry as described previously (Fung *et al.* 2001a). CB cells were dispersed by trituration and incubated with fura-2AM (Molecular Probes, Ore., USA) for 30 min. Following rinses, cells were seeded on cover-slip for the measurement. Glomus cells in clusters of 8-20 cells were studied.

The fabrication and calibration of the NO electrode has been described previously (Fung *et al.* 2001b). Briefly, a laboratory-made Pt wire insulated in a poly-ethylene tube was dipped in Nafion. The Nafion-coated electrode was further modified with palladium and iridium oxide particles for improving the sensitivity of the NO electrode. Then, a thin film of poly-*o*-aminophenol (POAP) was deposited in the outer layer to ameliorate the selectivity of the NO electrode and to avoid fouling by proteins. NO standards were prepared by serial dilution of a saturated NO solution. Electrochemical experiments were performed on a CHI 660A Electrochemical Analyzer (CH Instruments, USA) at room temperature in a three-compartment cell with a Ag/AgCl reference electrode, a Pt wire auxiliary electrode and a chemically modified electrode as working electrode. The NO electrode was calibrated with successive injections of various concentrations of NO to the Ringer's solution in the recording chamber.

The electrode and CB were equilibrated in the perfusate for 15-30 min. The tip of the NO electrode was gently inserted into the CB under visual guidance with a dissecting microscope. Following current recording in the resting condition for 10-15 min, hypoxia was induced for 5 min following by recovery for 20-30 min. For the drug treatment, L-NAME (500 μM) or *S*-methylisothiourea (SMT, 50 μM) was added freshly to the oxygenated Ringer's and perfused for 10 min before hypoxia. For the measure of NO release, the resting and peak values of the current were subtracted and calibrated in NO concentration (nanomoles) according to the current response curve of the NO electrode.

The rat Ringer's solution contained (mM): NaCl 125, KCl 3.1, $NaHCO_3$ 26, $NaH_2PO_4$ 1.25, $MgSO_4$ 1.3, $CaCl_2$ 2.4, D-Dextrose 10, pH at 7.35. $K_2IrCl_6$, $K_2PdCl_6$, *o*-Aminophenol and Nafion perfluorinated ion-exchange resin in alcohol were obtained from Aldrich. SMT was purchased from Tocris Cookson and the remaining chemicals were obtained from Sigma.

For data analysis, values were normalized as a percentage of control if necessary and presented as mean +/- SE. Means were compared with Student *t*-test or the non-parametric Wilcoxon signed-rank test. ANOVA with a post-hoc test (Dunnett's *t*-test) was used for multiple comparisons of values in studies among groups. Differences were considered significant at $P<0.05$.

Details for immunohistochemistry have been described previously (Chen *et al.* 2002). In brief, carotid bifurcations were fixed in formalin and serial sections of 5 μm thickness were cut and mounted. Subsequently, sections were immunostained with antiserum to ET-1 (polyclonal rabbit antibody; Peninsula Laboratories, Calif., USA), iNOS (polyclonal rabbit antibody; Transduction Laboratories, Lexington, KY, USA), HIF-1α (mouse

monoclonal IgG antibody, Calbiochem, CA, USA), VEGF (mouse monoclonal IgG antibody, Santa Cruz Biotechnology Inc., USA), VEGFR-1 (rabbit IgG antibody, Santa Cruz Biotechnology Inc., USA), VEGFR-2 (rabbit IgG antibody, Santa Cruz Biotechnology Inc., USA), using LSAB kit (Dako, Denmark) for HIF-1α and Dako envision kit (Dako, Denmark) for the others. To block endogenous peroxidase activity, the sections were immersed in hydrogen peroxide. All sections were immersed in a solution containing trypsin and $CaCl_2$. Sections were pre-incubated with normal horse serum to reduce non-specific binding of the antiserum. Then, sections were incubated with the corresponding primary antibodies in Tris-HCL buffer respectively containing bovine serum albumin. Sections were washed in PBS, then incubated with peroxidase labeled polymer conjugated to goat anti-rabbit IgG in Tris-HCL buffer. Finally, sections were washed and the peroxidase was visualized by immersing in diaminobenzidine containing hydrogen peroxide in Tris-HCl buffer. Sections were rinsed and counterstained with hematoxylin. Positive staining was indicated by a brown color. The specificity of the immunoreactivity was determined by substitution of buffer for the primary antibody. Control sections were incubated with normal rabbit IgG and stained uniformly negative.

## 3. RESULTS

Immunohistochemical study revealed that a strongly positive HIF-1α–immunostaining was observed in majority of cells throughout the CBs of CH rats and the staining was found primarily in nuclei of the cells. The nuclear staining was intense in round and in disk-shaped nuclei, as well as in nuclei surrounding vessels in the CB, suggesting HIF-1α protein was expressed in the glomus cell, sustentacular cell and in the vascular smooth muscle and endothelial cell. In contrast, a mild expression of HIF-1α protein was found in the normoxic group. The immunostaining was negative in CB sections with a replacement of either the primary or the secondary antibody with normal serum.

Cytoplasmic staining of VEGF-immunoreactivity was intense and ubiquitously found in cells with round nuclei and clustering in glomeruli in the CBs of CH rats but was absent in normoxic CBs. These suggest an increased expression of VEGF in the glomus cells during chronic hypoxia. For the VEGF receptors (VEGFR), the immunoreactivities of VEGFR-1 and VEGFR-2 in the CB were determined in normoxic and CH rats. For the VEGFR-1, a specific staining was strongly intense in lobules of glomus cells in the CBs of CH group and the staining was also found in cells adjacent to vessels, suggesting an expression in both parenchymal and vascular cells in

the CB. In contrast, the expression was relatively low and the positive staining was light in the parenchyma in normoxic controls. These indicate that the expression of VEGFR-1 was enhanced in chronic hypoxia. A positive staining of VEGFR-2 was strongly intense and distributed in cell clusters and in vascular linings in the CB of both the CH and normoxic group. Hence there was no major differences in the VEGFR-2 expression between the two groups.

Both ET-1 and iNOS were positively stained in most of the cells clustering in glomeruli in the CB of CH rats but were absent in normoxic group. Spectroflurometric studies showed that the intracellular calcium response to ET-1 (100 nM) in freshly dissociated CH rat glomus cells was augmented by about 50% compared with that of the ET-1 response in the normoxic group. These results suggest an enhancement of the paracrine/autocrine effect of ET-1 on the chemoreceptors for the increases of excitability and mitosis of the chemoreceptors during chronic hypoxia.

The amount of NO release induced by acute hypoxia in the ex-vivo CB was significantly augmented in the CH group (~470 nM) compared with that of the normoxic CB (~90 nM). The hypoxia-induced NO generation was markedly attenuated by pretreatment with L-NAME (500 μM), a non-selective NOS inhibitor, and also by *S*-methylisothiourea (SMT, 50 μM), a specific blocker for iNOS. These indicate that hypoxia-induced NO production increases in the rat CB adapted to chronic hypoxia and that iNOS is involved in the NO generation. In addition, electrophysiological studies in ex-vivo CB showed pre-treatment with L-NAME increased the hypoxic response of the sinus nerve, confirming the inhibitory role of endogenous NO generation for the chemoreception.

## 4. DISCUSSION

Chronic hypoxia increased the nuclear expression of HIF-1α protein in most of the CB cells. This finding is consistent with previous studies showing that protein expression of HIF-1α and DNA-binding activity of HIF-1 in the nucleus of cultured cells are increased by hypoxia (Jiang *et al.* 1996). Also, mRNA and protein expression of HIF-1α but not HIF-1β is elevated in the lung (Palmer *et al.* 1998) and brain (Chavez *et al.* 2000) of rats exposed to chronic hypoxia. Hence, results are in agreement with the hypothesis that HIF-1α plays an active role in the physiological adaptation in response to hypoxia.

The vascular volume increases in the CB of CH rats (Clarke *et al.* 2000) and this may be due to an increase in vascularity of the CB (Dhillon *et al.* 1984; McGregor *et al.* 1984; Bee *et al.* 1986) and in the diameter of the

large venous vessels (Clarke *et al.* 2000). The increased VEGF expression in the glomus cells may play a paracrine role in the angiogenesis that vascularizes the CB by capillary sprouting from the existing vascular network. It has been shown that VEGF increases the length of the endothelial cells and induces branches, i.e. increased number of the endothelial cells, in the rat brain during chronic hypoxia (Harik *et al.* 1995). In addition, VEGF increases the permeability of vessels which enhances the filtration of fluid out into the interstitium, and thus may be responsible for the increase in extravascular volume of the CB during chronic hypoxia (Clarke *et al.* 2000). Hence, the expression of VEGF in the glomus cells may involve in changes of the CB vasculature and may partially responsible for the enlargement of the CB in chronic hypoxia.

It is known that CH induces hypertrophy and hyperplasia in the CB. ET-1 expresses in the CB (He *et al.* 1996; Chen *et al.* 2000) and it stimulates the proliferation of cultured glomus cells (Paciga *et al.* 1999). Hence, the intracellular calcium response to ET-1 in the glomus cells may play a role in the proliferation and structural changes of the chemoreceptors during chronic hypoxia. In addition, the elevation of intracellular calcium is an essential step for vesicular release of neurotransmitters for the chemoreception. Thus, the enhancement of the sensitivity to ET-1 may increase the excitability of the chemoreceptors to hypoxia.

The hypoxia-induced NO generation augmented in the CB of CH rats suggesting an increased production of NO during the physiological adaptation to chronic hypoxia. The enhanced NO generation can be explained by an increased amount of NOS in the CB. In this regard, the CB enlarges in chronic hypoxia and the vasculature in the CB undergoes remodeling with formation of new vessels and increased density of the capillary (McGregor *et al.* 1984; Bee *et al.* 1986). The expression of eNOS has been reported in the endothelium of the CB (Gozal *et al.* 1996; Kline *et al.* 2000). Thus, an increased number of the endothelial cells and area of vascular endothelium in the CB may cause the increased expression of eNOS during chronic hypoxia (Prabhakar 1999) and this can increase the NO production in response to hypoxia. In addition, nNOS is expressed mainly in nerve fibres in the CB (see Wang *et al.* 1995 for review). With the vascular remodeling and the proliferation of the chemoreceptors in the CB during chronic hypoxia, the total number of nitrergic nerve fibers surrounding small arteries and arterioles and clusters of glomus cells may increase. In fact, the expression of nNOS increases in the CB during chronic hypoxia (Prabhakar 1999). Our study shows an increased iNOS expression in the CH CB, suggesting an involvement of iNOS. The enhanced production of NO plays a physiological role in the blunting of the hypoxic ventilatory response and chemosensitivity during chronic hypoxia. Also, the augmentation of NO

generation may enhance vasodilatation, thus increasing the blood flow and oxygen delivery in the CB during chronic hypoxia.

In conclusion, our results suggest that tissue hypoxemia induces the transcriptional activity of HIF-1 and regulates a spectrum of gene products involving in the structural remodeling and physiological adaptation of the CB to chronic hypoxia (Fig. 1).

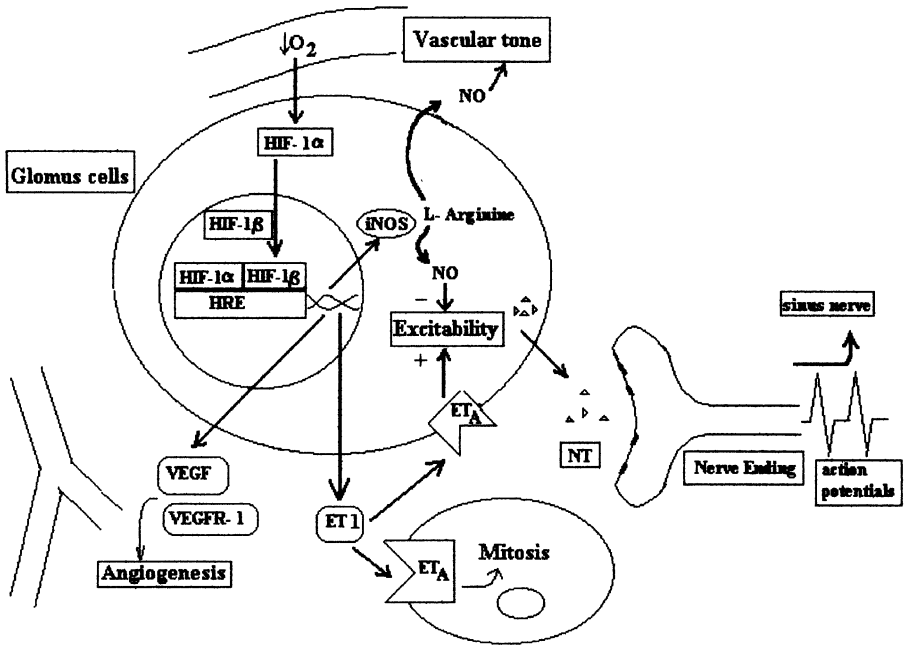


*Figure 1.* Summary of the putative roles of HIF-1 and its target gene products in the anatomical and physiological changes of the CB in chronic hypoxia. Chronic hypoxia increases HIF-1α level and HIF-1 activity, and these activate the mRNA expression of genes encoding ET-1, iNOS, VEGF, and VEGFR receptors in the CB. These proteins may be functionally important for the vascular remodeling of the CB in chronic hypoxia, and also for physiological changes including the increase of excitability and mitosis of the chemoreceptors and the blunting of the carotid response to hypoxia in chronic hypoxia. Abbreviations: arrows, directions of movement or signaling flow; ET-1, endothelin-1; $ET_A$, endothelin receptor A; HIF-1, hypoxia-inducible factor-1; HRE, hypoxia-response element; NO, nitric oxide; iNOS, inducible nitric oxide synthase; NT, neurotransmitter; VEGF, vascular endothelial growth factor; VEGFR-1, VEGF receptor 1.

## ACKNOWLEDGEMENTS

The authors thank W. B. Wong, K. M. Leung and J. Leung for their technical assistance. This work was supported by CERG grants of RGC, Hong Kong and UGC research grants of HKU (MLF)

## REFERENCES

Bee, D., Pallott, D. J., and Barer, G. R., 1986, Division of type 1 and endothelial cells in the hypoxic rat carotid body. *Acta. Anat.* 126: 226-229.

Bisgard, G. E., 2000, Carotid body mechanisms in acclimatization to hypoxia. *Resp. Physiol.*. 121: 237-246.

Chavez, J. C., Agani, F., Piciule, P., and LaManna, J. C., 2000, Expression of hypoxia-inducible factor-1α in the brain of rats during chronic hypoxia. *J. Appl. Physiol.* 89: 1937-1942.

Chen, J., He, J., Dinger, B., and Fidone, J., 2000, Cellular mechanisms involved in rabbit carotid bidy excitation elicited by endothelin peptides. *Respir. Physiol.* 121: 13-23.

Chen, Y., Tipoe, G. L., Liong, E., Leung, P. S., Lam, S.-Y., Iwase R., Tjong, Y.-W., and Fung, M.-L., 2002, Chronic hypoxia enhances endothelin-1-induced intracellular calcium elevation in rat carotid body chemoreceptors and up-regulates $ET_A$ receptor expression. *Pflügers Archiv* 443: 565-573.

Clarke, J. A., Daly, M. B., Marshall, J. M., Ead, H. W., and Hennessy, E. M., 2000, Quantitative studies of the vasculature of the carotid body in the chronically hypoxic rat. *Braz. J. Med. Biol. Res.* 33: 331-340.

Dhillon, D. P., Barer, G. R., and Walsh, M., 1984, The enlarged carotid body of the chronically hypoxic and hypercapnic rat: a morphometric analysis. *Q. J. Exp. Physiol.* 69: 301-317.

Fung, M.-L., Lam, S.-Y., Chen, Y., Dong, X., and Leung, P. S., 2001a, Functional expression of angiotensin II receptors in type-I cells of the rat carotid body. *Pflügers Archiv* 441: 474-480.

Fung, M.-L., Ye, J.-S., and Fung, P. C. W., 2001b, Acute hypoxia elevates nitric oxide generation in rat carotid body in vitro. *Pflügers Archiv* 442: 903-909.

Gonzalez, C., Almaraz, L., Obeso, A., and Rigual, R., 1994, Carotid body chemoreceptors: From natural stimuli to sensory discharges. *Physiol. Rev.* 74: 829-898

Gozal, D., Gozal, E., Gozal, Y. M., and Torres, J. E., 1996, Nitric oxide synthase isoforms and peripheral chemoreceptor stimulation in conscious rats. *Neuroreport* 7: 1145-1148.

Harik, S. I., Hritz, M. A., and LaManna, J. C., 1995, Hypoxia-induced brain angiogenesis in the adult rat. *J. Physiol. (Lond.)* 485: 525-530.

He, L., Chen, J., Dinger, B., Stensaas, L., and Fidone, S., 1996, Endothelin modulates chemoreceptor cell function in mammalian carotid body. *Adv. Exp. Med. Biol.* 410: 305-310.

Jiang, B. H., Semenza, G. L., Bauer C., and Marti H. H., 1996, Hypoxia-inducible factor 1 levels vary exponentially over a physiologically relevant range of $O_2$ tension. *Am. J. Physiol.* 271: C1172-1180.

Kline, D. D., Yang, T., Premkumar, R. D., Thomas, A. J., and Prabhakar, N. R., 2000, Blunted respiratory responses to hypoxia in mutant mice deficient in nitric oxide synthase-3. *J. Appl. Physiol.* 88: 1496-1508.

Lahiri, S., Rozanov, C., Roy, A., Storey, B., and Buerk, D. G., 2001, Regulation of oxygen sensing in peripheral arterial chemoreceptors. *Int. J. Biochem. & Cell Biol.* 33: 755-774.

McGregor, K. H., Gil, J., and Lahiri, S., 1984, A morphometric study of the carotid body in chronically hypoxic rats. *J. Appl. Physiol.* 57: 1430-1438.

Paciga, M., Vollmer, C., and Nurse, C., 1999, Role of ET-1 in hypoxia-induced mitosis of cultured rat carotid body chemoreceptors. *Neuroreport* 10: 3739-3744.

Palmer, L. A., Semenza, G. L., Stoler, M. H., and Johns, R. A., 1998, Hypoxia induces type II NOS gene expression in pulmonary artery endothelial cells via HIF-1. *Am. J. Physiol.* 274: L212-219.

Prabhakar, N. R., 1999, NO and CO as second messengers in oxygen sensing in the carotid body. *Resp. Physiol.* 115: 161-168.

Semenza, G. L., 2000, HIF-1: mediator of physiological and pathophysiological responses to hypoxia. *J. Appl. Physiol.* 88: 1474-1480.

Wang, Z.-Z., Dinger, B. G., Stensaas, L. J., and Fidone, S. J., 1995, The role of nitric oxide in carotid chemoreception. *Biol. Signals* 4: 109-116.

# Carotid Body HIF-1α, VEGF and NOS Expression during Aging and Hypoxia

DI GIULIO CAMILLO., BIANCHI GIUSEPPINA, CACCHIO MARISA., MACRÌ M.A.*, FERRERO G.°, RAPINO C., VERRATTI V., PICCIRILLI M. and ARTESE L.°

*Department of Biomedical Sciences, Centre of Excellence for Aging and ° Dept. of Odontostomatology "G. d'Annunzio" University, Chieti . * Dept. of Experiment Med. and Pathol. INFM Rome. Italy.*

## 1. INTRODUCTION

Carotid body (CB) undergoes several morphological, physiological and biochemical changes during aging, hypoxia and hyperoxia (Di Giulio *et al.*, 1998; Lahiri *et al.*,1990; Lahiri *et al.*,2000). CB releases several substances like dopamine, acetilcholine, nerpinephrine, erythropoietin, substance P, and it detects $pO_2$ and $pCO_2$ levels in the blood, it regulates ventilation according to oxygen needs and body requirements for homeostasis maintenence (Bunn *et al.*, 1996). The ventilatory response to hypoxia is characterised by increase in volume and ventilatory frequency in relation to the degree of hypoxia. This response is attenuated with aging (Fukuda 1992) and it is related to the age-dependent structures and function modifications (Guenard 1998), including the basal reduction of oxygen requirements (Sohalet.al,1986, Gunnarsson *et al.*, 1996).

During aging there is a reduction of nerve conductivity, the maximum number of impulses per minute generally decrease with lowering of sensitivity of peripheral receptor, so leading to a reduction of the homeostatic capacity and a higher latency in adaptation responses (Rivner *et al.*, . 2001). As a response to hypoxia, HIF-1α (Hypoxic Inducible Factor -1α) mediates transcriptional activation of a network of genes encoding for VEGF (Vascular Endothelial Growth Factor), NOS (Nitric Oxide Sintase), erythropoietin and several glycolytic enzymes (Iyer *et al*, 1998).

*Chemoreception*, Edited by Pequignot et al.
Kluwer Academic/Plenum Publishers, New York, 2003

Acute hypoxia increases impulses in chemosensory fibres, while chronic hypoxia leads to enlargement and hypertrophy of glomus cells, enhancement of catecholamine content and a blunted respiratory response. The response to chronic hypoxia suggests that a number of CB factors involved with growth and neurotransmission are released with time. Another consideration is that chronic hyperoxia attenuated the response to hypoxia, while the response to $CO_2$ remains unaltered (Lahiri *et al.*,1987), suggesting that the sensitive-mechanisms for carbon dioxide and oxygen are not the same. Generally growth, differentiation, aging and death of cells are related to a series of factors including oxygen consumption, intracellular pH, free radicals (Wickens 2001, Trounce et al,1989). During aging the antioxidant capacity is reduced and the $CO_2$-$O_2$ sensitivity is modified. Oxygen sensitive mechanisms are age-dependent and undergo several modifications (Trubiani *et al.*, 2002).

In our previous study we pointed out that chronic hypoxia induces an increase in the activity of NOS (Di Giulio et al., 2000, Zakrewicz et al., 2001). To test if oxygen-sensitive mechanisms are affected in an age-dependent fashion, we studied HIF-1α, VEGF and NOS after chronic hypoxia.

## 2. METHODS

Four groups of six male Wistar rats weighting 200-250 g. were used, according to the guidelines of the Declaration of Helsinki. Two age-matched groups (3 and 24 months old) were kept at room air (21 % $O_2$) used as control groups, the other two groups were kept in a Plexiglas chamber for 12 days in chronic intermittent hypoxia (10-12 % inspired oxygen for 12 hours for day). Chamber temperature and $CO_2$ were kept in physiological ranges. The rats were anaesthetized with Nembutal 40 mg/kg, i.p. and the CBs were dissected.

Immunohistochemistry for HIF-1α ,VEGF and -nitric oxide synthase (NOS-1) were evaluated by immunohistochemical analysis (Santa Cruz Biotech antibodies). Diaphorase activity were used to quantify the reaction from arginine to NO (Bredt *et al.*, 1990). Carotid body tissues were immersed over night in ice cold 4 % paraformaldehyde in 0.1 M phosphate buffered saline (PBS). Tissues were then rinsed in 15 % sucrose PBS (1 h) and stored at 4°C in 30 % sucrose PBS (2 h). Ten micrometer thick sections were cut using a cryomicrotome (Reichert-Jung Frigocut 2800), thaw-mounted onto microscope slides, fixed by immersion in acetone at 4°C for 5 min, and air-dried. Slides were stored at 4°C until used. For the immunohistochemical

staining of NO synthase, VEGF and HIF slides were preincubated in PBS for 5 min and then with NOS1 of rat origin ( R.20- Santa Cruz Biotech, Inc) which was diluted 1:100 in PBS and applied for 30 min. at 37 °C. Slices were then washed twice in PBS for 5 min. and in tris-HCl buffer, pH 7.6 for 10 min. A peroxidase-conjugated second antibody, goat antirabbit IgG, was added for 10 min. and slides were again washed in PBS. The peroxidase label was developed using diaminobenzidine (DAB) dissolved in imidazole buffer, pH 7.6 for 6-10 min , washed in tris-HCl buffer, and dehydrated.For histochemical staining of NADPH-diaphorase, slides were immersed for 30 min at 37 °C in 50 mM tris-HCl, pH 8.0, 1 mM-NADPH, 0.5 mM nitroblue tetrazolium (NBT), 0-2 % Triton X-100. The slides were briefly washed in PBS and dehydrated with a graded series of ethyl alcohols.

Slides from both staining procedures were mounted using Permount., cover-slipped and photographed through a Leitz Dialux microscope. CBs densitometric analyses were carried out randomly, using a Sony Video camera connected with a Quantimet 500 Plus (Leica) to determine the gray intensity levels.

## 3. RESULTS

HIF-1 α, VEGF and NOS are expressed in the carotid body and they are more expressed in the hypoxic carotid body as compared to the normoxic one (Fig 1,2,3 ). The increase in expression of HIF-1α, VEGF, NOS-1 is less evident in the CBs of old rats as compared to the young ones (Fig 4).

## 4. CONCLUSION

Time course of NOS, VEGF and HIF by CB depends on the level and on time of hypoxia exposure (Lahiri *et al.*, 2002) and age (Richmonds *et al.*, 1999). When we say "chronic hypoxia" we have to specify if we consider an "intermittent" situation, minutes, hours, days or months of hypoxia exposure (Schmidt 2002). Moreover, when evaluating hypoxic responses also gender (Soliz *et al.*, 2000, Loeppky *et al.*, 2001) and age differences should be considered.

Changes in oxygen supply such as chronic hypoxia or hyperoxia to CB could represent a model for studying aging. The lower increases in Hypoxia Inducible Factor-1α, Vascular Endothelial Growth Factor and Nitric Oxide Synthase-1 during aging are important tools for aging studies.

Normally acute hypoxia inhibits the activity of several enzymes, while others such as tyrosine hydroxylase are stimulated and represent a defence mechanism (Prabhakar *et al.*, 2001).Time course of hypoxia involves

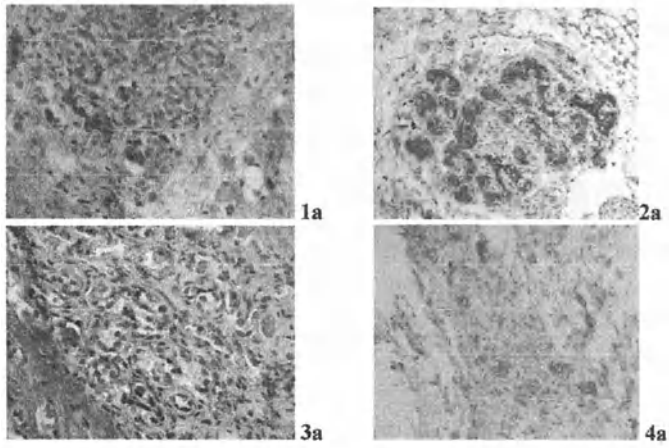


**Fig.1: Carotid Body HIF-1α expression:**
**1a normoxic young**
**2a hypoxic young**
**3a normoxic old**
**4a hypoxic old**

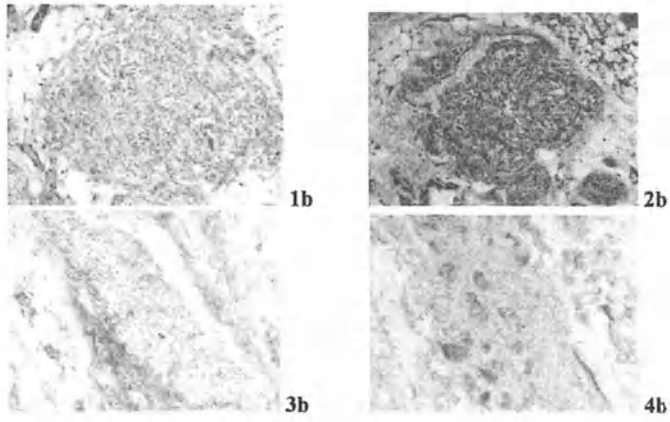


**Fig.2: Carotid Body VEGF expression:**
**1b normoxic young**
**2b hypoxic young**
**3b normoxic old**
**4b hypoxic old**

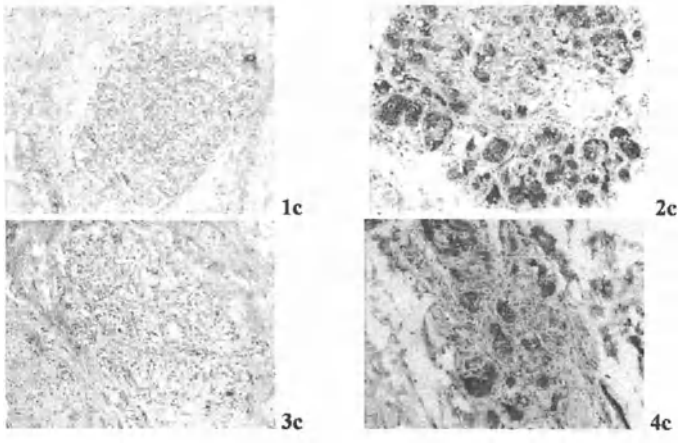


**Fig.3: Carotid Body NOS expression:**
**1c normoxic young**
**2c hypoxic young**
**3c normoxic old**
**4c hypoxic old**

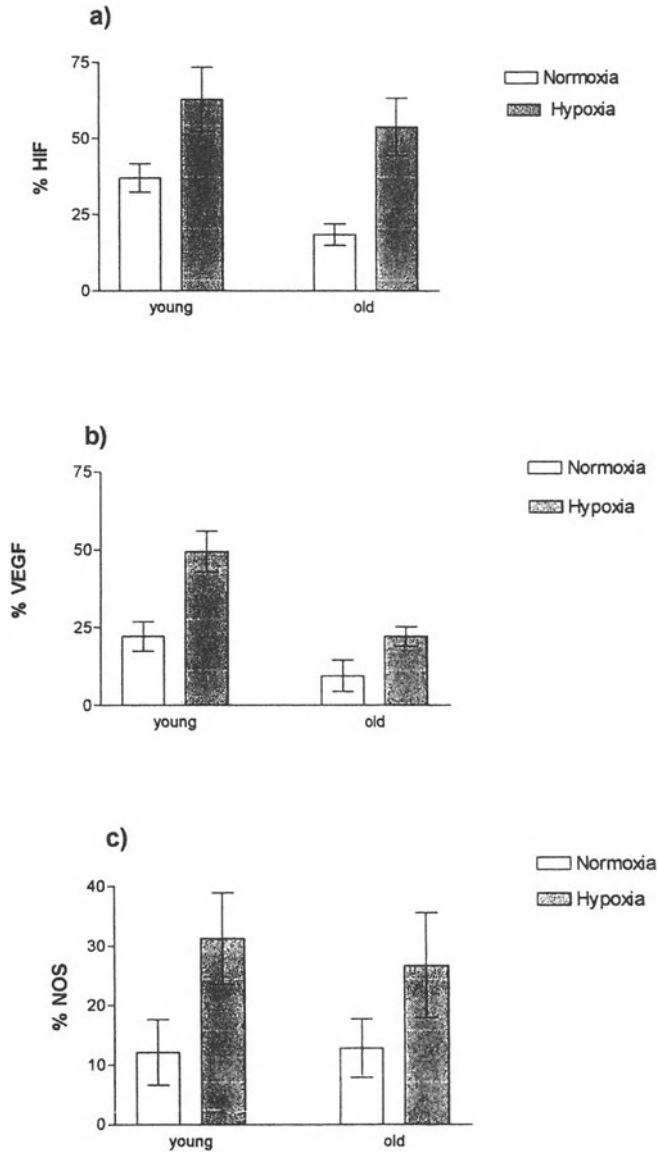


**Fig. 4: Carotid body HIF-1α, VEGF and NOS expression**

different pathways. The increase in HIF, NOS and VEGF could be responsible for the reduction in ventilatory response during chronic hypoxia and aging. These responses could be adaptations to long term stimulation by age or hypoxia, and hypoxia and aging could share some kind of link in the CB model. The CB hyperplasic effect during chronic hypoxia is less evident in aged CB than in young. Hypoxia stimulated release of several growth factors such as epidermal growth factor (EGF), nerve growth factor (NGF), erythropoietin (EPO) fibroblast growth factor, platelet derived growth factor (PDGF). During aging the release of these substances would be lower, so explaining the reduced hyperplasic effect due to hypoxia. (Di Giulio unpublished observation).

Hypoxia and aging (Martinelli *et al.*,1990, Cerretelli *et al.*, 1996) are considerable "stresses" for the CB. Free radical production (Jamieson 1989; Finkel *et al.*,2000) can interfere with oxygen sensitive mechanisms. The stimulatory effect of NOS, VEGF, HIF and tyrosine hydroxylase in CB helps to postulate the hypothesis that there might be a common mechanism for enzymatic activation during chronic hypoxia. It is possible that oxygen might keep these enzymes in physiological ranges. NOS, VEGF, HIF can act as putative modulators in CB, interacting with the oxygen sensor. Aging interplaying with of all these factors may modify CB structure and function, representing an adaptive process. The chromophore theory of chemoreception still remains, and NO, VEGF and HIF production is reduced in aged CB. In conclusion, CB is a model to study aging processes, since CB is endowed with high blood flow and metabolism, so strengthening its function as a tool for modulating aging processes which interfere with cell metabolism.

## ACKNOWLEDGMENTS

We would like to thanks Dr. F. Daniele for her help in correcting the manuscript

## REFERENCES

Bredt, D.S., Hwang, P.M., Snyder, S.H., 1990, Localization of nitric oxide synthase indicating a neuronal role for nitric oxide. *Nature* 347: 768.

Bunn, H.F., Poyton, R.O., 1996, Oxygen sensing and molecular adaptation to hypoxia. *Physiol Rev.* 76: 839-885.

Cerretelli, P., and Hoppeler, H., 1996, Morphological and metabolic response to chronic hypoxia: the muscle system. *Handbook of Physiology –Environment Physiology* 50: 1155-1181.

Di Giulio, C., Di Muzio, M., Sabatino, G., Spoletini, L., Amicarelli, F., Di Ilio, C., and Modesti, A.,1998, Effect of chronic hyperoxia on young and old rat carotid body ultrastructure. *Exp Gerontol.* 33: 319-329.

Di Giulio, C., Grilli, A., Ciocca, I., Macrì, M.A., Daniele, F., Sabatino, G., Cacchio, M., Da Porto, R., Di Natale, F., and Felaco, M., 2000, Carotid body NO-CO interaction and chronic hypoxia. In *Oxygen sensing: Molecule to Man* (S. Lahiri, N.R. Prabhakar, R.E. Forster, eds.), Kluver Press, New York, pp.685-690.

Finkel, T., and Holbrook, N.J., 2000, Oxidants, oxidative stress and the biology of ageing. *Nature* 408: 239- 247.

Fukuda, Y., 1992, Changes in ventilatory response to hypoxia in the rat during growth and aging. *Pflügers Arch.* 421: 200-203.

Guenard, H., 1998, Respiration and aging. *Rev Mal Respir.* 15: 713-721.

Gunnarsson, L., Tokics, L., Brismar, B., and Hedenstierna, G., 1996, Influence of age on circulation and arterial blood gases in man. *Acta Anaesthesiol. Scand.* 40: 237-243.

Habeck, J.O., Huckstorf, C., and Behm, R., 1988, The paraganglia within the carotid bifurcation regions of young and old spontaneously hypertensive rats (SHR) after exposure to chronic hypobaric hypoxia. I. The carotid bodies. *Anat. Anz.* 165: 45-54.

Iyer, N.V., Kotch, L.E., Agani, F., Leung, S.W., Laughner, E., Wenger, R.H., Gassmann, M., Gearhart, J.D., Lawer, A.M., Yu, A.Y., Semenza, G.L., 1998, Cellular and developmental control of $O_2$ homeostasis by hypoxia-inducible factor 1-$\alpha$ . *Genes Dev.* 12: 149-162.

Jamieson, D.,1989, Oxygen toxicity and reactive oxygen metabolites in mammals. *Free Radic. Biol. Med.* 7: 87-108.

Lahiri, S., Mulligan, E., Andronikou, S., Shirahata, M., and Mokashi, A.,1987, Carotid body chemosensory function in prolonged normobaric hyperoxia in the cat. *J. Appl. Physiol.* 62(5): 1924-1931.

Lahiri, S., Mokashi, A., Di Giulio, C., Sherpa, A.K., Huang, W.X., and Data, P.G.,1990, Carotid body adaptation: Lesson from chronic stimuli. In *Hypoxia: The Adaptations* (J.R. Sutton, G. Coates, J.E. Remmers and B.C. Dekker, eds.), Philadelphia, pp. 127-130.

Lahiri, S., Rozanov, C., and Cherniack, N.S., 2000, Altered structure and function of the carotid body at high altitude and associated chemoreflexes. *High Altitude Medic. & Biol.* 1: 63-74.

Lahiri, S., Di Giulio, C., and Roy, A., 2002, Lesson from chronic intermittent and sustained hypoxia *Respir Physiolo. and Neurobiol.* 130: 223-233.

Loeppky, J.A., Scotto, P., Charlton, G.C., Gates, L., Icenogle, M., Roach , R.C., 2001, Ventilation is greater in women than men, but the increase during acute hypoxia is the same. *Respir. Physiol.* 125: 225-237.

Martinelli, M., Winterhalder, R., Cerretelli, P., Howald, H., and Hoppeler, H., 1990, Muscle lipofuscin content and satellite cell volume is increased after high altitude exposure in humans. *Experientia* 46: 672-676.

Prabhakar, N.R., Fields, R.D., Baker, T., Fletcher, E.C., 2001, Intermittent hypoxia: cell to system. *Am. J. Physiol. Lung Cell Mol. Physiol.* 281: 524-528.

Richmonds, C.R., Boonyapisit, K., Kusner L.L., and Kaminski, H.J., 1999, Nitric oxide synthase in aging rat skeletal muscle. *Mech. Ageing Dev.* 109: 177-189.

Rivner, M.H., Swift, T.R., Malik, K., 2001, Influence of age and height on nerve conduction. *Muscle & Nerve* 24: 1134-1141.

Schmidt, W., 2002, Effect of Intermittent Exposure to High altitude on blood volume and erythropoietic activity. *High Altitude Medic. & Biol.* Vol.3: 167-176.

Sohal, R.S., Toy, P.L., and Allen, R.G., 1986, Relationship between life expectancy, endogenous antioxidants and products of oxygen free radical reactions in the housefly, musca domestica. *Mech. Aging Dev.* 36: 71-77.

Soliz, J.V., Pequignot, J., Sempre, B., Cottet-Emard, J.M., Dalmaz ,Y., Favier, R., Spielvogel, H., Pequignot, J.M., 2000, Gender differentiation on the chemoreflex during growth at high altitude: functional and neurochemical studies. *Am J. Physiol. Regul. Integr. Comp. Physiol.* 278: 806-816.

Trounce, I., Byrne, E., and Marzuki, S., 1989, Decline in skeletal muscle mitochondrial respiratory chain function: possible factor in aging. *Lancet* 8639: 637-639.

Trubiani, O., Di Giulio, C., Tripodi, D., Bianchi, G., Paganelli, R., and Di Primio, R., 2002, Thymic sensitivity to hypoxic condition in young and old rats: Age-dependent expression of NF-Kappa B. *Exp. Gerontol.* 37: 1077-1088.

Wickens, A.P., 2001, Ageing and the free radical theory. *Respir. Physiol.* 128: 379-391.

Zakrewicz, A., Secomb, T.W., Pries, A.R., 2001, Angioadaptation: keeping the vascular system in shape. *News Physiol. Sci.* 17: 197-201.

# Rat Carotid Bodies in Systemic Hypoxia

***Involvement of arterial CO2 tension in morphological changes***

[1]TATSUMI KUSAKABE, [2]HIDEKI MATSUDA, [3]YOSHIAKI HAYASHIDA

*[1]Department of Sport and Medical Science, Kokushikan University, Tokyo 206-8515, Japan; [2]Department of Otorhinolaryngology, Yokohama City University School of Medicine, Yokohama 236-0004, Japan; [3]Department of Systems Physiology, University of Occupational and Environmental Health, Kitakyushu 807-8555, Japan*

## 1. INTRODUCTION

It has been reported by many authors that the carotid bodies become enlarged several fold in rats exposed to long term hypoxia. As a result of enlargement, the carotid body takes on a spongy appearance with increased vascularization. In early studies, experimental animals were exposed to hypoxia equivalent to that of high altitudes (3800-7500m) in a hypobaric chamber (Blessing and Wolff, 1973; Heath *et al.*, 1973; Moller *et al.*, 1974; Laidler and Kay, 1975a, b, 1978; Barer *et al.*, 1976), and in later studies, the animals were also exposed to hypoxia in a normobaric hypoxic chamber (10% $O_2$) (Pequignot and Hellström, 1983; Dhillon *et al.*, 1984; McGregor *et al.*, 1984; Pequignot *et al.*, 1984; Kusakabe *et al.*, 1998a, b; 2000, 2002). In some studies the animals were exposed to hypoxia for short periods of 1-2 weeks, and in other studies for long periods of 2-3 months.However, most authors use the term "chronic hypoxia" in their publications.Thus, the condition and duration of experimental hypoxic exposure have been various, and it is difficult to compare these results.

On the other hand, most studies on hypoxic exposure have not referred to carbon dioxide levels except in a few instances (Dhillon *et al.*, 1984). In recent years there has been much concern over global warming caused by increased levels of carbon dioxide. Therefore it is meaningful to investigate the

*Chemoreception*, Edited by Pequignot et al.
Kluwer Academic/Plenum Publishers, New York, 2003

effects of hypoxia which could be induced by varying levels of this gas.

Three types of hypoxia with different levels of carbon dioxide (hypocapnic, isocapnic, and hypercapnic hypoxia) have been called systemic hypoxia (Hayashida *et al.*, 1997). More recently we reported the changes in general morphology and in peptidergic innervation in the carotid bodies of rats exposed to long term (3 months) hypocapnic (10% $O_2$ in $N_2$; Kusakabe *et al*, 2000), isocapnic (10% $O_2$ and 2-3% $CO_2$; Kusakabe *et al.*, 1998), and hypercapnic hypoxia (10% $O_2$ and 6-7% $CO_2$; Kusakabe *et al.*, 2002). In this review, we summarize the morphological changes in the hypoxic carotid bodies to evaluate different levels of arterial $CO_2$ tension.

## 2. MORPHOLOGICAL CHANGES IN THE CAROTID BODIES IN SYSTEMIC HYPOXIA

In hematoxylin and eosin stained sections through the center of normoxic rat carotid bodies, the bodies are oval and highly vascular (Fig.1). The mean short and long axes of the normoxic control carotid bodies are 329.0±35.3 μm and 439.7±28.5 μm, respectively (Fig.2a).

The carotid bodies of the systemic hypoxic rats were found to be enlarged several fold, but the degree of enlargement was different for each (Fig.1). The mean short and long axes of hypocapnic hypoxic carotid bodies were 518.7±37.1 μm and 782.7±92.2 μm, those of isocapnic hypoxic carotod bodies were 525.8±24.4 μm and 827.7±29.5 μm, and those of hypercapnic hypoxic carotid bodies were 390.6±37.9 μm and 664.5±59.6 μm, respectively (Fig.2a). All values in the systemic hypoxic carotid bodies were significantly ($p<0.005$) larger than those in the normoxic control ones.In addition, the hypercapnic hypoxic carotid bodies were significantly ($p<0.005$) smaller than the hypocapnic and isocapnic hypoxic ones (Fig.2a).

In the normoxic control carotid bodies, about 90% of blood vessels were small with diameters of less than 10 μm, and blood vessels with diameters greater than 15 μm were under 10% (Fig.2b).In the hypocapnic and isocapnic hypoxic carotid bodies, the percentage of small blood vessels less than 5 μm was reduced to under 20%, and blood vessels with diameters greater than 15 μm increased to about 40% (Fig.2b).In the hypercapnic hypoxic carotid bodies, the percentage of relatively small vessels and that of relatively large vessels were similar to that in normoxic control carotid bodies, although the carotid bodies themselves were significantly larger than in normoxic controls (Fig.2b).

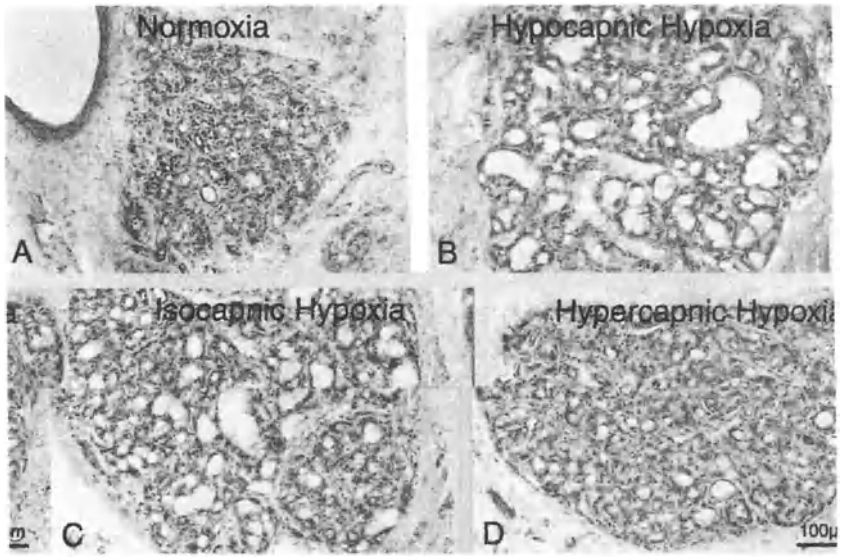


*Figure 1.* A comparison of hematoxylin-eosin stained sections of the control normoxic carotid body and systemic (hypocapnic, isocapnic, and hypercapnic) hypoxic carotid bodies (3 months).

## 3. CHANGES IN THE PEPTIDERGIC INNERVATION IN THE CAROTID BODIES IN SYSTEMIC HYPOXIA

Immunoreactivity of substance P (SP), calcitonin gene-related peptide (CGRP), vasoactive intestinal polypeptide (VIP), neuropeptide Y (NPY) was recognized in the nerve fibers distributed throughout the parenchyma of the normoxic control carotid bodies, although there were some differences in the abundance of immunoreactive fibers (Kusakabe *et al.*, 1998, 2000, 2002). They appeared as thin processes with many varicosities. NPY-immunoreactive varicose fibers were more numerous than SP-, CGRP-, and VIP-immunoreactive fibers. Most immunoreactive fibers were associated with the vasculature and some fibers were observed to surround the clusters of glomus cells. The mean density of varicosities in these neuropeptide-containing fibers per unit area ($10^4$ $\mu m^2$) was 6.47±1.03, 14.32±1.64, 12.54±1.79, and 45.63±5.28, respectively (Fig. 3).

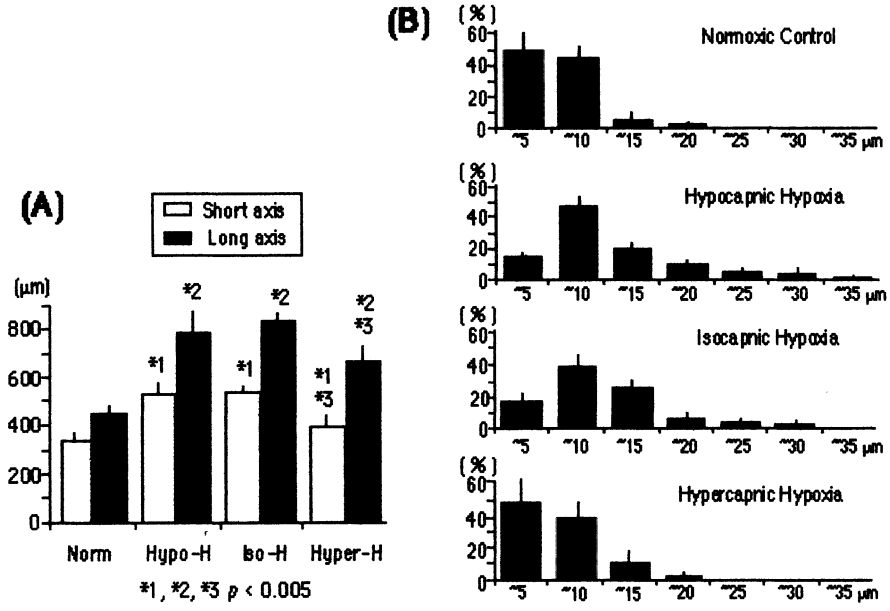


*Figure 2.* A comparison of the diameter of the carotid body (A) and the diameter (short axis) of blood vessels (B) within the carotid body in systemic hypoxia.

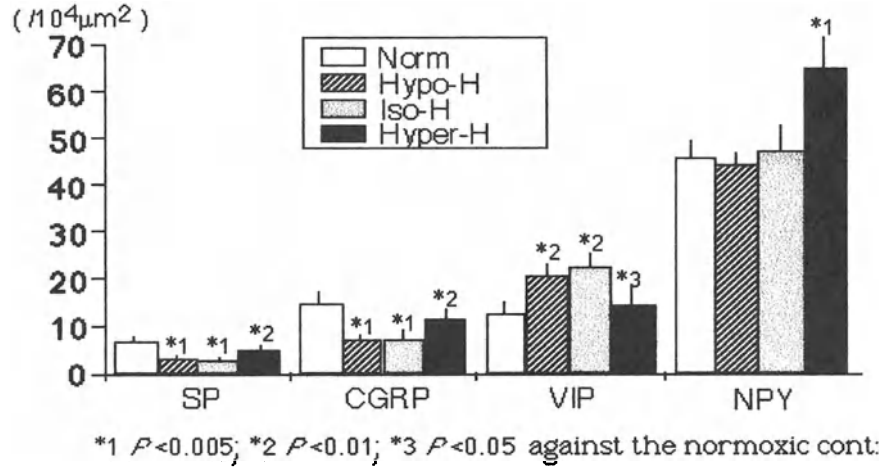


*Figure 3.* Histogram comparing the density of varicosities of SP, CGRP, VIP, and NPY immunoreactive fibers per unit area in normoxic (Norm) and hypocapnic (Hypo), isocapnic (Iso), and hypercapnic (Hyper) hypoxic carotid bodies.

In the chronically isocapnic hypoxic carotid bodies, SP, CGRP, VIP, and VIP immunoreactive fibers were mainly associated with enlarged vasculature (Kusakabe *et al.,* 1998). Especially, most VIP fibers were found around the vasculature. When the mean density of varicosities per unit area ($10^4$ $\mu m^2$) was compared in the same way, the density of VIP fibers was significantly ($p<0.01$) increased from 12.54±1.79 to 22.56±1.60, although that of NPY fibers was unchanged (Fig. 3). The mean density of SP and CGRP fibers per unit area was significantly ($p<0.01$) reduced from 6.47±1.03 to 2.24±0.34, and from 14.32±1.64 to 6.70±1.20, respectively (Fig. 3). The mean density of VIP fibers per unit area in chronically hypoxic carotid bodies was 1.80 (22.56/12.54) times higher than that of VIP fibers in normoxic carotid bodies, and the mean density of SP and CGRP fibers per unit area was 0.35 (2.24/6.47) and 0.47 (6.70/14.32) times higher than that of SP and CGRP fibers, respectively.

In chronically hypocapnic hypoxic carotid bodies, the density of VIP fibers was increased significantly 1.40 times, the density of SP and CGRP fibers was reduced significantly to under 50%, and the density of NPY was unchanged (Fig. 3) (Kusakabe *et al.,* 2000). Thus, changes in peptidergic innervation in chronically hypocapnic hypoxic carotid bodies was similar to changes in chronically isocapnic hypoxic bodies, although the individual rate was different for each.

In chronically hypercapnic hypoxic carotid bodies, however, the density of NPY fibers was significantly increased, and that of VIP fibers was unchanged (Fig. 3). Thus, the changes in the density of VIP and NPY fibers were reversed. The density of SP and CGRP fibers was reduced (Fig. 3).

No glomus cells with the immunoreactivity of these four neuropeptides were observed in the normoxic and chronically systemic hypoxic carotid bodies.

## 4. EFFECT OF CARBON DIOXIDE LEVELS

Considered together with the findings obtained from chronically systemic hypoxic rat carotid bodies, the rate of vascular enlargement in chronically hypercapnic hypoxic carotid bodies was smaller than in hypocapnic and isocapnic hypoxic carotid bodies. Furthermore, the density of NPY immunoreactive fibers in the hypercapnic hypoxic carotid bodies was significantly increased, and that of VIP was unchanged, although the density of NPY and VIP fibers was reversed in the chronically hypocapnic and isocapnic hypoxic carotid bodies. The difference in the density of NPY and VIP fibers between the hypercapnic and isocapnic and hypocapnic hypoxic carotid bodies suggests the involvement of a high level of arterial $CO_2$ tension (Kusakabe *et al.,*

2002).

We have suggested that at least part of the vascular expansion in the chronically hypocapnic and isocapnic hypoxic carotid bodies may be due to the vasodilatory effect of VIP, and concluded that VIP fibers around the blood vessels are indirectly involved in chemosensory mechanisms by controlling local carotid body circulation (Kusakabe *et al.*, 1998). More recently we also suggested that a low percentage of vascular enlargement in the chronically hypercapnic hypoxic carotid bodies may be due to the vasoconstrictory effect of the increased NPY resulting from hypercapnia (Kusakabe et al., 2002).

It has been generally suggested that $CO_2$ tension causes vasodilation in both central and peripheral vascular systems (Fensternacher and Rapoport, 1984). In hypercapnic hypoxic carotid bodies, however, the percentage of vascular enlargement is small. This may indicate that high $CO_2$ tension causes the carotid body vasculature to constrict. However, this finding may be restricted to the chronically hypoxic condition.

In conclusion, high $CO_2$ tension affects the peptidergic innervation in the carotid body during chronically hypoxic exposure. Altered innervation may regulate vascular tone in the chronically hypoxic carotid body.

## ACKNOWLEDGEMENTS

We are grateful to Ms. K. Haraguchi of the Department of Systems Physiology, University of Occupational and Environ-mental Health for hypoxic animal husbandry. This work was supported by grants-in aid 09670022, 11670015 and 13680048 from the Ministry of Education, Science, Sports, and Culture, Japan, and in part by grants in the project research at Kokushikan University.

## REFERENCES

Barer, G.R., Edwards, C., and Jolly A.I., 1976, Changes in the carotid body and the ventilatory response to hypoxia in chronically hypoxic rats. *Clinic Sci.* 50: 311-313.

Bleesing, M.H., and Wolff, H., 1973, Befunde an Glomus Caroticum der Ratte nach Aufenhalt im einer Simulierten Höhe von 7500m. *Virchows Arch. Pathol. Anat. Physiol.* 360: 78-97.

Dhillon, D.P., Barer, G.R., and Walsh, M., 1984, The enlarged carotid body of the chronically hypoxic and chronically hypoxic and hypercapnic rat: A morphometric analysis. *Quart. J. Exp. Physiol.* 69: 301-317.

Fenstermacher, J.D., and Rapoport, S.I., 1984, Blood-brain barrier. In: Handbook of Physiology. Volume IV. Microcirculation, Part 2. Waverly Press. Baltimore. Pp. 969-1000.

Hayashida, Y., Hirakawa, H., Nakamura, T. and Maeda, M., 1996, Chemoreceptors in autonomic responses to hypoxia in conscious rats. *Adv. Exp. Med. Biol.* 410:439-442.

Heath, D., Edwards, C., Winson, M., and Smith, P., 1973, Effects on the right ventricle, pulmonary vasculature, and carotid bodies of the rat of exposure to, and recovery from, simulated high altitude. *Thorax* 28: 24-28.

Kusakabe, T., Hayashida, Y., Matsuda, H., Gono, Y., Powell, F.L., Ellisman, M.H., Kawakami, T., and Takenaka, T., 1998, Hypoxic adaptation of the peptidergic innervation in the rat carotid body. *Brain Res.* 806: 165-174.

Kusakabe, T., Hayashida, Y., Matsuda, H., Kawakami, T., and Takenaka, T., 2000, Chenges in the peptidergic innervation of the rat carotid body a month after the termination of chronic hypoxia. *Adv. Exp. Med. Biol.* 475: 793-799.

Kusakabe, T., Hirakawa, H., Matsuda, H., Yamamoto, Y., Nagai, T., Kawakami, T., and Hayashida, Y., 2002, Changes in the peptidergic innervation in the carotid body of the rats chrnically exposed to hypercapnic hypoxia: an effect of arterial $CO_2$ tension. *Histol. Histopathol.* 17: 21-29.

Laidler, P., and Kay, J.M., 1975, A quantitative morphological study of the carotid bodies of rats living at a simulated altitude of 4300 meters. *J. Pathol.* 117: 183-191.

Laidler, P., and Kay, J.M., 1975, The effect of chronic hypoxia on the number and nuclear diameter of type I cells in the carotid bodies of rats. *Am. J. Pathol.* 79: 311-320.

Laidler, P., and Kay, J.M., 1978, A quantitative study of some ultrastructural features of the type I cells in carotid bodies of rats living at a aimulated altitude of 4300 meters. *J. Neurocytol.* 7: 183-192.

McGregor, K.H., Gil, J., and Lahiri, S., 1984, A morphometric study of the carotid body in chronically hypoxic rats. *J. Appl. Physiol.* 57: 1430-1438.

Molłer, M., Mollgard, K., and Sorensen, S.C., 1974, The ultrastructure of the carotid body in chronically hypoxic rabbit. *J. Physiol. (Lond).* 238: 447-453.

Pequignot, J.M., and Hellström, S., 1983, Intact and sympathectomized study of the carotid bodies of long-term hypoxic rats: A morphometric light microscopical study. *Virchow Arch. Pathol. Anat.* 400: 235-243.

Pequignot, J.M., Hellström, S., and Johanson, C., 1984, Intact and sympathectomized study of the carotid bodies of long-term hypoxic rats: A morphometric ultrastructural study. *J. Neurocytol.* 13: 481-493.

# Immunohistochemical Study of the Carotid Body just after Arousal from Hibernation

KOHKO FUKUHARA[1], HARUKI SENOO[1], KATSUAKI YOSHIZAKI[2] and KAZUO OHTOMO[3]

*Department of Anatomy, School of Medicine, Faculty of Medicine[1], Department of Physiology[2], Department of Anatomy[3], School of Health Science, Faculty of Medicine, Akita University, Akita 010-8543, Japan*

## 1. INTRODUCTION

Hibernation is a seasonal phenomenon by which some warm-blooded animal species adapt to the harsh environment prevailing during winter. In the cold season, hibernating animals substantially reduce their heart rate, respiratory rate, body temperature, blood flow and oxygen consumption; however, this suppressed physiological state does not persist because of the periodical arousal that returns the animals to euthermy (Daan, 1991; Waßmer *et al.*, 1997). Hibernation is initiated by a drop in heart rate, followed by a gradual decline in body temperature in ground squirrels (Frerichs, 1994), and in the African blue-naped mouse bird (Schaub *et al.*, 1999). The progression from euthermy to torpor during the hibernation season takes about 24 hours (Wang, 1988; Waßmer *et al.*, 1997), but arousal from hibernation takes only one hour. During arousal from hibernation, the respiratory rate, heart rate and oxygen consumption increase markedly and this is followed by an elevation in body temperature.

The carotid body, an arterial chemoreceptor organ that is sensitive to the oxygen and carbon dioxide concentrations in the blood, contains several neurochemical agents in the glomus cells (Lundberg *et al.*, 1979; Wharton et al., 1980; Kobayashi *et al.*, 1983; Fried et al., 1989; Oomori *et al.*, 1994). One of these agents, tyrosine hydroxylase (TH), the rate-limiting enzyme in the biosynthesis of catecholamines, is increased under hypoxic conditions (Fidone *et al.*, 1982 a, b; Kusakabe *et al.*, 1998; Kusakabe *et al.*, 2000; Schmitt *et al.*, 1992; Wang *et al.*, 1998). Hibernation is considered to be a state of hypoxia because of reduced blood flow and increased oxygen affinity of hemoglobin. Our previous study in chipmunks demonstrated that the immunoreactivity for TH in glomus cells of hibernating animals was

*Chemoreception*, Edited by Pequignot et al.
Kluwer Academic/Plenum Publishers, New York, 2003

higher than that in non-hibernating chipmunks. It is thought that TH in glomus cells of hibernating animals may be involved in maintenance of hibernation and the marked physiological changes during arousal from hibernation. In this study, we measured changes in body temperature, respiratory rate and heart rate during arousal from hibernation in the horseshoe bat. Moreover we examined the immunoreactivity for TH in bat carotid bodies in the hibernating state, one hour and two hours after onset of arousal from hibernation.

## 2. MATERIALS AND METHODS

### 2.1 Materials

Eighteen adult male horseshoe bats (*Rhinolophus ferrumequinum*) (mean body weight: 20 g) were used in this study. They were captured in July (5 non-hibernating bats) and in January (13 hibernating bats) in their natural habitat, according to the legal regulations stipulated in Japan. Each animal was placed in an individual chamber and transferred to the laboratory. Non-hibernating bats were rested in a cool damp place before samples were taken. Hibernating bats were placed in hibernation chambers in a refrigerator set at 5 ℃ and allowed to re-enter torpor for 3–4 days before sampling. Six hibernating bats were used for measurement of vital signs such as respiratory rate (Rr), heart rate (Hr), rectal temperature (Rt), and surface temperature at the nose (Ts) during arousal from hibernation. Five non-hibernating bats anesthetized with an intraperitoneal injection of sodium pentobarbital (50 mg/kg body weight) were used for measurements of the same vital signs.Seven hibernating bats were used for immunohistochemical experiments only.

### 2.2 Physiological measurements

An electrocardiogram was used to measure Hr. Rr was measured by attaching a strain gauge (D-FAE-5-512 T11, Minebea Co., Japan) to the chest of hibernating bats during arousal from hibernation (i.e., during re-warming). Rectal temperature was measured with a digital thermometer (SK-1250MC, Sato, Japan), and the surface temperature was measured indirectly at the animal's lips with an infrared-beam-type thermometer (Circle Thermo SK-8100, Sato, Japan). These vital signs were recorded on both a DAT recorder (PC208Ax, Sony, Japan) and a pen recorder (Omniace RT330, NEC, Japan). The measurements were taken with the bat in a natural posture hanging from a bar.

## 2.3 Tissue preparation

Animals were anesthetized with an intraperitoneal injection of sodium pentobarbital (50 mg/kg body weight). The carotid bodies were subjected to immunohistochemical investigation using specific antibody against tyrosine hydroxylase (TH). For fixation, these animals were perfused through the heart with ice-cold 4% (v/v) paraformaldehyde and 0.2% (v/v) picric acid in 0.1 M phosphate buffer (pH 7.4) at a constant flow rate. The bilateral carotid bodies and adjacent tissues containing the common carotid artery and its branches were dissected out from the fixed animals under a dissecting microscope. These tissues were post-fixed in the same fixative for 8–12 h at 4℃. After being washed briefly in 10 mM phosphate-buffered saline (PBS, pH 7.4), the carotid bodies were removed from adjacent tissues and rinsed for 12–24 h in 10 mM PBS containing 30% (w/v) sucrose. They were then frozen and sectioned at 10 μm with a cryostat (Histostat Microtome 2200, Meiwa Shoji Co. Ltd., Japan). The sections were mounted on silane-coated slides (Matsunami, Japan).

## 2. 4 Immunoreactibility

The sections were processed for immunohistochemistry according to the peroxidase–antiperoxidase method. First, endogenous peroxidase activity was quenched by treating the sections with 0.3% (v/v) hydrogen peroxide and 0.2% (v/v) Triton-X diluted in 10 mM PBS (PBS-T) for 30 min at room temperature. The sections were rinsed three times in PBS-T, then incubated at 4℃ for 18–24 h with primary antisera against TH (1:1000; Chemicon, USA) in a solution in 0.5% (w/v) bovine serum albumin and 3% (v/v) normal goat serum in 10 mM PBS-T (pH 7.4) at room temperature. The sections were rinsed with PBS-T, then incubated with goat anti-rabbit IgG (1:200; Jackson, USA) in 10 mM PBS-T (pH 7.4) for 2 h at room temperature. Next they were rinsed three times with PBS-T and then incubated with rabbit peroxidase-antiperoxidase complex (1:200; Dako, Denmark) in 10 mM PBS-T for 2 h at room temperature. The sections were rinsed three times with 50 mM Tris-HCl buffer at pH 7.5. The peroxide activity was visualized with 0.05% (w/v) 3,3'-diaminobenzidine tetrahydrochloride (Sigma, St. Louis, MO, USA) in 50 mM Tris-HCl buffer (pH 7.5) containing 0.01% (v/v) hydrogen peroxide for 10 min at room temperature (Graham and Karnovsky, 1966). The sections were dehydrated through a graded ethanol series (50–100%) and then mounted on Permount (Fisher, USA).

## 2.5 Measurements

Morphometric analysis of TH-immunostained sections was performed by using NIH-Image public domain software. The results are expressed as mean ±standard deviations of the percentage of immunoreactive areas per section from bats in hibernation, and 1 h and 2 h after the onset of arousal from hibernation; at least 16 sections were were examined. per group .

# 3. RESULTS

## 3.1 Physiological results

In non-hibernating bats, Rr was 120–170 breath/min, Hr was 440–660 beats/min. Tr was 36.8–37.1 ℃ and Ts was 28.9–32.1 ℃. The first measurements during the progression of arousal from hibernation were, Rr, 30–70 breath/min, Hr, 42-60 beats/min and Tr, 7.1–10.2℃ (Table. 1). Arousal from hibernation started with an increase in heart rate and respiratory rate, followed by a rise in body temperature. Measurements were taken until the recordings became unstable because the animal began to beat its wings; this occurred within 34–54 min at an environmental temperature of 10.5–11.5℃. The values at the end of the experiment were, Rr, 180–270 breath/min, Hr, 420–720 beats/min and Ts, 18.9–22.8℃.

During arousal from hibernation, the relationship between 1/Ts and ln (Hr) showed two linear components with a break point at 17℃ (Fig. 1).

*Table 1.* Respiratory rate (Rr), heart rate (Hr) and rectal (Tr) and surface (Ts) temperatures at the beginning and the end of arousal from hibernation in horseshoe bats.

| state | | Tr (℃) | Ts (℃) | Rr (breaths/ min) | Hr (beats/min) |
|---|---|---|---|---|---|
| arousal | beginning | 7.1-10.2 | 6.1-11.8 | 30-70 | 42-60 |
| | end | | 18.9-22.8 | 180-270 | 420-720 |
| non-hibernation | | 36.8-37.1 | 28.9-32.1 | 120-170 | 440-660 |

Non-hibernating control bats (n=5) and hibernating bats (n=6) were measured.
Measurements were taken until the recordings became unable because the animal began to beat its wings; this occurred within 34-54 min at an environmental temperature of10.5-11.5℃.

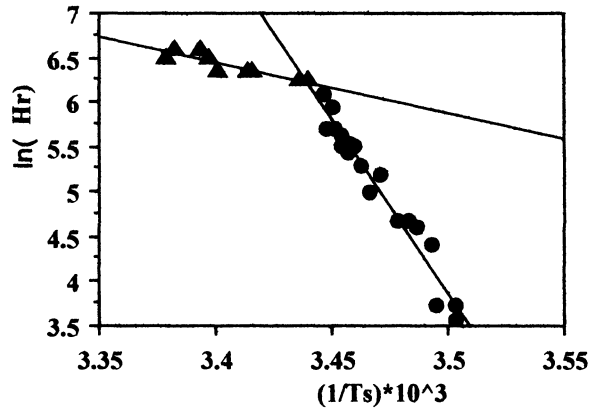


*Fig. 1.* Relationship between the surface temperature at lips (Ts) and heart rate (Hr) of bat during arousal from hibernation. Surface temperature was measured with an infrared-beam type thermometer. The relationship between 1/Ts and ln(Hr) showed two linear components with a break point at 17

## 3.2 Immunohistochemical results

During hibernation, the immunoreactivity for TH in glomus cells of bat carotid bodies increased in comparison with that in non-hibernating animals (Fig. 2). This increase was reduced markedly 1 h after the beginning of arousal from hibernation (Fig. 3). The percentage of immunostained areas per section from hibernating bats, 1 h or 2 h after the onset of arousal from hibernation was 28.6±6.5% (n=19), 17.1±4.7% and 18.2±7.1% (n=38), respectively (Fig. 4).

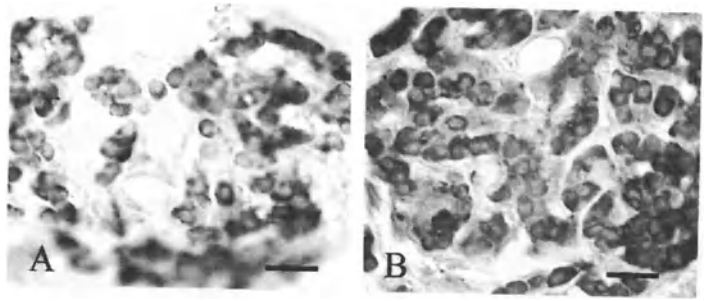


*Fig. 2.* TH immunoreactivities in bat carotid body during non-hibernation (A) and hibernation (B). Scale bar=20μm.

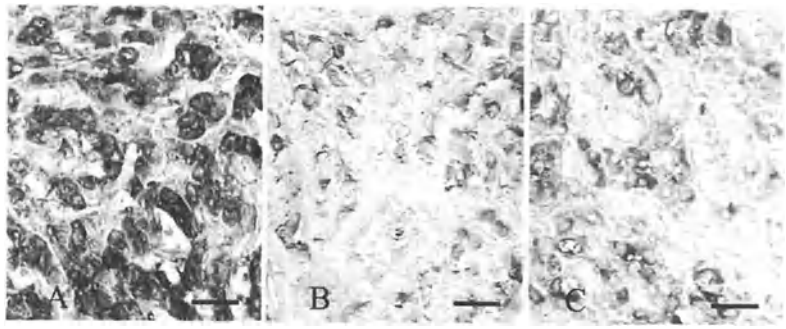


*Fig. 3.* TH immunoreactivities in bat carotid bodies at the state of hibernation (A), 1h (B) and 2h (C) after the onset of arousal from hibernation. Scale bar = 20μm.

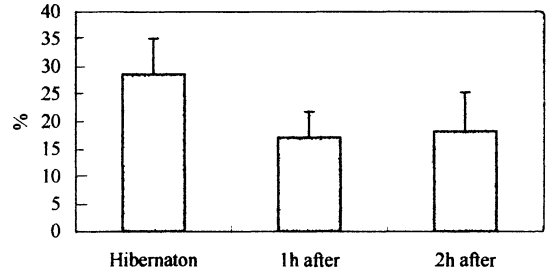


*Fig. 4.* The percentage of immunostained area per section from hibernating, 1h and 2h after the onset of arousal from hibernation were 28.6±6.5% (n=19),17.1±4.7% (n=16) and 18.2 ±7.1% (n=38), respectively

## 4. DISCUSSION

Hypothermia during hibernation is not continuous. Hibernating animals arouse periodically, and 80% of their winter energy budget is consumed during arousal (Wang, 1978). The onset of hibernation is characterized by a gradual decrease in heart rate, followed by a decline in body temperature over 24 hours (Wang. 1988; Frerichs et al., 1994). The length of the arousal phase is affected by ambient temperature (Strijkstra and Dann, 1997), but the time course of arousal from hibernation is about one hour (Wang. 1988; Frerichs et al., 1994). Our present study showed that the physiological changes that occurred during the progression from the state of hibernation to those in non-hibernation started with an increase in Hr and Rr, followed by a rise in body temperature, and the time course of these physiological changes required 34–54 minutes.

Our results for horseshoe bats were similar to those of Wang and Frerichs.

In addition, we examined the relationship between Ts at the lips and Hr of a bat during arousal from hibernation. The relationship between 1/Ts and ln (Hr) showed two linear components with a break point at 17℃.

There are two possible reasons for this break point. First, a difference in enzyme kinetic responses to changing temperature for several enzymes involved in thermogenesis (Storey, 1997). Arousal from hibernation requires thermogenesis in brown adipose tissue. The process of this thermogenesis is started by the stimulation of beta-adrenergic signals, followed by a rise in intracellular 3',5'-cyclic adenosine monophosphate (cAMP), activation of cAMP-dependant protein kinase A (PKA) and then activation of lipolysis and uncoupled respiration. The Arrhenius plots of enzymes for this process showed different, species-specific breakpoints (MacDonald and Storey, 1998). These results suggest that enzymes for this process in hibernating animals may be modulated by different temperatures. A second possible explanation is that there may be differences in the mechanism of heat production. Fons *et al.*, (1997) has demonstrated that the heat for rewarming was produced mainly in the brown adipose tissue up to a body temperature of approximately 17℃ and that further increases are enhanced by skeletal muscle. However, Geiser (1988) has suggested that reduction of metabolism in small hibernators is not only affected by temperature but also by metabolic inhibition. Therefore, the significance of this break point remains unclear.

The carotid body, which plays a regulatory function and is sensitive to oxygen and carbon dioxide in blood, contains several neurochemical agents in nerve fibers around blood vessels and glomus cells (Lundberg *et al.*, 1979; Wharton *et al.*, 1980; Kobayashi *et al.*, 1983; Kondo et al., 1986; Fried *et al.*, 1989; Oomori *et al.*, 1994). It has been reported that the amounts of these neurochemical agents change under hypoxic conditions (Fidone et al., 1982 a, b; Kusakabe *et al.*, 1998; Kusakabe *et al.*, 2000; Wang *et al.*, 1998). TH, the rate-limiting enzyme in the biosynthesis of catecholamines, increases during hypoxic conditions and dopamine is synthesized and released from glomus cells during hypoxia (Fidone et al., 1982a, b; Schmitt et al., 1992; Millhorn *et al.*, 1997). In addition, TH gene expression is stimulated by hypoxia in glomus cells (Czyzyk-Krzeska *et al.*, 1992). Hibernation is considered to be a state of hypoxia because of the decrease in blood flow and increase in oxygen affinity of hemoglobin in response to hypothermia. Our previous study in chipmunks has demonstrated that the immunoreactivity for TH in the carotid bodies of hibernating animals was more intense than that in

non-hibernating ones (Ohtomo *et al.*, 2000). In this study, we observed markedly lower immunoreactivity for TH in bat carotid bodies one hour after onset of arousal from hibernation. Analysis using NIH-Image showed that the ratio of the stained area to total area was significantly lower 1 h after onset of arousal from hibernation (40.2%).

Saitongdee *et al.*, (1999) have shown that immunoreactivities for TH and NPY of sympathetic nerve markers increased in both mesenteric and renal arteries of hibernating hamsters and that the increase was markedly lower 2 h after arousal from hibernation. Furthermore, they, concluded that the increase in immunoreactivities for TH and NPY in hibernating animals reflected their functions in mediating vasoconstriction and the reductions of TH and NPY due to the rapid return of sympathetic nerve activity to normality from hibernation. Stimulation of the sympathetic nerve innervating the carotid body induced vasoconstriction of the carotid body. Kondo *et al.*, (1986) indicated that NPY fibers in carotid bodies are considered to be postganglionic sympathetic noradrenergic fibers. The increase of TH as a sympathetic nerve marker in carotid bodies during hibernation may contribute to vasoconstriction, and the dramatic decrease during arousal may reflect vasodilator control accompanying the marked physiological changes.

These results indicate that TH of carotid bodies in hibernating animals may participate in the maintenance of hibernation and in the marked physiological changes at the onset of, and arousal from hibernation.

## REFERENCES

Czyzyk-Krzeska MF, Bayliss DA, Lawson EE, Millhorn DE (1992) Regulation of tyrosine hydroxylase gene expression in the rat carotid body by hypoxia. *J.Neurochem* 58: 1538-1546

Daan S, Barnes BM, Strijkstra AM (1991) Warming up for sleep? Ground squirrels sleep during arousals from hibernation. *Neurosci Lett* 128: 265-268

Fidone S, Gonzalez C, Yoshizaki K (1982a) Effects of hypoxia on catecholamine synthesis in rabbit carotid body *in vitro*. *J.Physiol* 333: 81-91

Fidone S, Gonzalez C, Yoshizaki K (1982b) Effects of low oxygen on the release of dopamine from the rabbit carotid body *in vitro*. *J Physiol* 333: 93-110

Fons R, Sender S, Peters T, Jurgens KD (1997) Rates of rewarming, heart and respiratory rates and their significance for oxygen transport during arousal from torpor in the smallest mammal, the Etruscan shrew *Suncus etruscus*. *J Exp Biol* 200: 1451-1458

Frerichs KU, Kennedy C, Sokoloff L, Hallenbeck JM (1994) Local cerebral blood flow during hibernation, a model of natural tolerance to cerebral ischemia. J Cereb *Blood Flow* Metab 14: 193-205

Fried G, Meister B, Wikstrom M, Terenius L, Goldstein M (1989) Galanin-, neuropeptide Y- and enkephalin-like immunoreactivities in catecholamine-storing paraganglia of the fetal guinea pig and newborn pig. *Cell Tissue Res* 255: 495-504

Geiser F (1988) Reduction of metabolism during hibernation and daily torpor in mammals and birds: temperature effect or physiological inhibition? *J Comp Physiol* B 158:25-37

Graham RC, Karnovsky MJ (1966) The early stages of absorption of injected horseradish peroxidase in the proximal tubles on mouse kidney: Ultrastructural cytochemistry by a new technique. *J Histochem Cytochem* 14: 291-302

Kobayashi S, Uchida T, Ohashi T, Fujita T, Nakao K, Yoshimasa T, Imura H, Mochizuki T, Yanaihara C, Yanaihara N (1983) Immunocytochemical demonstration of the co-storage of noradrenaline with Met-enkephalin-Arg6-Phe7 and Met-enkephalin-Arg6-Gly7-Leu8 in the carotid body chief cells of the dog. *Arch Histol Jpn* 46: 713-722

Kondo H, Kuramoto H, Fujita T (1986) Neuropeptide tyrosine-like immunoreactive nerve fibers in the carotid body chemoreceptor of rats. *Brain Res* 372: 353-356

Kusakabe T, Hayashida Y, Matsuda H, Gono Y, Powell FL, Ellisman MH, Kawakami T, Takenaka T (1998) Hypoxic adaptation of the peptidergic innervation in the rat carotid body. *Brain Res* 806: 165-174

Kusakabe T, Hayashida Y, Matsuda H, Kawakami T, Takenaka T (2000) Changes in the peptidergic innervation of the rat carotid body a month after the termination of chronic hypoxia. *Adv Exp Med Biol* 475: 793-799

Lundberg JM, Hokfelt T, Fahrenkrug J, Nilsson G, Terenius L (1979) Peptides in the cat carotid body (glomus caroticum): VIP-, enkephalin-, and substance P-like immunoreactivity. *Acta Physiol Scand* 107: 279-281

MacDonald JA and Storey KB (1998) cAMP-dependent protein kinase from brown adipose tissue: temperature effects on kinetic properties and enzyme role in hibernating ground squirrels. *J Comp Physiol* B 168: 513-525

Millhorn DE, Raymond R, Conforti L, Zhu W, Beitner Johnson D, Filisko T, Genter MB, Kobayashi S, Peng M (1997) Regulation of gene expression for tyrosine hydroxylase in oxygen sensitive cells by hypoxia. *Kidney* Int 51: 527-535

Ohtomo K, Fukuhara K, Yoshizaki K (2000) Immunohistochemical study of the carotid body during hibernation. *Adv Exp Med Biol* 475: 815-821

Oomori Y, Nakaya K, Tanaka H, Iuchi H, Ishikawa K, Satoh Y, Ono K (1994) Immunohistochemical and histochemical evidence for the presence of noradrenaline, serotonin and gamma-aminobutyric acid in chief cells of the mouse carotid body. *Cell Tissue Res* 278: 249-254

Saitongdee-P; Milner-P; Loesch-A; Knight-G; Burnstock-G (1999) Electron-immunocytochemical studies of perivascular nerves of mesenteric and renal arteries of golden hamsters during and after arousal from hibernation. *J. Anat* 195; 121-130

Schaub R, Prinzinger R (1999) Long term telemetry of heart rates and energy metabolic rate during the diurnal cycle in normothermic and torpid African blue-naped mousebirds (*Urocolius macrourus*). *Comp Biochem Physiol* A 124: 439-445

Schmitt P, Garcia C, Soulier V, Pujol JF, Pequigot JM (1992) Influence of long-term hypoxia on tyrosine hydroxylase in the rat carotid body and adrenal gland. *J. Auton .Nerv. Syst* 40: 13-19

Storey KB, (1997) Metabolic regulation in mammalian hibernation: Enzyme and protein adaptations. *Comp Biochem Physiol* 118A:1115-1124

Strijkstra-AM, Daan-S (1997) Ambient temperature during torpor affects NREM sleep EEG during arousal episodes in hibernating European ground squirrels. *Neurosci Lett* 221; 177-80

Wang LCH (1988) Mammalian hibernation: An escape from the cold. In: *Advances in*

*Comparative and Environmental Physiology* (Gilles R, ed.), Berlin, Springer, Vol 2, pp 1-45

Wang LCH (1978) Time patterns and metabolic rates of natural torpor in the Richardson's ground squirrel. *Can J Zool* 57: 149-15542)

Waβmer T, Wollnik F (1997) Timing of torpor bouts during hibernation in European hamsters (*Cricetus cricetus L.*). J Comp Physiol B 167: 270-279

Wharton J, Polak JM, Pearse AG, McGregor GP, Bryant MG, Bloom SR, Emson PC, Bisgard GE, Will JA (1980) Enkephalin-, VIP- and substance P-like immunoreactivity in the carotid body. *Nature* 284 (5753): 269-271

Wang ZZ, Dinger B, Fidone SJ, Stensaas LJ (1998) Changes in tyrosine hydroxylase and substance P immunoreactivity in the cat carotid body following chronic hypoxia and denervation. *Neuroscience* 83: 1273-1281

# Index